U.S. DEPARTMENT OF COMMERCE
National Technical Information Service

PB-260 384

Formation and Transport of Oxidants Along Gulf Coast and in Northern U.S

Research Triangle Inst, Research Triangle Park, N C

Prepared for

Environmental Protection Agency, Research Triangle Park, N C Office of Air Quality Planning and Standards

Aug 76

335125

EPA-450/3-76-033
August 1976

PB 260 384

FORMATION AND TRANSPORT OF OXIDANTS ALONG GULF COAST AND IN NORTHERN U.S.

U.S. ENVIRONMENTAL PROTECTION AGENCY
Office of Air and Waste Management
Office of Air Quality Planning and Standards
Research Triangle Park, North Carolina 27711

REPRODUCED BY
NATIONAL TECHNICAL
INFORMATION SERVICE
U. S. DEPARTMENT OF COMMERCE
SPRINGFIELD, VA. 22161

TECHNICAL REPORT DATA

(Please read Instructions on the reverse before completing)

1. REPORT NO. EPA-450/3-76-033	2.	3. RECIPIENT'S ACCESSION NO.
4. TITLE AND SUBTITLE Formation and Transport of Oxidants Along Gulf Coast and in Northern U.S.		5. REPORT DATE August, 1976 6. PERFORMING ORGANIZATION CODE
7. AUTHOR(S) Research Triangle Institute		8. PERFORMING ORGANIZATION REPORT NO.
9. PERFORMING ORGANIZATION NAME AND ADDRESS Research Triangle Institute Research Triangle Park, North Carolina 27709		10. PROGRAM ELEMENT NO. 2AH137, 2AE137, 2AC129 11. CONTRACT/GRANT NO. 68-02-2048
12. SPONSORING AGENCY NAME AND ADDRESS U.S. Environmental Protection Agency Office of Air Quality Planning and Standards Monitoring and Data Analysis Division Research Triangle Park, North Carolina 27711		13. TYPE OF REPORT AND PERIOD COVERED Final 14. SPONSORING AGENCY CODE

15. SUPPLEMENTARY NOTES

16. ABSTRACT

This publication reports on two concurrent sets of field measurements of ozone and precursors which were being conducted in separate regions of the United States from July 1 - October 31, 1975.

The first set of measurements spanned the northern portion of the United States from Montana to Pennsylvania. Three continuously operated ground stations (Wolf Point, Mt.; Creston, Ia.; Bradford, Pa.) were used to monitor ambient levels of ozone NO/NO_x and 24-hour suspended particulate levels plus the analysis of bag samples for organic pollutants. The main objective of the northern study was to determine the extent to which ozone buildup under conducive meteorological conditions differs in large areas having low and high precursor emission densities.

The second set of measurements were taken along the Gulf Coast, primarily in Texas and Louisiana. Continuous monitoring of ozone, NO/NO_x and 24-hour total suspended particulates plus collection of bag samples for analysis of organic pollutants was performed at a rural site near DeRidder, Louisiana. The objectives of the southern set of measurements were to document the extent to which ozone levels exceed the Federal ambient standard in this region and to assess the relative importance of long-range transport and local synthesis in determining the high levels of ambient ozone observed near several Texas cities.

17. KEY WORDS AND DOCUMENT ANALYSIS

a. DESCRIPTORS	b. IDENTIFIERS/OPEN ENDED TERMS	c. COSATI Field/Group
Photochemical Air Pollutants Precursors Ozone Nitrogen Oxides Organic Pollutants	Atmospheric ozone levels. Ozone formation and transport related to precursor levels and weather conditions.	Atmospheric Photochemistry/ Air Pollution

18. DISTRIBUTION STATEMENT Release Unlimited	19. SECURITY CLASS *(This Report)* Unclassified	21. NO. OF PAGES 473
	20. SECURITY CLASS *(This page)* Unclassified	22. PRICE 12.00/3.00

EPA Form 2220-1 (9-73)

*U.S. GOVERNMENT PRINTING OFFICE: 1976 641-317/5534

EPA-450/3-76-033

FORMATION AND TRANSPORT OF OXIDANTS ALONG GULF COAST AND IN NORTHERN U.S.

by

C.E. Decker, L.A. Ripperton, J.J.B. Worth
and
F.M. Vukovich, W.D. Bach, J.B. Tommerdahl, F. Smith, D.E. Wagoner

Research Triangle Institute
Research Triangle Park, N. C. 27709

Contract No. 68-02-2048
Program Element No. 2AC129

EPA Project Officer: Edwin L. Meyer, Jr.

Prepared for

ENVIRONMENTAL PROTECTION AGENCY
Office of Air and Waste Management
Office of Air Quality Planning and Standards
Research Triangle Park, North Carolina 27711

August 1976

1 a

This report is issued by the Environmental Protection Agency to report technical data of interest to a limited number of readers. Copies are available free of charge to Federal employees, current contractors and grantees, and nonprofit organizations - in limited quantities - from the Library Services Office (MD35), Research Triangle Park, North Carolina 27711; or, for a fee, from the National Technical Information Service, 5285 Port Royal Road, Springfield, Virginia 22161.

This report was furnished to the Environmental Protection Agency by Research Triangle Institute, Research Triangle Park, N. C. 27709, in fulfillment of Contract No. 68-02-2048. The contents of this report are reproduced herein as received from Research Triangle Institute. The opinions, findings, and conclusions expressed are those of the author and not necessarily those of the Environmental Protection Agency. Mention of company or product names is not to be considered as an endorsement by the Environmental Protection Agency.

Publication No. EPA-450/3-76-033

ACKNOWLEDGMENTS

This project was conducted by the Research Triangle Institute (RTI), Research Triangle Park, North Carolina, under Contract No. 68-02-2048 for the United States Environmental Protection Agency. The support of this agency is gratefully acknowledged as is the advice and guidance of the Project Officer, E. L. Meyer, Jr. and other staff members of the Office of Air Quality Planning and Standards.

Special acknowledgments are given to two laboratories of the United States Environmental Protection Agency--the Environmental Monitoring and Support Laboratory (EMSL) of the National Environmental Research Center, Research Triangle Park; and the Environmental Monitoring and Support Laboratory of National Environmental Research Center, Las Vegas. The EMSL-RTP participated in the quality assurance auditing program at cooperating state and local agency urban stations and at RTI rural stations and analyzed high volume particulate samples for sulfates, nitrates, and ammonium ion. Special recognition is given of the technical support provided by T. A. Hartlage, B. Martin, J. A. Fraser, and Dr. R. J. Thompson, as is the advice and assistance provided by officials of the EMSL, Dr. T. A. Hauser, and Laboratory Director, Dr. D. S. Shearer. The EMSL-LV provided RTI access to their environmental test chamber for altitude testing of air quality analyzers and their B-26 aircraft, pilots and instrument technicians for joint airborne measurement flights in the gulf coast area in October 1975.

Work on this project was performed by staff members of the Systems and Measurements and Energy and Environmental Research Divisions of RTI under the general direction of Mr. J. J. B. Worth, Group III Vice President. Mr. Worth was Laboratory Supervisor for this program. Mr. C. E. Decker served as Project Leader and was responsible for the coordination and conduct of the program. Staff members of RTI who contributed to the preparation of this report are recognized and listed in alphabetical order: Dr. W. D. Bach, Mr. C. E. Decker, Mr. R. B. Denyszyn, Mr. W. C. Eaton, Dr. L. A. Ripperton, Mr. F. Smith, Mr. J. B. Tommerdahl, Dr. F. M. Vukovich, Dr. D. E. Wagoner, and Mr. J. J. B. Worth.

TABLE OF CONTENTS

Page

ACKNOWLEDGMENTS iii

LIST OF FIGURES ix

LIST OF TABLES xvii

Section

1.0 EXECUTIVE SUMMARY 1

1.1 Introduction and Objectives 1

1.2 Design of Study/Field Measurement Program 1

1.3 Principal Findings 2

1.4 Conclusions 7

2.0 INTRODUCTION 9

2.1 Background 9

2.2 Research Objectives 10

3.0 DESIGN OF STUDY 11

3.1 Northern High Pressure Oxidant Study 12

3.1.1 Airborne Measurements 12

3.1.2 Ground Measurements 13

3.1.3 Ozonesonde Measurements 13

3.2 Gulf Coast Oxidant Study 15

3.2.1 Airborne Measurements 15

3.2.2 Ground Measurements 23

3.2.3 Ozonesonde Measurements 23

3.3 Analysis Procedure 23

3.3.1 Northern High Pressure Oxidant Study 23

3.3.2 Gulf Coast Oxidant Study 24

4.0 FIELD MEASUREMENT PROGRAM 25

4.1 Ground Stations 25

4.1.1 Sampling Protocol 25

4.1.2 Siting Considerations and Description of Monitoring Stations 26

4.1.3 Air Quality Measurements 32

4.1.3.1 Instrumentation 32

4.1.3.2 Instrument Calibration and Maintenance 35

TABLE OF CONTENTS (con.)

Section | Page
4.1.4 Data Acquisition and Data Processing 37
4.1.5 Data Validation and Quality Control 38
4.2 Airborne Measurements 39
4.2.1 Airborne Measurements System Description 39
4.2.1.1 Aircraft 39
4.2.1.2 Measurement System 42
4.2.1.3 Instrumentation 42
4.2.1.4 Data Acquisition System 47
4.2.2 Instrument Calibration and Pressure Effect Tests 49
4.2.2.1 Instrument Calibration 49
4.2.2.2 Pressure Effects Test 50
4.2.3 Operations Procedures and Data Validation Techniques 50
4.2.4 Data Reduction and Processing 55
4.2.5 Aircraft Flight Summary 63
4.3 Ozonesonde Measurement Program 63
4.3.1 Introduction 63
4.3.2 Instrumentation and Data Acquisition 63
4.4 Program Summary 72
5.0 QUALITY ASSURANCE PROGRAM 75
5.1 Quality Assurance Protocol 75
5.1.1 Qualitative Systems Audit 76
5.1.2 Performance Audit 77
5.2 Description of the Air Pollution Monitoring Network 77
5.3 Audit Procedures 81
5.3.1 RTI Ozone Auditing Procedures 81
5.3.2 EPA Ozone Auditing Procedures 82
5.3.3 EPA Oxides of Nitrogen Auditing Procedures 82
5.4 Analysis and Interpretation of Audit Data 83
5.4.1 Precision/Accuracy Estimated for Ozone Measurement 84

TABLE OF CONTENTS (con.)

Section Page

5.4.2 Precision/Accuracy Estimates for Nitric Oxide and Nitrogen Dioxide Measurements 89

5.5 Summary of Audit Results 89

6.0 SUMMARY OF DATA AND STATISTICS 91

6.1 Summary Statistics 91

6.2 Diurnal Patterns 100

6.3 Summary of Climatic Conditions 113

7.0 INTERPRETATION OF RESULTS: NORTHERN HIGH PRESSURE OXIDANT STUDY 121

7.1 Examination of Aircraft Ozone Measurements 121

7.1.1 Data Analysis Approach 121

7.1.2 Summary of Aircraft Ozone Measurements and Meteorological Conditions 122

7.2 The Relationship Between the High Ozone in the Rural Boundary Layer and High Pressure Systems 128

7.2.1 Introduction 128

7.2.2 Statistics on High Ozone Concentrations Versus High Pressure Systems 129

7.2.3 Distribution of Ozone Relative to a Moving High Pressure System 133

7.2.4 Source Regions and Residence Times of Air Relative to a Moving High Pressure System 139

7.2.5 Some Aspects of the Mechanism Governing the Chemistry of Ozone in High Pressure Systems 148

7.2.5.1 Theory 148

7.2.5.2 Variation of the Diurnal Cycle in a Moving High Pressure System 158

7.2.5.3 Variation of Ozone Chemistry in a High Pressure System in the Eastern Portion of the United States 161

7.2.6 Summary of Northern High Pressure Analysis 169

7.3 Chemistry of Ozone Generation 173

7.3.1 Relationship of Ozone and Population Density 177

7.3.2 Ozonesonde Releases 191

TABLE OF CONTENTS (con.)

Section Page

7.3.2.1 Ozonesonde Releases at Huron, South Dakota, September 5-7, 1975 192

7.3.2.2 Stratospheric-Tropospheric Ozone Distribution 192

7.3.2.3 Aircraft and Ozonesonde Profiles 196

7.3.3 Hydrocarbons and Halocarbons 196

7.3.3.1 Variation of Selected Hydrocarbons 196

7.3.3.2 Hydrocarbons: High Pressure System Flight of September 6-7, 1975 201

7.3.4 Particulates, Northern High Pressure Study 201

7.3.4.1 Ground Site Measurements 201

7.3.4.2 Aircraft Particulate Measurements, Northern Study 205

7.3.5 Summary of Ozone Generation (Northern High Pressure Oxidant Study) 207

8.0 INTERPRETATION OF RESULTS: GULF COAST OXIDANT STUDY 209

8.1 Examination of Ozone Measurements and Meteorological Conditions 209

8.1.1 Data Analysis Approach 209

8.1.2 High- and Low-Ozone Days 211

8.1.3 Summary of Aircraft Ozone Measurements and Meteorological Conditions 221

8.1.4 High Ozone Occurrences at Austin, Texas 255

8.1.5 Summary of Gulf Coast Aerial Survey 266

8.2 Chemistry of Ozone Generation 268

8.2.1 Bag Irradiation Experiments 280

8.2.2 Ozonesonde Releases 280

8.2.2.1 Introduction 280

8.2.2.2 Ozonesonde Releases at DeRidder, Louisiana, October 24-27, 1975 284

8.2.2.3 Stratosphere-Troposphere Ozone Distribution 284

8.2.2.4 Low Altitude Distribution of Ozone 287

8.2.3 Variation of Selected Hydrocarbons 289

TABLE OF CONTENTS (con.)

Section **Page**

8.2.3.1 Theoretical Considerations 289

8.2.3.2 Variation of Selected Hydrocarbons 291

8.2.4 Particulates 294

8.2.4.1 Total Suspended Particulates; Sulfate, Nitrate, Ammonium 294

8.2.4.2 Gulf Coast Aircraft Particulate Samples 294

8.2.5 Summary of Ozone Generation (Gulf Coast Oxidant Study) 297

9.0 CONCLUSIONS 299

10.0 REFERENCES 301

APPENDIXES

APPENDIX A. Calibration Systems/Procedures 305

APPENDIX B. Performance Characteristics and Operational Summaries for Instruments 315

APPENDIX C. Airborne Platform Air Sampling System Design 319

APPENDIX D. Ozone and Oxides of Nitrogen Analyzer Evaluation at Reduced Pressure 343

APPENDIX E. Summary Sheets for Aircraft Data and Selected Flights 353

APPENDIX F. Background Data and Emission Study for Texas Gulf Coastal Area 447

LIST OF FIGURES

Figure		Page
1	Site locations for ground station network.	14
2	Sea breeze flight plan.	16
3	Downwind plume flight plan.	18
4	Areal survey flight plan.	19
5	North-south survey flight plan.	20
6	Land-sea survey flight plan.	21
7	Double-box flight plan.	22
8	Air monitoring station, Bradford Regional Airport.	28
9	Interior view of air monitoring station.	28
10	Aerial view of Creston, Iowa (Creston Municipal Airport) site.	29
11	Air monitoring station, Creston Municipal Airport.	29
12	Aerial view of Wolf Point, Montana (Wolf Point International Airport) site.	30
13	Air monitoring station, Wolf Point International Airport.	30
14	Aerial view of Lewisburg, West Virginia (Lewisburg Airport) site.	31
15	Air monitoring station, Lewisburg Airport.	31
16	Aerial view of DeRidder, Louisiana (Beauregard Parish Airport) site.	33
17	Air monitoring station, Beauregard Parish Airport.	33
18	Instrumented aircraft.	40
19	Functional layout of airborne sampling system.	41
20	Block diagram, aircraft air sampling system.	43
21	Diagram of physical layout.	44
22	Diagram of grab sampling system for hydrocarbon sample collection.	46
23	Diagram of selective filter sampling system.	46
24	Sketch of airborne high volume sampler.	47
25	Aircraft vertical profile (typical flight track).	51
26	Example of ground measurement comparison.	53
27	Low pass pattern for aircraft/station comparison.	53

LIST OF FIGURES (con.)

Figure		Page
28	Comparison data during low passes.	54
29	Comparison data during low passes.	55
30	Normalized response versus altitude for Bendix ozone analyzer.	57
31	Normalized response versus altitude for Bendix oxides of nitrogen analyzer.	57
32	Example of initial data plots.	58
33	Sample flight track.	61
34	Vertical profile; flight 079 flown on September 21, 1975.	62
35	Gulf coast sea-breeze flights (6/28/75-10/21/75).	64
36	Gulf coast inland survey flights (6/25/75-10/31/75).	65
37	Northern high pressure flights (7/8/75-9/30/75).	66
38	Mean diurnal ozone concentrations at Bradford, Creston, and Wolf Point (June 27-September 30, 1975).	107
39	Mean diurnal ozone concentrations at Bradford, Lewisburg, and DeRidder (June 27-September 30, 1975 at Bradford; June 27-October 31, 1975 at Lewisburg and DeRidder).	108
40	Mean diurnal ozone concentrations at Pittsburgh, Columbus, and Poynette (June-September 1975).	109
41	Mean diurnal ozone concentrations at Omaha, Cedar Rapids, and Des Moines (June-September 1975).	110
42	Mean diurnal ozone concentrations at Nederland, Austin, Houston, and DeRidder (June 1-September 30, 1975, except DeRidder--July-October 1975).	111
43	Mean diurnal ozone concentrations at Kane (1973), DuBois (1974), and Bradford (1975) Pennsylvania.	112
44	Mean diurnal ozone concentrations at Columbus, Ohio for 1974 and 1975.	114
45	Mean diurnal nitrogen dioxide concentrations at Bradford, Creston, Wolf Point, and DeRidder (June 27-October 31, 1975)	115
46	Tracks of high pressure center (July 1975).	116
47	Tracks of high pressure center (August 1975).	117
48	Tracks of high pressure center (September 1975).	118

LIST OF FIGURES (con.)

Figure		Page
49	High pressure system flight on July 24, 1975.	124
50	High pressure system flight on July 25, 1975.	125
51	High pressure system flight on July 26, 1975.	126
52	Area averaged value of the daily maximum ozone concentration (solid line) and the area averaged surface pressure (dashed line) versus day of month for latter part of the summer of 1973 and 1974.	130
53	Daily maximum ozone concentration at Wolf Point, Montana; Creston, Iowa; and Bradford, Pennsylvania and the daily average pressure obtained from the nearest synoptic station for the summer of 1975.	131
54	Nine-point running average of the data presented in figure 53 and of the Bradford ozone data and the Pittsburgh pressure data presented in figure 53.	134
55	The temporal and spatial variation of the diurnal maximum ozone concentration through a high pressure system located in the east in the summers of 1973, 1974, and 1975.	135
56	The average temporal and spatial variation of the diurnal maximum ozone concentration through a high pressure system located in the east based on the 1973, 1974, and 1975 data.	137
57	The temporal and spatial variations of the diurnal maximum ozone concentration through a high pressure system based on the 1975 data at Wolf Point, Montana; Creston, Iowa; and Bradford, Pennsylvania.	138
58	Hypothetical high pressure system for which residence time were calculated.	141
59	The number of days air parcels, in various locations in a high pressure system, will spend within that system versus the speed of the system for a circular symmetric high pressure system.	143
60	The number of days air parcels in high pressure systems have spent (residence time) within the system versus the speed of the system for a circular symmetric high pressure time.	145

LIST OF FIGURES (con.)

Figure		Page
61	The number of days air parcels in various locations in a high pressure system will spend within that system versus differently shaped elliptical high pressure systems. The system speed is 7.5 ms^{-1}.	146
62	The number of days air parcels have spent (residence time) within a high pressure system versus differently shaped elliptical systems. The system speed is 7.5 ms^{-1}.	147
63	The diurnal variation of the transport and synthesis term in a rural boundary layer in North Carolina.	153
64	The variation of δ versus λ.	153
65	The variation of the concentrations of NO, NO_2, and α-pinene versus δ for various values of T.	154
66	The variation of β versus δ^* and δ^{**}.	157
67	The variation of the ratio, O_{3o}/O_{3max} versus δ.	157
68	The average diurnal variation of ozone concentration at Wolf Point, Creston, and Bradford based on eight high pressure systems which consecutively passed through these stations. The day with the largest diurnal maximum ozone concentration, when the high pressure system was in the vicinity of the station, was used to compute the average for all eight systems.	159
69	The average diurnal variation of ozone for those days when the diurnal maximum ozone concentration exceeded the NAAQS (solid line) and when the diurnal maximum was less than the NAAQS (dash-dot line) based on the data for August 1973 (A), 1974 (B), and 1975 (C) and at Kane, DuBois, and Bradford, Pennsylvania, respectively.	162
70	The average diurnal variation of ozone at Lewisburg, West Virginia for those days when the diurnal maximum ozone concentration exceeded the NAAQS (solid line) and when the diurnal maximum was less than the NAAQS (dash-dot line) based on data for August 1973 (A) and 1975 (B).	166
71	Population density by counties: 1970.	178
72	General equal response curves (0.08 ppm ozone) for an alkane-NO_2 system (solid line) and for an olefin-NO_2 system (broken line). The two diagonals with their indicated slopes define the HC/NO_2 ratios which correspond to maximum ozone production for each type of hydrocarbon.	182

LIST OF FIGURES (con.)

Figure		Page
73	Ozone versus median NO_x concentration range at Bradford, Pennsylvania and Wolf Point, Montana (July-September 1975).	190
74	Time-altitude cross section of ozone and potential temperature.	194
75	Vertical profiles of ozone at Huron, South Dakota.	197
76	Vertical profiles of ozone at Huron, South Dakota.	198
77	Bar graph showing propane and acetylene concentrations by day of week at Bradford, Pennsylvania, Creston, Iowa, and Wolf Point, Montana (July-September 1975).	199
78	Linearized plot of selected hydrocarbons from flight on September 6-7, 1975.	202
79a	Arriving air trajectories associated with lower decile concentrations of maximum ozone at DeRidder, Louisiana.	212
79b	Arriving air trajectories associated with upper decile concentrations of daily maximum ozone at DeRidder, Louisiana.	213
79c	Arriving air trajectories associated with lower decile concentrations of daily maximum ozone at Nederland, Texas.	214
79d	Arriving air trajectories associated with upper decile concentrations of daily maximum ozone at Nederland, Texas.	215
79e	Arriving air trajectories associated with lower decile concentrations of daily maximum ozone at Houston, Texas.	216
79f	Arriving air trajectories associated with upper decile concentrations of daily maximum ozone at Houston, Texas.	217
79g	Arriving air trajectories associated with lower decile concentrations of daily maximum ozone at Austin, Texas.	218
79h	Arriving air trajectories associated with upper decile concentrations of daily maximum ozone at Austin, Texas.	219

LIST OF FIGURES (con.)

Figure		Page
80	Ozone concentrations, air trajectories and sea level pressure distribution for August 7, 1975 flight.	222
81	Ozone concentrations, air trajectories and sea level pressure distribution for August 8, 1975 flight.	223
82	Ozone concentrations, air trajectories and sea level pressure distribution for August 9, 1975 flight.	226
83	Ozone concentrations, air trajectories and sea level pressure distribution for September 19, 1975 flight.	227
84	Ozone concentrations, air trajectories and sea level pressure distribution for September 21, 1975 flight.	229
85	Ozone concentrations, air trajectories and sea level pressure distribution for October 10, 1975 flight.	231
86	Ozone concentrations, air trajectories and sea level pressure distribution for October 13, 1975 flight.	232
87	Ozone concentrations, air trajectories and sea level pressure distribution for October 14, 1975 flight.	234
88	Time altitude cross section of potential temperature (°K) at Lake Charles, Louisiana. Dates are indicated at 0000 GMT.	236
89	Ozone concentrations, air trajectories and sea level pressure distribution for October 19, 1975.	237
90	Ozone concentrations, air trajectories and sea level pressure distribution for October 20, 1975 flight.	239
91	Ozone concentrations, air trajectories and sea level pressure distribution for October 21, 1975 flight.	242
92	Ozone concentrations and temperature from vertical profile flight of October 21, 1975 at DeRidder, Louisiana.	244
93	Ozone concentrations, air trajectories and sea level pressure distribution for October 22, 1975 flight.	245
94	Ozone concentrations, air trajectories and sea level pressure distribution for October 24, 1975 flight.	247
95	Air trajectories and sea level pressure distribution for October 30, 1975 flight.	249
96	Analysis of aerial ozone distribution as measured on EPA and RTI flight paths at 305 m near Port Arthur, Texas, October 30, 1975.	250

LIST OF FIGURES (con.)

Figure — Page

97 Vertical profile of ozone concentration, temperature, and winds at Lake Charles, Louisiana, October 30, 1975. 252

98 Ozone concentrations, air trajectories and sea level pressure distribution for October 31, 1975 flight. 253

99 Ozone concentrations, air trajectories and sea level pressure distribution of the August 8, 1975 flight and the trajectories of parcels arriving in Austin on the morning (□) and the evening (Δ) of August 9, 1975. 258

100 Ozone concentrations, air trajectories and sea level pressure distribution of the August 9, 1975 flight and trajectories of parcels arriving in Austin on the morning (□) and the evening (Δ) of August 10, 1975. 259

101 Temperature profiles at Victoria, Texas, August 9, 0000 GMT to August 10, 0000 GMT, Isothermal (C) are skewed. Dashed lines are the dry adiabats for the 0900, 1200 and 1500 CST temperatures at Austin, Texas on August 10, 1975. 260

102 Hourly average ozone concentrations, August 9, 10, 1975 at Austin, Texas and the mean hourly average concentration for July 1 to October 31, 1975. 261

103 Air trajectories arriving in Austin, Texas on September 3-4, 1975 (□ - morning, Δ - evening). 264

104 Hourly average ozone concentrations, September 3, 4, 1975 at Austin, Texas and the mean hourly average concentration from July 1 to October 31, 1975. 265

105 Ozone concentrations observed on sea-breeze flight of September 19, 1975. 270

106 Ozone concentrations observed on aerial survey flight on June 27, 1975. 271

107 Ozone concentrations observed on box flight pattern on October 19, 1975. 272

108 Ozone concentrations observed on aerial survey flight on June 26, 1975. 273

109 Ozone concentrations, transitions flight on August 5, 1975. 277

110 Ozone concentrations, transition flight on June 25, 1975. 278

LIST OF FIGURES (con.)

Figure		Page
111	Ozone increase as a function of initial NO_x concentration; captured air irradiation experiments, DeRidder, Louisiana (October 1-31, 1975).	282
112	Ozone increase as a function of initial ozone concentration; captured air irradiation experiments, DeRidder, Louisiana (October 1-31, 1975).	283
113	Time-altitude cross section of ozone and potential temperature, lower portion.	285
114	Time-altitude cross section of ozone and potential temperature, upper portion.	286
115	Vertical profile of ozonesonde data (solid) and best fit profile (dashed) 100 to 100 mb.	288
116	Vertical profile of ozone departures from best fit profile and time-altitude cross section of potential temperature.	290
117	Bar graph showing acetylene and propane concentrations by day of week at DeRidder, Louisiana (July-October 1975).	292

LIST OF TABLES

Table		Page
1	Pollutants measured at rural monitoring stations	26
2	Calibration techniques	35
3	List of data channels	48
4	Flight data, sea-breeze flight 079 (9/21/75)	59
5	Flight summary, northern route high pressure system surveys	67
6	Flight summary, gulf coast area	68
7	List of vertical profile flights	69
8	Flight summary, joint EPA-RTI gulf coast flights	70
9	List of location identifiers	71
10	Program schedule	73
11	Summary of ozone and oxides of nitrogen audit data	85
12	Statistical summary of hourly ozone concentration measurements by station	92
13	Summary of ozone data above NAAQS by station	93
14	Statistical summary of hourly oxides of nitrogen concentration measurements - rural stations (June 27 - September 30, 1975)	94
15	Statistical summary of selected hydrocarbon and halocarbon analyses	95
16	Summary of mean 24-hour particulate concentrations: (TSP, NH_4^+, NO_3^-, $SO_4^=$) for rural stations (July to September 1975)	96
17	Summary of mean ozone and oxides of nitrogen concentrations by month	97
18	Summary of mean hydrocarbon and halocarbon concentrations by month at rural stations (July - September 1975)	98
19	Cumulative frequency distributions of hourly concentrations of ozone - rural stations (June 27-September 30, 1975)	101
20	Cumulative frequency distributions of hourly concentrations of ozone - State/local stations (June-September 1975)	102
21	Cumulative frequency distribution of hourly concentrations of oxides of nitrogen - rural stations (June 27-September 30, 1975)	103

LIST OF TABLES (con.)

Table		Page
22	Means of hourly concentrations of ozone for each hour of day - RTI rural stations (June 27-September 30, 1975)	104
23	Means of hourly concentrations of ozone for each hour of day - State/local stations (June-September 1975)	105
24	Means of hourly concentrations of oxides of nitrogen for each hour of day - rural stations (June 27-September 30, 1975)	106
25	Candidate missions by sector	123
26	Average ozone concentration at mission altitude	123
27	Average ozone concentration for each operational sector	127
28	The relationship between the number of hours a high system is near a station and the number of hours of high ozone (greater than the NAAQS) observed at that station for the period 4 July to 3 September. In 1975, the station used was Bradford; in 1974, DuBois; and in 1973, Kane.	132
29	The values of t_{max}, $0_3*/0_3**$ (where 0_3* is Wolf Point ozone amplitude in all cases), β (estimated from t_{max} and letting t'_{max} = 1400 LDT), α, diurnal ozone amplitude (diurnal maximum ozone minus diurnal minimum ozone), and the diurnal minimum ozone concentration for Wolf Point, Creston, Iowa, and Bradford, Pennsylvania obtained from the diurnal curves given in figure 68.	160
30	The values of t_{max}, $0_3*/0_3**$ (0_3* is the amplitude of ozone for the high ozone case), β (using t_{max} and letting t'_{max} = 1400 LDT), and α for Kane, Pennsylvania obtained from the 1973 diurnal curves given in figure 69.	161
31	The values of t_{max}, $0_3*/0_3**$ (0_3* is the amplitude of ozone for the high ozone case), β (using t_{max} and letting t'_{max} = 1400 LDT), and α for DuBois, Pennsylvania obtained from the 1974 diurnal curves in figure 69.	163
32	The values of t_{max}, $0_3*/0_3**$ (0_3* is the amplitude of ozone for the high ozone case), β (using t_{max} and letting t'_{max} = 1400 LDT), and α for Bradford, Pennsylvania obtained from the 1975 diurnal curves in figure 69.	164

LIST OF TABLES (con.)

Table **Page**

33 The values of t_{max}, O_3*/O_3** (when O_3* was the amplitude of ozone in 1973 in all cases), β (using t_{max} and letting t'_{max} = 1400 LDT), α, the diurnal amplitude of ozone (ozone maximum minus the ozone minimum), and the diurnal minimum ozone concentration for the high ozone cases in 1973, 1974, and 1975 from figures 69A, B, and C. 165

34 The values of t_{max}, O_3*/O_3** (where O_3* is the amplitude of ozone in the high ozone case), β (using t_{max} and letting t'_{max} = 1400 LDT), and α for Lewisburg, West Virginia obtained from the 1973 diurnal curves given in figure 70. 167

35 The value of t_{max}, O_3*/O_3** (where O_3* is the amplitude of ozone in the high ozone case), β (using t_{max} and assuming t'_{max} = 1400 LDT), and α for Lewisburg, West Virginia obtained from the 1975 diurnal curves given in figure 70. 167

36 The values of t_{max}, O_3*/O_3** (where O_3* was the amplitude of ozone in 1973 in all cases), β (using t_{max} and letting t'_{max} = 1400 LDT), α, the diurnal amplitude of ozone (maximum ozone minus minimum ozone), and the diurnal minimum ozone concentration for the high ozone cases in 1973 and 1975 from figures 70A and 70B. 167

37 The average maximum concentration of NO_2 found between the time of maximum ozone and midnight using only the data on high ozone days for August 1974 at DuBois, Pennsylvania and in 1975 at Bradford, Pennsylvania; and the computed NO concentration at the time of maximum NO_2 assuming a three-gas system (NO, NO_2, and NO_3). 168

38 Population density for States west of Fargo, N.D. → Dallas, Texas line* 175

39 Population density for states between Fargo, N.D. → Dallas, Texas line and east of Chicago, Illinois → St. Louis, Missouri line* 176

40 Population density for states east of Chicago, Illinois → St. Louis, Missouri line* 176

41 Summary of ozone data for rural stations 179

42 Summary of aircraft ozone data for population density areas 179

LIST OF TABLES (con.)

Table		Page
43	Dark phase ozone half life	179
44	Results of computer simulation runs	181
45	Mean hydrocarbon and halocarbon concentrations for selected ozone concentration ranges at Wolf Point, Montana (July-September 1975)	183
46	Mean hydrocarbon and halocarbon concentrations for selected ozone concentration ranges at Creston, Iowa (July-September 1975)	184
47	Mean hydrocarbon and halocarbon concentrations for selected ozone concentration ranges at Bradford, Pennsylvania (July-September 1975)	185
48	Mean hydrocarbon and halocarbon concentrations for selected ozone concentration ranges for aircraft samples - Region 1 - west of Fargo, N.D. → Dallas, Texas	186
49	Mean hydrocarbon and halocarbon concentrations for selected ozone concentration ranges for aircraft samples - Region 2 - east of Fargo, N.D. and Dallas, Texas line and west of Chicago, Illinois → St. Louis, Missouri line	187
50	Mean hydrocarbon and halocarbon concentrations for selected ozone concentration ranges for aircraft samples - Region 3 - east of Chicago, Illinois → St. Louis, Missouri line	188
51	Summary of NO_x data	189
52	Comparison of ozone measuring techniques	193
53	Average daily total suspended particulate (TSP) by month at three sites (1975)	203
54	Sulfate as a percentage of TSP by month	203
55	Selected particulate constituents as percentages of gross suspended particulates (1966-1967)*	204
56	Nitrate as a percentage of TSP by month	205
57	Nitrate and sulfate: north high pressure flights	206
58	Summary of conditions accompanying upper decile ozone concentrations at Austin, Texas, July 1 to October 31, 1975	256
59	Mean hydrocarbon and halocarbon concentrations for ozone concentration ranges at DeRidder, Louisiana (July-October 1975)	274

LIST OF TABLES (con.)

Table		Page
60	Mean hydrocarbon and halocarbon concentrations for ozone concentration ranges, gulf coast - flights over land (July-October 1975)	275
61	Average hydrocarbon and halocarbon concentrations for ozone concentration ranges, gulf coast - flights over water (July-October 1975)	276
62	Population density for southeastern States*	279
63	DeRidder, Louisiana bag irradiation experiments, 1975, experimental data from bag irradiation	281
64	Average daily total suspended particulate (TSP) by month at DeRidder, Louisiana (1975)	287
65	Selected particulate constituents as percentages of gross suspended particulates (1966-1967)*	295
66	Nitrate and sulfate concentrations for samples collected during gulf coast flights	296

1.0 EXECUTIVE SUMMARY

1.1 Introduction and Objectives

During the summer of 1975, Research Triangle Institute (RTI) conducted a two-part field measurement program designed (1) to determine the change in the concentration of ozone in the center of a high pressure system, as the system moves from an area of low population density to an area of high population density; and (2) to determine the areal extent of high ozone concentrations in the northern gulf coast region of Texas.

In the Northern High Pressure System Oxidant Study, the objective was to determine the change in the concentration of ozone near the center of high pressure systems, as these systems traverse the northwestern, north-central, and northeastern areas of the United States. During their passage over the United States, these systems traverse, first, regions of low population density and little industrial activity--that is, regions having small emission densities of the hydrocarbon and nitrogen oxide precursors necessary for the production of the photochemical oxidants. During this initial period, low ozone concentrations were anticipated. As the systems move eastward, however, population density, industrial activity, and, consequently, emissions of oxidant precursors increase. It was anticipated that ozone levels would increase.

The objective of the Gulf Coast Oxidant Study was to document the areal extent of high ozone concentrations in the northern gulf coast region of Texas. Primary emphasis was on the roles and/or contribution of land-sea breeze circulations, of local emissions of ozone precursors, and of transport of ozone and ozone precursors within and downwind of the study areas.

1.2 Design of Study/Field Measurement Program

To accomplish the objectives described above at a minimum cost, two independent studies were designed that could be conducted concurrently and that employed similar measurement systems.

Based on the above considerations, two modes of measurement were employed: (1) a network of five, fixed, rural sites operated by RTI plus supplementary rural and urban ground-level sites operated by State/local/other agencies, and (2) an instrumented aircraft flying specified patterns. The field measurement program included continuous ozone and nitrogen dioxide measurements, collection of grab samples for selected hydrocarbon and halocarbon analyses, and 24-hour, total suspended particulate (TSP) samples at four manned, rural stations located in Bradford, Pennsylvania; Creston, Iowa; Wolf Point, Montana; and DeRidder, Louisiana. Ozone measurements were also made at an unmanned station at Lewisburg, West Virginia, and at supplementary stations located in the general study areas, which were operated by State and local governments or by private industry. Ozone and oxides of nitrogen were measured and grab samples collected during aircraft flights designed to accomplish specific objectives for each study area. Supplemental vertical ozone data were obtained from ozonesonde releases at Huron, South Dakota, and DeRidder, Louisiana. A joint RTI-EPA quality assurance program was designed and implemented to assure that high quality data were obtained.

The data acquisition program began at all stations before July 1, 1975. Data were collected and quality assurance performance audits were performed at specified intervals at each of the stations included in the monitoring network through September 30, 1975, at northern stations and through October 31, 1975, in the South.

Since only one aircraft was utilized for both studies, the aircraft was based in DeRidder, and flights were conducted in the gulf coast area until an appropriate high pressure system developed in the northern study area. A total of 111 individual aircraft flights were flown during the combined studies. These flights were flown under varying meteorological conditions and included sea breeze flights, coastal areal survey slights, downwind plume flights, vertical profile flights, double-box patterns around Nederland, Texas, calibration and instrument checkout flights, and northern high pressure system flights. During the month of October, several joint RTI-EPA/Las Vegas flights were flown in the gulf coast area.

1.3 Principal Findings

The data obtained during the field measurement program were summarized statistically and segmented into four general subject areas for analysis and interpretation. These areas are: (1) Northern High Pressure Oxidant Study, (2) Gulf Coast Oxidant Study, (3) Chemistry of Ozone Generation in Rural Areas, and (4) Quality Assurance Program. Data were analyzed and interpreted according to the objectives for each study and have been incorporated into a comprehensive section that combined both a chemical and meteorological interpretation of the results. Principal findings are presented separately below. Results of the Quality Assurance Program and an abbreviated statistical summary of the data are also included.

A. Quality Assurance Program

Based on the precision and bias estimates obtained from the audit data, it is concluded that the quality of the ozone and nitrogen oxides measurements was comparable to the quality of similar measurements made in other well managed networks and was sufficient to satisfy the summer study requirements. Estimates of the relative bias, the coefficient of variation and the 90 percent confidence interval for the error (deviation of the measured value from the audit value) in the O_3, NO, and NO_2 measurement data are presented in section 5.5 of the report.

B. Statistical Summary of Data

1. The mean hourly concentrations of ozone at rural stations ranges from a low of 58 $\mu g/m^3$ at Wolf Point to 81 $\mu g/m^3$ at Bradford. For urban stations the range for mean hourly concentrations was from 44 to 73 $\mu g/m^3$. The standard deviations for all stations, both rural and urban, were similar in magnitude. The overall ozone mean (i.e., ozone burden) was, in general, higher for rural stations than for urban stations.

2. Maximum hourly average ozone concentrations for rural stations ranged from a low of 128 $\mu g/m^3$ at Wolf Point to a high of 256 $\mu g/m^3$ at DeRidder. Maximum hourly averages at urban stations ranged from a low of 180 $\mu g/m^3$ to 629 $\mu g/m^3$.

3. The NAAQS for photochemical oxidants (160 $\mu g/m^3$) was exceeded approximately 4, 3, 1, 1, and 0 percent of the hours at Bradford, Lewisburg, Creston, DeRidder, and Wolf Point, respectively and from less than 1 to 8 percent of the hours at the urban stations.

4. Based on the percentage of days exceeding the NAAQS and hours above the standard a west-to-east gradient in ozone concentration was observed using northern rural stations data as follows:

Site	Hours above standard	Days above standard	Percent of days above standard
Wolf Point	0	0	0.0
Creston	17	7	8.0
Lewisburg	59	11	11.1
Bradford	100	18	18.5

5. Mean hourly concentrations of nitric oxide and nitrogen dioxide measured at the four rural stations (Bradford, Creston, Wolf Point, DeRidder) were in the noise or below the detectability level of the measurement method ($\leq 10\ \mu g/m^3$).

6. An increase in the percentage of sulfates and nitrates in the suspended particulate matter from west-to-east stations was observed. A definite trend was not observed in the hydrocarbon and halocarbon concentrations observed at the rural stations.

C. Northern Oxidant Study

Analyses of rural ozone concentrations were made for (1) four locations (Wolf Point, Creston, Bradford, and Lewisburg) and (2) three locations in northwestern Pennsylvania during comparable dates of 1973 (Kane), 1974 (DuBois), and 1975 (Bradford). The analyses were aided by simplified models of atmospheric synthesis and destruction of ozone and of the airflow near the ground in a transient anticyclone.

1. The analyses show that high ozone occurrences during the summer months are associated with high pressure systems. In the midwest and eastern United States, the lowest ozone concentrations are found in the leading portion of the system and the highest ozone concentrations in the trailing portion of the system. The airflow model shows that air parcels in the leading portion of the system have the shortest residence time in the system and those parcels in the trailing portion, the longest residence time. Ozone concentrations measured at Wolf Point show little variability as high pressure systems passed through that area.

2. Ozone--as indicated by the daily maximum concentration or the number of hours the NAAQS was exceeded--increased when the high pressure system was in the east compared to when it was in the west. The increase in ozone was apparently due to a west to east increase in the diurnal minimum rather than a substantial west to east increase in ozone production.

3. The data suggested that the west to east increase in the diurnal minimum can be attributed to lower concentration of ozone destructive agents in the west. This allowed a residual amount of ozone to remain after each diurnal cycle as the parcel drifted eastward.

4. The evidence indicates that there was a reversal of the role of synthesis and destruction of ozone in high pressure systems located in the east from 1973 to 1974 and 1975. Lower concentrations of ozone destructive agents and smaller amplitude of synthesis were found in 1973 compared to 1974 and 1975.

5. The summer of 1973 and the largest total number of runs of high pressure and high ozone compared to 1974 and 1975. The large number of hours of high ozone was summarized to be a result of the relatively stagnant condition allowing air parcels in the high pressure systems to have large residence times and to experience many diurnal cycles depleting the concentration of ozone precursors and destructive agents and increasing the level of diurnal minimum.

6. In 1975 fewer hours of high pressure, fewer hours of concurrant high ozone, and lower average ozone concentrations during high pressure were observed than in 1974 or 1973 in northwestern Pennsylvania. Macroscale high pressure systems were not as persistent in 1975 as in the two previous years.

7. Ozone data from all aircraft flights show an increase of afternoon (1300-1900 LDT) average concentrations from west to midwest to east sectors of the study area as follows:

Sector	Mean	Standard deviation
West	60 $\mu g/m^3$	4 $\mu g/m^3$
Midwest	96 $\mu g/m^3$	11 $\mu g/m^3$
East	106 $\mu g/m^3$	16 $\mu g/m^3$

8. Anthropogenic pollutants (acetylene and halocarbons) are present in all grab samples collected at northern rural ground stations and during aircraft flights. Mean hourly average oxides of nitrogen concentrations even though in the noise level of the measurement technique are higher on a relative basis at Bradford and at Creston than at Wolf Point. This observation is based on over two thousand samples at each site.

9. Analysis of a series of ozonesonde releases at Huron, South Dakota, does not indicate ozone intrusion from the stratosphere.

10. Ozone concentrations measured at ground stations and during aircraft flights and the sulfate and nitrate composition of total suspended particulates increase from west to east. This pattern is generally consistent with population density patterns.

D. Gulf Coast Oxidant Study

1. Air moving slowly over areas of large hydrocarbon emissions was associated with upper decile ozone concentrations at

urban and rural locations in the gulf coast area. In most cases, trajectory analysis showed air with high ozone concentrations arrived from nonprevailing directions.

2. Air that moved rapidly, showed weak anticyclonic curvature, and had long overwater fetches was associated with lower decile ozone concentrations at all of the ground station locations.

3. In most cases, trajectory analysis attributed the highest ozone concentrations to principal cities or areas of high precursor emissions located in the gulf coast study area. These observations suggest that ozone plumes commonly develop downwind of large precursor emission areas.

4. Aircraft ozone measurements clearly demonstrate an ozone plume (280 $\mu g/m^3$, maximum) upon a low (< 100 $\mu g/m^3$) background downwind of the petrochemical complex at Port Arthur, Texas. During the period observed, ground level ozone concentrations at a continuously operating ground station near the emission area were less than 100 $\mu g/m^3$.

5. Intercity urban plume transport of ozone or ozone precursor materials was evident. This was shown as a potential cause of some violations of the NAAQS at Austin.

6. In the survey flights, the mean ozone concentrations over water were usually found to be less than those over the land, regardless of the level of ozone encountered. When elevated ozone concentrations were measured over the water, the trajectory analyses usually showed the air parcel had a recent (< 24 hr) history over continental areas, usually over high precursor emission areas.

7. When areawide ozone concentrations exceeded the NAAQS, vertical mixing was usually restricted by a stable layer below 2 km.

8. Analysis of a series of ozonesonde releases at DeRidder, Louisiana, does not indicate ozone intrusion from the stratosphere. Mid-to-upper tropospheric ozone concentrations changed by 50 percent or more during a day, but they did not contribute to ozone changes at ground level.

9. Anthropogenic pollutants (acetylene and selected halocarbons were present in all grab samples collected at the DeRidder station and during aircraft flights. Examination of the data indicate that hydrocarbon and ozone concentrations are not linearly related at DeRidder.

10. Four distinct areal distributions of ozone were identified from aircraft flights:

    a) area-wide low concentrations (~70 $\mu g/m^3$),
    b) localized plumes downwind of precursor areas,
    c) elevated ozone concentrations, some exceeding NAAQS for ozone, usually increasing from west to east,
    d) area-wide (North Carolina to Louisiana) ozone concentrations exceeding the NAAQS for ozone.

1.4 Conclusions

The following conclusions derived from the data are listed separately for each of the two study areas. Section numbers are provided to refer to the section of the report that pertains to each conclusion.

A. Conclusions: Northern High Pressure Oxidant Study

1. In the summer, high concentrations of ozone (i.e., $\geq$ 160 $\mu g/m^3$) in the rural boundary layer and in the eastern portions of the United States are most often found within high pressure systems. Sustained periods of high ozone are associated with macroscale high pressure systems that persist for more than 20 days. (Section 7.2.2)

2. Highest concentrations of ozone were found in the back side of a high pressure system. A relative minimum is observed in the front side or near the center. (Section 7.2.3)

3. Locations of maximum and minimum ozone concentrations in a moving high pressure system correlate with the location of air having maximum and minimum residence time in that system. (Section 7.2.3)

4. The air initially in the northeastern quadrant of an eastward moving high pressure system has the longest residence time in that system. (Section 7.2.4)

5. Oxides of nitrogen concentrations in rural areas in the western section of the study area were apparently too low to promote the generation of ozone concentration equal to or greater than the NAAQS. (Section 7.3.1)

6. High ozone concentrations and the frequency of exceeding the NAAQS for photochemical oxidants are associated with increased population density (i.e., both increased from west to east). (Section 7.3.1)

B. Conclusions: Gulf Coast Oxidant Study

1. Ozone concentrations over the Gulf of Mexico usually were less than those over land. High ozone concentrations (i.e., $\geq 160\ \mu g/m^3$) that were measured over water or in air flowing off the Gulf of Mexico were associated with air that had previously passed over continental sources of pollution. (Section 8.1.3)

2. Changes in the vertical structure of ozone concentrations below 3 km are primarily controlled by boundary layer processes. (Section 8.1.2)

3. Elevated ozone concentrations (i.e., $\geq 160\ \mu g/m^3$) are frequently measured in plumes downwind of potential ground sources of precursors, i.e., cities, major refineries, and petrochemical installations. (Section 8.1.3)

4. Upper decile concentrations of ozone are associated with slow moving air that had passed over high precursor emission areas and arrived from a nonprevailing wind direction; lower decile concentrations are associated with faster moving air, having a long over-water fetch with a weak anticyclonic trajectory. (Sections 8.1.3 and 8.1.4)

2.0 INTRODUCTION

2.1 Background

Since the mid-1960's, surface concentrations of ozone greater than the National Ambient Air Quality Standard (NAAQS) (160 μg/m^3 hourly average not to be exceeded more than once a year)[1] have been reported at nonurban sites in many areas of the United States.[2-9] Prior to this time the range of surface ozone concentrations was considered to be 40-120 μg/m^3.[10] High concentrations of ozone are now being measured in areas which many consider remote, rural, or "clean" (i.e., devoid of anthropogenic pollution).

In 1970, in the Mt. Storm area[11] of West Virginia, high ozone concentrations were found to occur and persist for several days at a time. In 1972, it was predicted that the phenomenon was probably widespread.[3] In 1973,[4] it was determined that the phenomenon was widespread over at least a four-State area and was not confined to the vicinity of Mt. Storm. Stations located in southern West Virginia, western Maryland, central Ohio, and northwestern Pennsylvania all showed numerous simultaneous onsets of periods of high ozone. In 1974,[5] a study was conducted in Ohio to investigate the relationship between high rural ozidant levels and urban hydrocarbon control strategies. All data obtained in the 1974 study[5] showed strong evidence for the involvement of anthropogenic precursors and urban effluvia in the generation of the high ozone concentrations in rural areas. As a result of these investigations, it was postulated that the high concentrations of ozone (produced by photochemical processes) found in nonurban portions of the area studied are primarily an air mass characteristic and will occur when a slow-moving, high atmospheric pressure system passes over the region.

A series of studies[6, 12-15] conducted by the Air Control Board of the State of Texas have shown occurrences of concentrations of ozone in excess of 160 μg/m^3 in nonurban areas. Due to the short duration of the periods of measurement and the sequential mode of measurement at the several locations reported in these studies, the areal extent of the region of high ozone concentrations was not determined. Correspondingly, the source of the high concentrations of ozone was not determined.

Faced with the problem of devising strategies to reduce urban oxidants to concentrations conforming to the NAAQS, the Texas Air Control Board found that nonurban air entering the cities had ozone concentrations above the NAAQS. The board, therefore, concluded that strategies applied to the urban areas would not achieve oxidant levels at or below the NAAQS and that "In some areas of Texas, it appears likely that the photochemical oxidant standard would be exceeded even if emissions from human activity were reduced to zero."16/

2.2 Research Objectives

In response to the Environmental Protection Agency's interest in these areas, RTI planned and conducted a two-part study program: (1) to determine the change in the concentration of ozone in the center of a high pressure system as the system moves from an area of low population density to an area of high population density; and, (2) to investigate the areal extent of regions of high ozone concentrations in the northern gulf coast area of Texas, with particular attention being given to the determination of whether the high ozone concentrations extend over several contiguous States.

3.0 DESIGN OF STUDY

In order to accomplish the objectives set forth in section 2.2, it was necessary to design two independent studies that had different objectives but could be conducted concurrently and employed similar measurement systems.

The Northern High Pressure Oxidant Study focused on tracking the movement of high pressure systems originating in the Alberta-Saskatchewan region of Canada as the system moves southward over the northern Plains States, then eastward over the northern Midwest States and the northern mid-Atlantic States or New England States. During this slow passage over the United States, the air mass first traverses regions of low population density and little industrial activity--that is, regions having small emission densities of hydrocarbon and nitrogen oxide precursors necessary for the production of the photochemical oxidants. During this initial period, low ozone concentrations in high pressure systems are anticipated. As the air mass moves eastward, however, population density, industrial activity, and, consequently, emissions of oxidant precursors increase.

Primary emphasis for the Gulf Coast Oxidant Study was focused on the roles and/or contribution of land-sea breeze circulations, the local emissions of ozone precursors, and transport of ozone and ozone precursors to concentrations of ozone measured within and downwind of the study areas.

Based on the above considerations, two modes of measurement were employed to measure the concentration of ozone (O_3), oxides of nitrogen (NO_x), hydrocarbons (HC) and halocarbons (HCX), and particulates (TSP, $SO_4^{=}$, NH_4^+, NO_3^-): a network of five fixed, rural, ground-level stations and an instrumented aircraft flying specified patterns. Measurements at each ground-level station within the network were the same for both studies; however, the flight patterns were quite different. These are discussed separately in the following sections. In addition, vertical profiles of ozone were obtained from ozonesonde releases at Huron, South Dakota, and at DeRidder, Louisiana.

3.1 Northern High Pressure Oxidant Study

3.1.1 Airborne Measurements

Upon a forecast of a high pressure system moving out of the Canadian prairie provinces into the northern United States and having the potential to move in a desired manner across the eastern United States, the aircraft was dispatched from the gulf coast area to Sidney, Montana, arriving within 24 hours of notification. Beginning there, the aircraft flew a daily mission with a pattern based on weather information transmitted to RTI by the weather forecasting service of Murray and Trettel, Inc., Northfield, Illinois. Using this information, RTI then planned the flight to maximize the data collection in relation to the aircraft and crew capabilities.

In general, each flight was flown at altitudes between the morning inversion height and the afternoon mixing height. Normally, this altitude was about 1,520 m (5,000 ft) MSL or about 912 m (3,000 ft) above ground. Insofar as possible, the flight was flown under visual flight rules (VFR) to maintain maximum flexibility of flight plans. Depending upon conditions, takeoff was scheduled to occur after 1030 hours Local Daylight Time (LDT) and to terminate before 1830 LDT. The aircraft has a range of about 1,609 km (1,000 mi) or 5.1 hours of flight at 198 mph, before reaching a minimum of 45 minutes fuel reserve to reach an alternate destination.

Two modes of flight were used to acquire data in the vertical and the horizontal. Each day at approximately 1300 LDT, the aircraft was to be near the center of the high pressure system. At that time a vertical profile of ozone concentration was obtained. The aircraft altitude was then altered to 1,216 m (4,000 ft) MSL and sampled for 3 minutes at that altitude. The aircraft then ascended to 1,830, 2,135, 2,440, 2,745, and 3,050 m (6,000, 7,000, 8,000, 9,000 and 10,000 ft), sampled for 3 minutes at each altitude with ascent rates of 152 m (500 ft) per minute between levels. The aircraft then descended and sampled at these same altitudes. The flight continued at an altitude of 1525 m (5,000 ft) about 1 hour after the vertical profile began.

The horizontal transects flown across the high pressure system were determined by a combination of factors such as the location of the high pressure center relative to the aircraft's overnight position, the track the system was expected to follow, and the time required to be in position for the 1300 LDT sounding near the high pressure center. Based on experience gained through simulated flights in historical weather systems the following objectives were desired and achieved in most situations: (1) cross the high as it moves along the population gradient, (2) make a low pass tie-in with a ground sampling location, (3) make a tie-in with the ozonesonde location, (4) cross a major portion of the high pressure system, and (5) be in a good location to do one of the above on the following day (including becoming airborne in sufficient time to the vertical profile).

3.1.2 Ground Measurements

To support the airplane data-gathering program, four instrumented ground stations were established at airports near Wolf Point, Montana; Creston, Iowa; Bradford, Pennsylvania; and Lewisburg, West Virginia. These locations are depicted in figure 1. In addition, a 15-station monitoring network utilizing existing state and local agency stations was used to provide additional supporting data. These locations are also shown in figure 1.

Aerometric data, as listed in table 1 in section 4.0, were obtained at these ground stations. Day-by-day and diurnal behavior of the pertinent variables were observed. Details regarding the measurement parameters and sampling schedule are presented in section 4.0.

3.1.3 Ozonesonde Measurements

As an addition to the northern high pressure study, a program of serial ozonesonde soundings across high pressure systems which passed through the northern Great Plains was conducted. High pressure systems, which RTI identified for flight analysis, were investigated with releases from Huron, South Dakota. The objective of the program was to document the vertical ozone distribution and its changes, especially these changes that could be attributable to intrusion of stratospheric ozone into the troposphere across discontinuities in the tropopause. Secondarily, the influence of stable layers in the planetary boundary layer upon the diurnal ozone changes at the ground was sought.

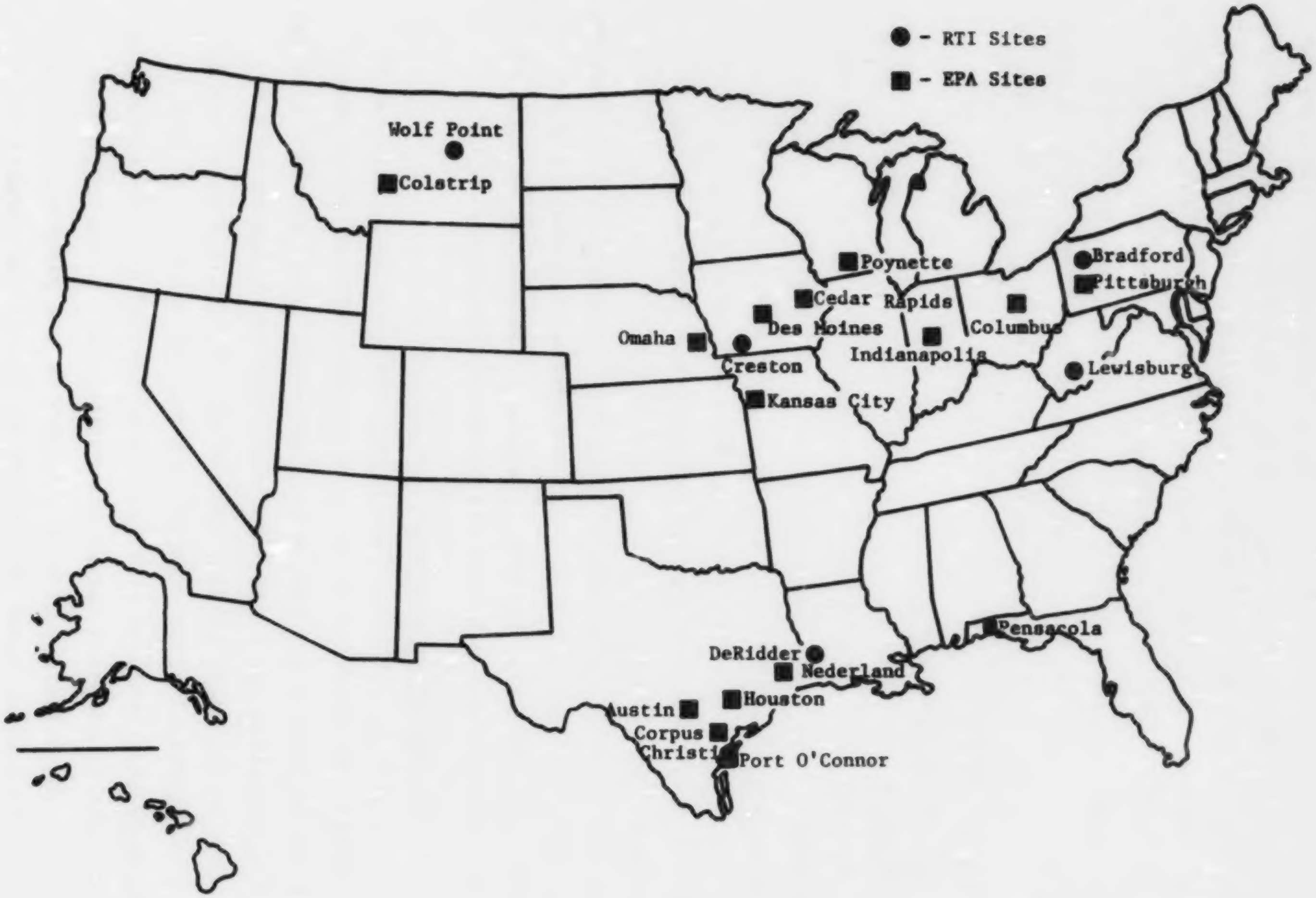
● - RTI Sites
■ - EPA Sites
Wolf Point
Colstrip
Poynette
Cedar Rapids
Des Moines
Omaha
Creston
Kansas City
Indianapolis
Columbus
Bradford
Pittsburgh
Lewisburg
Pensacola
DeRidder
Nederland
Houston
Austin
Corpus Christi
Port O'Connor

Figure 1. Site locations for ground station network.

3.2 Gulf Coast Oxidant Study

3.2.1 Airborne Measurements

The airborne operations in the gulf coast area were designed to document the areal extent of high ozone concentrations in the gulf coast area of Texas and to investigate the possible influence of four factors that could affect ground level ozone concentrations. These are: (1) a sea breeze, (2) a petrochemical complex, (3) a coastal areal ozone distribution, and (4) a vertical ozone distribution. Flight protocol required that crew and aircraft safety take precedence at all times. All flight patterns in the gulf coastal area were subordinate to aircraft operations associated with the northern high pressure oxidant study described in section 3.1. Area survey flight plans were normally scheduled for two consecutive days of operation. The flight patterns designed to be flown in the gulf coast area and the type of information sought from each type of flight are discussed below.

(1) Sea Breeze Flight

A flight pattern was designed to investigate the role that the land-sea breeze circulation may play in contributing to high ozone concentrations during the time of onshore winds. The occurrence of high ozone concentrations near the sea surface as compared to concentrations at higher altitudes and the change in concentration across the sea breeze front were of primary interest. The flight pattern shown in figure 2 was designed to be flown twice daily under the appropriate conditions of high ozone concentrations (i.e., $\geq$ 160 μg/m^3 hourly average at DeRidder, Louisiana, or Nederland, Texas, on the previous day) and when an identifiable sea breeze circulation could be expected. The flight track in the morning extended 321 km (200 mi) to sea at an altitude of 1,220 m (4,000 ft) MSL, well above the onshore flow. The return flight was at 244 m (800 ft) MSL, within the onshore component of the sea breeze. The afternoon flight was flown 321 km (200 mi) to sea at an altitude of 610 m (2,000 ft) MSL with an overwater vertical profile to 3,050 m (10,000 ft) as shown in figure 2.

(2) Petrochemical Complex Downwind Plume Flight

The extensive petrochemical complex along the Texas gulf coast provides a major source of ozone precursor materials, specifically hydrocarbons and oxides of nitrogen. The downwind plume flight pattern was designed to investigate

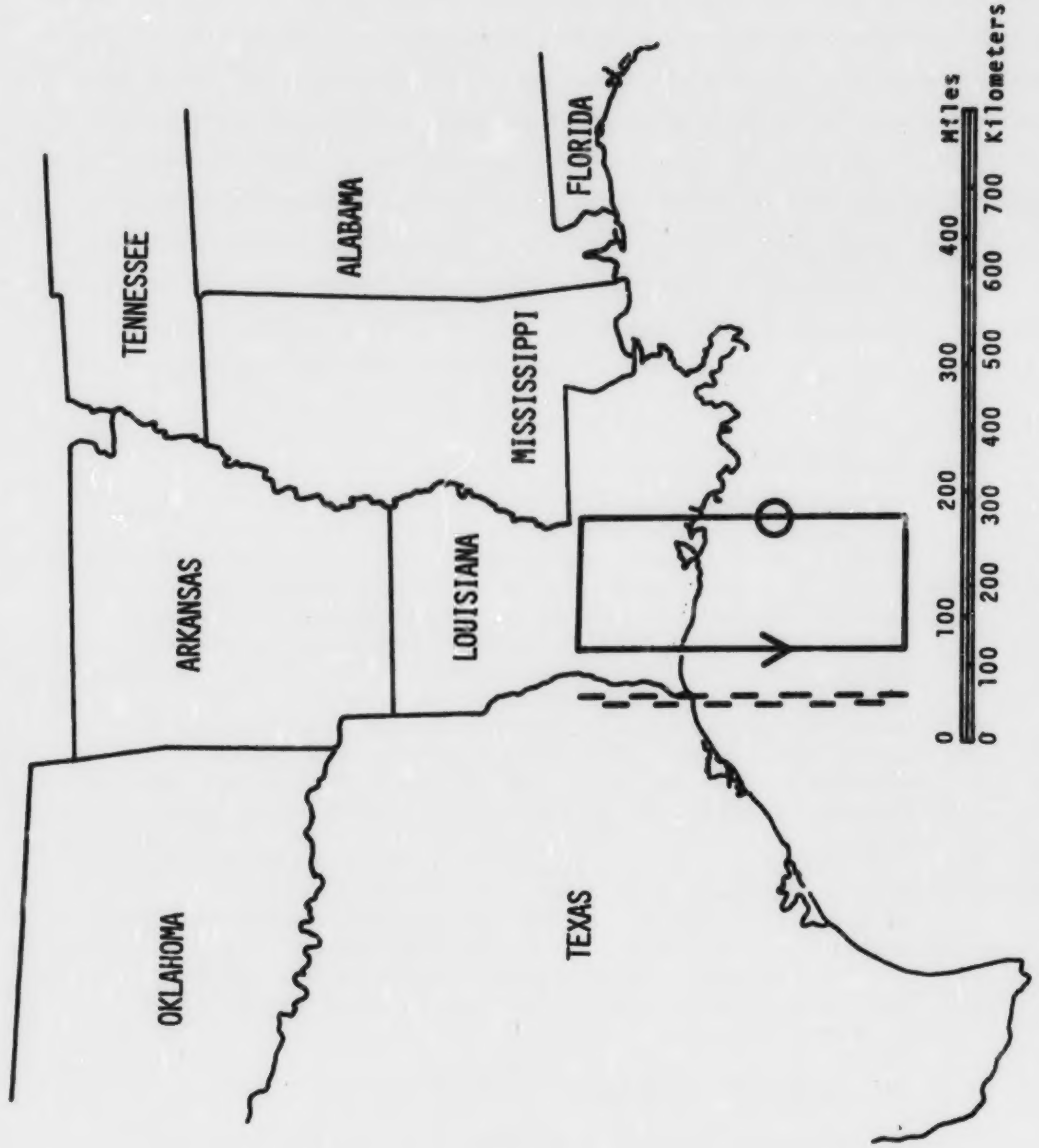
TENNESSEE
ALABAMA
FLORIDA
ARKANSAS
MISSISSIPPI
LOUISIANA
OKLAHOMA
TEXAS
0
100
200
300
400
Miles
0
100
200
300
400
500
600
700
Kilometers

Figure 2. Sea breeze flight plan.

and document the changing ozone and ozone precursor concentrations downwind of the complex.

The flight pattern, shaped like a parallelogram, is shown schematically in figure 3 and was flown downwind of the urban-industrial complex of the Freeport to Beaumont area. The flight plan was scheduled to be flown on two successive days; however, the orientation varied with the mean wind. The altitude for this pattern was 610 to 915 m (2,000 to 3,000 ft) MSL under VFR conditions.

(3) Coastal Areal Survey Flights

The areal extent of ozone concentration across the States bordering the Gulf of Mexico is largely unknown, especially in interior (noncoastal) areas. A prime objective of this study was to document the areal distribution of ozone and its precursors. Survey flights were designed to investigate the possibility of long-range transport of ozone and its precursors into the study area from Southeastern States, where high concentration of nonurban ozone have been documented, or from the Florida peninsula where occasional high ozone episodes have been reported. These flight tracks are shown in figures 4, 5, and 6.

Several missions were flown in conjunction with an EPA operated aircraft in October. This was done in order to extend the distance of the survey within the same time frame and also served as a comparative check of the aircraft measurement system. Included among the flights were a north-south survey, as shown in figure 5, a land-sea survey as shown in figure 6, and a superimposed set of "double-box" patterns about the Nederland, Texas, area to assess the influence of the petrochemical complex located there. This flight is diagrammed in figure 7.

(4) Vertical Profile Flights

The possibility of high ozone concentrations resulting from intrusion of stratospheric ozone into the troposphere and being transported to the ground was investigated using a vertical profile flight pattern.

The vertical distribution of ozone was examined by a series of flights with measurements made at prespecified altitudes to 6,100 m (20,000 ft). The airplane ascent rate was 152 m (500 ft) per minute. Ozone measurements were recorded at 305 m (1,000 ft) increments from the ground to 1,830 m (6,000 ft) and in 610 m (2,000 ft) increments from 1,830 m (6,000 ft) to 6,100 m (20,000 ft).

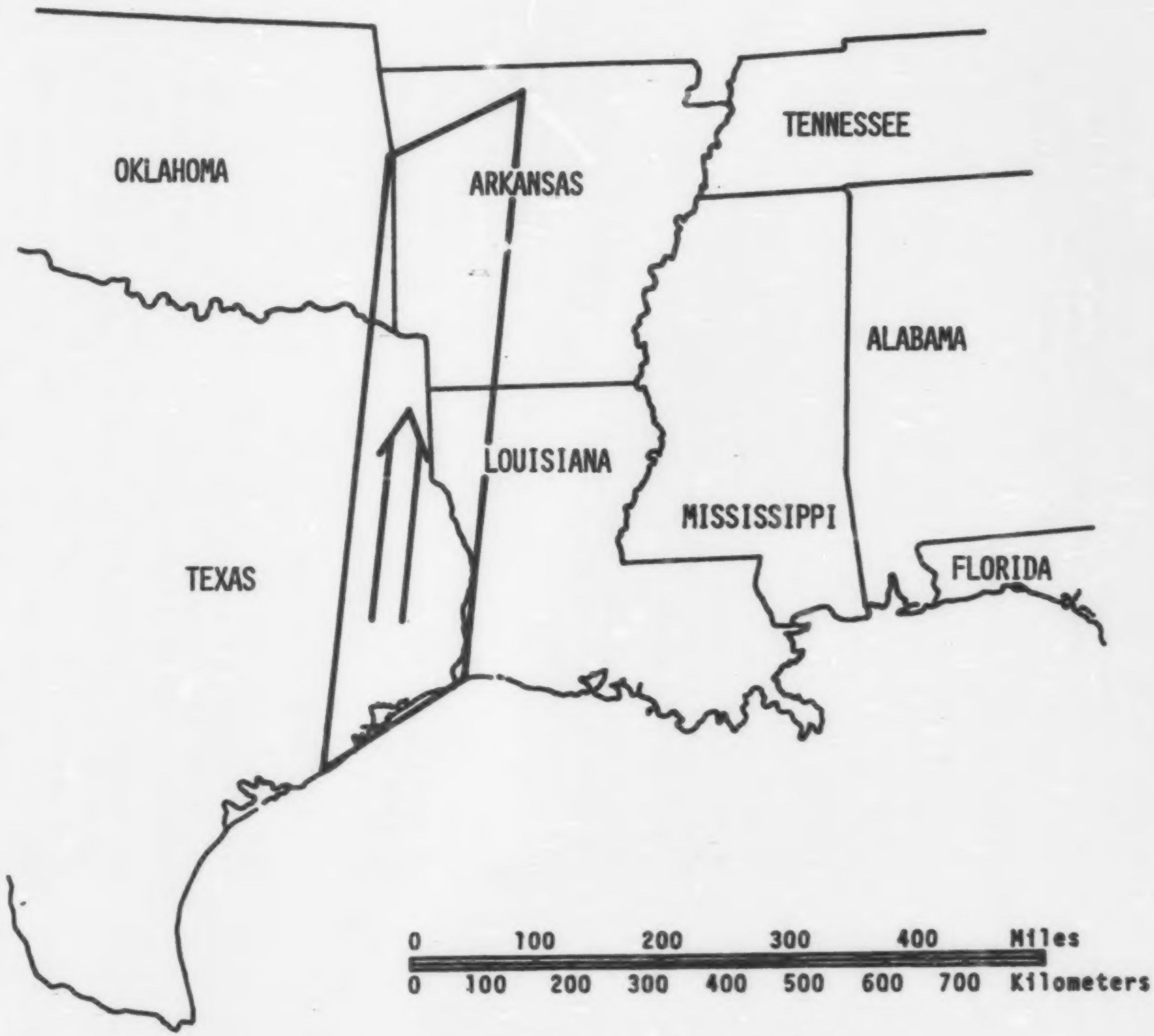
OKLAHOMA
ARKANSAS
TENNESSEE
ALABAMA
LOUISIANA
MISSISSIPPI
FLORIDA
TEXAS
0 100 200 300 400 Miles
0 100 200 300 400 500 600 700 Kilometers

Figure 3. Downwind plume flight plan.

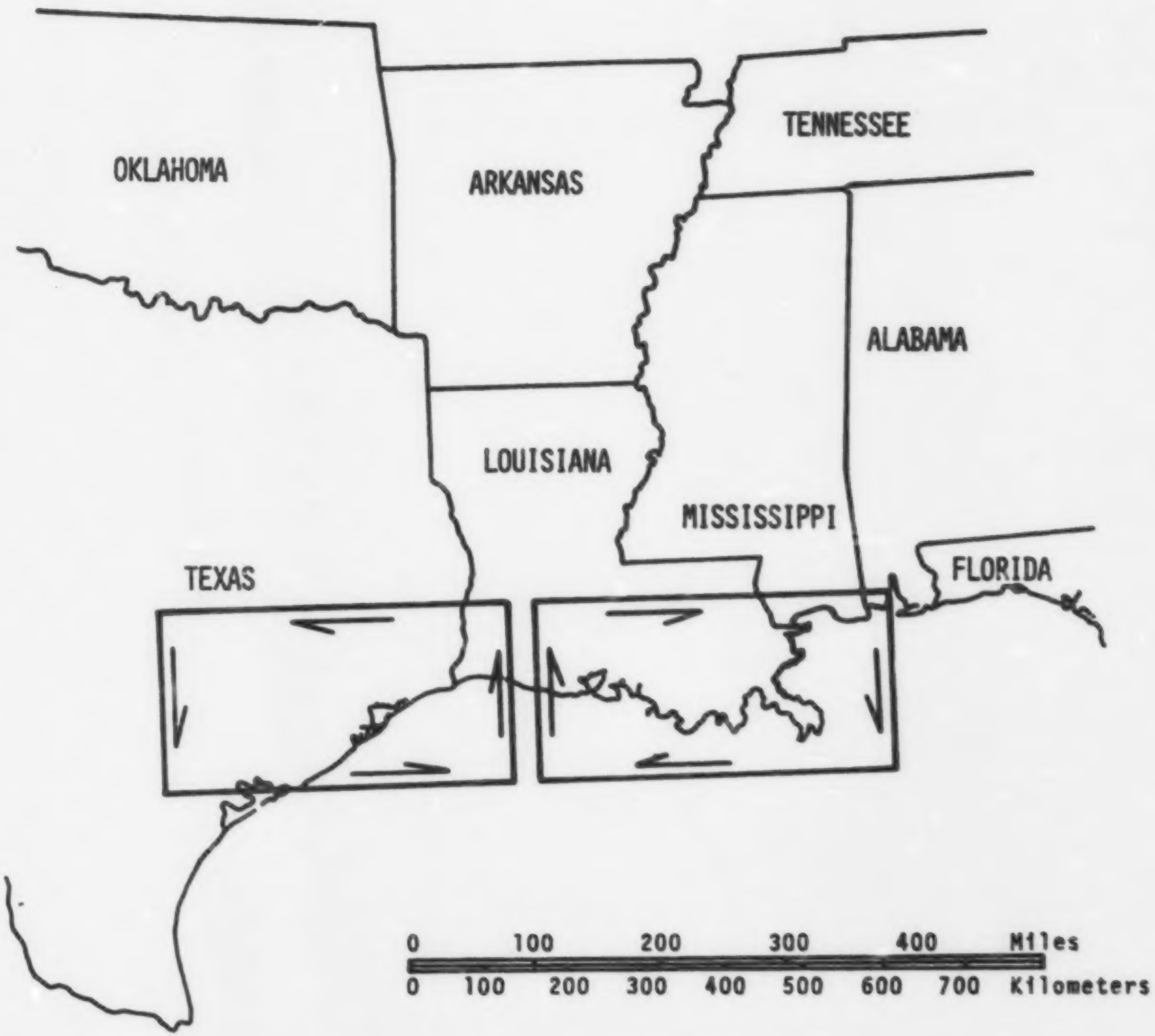
OKLAHOMA
ARKANSAS
TENNESSEE
ALABAMA
LOUISIANA
MISSISSIPPI
FLORIDA
TEXAS
0 100 200 300 400 Miles
0 100 200 300 400 500 600 700 Kilometers

Figure 4. Areal survey flight plan.

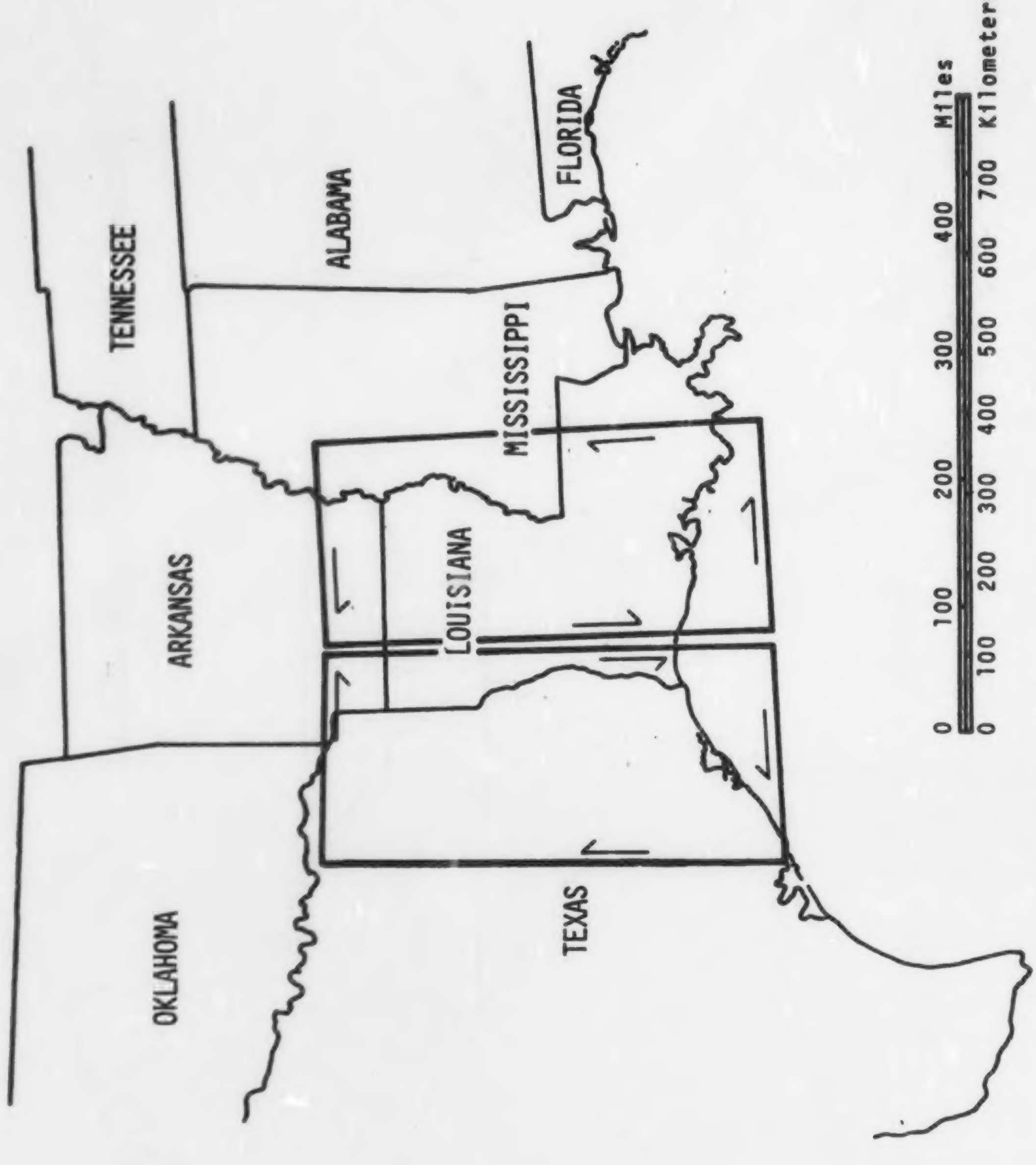
TENNESSEE
ALABAMA
FLORIDA
MISSISSIPPI
ARKANSAS
LOUISIANA
OKLAHOMA
TEXAS
0 100 200 300 400 Miles
0 100 200 300 400 500 600 700 Kilometers

Figure 5. North-south survey flight plan.

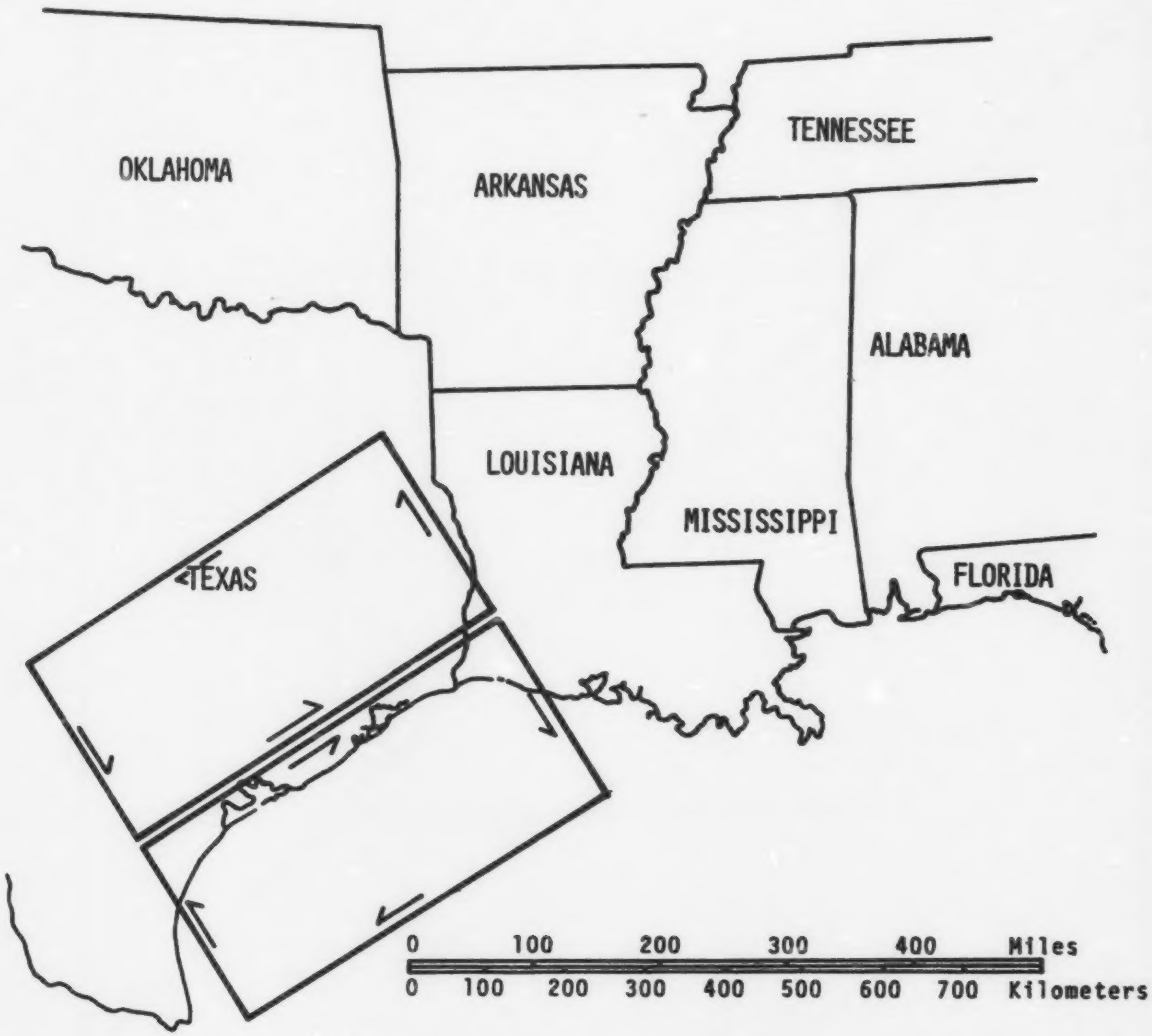
OKLAHOMA
ARKANSAS
TENNESSEE
ALABAMA
LOUISIANA
MISSISSIPPI
FLORIDA
TEXAS
0 100 200 300 400 Miles
0 100 200 300 400 500 600 700 Kilometers

Figure 6. Land-sea survey flight plan.

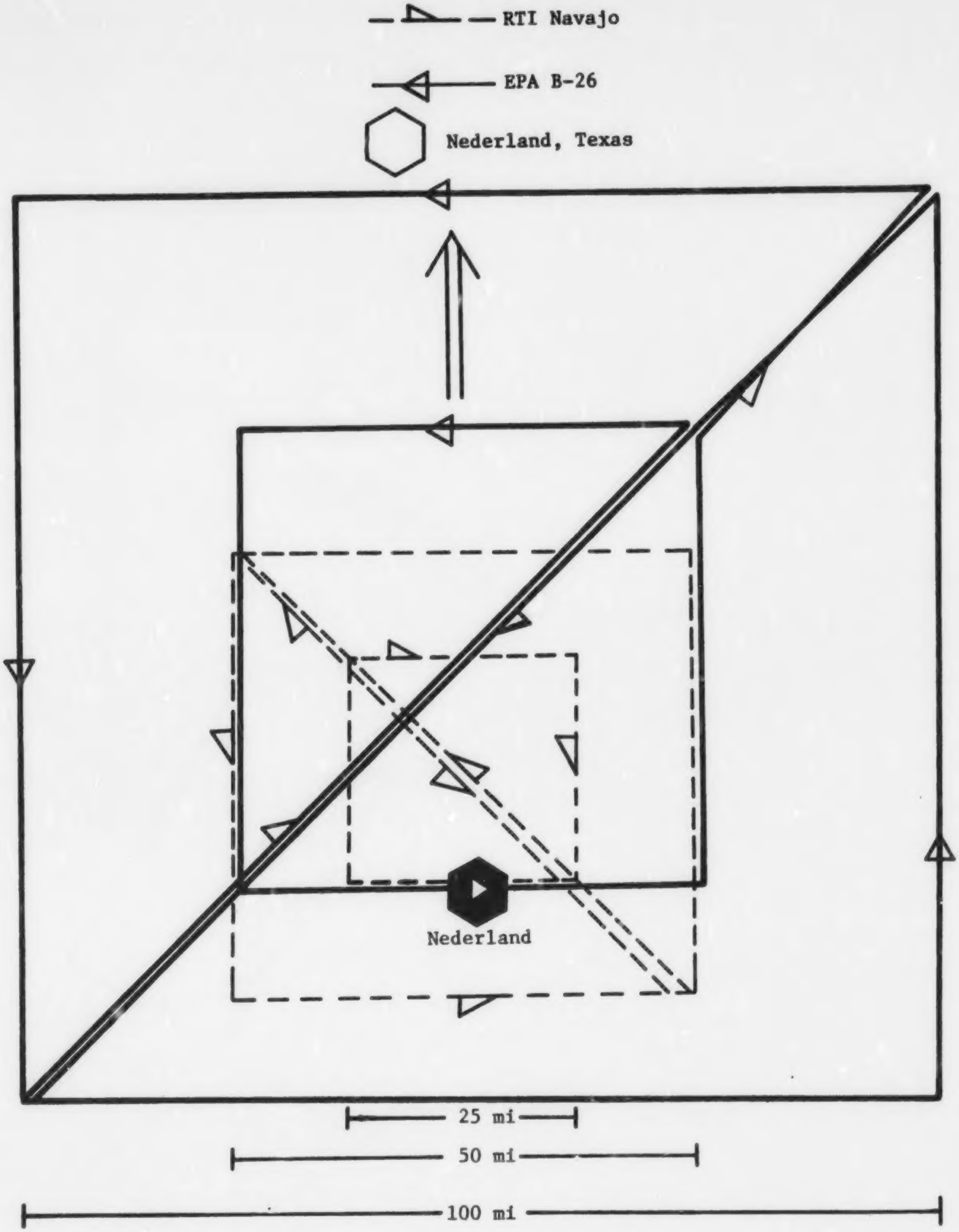
RTI Navajo
EPA B-26
Nederland, Texas
Nederland
25 mi
50 mi
100 mi

Figure 7. Double-box flight plan.

> Each profile flight required about 2 hours for completion. Because of restrictions on altitudes above 3,660 m (12,000 ft) in the DeRidder area, some profiles were flown near the Jasper, Texas, area about 31 km (50 mi) west.
>
> In addition, several vertical ozone distribution flights were carried out in support of the ozonesonde releases being conducted in the gulf coast area.

3.2.2 Ground Measurements

A single ground station was located at the DeRidder, Louisiana, airport for the gulf coast study. This station provided a continuity of aerometric information which, with the data obtained from the aircraft, was expected to provide insight into the areal extent of high ozone concentrations in the area. Day-by-day and diurnal behavior of the measured pollutants were observed. Details regarding the measurement parameters and sampling schedule are presented in section 4.0. In addition, ozone data from several urban stations operated by the Texas Air Control Board in the general study area were used by RTI in this investigation. These data are further described in sections 4.0 and 5.0.

3.2.3 Ozonesonde Measurements

An ozonesonde program was conducted to provide serial soundings from the DeRidder, Louisiana station in October 1975. This program was designed to expand the vertical dimension of the survey through the troposphere to the stratosphere and to provide another comparison of in-situ ozone measurements to altitudes of 6 km (~20,000 ft).

3.3 Analysis Procedure

The data analysis undertaken for the two studies described in this report have many elements in common; however, because of the vast difference in objectives, the analysis procedures for the two studies are discussed separately.

3.3.1 Northern High Pressure Oxidant Study

The Northern High Pressure Oxidant Study was designed to examine the change in ozone concentration within a high pressure system as that high pressure system moves from relatively large regions of low-density emissions of precursor materials into regions of successively greater densities of emissions of precursors.

The measurements made on successive days during airplane flights through the high pressure system should provide a data set in a quasi-Lagrangian coordinate system. Time-space sections of these measurements, in particular the ascents near the location of the day-to-day highest pressure, were analyzed to determine a measure of the change in the system's ozone concentration. Since ozone production within an air mass requires time, it may be that high concentrations can result without a progressive increase in the injected precursors. Accordingly, high pressure systems that remained over a region of low density of emissions of precursors were also analyzed.

Data from horizontal flights through the high pressure system were analyzed for discontinuities in systematic changes of, and symmetry of, ozone and ozone precursor concentrations to define the areal extent of regions of high ozone concentration. In addition, patterns suggested by these data were expected to offer clues to the processes taking place within the high pressure system that lead to the large areal coverage of high ozone concentrations.

3.3.2 Gulf Coast Oxidant Study

Concentrations of ozone and ozone precursor ratios along the flight paths and from the airplane ascents were examined for gradients and discontinuities. An attempt was made to relate departures from systematic changes to large-scale topographical features of the underlying surface of the earth, and/or to changes in the meterological conditions. Particular attention was given to nonsystematic changes evident in data from corresponding portions of both outbound and inbound (relative to the base station) flights or in corresponding regions (defined by altitude or by thermal structure) of ascents at the two extremities of the flight path.

4.0 FIELD MEASUREMENT PROGRAM

This section gives a description of the protocol for the establishment and operation of the ground station network, aircraft measurement program, and gas chromatographic analyses of selected hydrocarbons, acetylene, and halogenated compounds. Site locations, instrumentation, calibration, maintenance, data acquisition, and data processing procedures employed in each of the above-mentioned areas are described.

4.1 Ground Stations

4.1.1 Sampling Protocol

The field measurement program was designed to measure continuously the ambient concentration of ozone (O_3) and nitrogen dioxide (NO_2) at four manned stations located in rural areas in the States of Pennsylvania, Iowa, Montana, and Louisiana and ozone at an unmanned station in West Virginia. In addition to the continuous measurements for O_3 and NO_2, discrete grab samples were collected in Tedlar bags and on solid adsorption traps at specified intervals at four of the five rural sites and during aircraft flights. The samples were shipped to RTI for analysis of selected hydrocarbons, acetylene, and halogenated compounds by gas chromatography. Total suspended particulate (TSP) samples were also collected by the high volume sampler method at four sites on a daily basis for subsequent EPA analysis of sulfate, nitrate, and ammonium ions. Measurement parameters for each rural station are summarized in table 1.

Ozone was continuously measured at approximately 15 monitoring stations operated by State, local, or private industry. These data were provided to RTI by the Environmental Protection Agency. These State/local stations were located at: Colstrip, Montana; Indianapolis, Indiana; Columbus, Ohio; Pittsburgh, Pennsylvania; Northwest Houston (Aldine), Nederland, Austin, Corpus Christi, and Port O'Connor, Texas; Pensacola, Florida; Omaha, Nebraska; Des Moines and Cedar Rapids, Iowa; Kansas City, Missouri; and Poynette, Wisconsin. Figure 1 of chapter 3 showed the selected locations of fixed ground stations for the study (i.e., both rural and urban stations). Valid data from those sites that were received as of November 30, 1975, were employed in the present analysis.

Table 1. Pollutants measured at rural monitoring stations

Station	Pollutants*
Bradford, Pennsylvania	O_3, NO_2, HC and HCX by GC, SO_4^{2-}, NO_3^-, NH_4^+
Creston, Iowa	O_3, NO_2, HC and HCX by GC, SO_2^{2-}, NO_3^-, NH_4^+
Wolf Point, Montana	O_3, NO_2, HC and HCX by GC, SO_4^{2-}, NO_3^-, NH_4^+
DeRidder, Louisiana	O_3, NO_2, HC and HCX by GC, SO_4^{2-}, NO_3^-, NH_4^+
Lewisburg, West Virginia	O_3

*Hi Vol filters returned to EPA for analysis of SO_4^{2-}, NO_3^-, and NH_4^+.

4.1.2 Siting Considerations and Description of Monitoring Stations

The principal criteria for the selection of the rural monitoring station locations were: (1) that the location be free of natural and manmade obstructions to air movement, (2) that it be removed from local sources of ozone and ozone precursors, and (3) that it be readily accessible by aircraft in order to facilitate timely maintenance and routine calibration schedules. The locations selected meet these criteria.

Four rural ground stations were utilized in the ozone study in the north-central and north-east regions of the United States. These stations were situated approximately 1,200 km (750 mi) apart and are frequently located in the path of high pressure systems that enter the United States from Canada, move across the Plains towards the Ohio Valley and New York State. One rural ground station was located in the southern part of Louisiana and served as the base of operations in the Gulf Coast area.

A. Bradford, Pennsylvania, Monitoring Station

The monitoring station in Pennsylvania was located at the Bradford Regional Airport situated approximately 26 km (16 mi) south of Bradford. At an elevation of 653 m (2,143 ft) above mean sea level, the airport was well exposed to air flow from all compass points. The O_3 and NO_2 analyzers and associated equipment were housed in an environmentally controlled 2.4 m x 4.8 m (8 ft x 16 ft) Cortez van. The site is illustrated in figure 8. An interior view of the stations showing the analyzers and associated equipment is presented in figure 9. The interiors of the other three RTI rural stations were similar to the Bradford station.

B. Creston, Iowa, Monitoring Station

The Creston Municipal Airport, located approximately 5 km (3 mi) south of Creston, Iowa, was the site of a second rural monitoring station. The location was 394 m (1,293 ft) above mean sea level and was well exposed. Air quality analyzers and associated equipment were located in an environmentally controlled 2.4 m x 4.8 m (8 ft x 16 ft) Avion trailer which was located approximately 185 m (1,600 ft) away from the runway. An aerial and ground level view of the site are shown in figures 10 and 11.

C. Wolf Point, Montana, Monitoring Station

The northernmost monitoring station was located at the Wolf Point International Airport which is situated 3.2 km (2 mi) southeast of Wolf Point, Montana. The airport is located approximately 605 m (1,985 ft) above mean sea level. Exposure is excellent from all directions. Instrumentation and associated equipment were housed in an environmentally controlled 2.4 m x 4.8 m (8 ft x 16 ft) Avion trailer located 92 m (100 yd) southeast of a small terminal building. Aerial and ground-level views of the site are shown in figures 12 and 13. Although the airport is well-situated for an air monitoring site, the facilities are only marginally adequate for the aircraft. Therefore, all flight operations in the area were flown out of the Sidney-Richland Airport which is located 64 km (40 mi) southeast of Wolf Point, Montana.

D. Lewisburg, West Virginia, Monitoring Station

The fourth monitoring site for the study in the north-central and north-east regions of the United States was a cooperative station provided by Bendix Corporation at the Greenbriar Valley Airport, near Lewisburg, West Virginia. Situated at an elevation of 702 m (2,301 ft) above mean sea level, the Lewisburg site is well exposed and provided ozone data to the south of the anticipated path of high pressure systems. Aerial and ground-level views of the site are shown in figures 14 and 15.

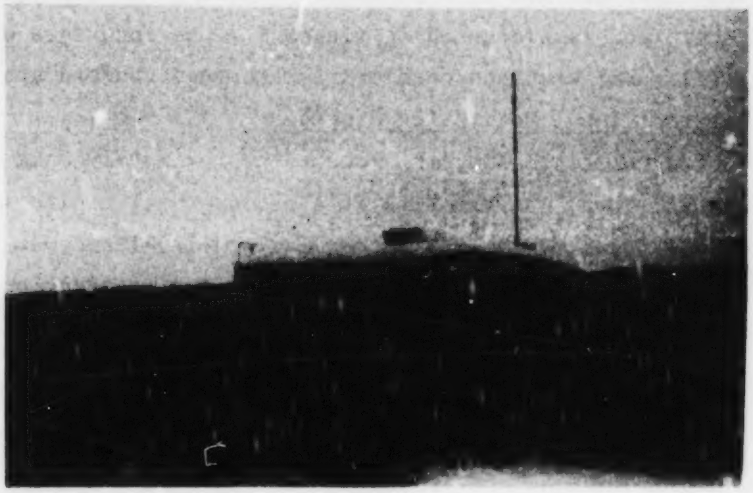

Figure 8. Air monitoring station, Bradford Regional Airport.

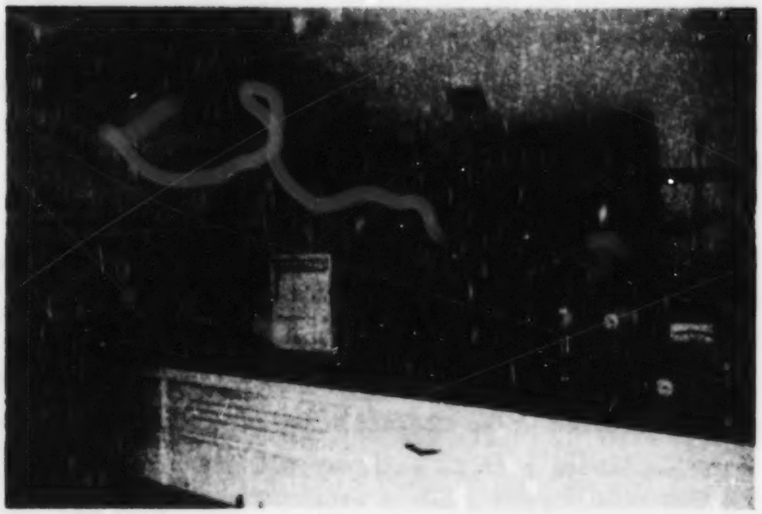

Figure 9. Interior view of air monitoring station.

Figure 10. Aerial view of Creston, Iowa (Creston Municipal Airport) site.

Figure 11. Air monitoring station, Creston Municipal Airport.

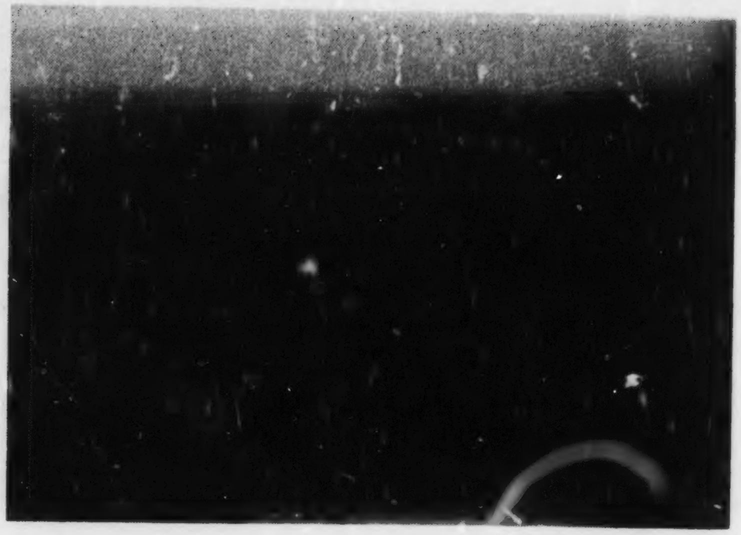

Figure 12. Aerial view of Wolf Point, Montana (Wolf Point International Airport) site.

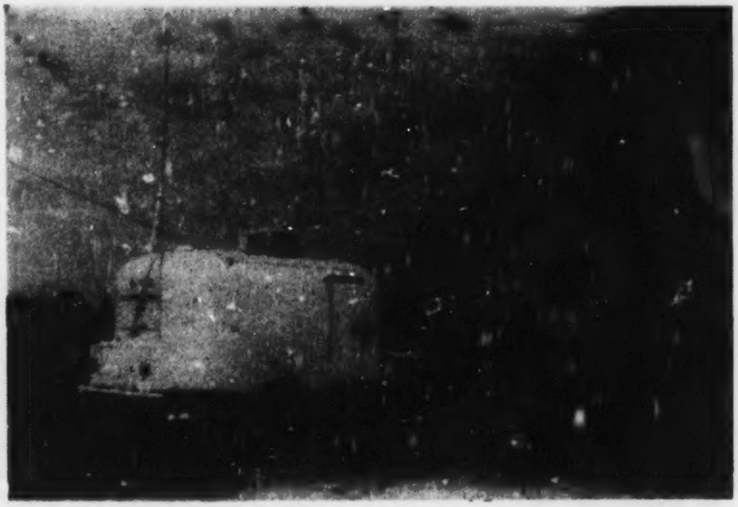

Figure 13. Air monitoring station, Wolf Point International airport.

Figure 14. Aerial view of Lewisburg, West Virginia (Lewisburg Airport) site.

Figure 15. Air monitoring station, Lewisburg airport.

E. DeRidder, Louisiana, Monitoring Station

The Beauregard Parish Airport, situated 8 km (5 mi) southwest of DeRidder, Louisiana, served as the base station for gulf coast operations during the summer study. The elevation of the airport is 62 m (203 ft) above mean sea level and exposure is excellent from all directions. Instrumentation and associated equipment were housed in the RTI Semi-Mobile Environmental Monitoring Laboratory. The leased aircraft used in this program for aerial measurements was based here. Aerial and ground-level views of the site are shown in figures 16 and 17. Beauregard Parish Airport is near a large air pollution source (a paper mill), which is situated approximately 3.2 km (2 mi) to the northwest. The prevailing wind direction during the summer months is from the southwest with flow out of the northwest occurring less than 5 percent of the time. Wind speed and direction were monitored continuously to identify periods of time when the sampling site might be under the influence of the paper mill plumes. No other airport sites examined in the Texas-Louisiana area were acceptable from the standpoint of remoteness from oil refineries (sources of hydrocarbons) or logistics [i.e., within 64 km (40 mi) of the Gulf Coast].

4.1.3 Air Quality Measurements

4.1.3.1 Instrumentation

Ambient ozone concentrations were measured at all rural ground stations using the Bendix Model 8002 Chemiluminescent Ozone Analyzer or an equivalent instrument. The principle of operation of this instrument is based on the gas-phase chemiluminescent reaction between ethylene and ozone. The reliability, stability, specificity, and precision of ozone measurements by this technique have been adequately demonstrated and described in the literature.[17/]

Nitric oxide and nitrogen dioxide concentrations were measured at four of the five rural stations using the Bendix Model 8101-B NO-NO_2-NO_x Analyzer. The principle of operation of this instrument is based on the gas-phase chemiluminescent reaction between NO and O_3. Measurement of the NO_2 concentration by this method requires that NO_2 be reduced to NO,

Figure 16. Aerial view of DeRidder, Louisiana (Beauregard Parish Airport) site.

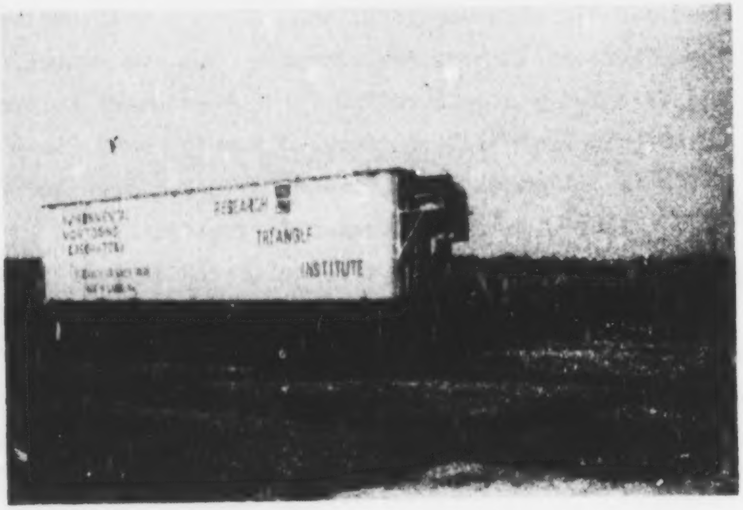
RESEARCH
TRIANGLE
INSTITUTE

Figure 17. Air monitoring station, Beauregard Parish Airport.

which then reacts with O_3. The sum of the initial NO measurement plus the NO produced by the reduction of NO_2 is the nitrogen oxides (NO_x) measurement. Electronic subtraction of the NO measurement from the NO_x measurement gives the NO_2 concentration.

Detailed hydrocarbon analyses of discrete grab samples collected during aircraft flights and at the four manned ground stations were performed by use of a modified Perkin-Elmer Model 900 gas chromatograph coupled to a Hewlett-Packard Model 2100A computer programmed for peak area analysis and quantification. Twelve nonmethane hydrocarbons were routinely analyzed and are listed below:

(1) ethane and ethylene
(2) acetylene
(3) propane
(4) propylene
(5) isobutane
(6) n-butane
(7) 1-butene
(8) isopentane
(9) cyclopentane
(10) n-pentane
(11) toluene
(12) o-xylene

The first ten compounds were separated on a 1.5 m x 0.15 cm i.d. Durapak n-Octane column operated at room temperature. The two aromatic compounds were separated on a 1.5 m x 0.15 cm i.d. stainless steel column packed with GP 5% SP-1200/5% Bentone 34 on 100/120 Supelcoport. Samples for these analyses were collected in the field in Tedlar bags and transported to the Research Triangle Institute campus for analysis.

Supplemental acetylene samples were collected at four ground stations and during aircraft flights using special traps containing silanized molecular sieve type 5A. Acetylene is quantitatively collected on the molecular sieve solid adsorbent, desorbed by heat, and separated from other hydrocarbons on an alumina-packed column at 175° C. Analyses were performed on a modified Beckman 6800 Air Quality Chromatograph. This technique was developed for the Environmental Protection Agency by Beckman Instruments, Inc., and is described in EPA Report 650/2-74-056.[18]

Concentrations of selected halocarbons were determined from bag samples collected at four ground stations and during aircraft flights using a Perkin-Elmer Model 900 gas chromatograph equipped with a ^{63}Ni electron-capture detector. The following halogenated compounds were analyzed: Freon-11, carbon tetrachloride, 1,1,1,-trichloroethane, and tetrachloro-ethylene. All four of these compounds are heavily used in industry and can be definitely labeled as anthropogenic pollutants, having no known natural sources. Separation of these compounds was made on a 1.5 m, 2 mm i.d. glass column packed with Chromosorb-W and coated with 10% DC-200.

4.1.3.2 Instrument Calibration and Maintenance

Dynamic calibration techniques were used to calibrate each analyzer at 3-week intervals during the approximately 100-day period of field operations. These techniques are outlined in table 2. Data obtained from these calibrations were used to provide transfer equations for converting analyzer voltage outputs to pollutant concentration ($\mu g/m^3$).

A brief description of the calibration techniques listed in table 2 is given below.

Ozone-Ultraviolet ozone generator referenced to the neutral-buffered potassium iodide (KI) method

Dynamic calibration of the ozone analyzers was accomplished by use of an ultraviolet ozone generator. The ozone generator consists of a 20 cm (8 in) length mercury vapor lamp which irradiates a 16 mm (5/8 in) diameter

Table 2. Calibration techniques

Pollutant	Calibration Technique
Ozone	Ultraviolet ozone generator referenced to the neutral buffered potassium iodide method (Federal Reference Method)
Nitric oxide/nitrogen dioxide	Gas phase titration technique
Selected hydrocarbons/freons/ acetylene	Mixtures prepared from pure hydrocarbons and dilution of certified mixtures

quartz tube through which clean (compressed) air flows at 5 ℓ/min. Variable ozone concentrations over the measurement range are generated by variable shielding of the mercury vapor lamp. Although the ultraviolet ozone generator has been shown to be quite stable and reproducible, the neutral-buffered KI method was used as the reference method. The ozone concentration of each calibration point was verified by the neutral-buffered KI method.[1/]

Nitric oxide/nitrogen dioxide--gas phase titration technique

The gas phase titration technique developed by Hodgeson et al[19/] of the Environmental Protection Agency was used for dynamic calibration of the chemiluminescent $NO-NO_x-NO_2$ analyzers. The technique is based on the application of the rapid gas-phase reaction between nitric oxide and ozone to produce a stoichiometric quantity of nitrogen dioxide. A certified tank of nitric oxide in nitrogen (of an approximate concentration of 50 ppm by volume) was diluted with zero air to provide NO concentrations in the range of 20 to 940 $\mu g/m^3$. Nitrogen dioxide concentrations are produced by the reaction of NO with ozone. Primary calibration of the NO in nitrogen concentration was accomplished by use of the gas phase titration technique.[19/] The NO concentration of each cylinder was determined prior to going to the field, once per month in the field, and at the conclusion of the study.

Selected hydrocarbons, freons, and acetylene

Hydrocarbon standards used to calibrate the Perkin-Elmer flame ionization detector gas chromatograph were obtained from Scott Research Laboratories as mixtures of hydrocarbons in hydrocarbon-free air. The concentration of these mixtures was certified to be accurate within ± 2 percent. Based on these concentrations, response factors were calculated by the computer system for subsequent use in the analysis routine. Comparison of the peak height, retention times, and peak area for hydrocarbons in standard mixtures were used to identify and quantify the various hydrocarbons collected in grab samples. A Perkin-Elmer electron-capture detector gas chromatograph was used for analysis of halocarbons. Halocarbon standards for calibration of the gas chromatograph were prepared by use of permeation tube devices and/or by quantitative dilution of pure liquids by injection of aliquots of liquid into Tedlar bags containing a known volume of hydrocarbon-free air.

A detailed discussion of all the calibration methods and procedures utilized during this program is given in appendix A.

Routine maintenance (excluding emergency trips for instrument failure) was performed by the station operator as required by each individual analyzer. Routine maintenance was performed on analyzers at the unmanned Lewisburg site during the regular dynamic calibration period. When failures occurred, an analyzer was brought back on-line in the most expedient manner by substitution or repair. A complete record of operational status (i.e., operational, repairs, maintenance, calibration, inoperative, etc.) was maintained for each analyzer throughout the duration of the project. This information was used in the data validation process.

4.1.4 Data Acquisition and Data Processing

Ozone, NO, and NO_2 concentration data at each station were recorded in analog form on strip chart recorders and in digital form on magnetic tape recorders. The strip chart recorders were used for backup in case of failure of the magnetic tape unit and, also, as a real-time record for assessment of the operational status of each analyzer. Primary data storage was on magnetic tape.

Since five identical data acquisition systems were not available, two different systems were used to record data at the five rural stations. A Metrodata DL-630 data logger was used at the DeRidder station, and Westinghouse Pulse-O-Matic recording systems were used at Bradford, Creston, Wolf Point, and Lewisburg. A brief description of each data acquisition system is presented in the following paragraphs.

The Metrodata Model DL-630 data system is a complete data-acquisition system capable of recording up to 40 channels of analog data plus a time code, station identification, and manual data entry on magnetic tape. Commands are locally selectable via front-panel, lighted push buttons. Channel selection allows the observation of the current signal of any channel as an electronic three-digit display on the front panel in real-time. The scan rate is 40 channels/second, and data are recorded on magnetic tape at 5-minute intervals.

The Westinghouse Pulse-O-Matic magnetic tape data acquisition system integrates the signal from the air quality analyzer for a 15-minute interval, thus providing a true 15-minute average. A battery backup unit is included in the recorder to preserve the time information on magnetic tape in the event of a power failure.

Magnetic tapes containing field data from the Metrodata and Westinghouse data acquisition systems were returned to Research Triangle Institute for processing on a weekly basis. The data manipulation required to retrieve the data stored on a magnetic tape consists basically of two phases:

(1) Translation of the tape to a form compatible with available data-processing equipment.

(2) Processing of the data on a computer to obtain pollutant concentrations in units of $\mu g/m^3$.

The end result was a hard-copy printout, which was then made available for inspection and validation. This printout consisted of the date, station identification, hourly average of 5- or 15-minute readings, and 24-hour average concentrations in $\mu g/m^3$ for each pollutant.

In order to obtain a printout of data that contains all the information, certain supplementary data must be supplied to the computer. These data include a listing of times when the instruments were inoperative or not functioning properly and linear best-fit equations relating the voltage output of the instrument to the concentration of the pollutant being measured. The times for instruments being inoperative were obtained from operator logs, calibration log sheets, quality control charts, examination of preliminary computer runs, and strip chart records. Linear best-fit equations were derived from data obtained during calibration--the known input gas concentrations and the resulting voltage output from the instrument. A regression analysis was performed on these points to obtain a best-fit equation characterizing the instrument's response.

4.1.5 Data Validation and Quality Control

In order to achieve and maintain a high level of confidence in air quality data, it was essential to routinely monitor critical instrument parameters and to maintain appropriate records. Quality control for the summer oxidant study included procedures for verification of calibration procedures, standards, and operating procedures, performance of dynamic calibrations at specified intervals, and maintenance of adequate records describing instrument performance as well as thorough training of field operators.

Calibration data, as well as daily zero and span information were examined for excessive zero and span drift. When zero drift exceeds ± 1 percent of full scale per 24-hour period, the data of the preceding 24-hour period was considered to be of questionable validity and was invalidated. Span drift was determined on a daily basis (ozone instruments) and from multipoint calibration data every 2 to 3 weeks. Span drift exceeding ± 1 percent per 24-hour period (ozone instruments only) or ± 3 percent per 2 weeks constituted grounds for invalidation of data. To verify accuracy of the data acquisition system, a constant voltage data input standard was recorded every 5 minutes on the Metrodata DL-630 data system in conjunction with the air quality data.

At the completion of each computer program set, the processed data were compared with strip-chart data for randomly selected periods. A typical check included comparison of computer-processed data and strip-chart data for six selected 1-hour averages per day. The recorded data on strip charts were also edited for signs of equipment malfunctions, excessive pollutant levels, or unusual diurnal patterns.

4.2 Airborne Measurements

4.2.1 Airborne Measurements System Description

4.2.1.1 Aircraft

A twin-engine light aircraft was instrumented to measure ozone, oxides of nitrogen, condensation nuclei, temperature, dew point, and pressure, and was also equipped to collect grab samples for HC analysis, selective filter samples for acetylene analysis, and high-volume filter samples for sulfate and nitrate analysis. The aircraft used was a Piper PA-31-350 Navajo Chieftain and is shown in figure 18 with the sampling

Figure 18. Instrumented aircraft.

probe and sulfate sampler in place. The aircraft was operated at a typical cruise speed of 180 mph (280 km/hr) and with an operational time of 3.5 hours. With 45 minutes of fuel reserve, a nominal range of 1,000 km was practical. The operational altitude was 22,000 feet (6,700 m) with a nominal climb rate of 1,000 ft/min (305 m/min). It was equipped with instrumentation and survival gear for night and over-water operations. Communication and navigation equipment included Dual VOR and VHF Communication, DME, ADF, Radar Altimeter, Weather Radar and Transponder.

The air sample intake system consisted basically of a 2.5-cm I.D. Teflon tube extending from approximately 60 cm in front of the nose of the aircraft to a stagnation type sample manifold on board the aircraft

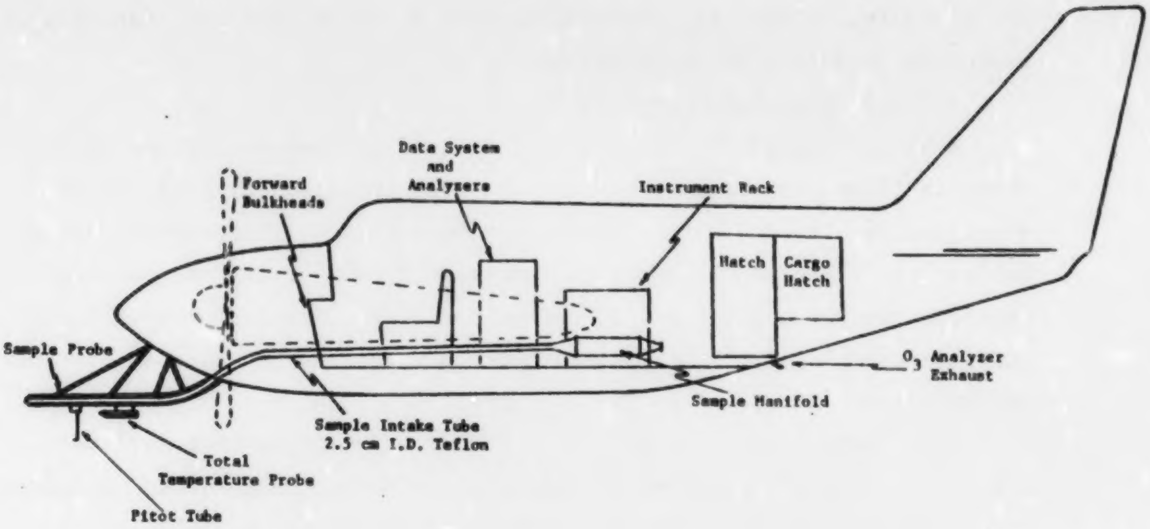
Data System and Analyzers
Forward Bulkheads
Instrument Rack
Hatch
Cargo Hatch
Sample Probe
O_3 Analyzer Exhaust
Sample Manifold
Sample Intake Tube 2.5 cm I.D. Teflon
Total Temperature Probe
Pitot Tube

Figure 19. Functional layout of airborne sampling system.

as shown in figure 19. The Teflon tube was inserted in a 3-cm I.D. steel tube mounted to the aircraft frame. A Pitot tube, a total temperature probe, and a high-volume particulate sampler were mounted to the sample probe.

The sample manifold was constructed of aluminum and coated internally with heat-cured Teflon. The manifold was designed with an inlet diverging diffuser section to allow deceleration of flow to a more controllable velocity, typically in the range of 1-2 m/sec.

Analyzer sample lines, temperature and dew point probes are situated along the main body of the manifold, an adequate distance from the diffuser, to allow unobstructed, isentropic flow of the air sample. Manifold velocity, monitored with a hot wire anemometer, was adjusted with an exit damper for variations in cabin pressure, altitude, and aircraft speed. A minimum flow velocity of 1 m/sec was maintained to insure a relatively rapid air sample exchange. In addition, the exhaust end of the manifold was designed to minimize the possibility of exhaust contamination from the aircraft. A detailed description of the sample probe and manifold design is presented in appendix C.

4.2.1.2 Measurement System

A block diagram of the aircraft air quality measurement system is shown in figure 20. Parameters continuously measured (directly or indirectly) were ozone, nitric oxide, nitrogen oxides, condensation nuclei, ambient air temperature, manifold temperature, dew point, ambient and manifold pressure, altitude, air speed and time. Samples were collected for laboratory analysis of hydrocarbons, halocarbons, acetylene, sulfates, and nitrates.

The physical position of the instruments and supporting equipment inside the aircraft is shown in figure 21. The instruments and equipment racks were mounted with Aeroflex steel rope shock absorbers bolted in place to the aircraft main frame.

The power supply system consisted of 28 Vdc to 115 Vac inverters that operated off of the aircraft Vdc power source. Two circuit breakers rated at 40 amps each were mounted in the pilot compartment along with an ammeter. One of the inverters was a surge-type which was used for the larger pumps. The system was wired such that it automatically switched over from aircraft power to ground power when external 115 Vac was connected. In addition, two 42 ampere-hour lead acid batteries provided power up to 2 hours when external power was not immediately available or impractical.

4.2.1.3 Instrumentation

Ozone was measured with a Bendix Model 8002 gas phase chemiluminescent ozone analyzer, operated continuously on the 0.2 ppm range. C. P. grade ethylene support gas for the analyzer was supplied from a size 3A gas cylinder. The instrument exhaust was routed through plastic tubing and dumped overboard through a bulkhead panel, to the rear and underneath the aircraft.

Oxides of nitrogen were initially measured with a Bendix gas phase chemiluminescent $NO-NO_2-NO_x$ analyzer, Model 8101-B. The instrument was operated in a cyclic mode with both the NO and NO_2 ranges set to 0.5 ppm

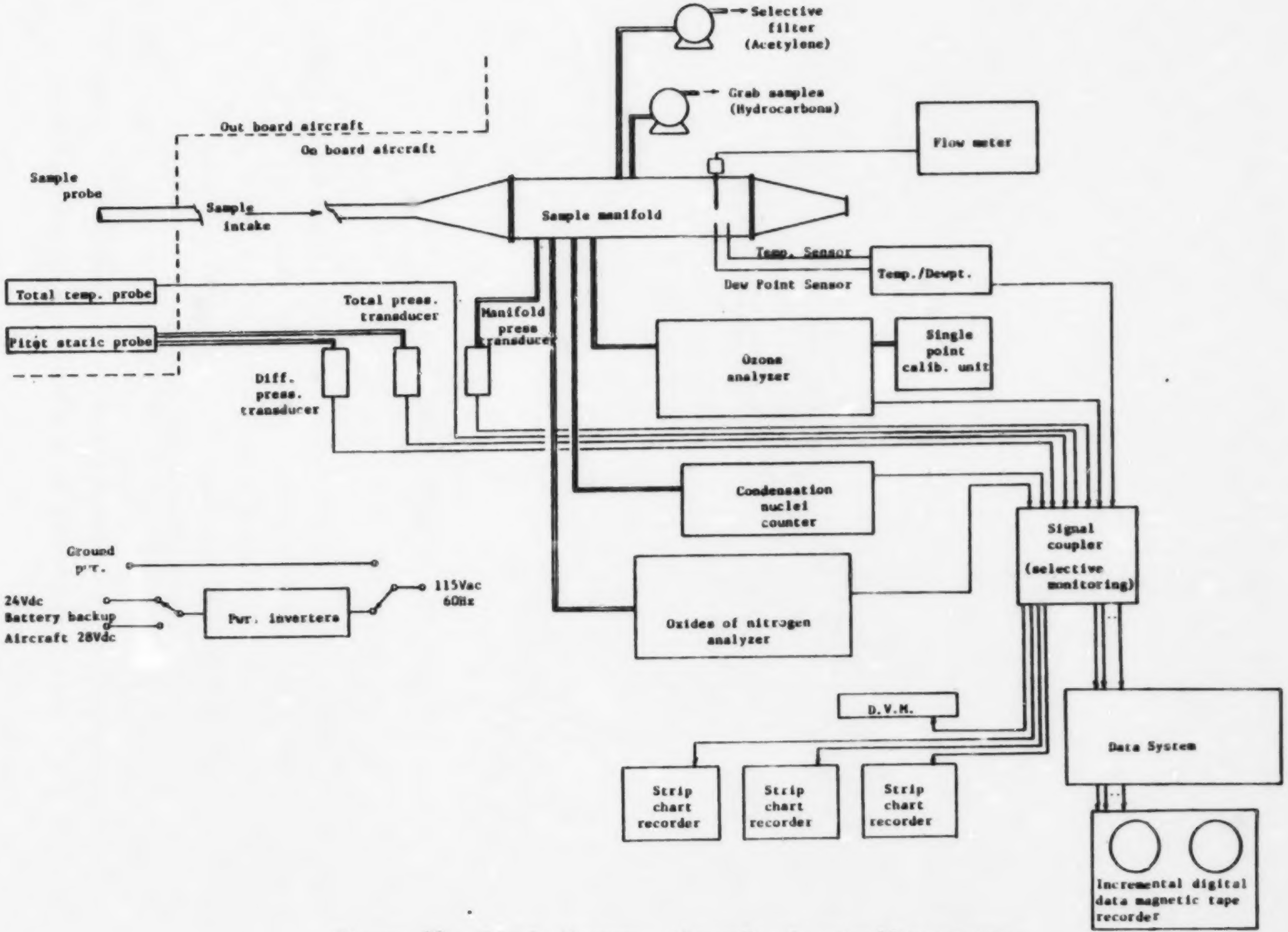
Selective filter (Acetylene)
Grab samples (Hydrocarbons)
Out board aircraft
On board aircraft
Sample probe
Sample intake
Sample manifold
Flow meter
Temp. Sensor
Dew Point Sensor
Temp./Dewpt.
Total temp. probe
Pitot static probe
Total press. transducer
Manifold press transducer
Diff. press. transducer
Ozone analyzer
Single point calib. unit
Condensation nuclei counter
Oxides of nitrogen analyzer
Signal coupler (selective monitoring)
Ground pwr.
24Vdc
Battery backup
Aircraft 28Vdc
Pwr. inverters
115Vac 60Hz
D.V.M.
Strip chart recorder
Strip chart recorder
Strip chart recorder
Data System
Incremental digital data magnetic tape recorder

Figure 20. Block diagram, aircraft air sampling system.

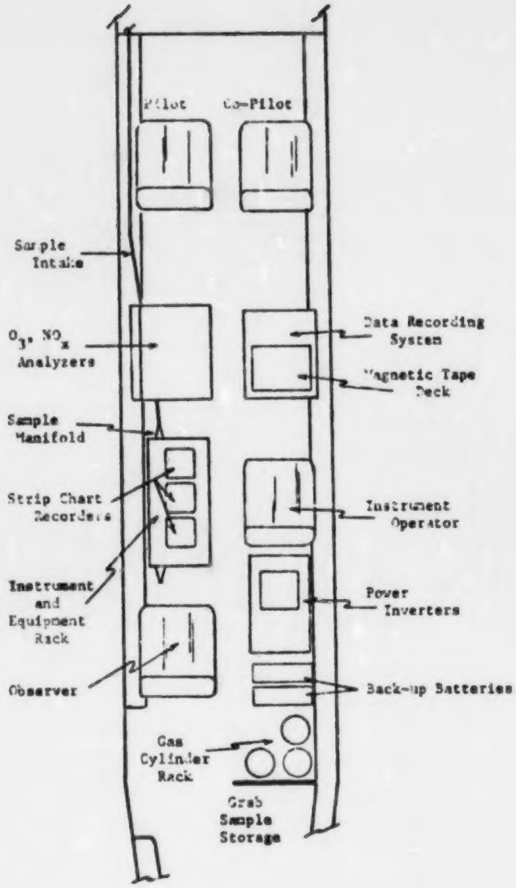
Pilot
Co-Pilot
Sample Intake
O_3, NO_x Analyzers
Sample Manifold
Strip Chart Recorders
Instrument and Equipment Rack
Observer
Gas Cylinder Rack
Grab Sample Storage
Data Recording System
Magnetic Tape Deck
Instrument Operator
Power Inverters
Back-up Batteries

Figure 21. Diagram of physical layout.

full scale. Oxygen support gas for the analyzer was supplied from a size 3A gas cylinder. Near the midpoint of the program, the Bendix NO_x analyzer was replaced with TECO Model 14-B chemiluminescent NO-NO_2-NO_x analyzer. This unit had the advantage of a more sensitive operating range, 0-0.1 ppm. The TECO instrument was operated continuously in the NO mode.

Condensation nuclei were measured with an Environment One, Model Rich 100, C.N. Counter. According to manufacturer specifications, the unit is capable of counting particles 0.0016 microns and larger in diameter, with a maximum concentration of 300×10^6 particles/cc and with a repeatability of ± 3 percent of full scale on all linear ranges.

Environmental characterization of the air being sampled included temperature and dew point measurements inside the sample manifold and measurements of the adiabatic stagnation temperature of the air relative to the moving aircraft. Manifold air temperature and dew point were monitored with a Yellow Springs Instrument Company Model 91 hygrometer. The temperature sensor, a 0.635-cm diameter bead thermistor, and the dew point sensor, a 0.9-cm diameter x 5.5-cm length lithium chloride probe, were mounted inside the sample manifold, downstream from the analyzer's sampling lines.

Ambient temperature measurements were made with a YSI bead thermistor, Type 44202, mounted in a total temperature probe, positioned in front of the aircraft, mounted to the sample probe. Design considerations for the total temperature probe are given in appendix C.

The Pitot tube was mounted on the sample probe a sufficient distance in front of the aircraft in order to eliminate erroneous measurements caused by aerodynamic distortion by the aircraft. The probe provided continuous measurements of the ambient static pressure, altitude, indicated air speed and Mach number.

A total pressure sensor was also used to continuously monitor manifold pressure, providing an additional measurement of the sample environment at the analyzer intake.

Bag samples for subsequent hydrocarbon analysis were collected with the apparatus shown in figure 22. Sample air was pumped from the manifold, through 0.635 mm I.D. Teflon tubing, through a manganese dioxide catalytic converter (for the purpose of converting ozone present in the sample to oxygen), into a 5 liter Tedlar bag. The bags were mated to the sampling system with stainless steel quick disconnect fittings.

A similar system was used to selectively trap acetylene from the sample air (fig. 23). A trap containing silanized molecular sieve was installed with stainless steel quick disconnect fittings between a metal bellows pump and the manifold. Flow rate was set for each filter by means

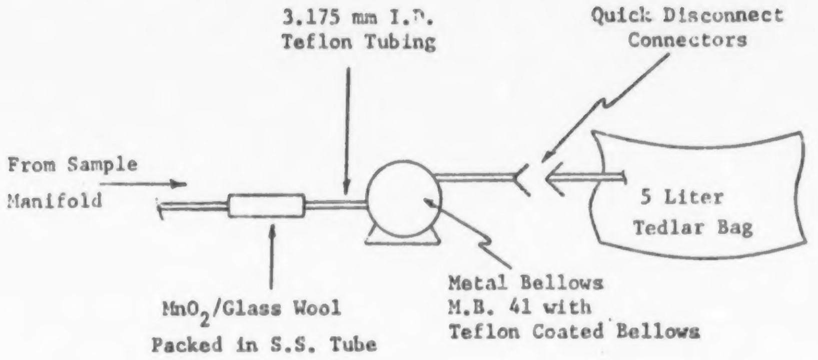
3.175 mm I.D.
Teflon Tubing
Quick Disconnect
Connectors
From Sample
Manifold
5 Liter
Tedlar Bag
Metal Bellows
M.B. 41 with
Teflon Coated Bellows
MnO_2/Glass Wool
Packed in S.S. Tube

Figure 22. Diagram of grab sampling system for hydrocarbon sample collection.

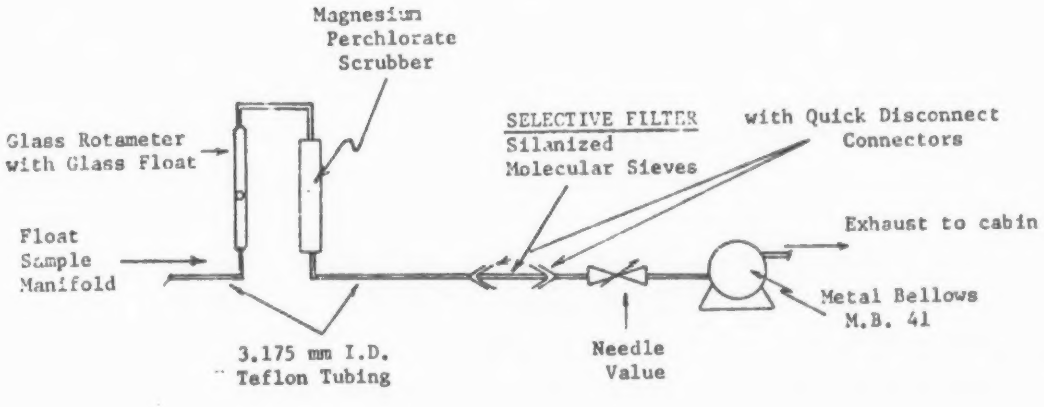
Magnesium
Perchlorate
Scrubber
Glass Rotameter
with Glass Float
SELECTIVE FILTER
Silanized
Molecular Sieves
with Quick Disconnect
Connectors
Exhaust to cabin
Float
Sample
Manifold
Metal Bellows
M.B. 41
3.175 mm I.D.
Teflon Tubing
Needle
Value

Figure 23. Diagram of selective filter sampling system.

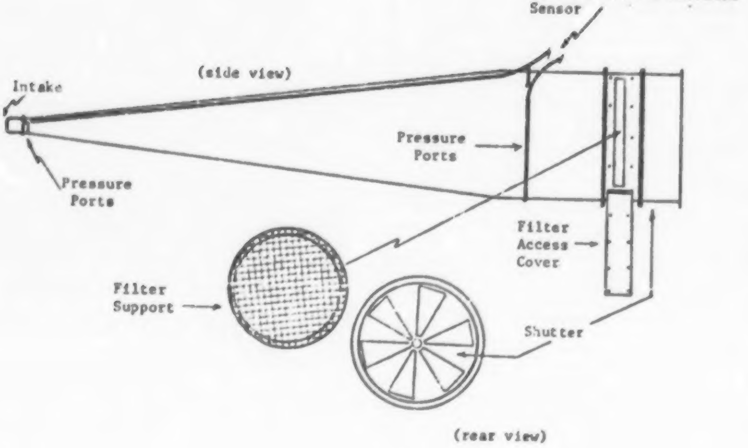
1/4" Copper Tubing
to Differential Pressure
Sensor
(side view)
Intake
Pressure
Ports
Pressure
Ports
Filter
Access
Cover
Filter
Support
Shutter
(rear view)

Figure 24. Sketch of airborne high volume sampler.

of a rotameter and needle value in series with the filter. A scrubber containing magnesium perchlorate removed moisture from the air sample prior to filter exposure. The filters were sealed prior to and immediately after exposure.

A high-volume filter type of sampler was designed to collect airborne particulates for sulfate and nitrate analysis. A probe was designed, which utilized aerodynamic pressure to cause a flow of approximately 35 cfm (1 m^3/min) through a standard high-volume glass filter which was trimmed to fit a circular holder approximately 18 cm (7 in) in diameter. A shutter was incorporated into the vent so that the flow through the filter was allowed only while in flight at altitude, not during takeoffs, landings or climbs or descents. A sketch of the unit is shown in figure 24. Design details are given in appendix C.

4.2.1.4 Data Acquisition System

The data acquisition system, shown in the overall system diagram, figure 20, consisted of a Monitor Labs Data Logger, System 9400, a Cipher,

Table 3. List of data channels

Channel No.	Instrument	Channel No.	Instrument
Time 2 x 10 digit words	Day:Hour:Min:Sec Manual data entry		
00	Ozone	15	Spare
01	NO	16	Spare
02	NO_2	17	Selective filter event
03	NO_x	18	Grab sample event
04	Condensation nuclei	19	Sulfate sampler timer
05	Manifold temperature	20	Bridge volt (ambient temp)
06	Dew point	21	Spare
07	Manifold flow rate	22	Spare
08	Spare	23	Spare
09	Spare	24	Spare
10	Total temperature	25	Spare
11	Manifold pressure	26	Spare
12	Static pressure	27	Short
13	Differential presure	28	10 mV (recorder span)
14	Spare	29	1.0 V (recorder span)

Model 85H magnetic tape recorder, a signal coupler and three Hewlett-Packard Model 680, strip chart recorders. Analog signals from the instruments were coupled to the data system through the signal coupler (junction box) that also housed all the necessary bridge circuits, scaling networks and voltage reference source. The analog signals were also available at a patch panel on the front of the signal coupler for purposes of maintenance and strip chart record selection. The panel included a simultaneous event marker and zero/span voltages for the three recorders and provided convenient access when checking instrument status with an external digital voltmeter.

The Monitor Labs data system included internal clock/control, a digital 18-column printer, a 20-digit manual data entry, and a 30-channel analog signal input capability. Channel number and utilization are listed in table 3.

The manual input data entry was used to indicate the operational status of the analyzers and instruments.

The Cipher tape transport system produced a computer-compatible, 1/2 inch, 7-track magnetic tape with a data storage density of 556 BPI.

4.2.2 Instrument Calibration and Pressure Effect Tests

4.2.2.1 Instrument Calibration

Dynamic calibration techniques were used to calibrate the ozone analyzer and the nitric oxide/nitrogen dioxide analyzer before and after each major survey conducted from the Raleigh-Durham area. Dynamic multipoint calibrations were also conducted during periods when the aircraft was stationed at DeRidder, Louisiana, where calibration equipment was maintained for the RTI field station. An ultraviolet ozone generator, referenced to the neutral-buffered potassium iodide (Federal Reference Method) was used to calibrate the ozone analyzer.[1/] The gas phase titration technique used to calibrate the nitric oxide/nitrogen dioxide analyzer was the tentative method reported in the Federal Register, Vol. 38, No. 110.[19/]

The condensation nuclei counter was calibrated at the factory by comparing instrument response to that of a Pollak Counter simultaneously sampling the same air source. The Pollak Counter was considered to be a suitable standard, and the Environment One instrument was adjusted to give comparable readout.

The thermistor temperature sensors used to measure ambient and manifold temperature were calibrated at the beginning and throughout the program by submersing the sensors in a water bath maintained over a range of temperatures and referenced to a laboratory-type mercury thermometer. The reference thermometer was calibrated in the laboratory against a Hewlett-Packard Quartz thermometer, Model 2801A.

Periodically, standard sling psychrometer readings were made and compared with the dew point sensor readings.

The pilot static pressure measurements were calibrated at the beginning of the program and involved repeated low passes over a runway of known length during a time when the meteorological conditions were reasonably stable. Several low passes were made from different directions, varying the aircraft speed over a maximum safe range. Each pass was timed with a stopwatch. Using airport temperature and barometric pressure readings, and time and distance measurements, the differential and total pressure sensor outputs were scaled to indicate ambient static pressure and true airspeed.

4.2.2.2 Pressure Effects Tests

The effects of changing altitude on instrument response have been previously investigated and reported in "EPA Contract No. 68-02-1286 Task 4, Final Report."[5] Prior to and at the conclusion of this program, additional tests were performed on the ozone and oxide of nitrogen analyzers used in this program. The environmental test chamber facility at NERC, Las Vegas, was used for these tests. The results of these tests produced a predictable decline in instrument response to a given concentration with increasing altitude (decreasing pressure). A detailed description of the chamber facility, the apparatus used, and the test results are presented in appendix D.

4.2.3 Operations Procedures and Data Validation Techniques

Specific operational and data validation procedures were routinely performed in order to insure uniform instrument operation and provide confidence in collected data beyond that established by the analyzer calibrations already described.

Preflight procedures

Analyzers, instruments, and data recording equipment were checked for proper operating modes. Time and altimeter readouts were synchronized with those reported by airport ground control. The strip chart recorders were zeroed and spanned with a known voltage source and adequately identified with time, flight notation, and parameter to be recorded. The data system time and manual input codes were preset, and the data system printout was identified with flight number and description.

Analyzer flow rates were checked with a soap bubble flow meter, and the ozone analyzer span/zero response was verified using a single point ozone generator and clean air source. The exceptions to the later procedure were flights preceded with a major analyzer calibration.

Inflight procedures

A flight log, which was maintained by the copilot throughout each flight, included time, course, airspeed, altitude, climb/descent, position information, and observed local weather observations. An instrument/systems log was maintained by the instrument technician, which included equipment performance or irregularities and inflight maintenance procedures. Additional logs were kept for grab sample and filter identification.

Inflight data validation procedures included span/zero checks for the ozone analyzer with the single point ozone generator, zero check for the nitric oxide/nitrogen dioxide analyzer, analyzer flowrate measurements, manifold flow measurements, wet and dry bulb temperature measurements inside the manifold and low pass air sampling at airports where RTI field stations were in operation.

Vertical flight profiles were made routinely and in general the flight pattern illustrated in figure 25 was followed.

Postflight checks

With the conclusion of each flight and after aircraft refueling and maintenance, the entire instrumentation system (with the exception of filter

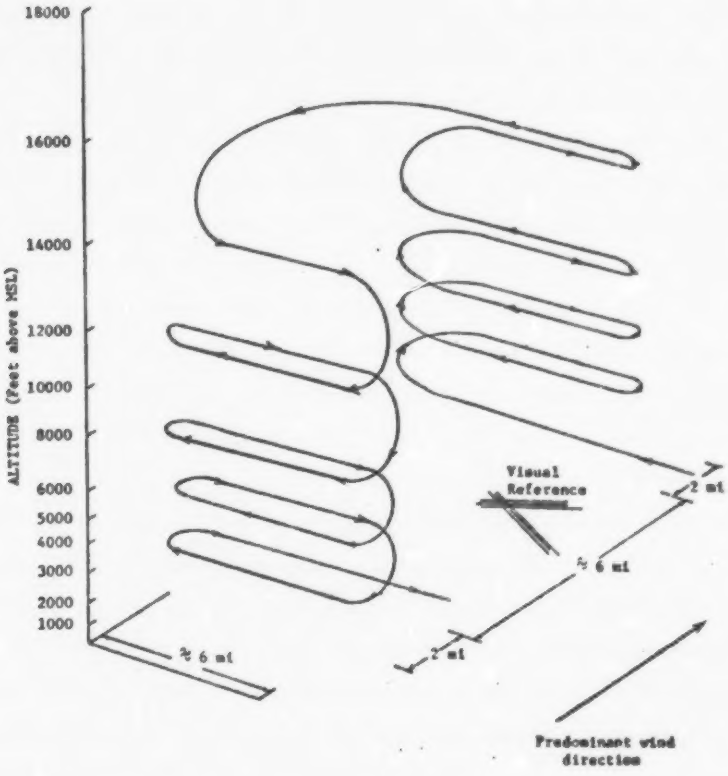
18000
16000
14000
12000
10000
8000
6000
5000
4000
3000
2000
1000
ALTITUDE (Feet above MSL)
Visual Reference
2 mi
≈ 6 mi
≈ 6 mi
2 mi
Predominant wind direction

Figure 25. Aircraft vertical profile (typical flight track).

and grab sample pumps) was switched to a 115 Vac ground power source. The instruments aboard the aircraft were then repaired or adjusted as indicated by operational checks.

The data for the preceding flight was spot-checked and documented and flight patterns were mapped with the appropriate time/position information.

Data validation techniques

In an effort to verify aircraft data other than by analyzer calibration procedures, comparative sampling in the vicinity of an RTI field station was conducted while the aircraft was on the ground and situated immediately next to the field station, and during inflight low-pass maneuvers.

An example of comparative ozone data from the aircraft and from the DeRidder station during simultaneous overnight sampling is shown in figure 26. During these sampling periods, the sample intake for the aircraft ozone analyzer was removed from the manifold and with Teflon tubing positioned approximately 1 meter above the top of the aircraft cabin. Sample intakes for the two systems were then separated by a distance of approximately 4 meters vertically and 20 meters horizontally.

Low-pass comparison of aircraft and field station data were conducted routinely during the program when the aircraft was based at DeRidder or when aerial surveys were in the vicinity of other RTI field stations and the weather permitted low-level flying. A typical low pass pattern is shown in figure 27 and consisted of the aircraft being flown approximately 50 ft (16 m) above the runway, maintaining a straight and level flight path as long as practical (generally approximately 30 seconds). Analyzer outputs were recorded near the end of the pass, which allowed the maximum stabilization time at the low altitude.

A plot of aircraft low-pass ozone data versus ground-station ozone data is presented in figure 28. Although these data were collected simultaneously during low-pass samplings, considerable scatter is evident. A review of the base station ozone strip-chart records frequently revealed a rapidly changing ozone concentration near the sampling times for many of the outlying data points on the graph. These departures from a homogeneous ozone concentration are not unexpected and often result from incomplete mixing during stagnation

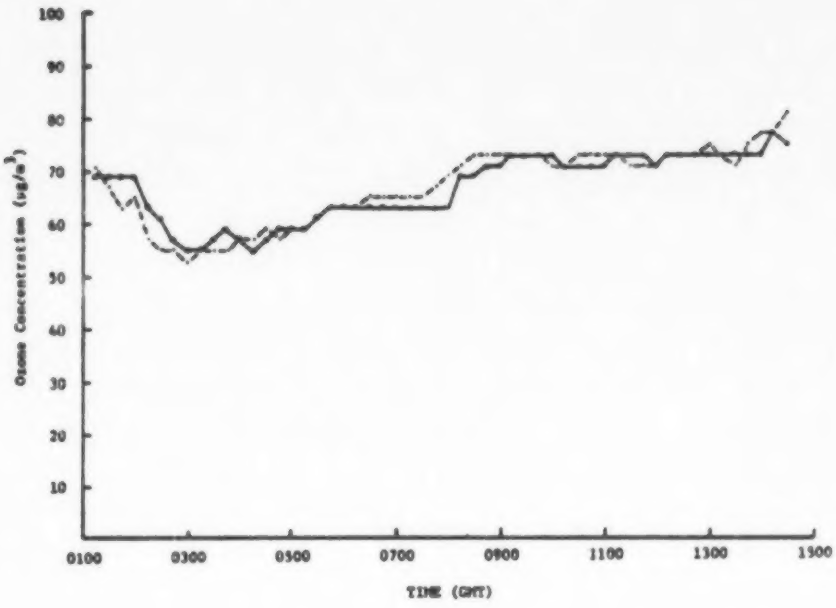

Figure 26. Example of ground measurement comparison.

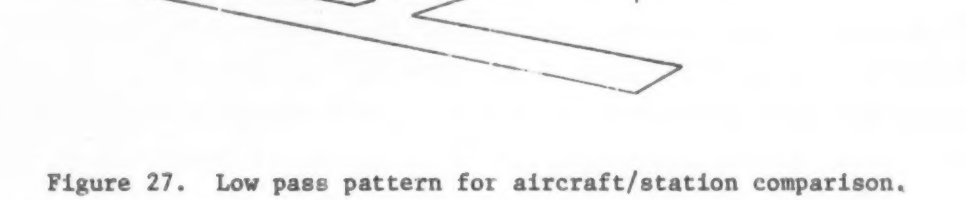
Down Wind Course
800'
Ground Station
Sample Port
50' Typical

Figure 27. Low pass pattern for aircraft/station comparison.

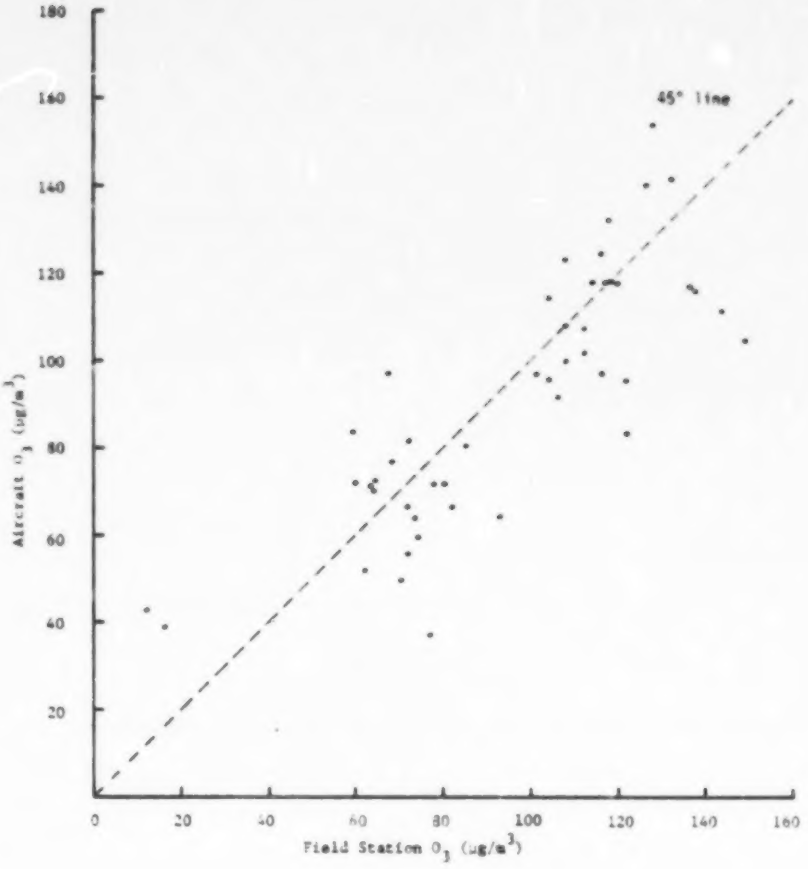

Figure 28. Comparison data during low passes.

periods or from rapid changes in concentration as a function of time, as evidenced by the ground-station data recordings.

During the latter part of the program the EMSL-LV aircraft, an instrumented B-26, was flown in support of the basic data acquisition program. Several comparison flights between the B-26 and the RTI Navajo were flown for purposes of obtaining inflight comparison of data. These were, in general, on flights between Lake Charles and DeRidder in wing-tip to wing-tip formation, typically at 305 m (1,000 ft) MSL. In addition, several low passes were made at DeRidder by sequencing both airplanes across the field with approximately 30 seconds time-spacing. These low pass comparison data are shown in figure 29.

4.2.4 Data Reduction and Processing

General reduction formulas

The following formulations were used in reducing signal output voltages for the ozone, nitric oxide/nitrogen dioxide analyzers, and the condensation nuclei counter.

Ozone and nitric oxide/nitrogen dioxide data are expressed in micrograms-per-cubic meter ($\mu g/m^3$) as follows:

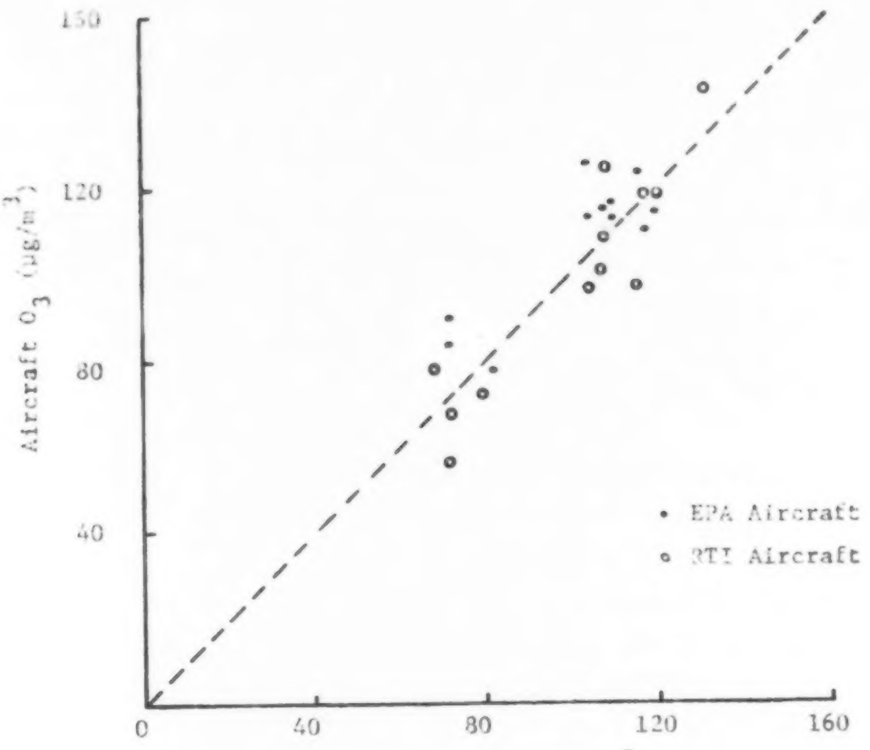

Figure 29. Comparison data during low passes.

$$c = \frac{m_c V_o + b_c}{K_a}$$

where

c = concentration in $\mu g/m^3$, corrected to standard pressure;

V_o = analyzer signal output in mV;

m_c, b_c = slope and constant respectively, representing analyzer calibration curve as determined during primary calibration; and

K_a = altitude correction.

Altitude correction factors (K_a) for the ozone and oxides of nitrogen analyzers were determined from analyzer response tests conducted in an environmental chamber at varying altitudes. These tests, described in detail in appendix D, provided the response versus altitude curves shown in figure 30 for the ozone analyzer and figure 31 for the oxides of nitrogen analyzer.

Condensation nuclei (CN) are reported as number-per-unit volume and are corrected for pressure as follows:

$$C = C' \quad \frac{P}{P_m}$$

where

C = number of CN per-unit-volume (CN/μl) corrected to standard pressure at sea level,

C' = number of CN as measured,

P = standard pressure at mean sea level, and

P_m = ambient static pressure.

Initial data plots

In order to provide a quick look at primary data and aid subsequent flight planning, flight tracks were initially traced to World Aeronautical Chart scales (1:1,000,000) (see example, fig. 32). The tracks include departure, ozone concentration at 2-minute intervals, and location of selective filter and grab samples.

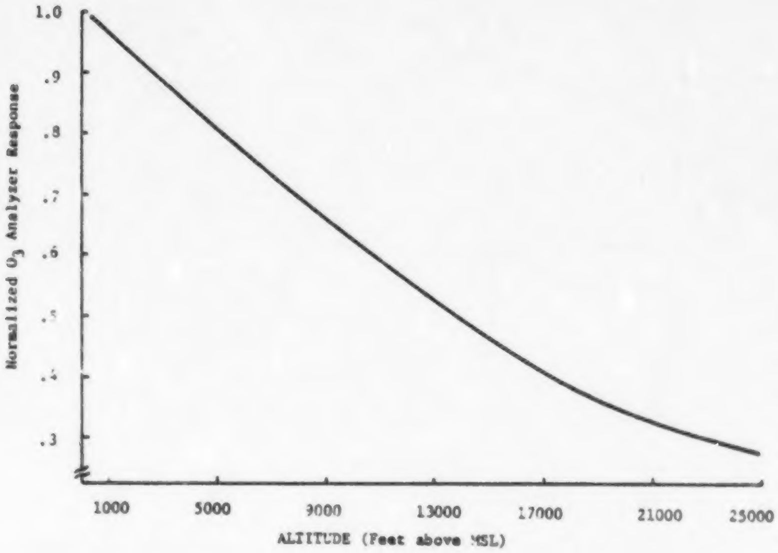

Figure 30. Normalized response versus altitude for Bendix ozone analyzer.

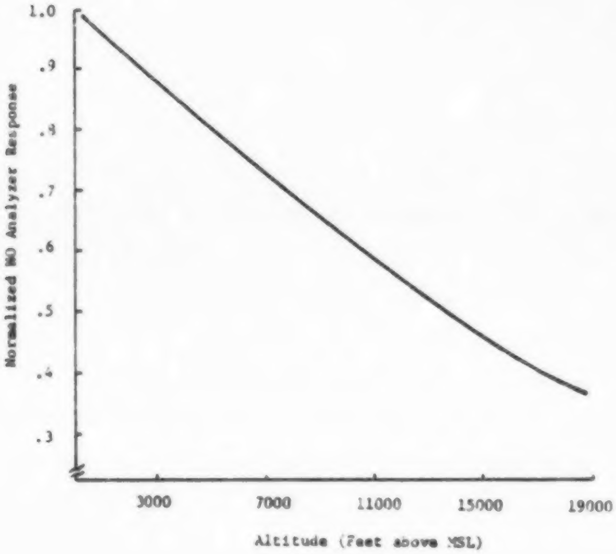

Figure 31. Normalized response versus altitude for Bendix oxides of nitrogen analyzer.

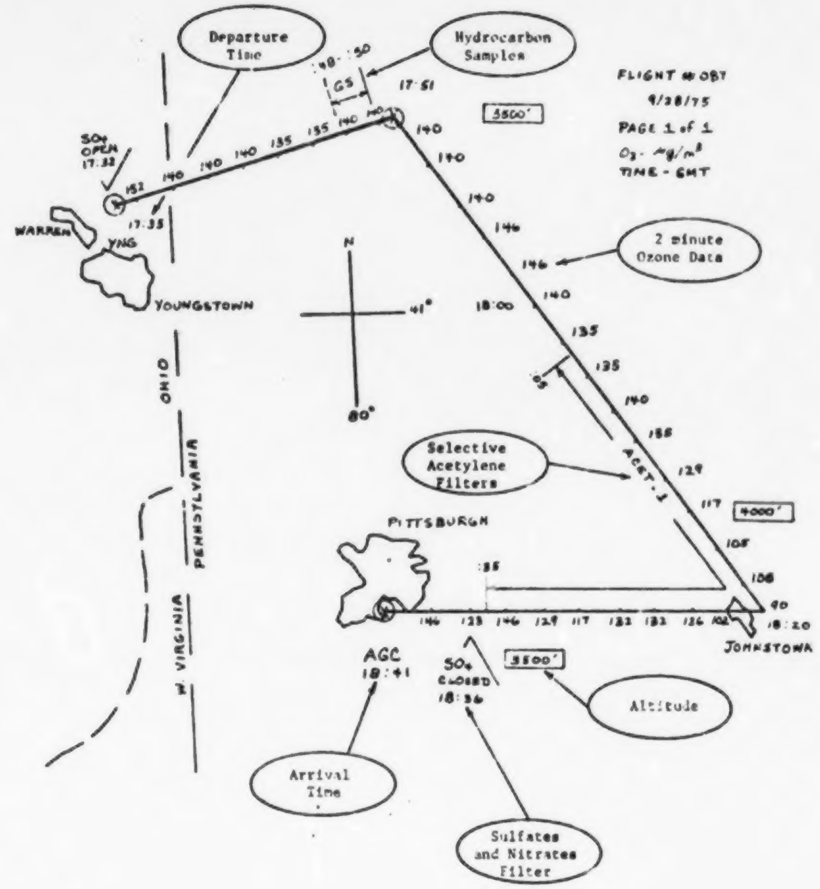
Departure Time
Hydrocarbon Samples
:48-:50
GS
17:51
3500'
FLIGHT # 087
9/28/75
PAGE 1 of 1
O_3 - µg/m³
TIME - GMT
SO4 OPEN 17:32
152
140
140
140
135
135
140
140
17:35
WARREN
YNG
YOUNGSTOWN
140
140
140
146
146
2 minute Ozone Data
N
41°
80°
18:00
140
135
135
:05
140
155
129
117
4000'
ACET.-1
Selective Acetylene Filters
OHIO
PENNSYLVANIA
W. VIRGINIA
PITTSBURGH
:35
105
108
90
18:20
146
123
146
129
117
132
132
126
102
JOHNSTOWN
AGC 18:41
SO4 CLOSED 18:36
3500'
Altitude
Arrival Time
Sulfates and Nitrates Filter

Figure 32. Example of initial data plots.

Final data format

A sample of the final data format is shown in table 4. The processed data were tabulated in a manner to facilitate future automatic flight plotting by computer. A ground track for the flight data presented in the tabulated data is shown in figure 33, and a graphic illustration of the ozone and ambient temperature data, measured during a vertical profile conducted during the flight, is shown in figure 34. Data for all the flights conducted during this program have been archived in the above manner and are available upon request.

Table 4. Flight data, sea-breeze flight 079 (9/21/75)

TIME (GMT)	POSITION	HEADING	ALTITUDE (ft)	O_3 ($\mu g/m^3$)	TEMP. (°C)	DEWPT. (°C)	MANIFOLD TEMP. (°C)	TRUE AIR SPEED (mph)
19:18	DRI	TAKEOFF	203	-	-	-	-	-
20	"	198°	750	92	24.8	11.6	28.3	151
22		"	-	93	-	-	-	-
24		"	2061	98	20.5	9.3	25.4	177
26		"	-	87	-	-	-	-
28		"	1954	87	20.5	10.8	25.7	185
30		"	-	87	-	-	-	-
32		"	2004	87	20.1	12.1	25.3	184
34		"	-	93	-	-	-	-
36		"	2001	87	20.6	12.7	25.3	181
38		"	-	109	-	-	-	-
40		"	2126	104	21.0	14.2	25.7	181
42		"	-	115	-	-	-	-
44		"	2021	131	20.8	15.7	25.8	184
46		"	-	125	-	-	-	-
48		"	2011	169	21.2	15.4	25.9	181
50		"	-	125	-	-	-	-
52		"	-	-	-	-	-	-
54		"	-	142	-	-	-	-
56		"	2060	115	22,0	15.1	26.7	181
58		"	-	131	-	-	-	-
20:00		"	2042	120	22.1	14.9	26.9	183
02		"	-	131	-	-	-	-
04	94°W; 29°N	090°	-	-	-	-	-	-
06		"	-	136	21.5	17.3	26.4	183
08		"	1046	125	-	-	-	-
10		"	-	125	-	-	-	-
12		"	2050	109	21.5	17.6	26.7	180
14		"	-	142	-	-	-	-
16		"	2051	169	20.7	18.0	26.0	181
18		"	-	136	-	-	-	-
20		"	2050	153	20.7	18.3	26.0	184
22		"	-	136	-	-	-	-
24		"	2043	158	20.5	17.7	26.0	184
26		"	-	158	-	-	-	-
28		"	2043	158	20.5	17.8	26.0	183
30		VERTICAL	-	158	-	-	-	-
32		"	3083	97	19.5	16.4	25.0	183
34		"	4108	90	18.8	13.3	24.4	175
38		"	5169	88	17.5	13.3	23.3	175
42		"	6127	93	15.4	10.9	21.7	180
46		"	8361	119	12.7	6.3	19.6	177
50		"	10409	118	9.6	0.8	17.5	174
54		"	8158	104	9.7	12.7	16.9	198
58		"	6017	99	14.3	10.5	20.3	194

Table 4 (con.). Flight data, sea-breeze flight 079 (9/21/75)

TIME (GMT)	POSITION	HEADING	ALTITUDE (ft)	O_3 ($\mu g/m^3$)	TEMP. (°C)	DEWPT. (°C)	MANIFOLD TEMP. (°C)	TRUE AIR SPEED (mph)
21:02		"	5059	88	15.9	14.7	21.7	188
06		"	4032	90	16.7	16.3	22.3	188
10		"	3008	103	18.4	17.7	23.9	188
14		"	1935	164	20.0	18.2	25.2	189
16	92°W; 29°N	360°	2018	164	21.3	17.2	26.0	184
18		"	-	164	-	-	-	-
20		"	2001	164	21.6	17.2	26.5	186
22		"	-	169	-	-	-	-
24		"	2022	185	21.9	17.4	26.9	184
26		"	-	196	-	-	-	-
28		"	2055	223	22.2	17.2	27.2	181
30		"	-	174	-	-	-	-
32		"	1289	153	23.0	17.2	28.2	187
34		"	-	147	-	-	-	-
36		"	633	131	25.0	17.1	28.7	122
37	LFT	LANDING		-	-	-	-	-
22:00	LFT	TAKEOFF		-	-	-	-	-
02	"	350°	-	104	-	-	-	-
04		"	2128	109	20.4	13.7	26.6	180
06		"	-	115	-	-	-	-
08		"	2080	109	19.7	13.7	26.0	179
10		"	-	109	-	-	-	-
12		"	2116	125	19.6	11.4	25.3	181
14		"	-	120	-	-	-	-
16		"	2098	115	19.6	10.3	25.4	181
18		"	-	109	-	-	-	-
20	92°W; 31°N	262°	2101	104	19.2	11.0	24.7	179
22		"	-	109	-	-	-	-
24		"	2125	104	19.1	9.4	24.6	183
26		"	-	104	-	-	-	-
28		"	2102	98	19.3	9.2	24.6	183
30		"	-	98	-	-	-	-
32		"	2081	98	19.0	10.5	24.2	181
34		"	-	98	-	-	-	-
36		"	2098	98	18.7	10.4	23.9	179
38		"	-	98	-	-	-	-
40		"	1029	104	19.9	11.9	24.8	173
42		"	-	104	-	-	-	-
45	DRI	LANDING	203	-	-	-	-	-

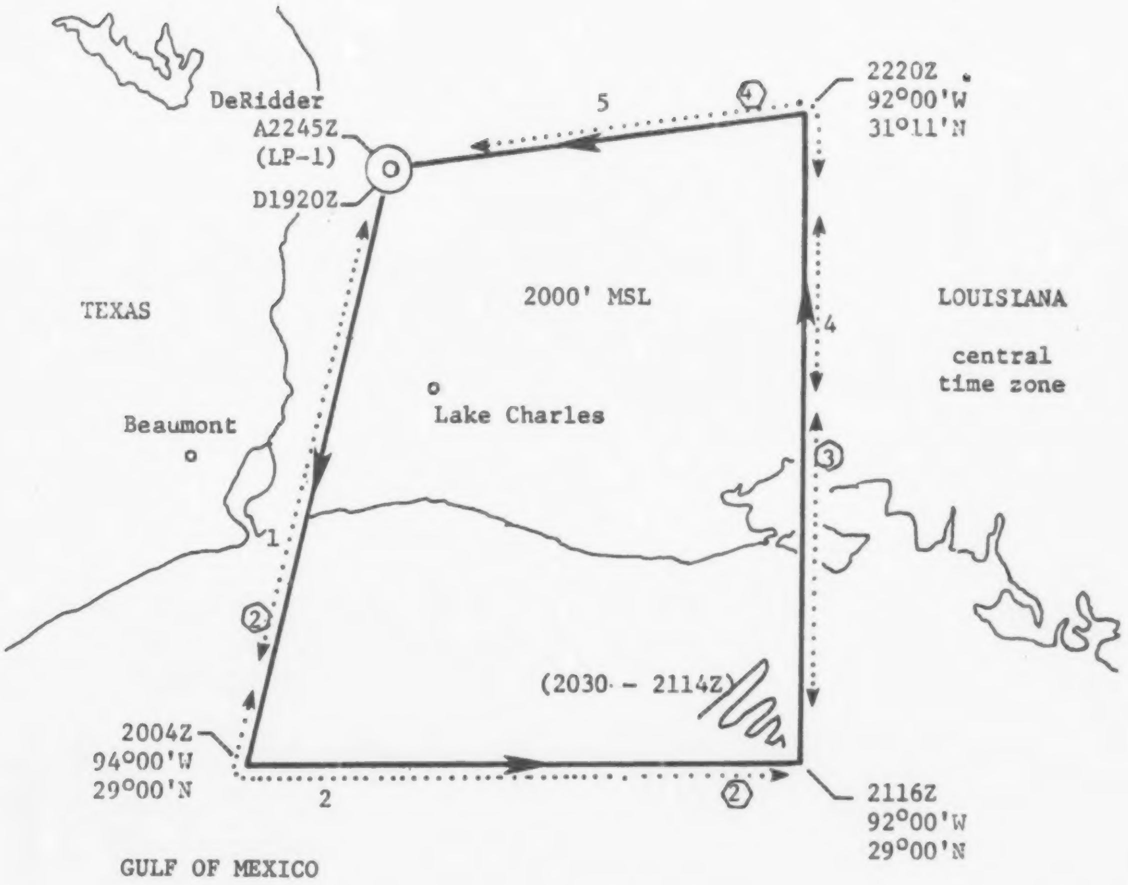
DeRidder
A2245Z
(LP-1)
D1920Z
2220Z
92°00'W
31°11'N
5
④
TEXAS
2000' MSL
LOUISIANA
central
time zone
Lake Charles
Beaumont
4
③
1
②
(2030 - 2114Z)
2004Z
94°00'W
29°00'N
2
②
2116Z
92°00'W
29°00'N
GULF OF MEXICO

SEA-BREEZE (079), 9/21/75
SCALE: 1 in = 35 mi
TIME: GMT
WEATHER: 200015

Figure 33. Sample flight track.

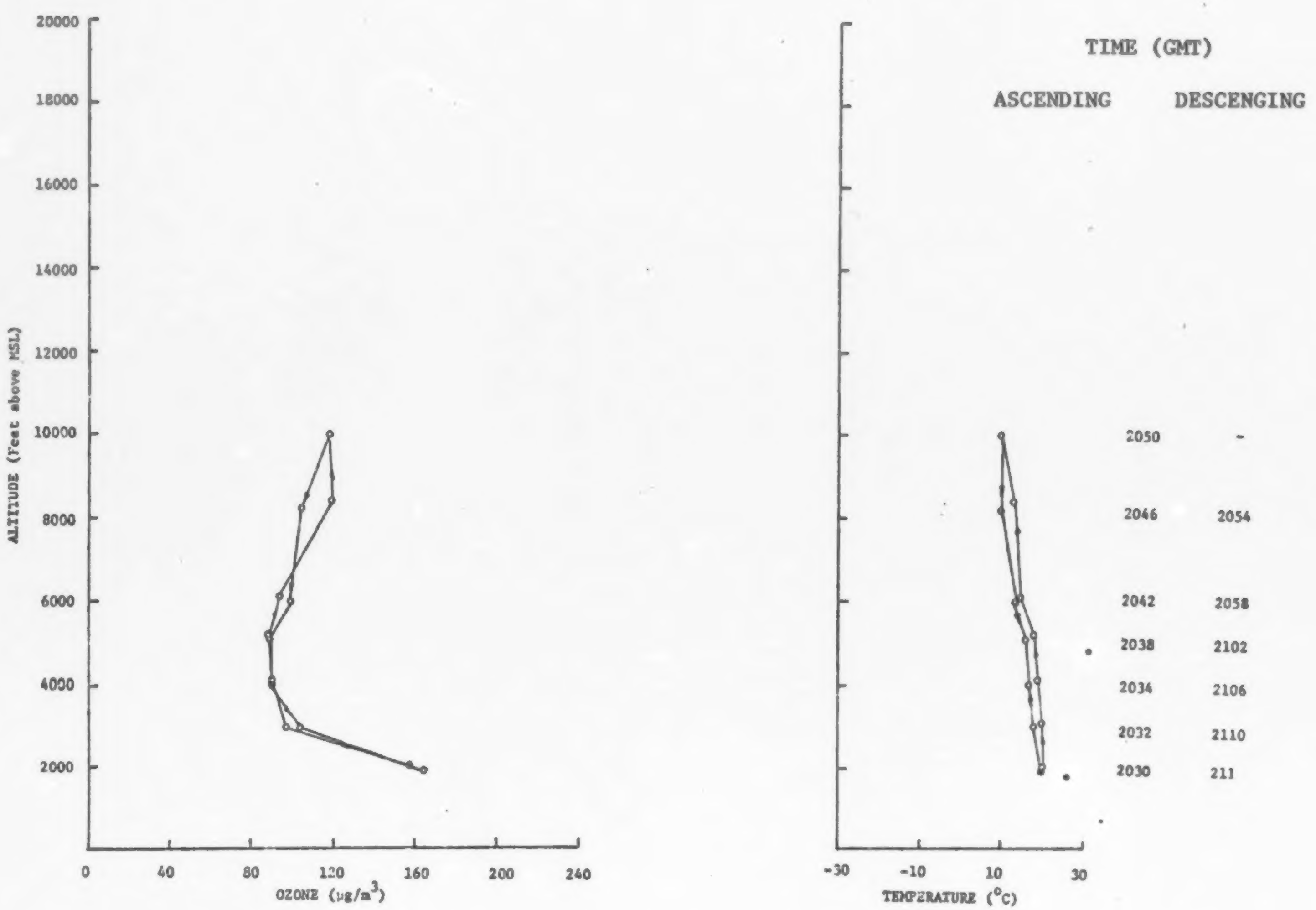

Figure 34. Vertical profile; flight 079 flown on September 21, 1975.

4.2.5 Aircraft Flight Summary

During the program, a total of 111 missions were flown for a total flight time of 292 hours, ranging from 1.5 to 4 hours (2.6 hour average) per flight. The type of flights included 34 gulf coast surveys (figs. 35 and 36), 28 high pressure surveys (fig. 37), plus transition and test flights.

Summaries of the northern route high pressure surveys and the Gulf Coast surveys are presented in tables 5 and 6, respectively. Table 7 lists the verticals conducted during the program and includes the locations where the vertical was performed and the maximum altitude surveyed. Table 8 lists joint EPA-RTI flights conducted in the Gulf Coast area during the latter part of October. A listing of location identifiers is given in table 9.

4.3 Ozonesonde Measurement Program

4.3.1 Introduction

To assess the role of the vertical distribution of ozone upon the ozone measurements near the ground, a special program of serial ozonesonde releases was initiated. These releases documented the vertical distribution of ozone and its changes. Special attention was given to any evidence of the intrusion of stratospheric ozone into the troposphere. The behavior of ozone in the planetary boundary layer was also investigated. Twenty-four ozonesondes were released during three program periods from Huron, South Dakota, and one period from DeRidder, Louisiana. These soundings were made sequentially, three times a day--near sunrise, in the early afternoon, and after sunset--showing the greatest contrasts of ground-level ozone during the day. Ozone data were taken during vertical profile flights, and a quality assurance program was conducted by the EPA.

4.3.2 Instrumentation and Data Acquisition

The ozonesonde consists of a regular radiosonde unit with a separate ozone sensor package attached. The radiosonde unit telemeters data from onboard temperature and humidity sensors at calibrated intervals of pressure changes. If the balloon carrying the package is accurately tracked, winds can be calculated. The ozone sensor package used in this study was the electrochemical concentration cell (ECC) developed by Komhyr and Harris.[20/] The ozone (oxidant) is measured by amount of current generated as ambient air is pumped through KI reagent in the sensing cell. The ozone partial

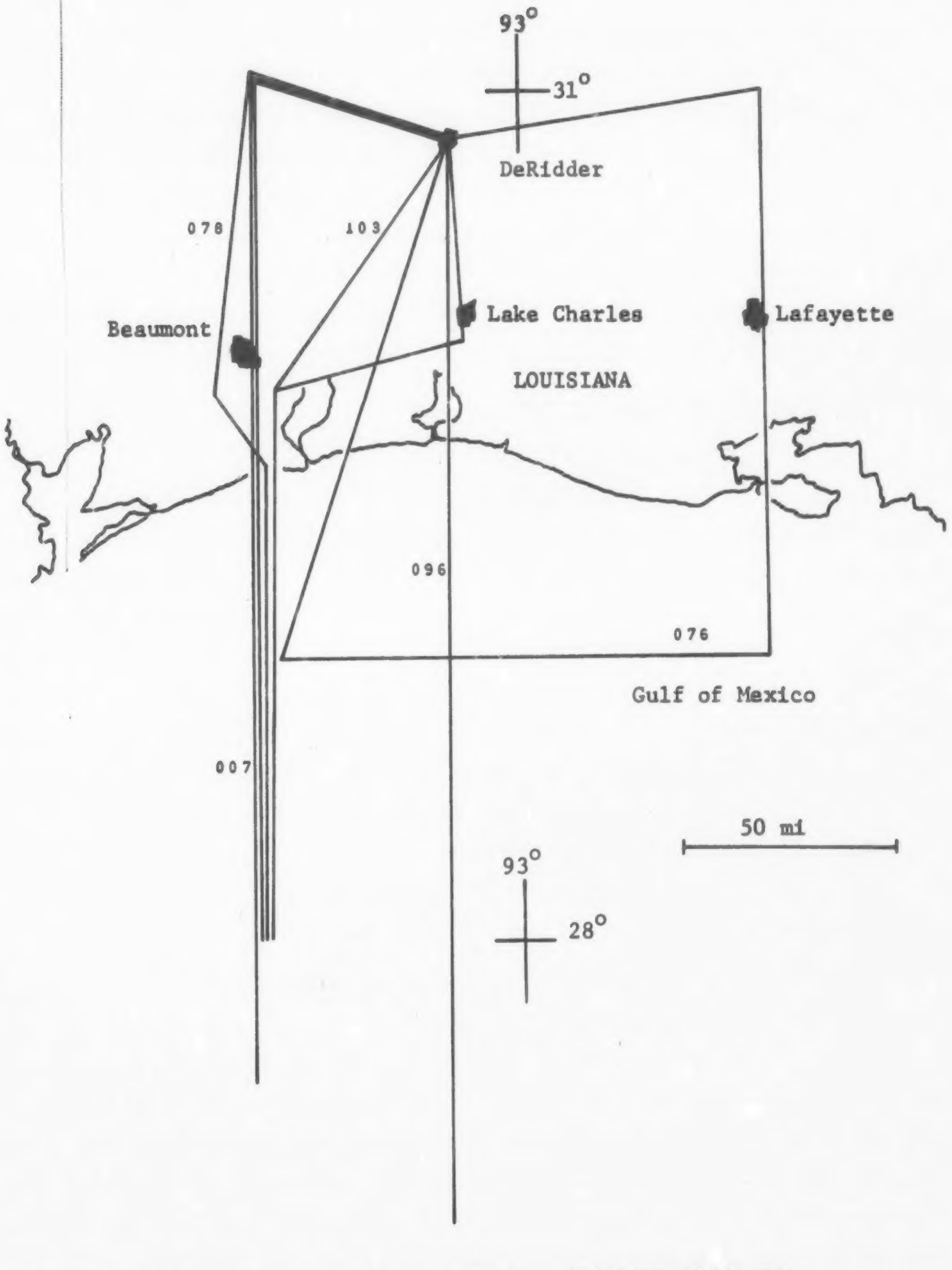
93°
31°
DeRidder
078
103
Beaumont
Lake Charles
Lafayette
LOUISIANA
096
076
Gulf of Mexico
007
50 mi
93°
28°

Figure 35. Gulf coast sea-breeze flights (6/28/75-10/21/75).

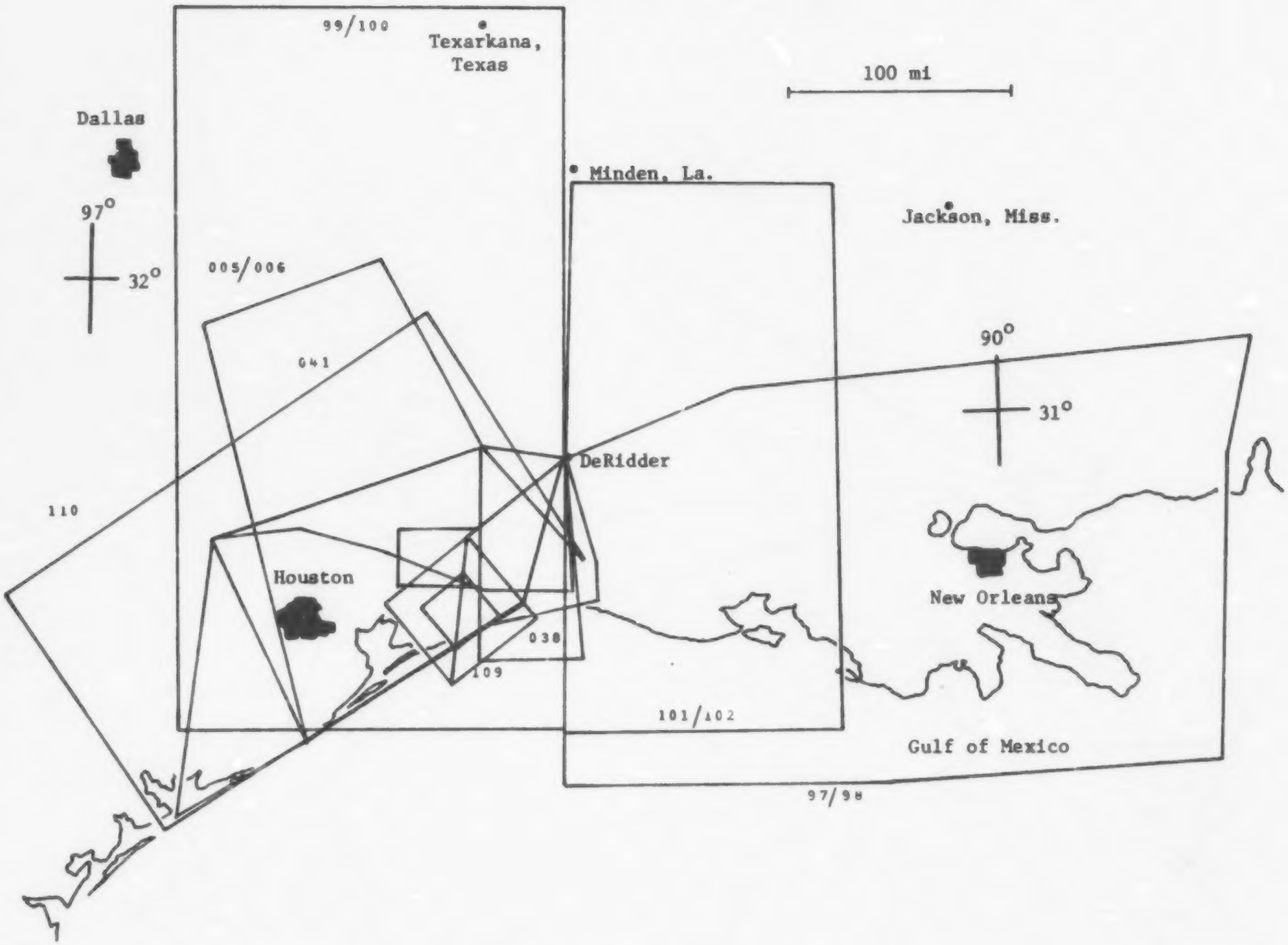
99/100
Texarkana, Texas
100 mi
Dallas
Minden, La.
Jackson, Miss.
97°
32°
005/006
041
90°
31°
DeRidder
110
Houston
New Orleans
038
109
101/102
Gulf of Mexico
97/98

Figure 36. Gulf coast inland survey flights (6/25/75-10/31/75).

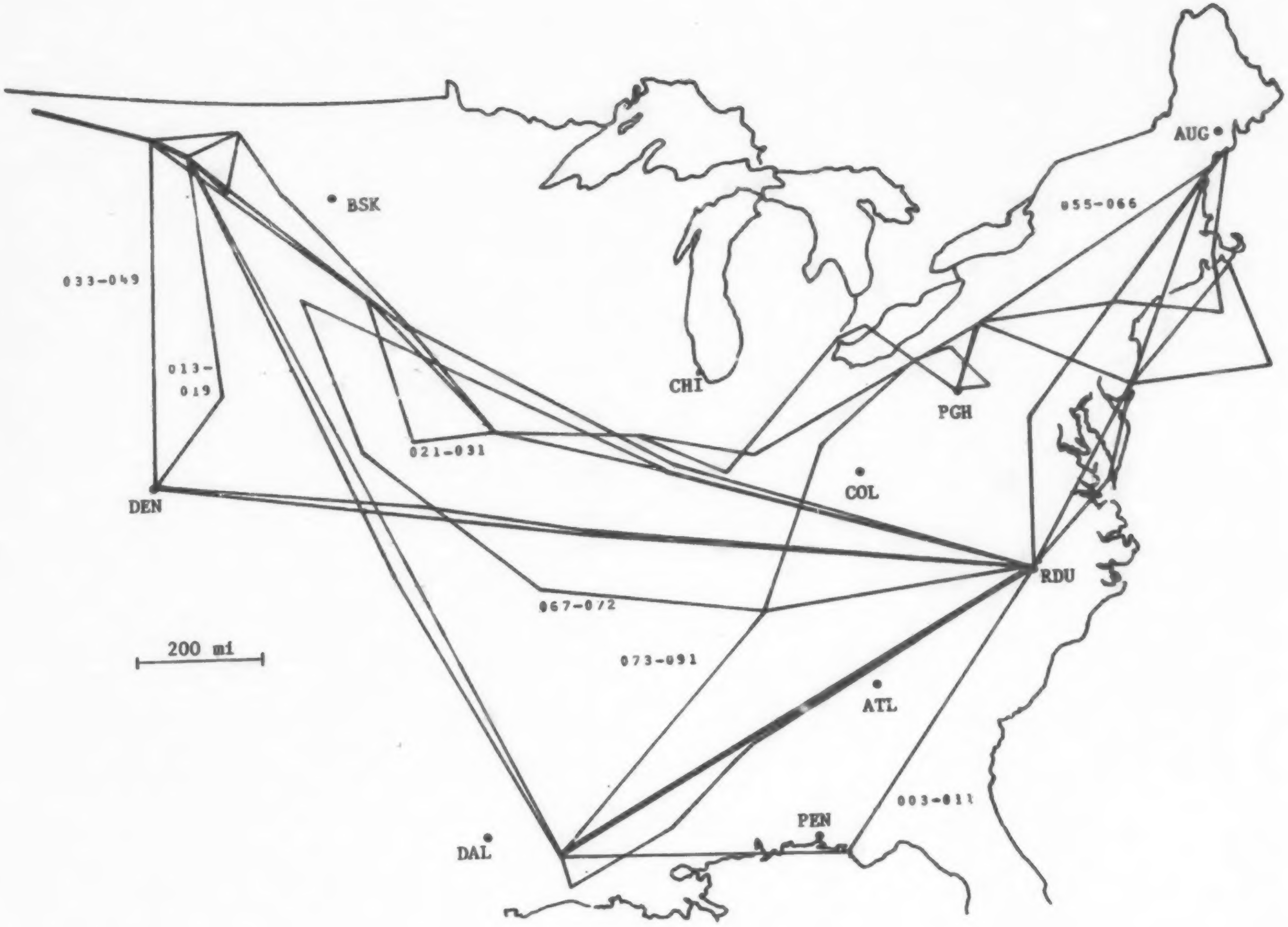
AUG
055-066
BSK
033-049
013-
019
CHI
PGH
021-031
COL
DEN
RDU
067-072
200 mi
073-091
ATL
003-011
PEN
DAL

Figure 37. Northern high pressure flights (7/8/75-9/30/75).

Table 5. Flight summary, northern route high pressure system surveys

Date 1975	No.	Type*
7/8	013	Transition, RDU-FSD
7/8	014	FSD-OLF-SDY
7/10	015	SDY-OLF-HARVE-OLF-SDY
7/11	016	SDY-OLF-STANLEY-OLF-SDY
7/12	017	SDY-AIA-DEN
7/13	018	DEN-FRI-JEF
7/14	019	Transition, JEF-RDU
7/22	012, 022	Transition, RDU-TCL-LCH
7/23	023, 024	Transition, LCH-ICT-SDY
7/24	025, 026	SDY-LNK
7/25	027	LNK-HUF
7/26	028	HUF-AGC
7/27	029, 030	AGC-ACK
7/27	031	Transition, ACK-RDU
8/12	042, 043	Transition, DRI-SDY
8/13	044, 045	SDY-OLF-SDY
8/14	046, 047	Transition, SDY-DEN
8/16	048, 049	Transition, DEN-RDU
9/4	055, 056, 057	Transition, RDU-BIS
9/5	058, 059	BIS-OLF-HON
9/6	060, 061, 062	HON-IND
9/7	063, 064	IND-PWM
9/8	065, 066	Transition, PWM-RDU
9/11	067, 068	Transition, RDU-CAP-PIR
9/12	069, 070	PIR-SGF
9/15	071, 072	Transition, SGF-BNA-RDU
9/27	084, 085	DRI-DAY
9/28	086, 087	DAY-AGC
9/29	088, 089	AGC-EWB
9/30	090, 091	Transition, EWB-RDU

*Identifiers listed in table 9.

Table 6. Flight summary, gulf coast area

Group	Date 1975	No.	Type*
1	6/25	003, 004	Transition, RDU-DRI
	6/26	005	Downwind Plume
	6/27	006	Downwind Plume
	6/28	007	Sea Breeze
	6/29	008	Vertical
	6/29	009	Vertical
	6/30	010, 011	Transition, LCH-RDU
2	8/5	033, 034	Transition, RDU-DRI
	8/6	035	Vertical
	8/6	036	Vertical
	8/7	037	Vertical
	8/7	038	Figure Eight
	8/8	039	Figure Eight
	8/9	040	Figure Eight
	8/11	041	Downwind Plume
3	9/18	073, 074	Transition, RDU-DRI
	9/19	075	Sea Breeze
	9/19	076	Sea Breeze
	9/20	077	Sea Breeze
	9/21	078	Sea Breeze
	9/21	079	Sea Breeze
4	10/9	092, 093	Transition, RDU-DRI
	10/10	094	Sea Breeze
	10/10	095	Sea Breeze
	10/13	096	Sea Breeze
	10/14	097, 098	Box Pattern
	10/19	099, 100	Box Pattern
	10/20	101, 102	Box Pattern
	10/21	103	Sea Breeze
	10/22	104	RTI/EPA Comparison
	10/24	105	RTI/EPA Comparison
	10/25	106	Vertical
	10/30	109	Box Pattern
	10/31	110	RTI/EPA Comparison, Box Pattern
	11/1	111	Transition, DRI-RDU

*Identifiers listed in table 9.

Table 7. List of vertical profile flights

Date 1975	Flight No.	Location	Max. Altitude Sampled (feet)
(Northern Route Verticals)			
7/9	014	Wolf Point, Mont.	10,000
7/10	015	Wolf Point, Mont.	10,000
7/11	016_A	Wolf Point, Mont.	12,000
7/11	016_B	Stanley	12,000
7/12	017	Alliance	18,000
7/13	018	Fort Riley	10,000
7/24	025	Huron	12,000
7/25	027	Peoria	12,000
7/26	028	Chatham, Canada	10,000
7/27	029	Atlantic City, N. J.	10,000
8/13	044	Wolf Point, Mont.	20,000
8/14	046	Wolf Point, Mont.	12,000
9/5	059_A	Dickenson	10,000
9/5	059_B	Huron	12,000
9/6	060	Huron	10,000
9/6	061	Peoria	10,000
9/7	063	Bradford	10,000
9/12	070	Concordia	12,000
9/27	085	Evansville	12,000
9/28	086	Parkersburg	10,000
9/29	089	Middletown, N. Y.	12,000
9/30	090	69°W, 43°N	10,000
(Gulf Coast Verticals)			
6/29	008	Jasper	10,000
6/29	009	Jasper	10,000
8/6	035	Jasper	20,000
8/6	036	DeRidder, La.	20,000
8/7	037	DeRidder, La.	20,000
8/11	041	Newton	12,000
9/19	076	92°W, 28°N	10,000
9/21	079	92°W, 29°N	10,000
10/10	095	92°W, 28°N	10,000
10/21	103	DeRidder, La.	10,000
10/22	104	DeRidder, La.	3,000
10/25	106	DeRidder, La.	22,000
10/30	109	S. W. Beaumont	5,000

Table 8. Flight summary, joint EPA-RTI gulf coast flights

Date 1975	No.	Type
10/20	01	Transition, LVN-LCH
10/27	02	RTI/EPA Comparison
10/27	03	Coastal Survey
10/24	04	RTI/EPA Comparison
10/29	05	RTI/EPA Comparison
10/30	06	Box Pattern
10/31	07	RTI/EPA Comparison
10/31	08	Box Pattern
11/1	09	Transition, LCH-LVN

pressure is proportional to the product of current generated, the sonde box temperature, and the time required to pump a given sample volume into the cell. The current output of the cell generates a signal, which is transmitted three times a minute by the rawinsonde transmitter when a pump-driven commutator interrupts the radiosonde data signal. A reference zero and span current are transmitted on alternate minute intervals. A detailed description of the sensor package has been given by Komhyr and Harris.[20] The system has compared favorably with other ozonesonde systems. Ozonesonde releases and data reduction were performed by Western Scientific Services, Inc., Fort Collins, Colorado, under subcontract to Research Triangle Institute.

The nominal ascent rate of 1,000 ft/min for the rawinsonde package was decreased to about 800 ft/min for this study to give better data resolution from the ground to 3 km (~700 mb, 10,000 ft). At that rate, an ozone reading was available each 90 m (~270 ft) during ascent, which is sufficient to resolve significant ozone strata in the boundary layer.

The ozonesonde data--pressure, temperature, ozone partial pressure and concentration ($\mu g/m^3$)--at significant levels of the sounding were reduced from strip chart records and tabulated. Audits of several of the soundings from the original strip charts and data work sheets showed less than five percent difference. All ozone data are reported in $\mu g/m^3$ at standard conditions (i.e., 25°C, 760 mmHg).

Table 9. List of location identifiers

Identifier	City/ Airport
ABR	Aberdeen, TX
ACK	Nantucket, MA
ACO	Akron, OH
ACY	Atlantic City, NJ
AEX	Alexander, VA
AGC	Pittsburgh, PA
AGS	Augusta, GA
AIA	Alliance, NE
ALB	Albany, NY
AND	Anderson, SC
ANW	Ainsworth, NE
ARB	Walnut Ridge, AR
BFD	Bradford, PA
BHM	Birmingham, AL
BIS	Bismarck, ND
BNA	Nashville, TN
BPT	Beaumont, TX
BRG	Whitesburg, KY
BRL	Burlington, IA
BTR	Baton Rouge, LA
CCT	Central City, KY
CLT	Charlotte, NC
CPR	Casper, WY
CSQ	Creston, IA
CTF	Chesterfield, SC
CYS	Cheyenne, WY
CZI	Crazy Woman, WY
DAY	Dayton, OH
DEC	Decatur, IL
DEN	Denver, CO
DGW	Douglas, WY
DIK	Dickinson, ND
DPR	Dupree, SD
DRI	DeRidder, LA
DYR	Dyersburg, TN
EVV	Evansville, IN
EWB	New Bedford, MA
FML	Fort Mill, SC
FOD	Fort Dodge, IA
FRI	Fort Riley, KS
FRR	Front Royal, VA
FSD	Sioux Falls, SD
GAD	Gadsden, AL
GBG	Galesburg, IL
GGG	Longview, TX
GGW	Glascow, MT
GLD	Goodland, KS
GRW	Greenwood, MS
GSO	Greensboro, NC
GSP	Greenville, SC
HCH	Hinch Mountain, VA
HCM	Harcum, VA
HEZ	Natchez, MS
HKY	Hickory, NC
HLC	Hill City, KS
HMV	Holston Mountain, TN
HON	Huron, SD
HSI	Hastings, NE
HUF	Terre Haute, IN
ICT	Wichita, KS
IND	Indianapolis, IN
IRK	Kirkville, MO
JAN	Jackson, MS
JAS	Jasper, TX
JEF	Jefferson City, MO
JST	Johnstown, PA
LCH	Lake Charles, LA
LEX	Lexington, KY
LFT	Lafayette, LA
LIB	Liberty, NC
LMN	Lamoni, IA
LNK	Lincoln, NE
LOU	Louisville, KY
LOZ	London, KY
LRP	Lancaster, PA
LUL	Lawrenceville, VA
LWM	Lawrence, MA
MCB	McComb, MS
MED	Mansfield, OH
MEI	Meridian, MS
MHE	Mitchell, SD
MKC	Kansas City, KS
MLC	McAlester, OK
MLS	Miles City, MT
MOB	Mobile, AL
MOT	Minot, ND
OKM	Oklahoma City, OK
OLF	Wolf Point, MT
OTM	Ottumwa, IA
PER	Poner City, OK
PFN	Panama City, FL
PIA	Peoria, IL
PIR	Pierre, SD
PKB	Parkersburg, WV
POU	Poughkeepsie, NY
PUD	Providence, RI
PWM	Portland, ME
RDU	Raleigh, NC
RMG	Rome, GA
SBI	Sabine Pass, LA
SDY	Sydney, MT
SGF	Springfield, MO
SLN	Salina, KS
SPA	Spartanburg, SC
SPI	Springfield, IL
SUX	Sioux City, IA
TCL	Tuscaloosa, AL
TKO	Mankato, KS
TNU	Newton, IA
TOC	Toccoa, SC
TYS	Knoxville, TN
UIN	Quincy, IL
VPS	Valparaiso, FL
YNG	Youngstown, OH

4.4 Program Summary

The program schedule and the sequence of events that occurred during the period of performance for field measurement activities (i.e., May 8-October 31, 1975) are presented in this section. The overall program schedule as originally projected at the beginning of the project and presented in the "Work Plan" for Contract 68-02-2048 is shown in table 10. Subsequent discussions related to the events that occurred during the ground-station and aircraft measurement phases of the project and the quality assurance activities are presented in the following paragraphs.

The schedule presented in table 10 for each task was met with respect to acquisition/checkout/preparation of equipment for ground stations; site selection; preparation/installation/checkout of equipment in the aircraft; installation of stations, analyzers, and equipment at the designated sites; and calibration of all analyzers. Each of the five rural stations was set up, calibrated, and brought on-line in a consecutive, orderly manner. The 15 selected stations operated by State, local, and private groups were operational, on-line stations. The field measurement program began at all stations on or before June 30, 1975. Since one aircraft was being utilized for both studies, e.g., northern high pressure and gulf coast oxidant studies, a decision was made to base the aircraft in DeRidder and conduct flights in the gulf coast area until an appropriate high pressure system developed in the northern study area. The aircraft was flown to DeRidder on schedule and subsequently prepared for routine aircraft flights, as dictated by meteorological conditions and the program plan. During the ensuing field measurement program, dynamic calibrations were performed on each analyzer on a monthly basis. Travel delays, instrument failures, and quality control/assurance procedures altered the schedule somewhat. Six quality assurance performance audits were conducted at each State/local agency station audited by RTI during the study. Monitoring and data acquisition continued through September 30, 1975, at the northern stations (Bradford, Creston, Wolf Point) and through October 31, 1975, in the gulf coast area (DeRidder).

During the 120-day field measurement program, a total of 111 individual aircraft flights were flown in support of ground-station measurements for the combined studies. These flights were flown under varying meteorological conditions and included sea breeze flights, coast areal survey flights,

Table 10. Program schedule

Date		Task
May 8, 1975		Start program/begin equipment acquisition.
	9	Begin preparation of comprehensive program plan.
	8-16	Conduct chamber tests at NERC, Las Vegas (O_3 and NO_2 analyzers).
	10+	Receive government furnished equipment
	12-16	Select sites for ground stations.
	15+	Begin checkout of equipment and training of operators/prepare equipment for installation in aircraft/develop flight protocol/begin background study.
	31	Submit monthly technical progress narrative (MTPN).
June	1-15	Organize and develop operational procedures/continue training of operators.
	10-12	Submit comprehensive program plan.
	10-20	Install equipment in aircraft/begin test flights.
	18	Transport equipment from RTI to field locations.
	21-25	Install and check out equipment at monitoring sites.
	23-30	Calibrate analyzers/begin field measurement program.
	23-25	Fly aircraft to base station/check out aircraft system/begin aircraft measurement program.
	30	Submit monthly technical progress narrative (MTPN).
July	7-15	Conduct first audit of state/local stations.
	15	Begin data reduction and processing.
	16-27	Calibrate analyzers at each RTI station.
	21-29	Conduct second audit of state/local stations.
	31	Submit monthly technical progress narrative (MTPN).
August	1-31	Continue data acquisition and processing.
	4-12	Conduct third audit of state/local stations.
	16-	Calibrate analyzers at each RTI station.
	18-26	Conduct fourth audit of state/local stations.
	30	Submit monthly technical progress narrative (MTPN).

Table 10 (con.). Program schedule

Date		Task
September	1-31	Continue data acquisition and processing.
	6-14	Conduct fifth audit of state/local stations.
	15-26	Calibrate analyzers at each RTI station.
	20-28	Conduct sixth audit of state/local stations.
	30	Terminate field measurement program at northern stations.
	30	Submit monthly technical progress narrative (MTPN).
October	1-31	Continue measurements in Gulf Coast area.
	1-5	Disassemble equipment at northern monitoring stations/transport equipment to RTI.
	15-20	Calibrate analyzers at DeRidder station.
	31	Terminate measurement in Gulf Coast area.
	31	Submit monthly technical progress narrative (MTPN).
November	1-5	Disassemble equipment/transport equipment to RTI.
	1-15	Complete data processing.
	15-31	Return GFE to EPA.
	31	Submit monthly technical progress narrative (MTPN).

dowwind plume flights, vertical profile flights, double-box pattern around Nederland, calibration and instrument checkout flights, and northern high pressure system flights. A listing of all flights was presented in section 4.2.5.

5.0 QUALITY ASSURANCE PROGRAM

5.1 Quality Assurance Protocol

A network of 19 ground stations was used to provide much of the data for the summer study. RTI was responsible for maintaining a quality assurance program for the ozone measurements made by 11 of the 19 stations. EPA was responsible for maintaining a similar quality assurance program for the ozone measurements made by the remaining eight stations, four of which were operated by the RTI. EPA also conducted performance audits of the $NO-NO_2-NO_x$ analyzers in the four RTI-operated stations.

The RTI quality assurance program consisted of a preliminary on-site systems audit of the equipment, facilities, procedures, and personnel to evaluate the capability of that station or agency to produce data of acceptable quality. A series of six performance audits were conducted at each station to assess and document the quality of the ozone measurements being made. The ozone measurement network for which RTI's quality assurance program was designed consisted of 11 ground stations operated by State or local agencies or private industries. Station locations and operating agencies or industries are:

Lewisburg, West Virginia	(Bendix Corporation)
Pittsburgh, Pennsylvania	(Local Agency)
Columbus, Ohio	(State Agency)
Indianapolis, Indiana	(State Agency)
Colstrip, Montana	(State Agency)
Pensacola, Florida	(State Agency)
Port O'Connor, Texas	(E. I. Du Pont de Nemours)
Houston, Texas	(State Agency)
Nederland, Texas	(State Agency)
Austin, Texas	(State Agency)
Corpus Christi, Texas	(State Agency)

The network of eight stations for which EPA maintained a quality assurance program included four stations operated by the RTI plus four stations operated by State or city agencies as follows:

Bradford, Pennsylvania	(Research Triangle Institute)
Creston, Iowa	(Research Triangle Institute)
Wolf Point, Montana	(Research Triangle Institute)
DeRidder, Louisiana	(Research Triangle Institute)
Omaha, Nebraska	(City Agency)
Cedar Rapids, Iowa	(City Agency)
Des Moines (Bondurant), Iowa	(City Agency)
Poynette, Wisconsin	(State Agency)

The qualitative systems audit and the quantitative performance audit are discussed in subsections 5.1.1 and 5.1.2, respectively.

5.1.1 Qualitative Systems Audit

The objective of the on-site/off-site qualitative systems audit was to assess the potential of that station and agency to generate ozone data of acceptable quality throughout the duration of the summer study.

The systems audit was conducted in two phases. Agencies operating the respective stations were contacted prior to the start of the summer program by telephone. Operation, calibration, and data validation procedures employed by the agency were discussed. Also, facilities and equipment in the station or used by the agency were reviewed. In preliminary discussions, no station or agency was judged to be deficient enough to constitute exclusion from the air monitoring network.

In concurrence with the first quantitative audit, an on-site systems audit was performed. This audit included:

1) Verification of the procedures used in calibration either through a review of their written procedures or through actual observation of a calibration or both.
2) A check, when applicable, of the station zero air supply by a visual inspection and by comparing analyzer responses to the auditor's clean air supply and the station's zero gas.
3) A check of the agency's capability to perform dynamic calibrations at suitable intervals.
4) A check of the agency's recordkeeping practices.
5) An inspection of the station, including sampling probe, manifold, inlet filter, and instrumentation.

5.1.2 Performance Audit

The objective of this task was to perform a series of systematic on-site quantitative performance audits to collect information on the precision and accuracy of summer study ozone measurements. During the summer study, EPA and RTI teams provided their own O_3 calibration systems and generated known O_3 concentrations on-site for audit purposes. EPA, in addition, provided a calibration system for auditing RTI's NO and NO_2 measurements.

Each respective analyzer audited by EPA and RTI for ozone or oxides of nitrogen was challenged, in most cases, at four upscale points. Stations within the EPA-RTI monitoring network were audited a minimum of two times and up to a maximum of six times. The responsible agency was notified by telephone any time an analyzer was found to differ more than ± 20 percent from the audit value. If the analyzer was within ± 20 percent of the audit value, the results of the audit were mailed to the agency after completing audit checks of all the stations.

5.2 Description of the Air Pollution Monitoring Network

Each station in the 19-station network is discussed here from a quality assurance point of view. Information given in each description includes geographical location, site characteristics, and station description.

The first 11 stations described form the 11-station monitoring network audited by RTI. The last eight stations, four of which were operated by RTI, were audited by EPA.

A. Lewisburg, West Virginia, Monitoring Station

The Lewisburg, West Virginia, station was located at the Greenbrier Valley Airport, approximately 160 km southwest of Garrett County, Maryland. The airport elevation is approximately 705 m MSL. The airport serves both private and commercial aviation. The valley surrounding the airport is rolling pastureland with some wooded areas. Analyzers and associated equipment were housed in an air-conditioned 2.5 × 9.2 m mobile laboratory owned by the Bendix Corporation, Lewisburg, West Virginia. A 1.25-cm diameter Teflon tube located 2 m above the laboratory served as the sample inlet line.

B. Pittsburgh, Pennsylvania, Monitoring Station

The Pittsburgh station was located in Penn Hills at 12245 Frankstown

Road. The analyzer, owned and operated by the Allegheny County Air Pollution Control Agency, was housed in a large air-conditioned room in the Penn Hills Municipal Building. A 0.6-cm OD Teflon line approximately 7.5 m long served as the sample inlet line with the sample inlet well below the building's roofline. The probe inlet had only about 270 degrees of exposure.

C. Columbus, Ohio, Monitoring Station

The Columbus station was located in the NE section of the city at the intersection of highway 161 and Maple Canyon Drive. The analyzer was housed in the bay of a fire station with no temperature control. A 0.6-cm OD Teflon line approximately 11 m long served as the sample inlet line. The probe inlet was above the roof line and had 360° of exposure.

D. Indianapolis, Indiana, Monitoring Station

The Indianapolis station was located in the NE section of the city at 71st and Tacona Avenue. The analyzer was located in a temperature-controlled (aluminum) shelter. A 0.6-cm OD heated Teflon line approximately 18 ft in length was mounted 1 m above the building and served as the inlet line. The sample inlet was an inverted glass funnel and had 360° exposure.

E. Colstrip, Montana, Monitoring Station

The Colstrip station was located approximately 3 km southeast of Colstrip, Montana (Burlington, Northern Site). The analyzer was housed in a temperature-controlled camper trailer. A 0.6-cm OD Teflon line was connected to a 2.54-cm glass manifold. The sample probe extended above the trailer and had 360° of exposure. The trailer was parked on a mesa approximately 30 m above the surrounding ground level.

F. Pensacola, Florida, Monitoring Station

The Pensacola station was located on Ellysen Naval Air Station. The analyzer was housed in a temperature-controlled trailer. Samples were taken from a glass manifold. The sample inlet line was wrapped with heat tape to prevent condensation in the inlet sample line.

G. Port O'Connor, Texas, Monitoring Station

The Port O'Connor station was located on the beach at the corner of Washington Boulevard and Harrison Street and is considered a rural station.

The analyzer, owned and operated by the Du Pont Company, was housed in a storage shed (2.4 × 2.4 × 2.4 m) under a beachhouse. The sample was obtained through a 9- to 10-m 0.6-cm OD Teflon line that extended 1 m above the roof with 360° exposure. There was no temperature control, and high humidity was experienced on all audit trips.

H. Texas Air Control Board Monitoring Stations

The Texas Air Control Board (TACB) stations are self-contained laboratories with the capability of performing over long periods of time. All stations were custom designed after the crew-shelters used by oil companies on the north slope in Alaska and in the Middle East. The windowless units are constructed of 7.6-cm pressure-bonded laminate and include 3.8 cm of styrofoam insulation. The stations are 3 m × 3 m × 7.3 m, with the interior divided into a 3 m × 6 m monitoring laboratory (main room) and a 3 m × 1.2 m utility room. The central air conditioning/heating unit provides a stable temperature (±1° C) and safety ventilation. The sample manifolds are glass and are heated by incandescent bulbs. Sample air and zero and span gases pass through the same filter before entering the ozone analyzer. The ambient sample intakes are inverted glass funnels approximately 3.6 m above the roof with 360° exposure.

Each of the Texas monitoring sites is described below.

H.1. Connie* 8: Aldine

Connie station 8 is located in Aldine, approximately 3 km north of the Houston city limits and about 20 km northwest of the Houston Ship Channel. Data reported from Aldine will be considered as data for Houston in this report.

The industries of the area emit primarily sulfur dioxide, carbon monoxide, nitrogen oxides, and various hydrocarbon compounds. Because of the prevailing winds (wind direction south to southeast 38 percent of the time), these emissions and photochemical oxidants are the principle pollutants measured at the monitoring site.

---

*For convenience, the TACB has given the continuous monitoring program the nickname of Project Connie and the individual sites are called Connie stations.

H.2. Connie 2: Nederland

Connie station 2 is located on the southeast corner of the public parking lot at the Jefferson County Airport in Nederland, Texas. Elevation of the site location is 5 m MSL. The Beaumont-Port Arthur-Orange area is moderately populated and heavily industrialized. Due to the type of industry in the area, there should be significant quantities of hydrocarbons and sulfur dioxide. The Jefferson County Airport is also the location of previous studies of photochemical oxidants. The wind direction is from the south approximately 15 percent of the time.

H.3. Connie 3: Austin

Connie station 3 is located in the south parking lot of the Texas Air Control Board, 8520 Shoal Creek Boulevard, Austin, with an elevation of 198 m MSL. The city of Austin has no heavy industry, chemical industry, or petroleum-related gaseous emission sources. The city has two electric generating plants. One plant is located in the center of the city on the Colorado River. Bergstrom Air Force Base lies approximately 1.6 km southeast from downtown. The University of Texas complex lies immediately to the north of the downtown areas. Emissions from these sources, as well as those of the downtown area, are carried to the Austin Connie station by southerly and southeasterly winds prevalent in the Austin area (37 percent of the time).

H.4. Connie 4: Corpus Christi

Connie station 4 is located in the southwest corner of the school grounds at the Robert Driscoll Junior High School in the 200 block of Old Robstown Road, Corpus Christi, Texas, and has an elevation of 12 m MSL. The area within a 1.2-km radius of the site is primarily residential, but schools, shopping centers, and light industry are also found within this area. Outside this radius and to the north are 12 major heavy industrial complexes, including chemical, petrochemical, and petrorefining facilities, nonferrous smelters, and cement plants. Grain storage and shipping areas and power-generating stations are also located to the north. Due to prevailing winds from the northwest 24 percent of the time, pollutants emitted from such industries reach the station.

I. Rural Monitoring Stations Operated by RTI

The RTI operated rural stations were located in: Bradford, Pennsylvania; Creston, Iowa; Wolf Point, Montana; and DeRidder, Louisiana. Descriptions of these stations were given in section 4.0 and are not repeated here.

J. Poynette, Wisconsin, Monitoring Station

This station is located at the edge of Poynette and is considered a rural station. The station has a heating system but no air conditioning. The sample line is a 0.9-cm ID Teflon line approximately 7.6 m long with a probe inlet height of about 9 m above ground.

K. Cedar Rapids, Iowa, Monitoring Station

This station was located about 3.2 km northeast (~20°) of the center of Cedar Rapids in a residential area. The station was air conditioned. The sample intake system consisted of a glass probe and manifold with a Teflon line from the manifold to the analyzer.

L. Des Moines (Bondurant), Iowa, Monitoring Station

The station was located in the center of Bondurant about 16 km northwest of Des Moines. A 9-m Teflon line 0.3 cm ID served as the sample inlet line. The station had a heating system but no air conditioning.

5.3 Audit Procedures

The equipment and procedures used by the RTI and EPA audit teams are discussed in the following subsections.

5.3.1 RTI Ozone Auditing Procedures

An ozone calibration system as described in appendix A of this report was used by the RTI audit team to generate test atmospheres of known ozone concentrations for challenging the ozone analyzers.

The ozone generator was calibrated in the laboratory at RTI using the 1% NBKI procedure prior to the field audits. When performing an audit the generator output as read from its laboratory developed calibration curve was taken as the reference O_3 value with 1% NBKI analyses performed in the station to verify that the calibration had not changed significantly during shipment and handling.

The NBKI sampling train used by RTI was the same as that in the Federal Register.[1/] The sampling train flow rate was controlled at about 500 cm^3/min with a critical orifice. A bubble flow meter (traceable to NBS) was used to determine the exact flow rate at each station. Ten-minute sampling periods (timed with a stopwatch) were used. An aneroid barometer and a mercury-in-glass thermometer were used to measure station pressure and temperature, respectively.

5.3.2 EPA Ozone Auditing Procedures

The calibration system employed by EPA for audit purposes was based upon reverse gas phase titration (RGPT) utilizing an NBS certified tank of nitrogen oxide. This audit technique was based upon the rapid gas phase reaction between O_3 and NO in accordance with the following equation:

$$NO + O_3 \rightarrow NO_2 + O_2,\ K = 1.0 \times 10^7 \ l\ mole^{-1}\ sec^{-1}$$

An O_3 concentration of unknown magnitude was generated and sufficient NO of known concentration was added in a dynamic calibration system to decrease the O_3 concentration by 90-95 percent of its original value as measured on the station chemiluminescent O_3 analyzer. The assay for the NO cylinder used in this technique was based on the gas phase titration (GPT) of NO with O_3 in which the O_3 concentrations were determined iodometrically using the 1 percent buffered potassium iodide procedure. The NO cylinder served as a transfer standard traceable to the primary standard used in the calibration procedure for the measurement of photochemical oxidants as specified in the Federal Register. The flow conditions in the dynamic calibration system were optimized to ensure the quantitative reaction of NO with O_3 and to minimize the reaction of NO_2 with O_3 which could cause errors in the audit procedure. Erroneous results will also result from this technique if the analyzer response is non-linear.

The ozone analyzers were challenged at two upscale points. These points were 40 percent and 80 percent of full scale.

5.3.3 EPA Oxides of Nitrogen Auditing Procedures

The EPA audit team utilized an NO cylinder with dilution to audit the

NO_x analyzers. Gas phase titration was used to generate known NO_2 samples. The gas phase titration system is illustrated in figure A-3 of appendix A. A detailed description of the technique is given in appendix A and is not repeated here.

Audit checks were generally made at 40 percent and 80 percent full scale for the NO_2 analyzers.

5.4 Analysis and Interpretation of Audit Data

The primary objective of the on-site performance audits was to allow estimates of the precision and accuracy of the O_3. NO_2 and NO measurements made by the monitoring network and subsequently used in the summer study.

General data analysis procedures used to estimate measurement precision and accuracy are discussed here. Quantitative information is given by pollutant in the following subsections.

The variable used in the analysis of audit data is the percent difference in the reference sample concentration and the analyzer response calculated by the relationship

$$d = 100(C_m - C_a)/C_a$$

where

d = difference in the analyzer response or measured value C_m and the reference or audit concentration C_a, percent

C_m = analyzer response or measured value, $\mu g/m^3$

C_a = reference or audit sample concentration, $\mu g/m^3$

The difference obtained at the i^{th} station on the j^{th} audit is represented by d_{ij}. The bias in the pollutant measurements for the network of stations over the audit period is estimated by

$$\hat{\tau} = \bar{d} = \frac{1}{nk} \sum_{i=1}^{k} \sum_{j=1}^{n} d_{ij}$$

and the standard deviation of the differences, s_d, is calculated by

$$s_d = \sum_{i=1}^{k} \sum_{j=1}^{n} \left[(d_{ij} - \bar{d})^2/(k \cdot n - 1)\right]^{1/2}$$

The above calculated standard deviation s_d is the standard deviation of the difference of two measurements; that is, for example, the difference in the O_3 concentration as determined by the auditor and the O_3 concentration as measured by the analyzer. To prevent overestimating the quality of the measurements, the "worst case condition" is assumed here. That is, it is assumed that all the variability in the differences (d_{ij}'s) is due to the measurement system. The audit value is assumed to be the true value. Under these assumptions, s_d is an estimate of coefficient of variation of the measurement data, i.e.,

$$s_d = \hat{CV}.$$

The coefficient of variation is used as a measure of the precision of the air pollution measurements. Two parameters are ordinarily needed to characterize the accuracy of a measurement process, one indicating its precision and the other its bias; therefore $\hat{\tau}$ and $\hat{CV}$ must be viewed together (in a confidence interval, for example) as a measure of accuracy.

Precision and accuracy of O_3 and oxides of nitrogen, i.e., NO and NO_2, are discussed in the following subsections.

5.4.1 Precision/Accuracy Estimated for Ozone Measurement

The ozone audit results are given by station, by concentration level, and by the date of the audit in table 11. The results are given as the relative difference between the measured and the audit (input) values. The station bias, d_i, is given in the right hand column of table 11.

It is noted here that the Pensacola, Florida, and Corpus Christi, Texas, stations were audited by RTI; however, the ozone data from these two stations were invalidated or received too late for inclusion in the

Table 11. Summary of ozone and oxides of nitrogen audit data

Station Location	Performance Audit													$d_{1.}$
	Audit Concentration μg/m^3	1		2		3		4		5		6		
		Date	d_{11}(%)	Date	d_{12}(%)	Date	d_{13}(%)	Date	d_{14}(%)	Date	d_{15}(%)	Date	d_{16}(%)	
RTI OZONE AUDIT RESULTS														
Lewisburgh, West Virginia	157	7/9/75	-21.2	8/18/75	-7.5	8/25/75	+5.0	9/8/75	0.0	9/15/75	+11.3	9/22/75	+2.5	-1.7
	392		-23.8		0.0		-3.1		-2.5		+6.9		+5.6	-1.0
Pittsburgh, Pennsylvania	157	7/10/75	+11.2	8/19/75	+14.5	8/26/75	-5.5	9/9/75	+13.6	9/16/75	+8.1	9/23/75	+9.8	+10.5
	392		+11.9		+17.5		-1.0		+24.0		+19.5		+19.5	+15.6
	784		+11.0		+18.5		-0.8		+27.5		+23.3		+22.5	+17.0
Columbus, Ohio	157	7/11/75	+11.3	8/9/75	-5.0	8/27/75	-12.5	9/10/75	-10.0	9/16/75	-7.5	9/24/75	-12.5	-6.0
	392		+8.1		-10.6		-16.3		-6.3		-6.9		-8.8	-6.8
Indianapolis, Indiana	157	8/5/75	-3.3	8/20/75	-27.2	8/28/75	-7.0	9/11/75	-17.1	9/17/75	-5.0	9/25/75	-15.3	-12.6
	392		+8.5		+6.0		-8.0		-8.0		-3.9		-4.5	-1.7
	784		+16.3		-17.0		-7.8		-4.8		-3.5		-1.3	+2.6
Colstrip, Montana	78	8/7/75	-3.8	8/21/75	-27.5	8/29/75	-10.0	9/12/75	-15.0	9/18/75	-20.0	9/26/75	-30.0	-17.5
Austin, Texas	157	7/16/75	+2.5	7/29/75	+6.8	8/21/75	+1.7	9/11/75	-9.4	10/14/75	-20.3	10/30/75	+9.9	-1.4
	789		-1.8		+4.3		+0.8		-10.8		-22.0		+2.8	-4.5
Houston, Texas	157	7/17/75	-1.6	8/1/75	-1.2	8/20/75	-10.4	9/10/75	-0.7	10/15/75	+5.0	10/28/75	-6.8	-2.4
	789		-0.5		-5.8		-14.0		-6.3		-1.0		-6.8	-5.7
Nederland, Texas	157	7/18/75	-9.1	7/31/75	-6.1	8/19/75	-21.2	9/9/75	+0.2	10/15/75	Analyzer Down	10/28/75	+8.8	-5.5
	785		-3.3		-8.5		-16.5		+0.5				+6.5	-4.3
Port O'Connor, Texas	157		Station Not Available	7/30/75	-21.6	8/20/75	+6.9	9/10/75	+33.9	10/15/75	-26.2	10/29/75	-12.7	-3.9
	392				-23.5		+5.5		+28.5		-22.0		-10.5	-4.4
	785				-24.0		+5.3		+26.5		-20.3		-10.0	-4.5

Table 11. Summary of ozone and oxides of nitrogen audit data (con.)

Station Location	Performance Audit														$d_{i.}$
	Audit Concentration µg/m^3	1		2		3		4		5		6		
		Date	d_{11}(%)	Date	d_{12}(%)	Date	d_{13}(%)	Date	d_{14}(%)	Date	d_{15}(%)	Date	d_{16}(%)	
EPA NITRIC OXIDE AUDIT RESULTS														
Creston, Iowa	100	8/1/75	-	8/19/75	-	9/1/75	-	9/12/75	-	9/25/75	+3.1			
	200 to 350		+0.7		-20.6		-		+4.0		-			
	400 to 600		+5.4		-25.3		-4.5		+4.0		+2.5			
Wolfpoint, Montana	345	7/13/75	-15.2											
DeRidder, Louisiana	200 to 350	7/23/75	+0.5	9/20/75	-	10/28/75	-10.1							
	400 to 600		+0.8		+2.1		-10.6							
Bradford, Pennsylvania	Not reported	8/20/75	+3.0											
EPA NITROGEN DIOXIDE AUDIT RESULTS														
Creston, Iowa	150 to 300	8/1/75	-13.0	8/19/75	-3.6	9/1/75	-	9/12/75	+4.0	9/25/75	+4.3			
	560 to 580		-9.3		-7.5		-15.0		+4.0		-0.2			
DeRidder, Louisiana	250 to 300	7/23/75	-0.0	9/20/75	+4.0	10/28/75	-							
	374		-		-		-0.8							
	450 to 550		-0.0		+12.8		-							
	765						-0.5							
Bradford, Pennsylvania	Not reported	8/20/75	+1.0											

Table 11. Summary of ozone and oxides of nitrogen audit data (con.)

Station Location	Performance Audit													$d_{1.}$
	Audit Concentration µg/m³	1		2		3		4		5		6		
		Date	d_{11}(%)	Date	d_{12}(%)	Date	d_{13}(%)	Date	d_{14}(%)	Date	d_{15}(%)	Date	d_{16}(%)	
	EPA OZONE AUDIT RESULTS													
Bradford, Pennsylvania	517 392	9/12/75	+6.3 -8.3	8/20/75	-5.1 -5.4									+0.6 -6.9
Wolfpoint, Montana	157 392	7/13/75	-17.7 -7.4	9/10/75	-17.8 -8.3									-17.8 -7.9
DeRidder, Louisiana	157 392	7/23/75	-21.3 -19.1	9/30/75	-15.7 -9.1									-18.5 -14.1
Omaha, Nebraska	392 785	8/5/75	+9.3 +18.0	8/19/75	+24.1 +22.7	9/2/75	+19.9 +18.3	9/9/75	+31.2 +35.4	9/26/75	-1.5 -3.4			+16.6 +18.2
Cedar Rapids, Iowa	392 785	7/30/75	-21.4 -20.4	8/13/75	-17.0 -17.3	8/28/75	-21.6 -20.7	9/16/75	-13.4 -17.0	9/23/75	-9.1 -12.2			-16.5 -17.5
Des Moines, Iowa	157 392 785	7/31/75	- +6.3 +8.3	8/14/75	-2.5	8/29/75	-2.9	9/15/75	-2.5	9/24/75	-1.3			-2.3 +6.3 +8.3
Poynette, Wisconsin	517 392	7/29/75	-14.7 -6.5	8/12/75	- -3.0	8/26/75	- +8.2	9/17/75	- +11.0	9/22/75	+3.7 +5.5			-5.5 +3.0
Creston, Iowa	157 392	8/1/75	+20.4 -14.9	8/15/75	-11.0 -17.3	9/1/75	-18.4 -16.2	9/12/75	-17.0 -9.9	9/25/75	-11.1 -17.1			-7.4 -15.1

summer study analysis. Therefore, these audit data are not included in this analysis.

The ozone audit data for the RTI-audited network yielded an overall bias of

$$\hat{\tau} = -1.8 \text{ percent},$$

and a coefficient of variation of

$$\hat{CV} = 13.5 \text{ percent}.$$

The combined data for the EPA ozone audits result in an overall bias of

$$\hat{\tau} = -4.3 \text{ percent},$$

and a coefficient of variation of

$$\hat{CV} = 14.9 \text{ percent}.$$

From the above estimated population parameters and under the assumption made previously concerning the accuracy of the reference samples, it can be stated that, for the summer study, the percent error in the measured value C_m of a true O_3 value for the RTI-audited network would be in the interval

$$\hat{\tau} - 1.645 \times \hat{CV} \leq \% \text{ Error} \leq \hat{\tau} + 1.645 \times \hat{CV},$$

or

$$-24\% \leq \% \text{ Error} \leq +20\%$$

approximately 90 percent of the time.

Similarly for the network audited by EPA the percent error would be within the interval

$$\hat{\tau} - 1.67 \times \hat{CV} \leq \% \text{ Error} < \hat{\tau} + 1.67 \times \hat{CV},$$

or

$$-29\% \leq \% \text{ Error} \leq +21\%$$

approximately 90 percent of the time.

An analysis of variance of the network audit data results in the following observations.

(1) The between-audits component of variability is negligibly small compared to the within- and between-station components of variability.

(2) Approximately 80 percent of the total variability is represented by the within-station component of variability.

(3) Approximately 20 percent of the total variability is represented by the between-station component of variability.

5.4.2 Precision/Accuracy Estimates for Nitric Oxide and Nitrogen Dioxide Measurements

The results of the NO and NO_2 audits of the RTI-operated ground stations are given in table 11. There were nine audit checks performed at different concentration levels for a total of 15 data points per pollutant for estimating bias and precision of the measurements reported by the network.

The available audit data for NO show an estimated network bias of

$$\bar{d} = -3.8 \text{ percent}$$

and a standard deviation of the differences of

$$s_d = 9.6 \text{ percent.}$$

The NO_2 audit data yield an estimated bias of

$$\bar{d} = -3.0 \text{ percent}$$

and a standard deviation of the differences of

$$s_d = 7.4 \text{ percent.}$$

5.5 Summary of Audit Results

Estimates of the relative bias, coefficient of variation, and 90-percent confidence interval for the error (deviation of the measured value from the audit value) in the O_3, NO, and NO_2 measurement data used in the summer study are as follows:

- Ozone. $\hat{\tau} = -2.6\%$, $\hat{CV} = 14\%$, $-26\% \leq \%$ error $\leq +20\%$.
- Nitric Oxide. $\hat{\tau} = -3.8\%$, $\hat{CV} = 9.6\%$, $-22\% \leq \%$ error $\leq +14\%$.
- Nitrogen Dioxide. $\hat{\tau} = -3.0\%$, $\hat{CV} = 7.4\%$, $-17\% \leq \%$ error $\leq +11\%$.

These bias and precision estimates based on the audit data compare favorably with the results from previous audits of similar monitoring networks.[5] Therefore, it is concluded that the quality of the O_3, NO, and NO_2 measurements made by the monitoring network and subsequently used in the summer study analysis is comparable to the quality of similar measurements made in other well-managed monitoring networks and sufficient to satisfy the summer study requirements.

6.0 SUMMARY OF DATA AND STATISTICS

The results of the field measurement program are presented in this section and include summary statistics, diurnal pollutant concentration patterns, and a meteorological summary for July, August, September, and October 1975. To facilitate discussion and interpretation of these results, detailed hydrocarbon and halocarbon analyses of grab samples from Bradford, Creston, Wolf Point, and DeRidder, and pertinent ratios of compounds in grab samples collected during aircraft flights are presented in sections 7.0 and 8.0.

6.1 Summary Statistics

Mean hourly ozone concentrations, standard deviations, and case counts for rural and urban stations, e.g., RTI and State/local agency stations, are shown in table 12. Valid and/or timely data were received from only 10 of the original 15 State/local agency stations shown in figure 1 (section 3.0) during the period June 1 to September 30, 1975. Consequently, only data for the monitoring stations listed in table 12 were considered in this section and for subsequent analysis and interpretation. Ozone data above the NAAQS for photochemical oxidants are summarized in table 13. Statistical data for nitric oxide and nitrogen dioxide, selected hydrocarbons and halocarbons, and particulates (TSP, NH_4^+, NO_3^-, $SO_4^=$) are presented in tables 14, 15, and 16, respectively. Mean ozone and oxides of nitrogen data are further summarized for each reporting station in table 17 and show a breakdown of means on a monthly basis. Table 18 also presents a similar summary for monthly mean hydrocarbon and halocarbon data.

The mean hourly concentrations of ozone at the rural stations ranged from a low of 58 $\mu g/m^3$ at Wolf Point to 81 $\mu g/m^3$ at Bradford. The range for mean hourly concentrations for urban stations was from 49 to 85 $\mu g/m^3$. The standard deviations for all stations, both rural and urban, were similar in magnitude (see table 12) with notable exceptions--Pittsburgh, Houston, and Nederland. The overall ozone mean (or ozone burden) for the rural stations was in most cases higher than for corresponding urban

Table 12. Statistical summary of hourly ozone concentration measurements by station

Station	Mean Hourly Concentration ($\mu g/m^3$)	Standard Deviation ($\mu g/m^3$)	Case Count
Bradford, Pennsylvania*	81.4	31.9	2332
Lewisburg, West Virginia*	76.3	39.2	2386
Creston, Iowa*	70.4	31.5	2117
Wolf Point, Montana*	57.6	25.3	2160
DeRidder, Louisiana*	61.2	38.0	2994
Poynette, Wisconsin*	75.8	43.0	2428
Port O'Connor, Texas*	55.3	43.9	2912
Pittsburg, Pennsylvania**	60.5	65.4	2841
Columbus, Ohio**	44.4	41.7	2885
Cedar Rapids, Iowa**	49.9	34.1	2781
Des Moines, Iowa**	72.9	44.1	2528
Omaha, Nebraska**	71.1	48.1	1787
Nederland, Texas**	54.6	52.5	2714
Austin, Texas**	49.2	35.7	2504
Houston, Texas**	51.3	65.0	2104

*Rural stations [June 27-September 30, 1975, except DeRidder (June 27-October 31, 1975)].

**Urban stations (June 1-September 30, 1975).

stations in the same general area. For example, the mean hourly ozone concentration at Bradford was 81 $\mu g/m^3$, while at Pittsburgh the mean was 61 $\mu g/m^3$. The lowest mean ozone for the rural stations was 58 $\mu g/m^3$ at Wolf Point. This mean was higher than the mean ozone concentration for the following urban stations: Columbus, Cedar Rapids, Nederland, Austin, and Houston. The higher ozone mean at rural stations results from higher minimum ozone concentrations persisting at night in the rural environment. Ozone concentrations at night at urban stations decreased to much lower values than at rural stations and decreased much more

Table 13. Summary of ozone data above NAAQS by station

Station	Maximum Hourly Average Concentration ($\mu g/m^3$)	99th Percentile ($\mu g/m^3$)	Days Exceeding Standard (Number)	Days Exceeding Standard (%)1/	Hours Above Standard (Number)	Hours Above Standard (%)
Bradford, Pa.*	248	200	18	18.5	100	4.3
Lewisburg, W. Va.*	225	180	11	11.1	59	2.5
Creston, Iowa*	245	155	7	7.9	17	0.8
Wolf Point, Mont.*	128	115	0	0.0	0	0.0
DeRidder, La.*	256	170	10	8.0	38	1.3
Poynette, Wis.*	243	205	22	21.7	121	5.0
Port C'Connor, Tex.*	259	200	15	12.4	99	3.4
Pittsburgh, Pa.**	490	300	41	34.6	227	8.0
Columbus, Ohio**	196	170	14	11.6	43	1.5
Cedar Rapids, Iowa**	180	140	1	0.9	6	0.2
Des Moines, Iowa**	196	185	22	20.9	124	4.9
Omaha, Nebr.**	216	180	15	20.1	64	3.6
Nederland, Tex.**	380	240	38	33.6	138	5.1
Austin, Tex.**	206	158	10	9.6	19	0.8
Houston, Tex.**	629	265	33	37.6	141	6.7

*Rural Stations [June 27-September 30, 1975, except DeRidder (June 27-October 31, 1975)].

**Urban Stations (June 1-September 30, 1975).

1/ Based on data available from each station.

Table 14. Statistical summary of hourly oxides of nitrogen concentration measurements - rural stations (June 27 - September 30, 1975)

Station	Mean Hourly Concentration ($\mu g/m^3$)		Standard Deviation ($\mu g/m^3$)		Case Count	
	NO	NO_2	NO	NO_2	NO	NO_2
Bradford, Pennsylvania	2.4	5.1	3.8	5.8	2265	2259
Lewisburg, West Virginia	N.A.	N.A.	N.A.	N.A.	N.A.	N.A.
Creston, Iowa	4.7	4.3	4.8	2.8	2162	2162
Wolf Point, Montana	<1.0	1.5	1.0	3.4	1318	2136
DeRidder, Louisiana*	1.9	4.9	8.1	9.4	2444	2444

N.A. - (NO_x not measured).

*June 27 - October 31, 1975.

rapidly in the afternoon. Maximum hourly ozone concentrations for the rural stations were 248 $\mu g/m^3$ at Bradford; 225 $\mu g/m^3$ at Lewisburg, 245 $\mu g/m^3$ at Creston, 256 $\mu g/m^3$ at DeRidder, 128 $\mu g/m^3$ at Wolf Point, 259 $\mu g/m^3$ at Port O'Connor, and 243 $\mu g/m^3$ at Pittsburgh. Maximum hourly ozone concentrations for urban stations were 629 $\mu g/m^3$ at Houston, 490 $\mu g/m^3$ at Pittsburgh, 380 $\mu g/m^3$ at Nederland, 216 $\mu g/m^3$ at Omaha, 206 $\mu g/m^3$ at Austin, 196 $\mu g/m^3$ at Columbus and Des Moines, and 180 $\mu g/m^3$ at Cedar Rapids.

The data summarized in table 13 show that the NAAQS for photochemical oxidants ($\geq$ 160 $\mu g/m^3$ hourly average) was exceeded approximately 4, 3, 1, 1, and 0 percent of the hours at the rural stations (i.e., Bradford, Lewisburg, Creston, DeRidder, and Wolf Point), and from less than 1 to 8 percent of the hours at the urban stations. Ozone measurements at Pittsburgh, Houston, Poynette, and Nederland exceeded the NAAQS approximately twice as frequently as did measurements at the other urban and the rural stations.

Table 15. Statistical summary of selected hydrocarbon and halocarbon analyses

Compound	Wolf Point		Creston		Bradford		DeRidder*	
	$\bar{x}$	cc	$\bar{x}$	cc	$\bar{x}$	cc	$\bar{x}$	cc
Ethane & Ethylene[1]	25.3	61	43.3	53	27.8	60	28.6	103
Propane	3.2	61	2.9	53	3.9	60	7.4	103
Propylene	1.3	61	1.5	53	1.2	60	1.9	103
Acetylene	2.4	61	3.4	53	3.4	60	3.2	103
n-Butane	2.1	61	1.2	53	4.5	60	2.9	103
1-Butene	0.1	61	0.4	53	0.2	60	0.1	103
Isobutane	0.8	61	0.5	53	2.3	60	2.1	103
Isopentane	1.7	61	1.0	53	2.6	60	1.6	103
Cyclopentane	0.1	61	0.1	53	0.2	60	0.2	103
n-Pentane	2.0	61	3.2	53	2.7	60	2.9	103
Toluene	8.9	47	5.8	45	5.3	36	8.0	83
o-Xylene	7.9	47	1.6	45	1.9	36	1.1	83
Freon-11[2]	278	42	293	45	271	50	373	95
Carbon Tetrachloride	72	61	47	45	61	50	77	95
1,1,1-Trichloroethane	1.5	61	1.0	45	1.1	50	1.4	95
Tetrachloroethylene	207	42	347	45	426	50	363	95

July - October, 1975

[1] Concentration Units are ppbv.

[2] Concentration units are pptv.

$\bar{x}$ - mean; cc - case count.

Table 16. Summary of mean 24-hour particulate concentrations: (TSP, NH_4^+, NO_3^-, $SO_4^=$) for rural stations (July to September 1975)

Station	TSP ($\mu g/m^3$)	NH_4^+ ($\mu g/m^3$)	NO_3^- ($\mu g/m^3$)	$SO_4^=$ ($\mu g/m^3$)	$\frac{NO_3^-}{TSP}$ (%)	$\frac{SO_4^=}{TSP}$ (%)
Bradford	34.2	0.4	0.9	10.1	2.6	29.5
Creston	74.5	0.1	1.8	6.2	2.4	8.3
Wolf Point	29.2	B.D	0.4	1.8	1.4	6.1
DeRidder	41.6	B.D	1.3	5.4	3.1	13.0

B.D - Below Detectable

*DeRidder - (July to October 1975)

Based on the percentage of days exceeding the standard and hours above the standard, a west-to-east gradient is observed in the data. Ozone measurements at Wolf Point did not approach the NAAQS for photochemical oxidants; the maximum hourly average was 128 $\mu g/m^3$, with the 99th percentile being 115 $\mu g/m^3$. For comparison, ozone measurements at Creston exceeded the NAAQS: (1) 17 hours; (2) 1 percent of the hours; and (3) 8 percent of the days during the period July 1 to September 30, 1975. Ozone measurements at Bradford exceeded the NAAQS: (1) 100 hours; (2) 4 percent of the hours; and (3) 19 percent of the days during the same period of time. Ozone measurements at Lewisburg were similar to those at Bradford and showed a definite increase in the number of hours exceeding the NAAQS for the eastern stations, as opposed to Creston. Ozone measurements at DeRidder were similar to those at Creston with respect to the frequency of levels exceeding the NAAQS, both on daily and hourly percentage basis. Measurements in DeRidder continued, however, for an additional 30-day period through October 31, 1975.

The mean hourly concentrations of nitric oxide and nitrogen dioxide measured at the four rural stations ranged from 1 to 10 $\mu g/m^3$, and fell

Table 17. Summary of mean ozone and oxides of nitrogen concentrations by month

Station	Pollutant	June	July	August	September	October
	Mean Monthly Concentration ($\mu g/m^3$)					
Bradford, Pennsylvania*	O_3	—	89.3	88.5	67.7	N.D.
	NO	—	2.7	<1.0	3.5	N.D.
	NO_2	—	4.7	6.4	5.2	N.D.
Lewisburg, West Virginia*	O_3	—	78.8	83.2	70.6	65.9
Creston, Iowa*	O_3	—	70.1	86.2	56.1	N.D.
	NO	—	<1.0	5.0	8.6	N.D.
	NO_2	—	2.1	5.5	5.3	N.D.
Wolf Point, Montana*	O_3	—	61.1	61.6	50.9	N.D.
	NO	—	<1.0	<1.0	<1.0	N.D.
	NO_2	—	2.6	<1.0	1.3	N.D.
DeRidder, Louisiana*	O_3	—	50.9	58.7	62.6	72.7
	NO	—				
	NO_2	—				
Pittsburg, Pennsylvania**	O_3	52.8	90.3	67.3	28.9	N.D.
Columbus, Ohio**	O_3	54.3	53.5	38.7	30.7	N.D.
Poynette, Wisconsin*	O_3	86.3	89.1	72.6	I.D.	N.D.
Omaha, Nebraska**	O_3	74.2	71.4	85.1		N.D.
Des Moines, Iowa**	O_3	52.3	92.2	84.4	51.9	N.D.
Cedar Rapids, Iowa**	O_3	51.0	63.7	52.0	32.6	N.D.
Nederland, Texas**	O_3	50.8	64.6	47.1	56.0	N.D.
Port O'Connor, Texas*	O_3	28.5	26.9	42.3	82.2	N.D.
Austin, Texas**	O_3	42.9	46.6	51.7	55.3	N.D.
Houston, Texas**	O_3	53.9	54.9	41.9	57.0	N.D.

*Rural Stations (June 27-September 30, 1975, except DeRidder and Lewisburg - Data Through October 31, 1975).

**Urban Stations (June 1-September 30, 1975).

N.D. - No Data - Field Program Concluded

Table 18. Summary of mean hydrocarbon and halocarbon concentrations by month at rural stations (July-September 1975)

Compound	Wolf Point, Montana			Creston, Iowa			Bradford, Pennsylvania			DeRidder, Louisiana*			
	July	August	September	July	August	September	July	August	September	July	August	September	October
Ethane and Ethylene[1/]	52.2	13.5	10.3	49.8	41.1	39.0	21.7	32.6	29.4	27.1	54.1	19.5	13.7
Propane	1.4	4.9	3.4	1.0	5.1	2.6	3.1	5.2	3.3	6.2	10.1	6.1	6.9
Propylene	1.4	1.4	1.2	3.0	0.6	0.9	1.5	1.3	0.8	1.3	2.9	1.7	1.8
Acetylene	4.0	1.7	1.5	1.5	2.2	6.5	2.9	4.5	2.9	4.2	4.0	2.7	2.1
n-Butane	0.6	1.9	3.9	1.7	0.6	1.2	5.0	5.5	2.8	2.1	3.5	3.0	2.9
1-Butene	<0.1	0.1	<0.1	1.2	0.0	<0.1	0.2	0.1	0.1	<0.1	0.1	<0.1	0.1
Isobutane	0.3	0.7	1.3	0.7	0.4	0.5	2.3	3.1	1.5	1.6	3.1	1.9	1.7
Isopentane	0.6	1.2	3.3	1.1	0.7	1.2	2.1	3.8	1.8	0.9	1.7	2.4	1.5
Cyclopentane	0.0	<0.1	0.3	0.2	0.0	<0.1	0.2	0.4	<0.1	0.0	0.3	0.2	0.1
n-Pentane	1.6	2.5	1.8	5.4	2.1	2.2	1.3	4.0	2.7	1.8	5.1	2.1	2.8
Toluene	6.3	5.4	15.2	4.1	4.6	8.7	—	3.7	7.0	4.8	5.6	8.5	13.1
o-Xylene	19.6	3.1	1.0	2.7	1.4	0.8	—	2.7	1.1	1.2	0.7	2.0	0.4
Freon-11[2/]	—	279	278	319	278	282	215	428	169	472	487	170	364
Carbon Tetrachloride	120	48	49	54	46	41	56	67	59	98	115	56	41
1,1,1-Trichloroethane	1.9	1.6	1.0	0.9	0.9	1.1	1.0	1.1	1.2	2.1	1.3	1.2	1.1
Tetrachloroethylene	—	180	234	413	299	328	348	447	484	403	664	185	200

[1/] Values are in parts-per-billion by volume, ppbv.

[2/] Values are in parts-per-trillion by volume, pptv.

*July-October 1975

for practical purposes within the noise or detectability level of the measurement method ($\approx$ 10 $\mu g/m^3$). These data, presented in table 14, are shown to emphasize the extremely low concentrations of measured NO_x in the environment at the rural stations. Maximum hourly nitric oxide and nitrogen dioxide concentrations were 34 and 68 $\mu g/m^3$ at Bradford, 28 and 25 $\mu g/m^3$ at Creston, 3 and 19 $\mu g/m^3$ at Wolf Point, and 17 and 43 $\mu g/m^3$ at DeRidder, respectively.

Grab samples collected at four of the five rural stations were analyzed for selected hydrocarbons and halocarbons. A summary of these data is presented in table 15. Each value represents the mean concentration over the measurement period for that component at the four stations. Averaged over the measurement period (July through September, except DeRidder), these data show similar concentrations for selected hydrocarbons and halocarbons. A definite trend is not apparent in these data.

Mean suspended particulate data given in table 16 show similar particulate loadings for Bradford and Wolf Point. Suspended particulates were as high at Bradford as at Wolf Point, with DeRidder falling in between. Further examination of the data shows a definite trend with respect to the sulfate and nitrate components of the suspended particulate matter; the percentage of sulfates and nitrates increases progressively from western to eastern stations. For example, sulfate represented 30 percent of total suspended particulate (TSP) at Bradford, 8 percent at Creston, and 6 percent at Wolf Point. Nitrates as a percentage of TSP showed a similar pattern, although not as dramatically.

Mean monthly ozone concentrations did not change significantly during the period July through September at Bradford, Creston, and Wolf Point, or at DeRidder from July through October; however, a gradual decrease was observed for Bradford, Creston, and Wolf Point and a gradual increase was observed for DeRidder. Mean monthly ozone concentrations at urban stations generally decreased during this period of time. Notable exceptions to this trend were observed at Houston, Austin, and Nederland. Mean monthly concentrations for nitric oxide and nitrogen dioxide at the four rural stations showed little variation during this period. Similar results were observed for mean monthly concentrations for selected hydrocarbons and halocarbons; these revealed no obvious trends.

Cumulative frequency distributions for hourly ozone concentrations for rural stations are presented for the entire period in table 19 and for State/local stations in table 20. Cumulative frequency distributions for hourly nitric oxide and nitrogen dioxide concentrations are given in table 21.

6.2 Diurnal Patterns

Mean ozone concentrations for each hour of the day for RTI rural stations are shown in table 22 and for State/local stations in table 23. Table 24 gives mean nitric oxide and nitrogen dioxide concentrations for each hour of the day for four of the five rural stations. Mean diurnal curves for ozone are shown for rural and urban stations in figures 38 to 42. Figures 38 and 39 present, respectively, the mean diurnal curves for Bradford, Creston, and Wolf Point, and for Bradford, Lewisburg, and DeRidder. Mean diurnal ozone curves for the stations at Pittsburgh, Columbus, and Poynette are presented in figure 40; at Des Moines, Cedar Rapids, and Omaha in figure 41; and at Nederland, Austin, Houston, and DeRidder in figure 42. The mean diurnal ozone curves for the rural and urban stations show the same general pattern; however, several observations can be made, as follows:

1. Mean hourly ozone concentrations for rural stations range from approximately 20-55 $\mu g/m^3$ in the morning to 80-115 $\mu g/m^3$ in the afternoon, while for urban stations, the mean ranges from 10-50 $\mu g/m^3$ to 70-130 $\mu g/m^3$.
2. The overall range or spread of mean ozone concentrations for both rural and urban stations (from low to high) was approximately the same (i.e., 60-70 $\mu g/m^3$).
3. Mean hourly ozone concentrations peaked in the afternoon, at rural stations from 1600-1700 and at urban stations from 1400-1700.

Figure 43 presents the mean diurnal ozone concentration curves for Kane, Pennsylvania, in 1973; for DuBois, Pennsylvania, in 1974; and for Bradford, Pennsylvania, in 1975. These curves represent ozone measurements during similar time periods at three sites that geographically, climatologically, and meteorologically are similar enough for comparison

Table 19. Cumulative frequency distributions of hourly concentrations of ozone - rural stations (June 27-September 30, 1975)

Concentration ($\mu g/m^3$)	Percent of Hourly Averages Greater Than Stated Concentration				
	Bradford, Pennsylvania	Lewisburg , West Virginia*	Creston, Iowa	Wolf Point, Montana	DeRidder, Louisiana*
	100.0	100.0	100.0	100.0	100.0
0	100.0	99.9	100.0	100.0	99.5
10	98.7	99.5	100.0	98.9	93.9
20	95.1	95.7	97.9	92.5	84.9
30	91.1	89.0	92.3	83.7	75.7
40	86.2	80.2	83.5	71.8	65.9
50	79.2	69.2	71.8	60.6	56.2
60	70.6	58.7	57.8	46.9	47.3
70	59.9	51.0	43.7	33.3	37.9
80	49.5	44.1	32.5	20.1	29.1
90	38.0	36.7	24.3	10.2	22.2
100	27.7	27.4	18.8	4.7	16.0
110	19.6	20.2	13.3	1.8	11.4
120	14.1	14.4	8.7	0.6	7.7
130	10.2	9.8	4.5	0.1	4.7
140	7.6	7.0	2.3	0.0	2.4
150	5.4	4.1	1.3	0.0	1.7
160	3.9	2.6	0.4	0.0	1.3
170	2.7	1.4	0.1	0.0	0.9
180	1.8	1.1	0.0	0.0	0.6
190	1.3	0.5	0.0	0.0	0.3
200	1.1	0.1	0.0	0.0	0.2
210	0.4	0.0	0.0	0.0	0.1
220	0.2	0.0	0.0	0.0	0.1
230	0.0	0.0	0.0	0.0	0.1
240	0.0	0.0	0.0	0.0	0.1
250	0.0	0.0	0.0	0.0	0.0

*June 27-October 31, 1975.

Table 20. Cumulative frequency distributions of hourly concentrations of ozone - State/local stations (June-September 1975)

Concentration ($\mu g/m^3$)	Percent of Hourly Averages Greater Than Stated Concentration									
	Pittsburgh, Pennsylvania	Columbus, Ohio	Poynette, Wisconsin	Omaha, Nebraska	Des Moines, Iowa	Cedar Rapids, Iowa	Nederland, Texas	Port O'Connor, Texas	Austin, Texas	Houston, Texas
	100.0	100.0	100.0	100.0	100.0	100.0	100.0	100.0	100.0	100.0
0	82.6	85.9	99.8	87.6	98.3	94.1	92.3	99.7	96.9	73.7
10	74.0	73.7	98.1	83.1	94.4	86.5	82.4	96.7	90.0	60.7
20	65.0	60.7	92.4	79.0	90.3	77.8	70.3	79.7	76.8	54.9
30	55.5	53.8	87.6	75.3	83.3	67.5	60.2	61.7	63.9	48.8
40	47.1	44.3	77.7	68.8	74.4	55.2	50.5	49.2	52.6	44.4
50	39.7	38.3	70.4	63.2	65.0	44.9	41.5	42.2	42.4	39.4
60	33.9	30.6	58.7	56.0	56.1	34.2	34.3	35.6	32.1	33.7
70	29.4	26.0	50.8	47.2	46.9	26.4	28.7	30.2	23.5	28.2
80	26.2	19.5	39.1	38.4	39.2	18.3	23.8	24.9	17.7	24.9
90	22.7	15.3	33.2	31.9	32.0	14.2	19.8	19.8	13.1	21.1
100	20.3	11.2	25.6	26.7	25.2	8.3	15.7	14.8	9.1	17.8
110	18.1	8.2	19.6	21.2	20.4	5.2	13.0	12.1	6.6	15.8
120	15.7	6.4	15.7	15.8	15.9	2.8	10.5	8.4	5.0	13.3
130	13.6	4.3	11.5	11.5	11.6	1.9	8.9	6.5	3.8	10.9
140	11.2	3.5	9.2	7.3	8.6	0.9	7.5	5.5	2.7	9.4
150	9.1	2.3	6.4	5.3	4.9	0.5	6.2	4.4	1.5	7.6
160	8.0	1.5	5.0	3.6	2.8	0.2	5.1	3.4	0.8	6.7
170	6.6	1.0	3.6	2.4	1.6	0.1	4.3	2.5	0.4	5.9
180	5.2	0.4	2.3	1.1	0.9	0.0	3.3	2.0	0.2	4.9
190	4.5	0.1	1.2	0.6	0.0	0.0	2.8	1.5	0.1	4.2
200	3.9	0.0	0.7	0.2	0.0	0.0	2.2	0.9	0.1	3.3
210	3.7	0.0	0.4	0.1	0.0	0.0	1.8	0.9	0.0	3.1
220	3.3	0.0	0.2	0.0	0.0	0.0	1.4	0.5	0.0	2.5
230	2.7	0.0	0.2	0.0	0.0	0.0	1.2	0.3	0.0	2.4
240	2.2	0.0	0.1	0.0	0.0	0.0	1.0	0.2	0.0	1.9
250	1.8	0.0	0.0	0.0	0.0	0.0	0.8	0.1	0.0	1.6
260	1.6	0.0	0.0	0.0	0.0	0.0	0.7	0.0	0.0	1.3
270	1.4	0.0	0.0	0.0	0.0	0.0	0.5	0.0	0.0	0.9
280	1.2	0.0	0.0	0.0	0.0	0.0	0.5	0.0	0.0	0.9
290	1.1	0.0	0.0	0.0	0.0	0.0	0.4	0.0	0.0	0.7
300	1.0	0.0	0.0	0.0	0.0	0.0	0.3	0.0	0.0	0.6
350	0.5	0.0	0.0	0.0	0.0	0.0	0.0	0.0	0.0	0.3
400	0.2	0.0	0.0	0.0	0.0	0.0	0.0	0.0	0.0	0.2
500	0.0	0.0	0.0	0.0	0.0	0.0	0.0	0.0	0.0	0.1
600	0.0	0.0	0.0	0.0	0.0	0.0	0.0	0.0	0.0	0.0

Table 21. Cumulative frequency distribution of hourly concentrations of oxides of nitrogen - rural stations (June 27-September 1975)*

Concentration ($\mu g/m^3$)	Percent of Hourly Averages Greater Than Stated Concentration							
	Bradford, Pennsylvania		Creston, Iowa		Wolf Point, Montana		DeRidder, Louisiana**	
	NO	NO_2	NO	NO_2	NO	NO_2	NO	NO_2
	100.0	100.0	100.0	100.0	100.0	100.0	100.0	100.0
0	50.6	73.9	75.0	91.8	9.7	33.2	19.2	48.0
10	4.8	15.1	6.1	1.6	0.1	3.9	9.1	13.1
20	0.5	2.1	3.0	0.2	0.1	0.4	0.4	4.8
30	0.0	0.5	0.0	0.0	0.0	0.0	0.1	1.0
40	0.0	0.1	0.0	0.0	0.0	0.0	0.1	0.3
50	0.0	0.0	0.0	0.0	0.0	0.0	0.0	0.2
60	0.0	0.0	0.0	0.0	0.0	0.0	0.0	0.0

*NO_x not measured at Lewisburg, West Virginia.

**June 27-October 31, 1975

Table 22. Means of hourly concentrations of ozone for each hour of day - RTI rural stations (June 27-September 30, 1975)

Hour	Concentration ($\mu g/m^3$)				
	Bradford, Pennsylvania	Lewisburg, West Virginia*	Creston, Iowa	Wolf Point, Montana	DeRidder, Louisiana*
0100	67.6	60.4	61.4	44.2	40.0
0200	62.0	54.3	59.0	43.1	35.4
0300	60.5	48.7	56.6	41.5	31.3
0400	57.4	45.0	54.4	39.2	27.6
0500	54.5	41.7	50.8	37.4	24.7
0600	53.6	37.9	48.3	34.4	22.6
0700	50.7	35.9	46.9	33.2	21.6
0800	54.0	36.4	46.2	35.4	23.6
0900	66.3	42.8	53.7	43.2	36.2
1000	81.0	55.2	64.5	53.2	55.8
1100	90.8	73.1	73.3	62.2	73.9
1200	97.9	93.5	80.3	69.6	87.4
1300	102.5	107.4	85.8	75.9	92.4
1400	106.0	111.8	90.7	80.1	95.4
1500	108.3	114.9	92.8	82.8	96.7
1600	108.8	115.4	93.6	84.4	97.4
1700	108.7	113.9	96.8	84.9	95.8
1800	108.4	111.6	96.8	83.1	94.2
1900	105.7	107.0	92.7	81.8	87.3
2000	98.2	102.5	83.1	74.7	73.2
2100	89.3	95.5	74.7	62.2	62.7
2200	81.8	86.7	70.1	51.4	52.7
2300	75.2	78.8	64.9	47.9	47.6
2400	70.9	67.7	62.7	44.2	43.8

*June 27-October 31, 1975.

Table 23. Means of hourly concentrations of ozone for each hour of day - State/local stations (June-September 1975)

Hour	Concentration (μg/m³)									
	Pittsburgh, Pennsylvania	Columbus, Ohio	Poynette, Wisconsin	Omaha, Nebraska	Des Moines, Iowa	Cedar Rapids, Iowa	Nederland, Texas	Port O'Connor, Texas	Austin, Texas	Houston, Texas
0100	31.1	24.1	65.6	52.8	52.3	35.1	24.8	54.5	30.2	9.5
0200	29.4	24.6	61.7	51.9	51.8	33.9	21.8	52.8	31.0	8.9
0300	28.7	25.5	57.9	51.8	49.4	34.4	19.5	51.3	31.4	8.6
0400	29.0	24.1	53.3	54.2	48.8	32.1	18.2	49.8	31.2	8.3
0500	24.9	23.1	50.9	52.7	48.0	31.5	14.2	48.1	29.4	7.0
0600	21.3	20.8	47.1	46.1	44.7	27.3	11.7	45.6	24.4	5.6
0700	15.8	18.2	44.9	38.5	41.8	22.7	14.8	42.8	15.9	6.1
0800	15.6	16.4	45.8	36.4	41.4	25.5	35.8	41.5	25.0	17.5
0900	23.3	22.2	53.8	45.3	53.2	35.6	69.2	41.2	41.2	43.5
1000	37.5	33.4	62.8	60.9	68.5	46.8	83.6	46.1	57.5	74.3
1100	58.7	46.5	74.4	73.8	81.7	57.2	93.7	54.1	70.4	96.7
1200	80.0	60.2	81.8	84.1	93.1	66.4	103.6	59.2	80.9	114.9
1300	102.4	71.7	89.8	96.9	102.1	72.3	104.5	63.5	82.6	127.4
1400	119.2	77.0	96.5	100.8	107.1	76.2	108.2	66.6	82.2	123.7
1500	123.4	80.8	100.4	106.2	109.9	78.2	103.1	66.1	82.9	129.1
1600	128.0	81.4	106.6	108.6	111.4	79.5	99.5	66.6	84.5	131.5
1700	124.0	82.6	106.7	108.2	111.5	80.3	90.7	66.3	80.3	118.4
1800	115.6	78.8	105.9	109.1	110.9	78.2	77.5	64.0	75.2	95.8
1900	99.3	72.7	103.5	101.6	105.0	74.4	62.6	60.5	61.0	61.3
2000	77.3	60.9	94.7	90.3	91.3	61.2	47.7	59.8	43.9	32.5
2100	56.9	44.6	85.9	73.2	73.2	45.3	36.0	58.4	35.3	17.4
2200	46.4	31.4	78.6	58.3	59.5	35.8	31.7	56.4	33.4	11.3
2300	39.1	25.1	73.3	52.2	53.2	32.4	27.3	55.8	33.5	10.7
2400	35.2	23.5	67.8	51.0	53.8	33.7	24.8	55.2	31.2	11.1

Table 24. Means of hourly concentrations of oxides of nitrogen for each hour of day - rural stations (June 27-September 30, 1975)[1]

Hour	Concentration (μg/m³)							
	Bradford, Pennsylvania		Creston, Iowa		Wolf Point, Montana		DeRidder, Louisiana*	
	NO	NO_2	NO	NO_2	NO	NO_2	NO	NO_2
0100	2.9	5.6	4.7	4.0	<1.0	<1.0	1.8	5.0
0200	2.9	5.3	4.7	4.0	<1.0	<1.0	1.7	4.3
0300	3.0	5.6	4.6	4.2	<1.0	<1.0	1.8	4.3
0400	3.1	5.8	4.5	4.0	<1.0	<1.0	2.2	4.6
0500	3.1	5.8	4.5	4.1	<1.0	<1.0	1.4	4.8
0600	2.9	5.7	4.5	4.1	<1.0	<1.0	1.4	5.0
0700	3.1	6.4	4.5	4.4	<1.0	<1.0	2.1	5.7
0800	3.5	7.0	4.7	4.4	<1.0	<1.0	3.0	7.9
0900	2.7	7.0	4.9	4.3	<1.0	<1.0	3.1	7.9
1000	2.3	6.2	4.9	4.3	<1.0	<1.0	2.2	6.1
1100	2.2	5.4	4.6	4.3	1.1	<1.0	1.8	6.8
1200	2.0	4.2	4.6	4.3	1.3	<1.0	1.8	5.6
1300	1.6	3.8	4.7	4.3	1.7	<1.0	4.4	4.6
1400	1.4	3.3	4.8	4.3	2.7	<1.0	2.7	5.4
1500	1.3	3.3	4.7	4.6	2.7	<1.0	1.4	2.7
1600	1.4	3.5	4.7	4.5	2.8	<1.0	1.4	3.0
1700	1.4	3.8	4.8	4.5	2.8	<1.0	1.5	3.0
1800	1.6	3.5	4.6	4.9	2.9	<1.0	1.7	3.3
1900	1.9	4.3	4.5	4.9	2.9	<1.0	1.6	3.7
2000	2.5	4.2	4.4	5.0	2.4	<1.0	1.5	3.8
2100	2.9	5.5	4.3	4.9	1.6	<1.0	1.6	4.5
2200	3.1	6.5	4.1	4.9	1.1	<1.0	1.6	5.9
2300	3.1	6.0	4.1	4.9	<1.0	<1.0	1.3	5.0
2400	2.9	5.4	4.1	4.9	<1.0	<1.0	1.3	4.4

*June 27-October 31, 1975.

[1] NO_x not measured at Lewisburg, West Virginia.

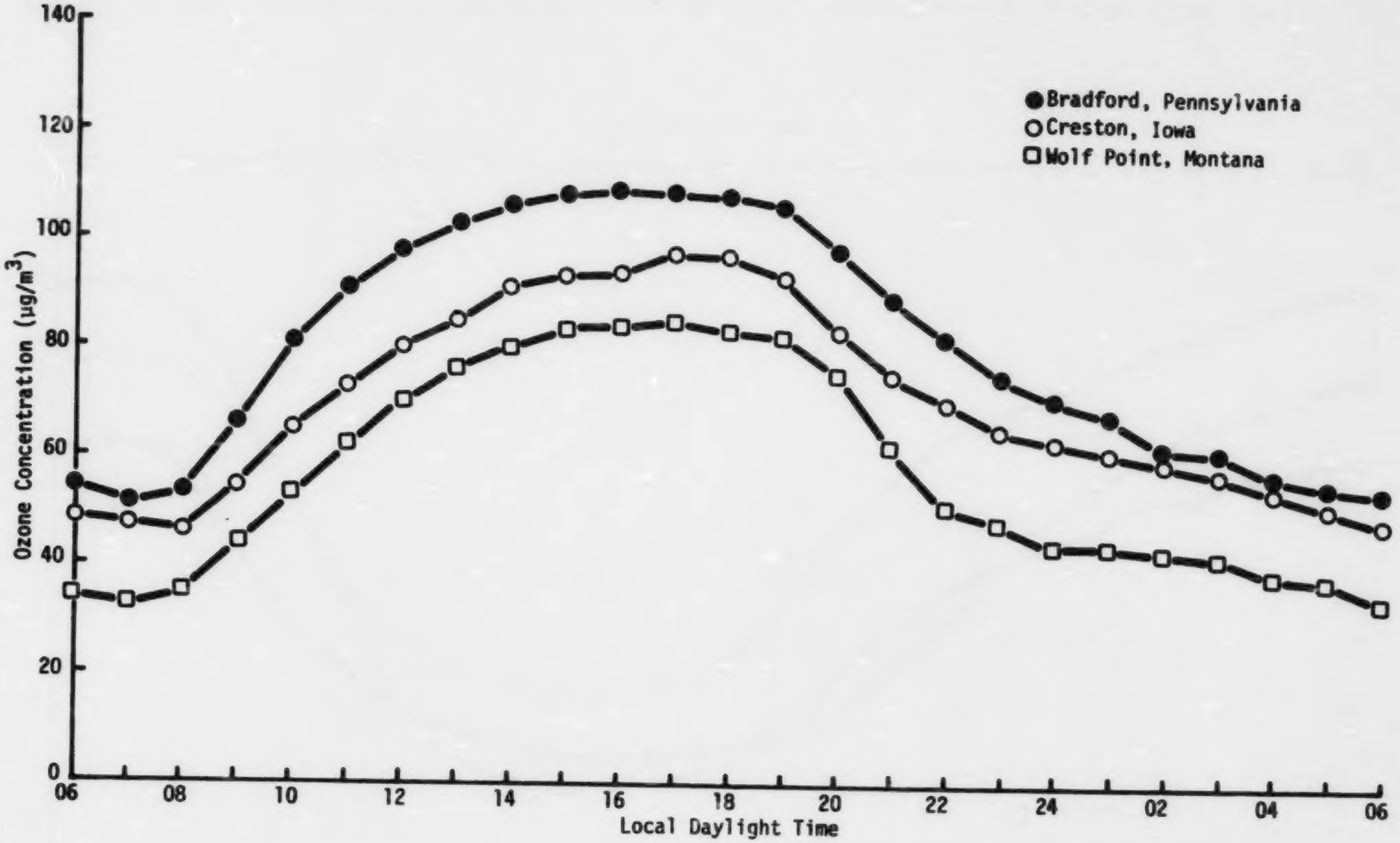

Figure 38. Mean diurnal ozone concentrations at Bradford, Creston, and Wolf Point (June 27-September 30, 1975).

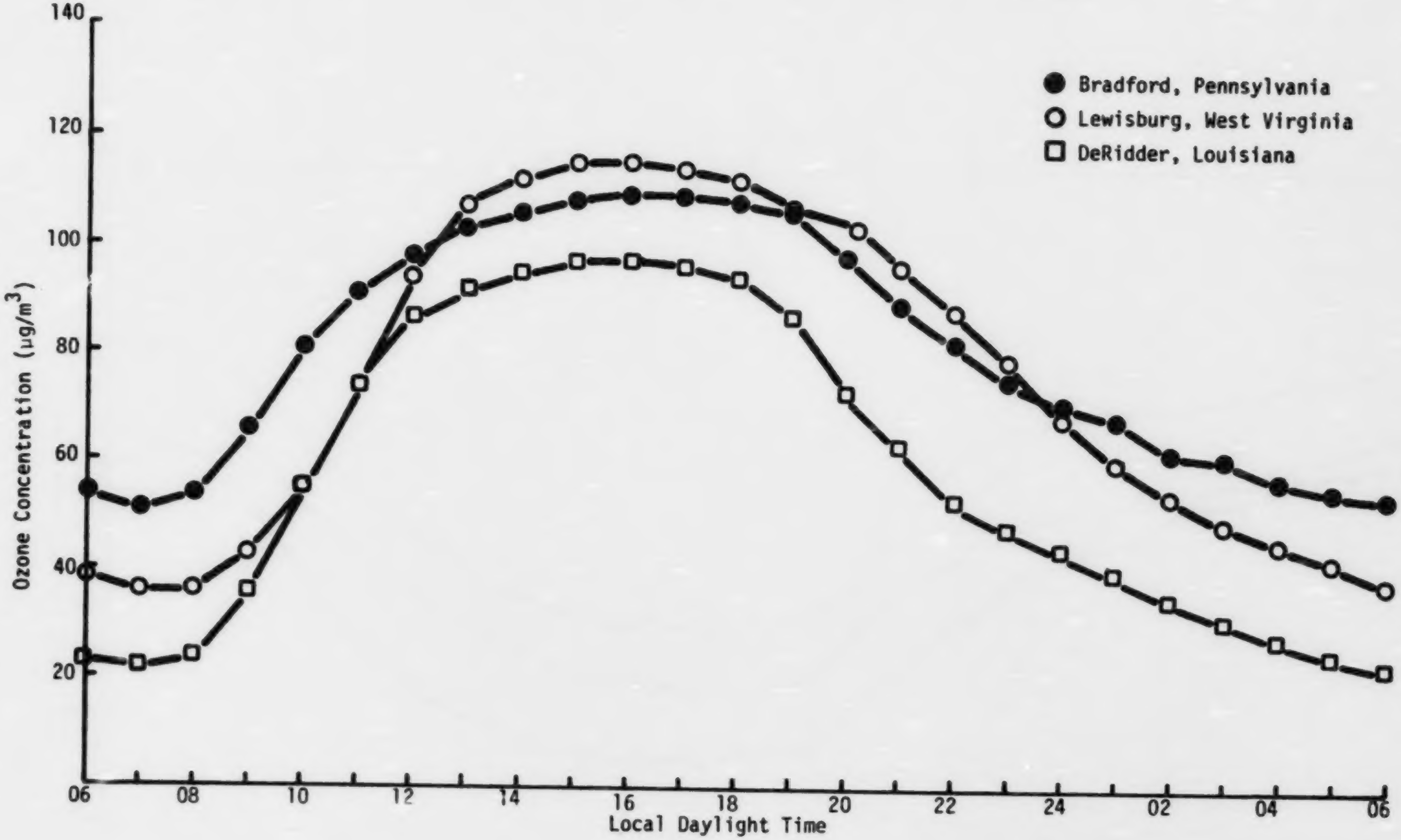

Figure 39. Mean diurnal ozone concentrations at Bradford, Lewisburg, and DeRidder (June 27-September 30, 1975 at Bradford; June 27–October 31, 1975 at Lewisburg and DeRidder).

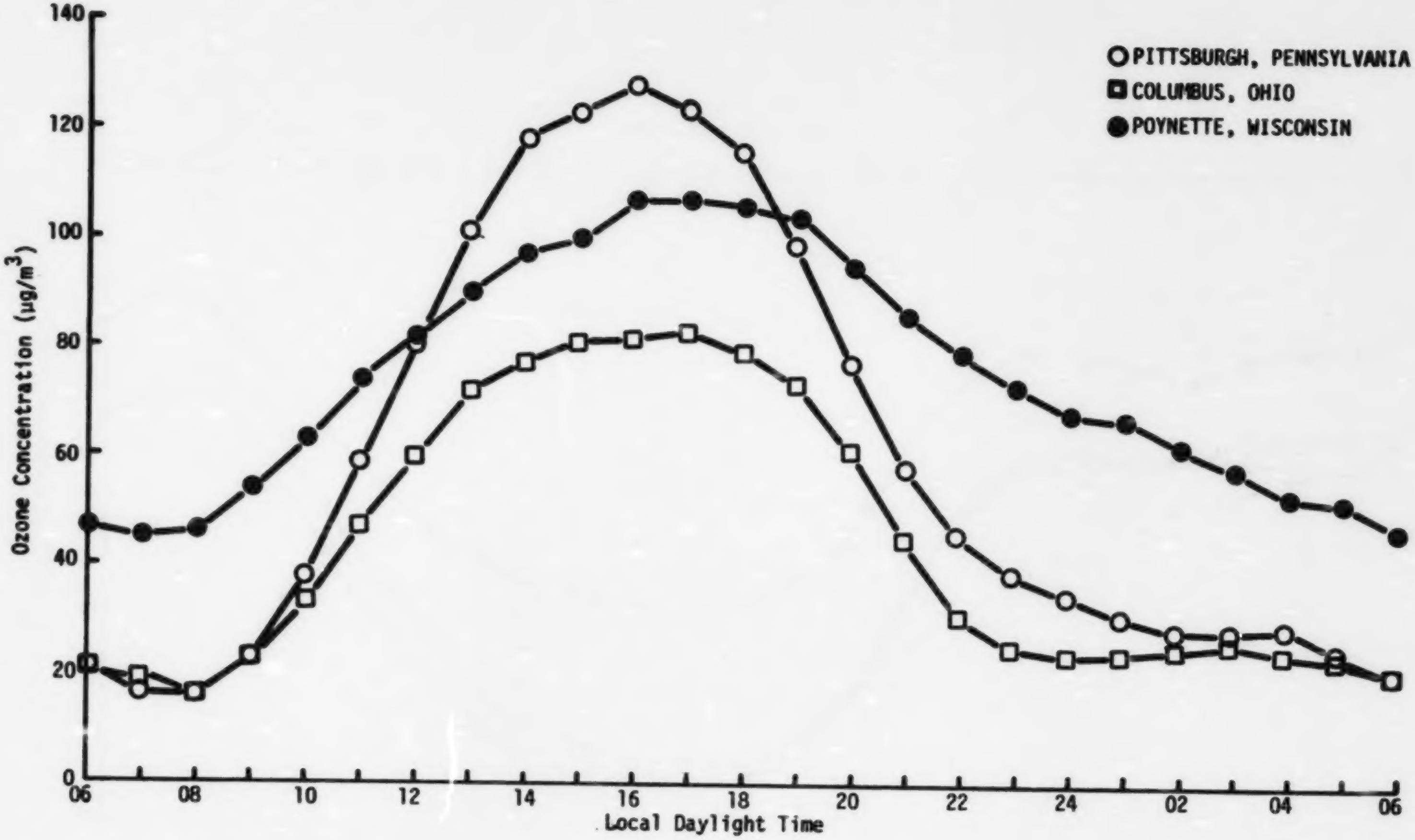

Figure 40. Mean diurnal ozone concentrations at Pittsburgh, Columbus, and Poynette (June-September, 1975).

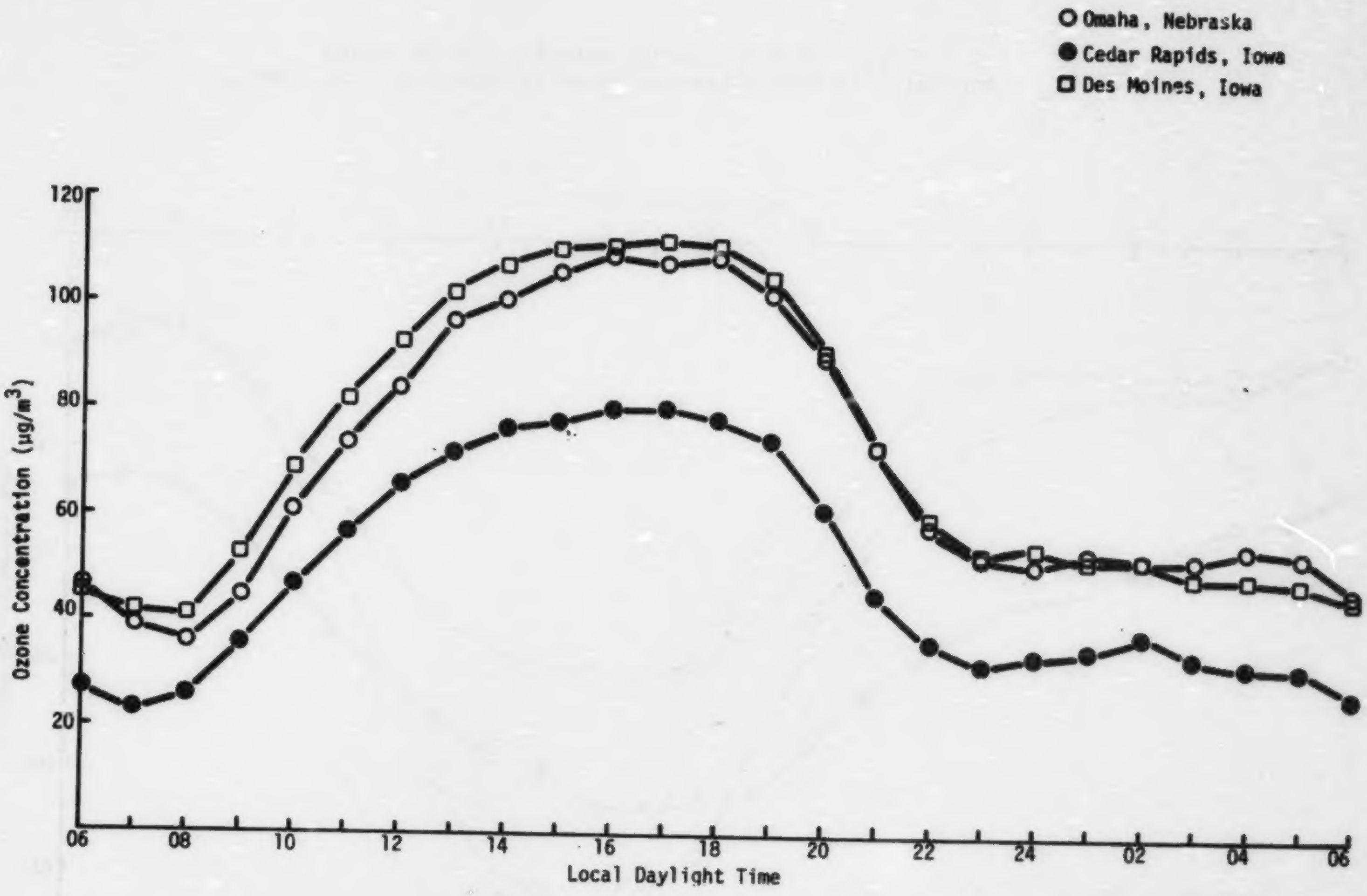

Figure 41. Mean diurnal ozone concentrations at Omaha, Cedar Rapids, and Des Moines (June-September 1975).

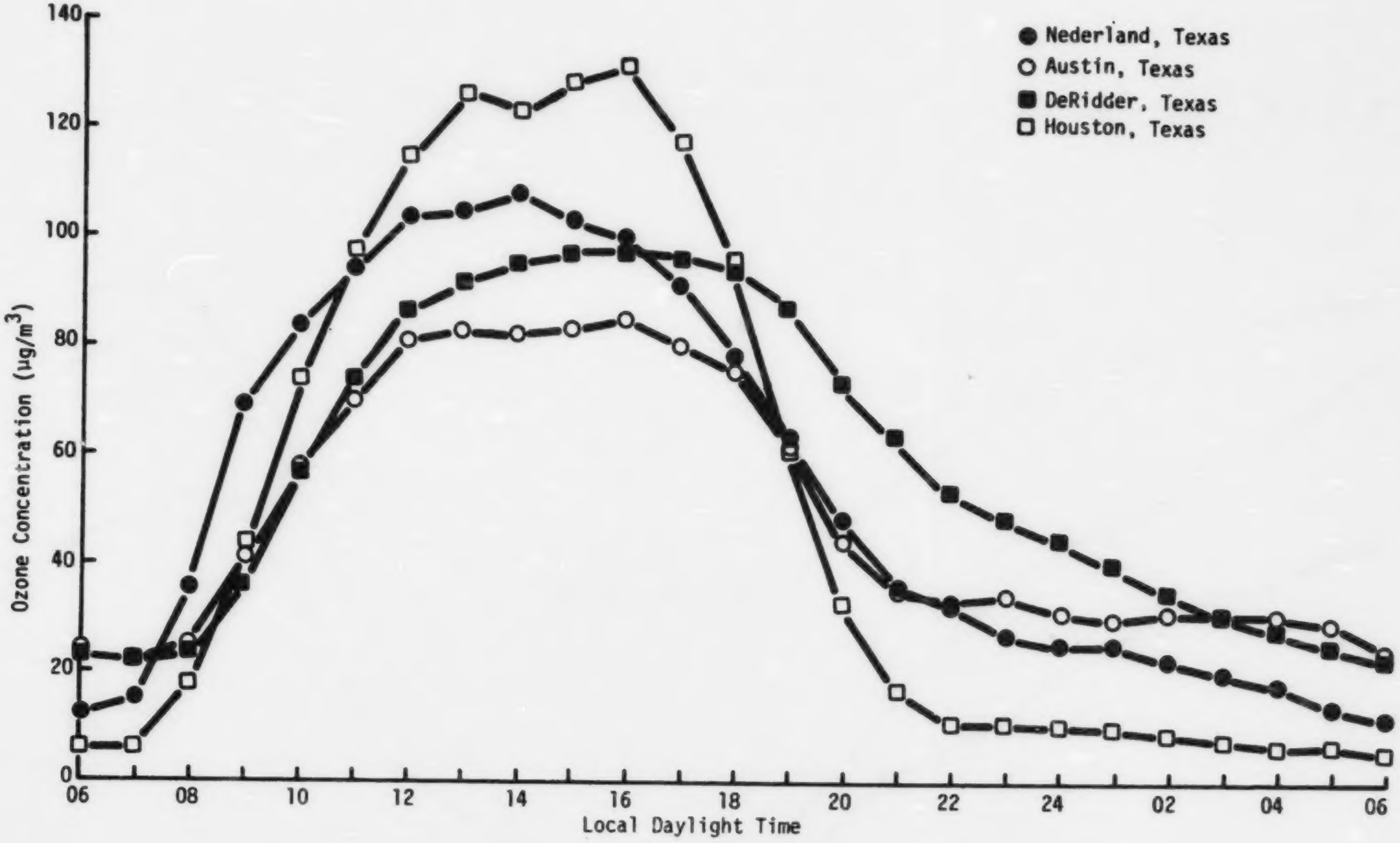

Figure 42. Mean diurnal ozone concentrations at Nederland, Austin, Houston, and DeRidder (June 1-September 30, 1975, except DeRidder--July-October 1975).

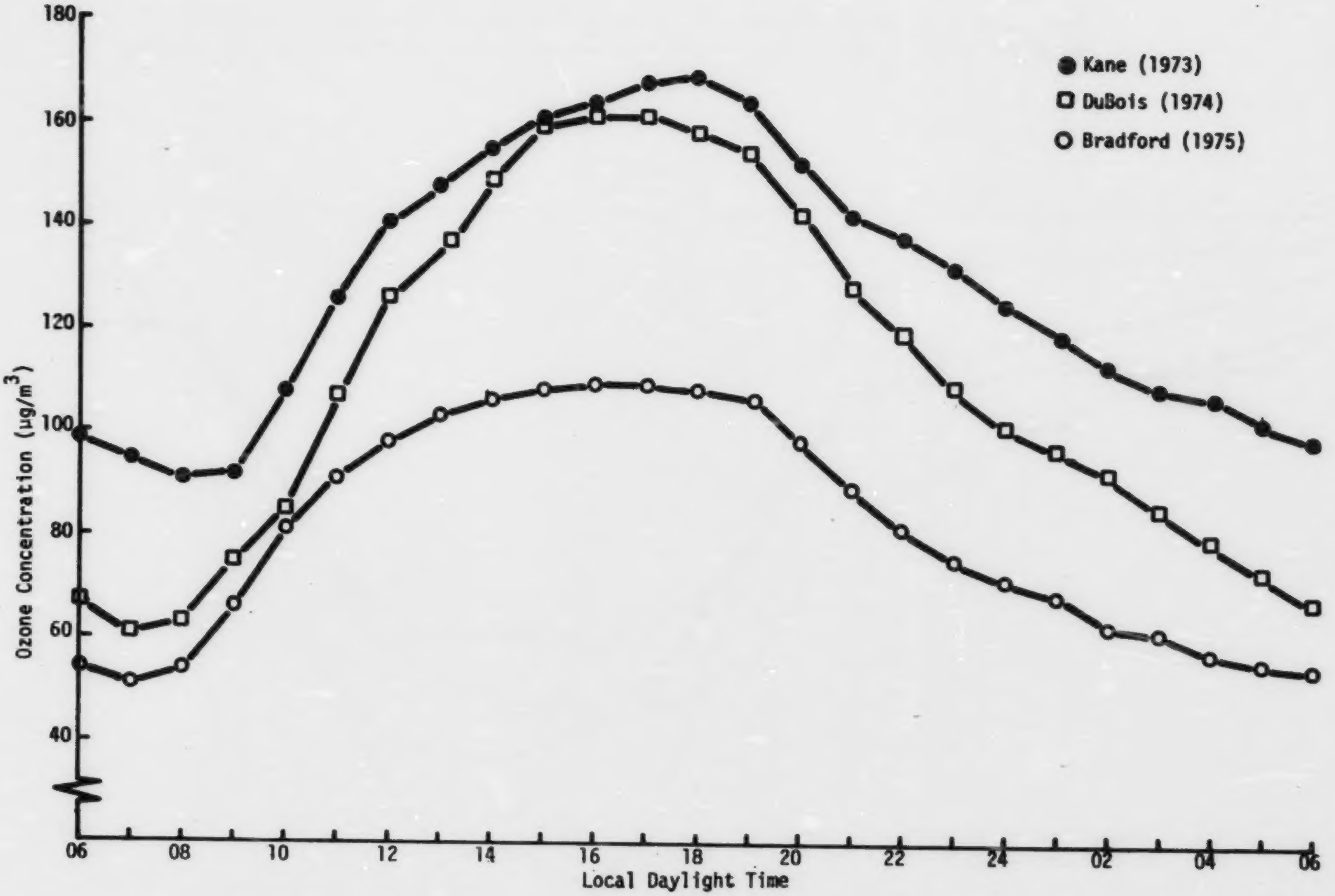

Figure 43. Mean diurnal ozone concentrations at Kane (1973), DuBois (1974), and Bradford (1975), Pennsylvania.

purposes. Figure 43 shows that the 1973 and 1974 diurnal curves are quite similar, while the diurnal curve for 1975 is substantially lower. The mean difference (diurnal variation) from ozone minimum to maximum for the 3-year period was 80 $\mu g/m^3$ for 1973, 100 $\mu g/m^3$ for 1974, and 60 $\mu g/m^3$ for 1975. Similar observations were observed in diurnal ozone trend at the urban station in Columbus from 1974 to 1975 (fig. 44).

For each of the four stations where measurements were made, mean diurnal curves for nitrogen dioxide are presented in figure 45. Mean hourly nitrogen dioxide concentrations ranged from < 1 to 8 $\mu g/m^3$. All of these measurements were at or below the generally accepted minimum detectable level of 10 $\mu g/m^3$ for the measurement method. These data are shown, as previously stated, to emphasize the extremely low concentrations of NO_x measured at these rural sites. Better resolution instrumentation with much lower minimum detectable levels are obviously needed for background measurements of NO_x in rural areas.

6.3 Summary of Climatic Conditions

In planning this study, RTI estimated that one to two candidate high-pressure systems could be anticipated for each of the 3 months, July through September. Six high-pressure systems were investigated. During the study, high-pressure systems tended to move south, to turn eastward in the central plains, and to move rapidly toward the east/northeast. It was difficult to keep up with the system and to perform the sampling at the desired locations. Of the systems studied using the aircraft, none stagnated. Secondary high-pressure systems following those studied did slow down and remain over the Eastern United States for a longer period of time. Movements of high-pressure systems for each of the 3 months are shown in figures 46, 47, and 48.

Due to the high mobility of the systems, annual changes in emission patterns or quantities are not routinely documented. The great year-to-year variability of ozone concentrations measured in the Eastern United States is usually attributed to changes in meteorological conditions. The correlation of ozone concentrations with climatic indices such as temperature, moisture, or wind over a long period of time is very poorly established;

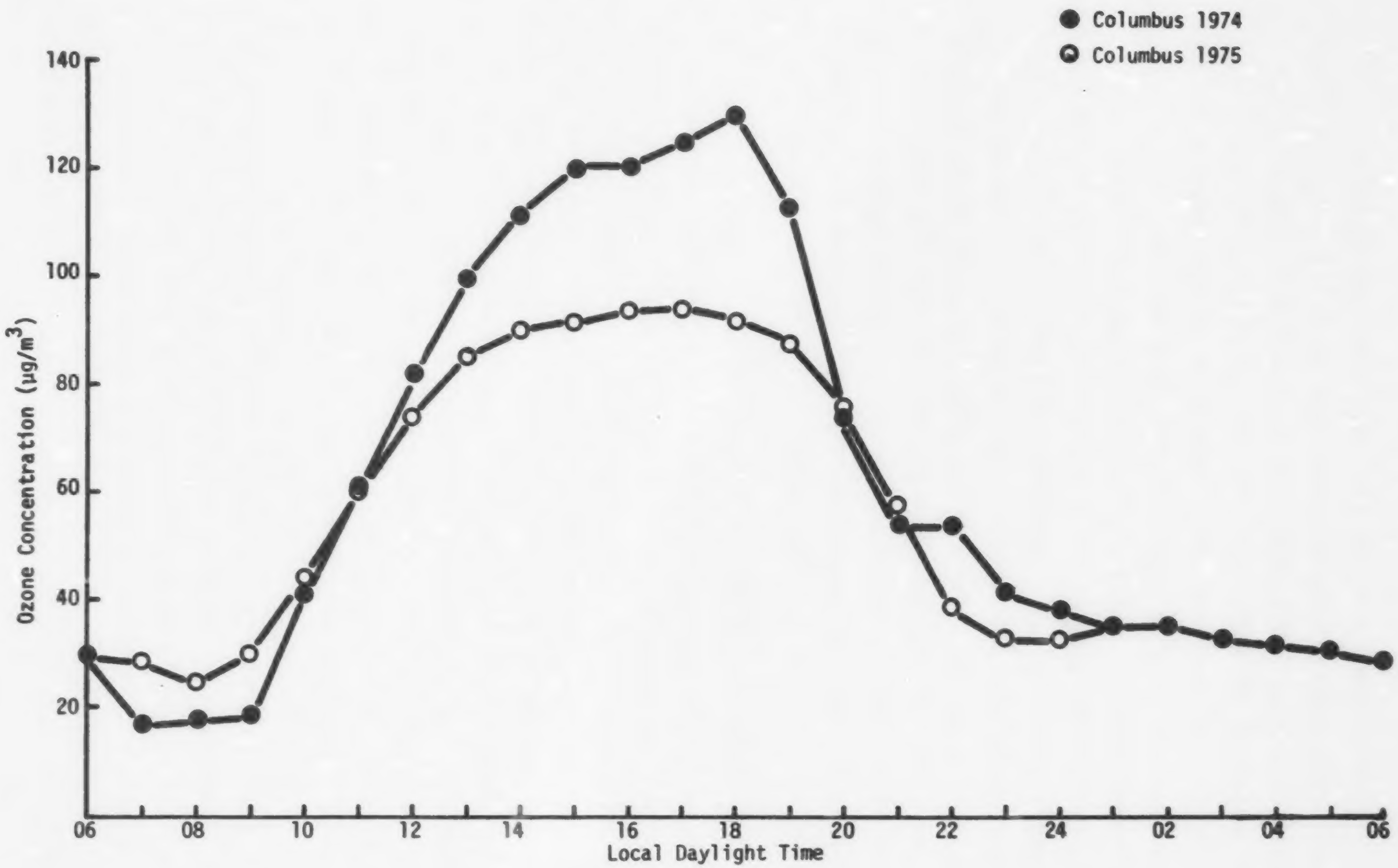

Figure 44. Mean diurnal ozone concentrations at Columbus, Ohio for 1974 and 1975.

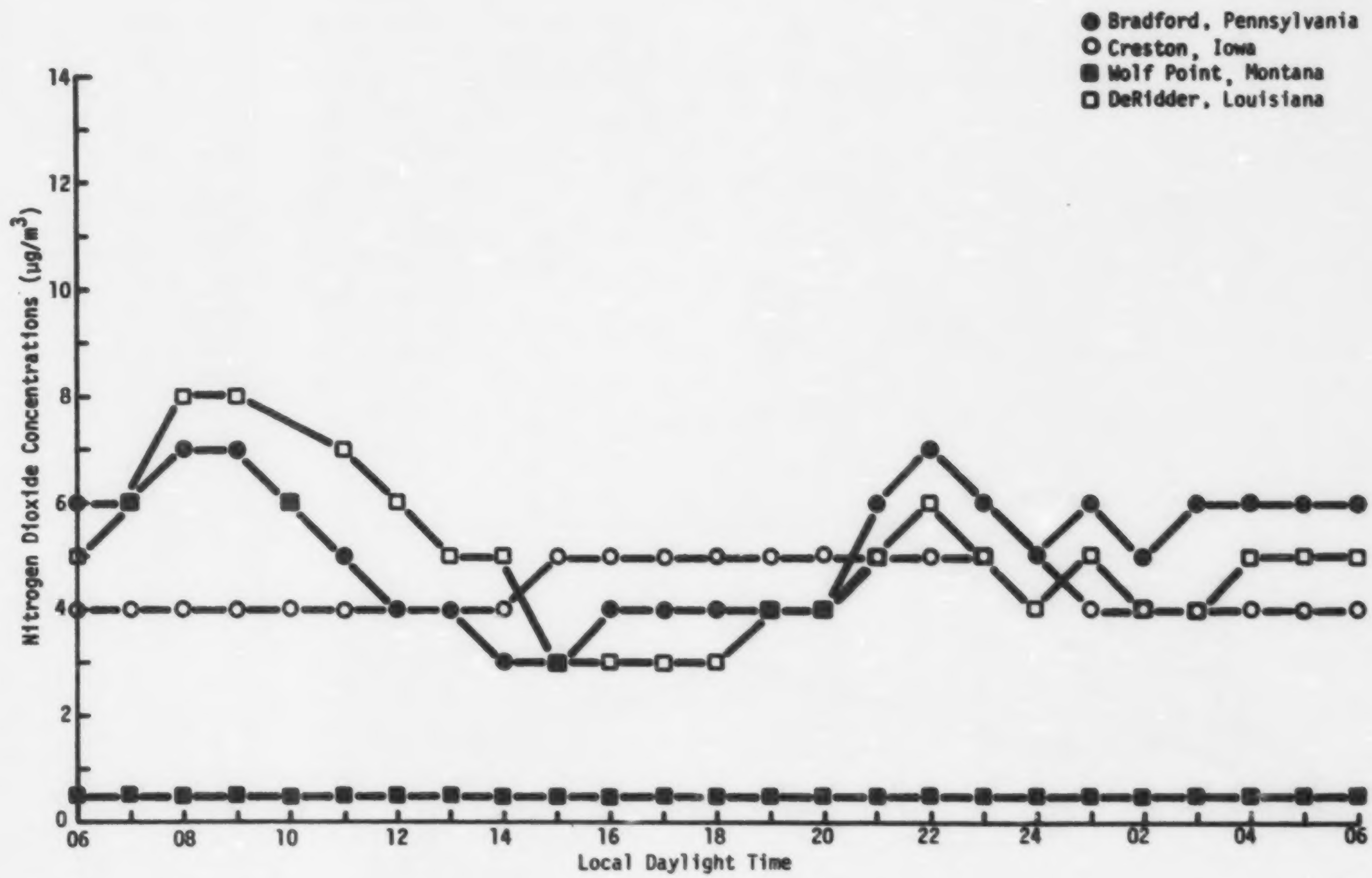

Figure 45. Mean diurnal nitrogen dioxide concentrations at Bradford, Creston, Wolf Point, and DeRidder (June 27-October 31, 1975).

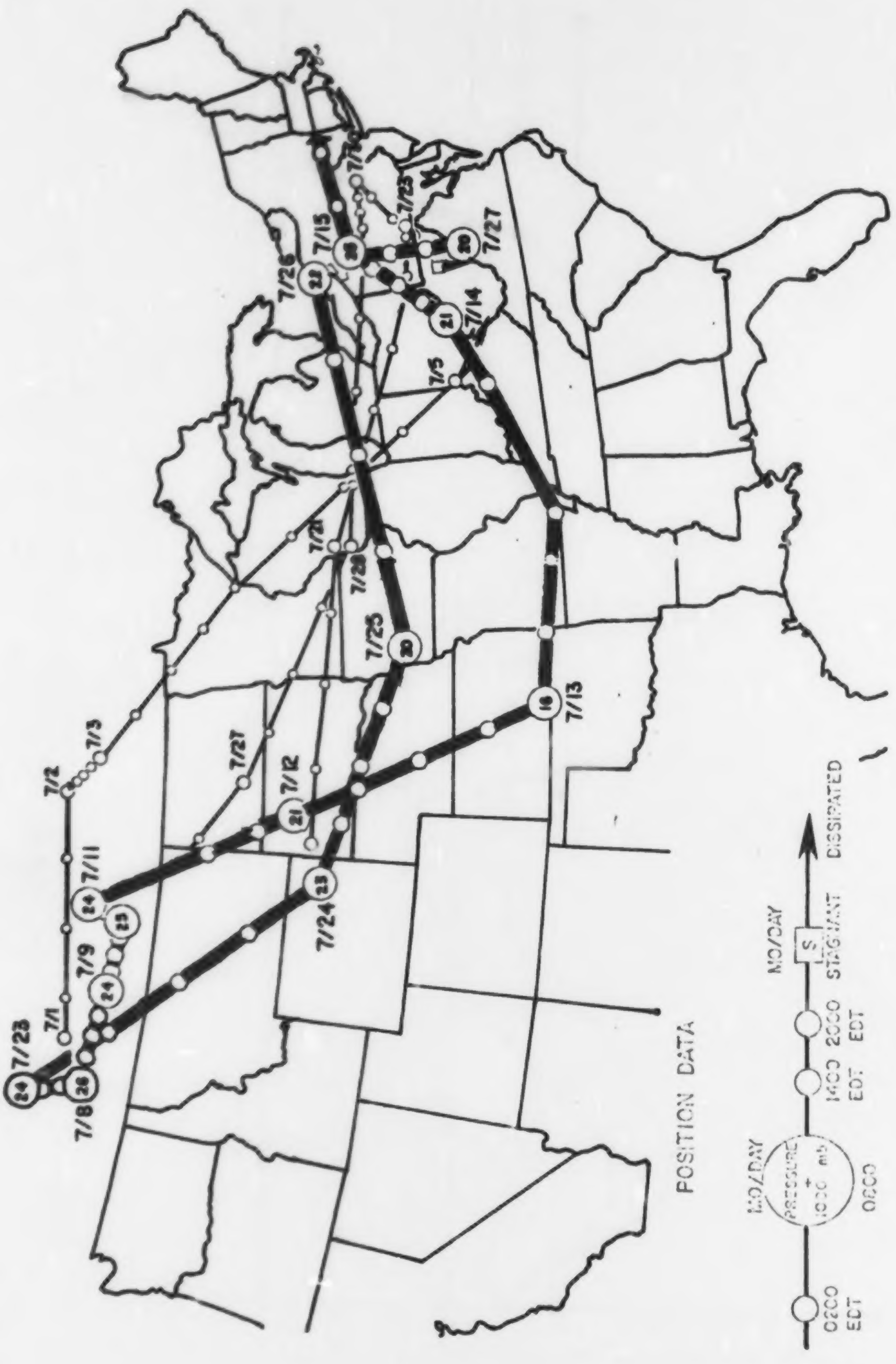
POSITION DATA
7/23
7/8
7/1
7/9
7/11
7/2
7/3
7/27
7/12
7/24
7/13
7/25
7/28
7/21
7/5
7/14
7/27
7/26
7/15
7/23
MO/DAY
PRESSURE + 1000 mb
0800 EDT
0800
1400 EDT
2000 EDT
MO/DAY
S
STAGNANT
DISSIPATED

Figure 46. Tracks of high pressure center (July 1975).

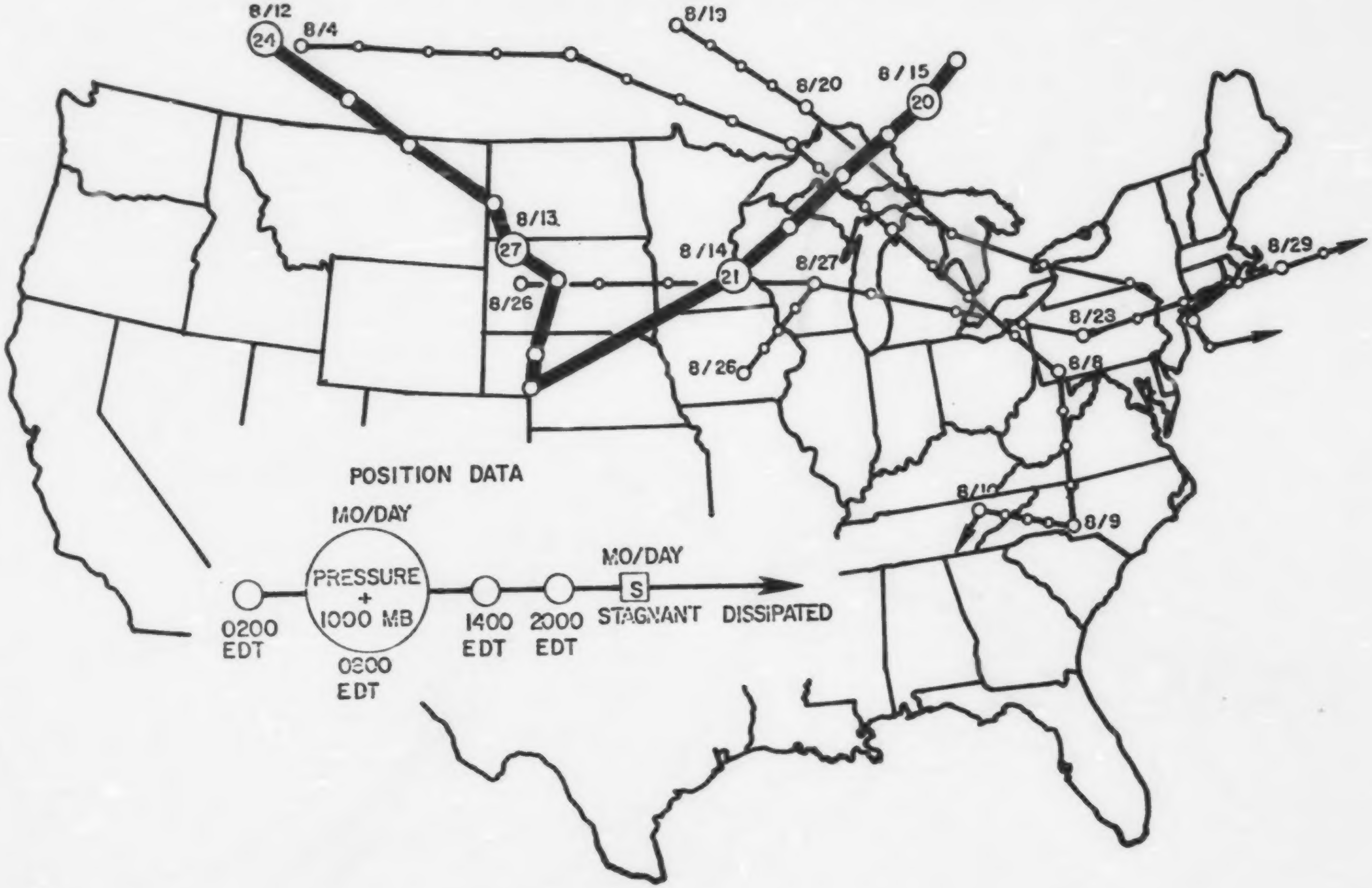
8/12
24
8/4
8/19
8/20
8/15
20
8/13
27
8/26
8/14
21
8/27
8/26
8/29
8/23
8/8
8/10
8/9
POSITION DATA
MO/DAY
PRESSURE + 1000 MB
0200 EDT
0800 EDT
1400 EDT
2000 EDT
MO/DAY
S
STAGNANT
DISSIPATED

Figure 47. Tracks of high pressure center (August 1975).

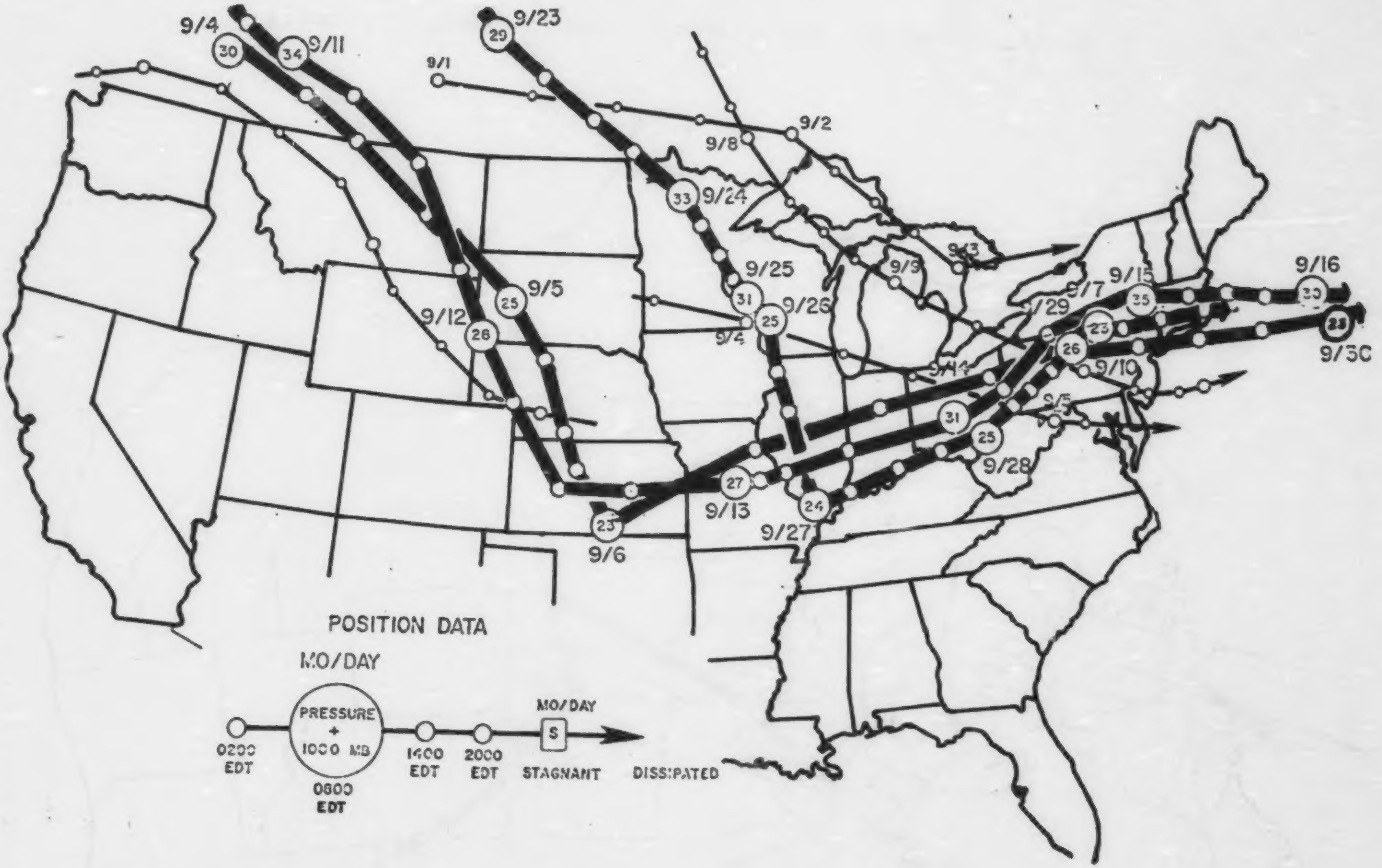
9/4
30
34
9/11
9/23
29
9/1
9/2
9/8
33
9/24
9/25
31
25
9/26
9/4
9/3
9/13
9/12
28
25
9/5
9/14
9/7
9/15
9/29
35
23
26
9/10
9/16
33
28
9/30
9/5
31
25
9/28
27
9/13
24
9/27
23
9/6
POSITION DATA
MO/DAY
PRESSURE
+
1000 MB
0200
EDT
0800
EDT
1400
EDT
2000
EDT
MO/DAY
S
STAGNANT
DISSIPATED

Figure 48. Tracks of high pressure center (September 1975).

as a consequence, it is difficult to assess the influence of climate upon these conditions. In section 8.0, some of the temporal relationships of ozone and meteorological conditions are examined.

High ozone concentrations have been associated with the transition of high-pressure systems in previous studies as well as in this study.[5/] The upper air flow patterns are examined for the 700-mb circulation difference for the year 1975 from the 30-year climatic norm.

A. July 1975[21/]

The average position of maximum winds at 700 mb during July lay just north of the Canadian border. A ridge line initially over the Midwestern United States retrograded to the Rocky Mountains by the end of the first week. The trough on the east coast moved to the central plains for most of the month. The subtropical ridge began to dominate the circulation patterns at 700 mb over the Southern United States later in the month. The ridge over the Rockies, trough over the Central, and ridge over the Eastern United States, gave greater north-south movement to systems than is usual. This situation provided the opportunity for more high-pressure systems to move southeastward out of Canada, into the Central United States, and northeastward from there. Temperatures were above normal by as much as 3.3° C in the eastern Dakotas and in southeastern Montana. Above normal temperatures were also found over most of Kentucky, eastern Ohio, New York State, and in New England.

B. August 1975[22/]

Pressure heights of 700 mb were higher than normal over the eastern half of the United States, the maximum departure being over the Ohio/Pennsylvania/West Virginia region. Lower than normal heights prevailed over the Rockies. The subtropical ridge extended along 32° N, with one center off the Carolinas coast and another center over Arizona. The resulting circulation pattern shows strong west-to-east flow from coast to coast at 42° N. Pressure systems moved quickly from west to east without north-south movement. None of the fronts penetrated south of 35° N during the month.

Lower ozone concentrations were generally found at urban and nonurban locations of the northern study. Increased ventilation by more transient systems may have been partly responsible. Temperatures were above normal east of the Mississippi River in all of Missouri, Kansas, Nebraska, Iowa, and in eastern South Dakota. Departures of more than 2.2° C occurred in the Creston area, about +1.0° C at Bradford and Lewisburg, and about -2.2° C at Wolf Point.

C. September 1975[23]

The trough at 700 mb was reestablished over the Central United States in September. The subtropical pressure ridge appeared slightly weaker near 30° N, with centers displaced farther eastward over the Atlantic. Pressure height departures from the mean are negative over the Central United States while they are most positive over British Columbia and off the Carolinas coast near 35° N, 70° W. The axis of maximum wind lies just north of the Canadian border but shows low speeds. The pattern of departures is more variable, farther west and farther north than in July. High-pressure systems followed the long wave pattern, entering the United States near Montana moving southeastward, then accelerating northeastward off the coast.

In September, there were few events of relatively high ozone concentration at both the urban and the nonurban locations. Most of the average afternoon concentrations were below mean value of the 3 months. Temperatures were cooler than normal east of the Rocky Mountains except on the South Atlantic coast. Departures of -2.8° C or more were common along a 240-km-wide swath from southwest Oklahoma to Detroit.

D. October 1975[24]

A southwesterly flow at 700 mb over the Gulf Coast area was induced by a long wave trough at latitudes near 30° N, situated near 115° W. Heavy precipitation was reported east of the study area. Temperatures were slightly warmer than normal over most of the area.

Four frontal systems passed the Gulf study area and one tropical storm moved out of the Yucatan Channel into the Mississippi coast. The fronts took a day or more to pass the area, since they were generally weak and did not penetrate much farther southward.

7.0 INTERPRETATION OF RESULTS: NORTHERN HIGH PRESSURE OXIDANT STUDY

7.1 Examination of Aircraft Ozone Measurements

7.1.1 Data Analysis Approach

The objective of the northern high pressure oxidant study was to gather aerometric data from an aircraft and strategically located ground stations to determine the change in the concentration of ozone in the center of a high pressure system, as the system moves from a region of low population density (Canada and northern great plains States), south of the Great Lakes (high population density), and out into the Atlantic Ocean. Thus, the mission area was bounded roughly by the Eastern Rockies to the west, the Canadian border to the north, the Atlantic Ocean to the east, and the 37th parallel to the south. This area was divided into three sectors, each with relatively uniform population density and similar land use patterns:

(1) Western sector: west of a line from Fargo, North Dakota, to Dallas, Texas, including the rather sparsely populated Great Plains;

(2) Midwestern sector: between longitudes 96° W and 86° W (between line from Fargo, North Dakota, to Dallas, Texas, and line from east of Chicago, Illinois, to St. Louis, Missouri) including the more densely populated midwestern farm belt;

(3) Eastern sector: east of the line from east of Chicago, Illinois, to St. Louis, Missouri, including the densely populated and highly industrialized area from Ohio to the eastern seaboard. All data from a flight were categorized by the sector containing the center of the high pressure system.

In an attempt to present a roughly homogeneous data set, the aircraft flights were then screened for altitude consistency, time of day, and distance to the center of high pressure.

(1) Altitude: due to the areal extent of these missions, terrain differences, air traffic density, and FAA controls, it was not always possible for the mission aircraft to maintain a constant altitude throughout the flight, or day after day. Thus, for analysis, only those flights that averaged 915 to 1220 m MSL were considered. Also, it was decided that the flight level (expecting approaches, departures, and vertical profiles) should not vary more than 305 m during a single mission. Data outside

this altitude range were not considered;

(2) Time of day: in order to minimize diurnal effects, only mission data taken between 1300 and 1900 local daylight time were included;

(3) Distance to high center: to be considered for analysis, the flight had to be almost wholly within an 800 kilometer radius of the center of the high pressure system.

7.1.2 Summary of Aircraft Ozone Measurements and Meteorological Conditions

Based upon this selection process, portions of 14 flights were chosen for analysis (table 25). Two of the six high pressure systems investigate produced data in each of the three geographical sectors: July 24-25-26 and September 5-6-7. Both of these cases showed ozone concentration increasing from west to east (table 26).

In the July case, the anticyclone moved southeastward out of Alberta at about 30 knots and was centered in central Nebraska at the time of the July 24 flight (figure 49). Ozone concentrations in these figures are for each 10 minutes of the flight which is shown in its entirety. The July 24 flight roughly paralleled the track of the cyclone some hundred kilometers to the east of the system's center. The July 25 flight also followed the tracks of the anticyclone, very nearly passing through the center of the system in south central Iowa (figure 50). On July 26 the aircraft trailed the high center into Pittsburgh after taking an excursion to the northeast into southern Ontario (figure 51). At this point, the high pressure system slowed drastically and dissipated as Tropical Storm Blanche moved up the eastern seaboard. In the September case, both anticyclone track and aircraft flights were geographically similar to the July mission except that the system was followed into southern Maine.

Ozone concentration was measured continuously during the flight. All measurements taken at mission altitude were averaged together for each flight to produce the data in table 27. Spikes associated with urban areas were not included in these averages. These data demonstrate the general increase in ozone concentration from the west to east. The average ozone concentration was computed for each flight. The results are presented in table 27 along with computed averages by geographical sector. An increasing west-east ozone

Table 25. Candidate missions by sector

Sector	Date	Local Daylight Time	Altitude(s) (Kft MSL)	Avg Speed of High Center (Knots)
WEST	09 Jul	1300 CDT - 1344 MDT	4.0	10
	10 Jul	1356 MDT - 1622 MDT	4.0	Stationary
	11 Jul	1300 MDT - 1442 MDT	4.0	10
	24 Jul	1300 CDT - 1416 CDT	4.0	27
	13 Aug	1608 MDT - 1900 MDT	4.0	22
	05 Sep	1326 MDT - 1718 CDT	4.0	Indeterminate
MID-WEST	13 Jul	1306 CDT - 1612 CDT	4.5 - 3.5	40
	25 Jul	1300 CDT - 1520 CDT	3.5	30
	06 Sep	1314 CDT - 1838 CDT	4.0	22
	27 Sep	1300 CDT - 1848 EDT	3.5-3.0-3.5	15
EAST	26 Jul	1300 EDT - 1548 EDT	3.5	13
	07 Sep	1300 EDT - 1856 EDT	3.5 - 4.0	38
	28 Sep	1336 EDT - 1430 EDT	3.5	17
	29 Sep	1304 EDT - 1558 EDT	3.0-3.5-4.0	33

Table 26. Average ozone concentration at mission altitude

CASE	WESTERN SECTOR	MID-WESTERN SECTOR	EASTERN SECTOR
July 24-25-26	38 $\mu g/m^3$	94 $\mu g/m^3$	101 $\mu g/m^3$
September 5-6-7	65 $\mu g/m^3$	80 $\mu g/m^3$	98 $\mu g/m^3$

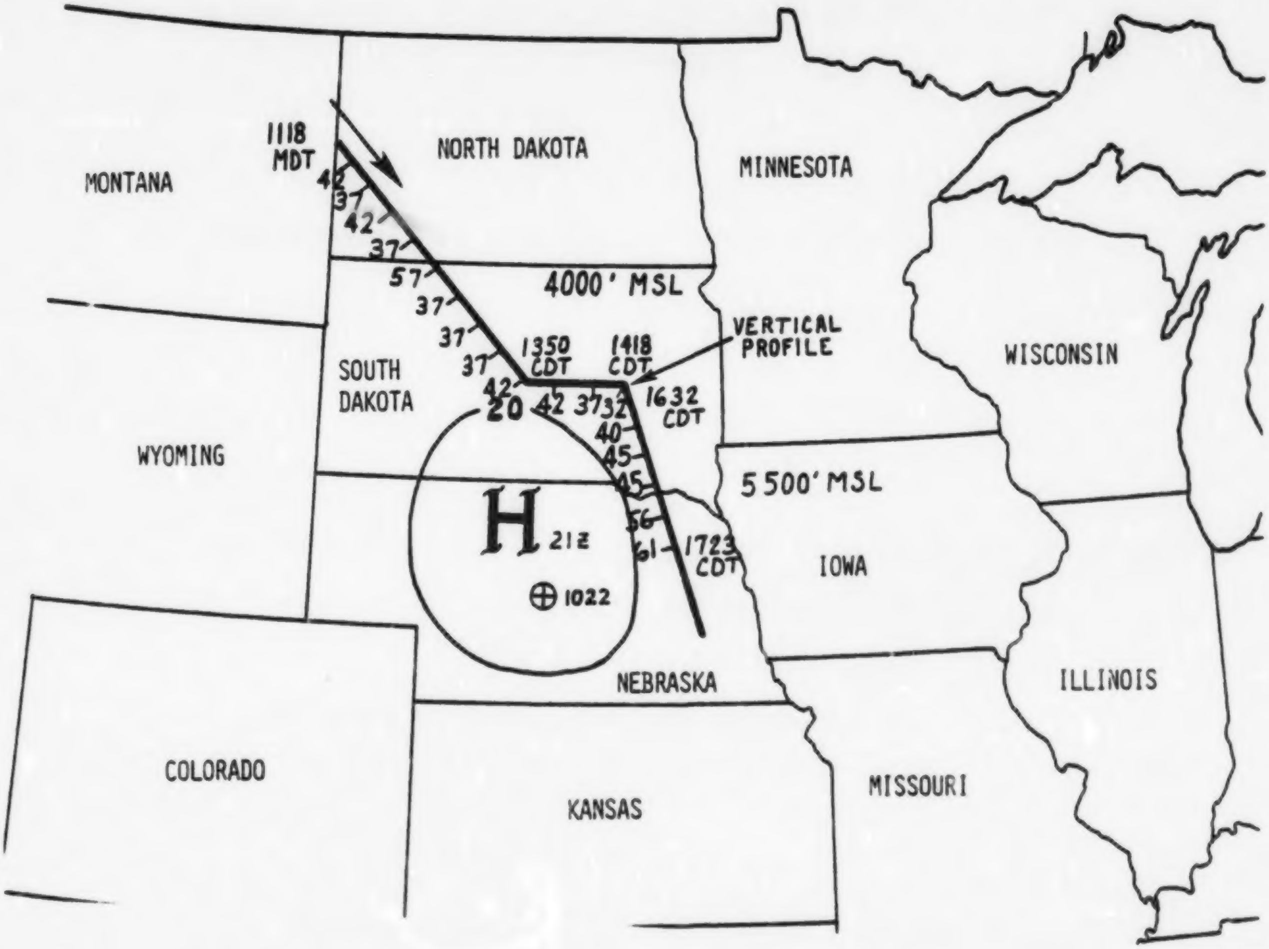
MONTANA
1118
MDT
NORTH DAKOTA
MINNESOTA
42
37
42
37
57
4000' MSL
37
37
37
VERTICAL
PROFILE
1350
CDT
1418
CDT
WISCONSIN
SOUTH
DAKOTA
42
20
42
37
32
1632
CDT
40
45
45
WYOMING
5500' MSL
H
212
56
61
1723
CDT
IOWA
⊕ 1022
NEBRASKA
ILLINOIS
COLORADO
KANSAS
MISSOURI

Figure 49. High pressure system flight on July 24, 1975.

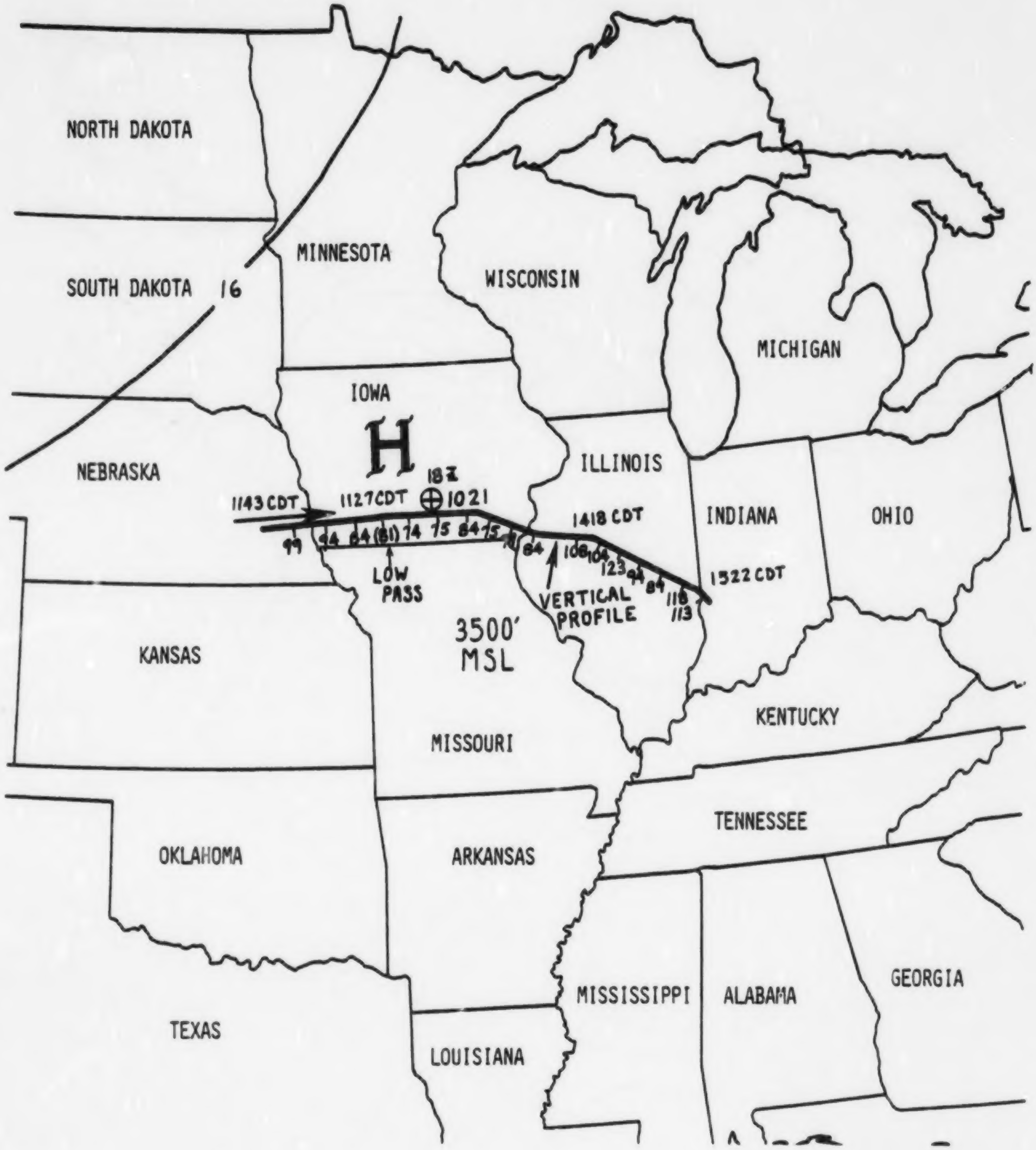
NORTH DAKOTA
SOUTH DAKOTA
16
MINNESOTA
WISCONSIN
MICHIGAN
IOWA
H
18Z
1021
NEBRASKA
ILLINOIS
INDIANA
OHIO
1143 CDT
1127CDT
1418 CDT
1522 CDT
99
94
84
(81)
74
75
84
75
84
108
104
123
94
84
118
113
LOW PASS
VERTICAL PROFILE
3500' MSL
KANSAS
MISSOURI
KENTUCKY
TENNESSEE
OKLAHOMA
ARKANSAS
MISSISSIPPI
ALABAMA
GEORGIA
TEXAS
LOUISIANA

Figure 50. High pressure system flight on July 25, 1975.

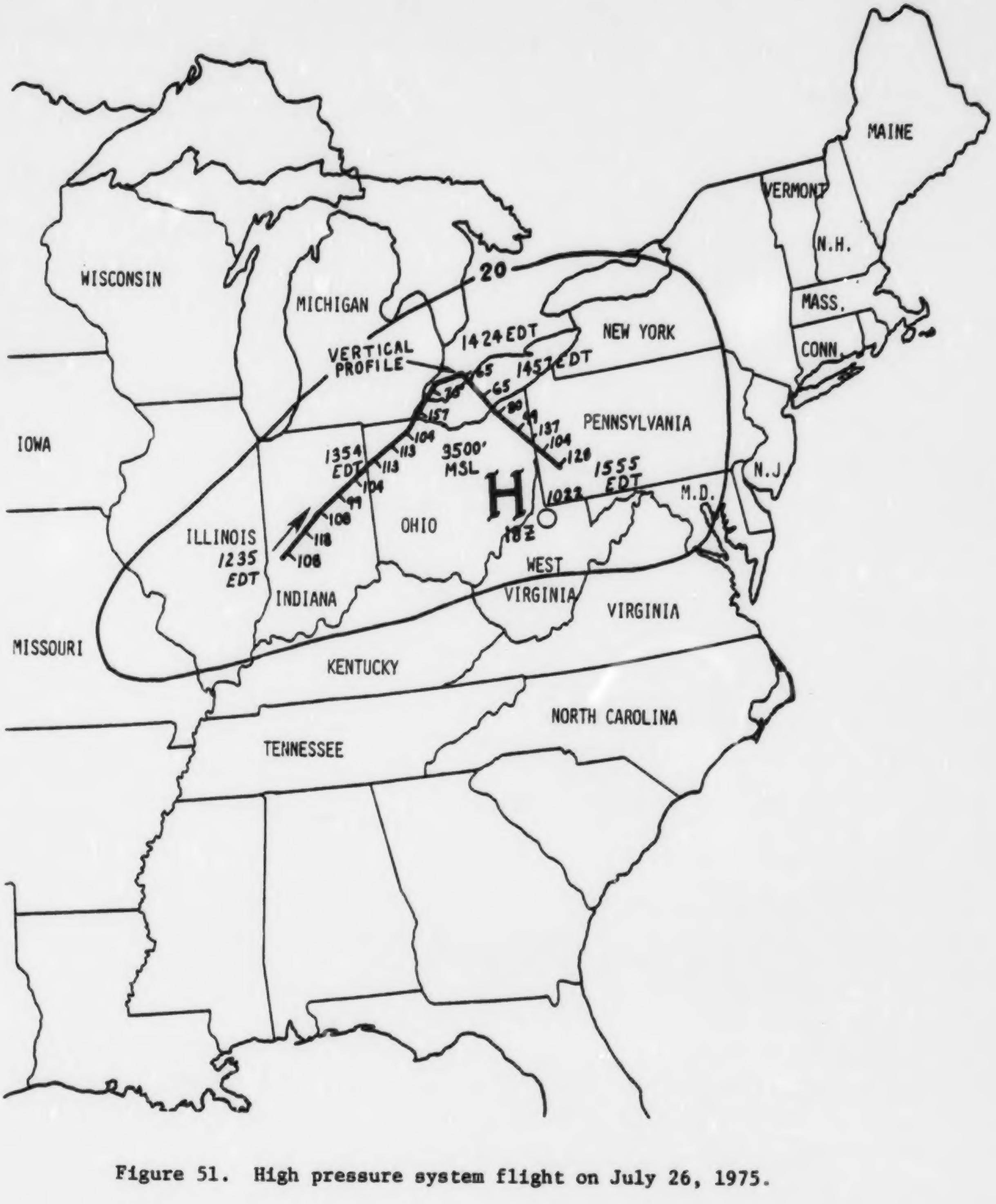
MAINE
VERMONT
N.H.
MASS.
CONN.
WISCONSIN
MICHIGAN
20
NEW YORK
1424 EDT
VERTICAL PROFILE
1457 EDT
165
65
75
80
99
157
137
104
120
IOWA
PENNSYLVANIA
1354 EDT
104
113
113
3500' MSL
1555 EDT
N.J.
104
H
1022
M.D.
99
108
118
108
ILLINOIS
1235 EDT
OHIO
182
WEST VIRGINIA
INDIANA
VIRGINIA
MISSOURI
KENTUCKY
NORTH CAROLINA
TENNESSEE

Figure 51. High pressure system flight on July 26, 1975.

Table 27. Average ozone concentration for each operational sector

SECTOR	DATE	NUMBER OF O_3 MEASUREMENTS	AVG O_3 FOR FLIGHT ($\mu g/m^3$)	STANDARD DEVIATION	MAX O_3 ($\mu g/m^3$)	MIN O_3 ($\mu g/m^3$)	RANGE ($\mu g/m^3$)
WEST	09 Jul	53	66	4.4	72	42	30
	10 Jul	70	72	6.0	81	57	24
	11 Jul	35	60	4.1	72	57	15
	24 Jul	39	38	2.9	42	32	10
	13 Aug	23	61	3.4	67	57	10
	05 Sep	66	65	5.3	78	60	18
	Totals & Avgs	286	60	4.4	69	51	18
MID-WEST	13 Jul	78	86	6.5	104	70	34
	25 Jul	43	94	12.9	123	75	48
	06 Sep	79	80	6.7	96	66	30
	27 Sep	72	124	19.6	170	74	96
	Totals & Avgs	272	96	11.4	123	71	52
EAST	26 Jul	59	101	18.2	157	55	102
	07 Sep	111	98	22.4	140	54	86
	28 Sep	26	131	14.5	146	90	56
	29 Sep	70	95	7.9	120	78	42
	Totals & Avgs	266	106	15.8	141	69	72

concentration for July and September cases (table 26 can still be seen even when all data from all flights are combined for averaging (table 27).

The spread between maximum and minimum ozone concentration values also increases west to east, which may be the result of a build-up of ozone on the back side of the high pressure system once it moves east of longitude 96° W. This phenomenon is discussed in Section 7.2.3. Other measures of ozone concentration that increased west to east were the average maximum and concentration variability as indicated by the average standard deviation of the mean values.

7.2 The Relationship Between the High Ozone in the Rural Boundary Layer and High Pressure Systems

7.2.1 Introduction

That high ozone (ozone concentrations in excess of the NAAQS--160 $\mu g/m^3$) exists in rural boundary layers is a well-established fact.[4,5,7,9,25] High ozone has been attributed to the formation of ozone by anthropogenic precursors and correlated with solar radiation and with wind speed; that is, high ozone concentrations are found with high levels of solar radiation (suggesting synthesis as a source of high ozone) and also with low wind speeds.

A more recent study has suggested that the occurrence of high ozone in the rural boundary layer is widespread in the eastern portions of the United States and is correlated with the presence of high pressure systems.[5] This study has shown that when a synoptic high pressure system moved into the eastern portions of the United States, high concentrations of ozone were reported at a number of rural stations scattered throughout the region. This condition persisted as long as the environmental conditions (e.g., high solar radiation, low wind speed) accompanying high pressure systems remained in the eastern portions of the United States. In this 1974 study, the five highest ozone concentrations were found at rural stations located near the central regions of the high pressure system. These regions were characterized by weak winds, disorganized flow, and relatively clear skies. The lowest ozone concentrations were found after frontal passages.

Data collected by the Research Triangle Institute in the summers of 1973, 1974, and 1975 have been used to investigate the relationship between high ozone and high pressure systems. In 1973 and 1974, the data were collected in the eastern portions of the United States at various stations located in rural boundary layers. However, in 1975 stations were located across the United States at Wolf Point, Montana; Creston, Iowa; Lewisburg, West Virginia; and Bradford, Pennsylvania. The following summarizes the results of the studies using these data.

7.2.2 Statistics on High Ozone Concentrations Versus High Pressure Systems

Figure 52 shows the daily area-averaged pressure and the daily maximum ozone concentration for the summers of 1973 and 1974. The ozone data represent the average value of the diurnal maximum ozone concentration observed at each available station. An averaging technique was used in order to remove local anomalies which may exist at a given time and station, and to demonstrate the systematic nature of the increase and decrease in ozone over a fairly large area. The rural stations used in 1973 were Kane, Pennsylvania; McHenry, Maryland; Lewisburg, West Virginia; and Coshocton, Ohio. In 1974, they were McHenry, Maryland; McConnelsville, Ohio; Wooster, Ohio; DuBois, Pennsylvania; and Wilmington, Ohio. The area-averaged pressure is the average of the daily average pressure for a synoptic weather station nearest to the respective rural stations. Figure 53 shows the daily ozone maximum and the average pressure from the nearest synoptic weather station to three of the ozone stations for the summer of 1975.

The data in figure 52 and 53 show the relationship between high ozone and high pressure systems; that is, high concentrations of ozone at the surface were found near the time a high pressure system was located in the region of interest. The 1975 data (figure 53) further indicate that high ozone concentrations were found in high pressure systems most often when these systems were located in the eastern part of the United States. This can be seen by noting that many high pressure systems pass through Wolf Point, Montana, but at no time did the concentration of ozone reach values greater than the NAAQS. However, relatively speaking, when the high pressure systems were found over that station, the ozone concentration at times exceeded the NAAQS at Creston, Iowa, when high pressure systems moved into the region, but not as often as when similar systems were located near Bradford, Pennsylvania.

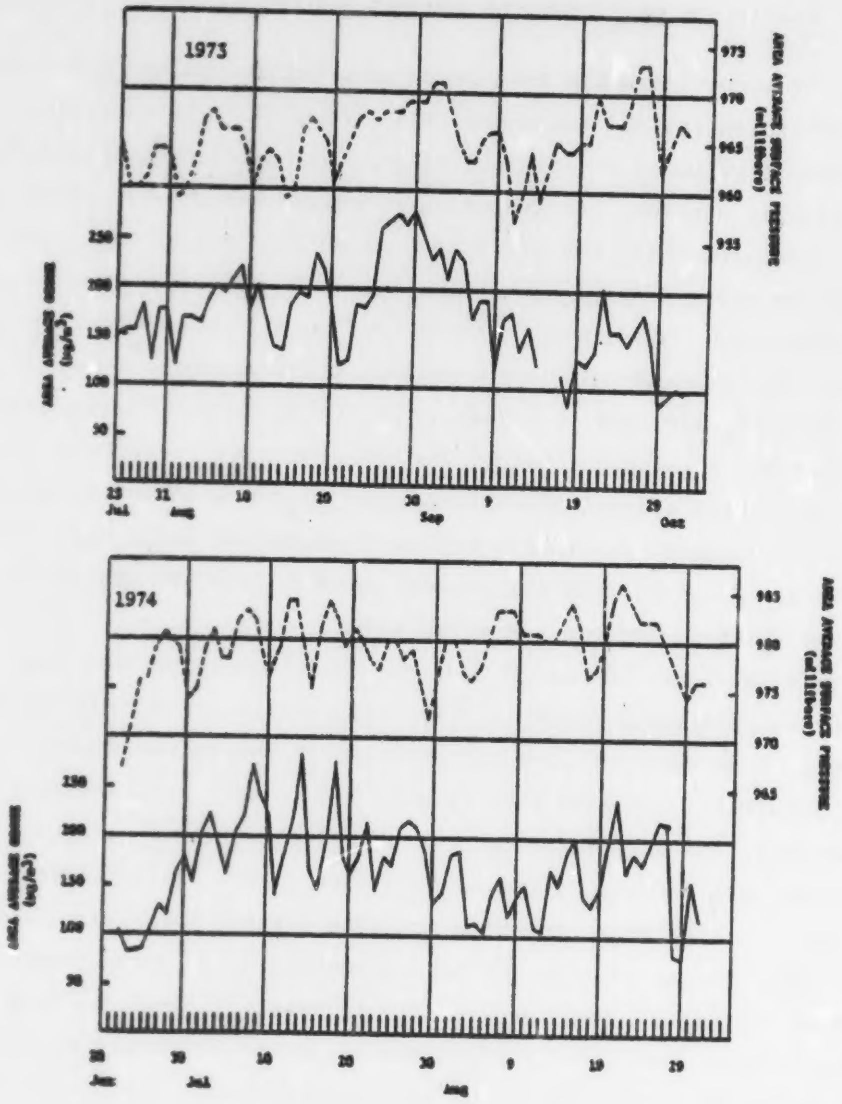

Figure 52. Area averaged value of the daily maximum ozone concentration (solid line) and the area averaged surface pressure (dashed line) versus day of month for latter part of the summer of 1973 and 1974.

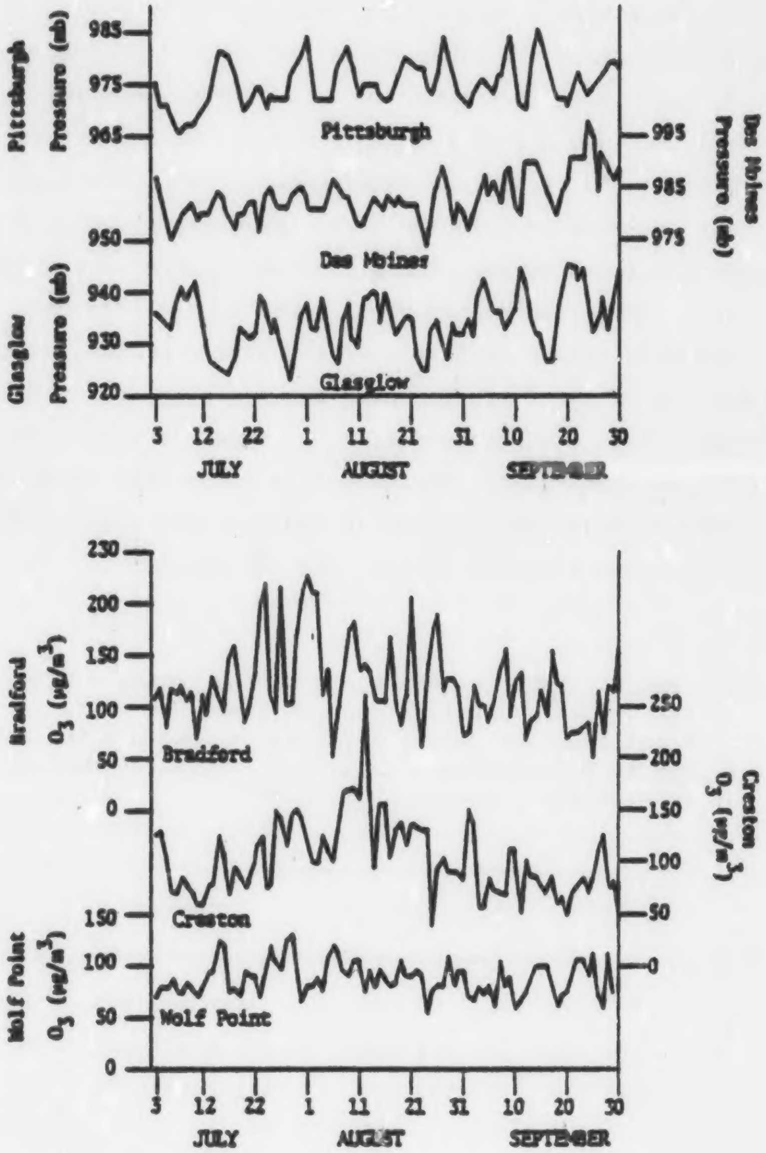

Figure 53. Daily maximum ozone concentration at Wolf Point, Montana; Creston, Iowa; and Bradford, Pennsylvania and the daily average pressure obtained from the nearest synoptic station for the summer of 1975.

The data in table 28 support the association between high ozone and high pressure systems. The table shows that in 1973, between July 4 through September 3, there were more hours in which a high pressure center or a ridge was within 720 km (450 mi) of the rural station in Pennsylvania than in 1974 or 1975. There is no significant difference between the total number of hours of high pressure in 1974 and 1975. However, there is a marked difference between the total number of hours ozone exceeded the NAAQS over the 3-year period. The greatest number of hours was in 1973, and the least was in 1975. The data also show that over the 3-year period, on the average, about 85 percent of the hours in which ozone was greater than the NAAQS occurred when a high pressure center or a ridge was within 720 km (450 mi) of the station. On the average, approximately 93 percent of the hours of high ozone occurred when the station was in the same air mass, regardless of the distance of the high pressure center from the station.

Table 28. The relationship between the number of hours a high pressure system is near a station and the number of hours of high ozone (greater than the NAAQS) observed at that station for the period 4 July to 3 September. In 1975, the station used was Bradford; in 1974, DuBois; and in 1973, Kane

YEAR	A*	B**	C***		D****	
1975	773 hrs	92 hrs	83 hrs	90%	87 hrs	95%
1974	781 hrs	346 hrs	277 hrs	80%	301 hrs	89%
1973	1015 hrs	552 hrs	471 hrs	85%	521 hrs	94%

*Column A gives the number of hours a high pressure center or a ridge is within 450 miles of the station.

**Column B gives the number of hours of high ozone. during the period 4 July-3 Sept.

***Column C gives the number of hours and the percentage of hours in Column B which coincide with a high pressure center or ridge within 450 miles of the station.

****Column D gives the number of hours and the percentage of hours in Column B which coincide the period the station remains in the same air mass regardless the distance of the high center from the station.

Though these data support the contention that high ozone is found in the presence of a high pressure system, they also suggest that the converse is not necessarily true; that is, the presence of a high pressure system does not necessarily imply the existence of high ozone. It is noted that in 1973 and 1974, high ozone occurred for about 50 percent of the total number of hours of high pressure. In 1975, it only occurred about 12 percent of those hours. If the ratio of hours of high pressure to that of high ozone is computed for daytime periods only, they are 65 percent for 1973, 50 percent for 1974, and 18 percent for 1975.

Figure 54 shows the results of computing a nine-point running mean using the data in figures 52 and 53. For 1975, the Bradford, Pennsylvania, data were used so that the figure shows variations in the eastern portion of the United States only. The nine-point running mean filters synoptic scale and mesoscale fluctuations, leaving only long-term trends (or macroscale fluctuations with periods greater than 9 days). In 1973 and 1974, the summer months were characterized by macroscale high pressure systems, which last for approximately 30 days or more. However, in 1975, they were characterized by a series of macroscale pressure systems, the longest of which was approximately 23 days and was centered around the 30th of July 1975. Coinciding with the pressure systems in 1973 and 1974 were macroscale ozone concentrations in excess of the NAAQS, which also lasted for approximately 30 days. However, in 1975, there was only one period, lasting approximately 4 days, in which the macroscale ozone exceeded the NAAQS centered at the 30th of July. These data suggest that ozone concentrations in excess of the NAAQS are associated with macroscale high pressure systems lasting longer than 20 days. If such systems do not develop, the occurrence of ozone concentrations greater than the NAAQS in rural regions appears to be minimized. This is supported by the facts that, though the number of hours a high pressure system or a ridge was near Bradford and Dubois in 1975 and 1974 were about equal, Bradford (1975) had considerably fewer number of hours of high ozone than DuBois (1974) (table 28).

7.2.3 Distribution of Ozone Relative to a Moving High Pressure System

Figure 55 shows the average daily variation of the diurnal ozone maximum relative to a moving high pressure system using data from Kane, Pennsylvania, in 1973, from DuBois, Pennsylvania, in 1974 and from Bradford,

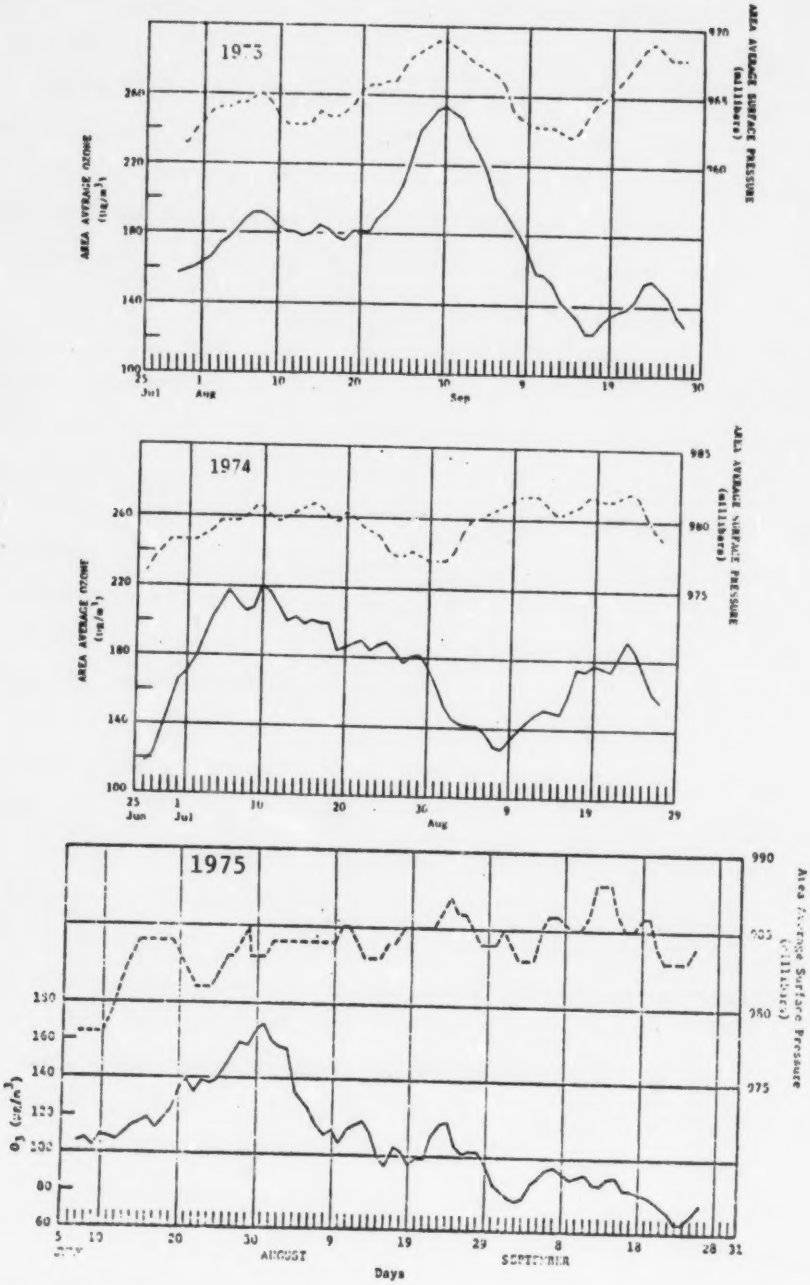

Figure 54. Nine-point running average of the data presented in figure 53 and of the Bradford ozone data and the Pittsburgh pressure data presented in figure 53.

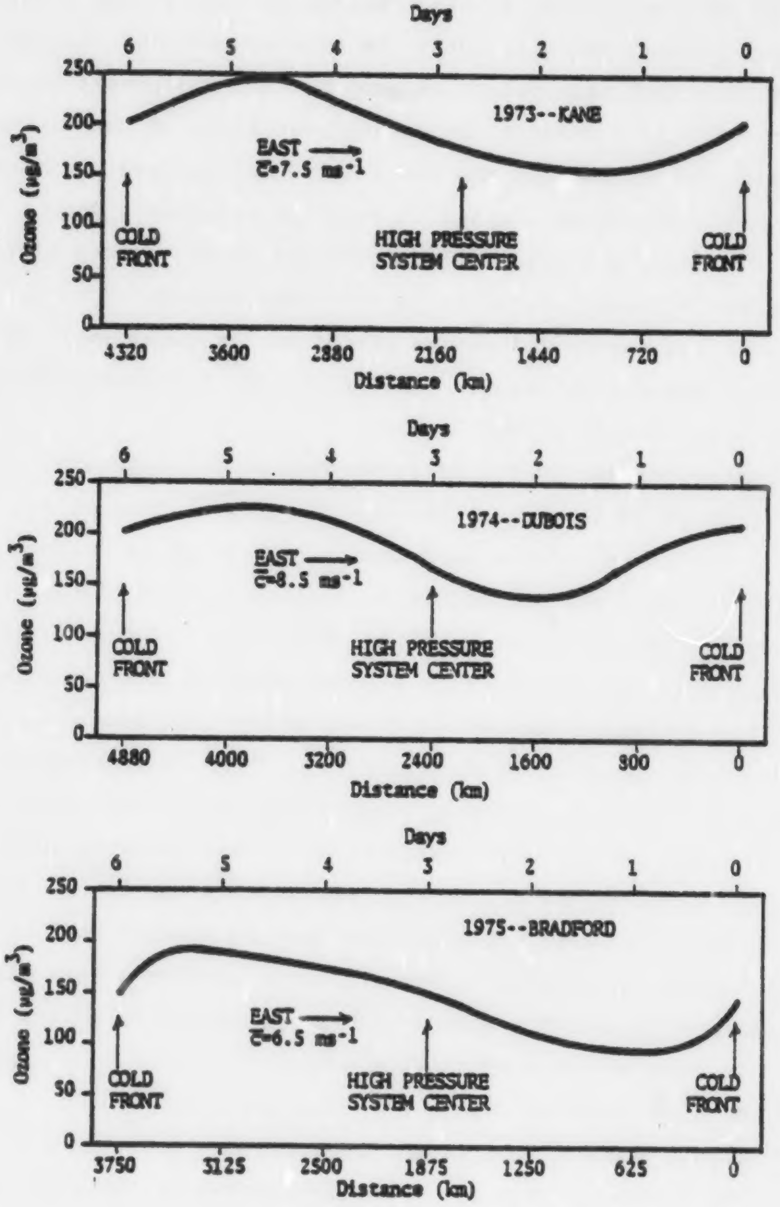

Figure 55. The temporal and spatial variation of the diurnal maximum ozone concentration through a high pressure system located in the east in the summers of 1973, 1974, and 1975.

Pennsylvania, in 1975. The period represented in the data coincides with the period from an initial frontal passage through a high pressure system to the next frontal passage. Only the data around 1700 EDT for each day represent an actual data point. A smooth curve was passed through these points in order to represent the average variation of the diurnal ozone maximum with distances from the initial frontal passage. Distances were computed based on the mean speed of the high pressure system. It is noted that the distances span the entire continent of the United States. These distances are representative of synoptic wave numbers three and four, which characterize the particular summer situations in each case. The mean period from frontal passage to frontal passage through the high pressure system was exactly 6 days in each of the 3 years.

The data indicate that a relative minimum in the diurnal ozone maximum occurs somewhere in the region between the initial frontal passage and the high pressure center. For a slow-moving high pressure system (the Bradford data), the relative minimum occurs soon after frontal passage (less than a day) or approximately 400 km upstream of the front. However, for fast-moving high pressure systems such as that found in 1974 (the DuBois data), the relative minimum occurs about 2 days after frontal passage or approximately 1,400 km upstream of the front. The 1973 data indicate that the position of the relative minimum (approximately 1.5 days after frontal passage or 1,000 km upstream) falls between that found in 1975 and that in 1974. The mean speed of the high pressure system in 1973 was greater than that found in 1975, but less than that found in 1974.

The largest value for the diurnal ozone maximum occurs after the high pressure center passes the station or on the back side of the high pressure system. In each of the 3 years, the concentration of ozone on the back side of the high pressure system exceeded the NAAQS.

These data support some of the conclusions resulting from the 1974 RTI summer field program,[5/] but are more significant in the statistical sense. However, one result of this study differs from that found in the 1974 summer study program. Though the 1974 data indicate that high ozone is found near the center of the high pressure system, the highest ozone is found on the back side of the high (or at least 2 days after the high pressure system passed the station). Distances given in the figures cannot be considered realistic because variations in the speed of the high pressure system could produce both larger and smaller distances. Differences between the results of this study and the 1974 study can be explained from the facts that the 1975 study dealt with time-dependent variations in ozone whereas the 1974 study dealt with space dependencies with no regard to time at all.

Figure 56 is the average variation of the diurnal ozone maximum relative to a moving pressure system determined using the 3 years of data in figure 55. These overall data summarize that found in figure 55.

Figure 57 is a similar representation to that of figure 56, except that the 1975 data for Bradford, Pennsylvania; Creston, Iowa; and Wolf

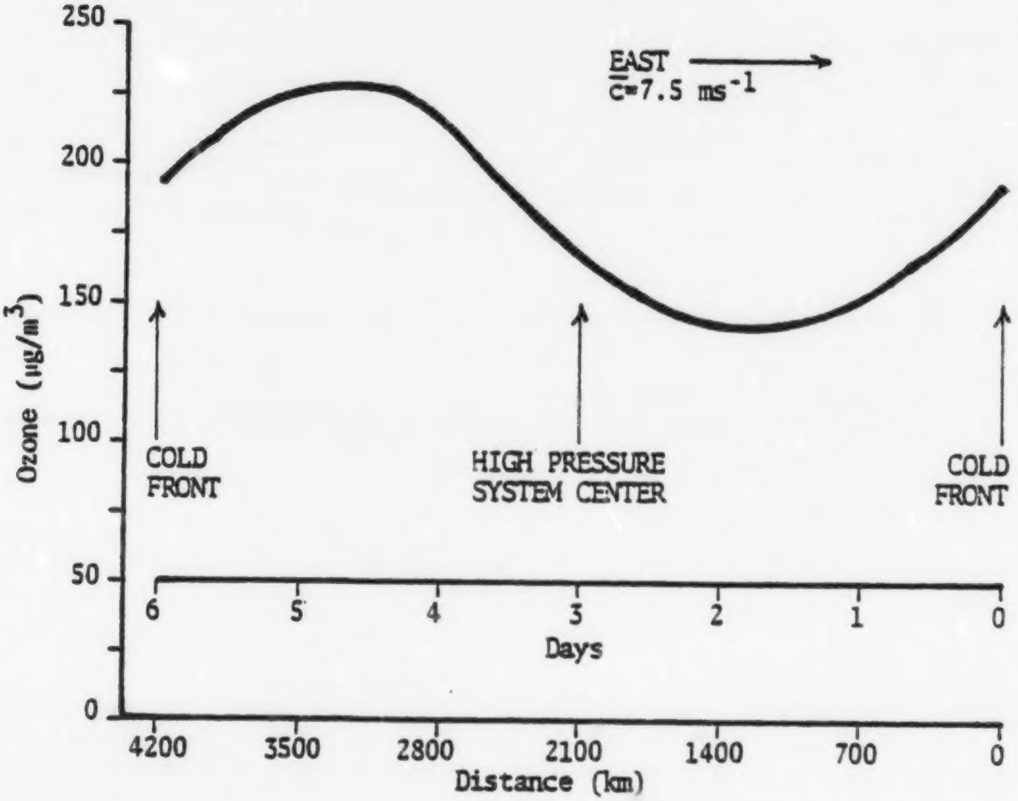

Figure 56. The average temporal and spatial variation of the diurnal maximum ozone concentration through a high pressure system located in the east based on the 1973, 1974, and 1975 data.

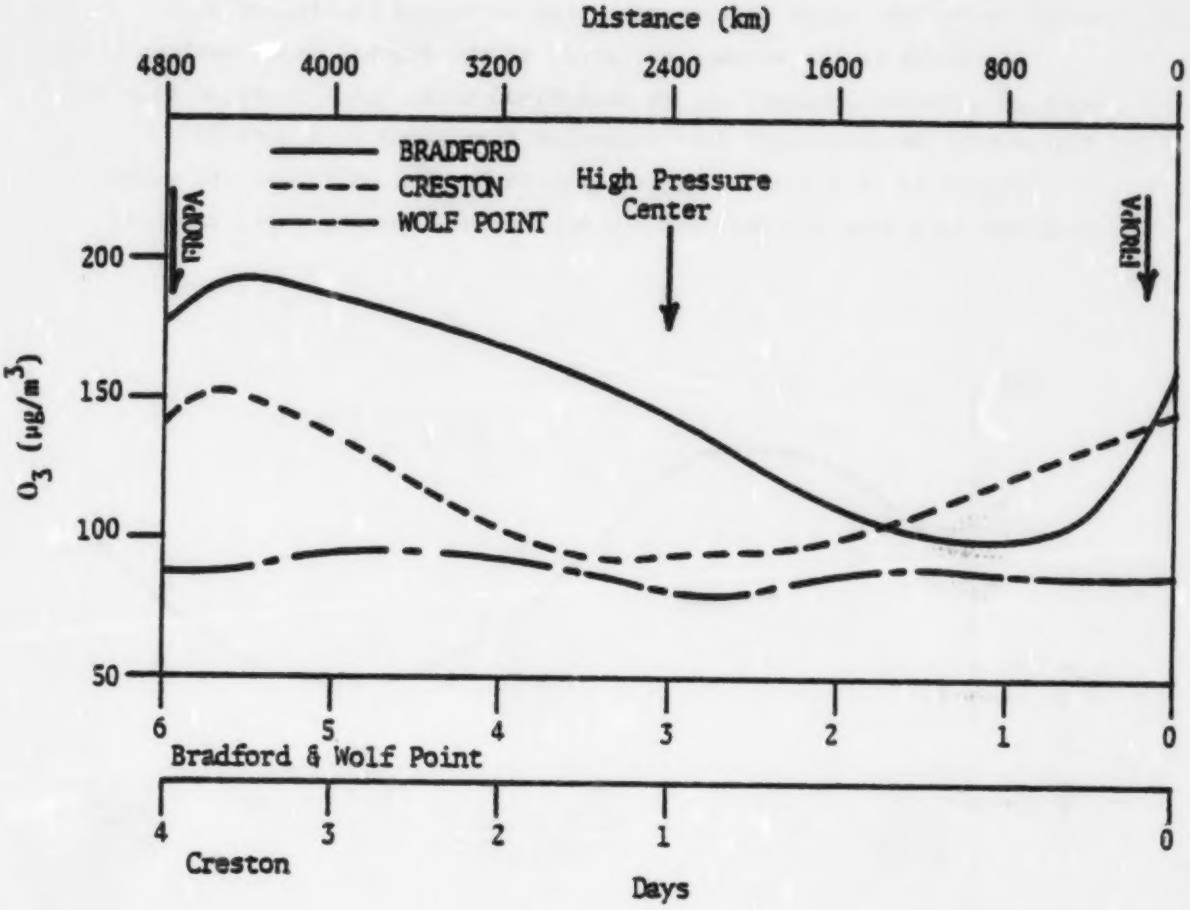

Figure 57. The temporal and spatial variations of the diurnal maximum ozone concentration through a high pressure system based on the 1975 data at Wolf Point, Montana; Creston, Iowa; and Bradford, Pennsylvania.

Point, Montana, are given. The period from frontal passage through the high pressure system to the next frontal passage was 6 days at Bradford and Wolf Point, but was approximately 4 days at Creston. At Creston it took, on the average, about 1 day for the high pressure center to reach the station after frontal passage, but the next front did not arrive until 3 days after the high pressure center arrived. Apparently, there was an initial acceleration of the high pressure system in the Great Plains regions of the United States. Distances were computed based on the mean speed of the high pressure system at Bradford.

The data indicate that there is no marked variation in the ozone concentration at Wolf Point as the high pressure system passes through that station. The ozone concentration was generally higher on the back side of the high, but only by approximately 10 percent of that in the front side. The variation of ozone concentration at Creston is similar to that shown in figures 55 and 56, except in this case the relative minimum was found when the high pressure center had passed the station and the ozone concentration on the back side of the high did not exceed the NAAQS. It was not until the high pressure system moved into the eastern portions of the United States that the ozone concentration on the back side of the high pressure system exceeded the NAAQS. This suggests an enhancement of a mechanism to increase the ozone concentration in local air parcels as the high pressure system moves eastward from Montana to Pennsylvania.

7.2.4 Source Regions and Residence Times of Air Relative to a Moving High Pressure System

A potential source for ozone is the upper atmosphere. However, analysis of available meteorological data did not show any evidence for an enhancement of downward transport of ozone, on the average, as a high pressure system moved from the west to the east by either subsidence or by vertical mixing. Low-level divergence and downward vertical motions are usually greatest near the center or in the forward portions of an eastward moving high pressure system, not on the back side. It could be hypothesized that the vertical gradient of ozone is greater through the troposphere in the East than in the West, which could be responsible for enhanced downward transport of ozone, but available vertical profile data from aircraft measurements did not support this.

Since vertical transport of ozone does not appear to be the mechanism to produce high ozone and since the number of industrial complexes and population centers (sources for ozone precursors) increases markedly from the west to the east, enhancement of tropospheric synthesis is suggested as the most probable mechanism. Since the industrial complexes and population centers are large in number and widespread in the East, injection of ozone precursors into the front side of a high pressure system should be identical to that into the back side. The fact that the ozone concentrations are larger in the back side of a moving high pressure system suggests a build-up of ozone precursors or the establishment of a critical distribution of ozone precursors takes place as parcels of air circulate in the high pressure system. It is important for air parcels to remain within the high pressure system since the system offers the critical environmental factor necessary for synthesis; that is, relatively cloudless skies which allow unimpeded exposure to solar radiation.[5] The longer parcels of air remain in the high pressure system and travel through the industrialized and highly populated eastern portions of the United States, the greater the potential is to increase significantly the concentration of ozone precursors and to produce high ozone. The following calculations offer some insight into the residence time of air parcels in high pressure systems.

It was assumed in the initial calculations that the pressure distribution, p, in the high pressure system may be expressed by the following equation:

$$p = p_o + p_1 \sin\ k(x - c_x t)\ \sin \lambda y, \qquad (1)$$

where

k is the wave number in the x direction (west-east direction),
$k = 2\ /L_x$ and L_x is the wavelength along x (see figure 58)
c_x is the wave speed assumed to have an x component only,
is the wave number in the y direction (south-north direction),
$= 2\ /L_y$ and L_y is the wavelength along y (see figure 58)
p_o is the mean of pressure,
p_1 is the amplitude of pressure for the harmonic, and p is pressure.

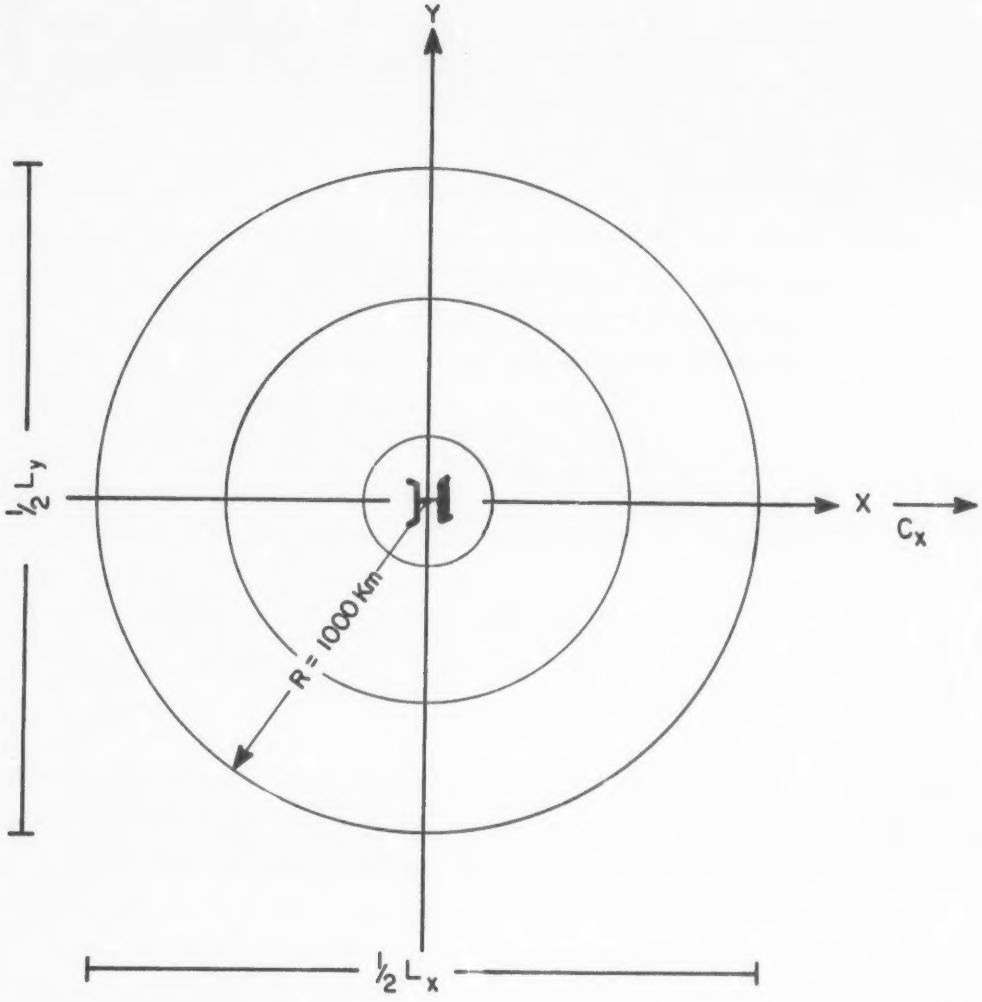
Y
X
C_x
H
R = 1000 Km
½ L_y
½ L_x

$L_x = L_y$
$L_x = 4R$

Figure 58. Hypothetical high pressure system for which residence times were calculated.

Accelerations were assumed to be zero, which yield the following equations of motion in the high pressure system

$$fv_g - fv + Ku = 0$$

$$fu_g - fu - KV = 0 \; ; \qquad (2)$$

where

f is the Coriolis parameter and is allowed to vary in the y direction

v is the south-north component of the wind (y-component),

u is the west-east component of the wind (x-component),

K is the friction coefficient,

u_g is the west-east component of the geostrophic wind, and

$$u_g = - \frac{\alpha}{f} \frac{\partial p}{\partial x} \, , \qquad (3)$$

v_g is the south-north component of the geostrophic wind, and

$$v_g = \frac{\alpha}{f} \frac{\partial p}{\partial y} \, , \text{ and} \qquad (4)$$

α is the specific volume.

This system of equations was used to compute the boundary layer trajectory of air parcels in a circular symmetric high pressure system which was used to determine the residence time for air parcels. All motion was constrained to be horizontal. The calculations were subject to the following conditions. The high pressure system had a radius of approximately 1,000 km and at that outer boundary, the geostrophic wind speed was set equal to 10 m/s. The value of the friction coefficient was 10^{-4} s^{-1}. These are typical parameters associated with high pressure systems.

Figure 59 shows the number of days air parcels that start at various locations in a high pressure system will spend within that system. Variations in the three high pressure systems are a result of differences in the speed of the systems. The system speeds were 5 m/s, 7.5 m/s and 10 m/s, and the direction of motion was to the east. Calculations indicate that, regardless of system speed, the source region for air parcels which will spend more

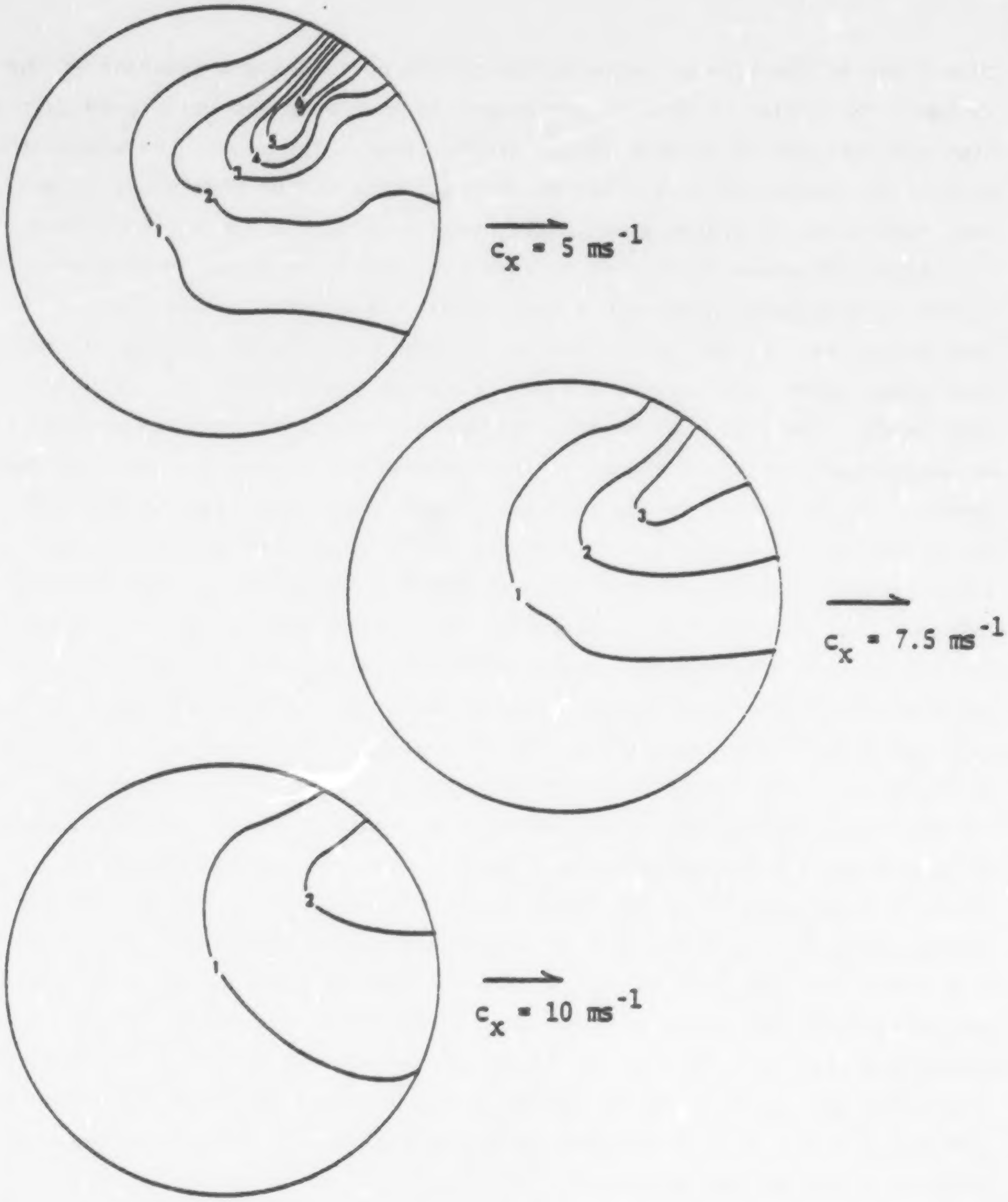

Figure 59. The number of days air parcels, in various locations in a high pressure system, will spend within that system versus the speed of the system for a circular symmetric high pressure system.

than 1 day in the high pressure system is the north-eastern quadrant of the system. The number of days an air parcel in that quadrant will spend in the high pressure system depends on the system speed. The slower the speed, the greater the number of days. Air in the back side of the high pressure system, regardless of system speed, will spend less than 1 day in the system.

Figure 60 shows the number of days air parcels in the high pressure system already have spent within the system. The system speeds are the same as before. On the whole, the air in the back side of the high pressure system has spent more days in the high pressure system than the air in the front side. The region of maximum residence time shifts from the south-western sector for small speeds to the northwestern sector for large system speeds. As the system speeds increase, the contour depicting one-day residence time shifts westward. This suggests the hypothesis that residence times greater than one day are required for air parcels in a high pressure system to build up critical concentrations of ozone precursors. Subsequently, the rise in ozone to the concentration experienced on the back side of the high pressure system should commence nearer to the leading edge of a high pressure system (soon after frontal passage) for a slow-moving system, and near or at the center of the high pressure system for faster-moving systems. This agrees well with the data in figure 55 which shows that the minimum concentration (afterwards there is a rise in the ozone concentration) is found soon after the front passed the station for the slow-moving system and nearer to the center of the high pressure system for the faster-moving system. The data in figure 57 shows that at Creston the ozone concentrations did not begin to rise until after the high pressure center passed the station. Whereas, at Bradford, the rise in concentration occurred soon after the initial frontal system passed the station. The difference is probably a result of the pressure system moving through Creston at twice the speed it moved through Bradford.

The distribution of residence times also is a function of the shape of the high pressure system. Figures 61 and 62 show similar distributions as those shown in figures 59 and 60 but for an elliptically shaped high pressure system. In the first case, the major axis (2,600 km) was oriented north-south, and the system was moving from west to east at a speed of 7.5 m/s. In the second case, the major axis was oriented west to east, and

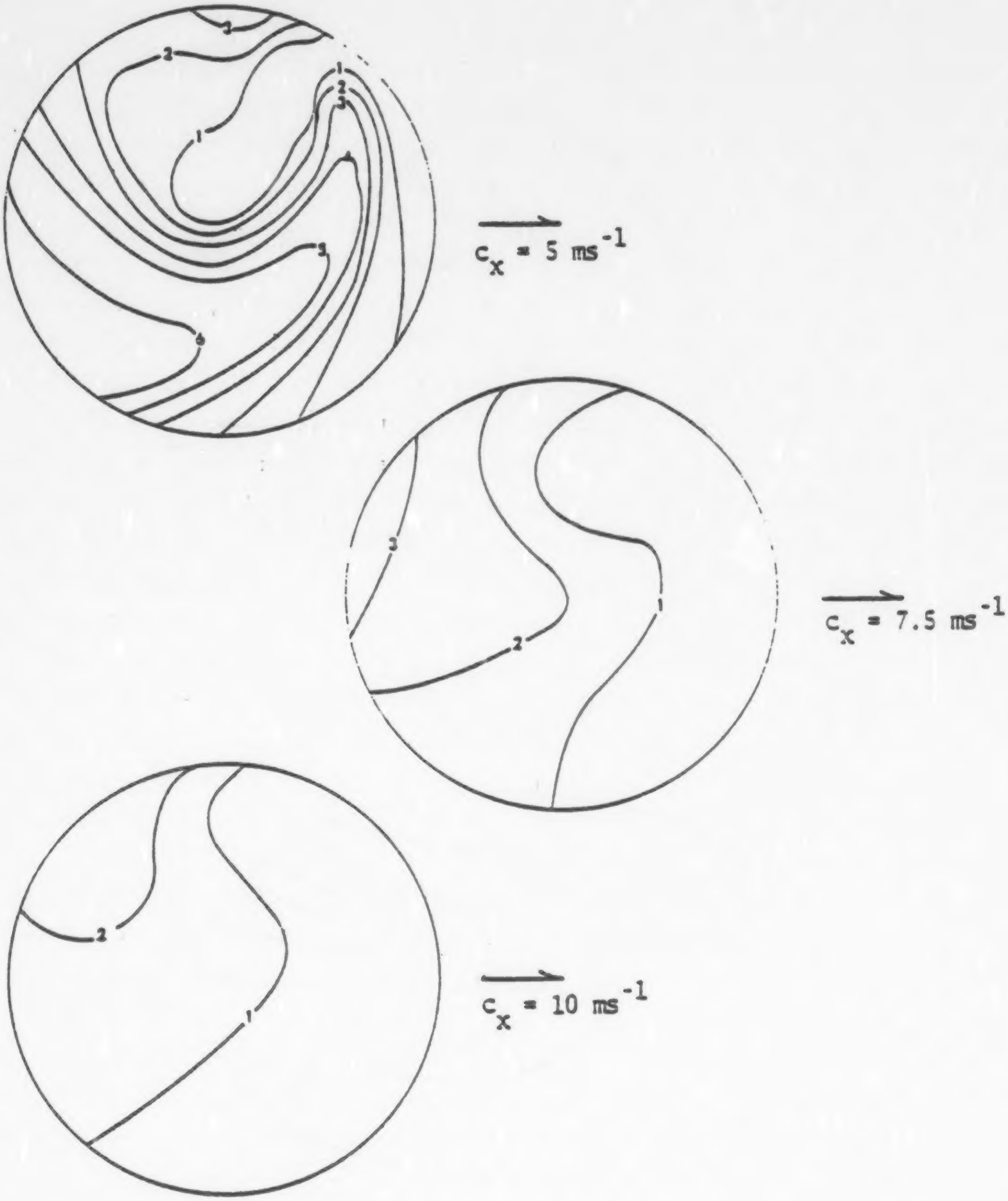

Figure 60. The number of days air parcels in high pressure systems have spent (residence time) within the system versus the speed of the system for a circular symmetric high pressure system.

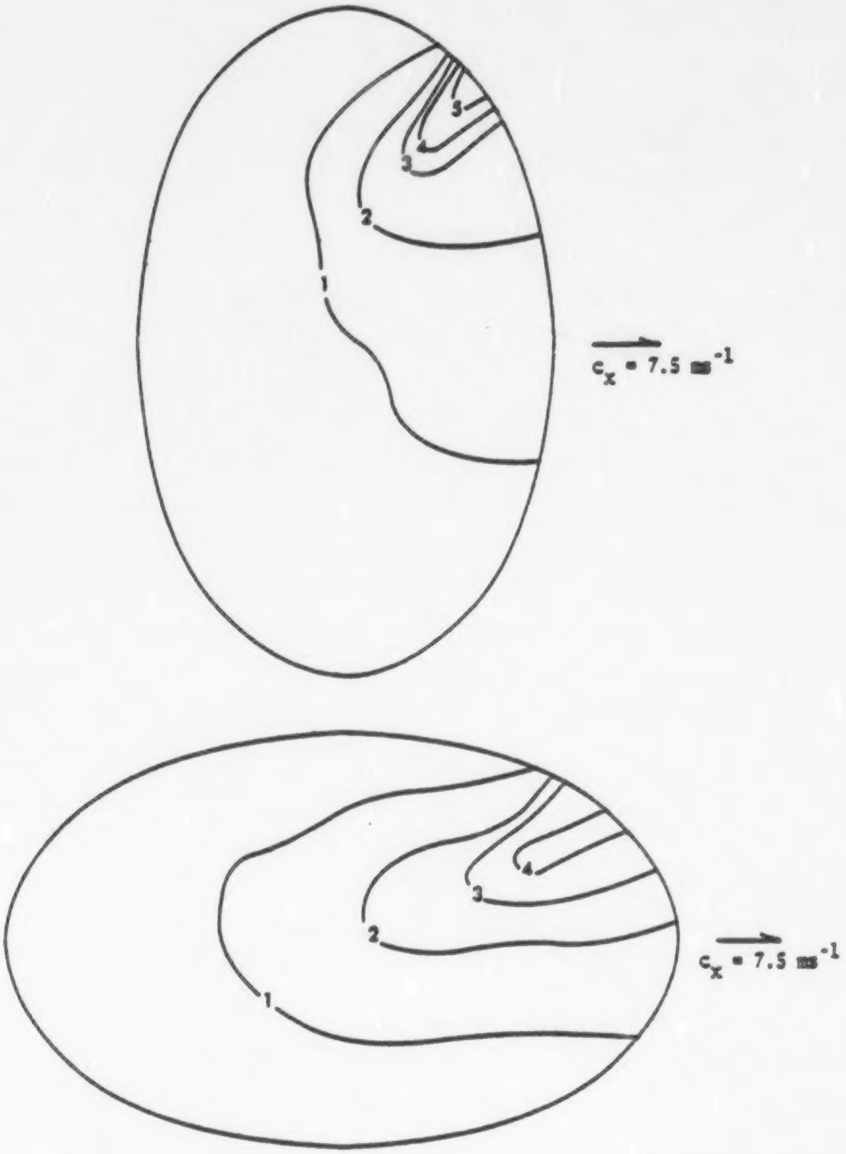
5
3
2
1
$\overrightarrow{c_x} = 7.5\ ms^{-1}$
4
3
2
1
$\overrightarrow{c_x} = 7.5\ ms^{-1}$

Figure 61. The number of days air parcels in various locations in a high pressure system will spend within that system versus differently shaped elliptical high pressure systems. The system speed is 7.5 ms^{-1}.

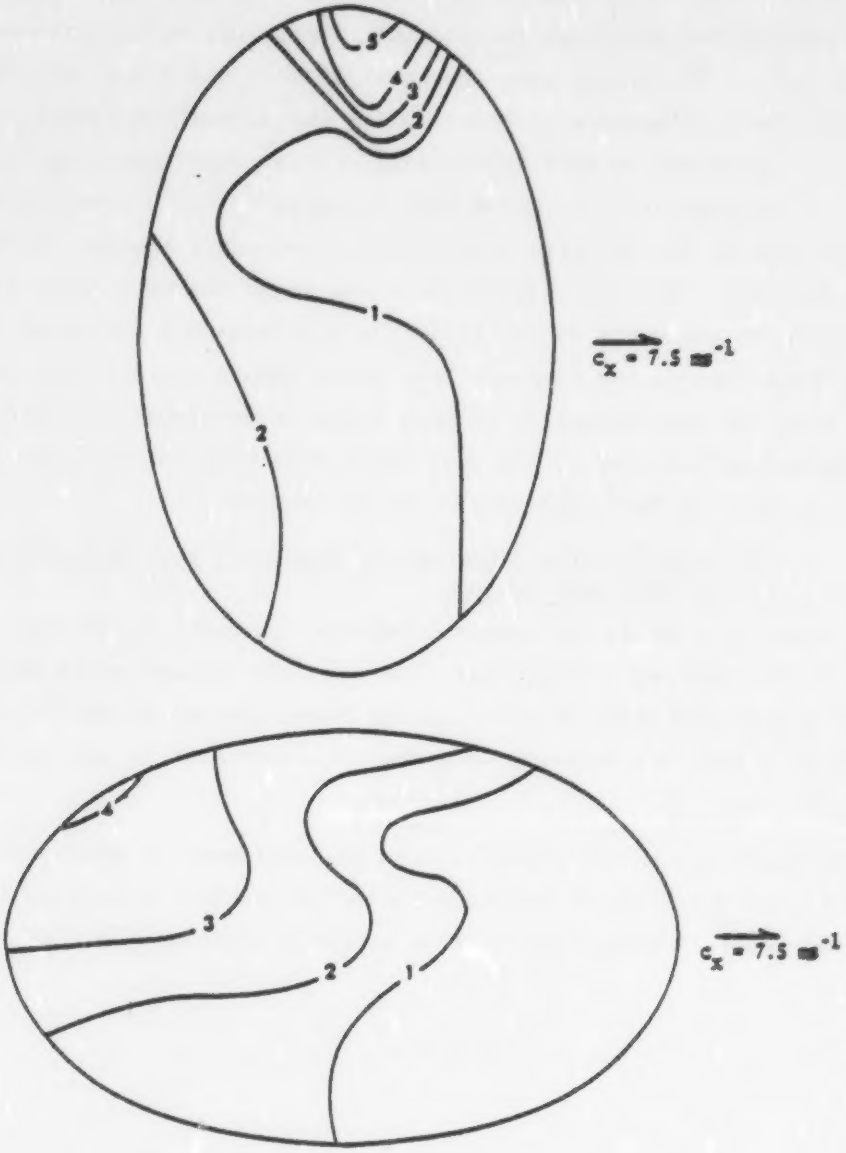

Figure 62. The number of days air parcels have spent (residence time) within a high pressure system versus differently shaped elliptical systems. The system speed is 7.5 ms^{-1}.

the system also was moving eastward at a speed of 7.5 m/s. The minor axis was 1,600 km. The source regions for air that will have large residence times remain in the northeastern quadrant, regardless of the orientation of the major axis. The system with the major axis oriented west to east has the air in the northwestern quadrant having the largest residence time (figure 62) identical to that found using the circular symmetric high pressure system; but systems with the major axis oriented south to north have the largest residence time in the northern sector with a secondary maximum in the southwestern quadrant. This portrays differences which can be encountered in the distribution of residence times within the high pressure system as the shape of the system changes and suggests that if residence times of air parcels are important in the production of high ozone as previously implied, there may be marked differences in the distribution of high ozone within the high pressure systems as the shape of the system changes.

7.2.5 Some Aspects of the Mechanisms Governing the Chemistry of Ozone in High Pressure Systems

In order to examine the chemical behavior of ozone in the high pressure system, it was necessary to examine theoretically the governing equation for the mean diurnal behavior of ozone in the lower portion of the boundary layer (e.g., first 100 meters). The theoretical effort is described below.

7.2.5.1 Theory

A chemical and environmental system is considered in which synthesis, transport, and destruction are the principal mechanisms governing the behavior of ozone. Mathematically, this can be described by the following equation:

$$\frac{\partial O_3}{\partial t} = G + M - D \, , \qquad (5)$$

where

$\partial O_3/\partial t$ is the local rate of change of ozone,

G is a contribution to the local rate of change due to synthesis of ozone,

M is the contribution to the local rate of change due to transport of ozone, and

D is the contribution to the local rate of change due to destruction of ozone either in the gas phase or at the surface.

The mean diurnal variation of ozone is usually determined by averaging of the hourly value over a very large number of days. In the summation of daily data, most synoptic weather regimes should be representative. In the average, therefore, the contribution due to horizontal transport is minimized since it is doubtful that horizontal gradients of ozone would exist over continental regions such that mean positive or negative contributions would exist. Furthermore, Bach[26] has shown that there is no unique correlation between air trajectories and high or low ozone over the eastern half of the United States. It should be pointed out that earlier in this report, it was shown that ozone gradients may exist between oceanic regions and continental regions, due apparently to a lack of ozone precursors in the oceanic regions. However, in this case we are dealing only with continental regions sufficiently inland so the influence of the oceanic regions would not affect the distribution of ozone. Since on the average, ozone does increase upward through the boundary into the mid and upper troposphere,[27] positive contributions through vertical transport could exist.

If a point in space is considered not at the surface, then gas phase destruction is a process which dominates the destruction term. The predominant reactions are second-order; that is, the reaction of ozone with one other gas. This can be expressed mathematically by the following expression:

$$D = \sum_{n} k_n \Psi_n O_3 \tag{6}$$

where

k_n is the rate constant,

Ψ_n is the concentration of destructive agents, and

n is the index of summations since there is more than one destructive agent for ozone.

It is assumed that the concentration of destructive agents is independent of time. This assumption severely limits the quantitative results, but it should allow reasonable qualitative results and also greatly simplifies the mathematics. Based on this assumption, a pseudo-first-order rate constant can be defined such that

$$K_o = \sum_n k_n \Psi_n \, , \tag{7}$$

where

K_o is the first-order rate constant.

Therefore, the resultant expression for the destruction term is

$$D = K_o \, O_3 \; . \tag{8}$$

Figure 63 shows the average daytime variability of the magnitude of the synthesis and of the (vertical) transport term in equation of continuity for ozone determined from data collected by Jeffries[28] in a rural North Carolina boundary layer near the surface. Jeffries data have been smoothed and normalized to produce the curves in figure 63. At night (2100 to 0800 EST), the synthesis term is 0 and the magnitude of the transport term was relatively small. The nighttime value of the transport term was subtracted from the data to produce a system governed by destruction at night in order to simplify the mathematics. Generally, the nighttime behavior of ozone is governed by destruction, although some vertical transport exists.[29]

Both the transport and synthesis terms begin to increase after 0800 EST, reach a maximum at 1500 EST, and return again to zero at 2100 EST. Figure 63 also contains a truncated Fourier series made up of the mean value and one harmonic. The Fourier series preserves the initial time and the time of maximum for both the transport and synthesis terms, but the evening minimum occurs 1 hour later (2200 EST). The truncated Fourier series represents the variations observed by Jeffries reasonably well and will be used as a mathematical representation of the daytime contribution for both the transport and the synthesis term to the diurnal variation of ozone.

Therefore, the continuity equation, which governs the daytime behavior of ozone and which is valid from $t = t_o$ to $t_o = t_o + T$, is

$$\frac{\partial O_3}{\partial t} + K_o O_3 = A \{1 - \cos [\omega (t - t_o)]\} \; . \tag{9}$$

The equation governing nighttime behavior of ozone, which is valid from

$t = t_o + T$ to t_o, is

$$\frac{\partial O_3}{\partial t} + K_o O_3 = 0 \; ; \tag{10}$$

where $A = a + b$, a is the amplitude of the transport term, b is the amplitude of the synthesis term, $\omega = 2\pi/T$, and is the frequency for synthesis and/or transport, T is the period for both the transport and the synthesis term, and t_o is the initial time for both the synthesis and transport term and in the applied sense, can be considered the time of minimum ozone. The righthand side of equation 10 is zero because at night the synthesis term is zero and the vertical transport term is negligible. Under conditions $a > b$, $b > a$, or $a = b$, the qualitative behavior of equation 9 will be unchanged, provided the period is the same for both the synthesis and the transport terms.

The solutions of the equations 9 and 10 were found subject to the following boundary conditions:

$$\begin{array}{ll} O_3 = 0 \text{ at } t = t_o & \text{for equation 9,} \\ O_3 = O_{3E} \text{ at } t = t_o + t & \text{for equation 10,} \end{array} \tag{11}$$

where O_{3E} is the value of O_3 at $t_o + T$ and is obtained from the solution of equation 9. These boundary conditions deal with variations observed in the lower boundary layer only.

The solution to equation 9 under the boundary condition is:

$$O_3 = \frac{A\lambda}{\omega} \{1 - \lambda_o \cos [\omega(t - t_o) - \theta]\} \; . \tag{12}$$

$$\lambda = \omega/K_o, \; \lambda_o = (\lambda^2 + 1)^{-1/2}, \text{ and } \theta = \arctan(\lambda).$$

The above solution is valid under the condition that $t > t_o$ (for example, t = time of maximum synthesis and/or transport). According to equation 12, ozone is a maximum when the argument of the cosine is pi (π). The time of maximum ozone (t_{max}) is defined by the following formula:

$$\sim \omega(t_{max} - t_o) - \theta = \pi$$

or (13)

$$t_{max} = t'_{max} + \delta$$

where

$t'_{max} = t_o + 0.5\ T$ which is the time of maximum transport and/or synthesis,

$\delta = \theta/\omega$ which is the difference between the time of maximum ozone and the time of maximum transport and/or synthesis.

Figure 64 shows the variations of δ with λ for periods $T = 10$ hours, $T = 12$ hours, and $T = 14$ hours. Variations in the period are due primarily to durations of daylight and represent seasonal influences. The figure shows that when $\lambda = 0$, $\delta = 0$. Since T is finite and greater than zero, ω is finite and greater than zero. Therefore, if $\lambda = 0$ ($\lambda = \omega/K_o$), K_o must be infinite which requires an infinite concentration of destructive agents since the rate constants are finite. As λ approaches infinity, δ approaches a maximum value which depends on the period. K_o must approach zero or the concentration of destructive agents approaches zero in order for λ to approach infinity. These results indicate that if large amounts of ozone-destructive agents are present, the time of maximum ozone approaches the time of maximum synthesis and/or transport. However, if the concentration of ozone destructive agents is small, there will be a lag between the time of maximum ozone and the time of maximum synthesis and/or transport with the time of maximum ozone occurring later in the day.

Figure 65 gives theoretically derived concentrations of NO, NO_2, and α-pinene as a function of δ for various values of T, using data in figure 64. These concentrations were computed under the assumption that the particular gas was the only available ozone-destructive agent. Though the specific values of the concentrations computed are unreliable due to the simplifications made, it is believed that the order of magnitude may be reasonable. This point will be clarified later. The figures show that NO must be of

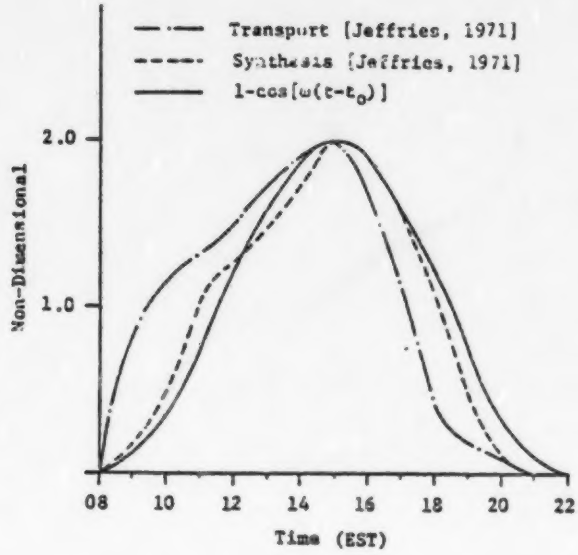

Figure 63. The diurnal variation of the transport and synthesis term in a rural boundary layer in North Carolina.

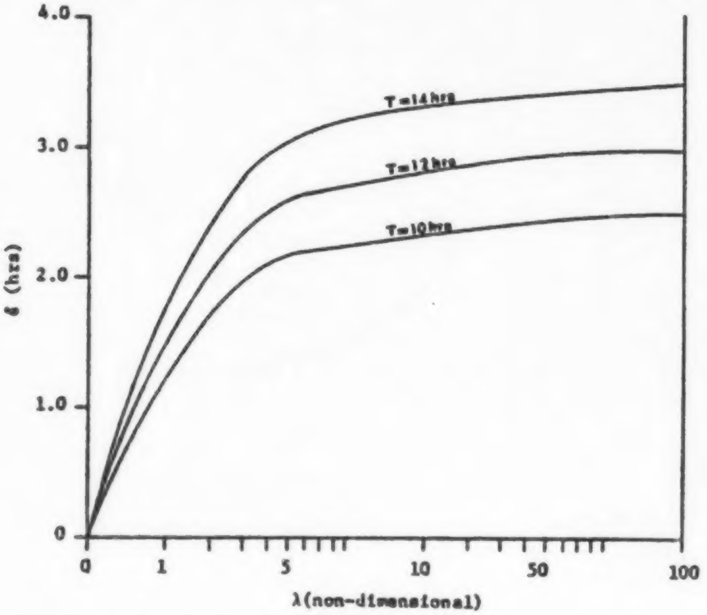

Figure 64. The variation of δ versus λ.

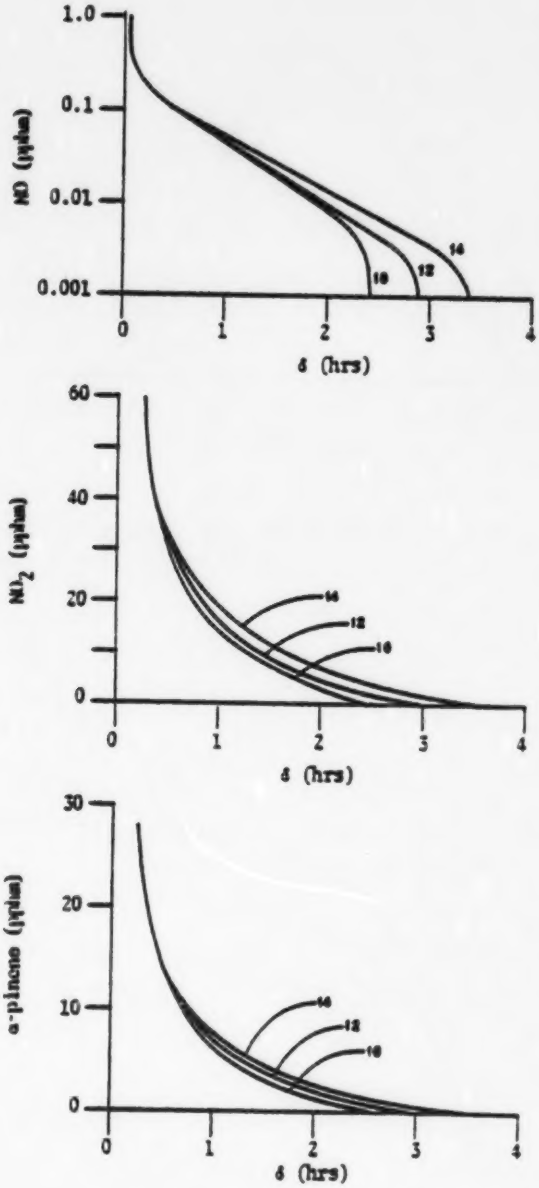

Figure 65. The variation of the concentrations of NO, NO_2, and α-pinene versus δ for various values of T.

the order of 0.07 to 0.006 pphm to produce δ's of the order of 1 hour to 3 hours, respectively; NO_2 must be of the order of 17 pphm to 2 pphm; and α-pinene must be of the order of 14 pphm to 1 pphm. The data indicate that extremely small and normally undetectable changes in the NO concentration can produce large differences in δ. However, large and detectable changes in the concentration of both α-pinene and NO_2 must occur in order to produce similar changes in δ.

According to equation 12, the maximum concentration of ozone at t_{max} (that is, when the argument of the cosine is equal to π) is given by the following formula

$$O_{3max} = \frac{A\lambda}{\omega}\,[1 + \lambda_o] \;. \tag{14}$$

Consider two regimes, which are defined by the following set of parameters.

REGIME #1	REGIME #2	
$O_3^* = O_{3max}$ in #1	$O_3^{**} = O_{3max}$ in #2	
$t^* = t_{max}$ in #1	$t^{**} = t_{max}$ in #2	
A^* = amplitude of synthesis and/or transport in #1	A^{**} = amplitude of synthesis and/or transport in #2	(15)
$\delta^* = \delta$ in #1.	$\delta^{**} = \delta$ in #2.	

If ω was identical in each regime, then the ratio of the maximum concentrations is given by

$$\frac{O_3^*}{O_3^{**}} = \alpha\beta \;; \tag{16}$$

where

$$\alpha = \frac{A^*}{A^{**}} \;, \tag{17}$$

and

$$\beta = \frac{\lambda^*}{\lambda^{**}}\,\frac{(1 + \lambda_o^{**})}{(1 + \lambda_o^*)} \tag{18}$$

The parameter, α, treats the differences in synthesis and/or transport in the two regimes, and β, the differences in the destruction in the two regimes.

Figure 66 yields the variation of β as a function of the differences in δ in the two regimes. The data generally show that for large differences in δ, with the δ in regime #1 greater than the δ in regime #2, β is much greater than 1. For example, if $\delta^* = 3$ hours and $\delta^{**} = 1$ hour, $\beta = 6.7$. This suggests that in the comparison of two regimes, one having smaller concentrations of ozone destructive agents than the other, the regime having the small concentration of ozone destructive agents has the potential to allow the achievement of a larger maximum ozone concentration. Whether or not the regime with the small concentration of ozone-destructive agents actually produces a larger maximum ozone concentration will depend on the parameter, α.

The solution to equation 10, the governing equation for the nighttime behavior of ozone, is

$$0_3 = 0_{3E} \exp \left[- K_o (t - t_o) \right] \ . \tag{19}$$

The expression for 0_{3E} is determined from equation 12 and is the value of equation 12 at $t = t_o + T$; that is,

$$0_{3E} = \frac{A\lambda}{\omega} \ \frac{\lambda^2}{\lambda^2 + 1} \tag{20}$$

The value of the ozone concentration at the end of the diurnal cycle (0_{3o}) was calculated using equation 19. The results are expressed in terms of the ratio $0_{3o}/0_{3max}$; that is,

$$\frac{0_{3o}}{0_{3max}} = \frac{(\lambda^2/\lambda^2 + 1)}{1 + \lambda_o} \exp \left[- K_o \Delta t \right] \ , \tag{21}$$

where Δt is the time interval over which equation 10 is valid.

Figure 67 yields the variations of the ratio $0_{3o}/0_{3max}$ as a function of δ and T. The data indicate that for small values of δ, or large concentrations of destructive agents, the concentration of ozone at the end of

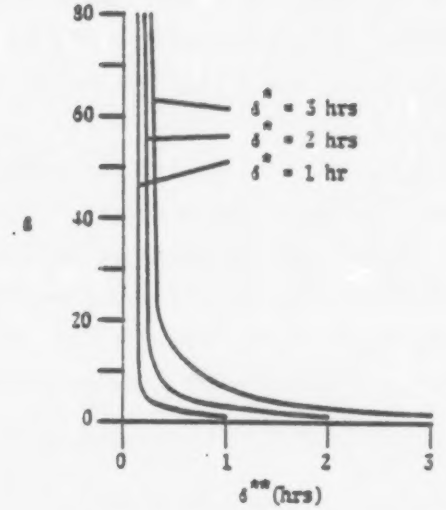

Figure 66. The variation of β versus δ^* and δ^{**}.

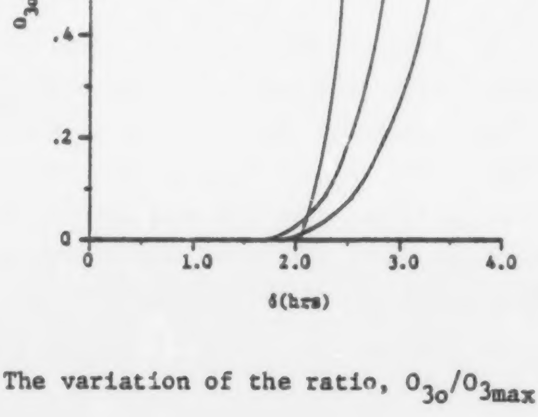

Figure 67. The variation of the ratio, O_{3o}/O_{3max} versus δ.

the diurnal cycle is zero. However, for large values δ, or small concentrations of destructive agents, a residual ozone concentration will remain at the end of the diurnal cycle. It appears that $\delta = 2$ hours is the critical value. It should be noted that the actual amount of the residual will depend on the value of O_{3max}.

Due to the assumptions required to linearize governing equations for the diurnal behavior of ozone, the resulting model is an oversimplification of ozone behavior. However, though the quantitative results stemming from this modeling effort are unreliable, it is believed that the qualitative results are reasonable. The results of the model effort will now be applied to examine the chemistry of ozone in high pressure systems.

7.2.5.2 Variation of the Diurnal Cycle of Ozone in a Moving High Pressure System

The synoptic surface weather data for the period 4 July through 30 September 1975 were examined to determine when a high pressure system moved out of Canada and passed consecutively over Wolf Point, Montana; Creston, Iowa; and Bradford, Pennsylvania. During the period, eight such systems were found. At each of these locations, the diurnal ozone distributions were examined during the period the high pressure system was in the vicinity of the station, and the day having the largest diurnal maximum ozone concentration for each system was used to compute the average diurnal variation over all eight systems. Figure 68 shows the results of the computations. As the high pressure system moved through Wolf Point and Creston to Bradford, the ozone concentration increased. The percent of increase was greater between Creston and Bradford than between Wolf Point and Creston. It is noted again that only at Bradford was the ozone concentration about equal to the NAAQS.

Table 29 summarizes some of the significant data in figure 68. The t_{max} at Wolf Point and Creston are identical, but the t_{max} at Bradford is 3 hours earlier in time. Assuming that the time of maximum transport and/or synthesis are identical and that this time is near the time of maximum solar radiation (t'_{max} = 1400 LDT), the data indicate that there were larger concentrations of ozone destructive agents at Bradford (δ = 1/2 hr) than at either Creston or Wolf Point (δ = 3 1/2 hrs.).

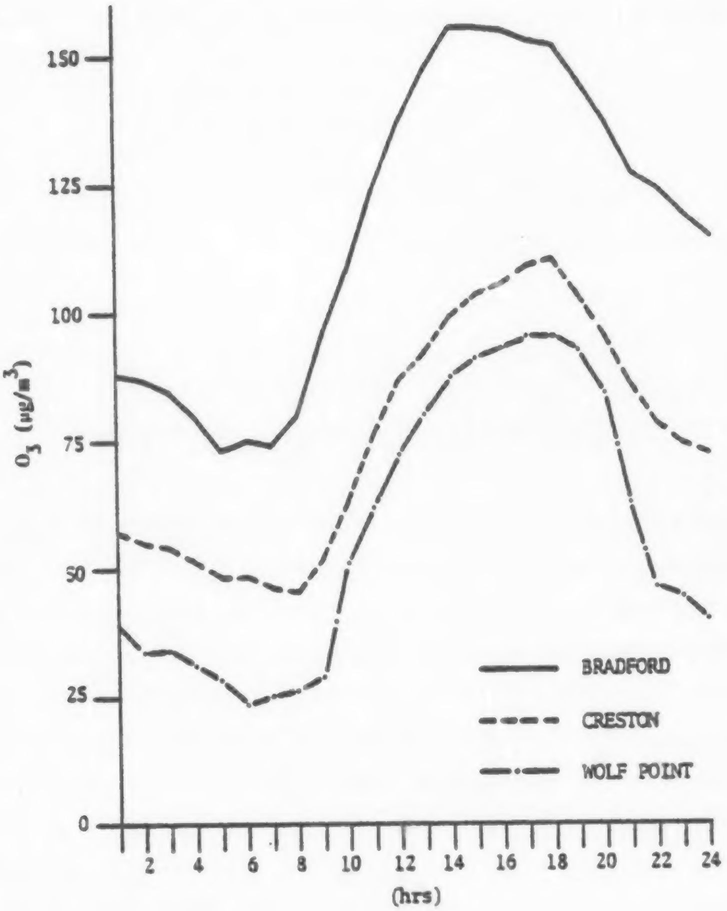

Figure 68 . The average diurnal variation of ozone concentration at Wolf Point, Creston, and Bradford based on eight high pressure systems which consecutively passed through these stations. The day with the largest diurnal maximum ozone concentration, when the high pressure system was in the vicinity of the station, was used to compute the average for all eight systems.

Table 29. The values of t_{max}, O_3*/O_3** (where O_3* is Wolf Point ozone amplitude in all cases), β (estimated from t_{max} and letting t'_{max} = 1400 LDT), α, diurnal ozone amplitude (diurnal maximum ozone minus diurnal minimum ozone), and the diurnal minimum ozone concentration for Wolf Point, Montana, Creston, Iowa, and Bradford, Pennsylvania obtained from the diurnal curves given in figure 68

STATIONS	t_{max}	O_3^{*}/O_3^{**}	β	α	Ozone Amplitude (μg/m^3)	Diurnal Minimum (μg/m^3)
Wolf Point	1730 MDT	1.0	1.0	1.0	71	24
Creston	1730 CDT	1.1	1.0	1.1	65	45
Bradford	1430 EDT	0.85	20.0	0.04	83	73

Table 29 also gives the values of the ratio O_3*/O_3** where Wolf Point was considered to be Regime #1 in each case, estimates of β based on values of δ (computed using the values of t_{max} and assuming a value of 1400 LDT for t'_{max}) and on data in figure 66, and the computed values of α. The ratio O_3*/O_3** was computed using the ozone amplitude (maximum minus minimum) in this case and in all following cases because the theory requires that the initial value of ozone is zero. This requirement can be satisfied by subtraction of the minimum ozone concentration. The calculations indicate that the amplitude of synthesis and/or transport at Creston and Wolf Point are identical; however, for Bradford the amplitude is considerably larger. Since available meteorological evidence does not support a larger vertical transport when the high pressure system was in the eastern portion of the United States than in the western portion, the ratio α must treat only amplitudes of tropospheric synthesis.

These data indicate that as the high pressure system moves from the western portions of the United States to the eastern portions, there is a marked change in the local ozone chemistry. Both destruction and synthesis of ozone are larger when the high pressure system is in the eastern portions of the United States. This supports the notion that there is widespread injection of ozone precursors, and apparently ozone-destructive agents also, in the east.

Table 29 also presents the amplitude of ozone (maximum ozone concentration minus minimum ozone concentration) and the minimum ozone concentration for each of the three stations. These data indicate that though there is a larger synthesis of ozone at Bradford, the amplitude of ozone is not much different than at Creston and Wolf Point. This is due to the increased (decreased) ozone destruction at Bradford (Wolf Point and Creston). The overall increase in ozone appears to be due to a buildup of the minimum ozone concentration. Since theory indicates that a residual ozone concentration will be found at the end of a diurnal cycle when δ is of the order of two hours or greater, it is suggested that the small concentrations of ozone-destructive agents in air parcels in the west allowed a buildup of the minimum ozone concentrations as they drifted westward. (Nota Bene: an air parcel does not travel with a high pressure system across the United States. It would take the circulation associated with six simultaneous high pressure systems moving from Wolf Point through Creston and Bradford at a speed of 10 ms^{-1} to transport a parcel from Wolf Point to Bradford.) In the east, injection of ozone destructive agents reduced δ to less than 2 hours, and no further build-up of the minimum concentration was allowed.

7.2.5.3 Variation of Ozone Chemistry in a High Pressure System in the Eastern Portion of the United States

Figure 69A gives the average diurnal variation of ozone for days when the maximum ozone concentration exceeded the NAAQS and for the remaining days when it was less than the NAAQS at Kane, Pennsylvania, during August 1973. Table 30 summarizes pertinent data from figure 69A. The t_{max} for

Table 30. The values of t_{max}, O_3^*/O_3^{**} (O_3^* is the amplitude of ozone for the high ozone case), β (using t_{max} and letting t'_{max} = 1400 LDT), and α for Kane, Pennsylvania obtained from the 1973 diurnal curves given in figure 69

CASE	t_{max}	O_3^*/O_3^{**}	β	α
High Ozone	1630 EDT	1.0	1.0	1.0
Low Ozone	1430 EDT	1.59	9.6	0.19

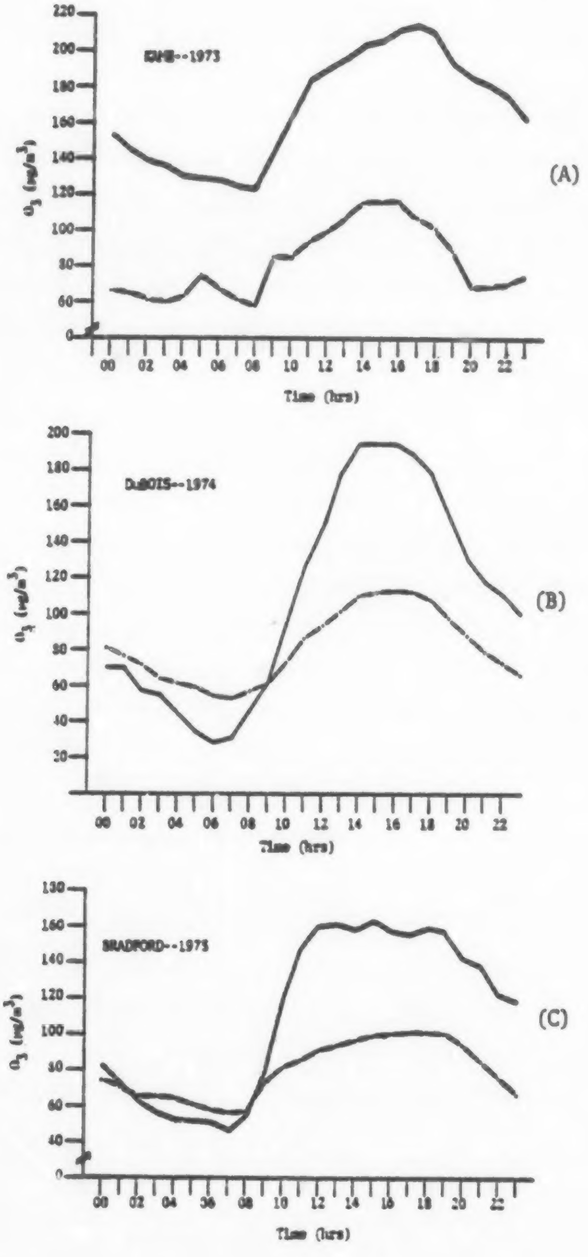

Figure 69. The average diurnal variation of ozone for those days when the diurnal maximum ozone concentration exceeded the NAAQS (solid line) and when the diurnal maximum was less than the NAAQS (dash-dot line) based on the data for August 1973(A), 1974(B), and 1975(C) and at Kane, DuBois, and Bradford, Pennsylvania, respectively

the high ozone curve (greater than the NAAQS) occurs later in the day than that for the low ozone curve. Assuming that t'_{max} = 1400 LDT, the data indicate that there were more ozone destructive agents on the days of low ozone (δ = 1/2 hr) than the days of high ozone (δ = 2 1/2 hrs). Also shown in the table is the ratio O_3*/O_3** where the high ozone curve was Regime #1, estimates of β, and the computed value of α. These data indicate that there was considerably more synthesis of ozone (vertical transport being ruled out) on days of low ozone than days of high ozone. The small concentrations of ozone destructive agents on days of high ozone versus days of low ozone is further supported by the fact that the minimum value on high ozone days is considerably greater than the minimum value on low ozone days (see figure 69A).

Figure 69B yields data similar to figure 69A except these data were obtained at DuBois, Pennsylvania in August 1974. Table 31 summarizes the pertinent data in the figure. The t_{max} for the low ozone curve occurred later in the day than for the high ozone curve which indicates more ozone destructive agents on days of high ozone than on days of low ozone. This is further supported by the fact that the minimum concentration for the high ozone curve is less than the minimum concentration for the low ozone curve (see figure 69B). Table 31 also gives the values of the ratio O_3*/O_3**, estimates of β, and the computed value of α. Results indicate that the synthesis of ozone was greater on days in which the ozone was high than days when the ozone was low. This is a complete reversal of the role of destruction and synthesis found in 1973.

Table 31. The values of t_{max}, O_3*/O_3** (O_3* is the amplitude of ozone for the high ozone case), β (using t_{max} and letting t'_{max} = 1400 LDT), and α for DuBois, Pennsylvania obtained from the 1974 diurnal curves in figure 69

CASE	t_{max}	O_3^*/O_3^{**}	β	α
High Ozone	1430 EDT	1.0	1.0	1.0
Low Ozone	1530 EDT	3.36	0.33	10.3

Figure 69C yields data identical to figure 69A, except in this case the data were collected at Bradford, Pennsylvania, in August 1975. Table 32 summarizes the pertinent data in the figure. As in the case of the 1974 data, the low ozone curve has a t_{max} that occurs later in the day than the high ozone curve, which indicates that the concentration of ozone destructive agents was greater on days of high ozone than on days of low ozone. That there were larger concentrations of ozone destructive agents on days having high ozone is supported by the fact that the minimum value on days of high ozone is smaller (see figure 69C). Also shown in table 32 is the value of the ratio O_3*/O_3**, the estimated value of β, and the computed values of α. In this case as in the case of 1974, the synthesis of ozone was greater on days having high ozone concentration than on days having low ozone concentration. These data, too, show a complete reversal of the role of destruction and synthesis found in 1973.

Table 33 summarizes pertinent data from figures 69A, B, and C using the high ozone curve only. The t_{max} for 1973 occurs later in the day than that for 1974 and 1975, indicating larger concentration of ozone destructive agents in 1974 and 1975. The calculated values of α indicate that synthesis of ozone was greater in 1974 and 1975 than in 1973. The amplitude of ozone supports the contention that there was greater synthesis of ozone in 1974 and 1975 than in 1973. The data also show that the high ozone in 1973 is basically a result of having a large minimum concentration of ozone. The large minimum concentration of ozone is due to the lack of a large concentration of ozone destructive agents, and suggests that in 1973 minimum value

Table 32. The values of t_{max}, O_3*/O_3** (O_3* is the amplitude of ozone for the high ozone case), β (using t_{max} and letting t'_{max} = 1400 LDT), and α for Bradford, Pennsylvania obtained from the 1975 diurnal curves in figure 69

CASE	t_{max}	O_3^*/O_3^{**}	β	α
High Ozone	1430 EDT	1.0	1.0	1.0
Low Ozone	1630 EDT	2.64	0.1	26.4

Table 33. The values of t_{max}, O_3*/O_3** (when O_3* was the amplitude of ozone in 1973 in all cases), β (using t_{max} and letting t'_{max} = 1400 LDT), α, the diurnal amplitude of ozone (ozone maximum minus the ozone minimum), and the diurnal minimum ozone concentration for the high ozone cases in 1973, 1974, and 1975 from figures 69A, B, and C

YEAR	t_{max}	O_3^*/O_3^{**}	β	α	Ozone Amplitude (μg/m^3)	Minimum Ozone (μg/m^3)
1973	1630 EDT	1.0	1.0	1.0	92	123
1974	1430 EDT	0.55	9.6	0.04	168	28
1975	1430 EDT	0.77	9.6	0.08	119	46

continued to increase in the eastern portions of the United States. Though the 1975 data (figure 69) indicated that there is a buildup of the diurnal minimum ozone concentration in the West, the buildup ceased in the East where air parcels in the system had acquired larger concentrations of ozone destructive agents. The smaller concentrations of ozone destructive agents, the smaller value of the synthesis term for ozone, and the larger number of hours of high pressure in the eastern portions of the United States suggests that the ozone system in 1973 may have been a spent system; that is, the high pressure systems in 1973 were relatively stagnant compared to those in 1974 and 1975, and the ozone precursors and ozone destructive agents were depleted as a result of the large number of diurnal processes experienced.

Figures 70A and 70B show the average diurnal variation of ozone on days of high ozone and on days of low ozone at Lewisburg, West Virginia, in August 1973 and 1975, respectively (1974 data are not available for this station). Tables 34, 35, and 36 summarize the pertinent data from these figures. Though specific factors on the year-to-year variation of high and low ozone do not coincide exactly with those found at the Pennsylvania stations, these data do show that there were greater synthesis and larger concentrations of ozone destructive agents on high ozone days in 1975 than in 1973, and that the minimum ozone concentration in 1973 was almost three

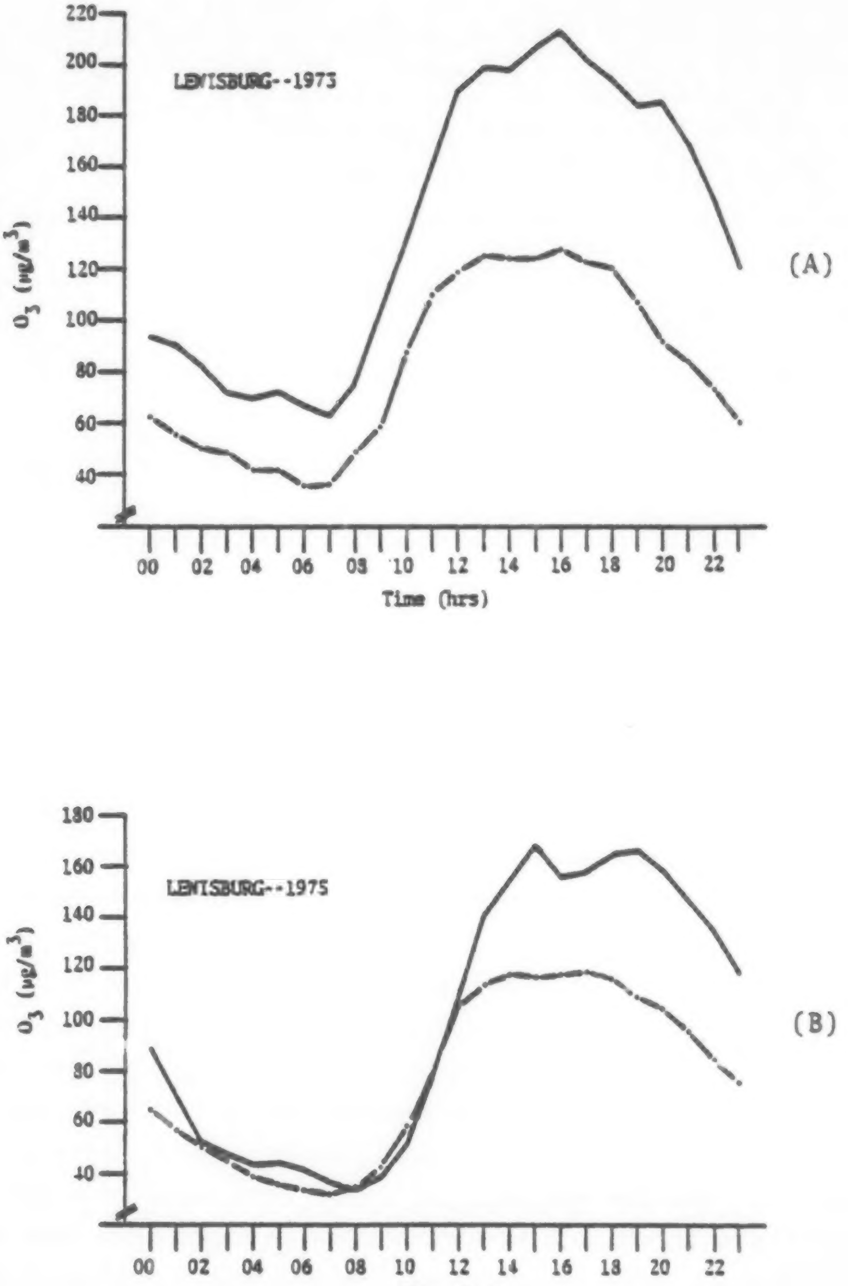

Figure 70. The average diurnal variation of ozone at Lewisburg, West Virginia for those days when the diurnal maximum ozone concentration exceeded the NAAQS (solid line) and when the diurnal maximum was less than the NAAQS (dash-dot line) based on data for August 1973(A) and 1975(B).

Table 34. The values of t_{max}, O_3*/O_3** (where O_3* is the amplitude of ozone in the high ozone case), β (using t_{max} and letting t'_{max} = 1400 LDT), and α for Lewisburg, West Virginia obtained from the 1973 diurnal curves given in figure 70

CASE	t_{max}	O_3^*/O_3^{**}	β	α
High Ozone	1530 EDT	1.0	1.0	1.0
Low Ozone	1530 EDT	1.8	1.0	1.8

Table 35. The values of t_{max}, O_3*/O_3** (where O_3* is the amplitude of ozone in the high ozone case), β (using t_{max} and assuming t'_{max} = 1400 LDT), and α for Lewisburg, West Virginia obtained from the 1975 diurnal cirves given in figure 70

CASE	t_{max}	O_3^*/O_3^{**}	β	α
High Ozone	1430 EDT	1.0	1.0	1.0
Low Ozone	1630 EDT	1.5	0.1	15.0

Table 36. The values of t_{max}, O_3*/O_3** (where O_3* was the amplitude of ozone in 1973 in all cases), β (using t_{max} and letting t'_{max} = 1400 LDT), α, the diurnal amplitude of ozone (maximum ozone minus minimum ozone), and the diurnal minimum ozone concentration for the high ozone cases in 1973 and 1975 from figures 70A and 70B

YEAR	t_{max}	O_3^*/O_3^{**}	β	α	Ozone Amplitude (μg/m^3)	Minimum Ozone (μg/m^3)
1973	1530 EDT	1.0	1.0	1.0	148	64
1975	1430 EDT	1.02	3.0	0.34	144	24

times larger than in 1975. This suggests that the change in mechanisms between 1973 and 1974 or 1975 was not a localized phenomena in Pennsylvania but was widespread.

Table 37 contains the average maximum concentration of NO_2 found in the period between the time of maximum ozone and midnight of the same day, using data for August 1974 at DuBois and 1975 at Bradford (NO_2 data were not available at Kane in 1973). The average NO_2 data represent only days when the maximum diurnal ozone concentration exceeded the NAAQS. Comparison of these concentrations with the data in figure 65 suggests that NO_2 alone could not be responsible for the shift of t_{max} from late afternoon to mid-afternoon between 1973 and 1974 or 1975.

The NO concentrations given in the table were computed assuming a three-gas system containing O_3, NO and NO_2 in which NO_2 is produced through the reaction of NO with O_3. The concentrations of NO are based on the values of NO_2 given in the table which are the maximum concentrations [that is, the local rate of change of NO_2 is zero ($\partial NO_2/\partial t = 0$) when the concentration of NO_2 is a maximum]. The order of magnitude of the computed concentration of NO compares well with that required to produce a δ of the order of 2 hours or more, according to figure 65.

For NO to account for most, if not all, of the destruction of ozone between the time of maximum ozone and the time of minimum ozone (approximately 80 percent of the maximum concentration of ozone was destroyed in

Table 37. The average maximum concentration of NO_2 found between the time of maximum ozone and midnight using only the data on high ozone days for August 1974 at DuBois, Pennsylvania and in 1975 at Bradford, Pennsylvania; and the computed NO concentration at the time of maximum NO_2 assuming a three-gas system (NO, NO_2, and NO_3)

YEAR	NO_2 (pphm)	NO (pphm)
1974	1.0	.004
1975	0.5	.002

that period according to the 1974 and 1975 data, and on the average the maximum concentration of ozone was approximately 10 pphm) would require a continuous injection of NO to replenish that destroyed if NO were at the small concentrations indicated in table 37. The reaction of NO with ozone would produce NO_2 one-for-one for each reaction. The 1974 and 1975 data suggest that approximately 8 pphm of NO_2 should be found some time in the period during which the ozone is being destroyed. Since the observed concentrations of NO_2 were never much more than 1 pphm, it must be concluded that either reaction with NO is not the mechanism by which ozone is being destroyed or that NO_2 is being removed almost as fast as it is being produced Data do not exist from the field programs accomplished over the 3 years to discriminate which condition is real.

There is, of course, the question of whether the requirement that NO is replenished by continual injection, presumably from the surface, could be satisfied. If it were not, this would lend support to the notion that the ozone is destroyed through reactions with gases other than NO. Again, this is a point which could not be resolved with available data. However, since the required concentrations of NO appear to be very small (the order of 1/100 ppb), it is certainly possible that continual injection of NO could replenish such small concentrations.

7.2.6 Summary of Northern High Pressure Analysis

Many of the results obtained in the preceding analysis were based on a comparison between the results of a linearized mathematical model which demonstrated the diurnal behavior of ozone and observed data in various rural regions of the United States. The model mainly treated the mechanisms synthesis and destruction of ozone, with no regard for the vast number of chemical processes required to produce, accumulate, and destroy ozone. The amplitude of synthesis treated the production of ozone, and the parameter λ treated the existing concentration of ozone destructive agents. Because of the assumption made in the model, specific numerical values are unreliable. However, application of the model results was in the domain of comparison between two ozone regimes using observed data. In the relative sense (e.g., stating one regime has more ozone destructive agents than another regime), these results are believed to be reliable. Furthermore, some of the explicit results determined by applying model results with observed data could have just as easily been determined by deductive reasoning. The use of the model simplified this effort.

One important assumption made in applying modeling results with observed data was that the time of maximum synthesis (t'_{max}) was near the time of maximum solar radiation. The absolute rate of synthesis is closely related to the interactions between solar radiation and NO_2. Since observed diurnal variations of the NO_2 in rural regions[4] show that NO_2 varies by about 10 to 20 percent of its mean value, and the mean value is approximately 1 pphm or less, this suggests strongly that the time of maximum synthesis is related to the time of maximum solar radiation.

The data presented support the premise that high ozone (ozone concentrations in excess of the NAAQS) found in the summer months is associated with high pressure systems. The data further indicate that sustained periods of high ozone are associated with a macroscale high pressure system having periods greater than 20 days. The largest concentrations of ozone were found on the back side of a moving high pressure system, and a relative minimum was found on the front side or near the center when the system was in the Midwest and East. The location of the maximum and minimum concentration of ozone in a moving high pressure system correlated with the location of air having maximum and minimum residence time in that system; that is, largest concentrations of ozone occurred on the back side of a high pressure system where air parcels had the largest residence time, and the smallest concentration of ozone was found in the front side of the system where the air parcel had the smallest residence time. For an eastward moving high pressure system whose speed is of the order of 5 m/s or more, the air initially in the northeastern quadrant of that system will have large residence times.

The data from the stations in the western portions of the United States did not display a preference for high ozone in the back side of the high pressure system. This suggested that a mechanism which increases the ozone concentrations in air parcels was enhanced as they moved from the west to the east. Meteorological analysis did not reveal any reason why, on the average, downward transport in high pressure systems, either by the general subsidence or by enhanced vertical mixing, should increase the ozone concentration in the back side of the system. Low-level divergence and downward motions are usually greatest near the center or in the front side of an eastward moving high pressure system. Furthermore, available aircraft data showed no evidence that, on the average, the vertical gradient of ozone through the troposphere is greater in the eastern portions of the United States than in the western portions so that this factor could not be responsible for enhanced transport. It can only be concluded that transport of ozone was not the mechanism creating the larger concentrations on the back side of the high pressure system, leaving enhancement of the synthesis of ozone as the potential mechanism.

Examination of the change in the diurnal variation of ozone using the linearized model and the 1975 data indicated that both the concentration of destruction agents and the synthesis of ozone were larger when the high pressure system was in the East than in the West. This suggested that the concentration of ozone precursors and ozone destructive agents (often ozone precursors and ozone destructive agents are identical) were larger when the system was in the east than in the west. The number of industrial complexes and population centers is considerably larger in the East, suggesting that the source of the ozone precursors and destructive agents is anthropogenic. Ozone concentrations were highest on the back side of a high pressure system, where air parcels had the largest residence time. This suggests that synthesis of high ozone requires sufficient time for injection of sufficient amounts of ozone precursors in the system where proper environmental conditions exist.

Even though there was a significant increase in synthesis when the high pressure system was in the East, the amplitude of the diurnal curve for ozone in the East was not significantly greater than that in the West. This is thought to be a result of the increased destruction of ozone. The larger maximum ozone concentration found when the high pressure system was in the east was a result of a diurnal minimum ozone concentration. The data combined with the modeling results indicated that the diurnal minimum could be increased due to the small concentrations of ozone destructive agents in local air parcels in the western portions of the United States. The negligible ozone destruction will allow ozone residuals to exist at the end of a diurnal cycle which can "pump up" the level of minimum ozone concentrations as these air parcels drift eastward. (Nota Bene: air parcels do not move with high pressure systems since their residence time is much less than the period of the system. See section 7.2.4.) The data further indicate that the apparent injection of ozone destructive agents into the system in the East should prevent further build-up of minimum concentrations. The building up of the level of the diurnal minimum ozone concentration and the diurnal synthesis of ozone were sufficient to produce ozone concentrations in excess of the NAAQS in high pressure systems located in the East.

The evidence further indicates that there has been a reversal of the role of synthesis and destruction of ozone in high pressure system located in the East from 1973 to 1974 and 1975. Smaller concentrations of ozone destructive agents in 1973 allowed a larger build-up of the level of the diurnal minimum ozone concentration and were influential in producing a reasonable diurnal amplitude for ozone (the maximum ozone concentration minus the minimum ozone concentration). These two factors combined to produce diurnal maximum ozone concentrations in the boundary layer in excess of the NAAQS. In 1974 and 1975, the concentration of ozone destructive agents was considerably larger such that the level of the minimum was somewhere between one-half and one-fourth that found in 1973. However, there was a marked increase in the synthesis of ozone in 1974 and 1975 compared to 1973, which produced ozone in excess of the NAAQS. The maximum value of ozone and the number of hours of high ozone in 1973 were greater than that found in 1974 and 1975, suggesting that the mechanism of producing a very high level for the diurnal minimum ozone concentration was more important in terms of producing a greater number of hours [this was not only true for the Pennsylvania stations, but Lewisburg, West Virginia, also had a greater number of hours of high ozone in 1973 (156 hrs) than in 1975 (26 hrs)] and larger concentrations of high ozone.

The summer of 1973 was characterized by having the largest total number of hours of high pressure and the largest total number of hours of high ozone in the east, compared with that of 1974 and 1975. Some of these high pressure systems became relatively stationary. In particular, one high pressure system remained stationary in the East for approximately 14 days in August. Long periods of relatively stagnant conditions would allow air parcels within the high pressure system to have large residence times and to experience many diurnal ozone cycles increasing the level of the diurnal minimum and depleting the concentration of ozone precursors and ozone destructive agents. The results would be to produce a mean diurnal cycle for ozone similar to that obtained for high ozone days in 1973 (fig. 69A). However, this requires that the injection of ozone precursors and ozone destructive agents was not large enough to compensate for the depletion of these constituents. It may also be possible that the high level of ozone, both day and night, removed both NO and NO_2 (where NO is an important destructive agent, and NO_2 is not only a destructive agent, but also an important ozone precursor) after it was injected into the system without markedly affecting the ozone concentration.

An alternative hypothesis to that dealing with differences in high pressure systems, which might explain the differences in 1973 compared to 1974 and 1975, is that there was an increase in the injection of ozone destructive agents from anthropogenic sources in 1974, and a further increase in 1975. This hypothesis would explain the systematic decrease in the value of the diurnal maximum ozone concentration and the decrease in the total number of hours of high ozone. Data were not available to examine this hypothesis completely.

The results of the analysis are highly indicative of the nature of ozone behavior in a rural boundary layer and in the presence of a high pressure system. However, since many of the results of the analysis are based on a simplified and unvalidated mathematical model, they are not conclusive. It is suggested that in the future, a more sophisticated mathematical model, which describes the ozone chemistry in considerably more detail, be used to test some of the hypothesis concerning the synthesis and destruction of ozone made in this analyses. It is further recommended that the results of the more sophisticated mathematical model be used as a guideline for a limited number of chamber experiments to validate the mathematical model. It is only in this manner that the chemistry of ozone in the rural boundary layer and in the presence of a high pressure system can be completely understood.

7.3 Chemistry of Ozone Generation

In the 1950's, many writers spoke of the "smog barrier." This was the point at which emission of pollutants to the air or concentration of pollutants in the atmosphere was presumed to reach such a level as to produce the symptoms of photochemical smog.

Today, 20-odd years later, a satisfactory three-dimensional characterization has not been made of the conditions of precursor identity, concentrations, ratios, time, and physical environment needed to produce certain objectionable levels of photochemical smog. The inflection point which would locate the "smog barrier" has turned out to be more nebulous than earlier optimism would have imagined. With the 1975 summer data, however, a fairly clear verbal model and some quantitative limitation for the generation of high ozone concentrations in rural areas in the Midwest and Mid-Atlantic areas of the United States can be constructed.

As a result of data collected in the northern part of this study, an explanation of observed ambient ozone levels in high pressure systems was given in section 7.2. Within a high pressure system the ozone concentrations begin to drop after the passage of the leading front. After the frontal passage the ozone concentration drops to a minimum for that high pressure system, then begins to rise before the passage of the center of the high. The ozone concentration continues to rise to a maximum for the system in the backside of the high (i.e., western side of an eastward-moving high pressure system).

On the front side of the high, the air has been in the system usually less than a day. Theoretical treatment indicates that the air in the trailing side of the high has remained in the system 2 or more days and has moved from 0 to 160 km per day, depending on the speed of the high pressure system and the location of the air parcel at the beginning of the period of calculation.

Additionally, it was pointed out that in 1975, while approximately 95 percent of the hours of high ozone concentrations ($\geq 160\ \mu g/m^3$) occurred in a high pressure system regardless of the distance of the high pressure center from the station, only 12 percent of the hours of high pressure were associated with high ozone. This can be related to the fact that air on the backside of the high has had more time to accumulate ozone precursors and more reaction time for ozone to be generated and accumulated.

The probable chemistry of ozone generation as it relates to the movement of a high pressure system from the northern Great Plains, south of the Great Lakes, and on to the eastern seaboard can be explained in general terms.

In the western Plains area away from large cities like Denver there are few people and few precursor emissions. As a high pressure system moves through this area, the precursor concentrations tend to increase and with the extended period of limited ventilation (and therefore greater times of reaction) ozone concentrations will tend to increase. Seldom if ever, however, will the ozone concentrations reach the NAAQS. The key here is that the emission rates of precursors are not sufficient enough to allow the generation of high concentrations (i.e., ≥ 160 $\mu g/m^3$) of ozone.

Somewhere along a line drawn from Fargo, North Dakota, to Dallas, Texas, the population density (going from west to east) increases by nearly 16-fold (~13 to ~213 people per square mile) (tables 38, 39, and 40). Because of the increase in population density, there is a substantial increase in anthropogenic pollution emissions so that, under a high pressure system, the pollution emissions are sufficient enough and have time, occasionally, to concentrate and react to form net ozone concentrations equal to or surpassing the NAAQS.

At this point, the role of ozone in "spent" photochemical systems and of ozone left over from the previous day's generation should be described.

Table 38. Population density for States west of Fargo, N.D. → Dallas, Texas line*

States	Population	Density of Population (By Square Mile, 1970)	Area (Square Miles)
Montana	694,409	4.8	145,587
Wyoming	332,416	3.4	97,203
Colorado	2,207,259	21.3	103,766
North Dakota	617,761	8.9	69.273
South Dakota	666,257	8.8	75,955
Nebraska	1,483,791	19.4	76,483
Kansas	2,249,071	27.5	81.787
Total	8,250,964		
Average Density	12.7		

*U.S. Bureau of the Census, Census of Population and Housing: 1970.

Table 39. Population density for states between Fargo, N.D. → Dallas, Texas line and east of Chicago, Illinois → St. Louis, Missouri line*

States	Population 1970 Census	Density of Population (By Square Mile, 1970)	Area (Sq. Miles) Land Area Only
Iowa	2,825,041	50.5	55,941
Missouri	4,677,399	67.8	68,995
Illinois	11,113,976	199.4	55,748
Total	18,616,416		
Average Density	103.0		

*U.S. Bureau of the Census, Census of Population and Housing: 1970.

Table 40. Population density for states east of Chicago, Illinois → St. Louis, Missouri line*

States	Population 1970 Census	Density of Population (By Square Mile, 1970)	Area (Sq. Miles) Land Area Only
Maine	993,663	32.1	30,920
New Hampshire	737,681	81.7	9,027
Vermont	444,732	47.9	9,267
Massachusetts	5,689,170	727.0	7,826
Rhode Island	949,723	905.0	1,049
Connecticut	3,032,217	623.7	4,862
New York	18,241,266	381.3	47,831
New Jersey	7,168,164	953.1	7,521
Pennsylvania	11,793,909	252.3	44,966
Ohio	10,652,017	260.0	40.975
Indiana	5,193,669	143.9	36,097
Michigan	8,875,083	156.2	56,817
Delaware	548,104	276.5	1,982
Maryland	3,922,399	396.6	9,891
Virginia	4,648,494	116.9	39,780
West Virginia	1,744,237	72.5	24,070
Kentucky	3,219,311	81.2	39,650
Total	87,853,839		412,531
Average Density	213.0		

*U.S. Bureau of the Census, Census of Population and Housing: 1970.

In an urban air pollution system there is continued input of ozone precursors, many of which are also ozone destructive agents (e.g., NO, alkenes) throughout the 24-hour day. In an urban area these ozone destructive agents frequently are produced in quantities sufficient enough to drive the ground-level ozone concentration to a measured zero at night. As a photochemical system moves out of the urban area, the rate of injection of fresh reactants decreases, and, when the reactant injection rate is relatively low enough, some ozone concentration is maintained overnight. Aloft, between the top of the previous day's mixing layer and the top of the ground-based radiation inversion, the ozone concentration is often higher than it is at the ground, since it is temporarily out of contact with sources of pollution at the ground. After the sun rises, the incident solar irradiation begins both to erode the radiation inversion, bringing higher ozone concentrations to the ground, and to initiate photochemical activity, which leads to ozone generation. Often, but not necessarily always, exceeding the NAAQS is a matter of de novo synthesis of only a relatively small amount of ozone, which, added to the ozone left in the air overnight, allows the atmospheric ozone concentration to reach or exceed the NAAQS.

7.3.1 Relationship of Ozone and Population Density

Consideration of the following data was instrumental in deriving the foregoing picture of the ozone behavior with the progression of a high pressure system from the northern Plains to the Atlantic Ocean.

The major objective around which the northern high pressure study was designed was that, under conditions of high pressure, ozone concentration is correlated with population density. Based on visual observation of a number of population maps, the study area was divided into three parts. This was done by drawing two lines, one from Fargo, North Dakota, to Dallas, Texas, and one from Chicago to St. Louis (fig. 71). The western area, containing Wolf Point, Montana, was the least populous (~13 persons mi^{-2}, table 38); the middle portion, containing Creston, Iowa, was intermediate in population density (~103 persons mi^{-2}, table 39); and the eastern portion containing Bradford, Pennsylvania, (~213 persons mi^{-2}, table 40) had the highest population density. Only the States over which the plane actually flew were considered in this analysis.

The ozone concentrations associated with the various stations and areas are presented in tables 41 and 42. Table 43 summarizes the ozone half-life information. Half-life was calculated from the 0200 to 0500 data, assuming a first-order decay rate. (A number of cases were not counted, those in which ozone concentration increased and several in which the $t_{1/2}$ was ~1700 hours.)

It is unlikely that the ozone destruction is entirely gas phase, and it is probable that fresh material injected into the air near the ground in addition to residual pollution left from the previous day has reacted with the ozone at night. Undoubtedly the air above the radiation inversion was less affected by ozone destruction. The numbers presented in table 43, however, do represent an upper limit for the destruction of ozone by residual

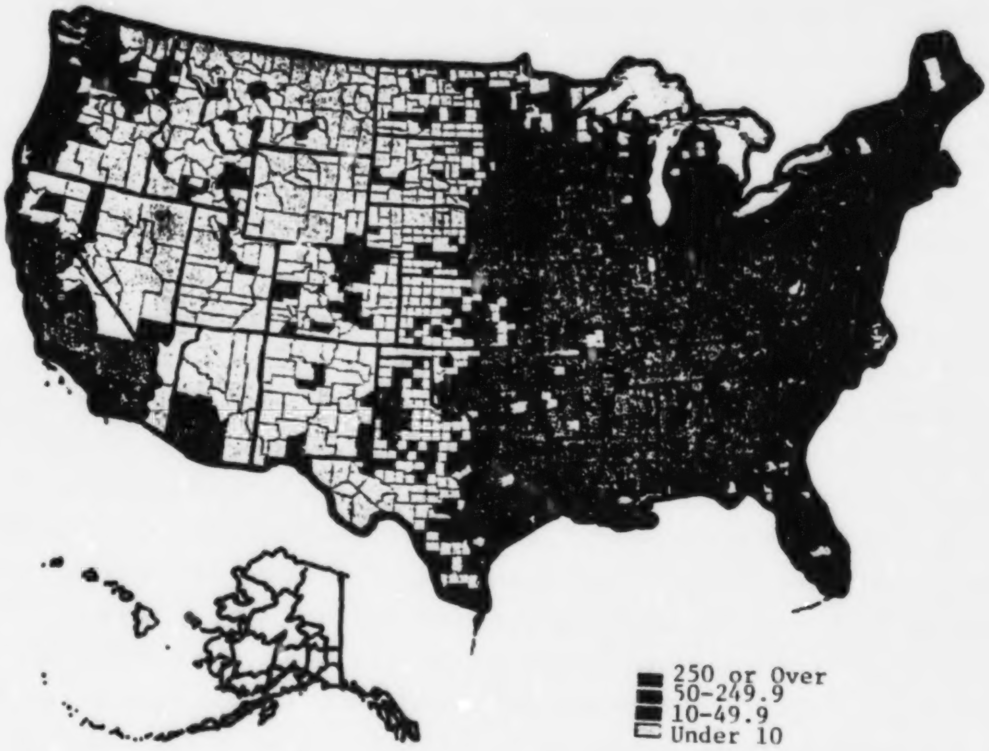

Figure 71. Population density by counties: 1970.

Table 41. Summary of ozone data for rural stations

Stations	Average O_3 μgm^{-3}	No. of Hours >160 μgm^{-3} June-September	Number of Hourly Samples
Wolf Point, Montana	57.6	0	2160
Creston, Iowa	70.4	17	2116
Bradford, Pennsylvania	81.4	100	2332

Table 42. Summary of aircraft ozone data for population density areas

Sample Area	Average O_3	No. of Samples >160 μgm^{-3}	Number of Individual Samples
Least Populous Area	68.0	3*	1429
Intermediate	88.0	0	578
Most Populous Area	105.8	95	1163

*These samples were taken between Sioux Falls and Sioux City almost on the Fargo-Dallas line.

Table 43. Dark phase ozone half life

Station	Half-Life Mean (hrs)	Std. Dev.	Range	Case Count
Bradford, Pennsylvania	13.1	15.2	2.8-75.9	65
Creston, Iowa	20.4	28.5	3.4-180.9	60
Wolf Point, Montana	15.4	15.9	3.6-70.7	61

gases from the day before. The actual half-lives calculated should at times allow enough ozone to remain overnight to furnish a significant base on which to build a concentration over the NAAQS the next day.

The concentration of O_3 occasionally increased from 0200 to 0500 LT. Since there was no sunlight to initiate photochemical reactions, this is an indication of the advection or movement of air containing high concentrations of ozone into the vicinity of the sampling site.

With minor variations the population density and pollution emission rates increase from the Great Plains to the Atlantic seaboard. In general, the farther east the more quickly the pollution concentration conditions which will generate concentrations of 160 $\mu g/m^3$ of ozone are achieved, so that both the average concentration of ozone and the frequency of exceeding the standard should increase. The data substantiate this reasoning.

The nature of the high ozone system in the midwest is that of an air mass characteristic rather than an urban plume or "ozone-shadow." Although the Bell Telephone interpretation[25/] shows a large urban effect of the New York Megalopolis, cities in other areas usually show only as perturbations in areawide systems, which extend upwind, downwind, and crosswind of the city. No individual area appears to be the sole source of the plume that trails across half the continent, but the air on the backside of the high pressure could have come from several areas from a few kilometers to a few hundred kilometers away.

The amount of ozone generated, as well as the concentrations of ozone generated, may depend more on the mass of injection of pollutant precursors (particularly NO_x) than on the concentrations of these materials at any given time. Thus, one might find that ozone concentration correlates better with population density than NO_x concentration correlates with either ozone or population density. Computer simulation shows that under some circumstances the same mass of precursors can generate higher concentrations of ozone with lower ambient concentrations of NO_x. Computer simulations were run with the following parameters: hydrocarbon at 0.25 ppmC; .071 ppm batch NO_x and .005 ppm initial NO_x ($NO + NO_2$) with an injection of .001 ppm m^{-1} for 660 min. (total 0.071 ppm NO_x calculated). The results are presented in table 44.

Table 44. Results of computer simulation runs

HC ppmC	Initial NO_x $(NO + NO_2)$ (ppm)	Rate Injection (ppm m^{-1})		Total NO_x (Calc.) (ppm)	Avg. NO_x (Conc.) (ppm)	Max. O_3 ppm
		[NO]	$[NO_2]$			
0.25	0.005	—	—	0.005	0.003	0.07
0.25	0.005	—	$1x10^{-4}$	0.071	0.023	0.17
0.25	0.005	$1x10^{-4}$	—	0.071	0.023	0.13
0.25	0.071	—	—	0.071	0.045	0.11

There are considerable difficulties in relating aerometric data to ozone concentration, especially on a one-to-one basis. First, it is well known that, even in a batch ozone-generating system, the ozone increases with time up to a point, while hydrocarbon and NO concentrations decrease. Nitrogen dioxide, if not present initially, will increase, then decrease. The ratio of alkenes to alkanes will decrease as will the ratio of NO to NO_2. The $NMHC/NO_x$ ratio will increase. Depending on the nature of the hydrocarbons emitted to the atmosphere and the length of time reactions have been occurring, the maximum ozone generable by a system will change. Figure 72 is a comparison of the 0.08 ppm isopleths for ozone concentration obtained with a computer model utilizing propylene only and using isopentane only as the hydrocarbon. It can easily be seen that the ozone-hydrocarbon relationship is different for the two hydrocarbons. The relationship, O_3-NMHC, will shift with time from somewhere near the alkene (as one extreme) to near the alkane (as the other extreme). The downtown city system should be closer to the propylene-NO_x system, and the rural high ozone system closer to the isopentane-NO_2 system. Tables 45 through 50 show the variation in relationship between hydrocarbon and ozone at different times at the sampling station and in the aircraft samples. A relationship with ozone generation is not readily apparent, but the major purpose of the hydrocarbon sampling was not elucidation of the chemical mechanisms of ozone generation, but to demonstrate the presence or absence of an anthropogenic input.

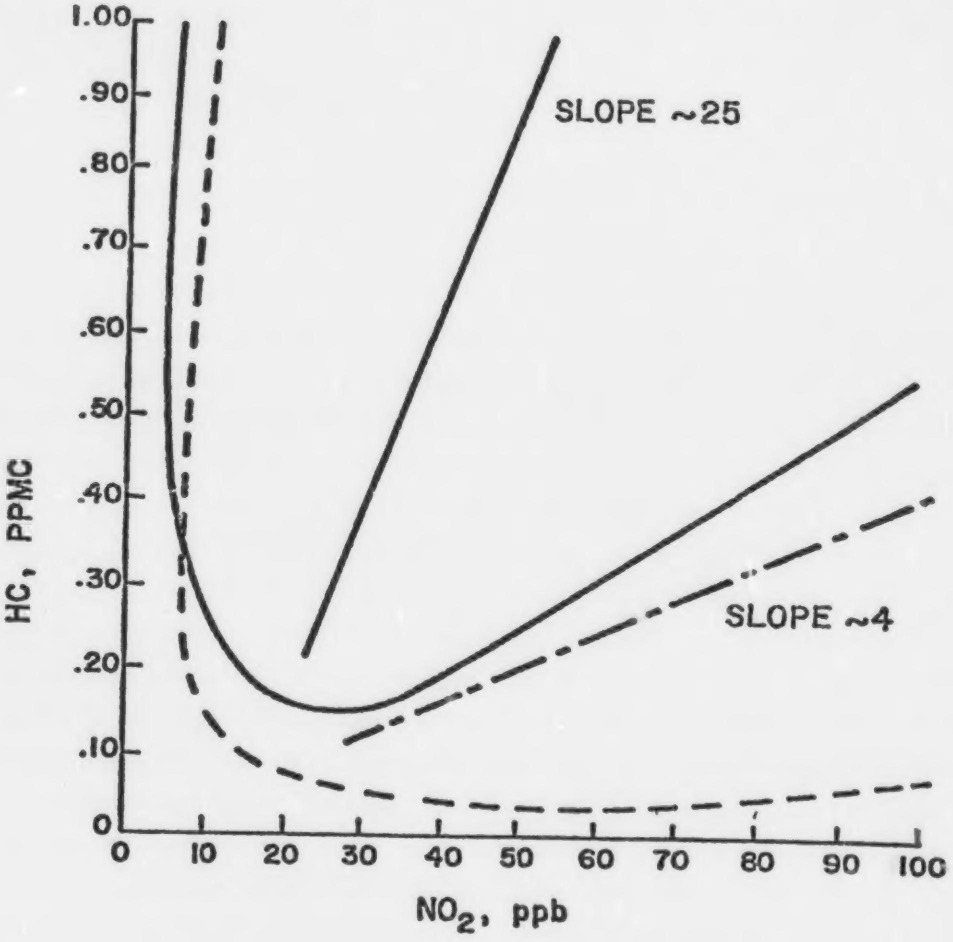

Figure 72. General equal response curves (0.08 ppm ozone) for an alkane-NO_2 system (solid line) and for an olefin-NO_2 system (broken line). The two diagonals with their indicated slopes define the HC/NO_2 ratios which correspond to maximum ozone production for each type of hydrocarbon.

Table 45. Mean hydrocarbon and halocarbon concentrations for selected ozone concentration ranges at Wolf Point, Montana (July-September 1975)

Compound	O$_3$ Maximum Hourly Average Concentration Range			
	0-53 (μg/m^3)	54-106 (μg/m^3)	107-159 (μg/m^3)	≥ 160 (μg/m^3)
Ethylene/Ethane (ppbV)	6.4	28.2	10.0	No Samples In This Range
Propane	0.3	3.3	5.2	
Propulene	0.8	1.3	1.4	
Acetylene	1.8	2.5	1.5	
n-Butane	0.6	2.3	5.6	
1-Butene	Not Detected	0.1	Not Detected	
Isobutane	0.2	0.8	1.8	
Isopentane	0.4	2.0	2.1	
Cyclopentane	Not Detected	0.2	0.2	
n-Pentane	2.1	1.9	2.1	
Toluene	35.6	3.8	29.9	
o-Xylene	2.1	3.5	1.5	
Freon-11 (pptV)	219.0	279.0	69.7	
Carbon Tetrachloride	53.0	58.0	78.2	
1,1,1-Trichloroethane	1.0	1.7	1.7	
Tetrachloroethylene	568.0	153.0	402.0	

Table 46. Mean hydrocarbon and halocarbon concentrations for selected ozone concentration ranges at Creston, Iowa (July-September 1975)

Compound	O_3 Maximum Hourly Average Concentration Range			
	0-53 ($\mu g/m^3$)	54-106 ($\mu g/m^3$)	107-159 ($\mu g/m^3$)	$\geq$ 160 ($\mu g/m^3$)
Ethylene/Ethane (ppbV)	13.2	36.8	51.1	24.6
Propane	1.6	2.3	3.0	2.0
Propylene	1.2	0.8	2.8	0.7
Acetylene	1.2	4.0	2.3	2.6
n-Butane	0.8	0.9	0.9	0.8
1-Butene	Not Detected	<0.1	1.1	Not Detected
Isobutane	0.4	0.4	0.7	0.4
Isopentane	0.3	1.1	1.0	0.4
Cyclopentane	Not Detected	0.1	0.2	Not Detected
n-Pentane	2.5	1.8	5.6	4.1
Toluene	5.7	8.4	2.3	0.5
o-Xylene	2.2	0.8	1.1	Not Detected
Freon-11 (pptV)	103.0	300.0	178.0	423.0
Carbon Tetrachloride	28.0	43.0	51.0	46.0
1,1,1-Trichloroethane	0.6	1.0	0.9	1.5
Tetrachloroethylene	161.0	327.0	286.0	425.0

Table 47. Mean hydrocarbon and halocarbon concentrations for selected ozone concentration ranges at Bradford, Pennsylvania (July-September 1975)

Compound	O_3 Maximum Hourly Average Concentration Range			
	0-53 ($\mu g/m^3$)	54-106 ($\mu g/m^3$)	107-159 ($\mu g/m^3$)	$\geq$ 160 ($\mu g/m^3$)
Ethylene/Ethane (ppbV)	51.7	26.6	30.0	15.3
Propane	2.7	3.8	4.4	3.1
Propylene	0.9	1.0	1.3	2.1
Acetylene	4.6	3.0	2.6	6.5
n-Butane	2.0	2.0	4.6	8.8
1-Butene	0.3	0.1	0.1	0.2
Isobutane	0.9	0.8	2.6	4.1
Isopentane	3.5	1.1	2.1	7.0
Cyclopentane	Not Detected	Not Detected	Not Detected	1.3
n-Pentane	9.3	2.4	1.8	3.2
Toluene	6.6	7.4	4.0	2.3
o-Xylene	3.6	2.3	1.4	2.7
Freon-11 (pptV)	213.0	196.0	409.0	1022.0
Carbon Tetrachloride	216.0	59.0	53.0	69.0
1,1,1-Trichloroethane	2.3	0.9	1.3	0.8
Tetrachloroethylene	791.0	385.0	400.0	2322.0

Table 48. Mean hydrocarbon and halocarbon concentrations for selected ozone concentration ranges for aircraft samples - Region 1 - west of Fargo, N.D. → Dallas, Texas

Compound	O_3 Maximum Hourly Average Concentration Range			
	0-53 ($\mu g/m^3$)	54-106 ($\mu g/m^3$)	107-159 ($\mu g/m^3$)	$\geq$ 160 ($\mu g/m^3$)
Ethylene/Ethane (ppbV)	11.6	177.4	No Samples In This Range	No Samples In This Range
Propane	0.4	0.4		
Propylene	0.7	0.7		
Acetylene	0.4	1.0		
N-Butane	0.4	0.7		
1-Butene	Not Detected	0.1		
Isobutane	0.1	0.3		
Isopentane	0.6	1.4		
Cyclopentane	Not Detected	Not Detected		
N-Pentane	0.7	0.8		
Toluene	3.4	95.3		
O-Xylene	Not Detected	67.8		
Freon 11 (pptV)	156.0	92.0		
Carbon Tetrachloride	50.0	38.0		
1,1,1-Trichloroethane	7.3	1.1		
Tetrachloroethylene	976.0	152.0		

Table 49. Mean hydrocarbon and halocarbon concentrations for selected ozone concentration ranges for aircraft samples - Region 2 - east of Fargo, N.D. and Dallas, Texas line and west of Chicago, Illinois → St. Louis, Missouri line

Compound	O_3 Maximum Hourly Average Concentration Range			
	0-53 ($\mu g/m^3$)	54-106 ($\mu g/m^3$)	107-159 ($\mu g/m^3$)	$\geq$ 160 ($\mu g/m^3$)
Ethylene/Ethane (ppbV)	11.9	8.4	9.4	No Samples In This Range
Propane	1.5	0.4	0.1	
Propylene	1.6	1.1	0.2	
Acetylene	1.0	0.4	0.7	
N-Butane	6.3	1.3	0.0	
1-Butene	0.7	0.2	Not Detected	
Isobutane	0.2	0.1	0.0	
Isopentane	4.5	1.3	0.2	
Cyclopentane	0.1	Not Detected	0.0	
N-Pentane	1.7	0.7	0.2	
Toluene	5.7	1.5		
O-Xylene	Not Detected	0.2		
Freon 11 (pptV)	88.0	103.0	253.0	
Carbon Tetrachloride	21.0	56.0	50.0	
1,1,1-Trichloroethane	1.0	1.0	Not Detected	
Tetrachloroethylene	218.0	224.0	133.0	

Table 50. Mean hydrocarbon and halocarbon concentrations for selected ozone concentration ranges for aircraft samples - Region 3 - east of Chicago, Illinois → St. Louis, Mo. line

Compound	O_3 Maximum Hourly Average Concentration Range			
	0-53 (μg/m^3)	54-106 (μg/m^3)	107-159 (μg/m^3)	≥ 160 (μg/m^3)
Ethylene/Ethane (ppbV)	No Samples In This Range	13.3	22.1	11.9
Propane		0.9	1.2	1.4
Propylene		0.7	0.8	0.6
Acetylene		1.5	1.4	2.0
N-Butane		1.2	1.5	1.6
1-Butene		< 0.1	0.1	< 0.1
Isobutane		0.2	0.4	0.6
Isopentane		2.1	2.4	1.4
Cyclopentane		0.1	0.1	0.3
N-Pentane		1.2	1.0	1.4
Toluene		4.8	6.3	3.5
O-Xylene		0.5	1.1	0.2
Freon 11 (pptV)		136.0	214.0	182.0
Carbon Tetrachloride		29.0	41.0	35.0
1,1,1-Trichloroethane		0.9	2.2	0.9
Tetrachloroethylene		98.0	353.0	116.0

The NO_x-O_3 relationship is apparent from aerometric data as one moves from Wolf Point to Creston (table 51). Although the concentrations of NO_x measured were within the noise level of the instrumentation (i.e., $\approx 10\ \mu g/m^3$), it is a fair assumption that the reason ozone concentrations at Wolf Point never reached the NAAQS was that the air at Wolf Point was deficient in NO_x. Somewhere between Wolf Point and Creston, the air occasionally began to pass the point of NO_x concentration in which O_3 generation was very sensitive to NO_x concentration. Figure 73 shows the relationship between NO_x and O_3 at Creston and Bradford; O_3 concentration as indicated by these data does not appear to be particularly sensitive to NO_x concentration. As stated above, however, the O_3 concentration attained at any given point may be more sensitive to the mass of NO_x emitted to the air than to the observed concentrations. Computer simulation results (table 44) show how this can occur.

The above discussion for NO_x is a reminder that from 1960 to 1970 the anthropogenic emissions of NO_x doubled in the United States. This is the period in which high nonurban concentration of ozone came forcibly to the attention of atmospheric chemists and control officials. Although the increased NO_x output is not at this time offered as the explanation of the increased rural O_3 concentration, it is, however, the only increase in anthropogenic activity that tends to correlate with the apparent spread of high rural ozone concentration.

Table 51. Summary of NO_x data

Station Location	NO_x (average) $\mu g/m^3$	NO_x (6 to 9 a.m. average) $\mu g/m^3$	NO_x emissions tons $mi^{-2} yr^{-1}$*
Wolf Point, Montana	1.5	<1.0	0.5
Creston, Iowa	9.0	9.2	5.4
Bradford, Pennsylvania	7.5	9.6	15.0

*Average of all counties wholly or partially within a 100 mile radius of the station; Source - NEDS Files (1975).

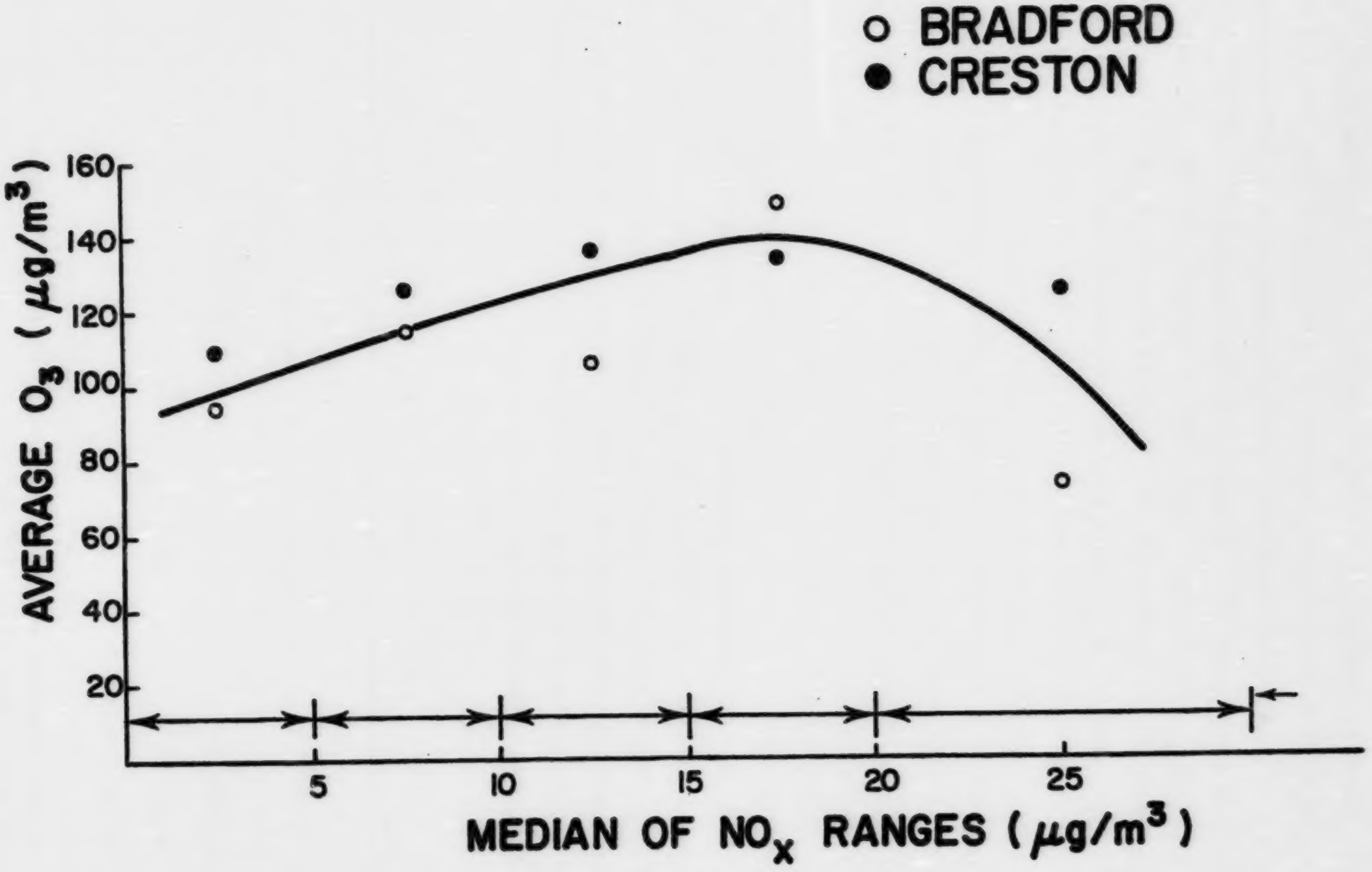

Figure 73. Ozone versus median NO_x concentration range at Bradford, Pennsylvania and Creston, Iowa (July-September 1975).

As indicated above, there are limitations that can be proved by the kind of data obtained in most aerometric studies. Two kinds of compounds should be measured for better modeling and understanding of ozone behavior. First, the ozone destructive capacity of the air needs to be known, especially at night. It is possible that no single ozone destructive agent is concentrated enough to produce the observed decrease in ozone at night, but that a great number of compounds may be involved. (Heterogeneous destruction at the surface of the earth has been shown not to account for all dark phase ozone destruction.[4/] Atmospheric gas phase destruction of ozone can easily be detected and monitored.

Another group of compounds that is important is the stable intermediates of the smog reactions--those which lead readily to hydroxyl, hydroperoxy and organic peroxy radical formation. The cumulative burden of these compounds may be important in the difference between Creston's and Bradford's O_3 concentrations even though the concentration of a single individual compound such as formaldehyde might be in the noise level of the analytical technique at both sites. The study of this possibility should be initiated.

When the efficacy of a control program or the legal aspects of control are being considered, the differences in ozone concentrations that exceed the NAAQS from one year to another should be studied carefully in an effort to determine whether they are due to differences in emissions, control measures, or meteorological variables. The difference in frequency between 1974 and 1975 of exceeding the NAAQS at various stations is explained as a meteorological phenomenon in section 7.2. In any event, this study adds to the already almost-overwhelming evidence that high ozone concentrations in the lower troposphere can be correlated positively with population density.

7.3.2 Ozonesonde Releases

To assess the role of the vertical distribution of ozone upon the ozone measurements near the ground, a special program of serial ozonesonde releases was initiated. These releases documented the vertical distribution of ozone and its changes. Special attention was given to any evidence of the intrusion of stratospheric ozone into the troposphere. The behavior of ozone in the planetary boundary layer was also investigated. Ozonesondes were released during three program periods from Huron, South Dakota. These soundings were made sequentially three times a day--near sunrise, in the early afternoon, and after sunset--and show the greatest contrasts of ground-level ozone during the day. Ozone data were taken during vertical profile flights, and a quality assurance program was conducted by the EPA.

7.3.2.1 Ozonesonde Releases at Huron, South Dakota, September 5-7, 1975

On September 4, a high pressure center moved southeastward through eastern Montana. It moved through the Black Hills and into northern Nebraska by the evening of September 5. As the high pressure continued its southeastward movement away from Huron, a trough of low pressure in western North Dakota developed into a weak cold front. The front passed Huron at about 2100 CDT on September 6, bringing a wind change from southerly to north and northeasterly at the ground, which persisted into the following day.

The RTI aircraft arrived in Huron at 1730 CDT on September 5. Just prior to landing, an ascent to 3 km MSL was made. Ozone measurements were made continuously but are reported only during level flight near 1.2, 1.5, 1.8, 2.4 and 3.0 km as the airplane ascended. On the next morning, another vertical profile was made to 3 km with ozone measurements reported during ascent and descent. During the same period, an EPA team performed a quality assurance of the ozonesonde system at Huron. Their mobile unit was set up and operative by early morning of September 6.

In the first comparison, simultaneous ozonesonde and chemiluminescence ozone analyzer measurements were taken on ambient air. The ozonesonde gave an ambient concentration of 76 $\mu g/m^3$ while the ozone analyzer gave a concentration of 73 $\mu g/m^3$. The RTI airplane recorded concentrations of 72 and 77 $\mu g/m^3$ on two low passes at 50 ft before and after a vertical profile flight.

On the next day, the ozone analyzer was audited by the EPA team on the 0.100 ppm range. The Percent Audit Error generated was -9.0 percent. Shortly after noon, simultaneous measurements of ambient concentration were taken using the ozonesonde and the Bendix ozone analyzer. The ozonesonde and the Bendix analyzer were connected to the calibrator manifold, and several ozone concentrations were generated. The ozonesonde data were computed without prior knowledge of the analyzer measurements; the results are given in table 52. The ozonesonde was subsequently launched.

7.3.2.2 Stratospheric-Tropospheric Ozone Distribution

A time-altitude cross-section of ozone concentration and of potential temperature from the ground to 100 mb was constructed. Potential tempera-

Table 52. Comparison of ozone measuring techniques

Ozonesonde ($\mu g/m^3$)	Chemiluminescent Analyzer ($\mu g/m^3$)
49	53
127*	176
370	373
559	559

*The ozonesonde fell over in high wind during the comparison and was not transmitting properly at this time.

ture, θ, is the absolute temperature an air parcel would have if it were brought adiabatically to a pressure of 1,000 mb. It is a particularly useful descriptor of the state of the atmosphere. In the absence of heat input or removal, θ is conserved. Rising or descending adiabatic motion can be deduced by the vertical displacements of the θ isopleths. When ozone concentration is expressed in conservative units, i.e., units which are independent of pressure or altitude, the ozone isopleths should be moved upward and downward with the adiabats unless ozone is being generated, destroyed, or horizontally advected into an area.

The static stability of the air is proportional to the vertical gradient of θ. The greater the stability, the more resistive the air becomes to vertical motion or diffusion, often trapping materials in an inversion.

The analyzed cross-section is shown in figure 74. The ozonesonde releases are indicated by the black triangles at the top and bottom of the figure. The National Weather Service radiosondes from Huron are indicated by the open triangles. The analysis of potential temperature uses both data sets. The θ contours are very continuous in time at all altitudes. The continuity shows that the independent measuring systems function and correlated well and that the atmosphere did not undergo any major perturbations in its structure, especially above 300 mb.

The tropopause separates the troposphere and stratosphere. It is identified by the minimum temperature of the sounding and is very well de-

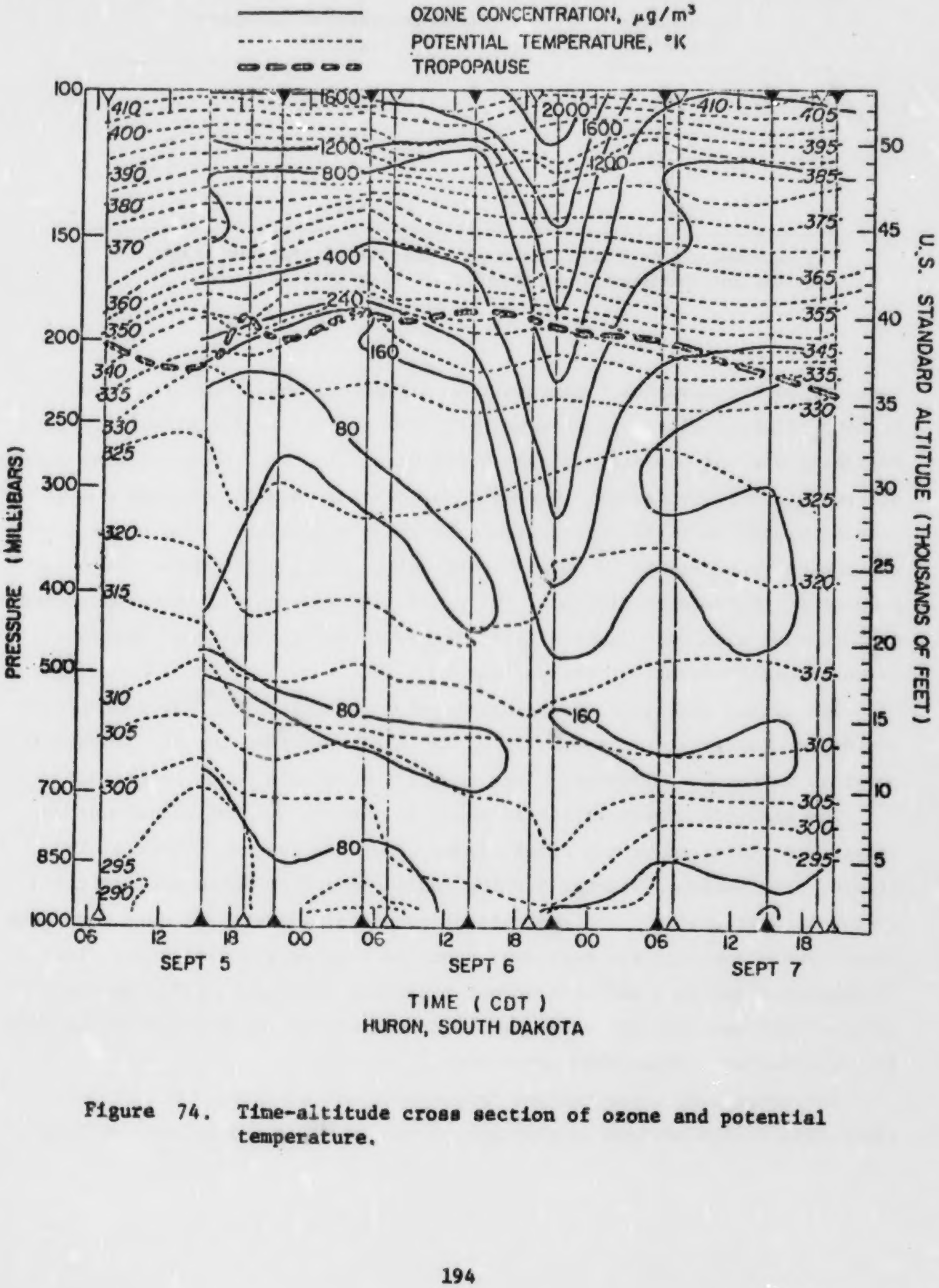

Figure 74. Time-altitude cross section of ozone and potential temperature.

fined from sounding to sounding near the 200-mb level. The static stability and the ozone gradient increase rapidly just above the tropopause in the 0500 September 6 sounding.

The most outstanding feature of the cross-section is the apparent dramatic increase of ozone above 500 mb at 2100 CDT on September 6. According to the data, ozone increased, 1,000 $\mu g/m^3$ in 7 hours at 40,000 ft, which was followed by an equally dramatic decrease over the next 9 hours. Below the tropopause at 36,000 ft, the data show an increase from 160 $\mu g/m^3$ to almost 800 $\mu g/m^3$, followed by a similar decline. This large impulse of ozone occurs at night, without perceptably affecting the atmospheric structure as defined by five soundings. Thunderstorms were not reported, so lightning-generated ozone is discounted. Winds above 700 mb show no meaningful change of wind speed or direction through the entire period, so a change in advection characteristics or a "source region" is an unlikely explanation. Since in the next sounding, the ozone has returned to concentrations similar to those observed at the same altitude and potential temperature as before the event, it is highly unlikely that the apparent event occurred.

An intensive investigation of the data-reduction process, beginning with the strip chart record, proved futile. Possible ozonesonde malfunctions, such as a restricted air intake, a battery deterioration, a reduced pump speed, or an erroneous sonde temperature indication, were investigated without providing a feasible explanation for the high concentrations. The sonde unit was not recovered. The temperature and pressure data agree extremely well with the data taken just 2 hours before by an unbiased party.

In the lower atmosphere, these soundings clearly show the destabilization of the air as the high pressure system of September 5 moved and the cold front passed near 2100 on the sixth. Analysis of winds above Huron showed the effect of the passing front only below 700 mb. It would be easy to suggest that the changes from a relative minimum ($< 80\ \mu g/m^3$) in the 700-mb to 500-mb layer to a relative maximum ($> 160\ \mu g/m^3$) is a result of the frontal passage. The change is supported by three different soundings before and after the frontal passage. It is probably real; however, the atmospheric structure does not give a clue to the reason for the change. This change does not affect the ozone distribution at the ground.

7.3.2.3 Aircraft and Ozonesonde Profiles

Vertical profiles of ozone as measured onboard the airplane, and the preceding and following ozonesonde releases are shown in figures 75 and 76. In figure 75, ozone concentrations are in an expected range of values. The ozonesonde profiles suggest that ozone is increasing with time aloft while it is being destroyed near the ground. The aircraft profile suggests that the transition could be ongoing. Both the first ozonesonde and the aircraft profile suggest a well-mixed afternoon convective layer, which the sounding verified. The nocturnal ozonesonde shows a typical destruction of ozone at the ground at night in the lowest part of a radiative inversion. Aloft at night, the ozone is insulated from the ground and not destroyed.

The early ozonesonde of September 6 (figure 76) substantiates the concept of a nocturnal decrease at the ground and persistence of ozone aloft. It does suggest a return toward lower concentration at 3 km from the previous nocturnal sounding. The later ozone profile suggests a well-mixed layer of ozone, probably locally synthesized. The aircraft profiles, going up and coming down, agree well with each other. They show a shallow layer of higher ozone near 1.2 km (4,000 ft). These profiles agree quite well with the one made on September 5 in magnitude and shape. The low pass values 72 and 77 $\mu g/m^3$ are in excellent agreement with the concurrent sonde and analyzer concentration reported in the quality assurance program. These aircraft soundings also agree quite well with early sonde measurements near 1.4 km. At noon, the mixing depth was probably not to that altitude.

7.3.3 Hydrocarbons and Halocarbons

7.3.3.1 Variation of Selected Hydrocarbons

A. Acetylene

Figure 77 shows the average acetylene concentration for each day of the week at the three ground stations. Wolf Point showed a fairly uniform concentration of acetylene during the week. Creston tended to have higher acetylene concentrations during the middle part of the week (Tuesday, Wednesday, and Thursday). Thursday was the highest (9.0 ppb) and Sunday the lowest (1.3 ppb). At Bradford, acetylene concentrations increased in an orderly fashion from Sunday through Saturday. Acetylene concentrations on Sunday were the lowest and were highest on Saturday.

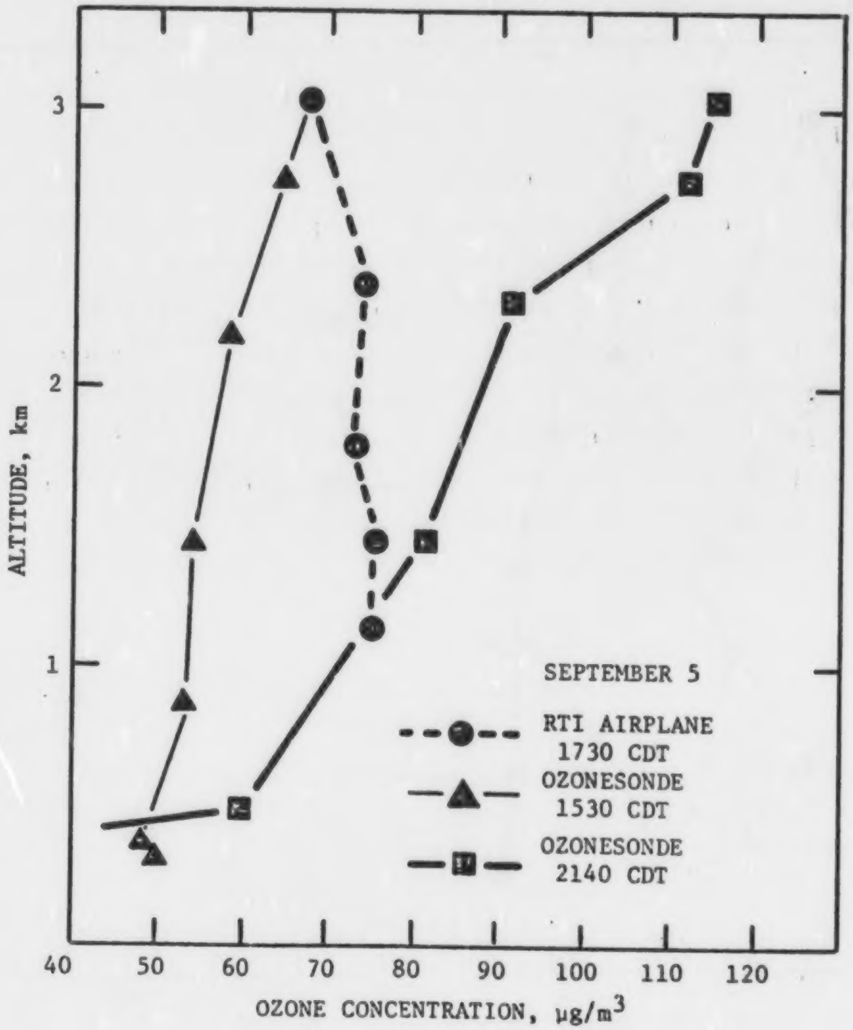

Figure 75. Vertical profiles of ozone at Huron, South Dakota.

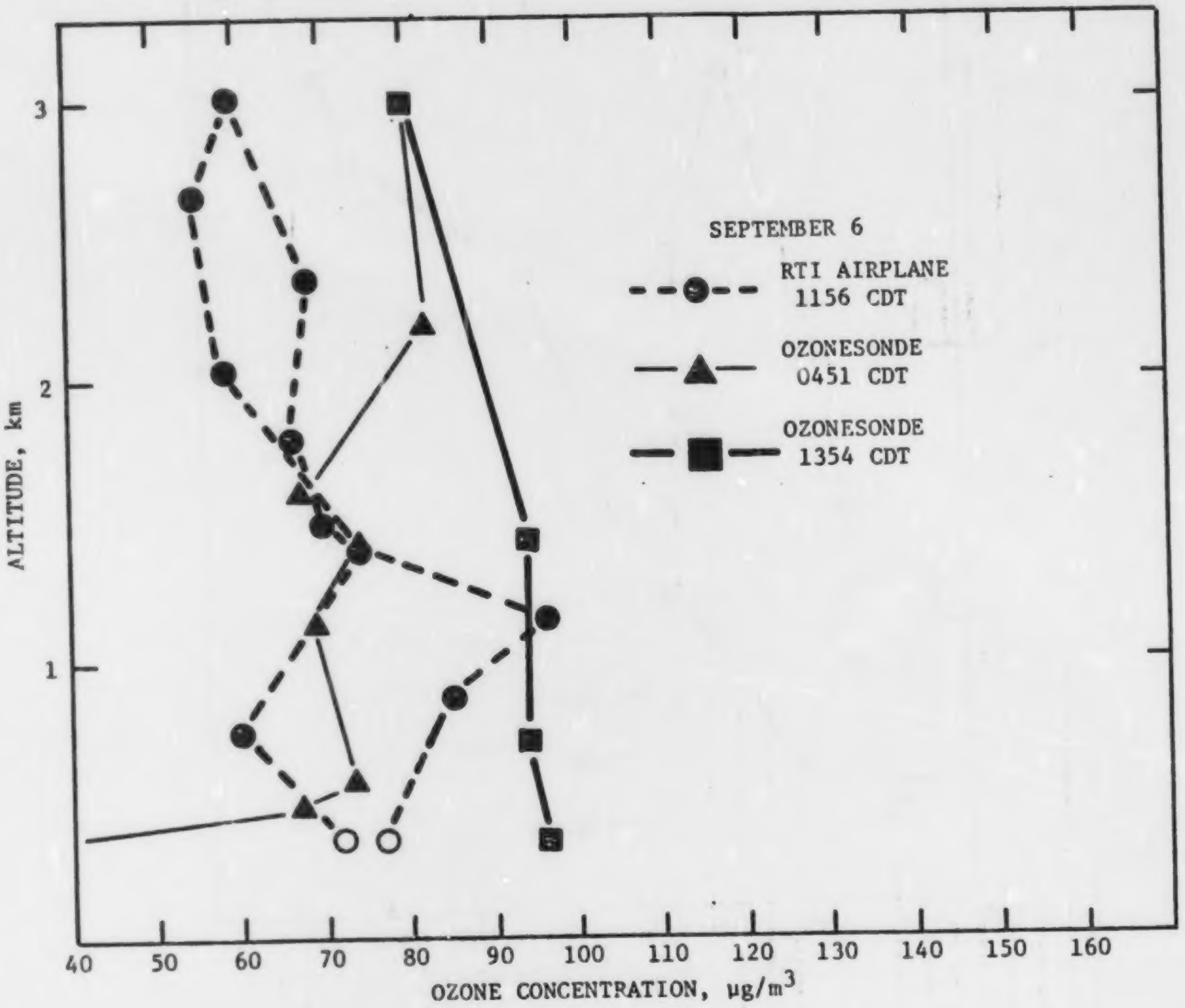

Figure 76. Vertical profiles of ozone at Huron, South Dakota.

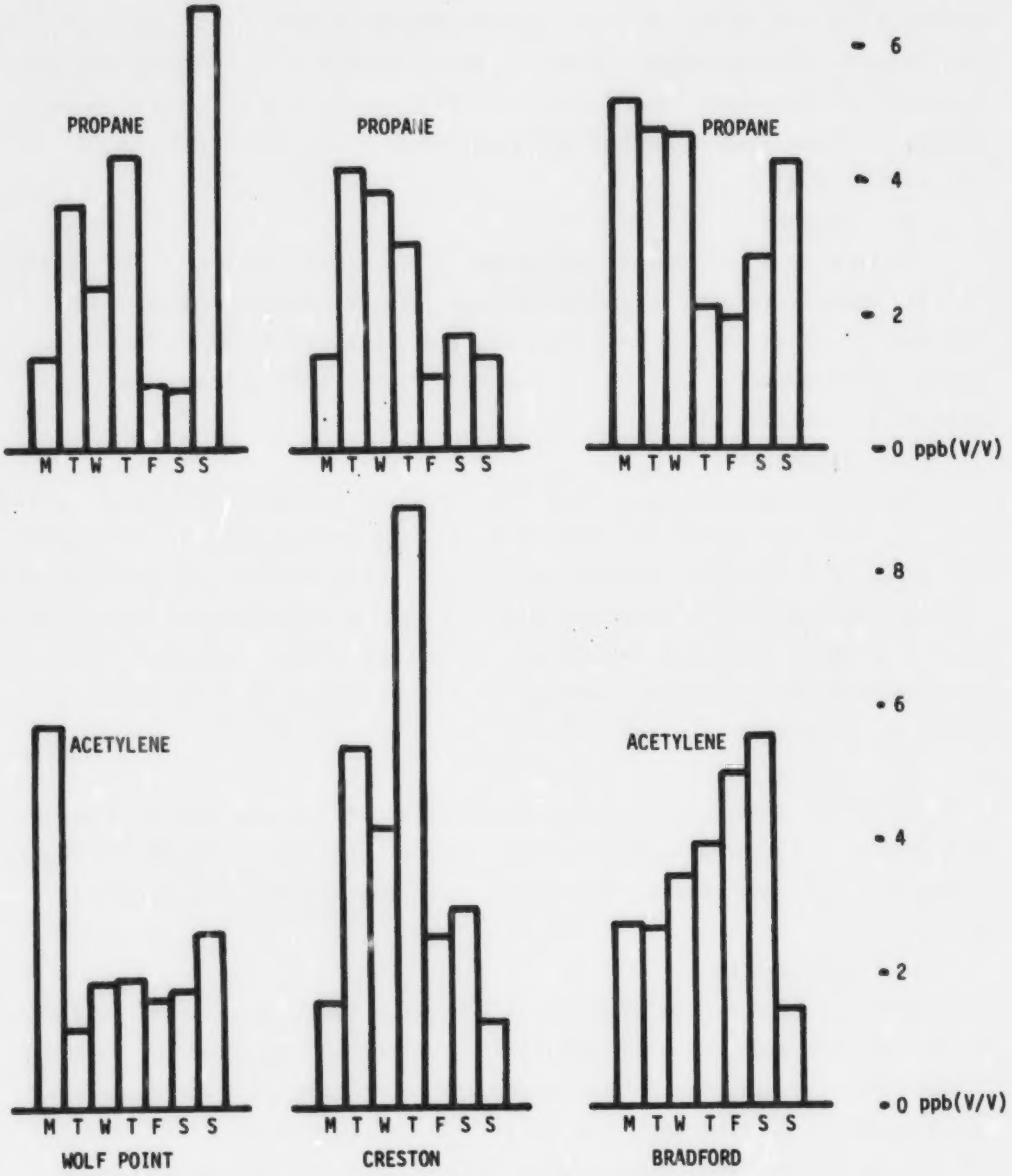

Figure 77. Bar graph showing propane and acetylene concentrations by day of week at Bradford, Pennsylvania, Creston, Iowa, and Wolf Point, Montana (July-September 1975).

Average monthly acetylene concentrations at Wolf Point show a rapid decrease for the months of July, August, and September (i.e., 4.0, 1.8, and 1.5 ppb, respectively). Creston, Iowa, showed an increase in acetylene from July to September, (1.5, 2.0, 6.5 ppb). Acetylene concentration at Bradford, Pennsylvania, peaked in August (i.e., 2.9, 4.5, 2.9) (table 18, section 6.1).

B. Propane

Propane is a hydrocarbon not found in automobile exhaust. Its presence is thus associated with an industrial user, petrochemical processes, natural gas, or other natural emissions sources. Figure 77 shows the average levels of propane for each day of the week at the three ground stations (table 18, section 6.1).

C. Butane

Butane concentrations at Wolf Point rapidly increased during the period July to September (table 18, section 6.1). The increase can be attributed to increased use of the compound as a fuel. Other closely related compounds such as isobutane and isopentane also increase in concentration from July to September while acetylene decreases. At the other two stations, butane concentration follows the acetylene concentration (i.e., increase in acetylene shows an increase in butane).

D. Toluene

As the DeRidder station, two of the northern stations showed a gradual increase in toluene concentration from July to September. Bradford, Pennsylvania, was the only station where this trend was not observed (table 18, section 6.1).

E. Halocarbons

Selected halocarbons measured at the three rural sites were, in general, at or near the accepted quasi-geochemical background reported for each compound. For example, the following percent of samples were at the quasi-geochemical background for Freon 11 at Wolf Point, Creston, and Bradford: 60, 51, and 50 percent, respectively. The highest percentage of samples near these background levels occurred at Wolf Point. This is not surprising, since the population density is much lower than at the other sampling sites.

Concentration gradients for certain halocarbons were observed in the data. For example, tetrachloroethylene showed a concentration gradient from west to east. Mean concentrations measured at the respective stations from west to east were 234, 328, and 484 ppt (table 18, section 6.1).

7.3.3.2 Hydrocarbons: High Pressure System Flight of September 6-7, 1975

This series of flights began in Des Moines, Iowa, and ended at Portland, Maine. The flight passed over parts of Iowa and Indiana, the Ohio Valley, the upper part of Pennsylvania, through New York State (passing near Albany, New York) and into Maine. The flight passed over some highly populated and industrialized areas.

Concentrations of several of the hydrocarbons (from bag samples) are plotted in figure 78 in a linearized fashion from west to east. The first sample was taken about 50 miles south of the Des Moines, Iowa, area and may show some influence from this city. Hydrocarbon concentrations in the second and third samples which were taken in an unpopulated area are substantially lower. On the next day, September 7, a sample was taken upwind of Indianapolis. Hydrocarbon concentrations were generally higher than the last two HC samples taken on the previous day.

An increasing trend is shown as the plane flies from west to east. For example, propane concentration increases slowly as the plane approaches the Ohio Valley, then increases rapidly in samples taken in this area. Propane concentration falls off again in the sample taken between Columbus and Pittsburgh and remains low for the remainder of the flight. Acetylene and isopentane also increase in air samples taken over the Ohio Valley area.

The last two samples were taken upwind and downwind of Albany, New York. The concentrations of several of the hydrocarbons increase (but not propane) in the downwind sample. This may reflect the influence of Albany, or conceivably the influence of the metropolitan New York City-New Jersey area.

7.3.4 Particulates, Northern High Pressure Study

7.3.4.1 Ground Site Measurements

A. Total Suspended Particulates

Twenty-four-hour high-volume samples were collected daily at the three ground sites at Wolf Point, Creston, and Bradford. Table 53 presents monthly and overall averages for the three northern area sites.

TSP was by far the highest at Creston in July and August. This could be a reflection of increased agricultural activity and/or an expression of

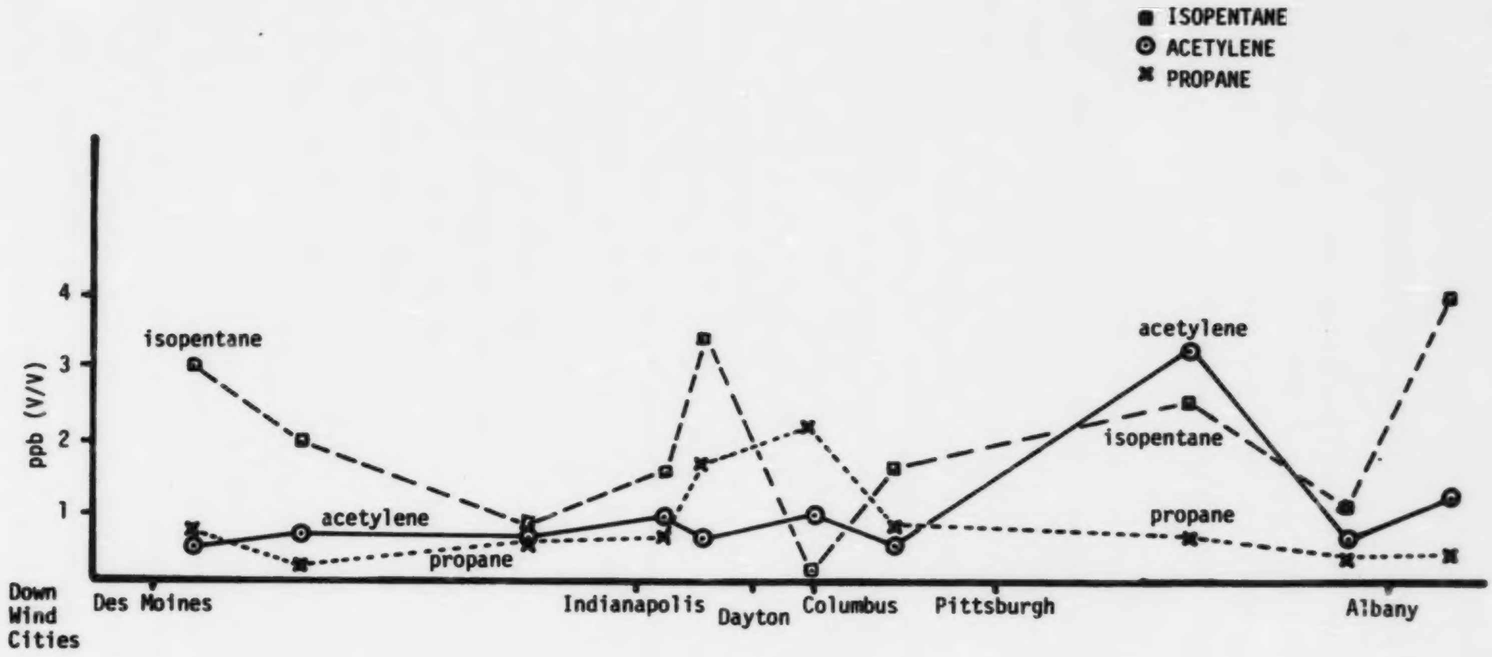

Figure 78. Linearized plot of selected hydrocarbons from flight on September 6-7, 1976.

Table 53. Average daily total suspended particulate (TSP) by month at three sites (1975)

Month	Average daily TSP, µg/m^3		
	Wolf Point	Creston	Bradford
July	36.8	92.8	40.9
August	23.0	88.4	38.1
September	27.9	48.8	25.2
October			
Overall Avg.	29.0	78.0	34.0

the topography and degree and type of plant life in the area, i.e., how well the soil is held against erosion and winds.

B. Sulfate as a Percentage of TSP

Table 54 shows that TSP at the Bradford site contained the highest percentage of SO_4^{2-} by weight, 29 percent on the average, for the study period. Creston had 9.2 percent and Wolf Point, 6.2 percent. The highest monthly SO_4^{2-} percentage was at Bradford in August (32 percent); the lowest at Wolf Point in August (5.6 percent).

The high percentage of SO_4^{2-} at Bradford is attributed to the large concentration of coal-burning installations in this region. Based on data in table 55, Bradford would be classed as a nonurban station proximate to

Table 54. Sulfate as a percentage of TSP by month

Month	Wolf Point	Creston	Bradford
July	6.3	9.8	26.3
August	5.6	7.2	32.2
September	6.4	6.9	29.8
Overall	6.2	9.2	29.0

Table 55. Selected particulate constituents as percentages of gross suspended particulates (1966-1967)*

	Urban		Nonurban					
	(217 Stations)		Proximate[a] (5)		Intermediate (15)		Remote[b] (10)	
	μg/m^3	%	μg/m^3	%	μg/m^3	%	μg/m^3	%
Suspended Particulates	102.0		45.0		40.0		21.0	
Benzene soluble Organics	6.7	6.6	2.5	5.6	2.2	5.4	1.1	5.1
Ammonium ion	0.9	0.9	1.22	2.7	0.28	0.7	0.15	0.7
Nitrate ion	2.4	2.4	1.40	3.1	0.85	2.1	0.46	2.2
Sulfate ion	10.1	9.9	10.0	22.2	5.29	13.1	2.51	11.8
Copper	0.16	0.15	0.16	0.36	0.078	0.19	0.060	0.28
Iron	1.43	1.38	0.56	1.24	0.27	0.67	0.15	0.71
Manganese	0.073	0.07	0.026	0.06	0.012	0.03	0.005	0.02
Nickel	0.017	0.02	0.008	0.02	0.004	0.01	0.002	0.01
Lead	1.11	1.07	0.21	0.47	0.096	0.24	0.022	0.10

---

*Data from United States National Air Sampling Network, 1966-1967.

[a] Near urban areas.

[b] Far from urban areas.

an urban area. In fact, it was quite far from an urban center. This high value reflects the general high-level concentrations of SO_4^{2-}, which are probably found throughout the western part of Pennsylvania. Both Creston and Wolf Point are in line with other remote rural locations.

C. Nitrate as a Percentage of TSP

Table 56 shows that TSP at the Bradford site contained the highest percentage of NO_3^- by weight, 2.7 percent on the average for the study period. Creston had 2.5 percent and Wolf Point 1.3 percent. The highest monthly NO_3^- percentage was at Bradford in September (4 percent); the lowest at Wolf Point in September (1.1 percent).

7.3.4.2 Aircraft Particulate Measurements, Northern Study

High-volume particulate samples were collected by aircraft on at least nine of the northern high pressure study flights. Collection occurred during the entire flight. These flights are listed in table 57 with the corresponding analyses for nitrate and sulfate. Ammonium ion was below detectable limits in all cases.

The overall average for nitrate and sulfate ion components of particulate matter was lower in samples from the nothern flights than in the Gulf Coast flights over land surfaces. The nitrate and sulfate levels were higher at lower flight altitudes 915 to 1220 m (3,000-4,000 ft msl) and diminished at 1830 m (6,000 ft) and higher altitudes.

The highest nitrate and sulfate levels on the northern flights occurred in a flight (086, 087) from Dayton, Ohio, to Pittsburgh, Pennsylvania, which

Table 56. Nitrate as a percentage of TSP by month

	Wolf Point	Creston	Bradford
July	1.5	2.4	2.3
August	1.3	2.0	2.1
September	1.1	2.9	4.0
October			
Overall	1.3	2.5	2.7

Table 57. Nitrate and sulfate: north high pressure flights

Date	Flight	Altitude (ft)	NO_3^-	$SO_4^=$
			($\mu g/m^3$)	
9/4	RDU-Bismarck (055, 056, 057)	6000	2.7	6.5
9/6	Huron-Indianapolis (060, 061, 062)	4000	2.4	1.4
9/7	Indianapolis-Portland (063, 064)	3500	3.9	14.5
9/11	Raleigh-Huron (Pierre) (067, 068)	8000	1.3	0.7
9/12	Pierre-Springfield (069, 070)	3000	1.1	BD
9/15	Springfield-RDU (071, 072)	9000	0.6	BD
9/28	Dayton-Pittsburgh (086, 089)	3500	9.8	22.2
9/29	Pittsburgh, Bedford (088, 089)	3500	1.5	0.2
9/30	Bedford-Raleigh (090, 091)	3500	5.6	18.6
Overall Average			3.2	7.1
Average of 3000, 3500, 4000			4.1	9.5
Average of 6000, 8000, 9000			1.5	2.4

BD - below detectable

crossed the Ohio Valley. The lowest values were found in the flight (071, 072) from Springfield, Missouri, to Raleigh, North Carolina.

7.3.5 Summary of Ozone Generation (Northern High Pressure Oxidant Study)

Under certain conditions of high pressure, ozone concentrations and the frequency of ozone concentrations exceeding the NAAQS increases with increasing population. As a high pressure system moves past a sampling station, ozone concentration decreases behind the leading front and reaches a minimum before the passage of the center of the high. In an eastward moving high, the maximum ozone concentration in the system occurs on the back or west side of the high pressure system. This behavior is explained in part by the fact that air in the front half of a high has been there a day or less whereas air on the back side has been in the high pressure system 2 or more days. This extra time allows precursors to accumulate and provides time for the generation and accumulation of high ozone concentrations.

In "spent" photochemical systems as they occur in rural areas, ozone left over from the previous day is destroyed slowly so that frequently sufficient ozone is left the next day to help attain and exceed the NAAQS with a large net ozone generation for the day. It was judged that the reason the air in the western part of the northern high pressure study and at Wolf Point never reached the NAAQS was that it was deficient in NO_x and never contained the requisite amount of the precursors to exceed the standard.

8.0 INTERPRETATION OF RESULTS: GULF COAST OXIDANT STUDY

8.1 Examination of Ozone Measurements and Meteorological Conditions

Ground and aircraft measurements were made to characterize the ozone concentrations in the northern gulf coast area.

The spatial variability on a given day among ground stations and aloft along flight tracks, and the temporal variability at a given station over the course of a given day or over the study period (e.g., diurnal variation) were examined and documented. Once these characterizations were made, the data could be interpreted and plausible explanations of observed phenomena could be offered.

Ozone in the lowest 3 km of the atmosphere is postulated to be a result of (1) generation/destruction from emitted precursors/destructive agents--local or distant, natural or anthropogenic; (2) lateral transport of ozone from one location to another; or (3) downward diffusion of ozone having stratospheric origin. All of these processes continually affect the ozone concentration, but they are not completely independent.

Under "normal" conditions (if there exists such a state), ozone concentrations are of the order of 40 to 120 $\mu g/m^3$. Principally, extreme concentrations of ozone (i.e., concentrations exceeding the NAAQS), large gradients of ozone, or upper/lower deciles of concentration were examined in these analyses. These extremes suggest an anomaly in one or more of the three contributory processes.

8.1.1 Data Analysis Approach

To examine the role of horizontal transport of ozone or ozone precursors, two sets of air parcel trajectories arriving in Austin, Houston, and Nederland, Texas, and in DeRidder, Louisiana, were computed at 0000 and 1200 GMT for each day between July 2 and October 31. One set used winds vectorally averaged over the lowest 200 m of the air; the other set, from the ground to 2 km MSL. The averaging depths were chosen to agree with trajectory analyses of Heffter.[30/] The lower wind is far more sensitive to frictional influences and diurnal changes than the other winds. The formation of a nocturnal radiative temperature inversion stabilizes the layer of air above the ground. The inversion inhibits the transfer of momentum to the

Preceding page blank

ground, thereby reducing the near-ground wind speed at night. In the absence of a well-defined pressure pattern, thermally driven local circulations like land-sea breeze circulations or urban heat islands can develop. (The trajectory analysis cannot be expected to reveal those circulations, since the upper air data are available only at 12-hour intervals and at widely spaced locations, 36 km (20 miles) or more inland from the coast).

The surface to 2-km wind is a good indicator of the mesosynoptic scale wind field of the lower atmosphere. Since wind speed usually increases with altitude, the trajectories computed with these winds show greater movement than at the lower level. During the summer afternoons, the lowest 2 km of the atmosphere is usually well mixed, and there is little change of wind direction with altitude.

Air parcel trajectories were also computed for morning (0700 CDT) and evening (1900 CDT) arrivals using the upper level winds for four points along each day's flight path. Usually these points were chosen at major changes in course direction. Occasionally trajectories were computed for locations where rapid changes in ozone concentrations were observed. These trajectories show spatial variability of the flow patterns, enable examination of the history of the air prior to a measurement, and broaden the assessment of the role of horizontal transport in the boundary layer. The trajectories give a reasonable, although inexact indication of where the air has been over the previous 48 hours.

Time-altitude cross sections of potential temperature, wind component perpendicular to the gulf coast, inversion layers, and afternoon mixing heights were computed for the first 3 km of the atmosphere above Houston and Lakes Charles. The Houston data were taken at 1200 GMT (0700 CDT) each morning at the Environmental Monitoring Support Unit (EMSU) at Houston Intercontinental Airport on weekdays only, excepting holidays. The Lake Charles cross sections were developed only for October. They were based on the 0000 GMT (1900 CDT) and 1200 GMT (0700 CDT) soundings by the National Weather Service at Lake Charles. Afternoon mixing depths at Houston were defined as the altitude of the intersection of the adiabatic lapse rate of the maximum daily temperature with the morning sounding. The same procedure was used at Lake Charles for both morning and afternoon soundings. Only those cross sections relevant to cases in point are presented.

The analysis permits an examination of ground and airborne measurements in the context of the past history of the air, of the possibilities for generating ozone or injecting ozone precursors en route to sampling points, and of the implications for ozone advection in the study area.

Ozone concentrations at 10-minute intervals along the flight path, surface pressure distributions near the flight time, and appropriate air parcel trajectories are incoporated into a single figure for each day's flight.

8.1.2 High- and Low-Ozone Days

The maximum daily ozone concentration at each of the four stationary monitoring locations (i.e., Nederland, Houston, Austin, and DeRidder) were tabulated. The upper and lower deciles of the distribution were determined at each location. Upper level trajectories arriving in the late afternoon (1900 CDT or 0000 GMT the next date) were plotted for the days of the upper or lower decile concentrations. The trajectories and the associated ozone concentrations are shown in figures 79a through 79h.

Trajectories associated with high ozone concentration at DeRidder characteristically have anticyclonic curvature indicative of flow in high pressure systems. The curvature is greater than with the lower decile concentrations--indicating transitory, not stationary, pressure systems. The location of parcels 12 hours prior to arrival are clustered within 100 miles of DeRidder. Some parcels show almost no movement. In most cases, the high ozone can be identified with trajectories from a potential source of ozone precursor material, i.e., Nederland, Houston, or Lafayette, Louisiana, during the 24 hours prior to arrival.

The trajectories on low-ozone days show a preference for overwater paths, with small curvature and faster air movement. The overland air parcels move over potential anthropogenic precursor sources quickly, reducing opportunities for injection of ozone precursors in large concentrations.

Trajectories on high-ozone days at Nederland also show the large curvature and slow-moving character, with a tendency for the air to move

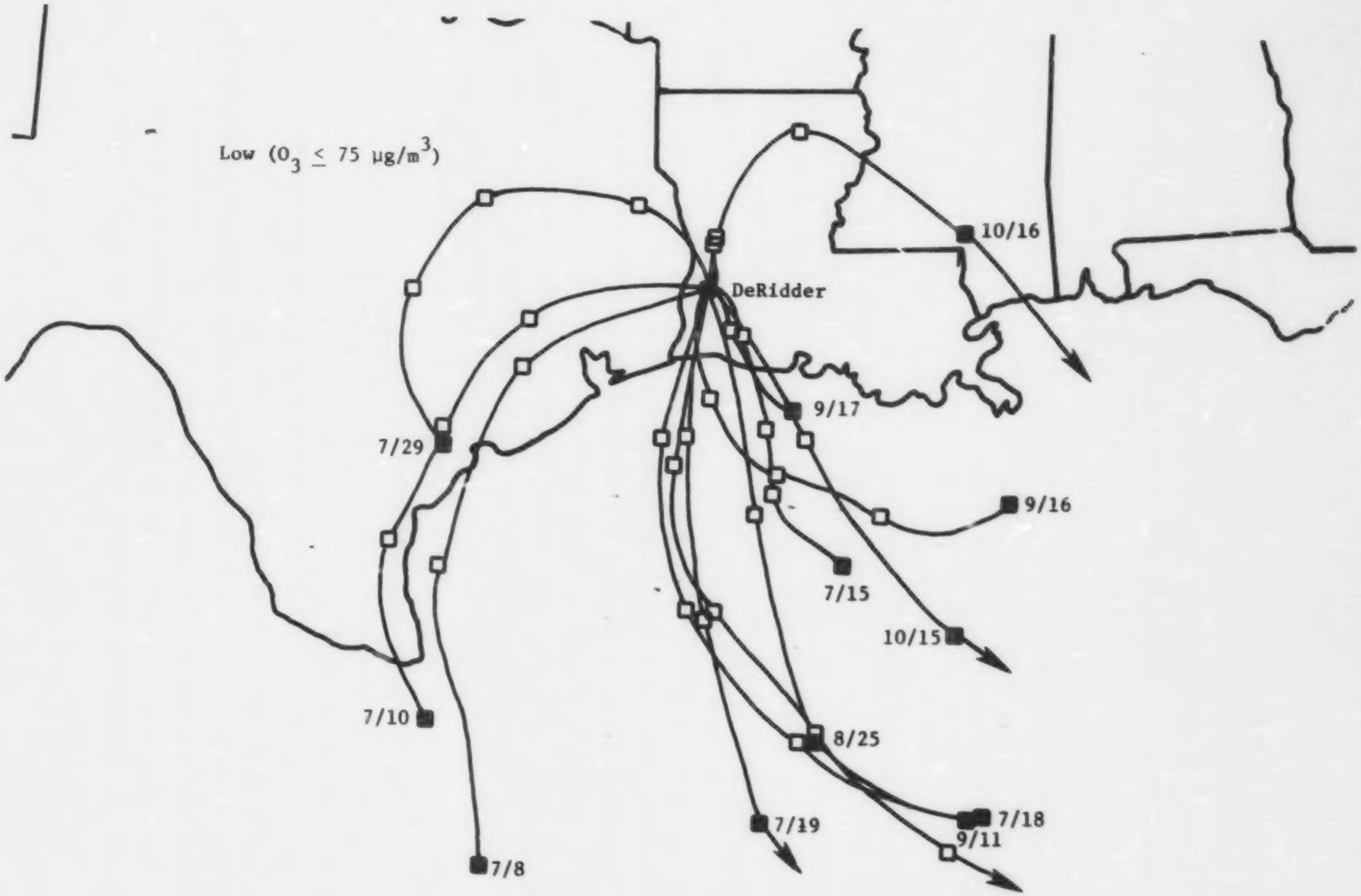
Low ($O_3 \leq 75\ \mu g/m^3$)
DeRidder
10/16
9/17
9/16
7/15
10/15
7/29
7/10
8/25
7/18
9/11
7/19
7/8

Figure 79a. Arriving air trajectories associated with lower decile concentrations of maximum ozone at DeRidder, Louisiana.

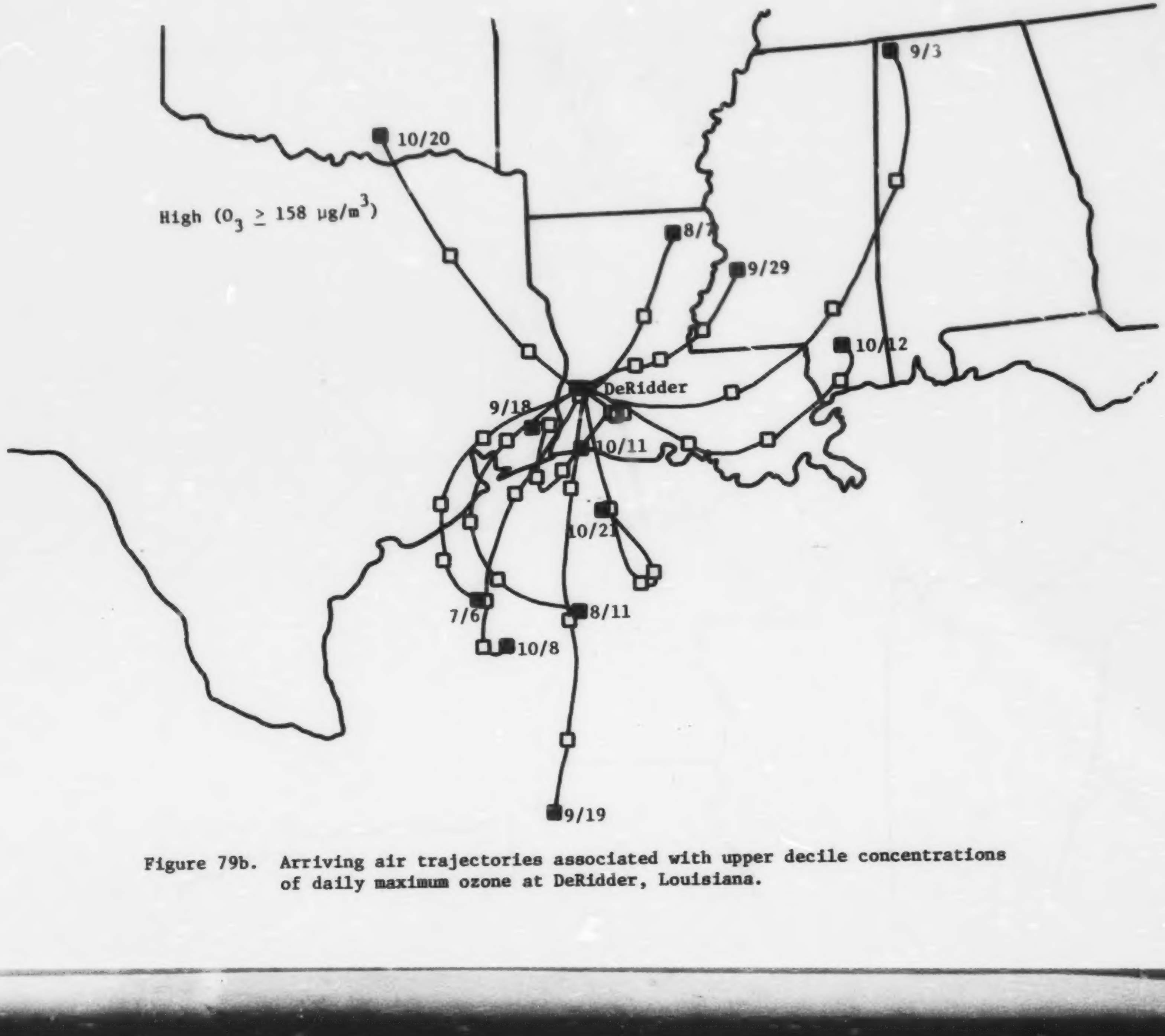
High ($O_3 \geq 158\ \mu g/m^3$)
10/20
9/3
8/7
9/29
10/12
DeRidder
9/18
10/11
10/21
7/6
8/11
10/8
9/19

Figure 79b. Arriving air trajectories associated with upper decile concentrations of daily maximum ozone at DeRidder, Louisiana.

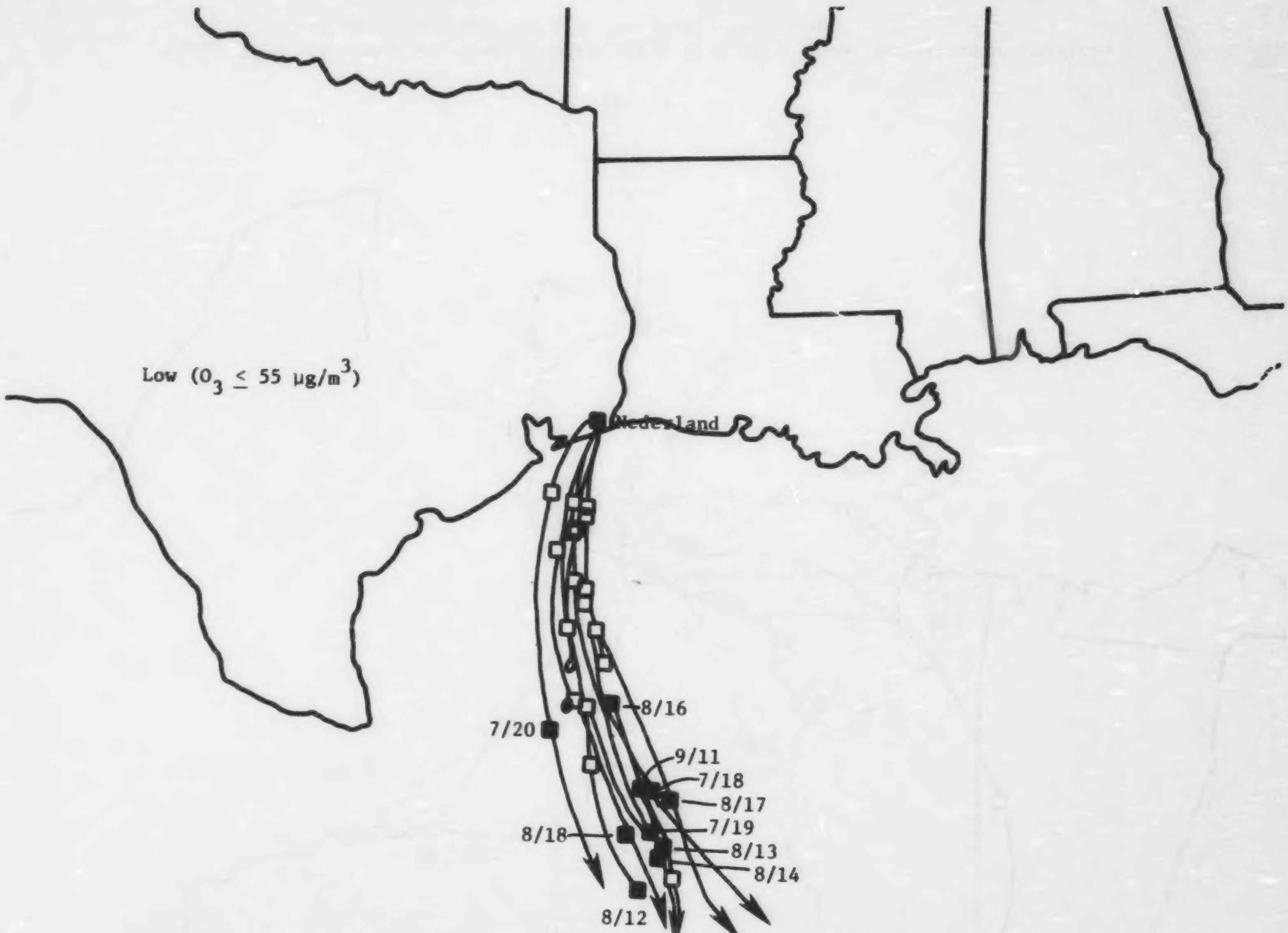
Low ($O_3 \leq 55$ μg/m^3)
Nederland
8/16
7/20
9/11
7/18
8/17
7/19
8/18
8/13
8/14
8/12

Figure 79c. Arriving air trajectories associated with lower decile concentrations of daily maximum ozone at Nederland, Texas.

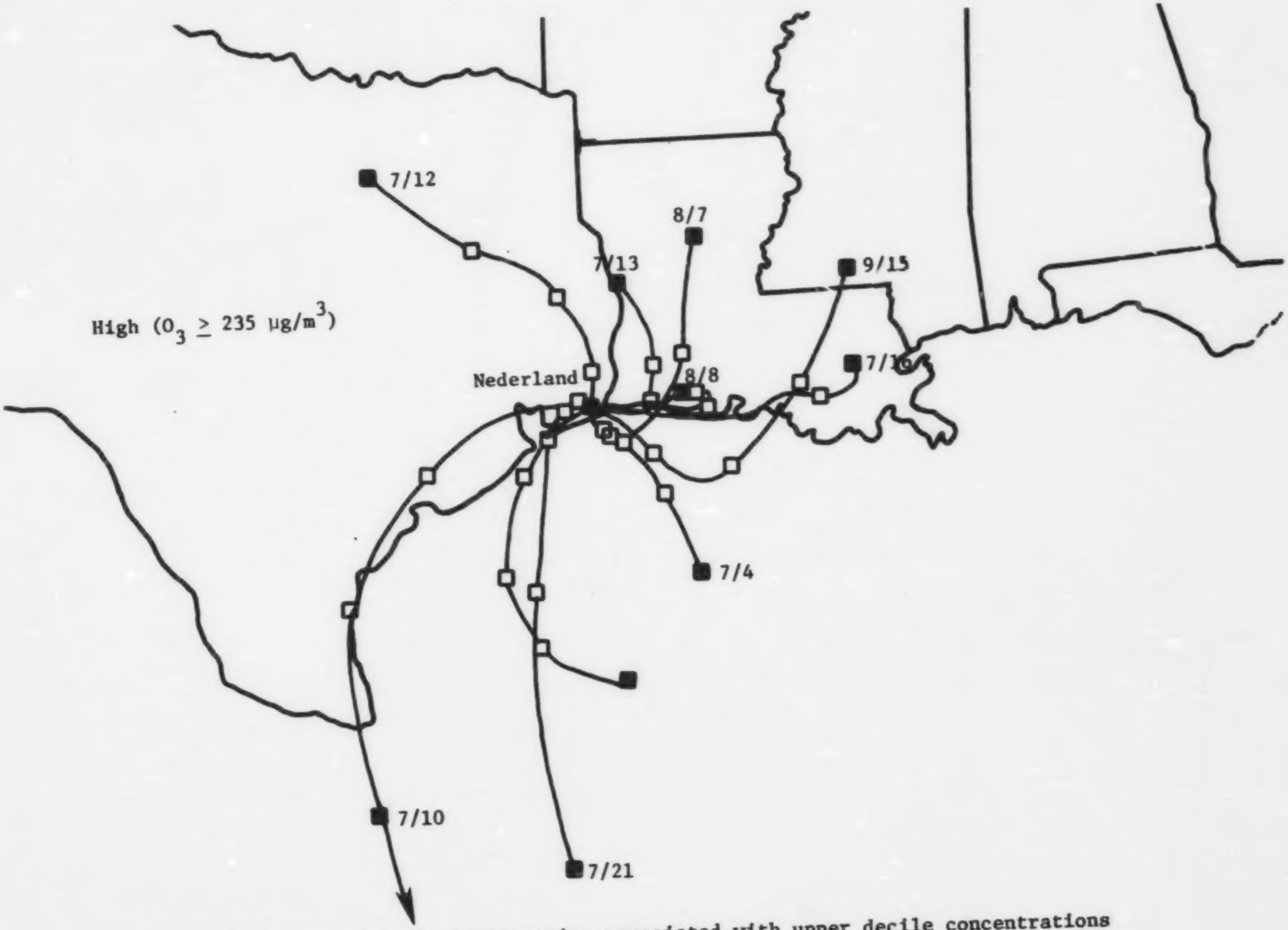
High ($O_3 \geq 235$ µg/m^3)
7/12
8/7
7/13
9/15
Nederland
8/8
7/16
7/4
7/10
7/21

Figure 79d. Arriving air trajectories associated with upper decile concentrations of daily maximum ozone at Nederland, Texas.

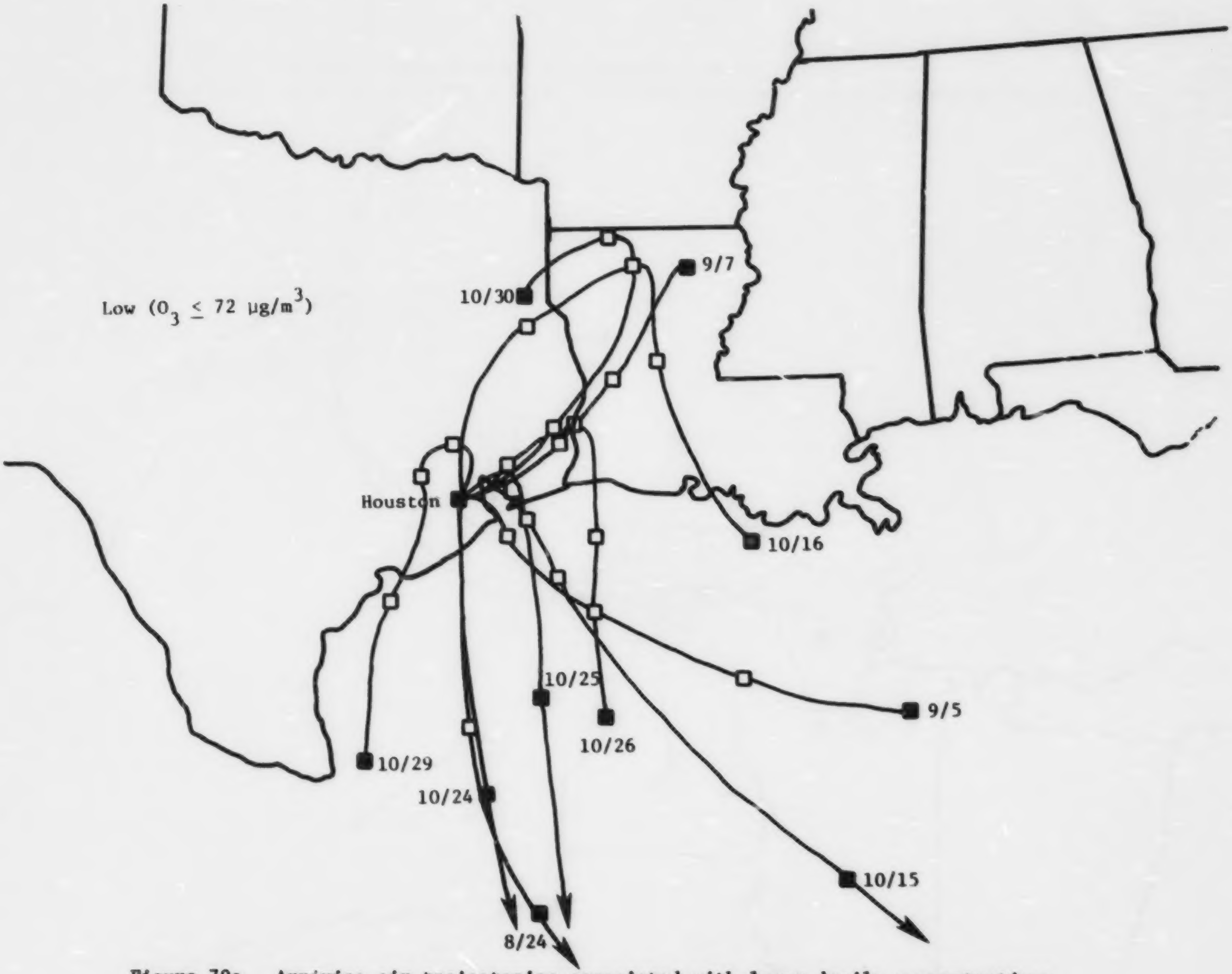
Low ($O_3 \leq 72$ µg/m^3)
10/30
9/7
Houston
10/16
10/25
9/5
10/26
10/29
10/24
10/15
8/24

Figure 79e. Arriving air trajectories associated with lower decile concentrations of daily maximum ozone at Houston, Texas.

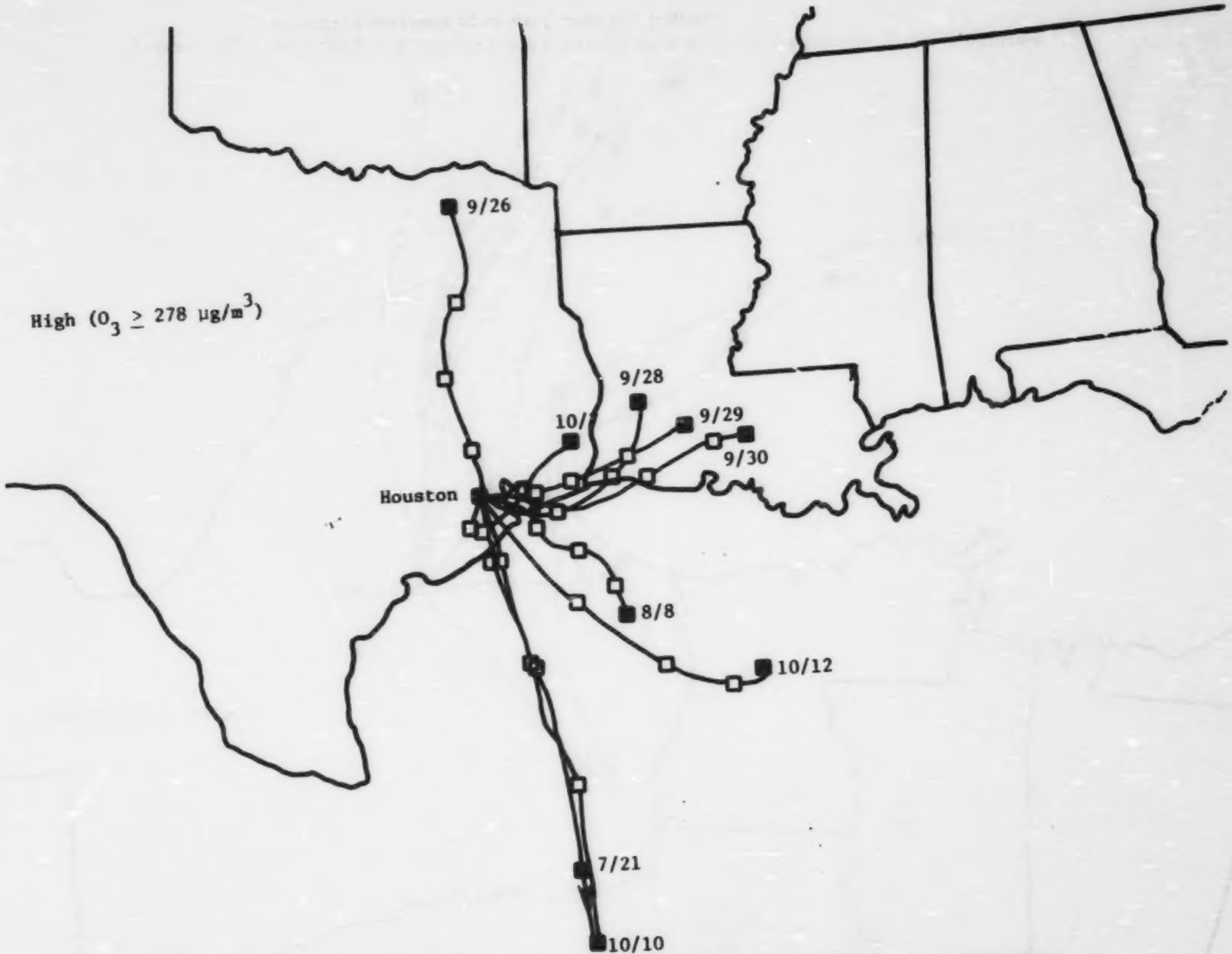
High ($O_3 \geq 278$ µg/m^3)
Houston
9/26
9/28
10/7
9/29
9/30
8/8
10/12
7/21
10/10

Figure 79f. Arriving air trajectories associated with upper decile concentrations of daily maximum ozone at Houston, Texas.

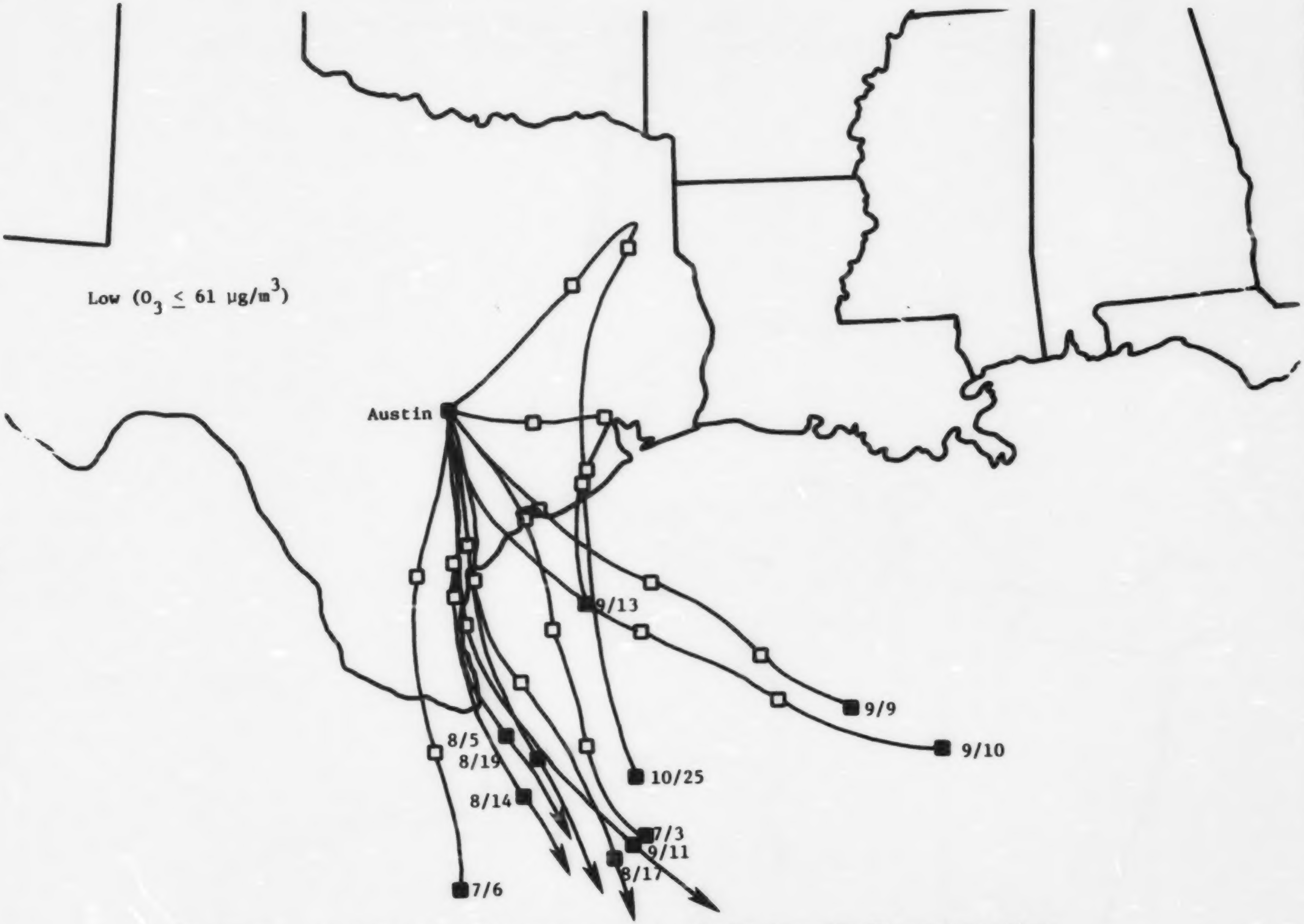
Low ($O_3 \leq 61$ µg/m^3)
Austin
9/13
9/9
9/10
10/25
8/5
8/19
8/14
7/3
9/11
8/17
7/6

Figure 79g. Arriving air trajectories associated with lower decile concentrations of daily maximum ozone at Austin, Texas.

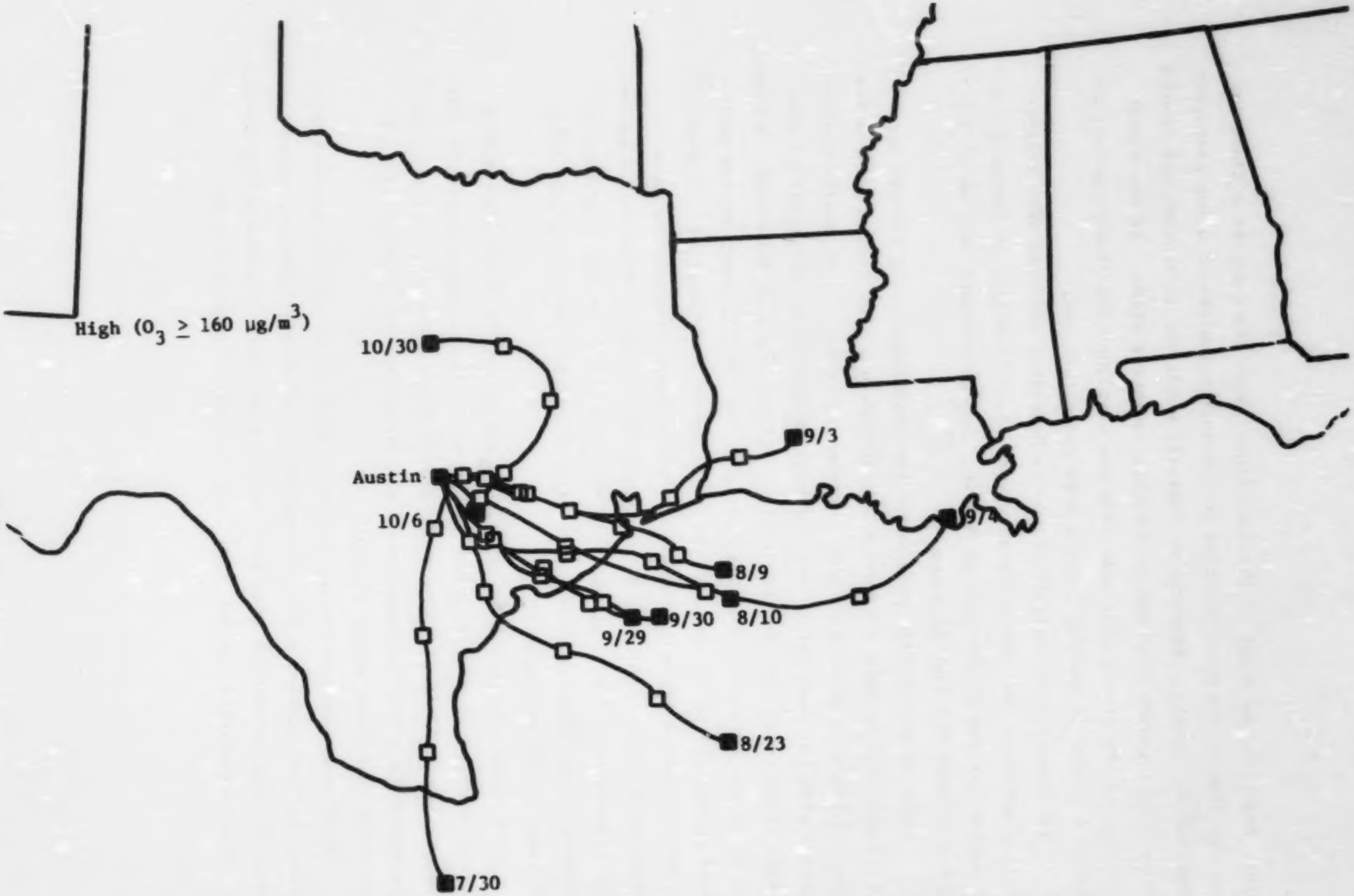
High ($O_3 \geq 160$ µg/m^3)
10/30
Austin
10/6
9/3
9/4
8/9
8/10
9/30
9/29
8/23
7/30

Figure 79h. Arriving air trajectories associated with upper decile concentrations of daily maximum ozone at Austin, Texas.

into Nederland parallel to the coastline. High ozone may be a function of the station location relative to the nearby sources of ozone precursor/destruction agents. Easterly or westerly winds are infrequent and usually have slower speeds than the predominant southerly winds. At the slower speed, the precursors move away from the sampling site slowly, giving the ozone a chance to develop locally high concentrations.

The lowest ozone concentrations in Nederland occurred with trajectories arriving from the south-southwest after traveling exclusively over a narrow portion of the Gulf of Mexico. Speeds averaged only about 3.5 m/s (~8 mph) over the last 12 hours.

There is very little preference for trajectory paths between upper and lower decile ozone concentrations at Houston. Low wind speeds in the past 12 hours occurred with both extremes of ozone. Upper decile trajectories with the long fetch over the Gulf of Mexico are difficult to understand after examining the trajectories for low ozone at Nederland. However, in these two instances, the air had spent the last 12 hours moving northward across the petrochemical complex at Texas City/LeMarque. MacKenzie[31/] indicates that a large variance among ozone concentratiohs has been measured at stations within 2 to 4 miles of the Aldene (Houston) location. The orientation of the receptors to the source and the reaction time to produce ozone from precursors strongly control the day-to-day variation of ozone maxima and minima.

Low ozone concentrations at Austin are primarily associated with a strong southerly flow over areas of low anthropogenic emissions. The air reaches Austin 12 to 15 hours after crossing the coastline. In only one trajectory is there a suggestion of slow movement over a large area of precursor emissions before arrival.

High ozone concentrations at Austin occur in an east-to-southeasterly flow. In four instances the air apparently moved over Houston, which suggests that horizontal transport of ozone or ozone precursors from Houston could be responsible for the high ozone measured (section 8.1.4).

8.1.3 Summary of Aircraft Ozone Measurements and Meteorological Conditions

1) August 7, 1975, Case Study

The simple flight plan (fig. 80), flown in the afternoon, was designed to determine if a plume could be found downwind--to the west--of the Nederland refinery area. The arriving air parcels had moved slowly over central Louisiana on a southwesterly heading. During the past 12 to 24 hours, the air parcels turned, arriving at the locations along the flight track from the southeast.

Upwind of Nederland, ozone concentrations were 80 $\mu g/m^3$. On the south-north leg of the flight across Nederland at 225 m above ground, ozone concentrations remain low except immediately over the city, where concentrations exceeded the NAAQS. Along the north to south leg, downwind of Nederland, ozone concentrations rose from approximately 90 $\mu g/m^3$ to near the NAAQS, suggesting that the plume may have a spread of approximately 24 km at that distance downwind. Ozone concentrations continued to rise as the aircraft turned eastward towards Nederland, and remained above the NAAQS until the aircraft passed east of Nederland. Ozone concentrations then decreased to approximately 90 $\mu g/m^3$.

The trajectories indicated a more southeasterly flow while the distribution of ozone suggested a more easterly flow. The low-altitude trajectories also indicated a turn to more southerly flow, but wind speeds were very light. The weak winds may have accounted for the high ozone concentrations measured directly over Nederland. The Nederland ground station reported a maximum of 237 $\mu g/m^3$.

Data from this flight clearly demonstrated that a plume existed downwind of the petrochemical complex of the Nederland area. Concentrations within the plume were more than 100 $\mu g/m^3$ greater than those found upwind or cross wind.

2) August 8, 1975, Case Study

The weak circulation pattern of the previous days continued; therefore, easterly to southeasterly flow was anticipated through the flight track area, as shown in figure 81. This particular flight pattern was chosen to survey the air flow onshore along the Texas gulf coast, to survey the

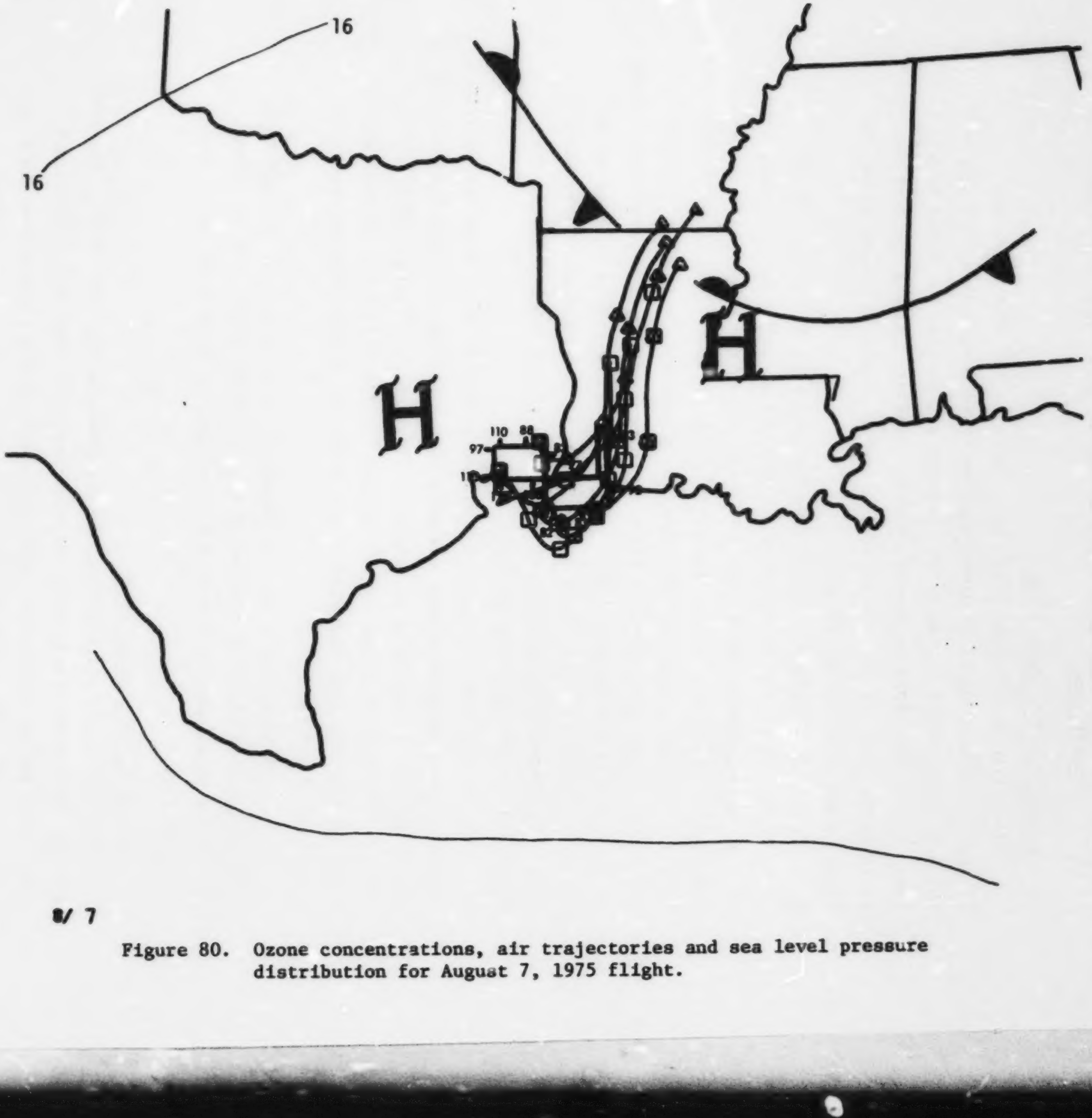
16
16
H
H
110
88
97
8/ 7

Figure 80. Ozone concentrations, air trajectories and sea level pressure distribution for August 7, 1975 flight.

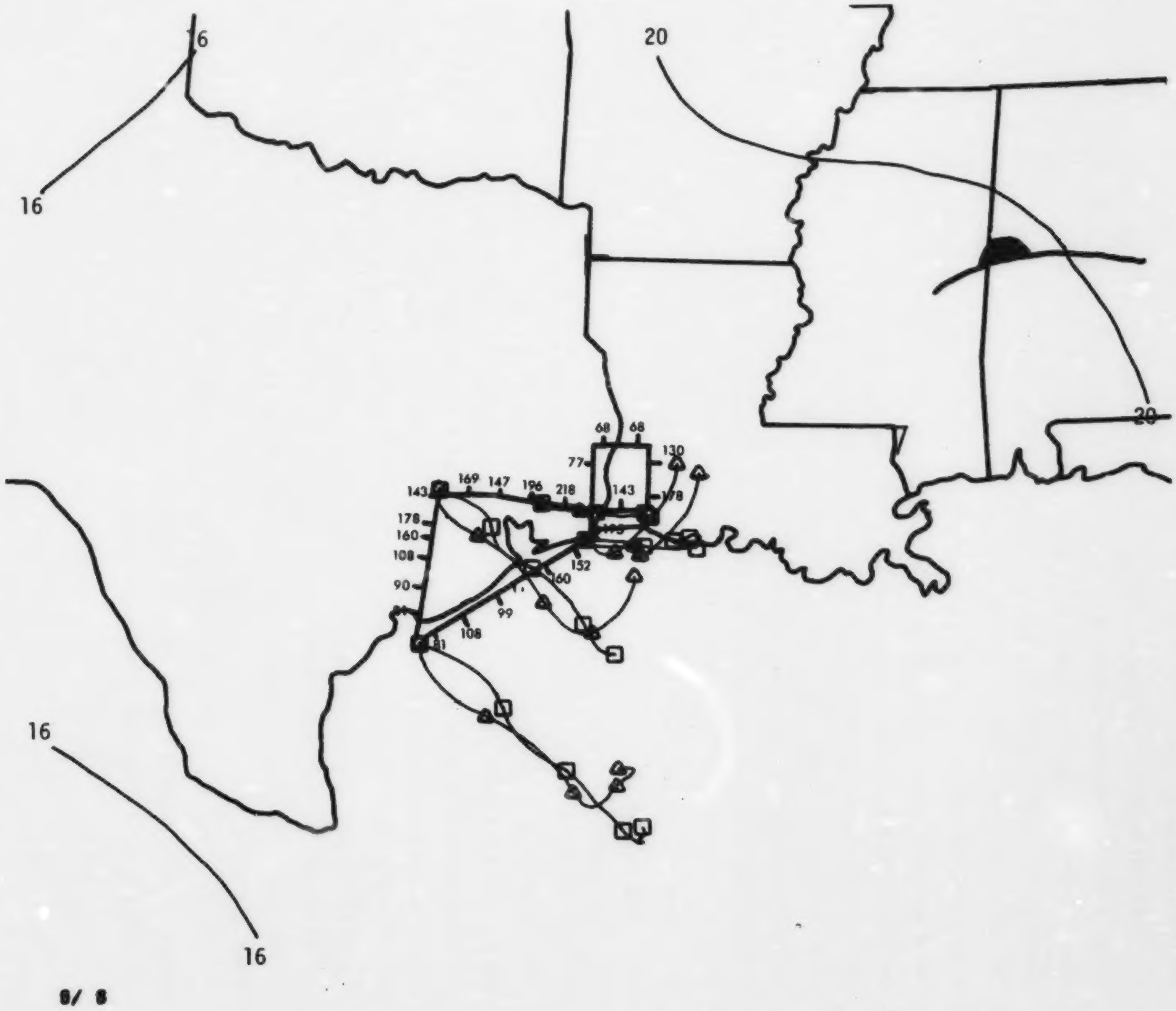
16
16
20
20
16
16
68
68
77
130
143
169
147
196
218
143
178
178
160
108
90
152
160
99
108
8/ 8

Figure 81. Ozone concentrations, air trajectories and sea level pressure distribution for August 8, 1975 flight.

air flow downwind of Houston, and to sample again for a plume downwind of the Nederland area.

The ozone distribution encountered along the flight was complex. After leaving DeRidder and heading southward toward the coast, high ozone concentrations above the NAAQS occurred at an altitude of 600 m MSL while passing over the Nederland area, and diminished to below the NAAQS upon reaching the coast. On the southwestward leg, ozone concentrations approached the NAAQS, then diminished rather rapidly after passing the Galveston Bay area. From there to Port O'Connor on Matagorda Bay, ozone concentrations decreased by 50 percent. On the northward leg, ozone concentrations increased toward Navasota, rising rapidly within 2 minutes from 40 $\mu g/m^3$ to 160 $\mu g/m^3$, and then 2 minutes later reaching 178 $\mu g/m^3$. Concentrations then decreased about 30 $\mu g/m^3$ for the duration of the leg. On the eastbound portion of the flight, ozone concentrations were 160 ± 15 $\mu g/m^3$. About 6 miles downwind of Nederland, ozone concentrations decreased to approximately 140 $\mu g/m^3$ and generally remained there except over Lake Charles.

The trajectory pattern provides some insight into the distribution of high ozone concentrations. In the southwestern corner where lower ozone concentrations were observed, the air arrived from the southeast, having traveled that way for approximately 36 hours. Air arriving in the northwestern corner apparently had a 24-hour period over land and passed through the Houston metropolitan area. The trajectories suggest that the air with high ozone concentrations farther east had a recent history over the precursor source regions of southeast Texas. Air flow in the southeast was quite slow and offered the potential for local ozone production. The largest concentrations were found directly upwind of the Nederland area.

On this day the second highest maximum daily ozone concentration observed were reported at Nederland (347 $\mu g/m^3$) and at Houston (378 $\mu g/m^3$). Concentrations at DeRidder, however, remained below 140 $\mu g/m^3$.

3) August 9, 1975, Case Study

The flight pattern of August 9 duplicated the previous day's flight, but ozone concentrations were quite different from those observed before (fig. 82). The air flow was from the east southeasterly with a long but slow fetch over water. On the southwestern heading of the flight, along the coastline, ozone concentrations were generally between 60 and 80 μg/m^3, indicating that all the onshore flow had low ozone concentrations. Immediately inland from Port O'Connor, ozone concentrations quickly increased to 200 μg/m^3 before slowly decreasing further northward. In the flight leg eastward into the wind, ozone concentrations remained low, even across the Nederland area. The trajectory of the air arriving along that part of the flight may have come inland between Nederland and Houston; the resolution of the trajectories, however, does not allow that distinction. Nevertheless, it is difficult to understand the lowered ozone concentrations of this day from those observed the day before along the same path at the same time. Further discussions of the data obtained on this day are included in section 8.1.4.

4) September 19, 1975, Case Study

A standard sea breeze flight was flown in the morning and afternoon of September 19. Pressure gradients were generally weak all along the gulf coast area. Low-level wind flow was onshore, as it was for the past several days (fig. 83). Throughout the entire flight, ozone concentrations were among the lowest found during the study.

At the ground stations, only a very few concentrations above 100 μg/m^3 were reported. Maximum concentrations in Austin on this day were 80 μg/m^3; in Nederland, 70 μg/m^3, and in DeRidder, 123 μg/m^3.

The vertical profile of ozone concentrations taken in the southeastern corner of the flight path showed very well-mixed profiles with ozone concentrations less than 100 μg/m^3.

5) September 21, 1975, Case Study

The frontal system that 2 days before was poised to the west of the study area passed through and a high pressure system began pushing down

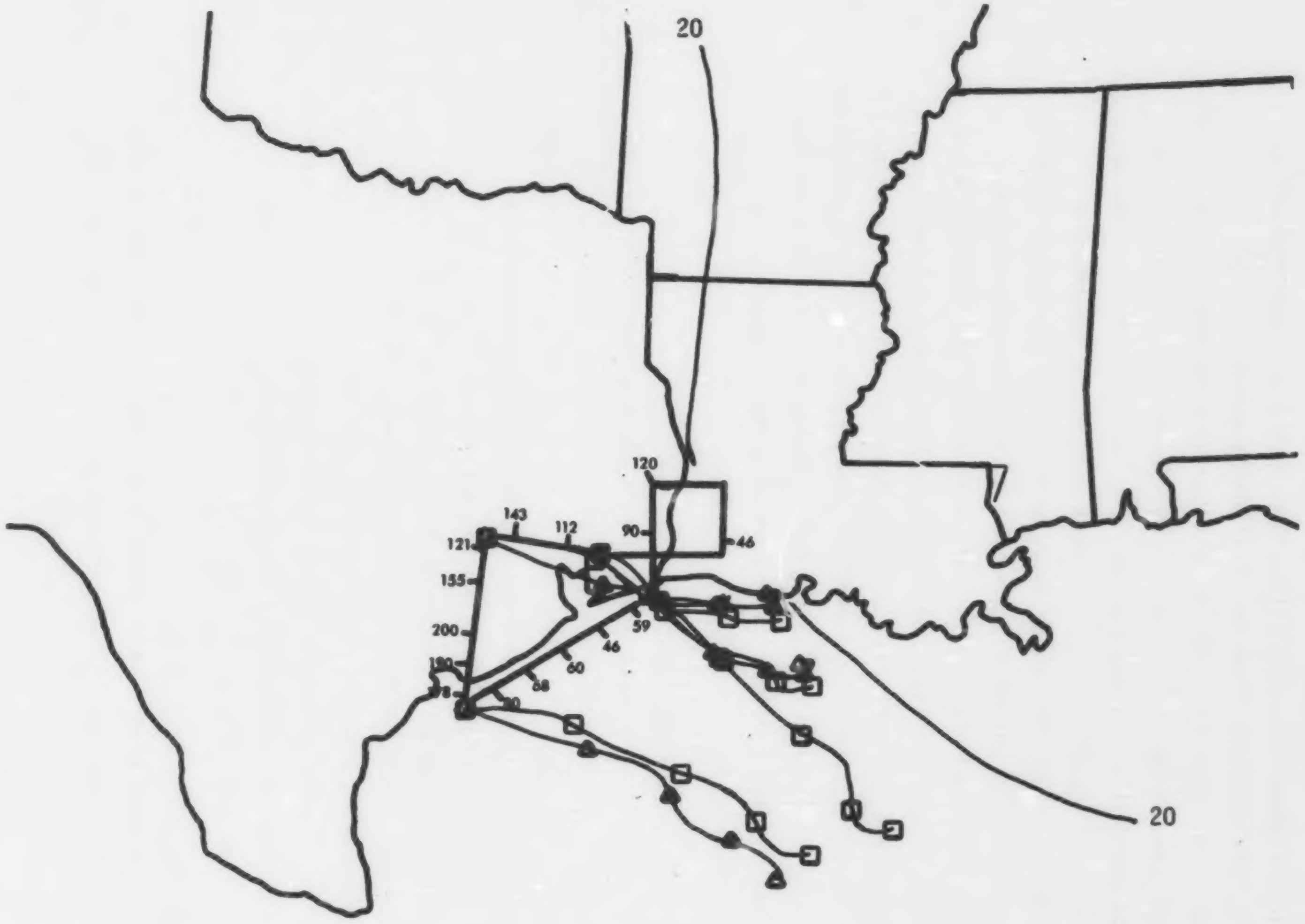
20
20
120
143
112
90
46
121
155
200
190
59
46
60
68
90

8/ 9

Figure 82. Ozone concentrations, air trajectories and sea level pressure distribution for August 9, 1975 flight.

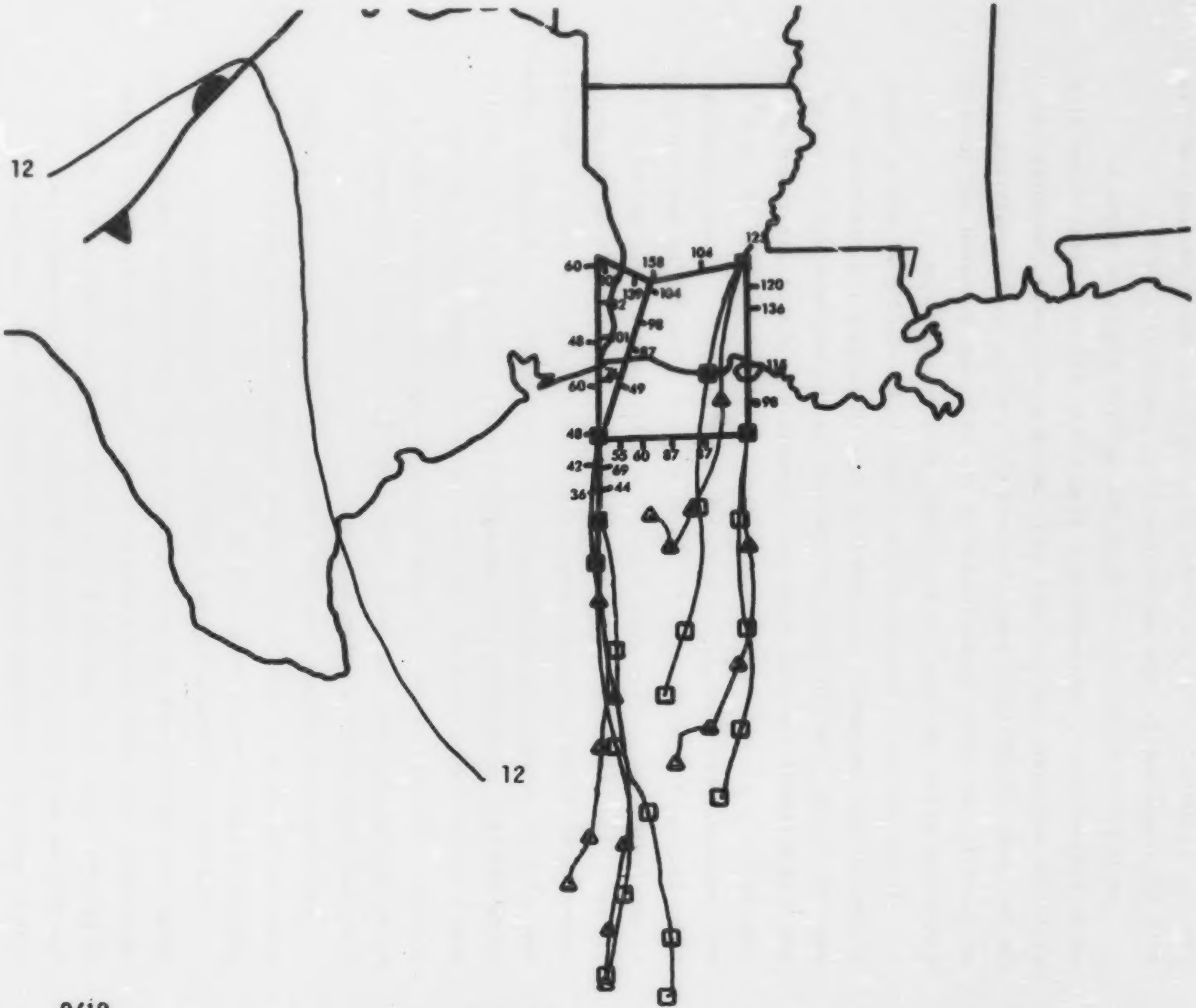
12
12
12
104
158
60
120
136
104
139
82
98
48
101
87
60
49
116
98
48
55
60
87
87
42
69
36
44

9/19

Figure 83. Ozone concentrations, air trajectories and sea level pressure distribution for September 19, 1975 flight.

from the northwest. The sea breeze flight pattern was flown for contrast with the measurements made before the front passed (fig. 84).

On the outward bound portion of the morning flight at 1,300 m, ozone concentrations decreased away from the coastline. After descending to 165 m, and retracing the same path toward shore, ozone concentrations on the order of 120 $\mu g/m^3$ were observed all the way to the coastline. Just at landfall, an ozone concentration of 164 $\mu g/m^3$ was measured but quickly dropped to below 100 $\mu g/m^3$ as the flight progressed inland.

On the afternoon portion of the flight from DeRidder at 600 m, ozone concentrations increased, and remained high throughout the eastbound leg over the water. The vertical profile made in the southeastern corner of the flight showed the high ozone concentrations at flight level; but at approximately 1.0 km, ozone concentrations decreased to below 100 $\mu g/m^3$ and remained there through the next 1.0 km of altitude. Ozone concentrations increased from 95 $\mu g/m^3$ to 120 $\mu g/m^3$ just below 2.5 km and continued to the top of the profile near 3 km. The shift toward lower values below 2.5 km to approximately 1.0 km was seen in the descent phase of the profile. Returning to flight altitude, ozone again increased to 164 $\mu g/m^3$. Neither the aircraft temperature measurements nor the Boothville, Louisiana, rawinsonde indicate the presence of inversion layers. It is possible, however, that a stable layer may have been present in the upper portion of the profile. The surface frontal zone sloped toward the north, and with a storm approaching from the south, the front could have been farther north than indicated on the weather maps.

Proceeding northward from the vertical profile, ozone concentrations again increased at flight level. After passing inland of Lafayette, ozone concentrations never exceeded 125 $\mu g/m^3$.

Trajectory analysis suggests that the air which had been over a relatively unpopulated region (e.g., Arkansas, Mississippi, Louisiana) was associated with lower ozone concentrations. Higher concentrations appear to be associated with northeast flow of air that had been in the Mobile or New Orleans area over the previous 24 hours. Ozone concentrations at the fixed monitoring locations in Texas and Louisiana were less than 130 $\mu g/m^3$.

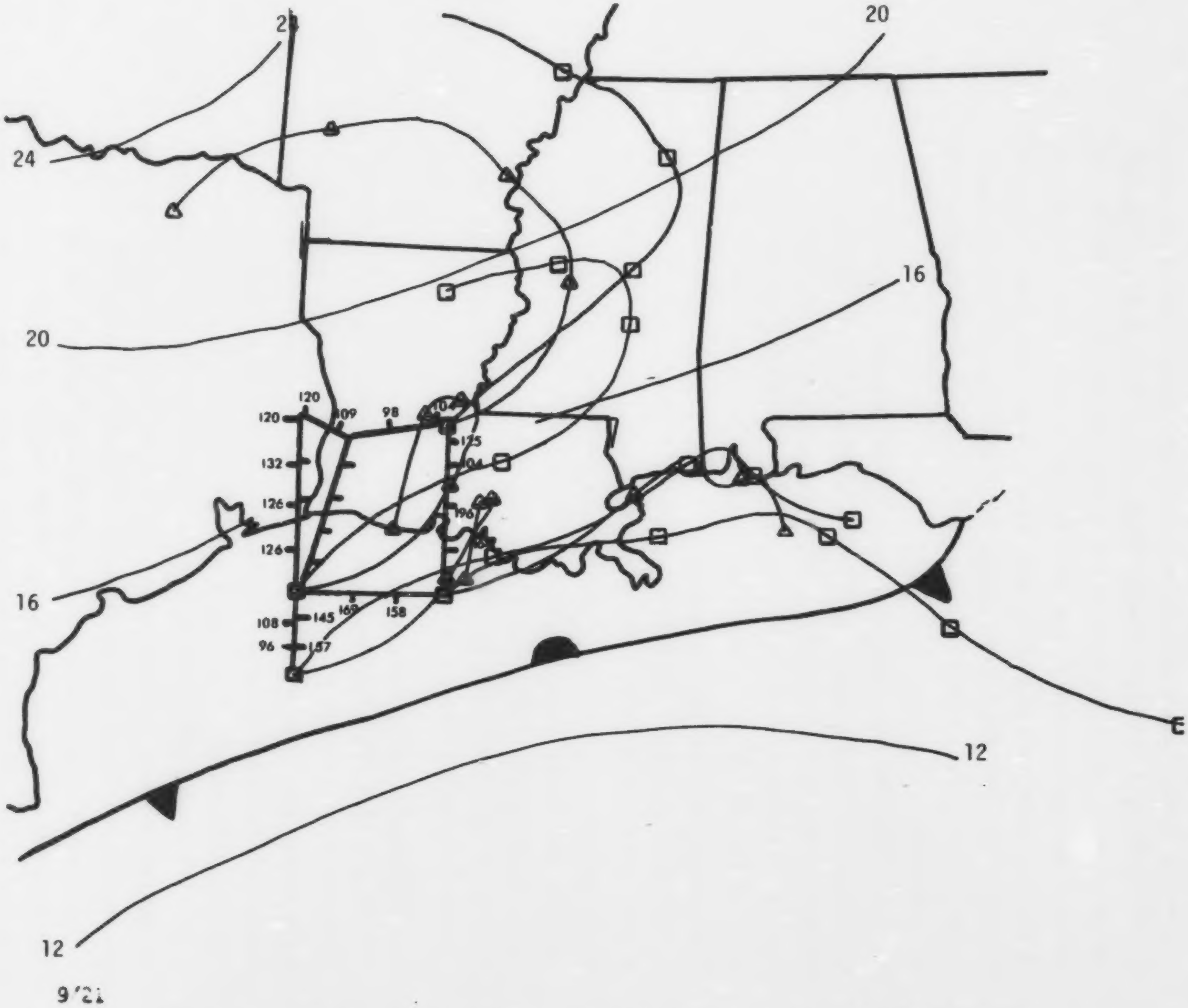
20
24
16
12
20
16
12
24
120
120
109
98
104
125
104
132
126
196
126
108
145
169
158
96
157
9'21

Figure 84. Ozone concentrations, air trajectories and sea level pressure distribution for September 21, 1975 flight.

6) October 10, 1975 Case Study

A sea breeze flight pattern was initiated under conditions conducive to establishing a land-sea breeze circulation. Very little difference was observed in ozone concentrations during the sea breeze flight until the very southern extent of the morning flight (fig. 85). During the afternoon, ozone concentrations near Lake Charles were high (371 $\mu g/m^3$) but decreased over the water. Along the eastern leg of the afternoon flight, high ozone concentrations were encountered, with landfall south of Lafayette.

Air flow into that region is very poorly defined. Lake Charles soundings indicated a southerly flow at about 3 m/s. Boothville, Louisiana, farther to the east, indicates a northeasterly wind about 5 m/s. Consequently, the trajectories show very little air motion over the past 12 hours along the eastern side of the flight path, where some of the high ozone concentrations were encountered.

Both portions of the vertical profile of ozone taken in the southeastern corner of the flight path are consistent above 2 km (above the mixing height). A low-level inversion is apparent in the Boothville sounding and in the aircraft temperature profile. Below the inversion layer, ozone concentrations on the ascent and the descent of the vertical profile differ in quantity by about 80 $\mu g/m^3$; but they agree on the rate increase of ozone between 1.0 and 1.3 km.

7) October 13, 1975, Case Study

As the high pressure system moved northeastward into the Carolinas, southerly flow returned to the coastal areas of Louisiana and Texas. The RTI aircraft flew approximately 200 miles out into the Gulf of Mexico to sample the air being returned to the area on the southwestern side of the high pressure system. The flight out was made at 650 m and the return flight 165 m. At both altitudes ozone concentrations decreased with increasing distance from the shore. No substantial difference in ozone concentration between altitudes could be determined (fig. 86).

Air parcel trajectories were markedly uniform over the period (possibly because of the influence of the Boothville, Louisiana, sounding upon the trajectories; they remained over water during the 48-hour period.

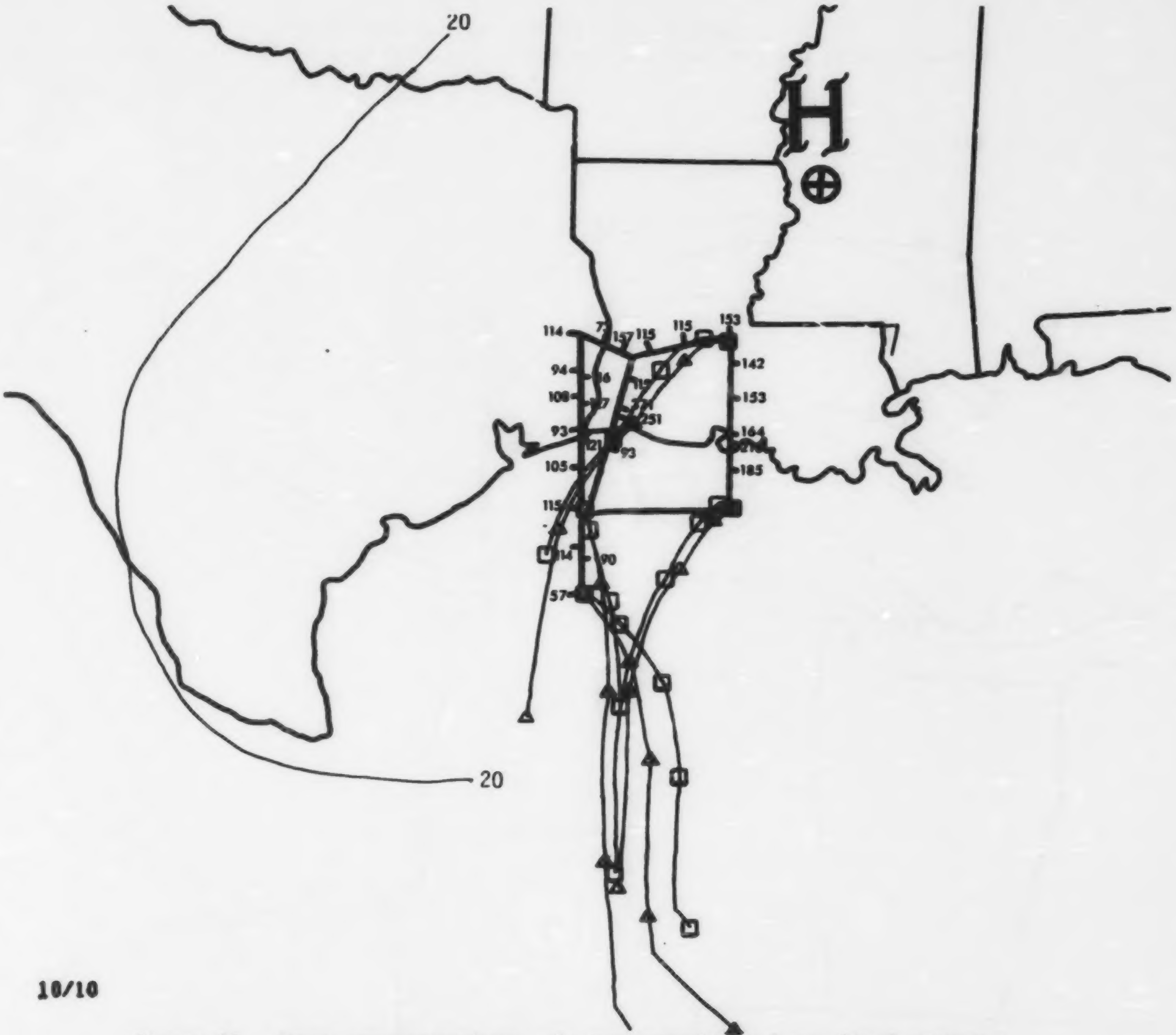
20
H
20
114
157
115
115
153
94
108
93
121
93
251
105
115
114
90
57
142
153
164
185
10/10

Figure 85. Ozone concentrations, air trajectories and sea level pressure distribution for October 10, 1975 flight.

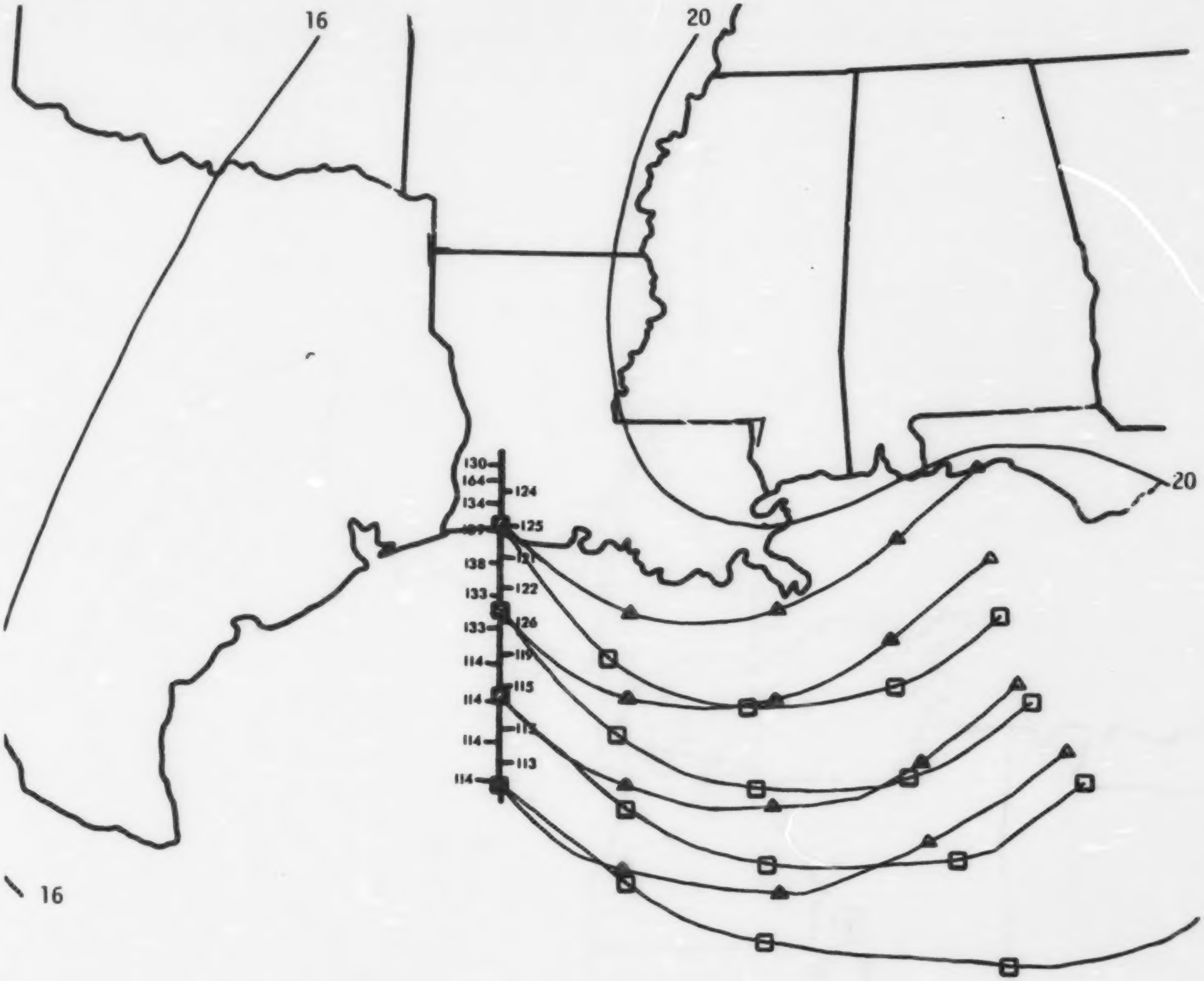
16
20
20
16
130
164
124
134
125
121
138
122
133
126
133
119
114
115
114
112
114
113
114

10/13

Figure 86. Ozone concentrations, air trajectories and sea level pressure distribution for October 13, 1975 flight.

The data associated with this flight give no indication of advection of high ozone into the northern gulf coast from potential source regions in the Florida panhandle or peninsula.

8) October 14, 1975, Case Study

An east-west survey flight shown in figure 87 was flown during the afternoon of October 14. A ridge of high pressure extended westward from a high pressure center on the Carolinas coast, north of the gulf coastal area. Winds aloft were southeasterly at about 10 m/s at most locations along the gulf coast. Air parcel trajectories arriving at locations along the flight path showed rapid movement. Ozone concentrations measured over the water had only minor variability, although the "source regions" of those trajectories were quite different. The air parcels arriving in the southwestern corner of the flight path had been exclusively over the Gulf of Mexico for the past 48 hours. Trajectories arriving in the southeastern corner had come from the Florida peninsula during the same period. There seemed to be no substantial difference in the ozone concentrations associated with these two trajectories. In south Alabama, air parcels spent a longer period over land areas closer to the high pressure center. The air parcel arriving on the Mississippi-Louisiana border was chosen to investigate the role of transport in the high ozone concentration (174 $\mu g/m^3$) found nearby. That air moved quite rapidly, passing over the Baton Rouge, Louisiana, area prior to being sampled.

In general, ozone concentrations over the water were lower than those found over land. These were also typical of afternoon concentrations found at DeRidder and Austin during the study period. The higher concentrations found over land may be due to low-volume emissions from anthropogenic sources near coastal areas, or may be due to some enhancement from natural sources such as the pine forests of the coastal plain.

9) October 19 to 24, 1975, Case Study

From the afternoon of October 19 to the afternoon of October 24, daily flights at low altitudes were conducted in east Texas, most of Louisiana, and areas of the Gulf of Mexico adjacent to these States. During this

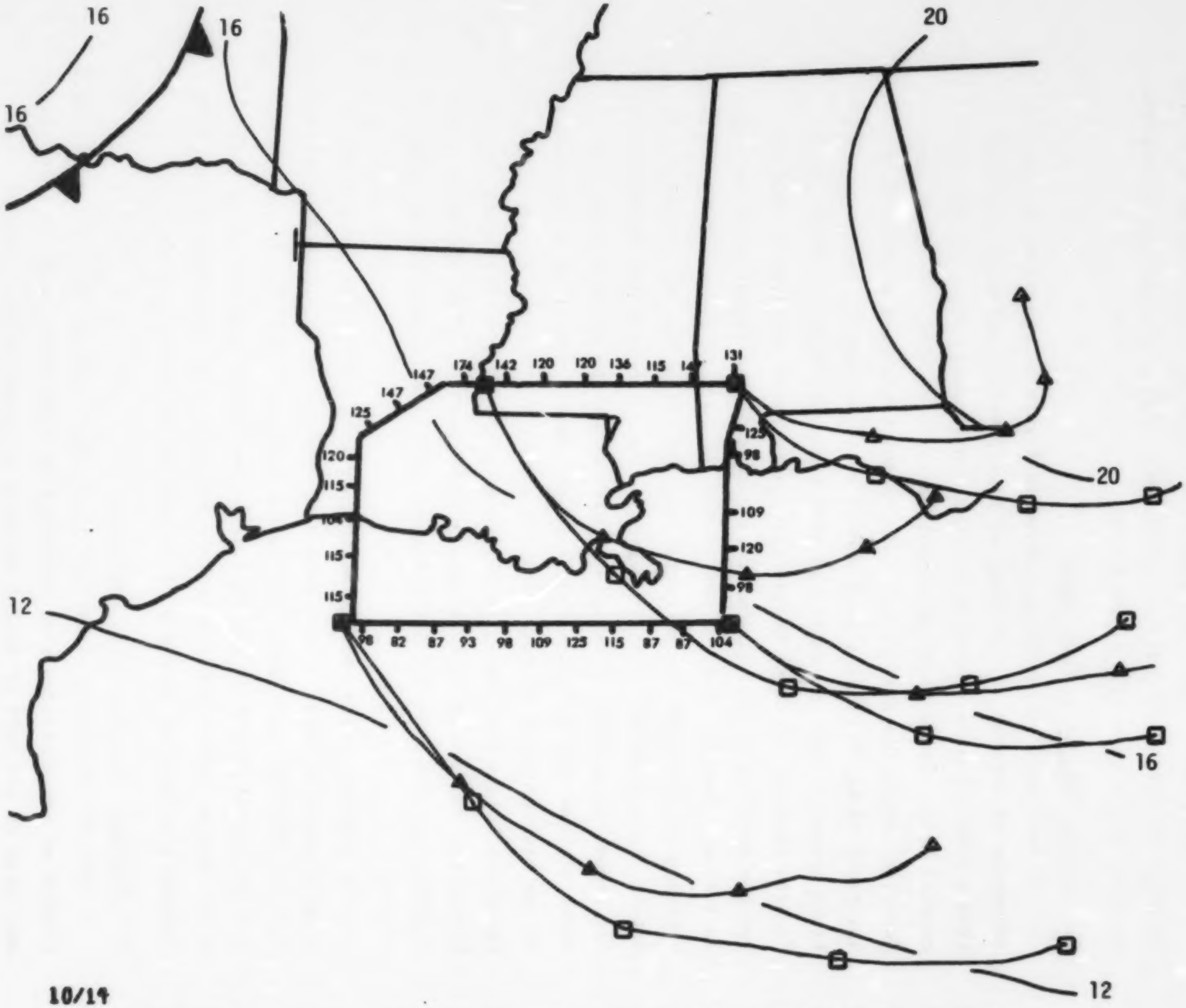
16
16
16
20
20
16
12
12
147
147
125
174
142
120
120
136
115
14
131
125
98
109
120
98
104
120
115
104
115
115
98
82
87
93
98
109
125
115
87
87

10/14

Figure 87. Ozone concentrations, air trajectories and sea level pressure distribution for October 14, 1975 flight.

6-day period, high ozone concentrations were found over large portions of the flight tracks in all the sectors investigated. High ground-level concentrations of ozone were observed at DeRidder, Nederland, Houston, and Austin. A high pressure system developed and moved east-northeastward, leaving the area under the influence of a ridge line. Time-altitude cross sections of air properties at Houston and Lake Charles showed very unusual conditions near 1.5 km.

On the evening of October 18, the atmosphere at Lake Charles was well mixed to approximately 1.7 km (fig. 88). Above 1.7 km, large-scale subsidence which began 12 hours before was developing a stable layer. A complex pattern of warming and cooling in and above that layer indicated an ongoing dynamic process. The subsidence continued, lowering of the mixing height and inversion layer until the morning of October 21 (1200 GMT); thereafter, the subsidence diminished. The stable layer began to rise, but its intensity did not diminish until the afternoon of October 22. By morning of October 23, the stable layer was effectively broken and the concentration of ozone near the ground decreased.

On the morning of October 19, a weak high pressure center was forming in southeastern Texas and western Louisiana. The western half of the north-south survey flight was initiated to document the gradient of ozone which might occur with the predominantly northerly flow of air. By midafternoon, the high pressure center was located to the south-southeast of Lake Charles, but the pressure gradient was weak. Low altitude air flow into the four ground locations had first been northerly, but had returned to a weak southerly flow the latter 12 hours.

Air flow aloft began northerly, turning westerly during the course of the day (fig. 89). The predominance of a northerly flow even in a developing anticyclone indicated an unusual situation. Anticyclonically curved trajectories are expected with the transient high pressure system. The curvature of these trajectories was cyclonic, suggesting that the high pressure system was being formed and had only recently begun to establish its influence in the flow regime.

Ozone concentrations meausured during the eastern half of the flight were of the order of 125 $\mu g/m^3$, while in the western half, concentrations

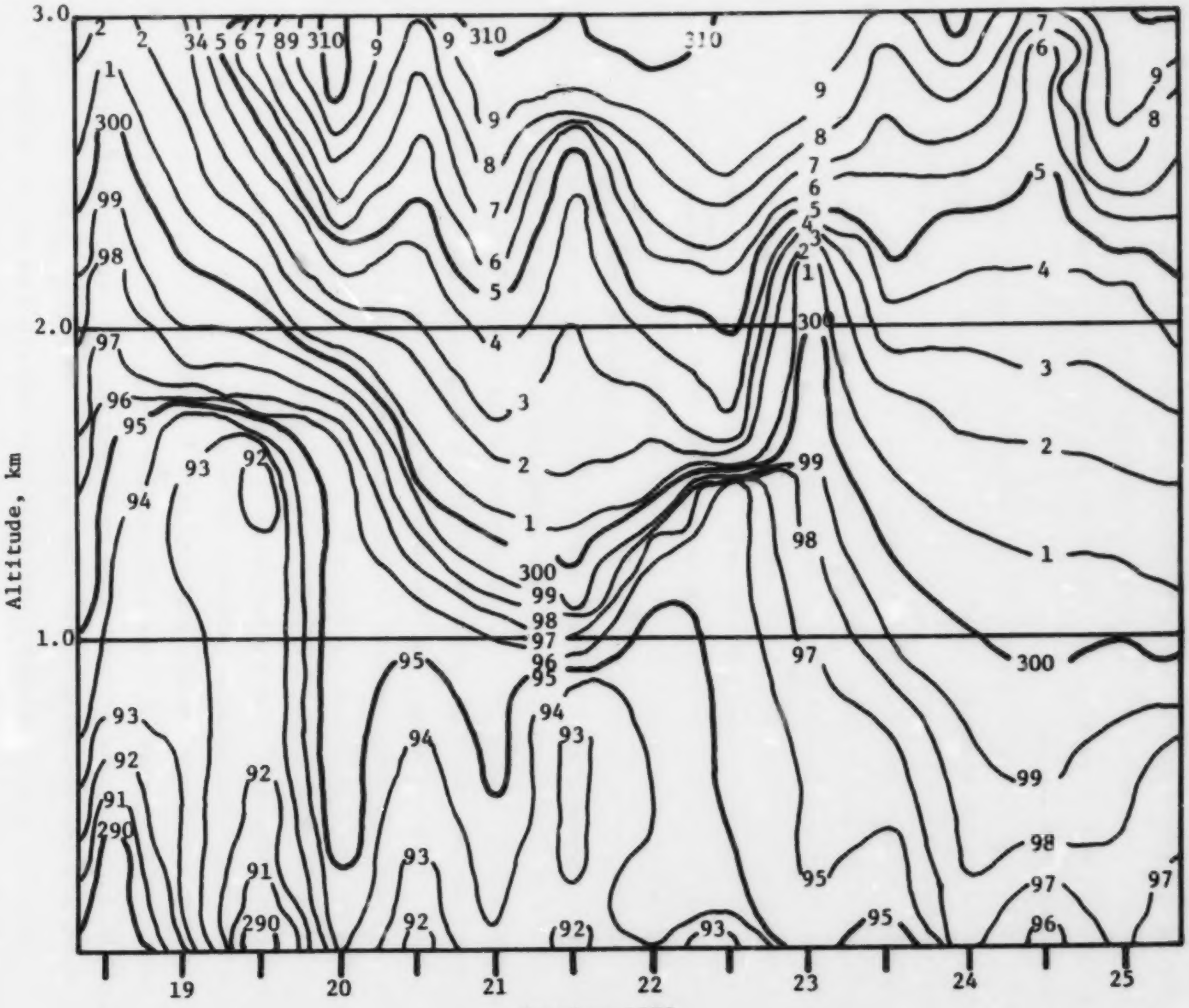

Figure 88. Time altitude cross section of potential temperature (°K) at Lake Charles, Louisiana. Dates are indicated at 0000 GMT.

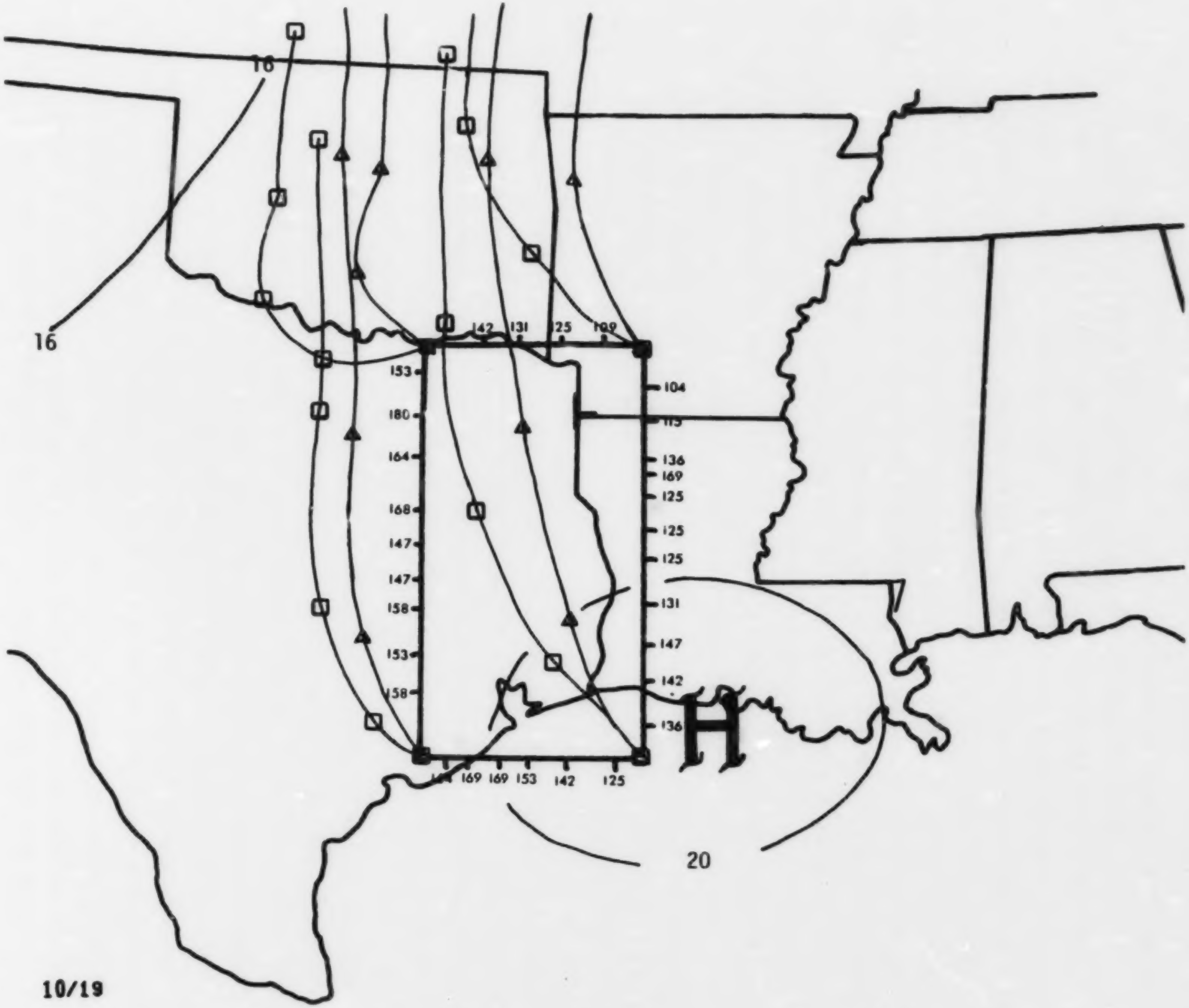
16
16
142
131
125
109
153
180
164
168
147
147
158
153
158
104
115
136
169
125
125
125
131
147
142
136
H
169
169
153
142
125
20
10/19

Figure 89. Ozone concentrations, air trajectories and sea level pressure distribution for October 19, 1975.

were mostly at or above the NAAQS. Clearly, the western half of the flight shows an area-type distribution rather than a plume-type distribution of ozone from a localized source.

Ozone concentrations of 180 $\mu g/m^3$, near the northwest corner of the flight path could be interpreted to be a result of ozone transport from the Dallas-Forth Worth metropolitan area. The afternoon trajectory indicates that winds in north central Texas had turned to a westerly component for the previous 12 hours. Assuming that a trajectory arriving at the location of the high ozone reading paralleled the path of the more northerly parcel, the air would have passed over the Dallas-Fort Worth metropolitan area about 12 hours before. However, the crosswind width of the plume, about 29 km at a distance of 96 km from Dallas, suggests no plume spreading en route since the metropolitan area is about the same cross wind width. The evidence of a plume downwind of Dallas was inconclusive.

The change of concentration from the northwest to the northeast corner of the flight is not easily interpreted from the viewpoint of the trajectories. The air arriving in the northwestern corner had a path roughly over the Oklahoma City area 24 to 36 hours before the aircraft reached this point. The air arriving in the northeastern corner passed over the Tulsa, Oklahoma, area, also an oil refining area, 24 hours before. On the southbound leg of the flight, the aircraft apparently passed through a narrow plume southwest of the Shreveport, Louisiana, area and measured ozone concentrations as high as 169 $\mu g/m^3$ for a brief period.

By the afternoon of October 20, the high pressure center had moved some 300 miles to the east-northeast to a position just north of Mobile, Alabama. Central pressures increased to 1,023 mb and the 1,020-mb isobar extended from west of Austin, Texas, to central Georgia. A high pressure ridge extended southeastward from the high center to south of the flight area. Southerly winds had persisted for the previous 24 hours at all of the ground monitoring stations. Farther away from the high pressure center, more air movement had occurred for the air arriving at Austin and Houston than for the air arriving at DeRidder and Nederland. The eastern portion of the north-south survey blocks was flown at 650 m along the path shown in figure 90. The area covered was reduced from the previous day for

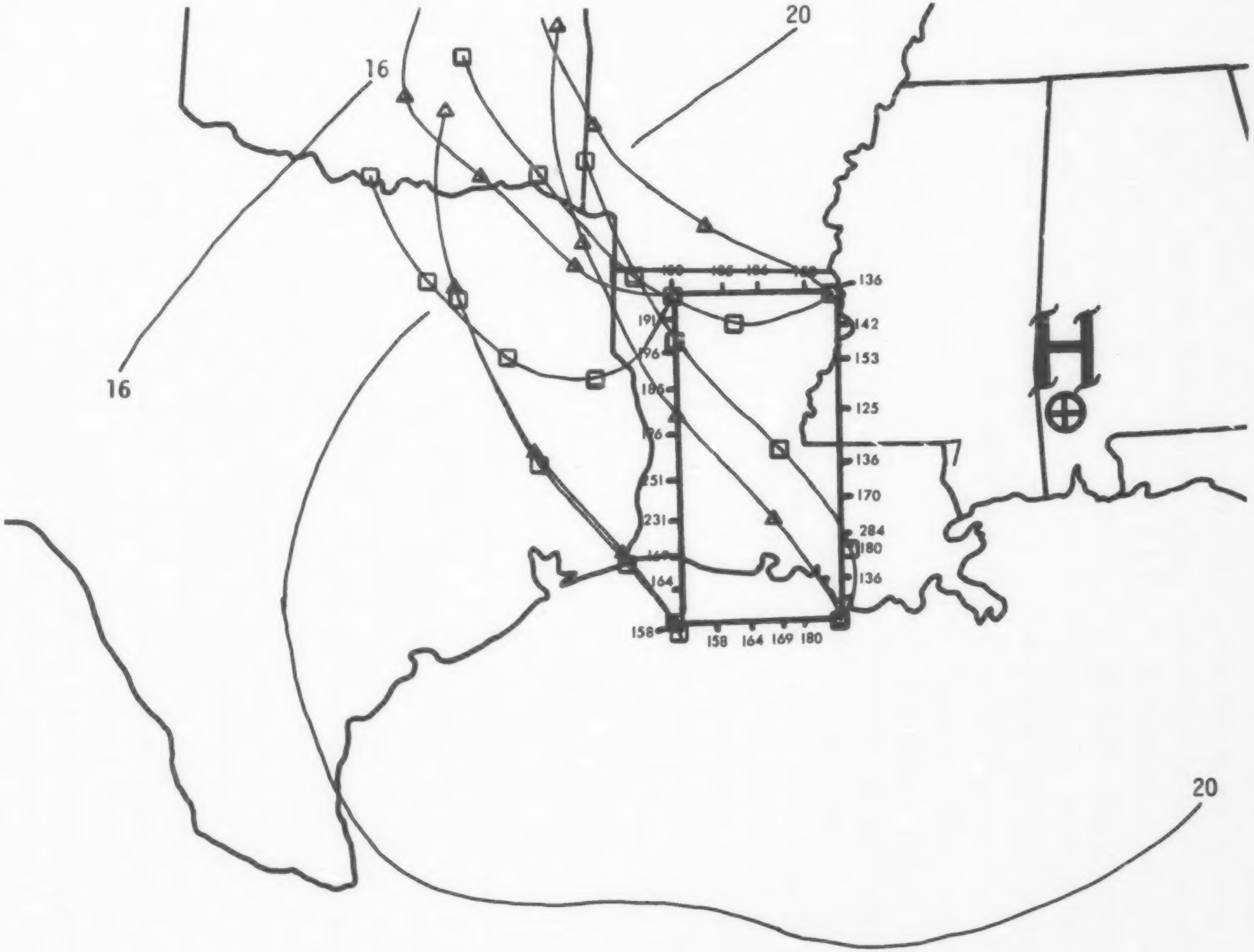

16
16
20
20
H
136
142
153
125
136
170
284
180
136
191
196
186
196
251
231
164
158
158
164
169
180

10/20

Figure 90. Ozone concentrations, air trajectories and sea level pressure distribution for October 20, 1975 flight.

operational reasons. Ozone concentrations near 160 $\mu g/m^3$ were encountered on all legs of the flight and were persistent in the northern, western, and southern portions of the flight. Again, eastern portions remained low. Highest ozone concentrations were recorded near Lafayette (284 $\mu g/m^3$).

Of the ground stations, only DeRidder (256 $\mu g/m^3$) showed ozone concentrations above NAAQS. Low altitude trajectories showed that air arriving at DeRidder in the late afternoon had been in transit from the Nederland area for the previous 24 hours. Concentrations measured there were among the highest along the flight path. The air which arrived at Nederland had passed over the Gulf of Mexico. An ozone concentration of 224 $\mu g/m^3$ was noted along the northern perimeter of the flight path approximately downwind of a refining complex at Monroe, Louisiana.

Persistent high ozone concentrations during a period of north-to-westerly flow across areas of low emission densities are difficult to understand or to explain. The air parcels arriving in the northeastern corner of the flight suggests an increase of concentration with time. Twenty-four hours previously, the parcel was near the Arkansas-Louisiana border, roughly in the area where ozone concentrations on the order of 110 $\mu g/m^3$ were sampled. At flight altitude 24 hours later, concentrations on the order of 145 $\mu g/m^3$ were encountered. Air parcels arriving in the northwestern corner on this evening came from areas of east Texas where ozone concentrations were equal to the NAAQS. Upon arrival, these concentrations increased to about 190 $\mu g/m^3$.

The upper air trajectory in the southwestern corner of the flight path showed air flow across Nederland to the sample point, where it had remained nearly stagnant for about 12 hours. Ozone concentrations at flight level were just below the NAAQS and were the lowest of those encountered. It may be improper to use winds integrated to 2 km in this situation since the subsidence inversion was present at approximately 1.2 km. Wind speeds below the inversion had a southerly component of about 6 m/s while those above, about 2.5 m/s. Southerly flow as suggested by the lower altitude trajectories are probably more appropriate in this situation. The subsidence inversion covered the Gulf Coastal Plain from Victoria, Texas, to Centerville, Alabama. Consequently, vertical motion probably was restricted to 1.5 km or less.

On October 22, the high pressure center had proceeded further eastward, leaving only a ridge line with a northeastward axis. Measurements of high ozone concentrations on the previous day at DeRidder, and the high concentrations already observed early in the afternoon indicated that a flight was necessary. The RTI aircraft left Lake Charles for Nederland, then went 160 km south out over the Gulf of Mexico before returning to Lake Charles via Nederland and DeRidder. A vertical profile was flown at DeRidder. This flight track is shown in figure 91.

Ozone concentrations exceeded the NAAQS throughout the flight except at the southern tip of the flight, where ozone decreased by about 20 $\mu g/m^3$. The over-water flight was made along the axis of the wind into Nederland at both the lower and upper levels. Trajectories suggest that advection of air having lower ozone concentrations into the Nederland area might have been expected within about 12 hours. The ground-level concentrations in Nederland decreased over the next 12 hours; but more probably in response to local nocturnal ozone destruction, rather than advection. On the following day, the maximum ozone concentration was 62 $\mu g/m^3$ lower, indicating a change of air mass.

Trajectories at the higher levels indicate that the air reaching Nederland had been carried out to sea approximately 24 hours before a reversal of wind initiated a return flow into the Nederland area. Though initially it might appear that the high ozone concentrations were associated with air flow from the Gulf of Mexico, the trajectory analysis clearly shows that the air is only returning after having passed over sources of ozone and ozone precusors.

The low-level trajectories into the DeRidder area show a slow movement of air from the Gulf of Mexico northward across Lake Charles into DeRidder over the past 24 hours. The upper air flow on October 21 indicates the air had begun to return northward during the past 12 hours. Time cross-sections of wind directions perpendicular to the coast at Lake Charles showed that wind speed was in a transition period from northerly to southerly on the morning of October 21, while it had had a southerly component for the past 36 hours in the very lowest layers.

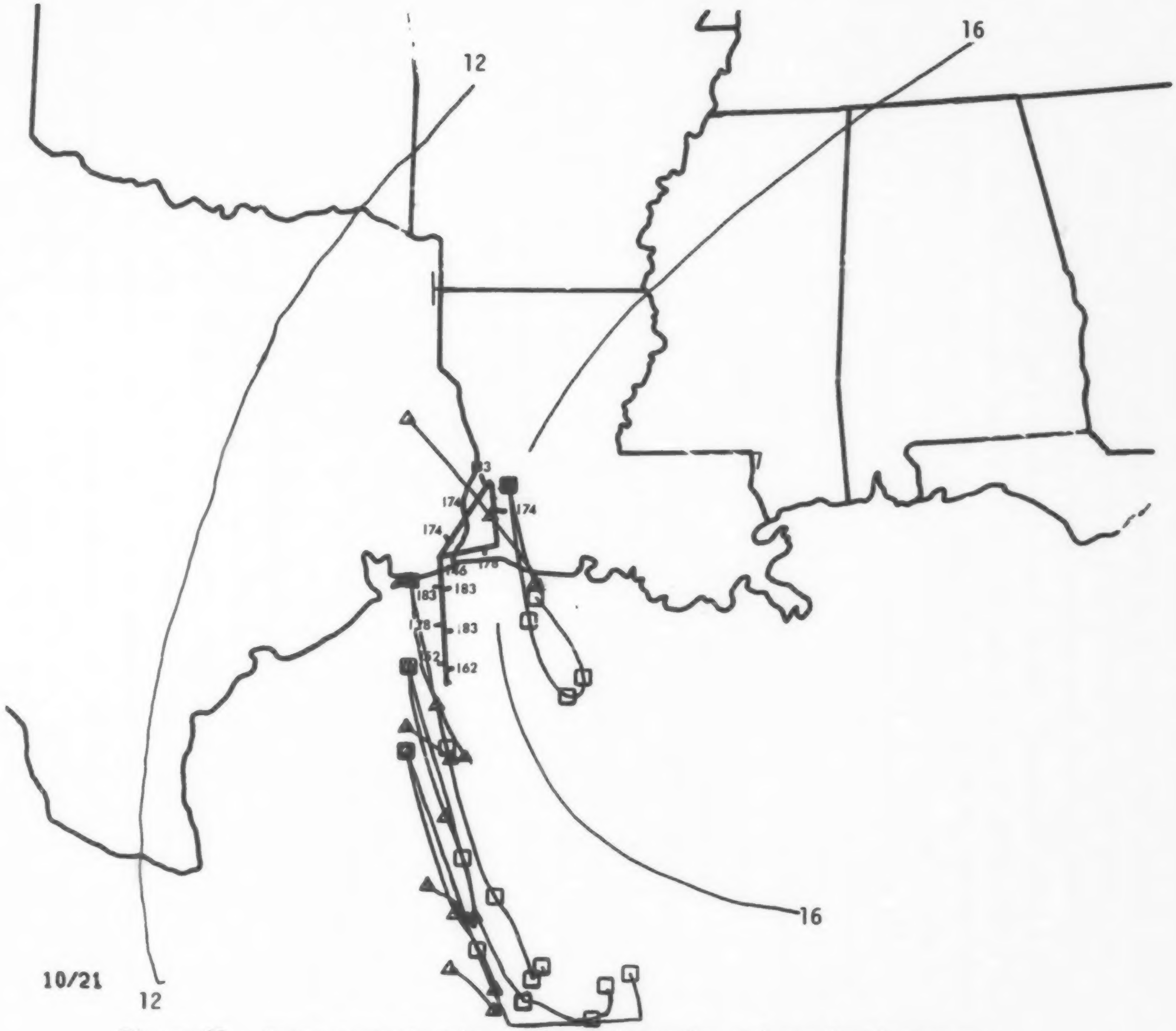
12
16
83
174
174
174
146
178
183
183
183
178
152
162
16
10/21
12

Figure 91. Ozone concentrations, air trajectories and sea level pressure distribution for October 21, 1975 flight.

With the advent of the southerly wind flow, the mixing depth of Lake Charles rose from 1.2 km in the morning to 1.45 km in the afternoon. The potential temperature (298.3°K) associated with the mixing depth, however, did not change. The mixing depth and the potential temperature at Houston were only slightly higher and were increasing.

The airplane flew a vertical profile to approximately 3 km at DeRidder (fig. 92). Ozone concentrations increased with altitude to 1.2 km. At 1.55 km, ozone concentrations decreased and remained constant thereafter to the top of the sounding. The ambient temperature decreased with altitude to 1.55 km. Over the next 300 m, the temperature was isothermal and the dew point temperature decreased by 11.2° C. On the way down, ozone concentrations remained below 110 $\mu g/m^3$ above 1.5 km. In the next 300 m of descent, ozone doubled to 216 $\mu g/m^3$, and slowly decreased to 178 $\mu g/m^3$ in the lowest 300 m of the air. The aircraft temperatures are in reasonably good agreement with the late afternoon soundings taken at Lake Charles, which showed a nearly isothermal layer extending from 1.0 km to about 1.7 km. On the return trip from DeRidder to Lake Charles, ozone concentrations also remained above the NAAQS between 300 and 600 m above the ground.

On this day, trajectories arriving at Houston and Austin showed a well-developed southerly flow, having been on the back side of the high pressure system for a longer time. Afternoon concentrations in the Houston area were 137 $\mu g/m^3$, a fairly low value for that station, and concentrations at Austin had decreased to 124 $\mu g/m^3$ from a previous day of 156 $\mu g/m^3$.

By the afternoon of October 22, the influence of the high pressure ridge had weakened through the area. The pressure gradient had increased and a strong southerly flow into Lake Charles and Houston had developed through all levels of the atmosphere. Ozone concentrations between 99 and 122 $\mu g/m^3$ were recorded during the EPA aircraft flight on October 22 with no particular pattern to the concentrations measured (fig. 93). Ground-level ozone concentrations at the four stations were comparable to those measured by the EPA aircraft. These measurements indicate a relatively uniform distribution of ozone in the air mass.

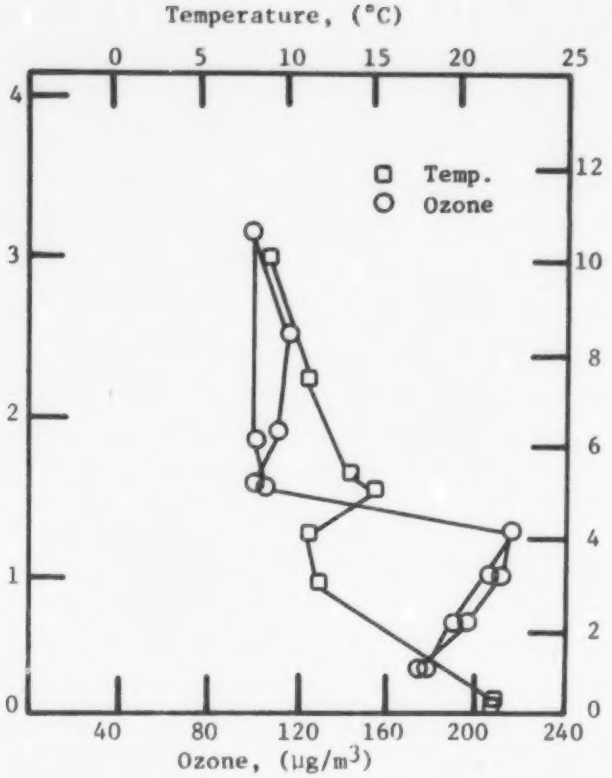

Figure 92. Ozone concentrations and temperature from vertical profile flight of October 21, 1975 at DeRidder, Louisiana.

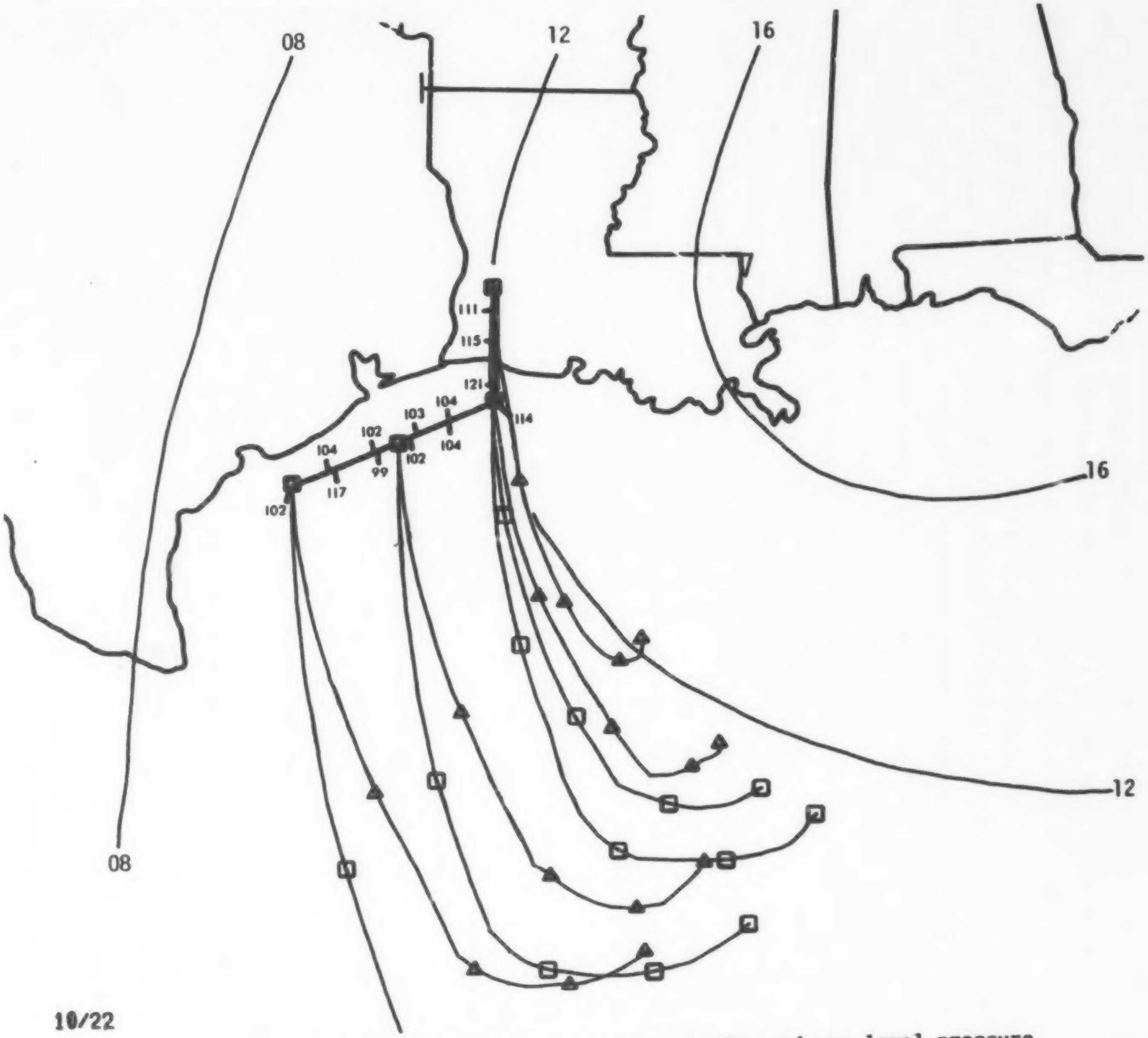
08
12
16
111
115
121
114
104
103
102
104
102
104
99
117
102
16
12
08
10/22

Figure 93. Ozone concentrations, air trajectories and sea level pressure distribution for October 22, 1975 flight.

The air parcel trajectories indicate a long fetch over water preceded by a turning from a northeasterly flow into a southeasterly to southerly flow. The ozone concentrations were slightly higher than "background" concentrations. The turning of the trajectories from the northeastern into a southerly flow suggests that the air might have had an earlier origin over the gulf coast region. (Caution is advised since air in the central Gulf of Mexico is distant from the sounding stations). Mixing depth increased slightly to about 1.75 km in the morning sounding at Lake Charles, slightly higher than the day before and penetrated slightly into the base of the inversion layer aloft at 1.6 km. By afternoon, the stable layer had arisen to around 2.2 km, and the afternoon mixing depth reached only about 1.8 km. Warm air apparently associated with the increased onshore flow left a relatively unstable column of air within the mixed layer. The ventilation of the near coastal area had increased substantially, and ozone concentrations decreased.

For the next 2 days, October 23 and 24, strong onshore winds persisted. Throughout the first 3 km of the air, mixing prevailed. Winds aloft exceeded 10 m/s through most of the first 2 km of the atmosphere. The lowest maximum ozone concentrations reported during the measurement program occurred at Nederland and Houston. The increased wind speeds have reduced the local residence time of injected ozone precursors, increased the turbulence of the atmosphere giving better dispersion, and probably have inhibited development of the oxidant potential on the Texas gulf coast.

Ozone concentrations between 68 and 93 $\mu g/m^3$ were measured during EPA Flight Pattern No. 4, flown on October 24 (fig. 94). These values were consitent with concentrations found onshore at ground measurement stations. The strong southerly flow at this time gives no indication of having had any recent history over any continental areas.

10) October 30, 1975 Case Study

A double-box pattern was shown in section 3.1 (fig. 6). It was designed to give maximum coverage over an area close to a suspected source of precursor pollutants. By enclosing a box within a box, at least two measures of a downwind plume were possible during the course of the flight.

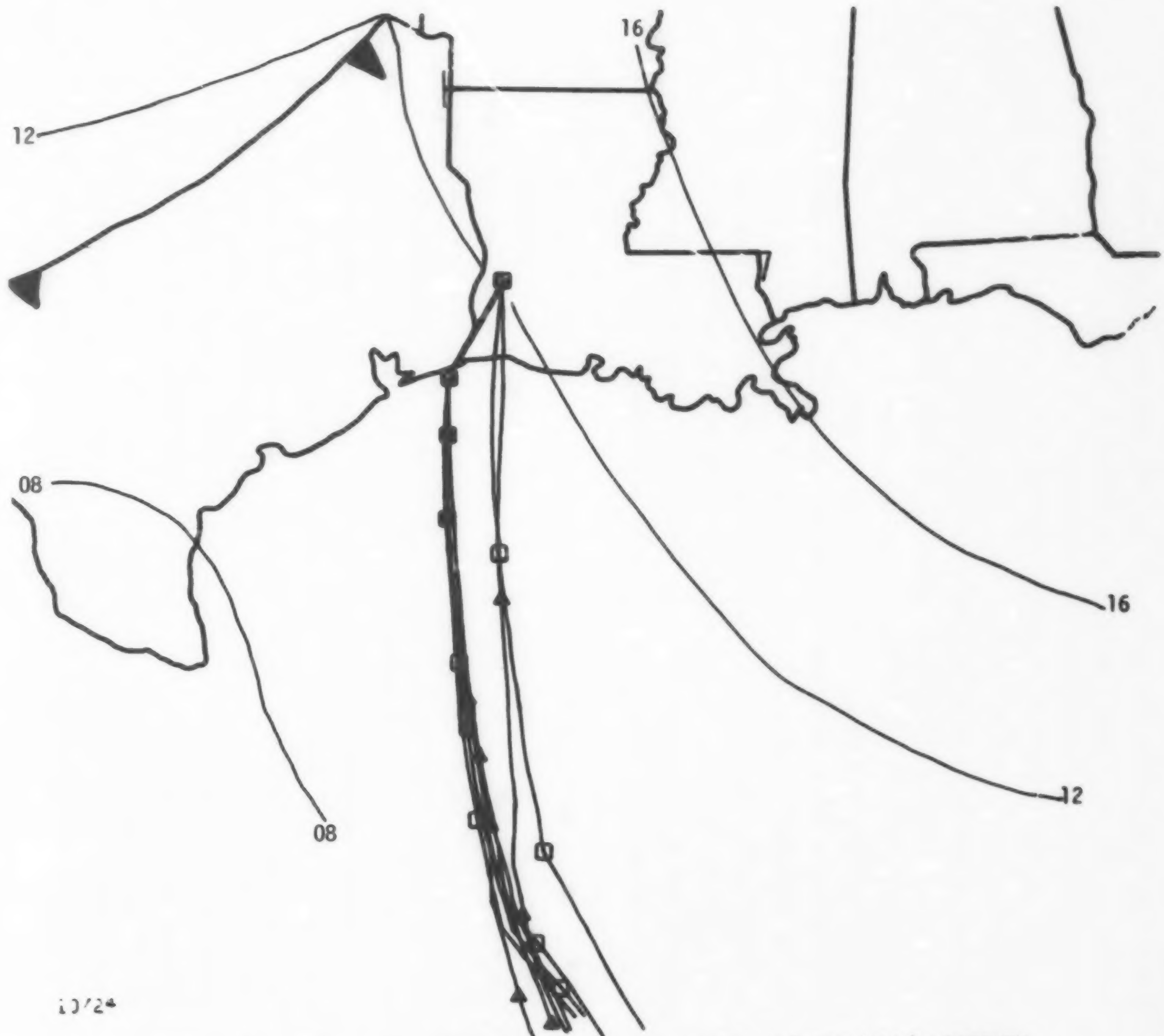
12
16
08
08
16
12
10/24

Figure 94. Ozone concentrations, air trajectories and sea level pressure distribution for October 24, 1975 flight.

Measurements upwind of source regions and to the outer edges of the box parallel to the wind help delineate the influence of the source region. Across the diagonal, measurements were made at different times in the same location to help identify changes of concentrations during the elapsed time and/or variances in the measurement techniques. A vertical profile was flown in an area where the plume was identified on a previous pass through the area.

On October 30, a ridge of high pressure extended southwestward to the west of the gulf coast area. Ahead of the ridge line, large-scale subsidence of the air established an inversion over the study area. The morning sounding at Houston showed two stable layers, the upper one slightly above 500 m, which defined the afternoon mixing for the station. The mixing height at Lake Charles was below 1.0 km with an inversion layer extending from 425 m (1,400 ft) to 760 m (2,500 ft). During the course of the day, the inversion layer actually lowered to 370 m (~ 1,200 ft) with the top at 500 m (1,500 ft), but was not destroyed by heating. Winds remained northeasterly to northerly in the mixed layer at about 6 m/s.

The double-box pattern was a joint RTI-EPA flight effort, with RTI flying a double-box pattern, which was enclosed by a larger double-box pattern flown by EPA. The boxes were oriented along the northeasterly flow of air with the longer sides of the boxes to the southwest of Nederland. The upper-level trajectories associated with this flight show a persistent northeasterly flow for 24 to 36 hours before arrival (fig. 95). Below 200 m, air flow is not as strong, but it is persistent.

Combined analysis of ozone concentration using the RTI and EPA aircraft are given in figure 96. Ozone concentrations of the order of 120 $\mu g/m^3$ or less, prevail throughout much of the study area. Immediately downwind of the Port Arthur area, a very distinct plume of ozone with concentrations as high as 280 $\mu g/m^3$ and a width of 48 km at 48 km downwind of Nederland. Gradients of ozone concentrations across the plume boundaries are of the order of 40 $\mu g/m^3$ per 10 km. Outside of the plume, concentrations remained below 120 $\mu g/m^3$. A brief vertical profile flown by the RTI aircraft near the center of the plume showed ozone concentrations of

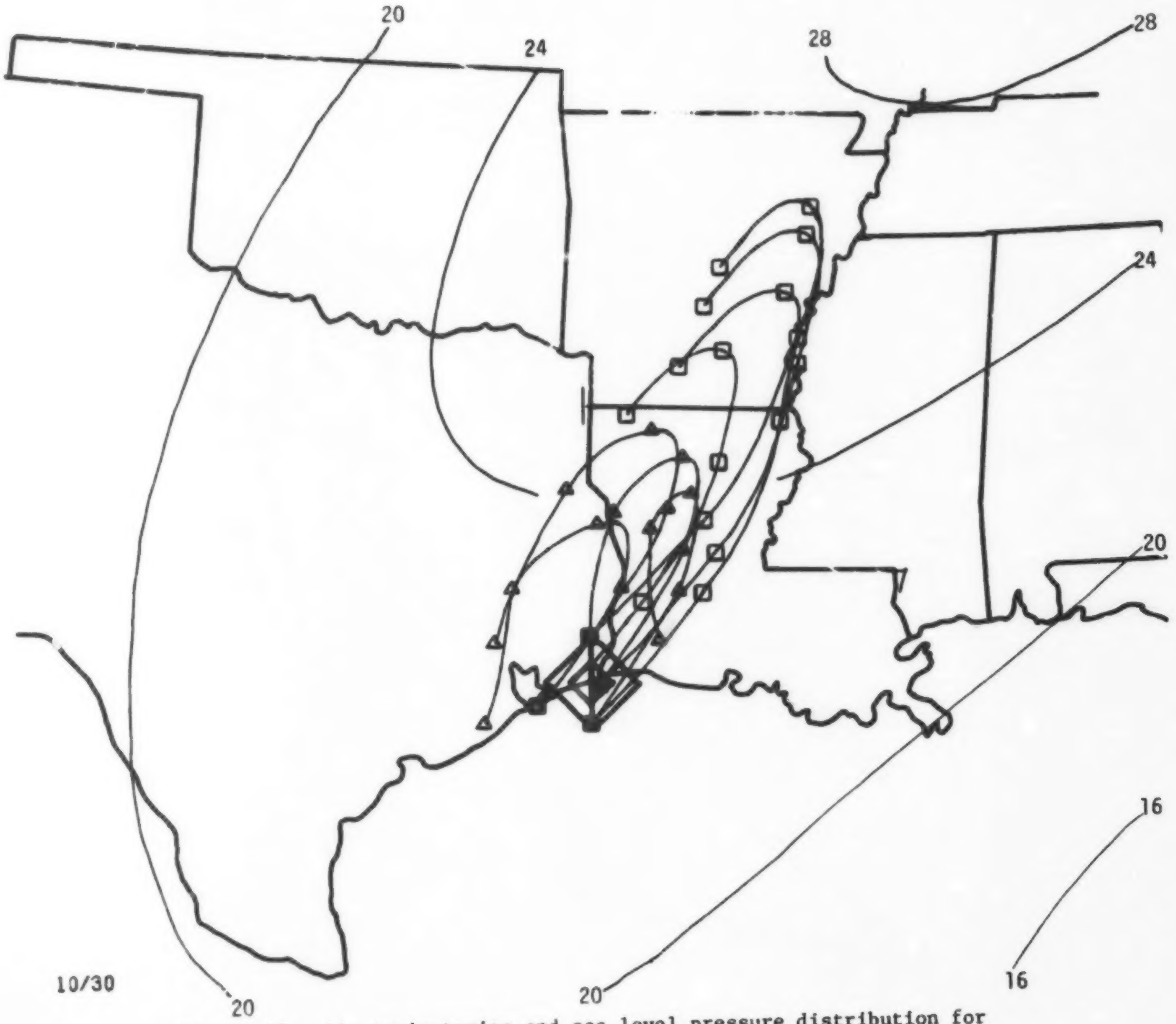
20
24
28
28
24
20
16
16
20
20
10/30

Figure 95. Air trajectories and sea level pressure distribution for October 30, 1975 flight.

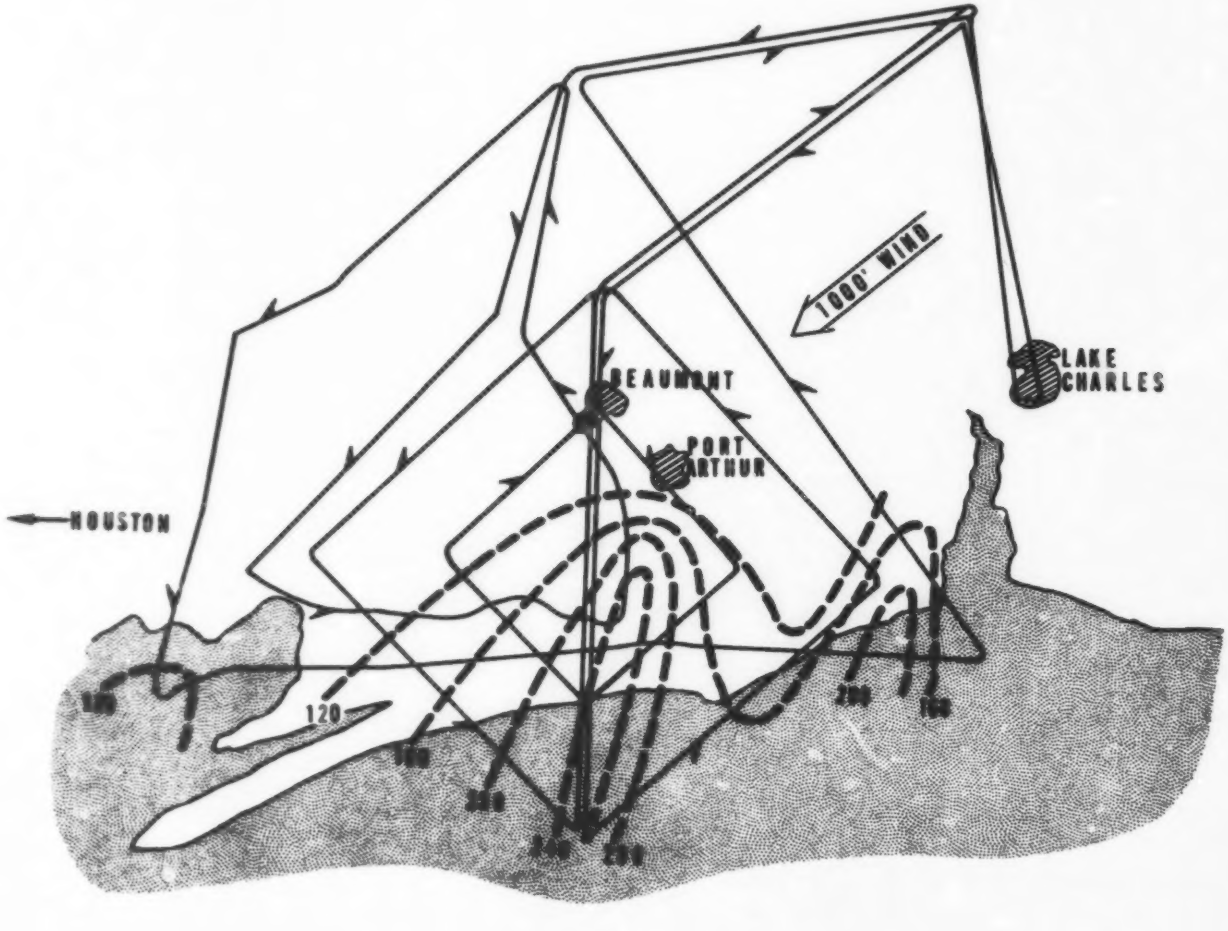
HOUSTON
1000' WIND
BEAUMONT
PORT ARTHUR
LAKE CHARLES
120

Figure 96. Analysis of aerial ozone distribution as measured on EPA and RTI flight paths at 305 m near Port Arthur, Texas, October 30, 1975.

236 μg/m^3 at 305 m (1,000 ft), decreasing to 124 μg/m^3 at 600 m (2,000 ft), and remaining below 120 μg/m^3 to 1.5 km (5,000 ft) (fig. 97).

The emergence of the plume immediately downwind of the Nederland area suggests that the ozone was formed quite rapidly in the 24-km flight distance between Port Arthur and the 236 μg/m^3 measurement. With a wind speed of 6 m/s (~13 mph), the travel time is slightly over an hour. The reactions continue even further downstream so that the 280 μg/m^3 might be representative of a 3.5 hour transport from the petrochemical complex near Nederland. Plume dimensions stay farily uniform showing only moderate spreading from a point downwind of Nederland.

There is no question that the petrochemical complexes surrounding Nederland supplied the necessary precursor materials for the resulting ozone plume. Background values of ozone are not high. There is no apparent mixing with the air above the inversion. The plume can only be generated by synthesis from the local emissions.

This regime emphasizes one of the difficulties in measuring ozone or oxidants near sources of precursors. The maximum ozone concentration recorded at Nederland on this day was 96 μg/m^3. In Houston, the Aldene station attained the maximum value of 72 μg/m^3, while DeRidder, upwind of both locations, had a maximum value of 107 μg/m^3, On the basis of the surface ozone measurements, this day would probably have been classified as a "low ozone case" for the gulf coast area. It is one of the lower decile concentration days at Houston. It is one of the upper decile concentration days at Austin, for reasons unrelated to the Nederland area.

11) October 31, 1975, Case Study

Area surveys were concluded on October 31 with the RTI and EPA aircraft flying complimentary box patterns over the land (RTI) and over the water (EPA) as shown in figure 98. The common leg of the flight from Matagorda Bay to Sabine Pass was flown by the two aircraft at different times as they returned to Lake Charles via DeRidder.

The high pressure system of the previous day had moved further northeastward. Air flow was changing from a northeasterly flow into a southeasterly flow on this morning. The ridge line had moved southeast-

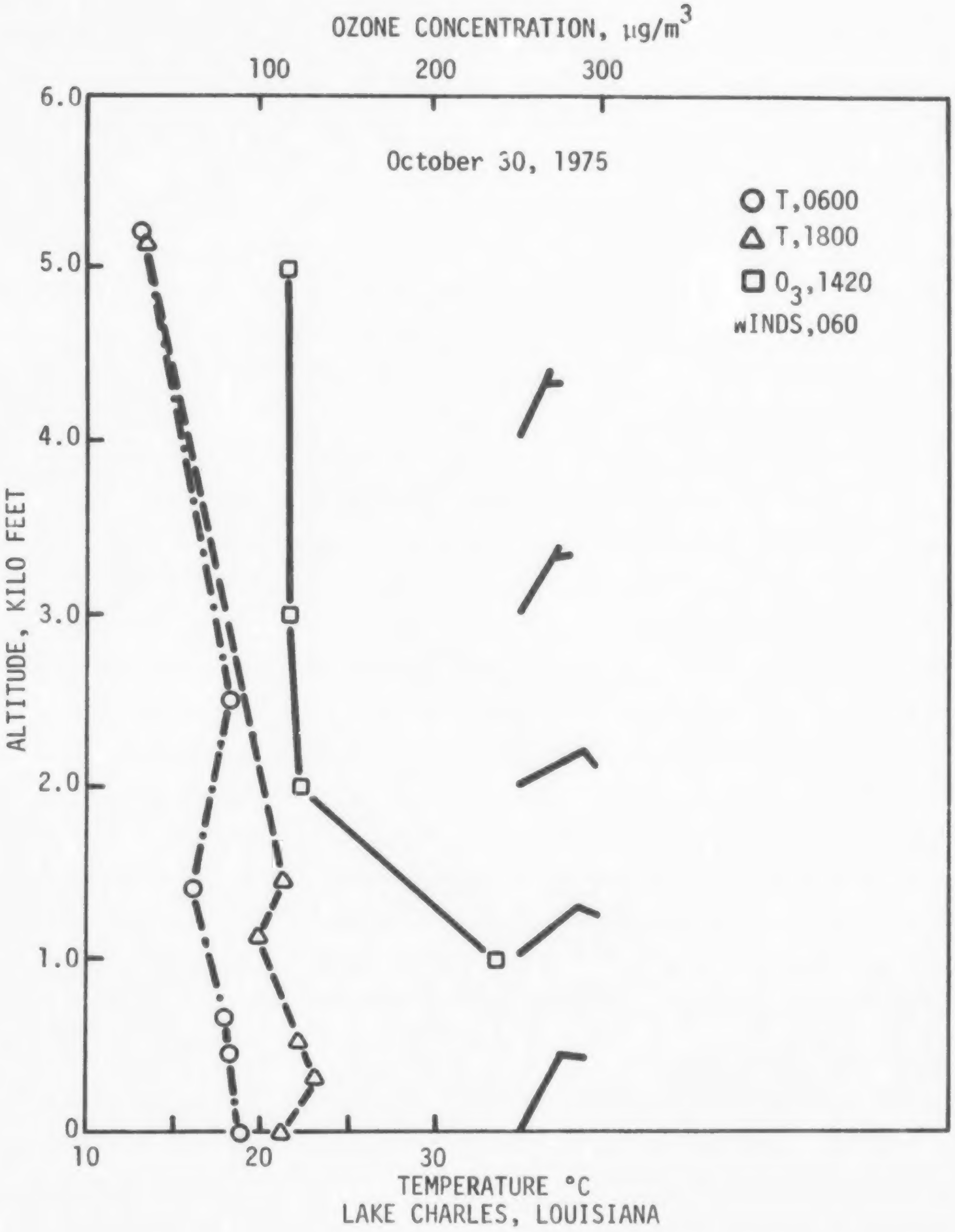

Figure 97. Vertical profile of ozone concentration, temperature, and winds at Lake Charles, Louisiana, October 30, 1975.

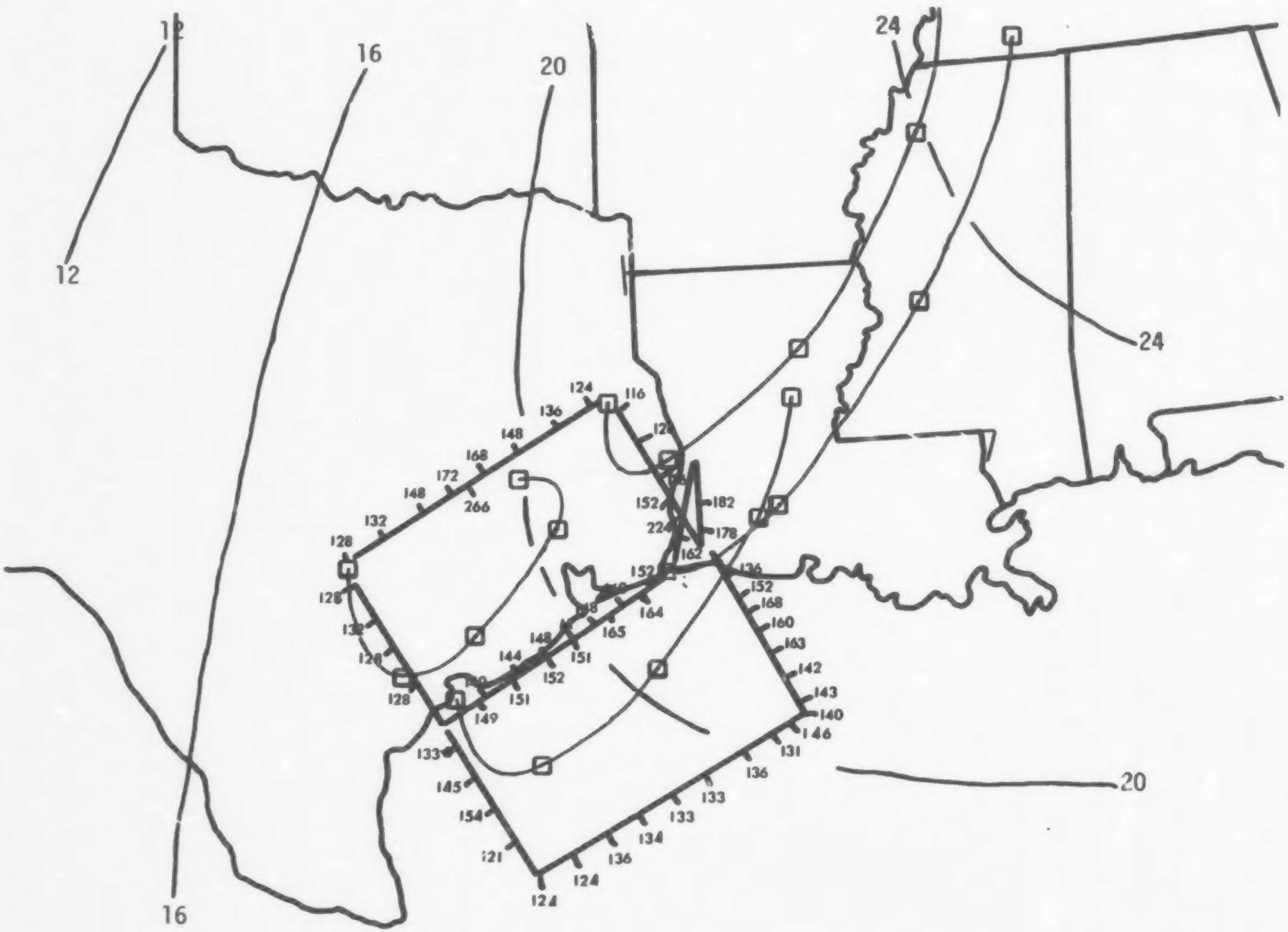
12
12
16
16
20
20
24
24
124
116
136
148
168
172
148
266
132
128
128
132
128
128
12
152
182
224
178
162
152
136
152
168
160
163
142
143
140
146
131
136
133
133
134
136
124
124
121
154
145
133
149
151
152
144
148
151
165
164

Figure 98. Ozone concentrations, air trajectories and sea level pressure distribution for October 31, 1975 flight.

ward, permitting the return flow. Pressure gradients and, hence, wind speeds were beginning to increase. No significant weather was encountered during the flight at 305 m. Upper air data indicated that the subsidence so prevalent from the day before, had broken and that vertical mixing was less restricted, once the heating processes had begun.

On the landward box pattern, the RTI aircraft encountered a brief period of high ozone concentrations along the Texas-Louisiana border. It is not clear from the available trajectories exactly where that air came from since in the very lowest layers morning sounding (the only sounding for the day available from Lake Charles) showed an east-to-northeast flow of air at flight altitudes.

Another brief encounter of high ozone (~15-minute duration and 72 km or 45 mi wide) occurred over Bryan, Texas, midway along the northwestern leg of the flight path. Morning winds at Houston showed a southeasterly wind at 8 m/s at flight level. Upper air data from Victoria, Texas showed south southeasterly winds at about 7.5 m/s at flight level. A simple calculation taking Houston as an area source 20 km wide, suggests that the air encountered over Bryan may be a downwind plume from the Houston area. At the indicated wind speed, transport time from Houston to Bryan (~160 km) would be on the order of 6 to 8 hours. The aircraft passed through the plume at approximately 1400 CST. The measured ozone had ample time to be synthesized in the air flow. Although these suppositions are quite reasonable, it is difficult to establish that emissions from the Houston area are responsible for the high ozone encountered.

Ozone concentrations decreased almost as rapidly as they increased and remained below 140 $\mu g/m^3$ until the flight path began paralleling the coastline. From Matagorda Bay northward to Galveston, ozone concentrations remained in 145 $\mu g/m^3$ range and increased to almost the NAAQS on approach to Galveston. During the remainder of the flight, ozone concentrations remained around the NAAQS and exceeded it in western Louisiana. It is difficult to postulate any particular reason for the high ozone concentrations in the eastern edge of the flight pattern. As suggested by the trajectories and the wind observations, a southerly flow of air returned, but it seems unlikely that these high ozone concentrations resulted from local transport. The eastern end of the flight pattern changes to southerly flow later than other locations. Opportunities for recirculation of the previous day's high ozone concentrations into the area are small.

8.1.4 High Ozone Occurrences at Austin, Texas

Austin is a city of 250,000 people in Travis County, Texas. It is 130 km northeast of San Antonio, the nearest population center in south central Texas. Houston is approximately 200 km to the east southeast, and Dallas-Fort Worth about 320 km north. The annual hydrocarbon emission density (all hydrocarbons) for Travis County is approximately 22.5 tons/mi^2, placing the county in approximately the upper 94 percentile of manmade hydrocarbon emissions within the United States.* A vast majority of these emissions is associated with fuel useage for transportation. The estimated annual NO_x emissions are between 13 and 24 tons/mi^2 within the upper 91 percentile of all counties within the United States. Emissions of hydrocarbons and NO_x within surrounding counties are almost an order of magnitude less. The Austin emissions are almost an order of magnitude less than those found in Harris and Jefferson Counties (Houston and Nederland).

The most frequently occuring values of daily maximum ozone were between 80 and 90 $\mu g/m^3$ during the study. The arithmetic mean is 103 $\mu g/m^3$ with a standard deviation of 38 $\mu g/m^3$. The geometric mean is 96.5 $\mu g/m^3$ with standard deviation values of 67 and 137 $\mu g/m^3$. The upper decile of daily maximum ozone concentrations at Austin exceeded 160 $\mu g/m^3$, which was achieved on 10 days. The dates and times of occurrences are summarized in table 58. On four of those occurrences, the air parcel trajectories indicate that the air had come from the Houston area during the past 24 to 48 hours. Those cases were examined for more evidence of transport from the Houston area. These 4 days actually comprise two cases, August 9 and 10 and September 3 and 4. In these cases, the hour of maximum concentration occurred at 1200 Or 1300 CDT, before the sun reached its zenith. In

---

*From National Emissions Data Summary as of May 1975.

Table 58. Summary of conditions accompanying upper decile ozone concentrations at Austin, Texas, July 1 to Oct. 31, 1975

Date	Austin Ozone			Trajectory from Houston	Houston Ozone, Maximum	
	Max ($\mu g/m^3$)	Hour of Max	Hours above NAAQS		1 Day Before	2 Days Before
July 30	206	1600	≥ 2	No	235	120
August 9	184	1200	1	Yes	378	186
August 10	176	1200	2	Probably Yes	190	378
August 23	171	1400	1	No	155	245
September 3	167	1200	1	Yes	151	216
September 4	174	1300	3	Probably Yes	82	151
September 29	178	1600	3	No	300	280
September 30	202	1200	1	No	418	306
October 6	222	1300	5	No	174	146
October 30	162	1700	≥ 1	No	72	114

most of the other cases, the ozone concentration reached its maximum at a later time of day. Although the maximum concentrations did not exceed the standard by large amounts, the violations present a significant problem in developing control strategies.

1) August 9 and 10 Case Study

The air parcel trajectories arriving in Austin in the morning and afternoon of August 9 have been added to the analysis of figure 81 giving figure 99. The parcel arriving in Austin on the afternoon of August 9 was within the plume identified downwind of Houston on the previous afternoon. The air arriving in Austin late on the afternoon of the 10th, was also sampled approximately 24 hours before in the area of high ozone concentrations in the southwest corner of the flight pattern (fig. 100). Trajectories of air parcels computed for the lower level of winds indicate 24-hour transport from the Houston area to Austin across the area where the higher ozone concentrations were measured by the aircraft on the day before high ozone concentrations were measured in Austin.

Temperature profiles taken at Victoria, Texas indicate a stable layer aloft near flight level on the afternoon of August 8 when low concentrations were reported at altitude and at the ground (fig. 101). On the morning of August 9, an inversion layer at Victoria, extended to approximately 300 m (1,000 ft) above the ground. With clear skies during the night, a temperature inversion, comparable in intensity and depth for the Austin area is quite reasonable. Beginning at the 0700 CDT surface temperature, a temperature profile for Austin was extrapolated upward for 300 m to approximate the inversion conditions. By 1000 CDT, the surface temperature had increased enough to dissipate the inversion. The temperature continued to increase rapidly, but by 1300 CDT adiabatic vertical mixing to a depth of approximately 1.5 km MSL had taken place. By 1600 CDT, mixing to near 2 km was indicated.

The hourly ozone concentration measured at Austin on August 9 and 10 are shown with the average diurnal curve for the 4-month period in figure 102. In the early morning hours of August 9, the ozone concentration at Austin increased at a rate slightly greater than the diurnal curve between 0700 and 1000. After 1000, ozone concentrations more than doubled in two

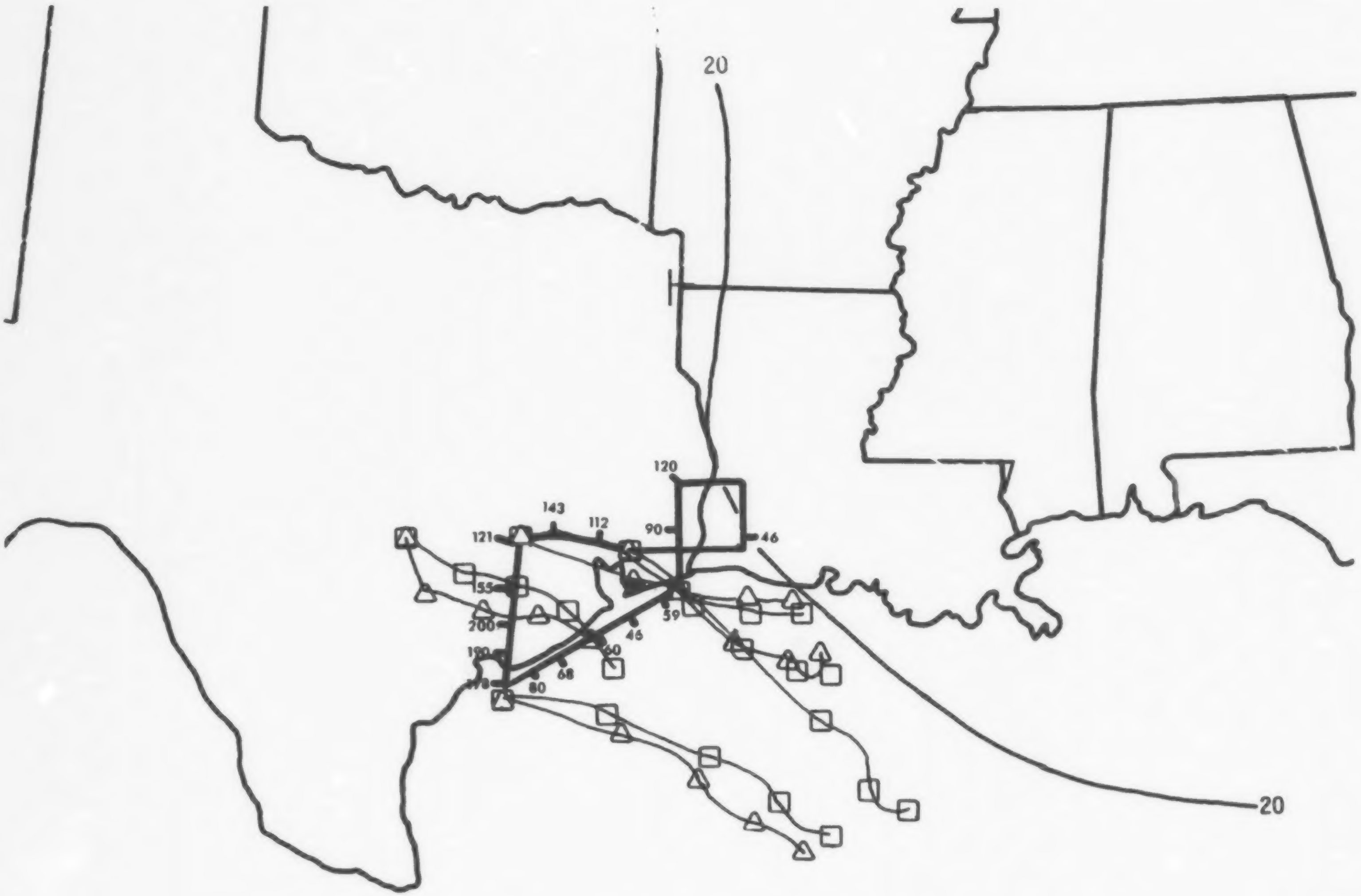
20
120
143
112
90
46
121
55
200
190
80
68
60
46
59
20

Figure 99. Ozone concentrations, air trajectories and sea level pressure distribution of the August 8, 1975 flight and the trajectories of parcels arriving in Austin on the morning (□) and the evening (Δ) of August 9, 1975.

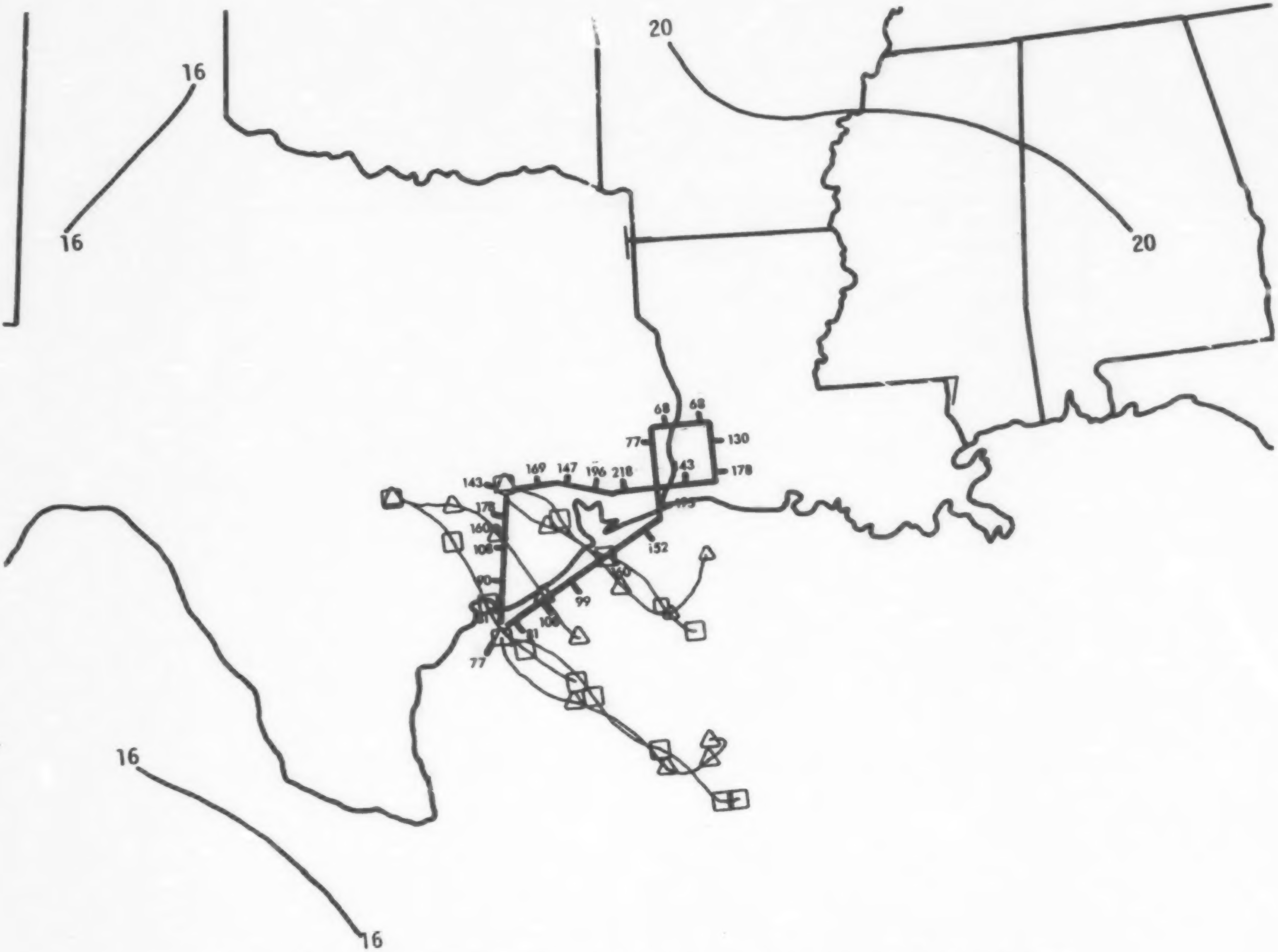
20
20
16
16
16
16
68
68
77
130
143
178
143
169
147
196
218
178
160
108
90
152
160
99
108
91
77

Figure 100. Ozone concentrations, air trajectories and sea level pressure distribution of the August 9, 1975 flight and trajectories of parcels arriving in Austin on the morning (□) and the evening (Δ) of August 10, 1975.

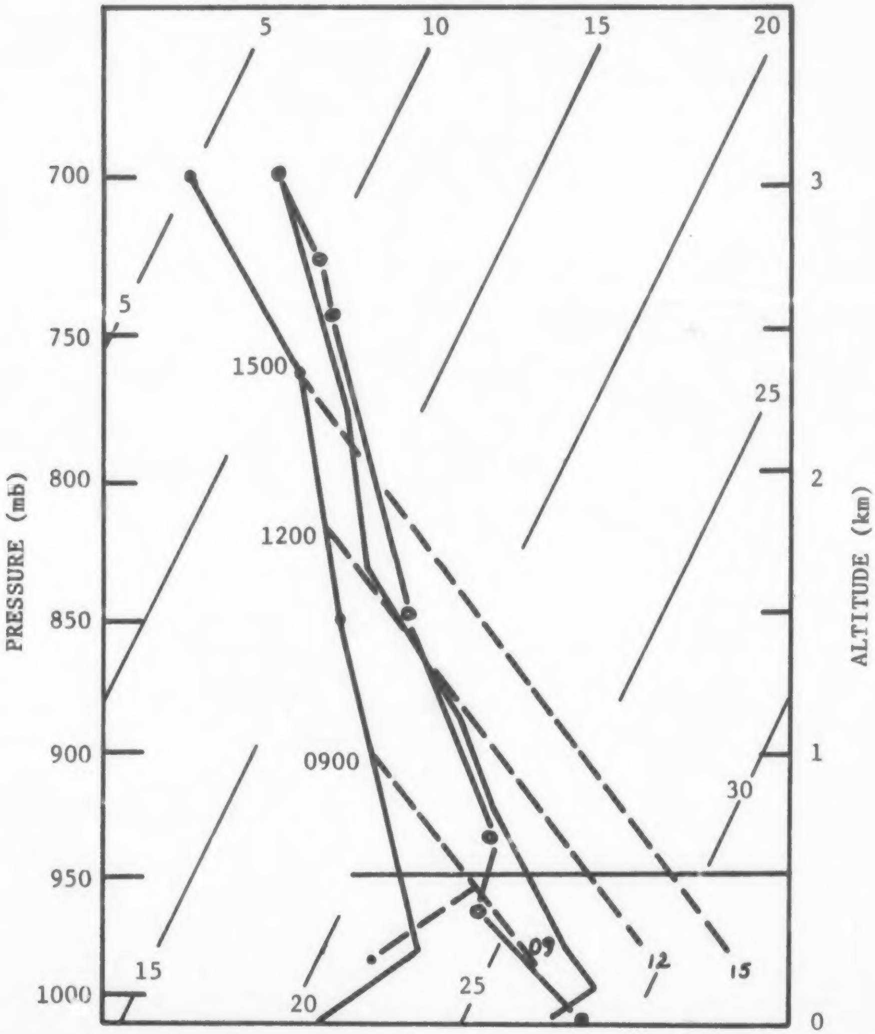

Figure 101. Temperature profiles at Victoria, Texas, August 9, 0000 GMT to August 10, 0000 GMT, Isothermal (C) are skewed. Dashed lines are the dry adiabats for the 0900, 1200 and 1500 CST temperatures at Austin, Texas on August 10, 1975.

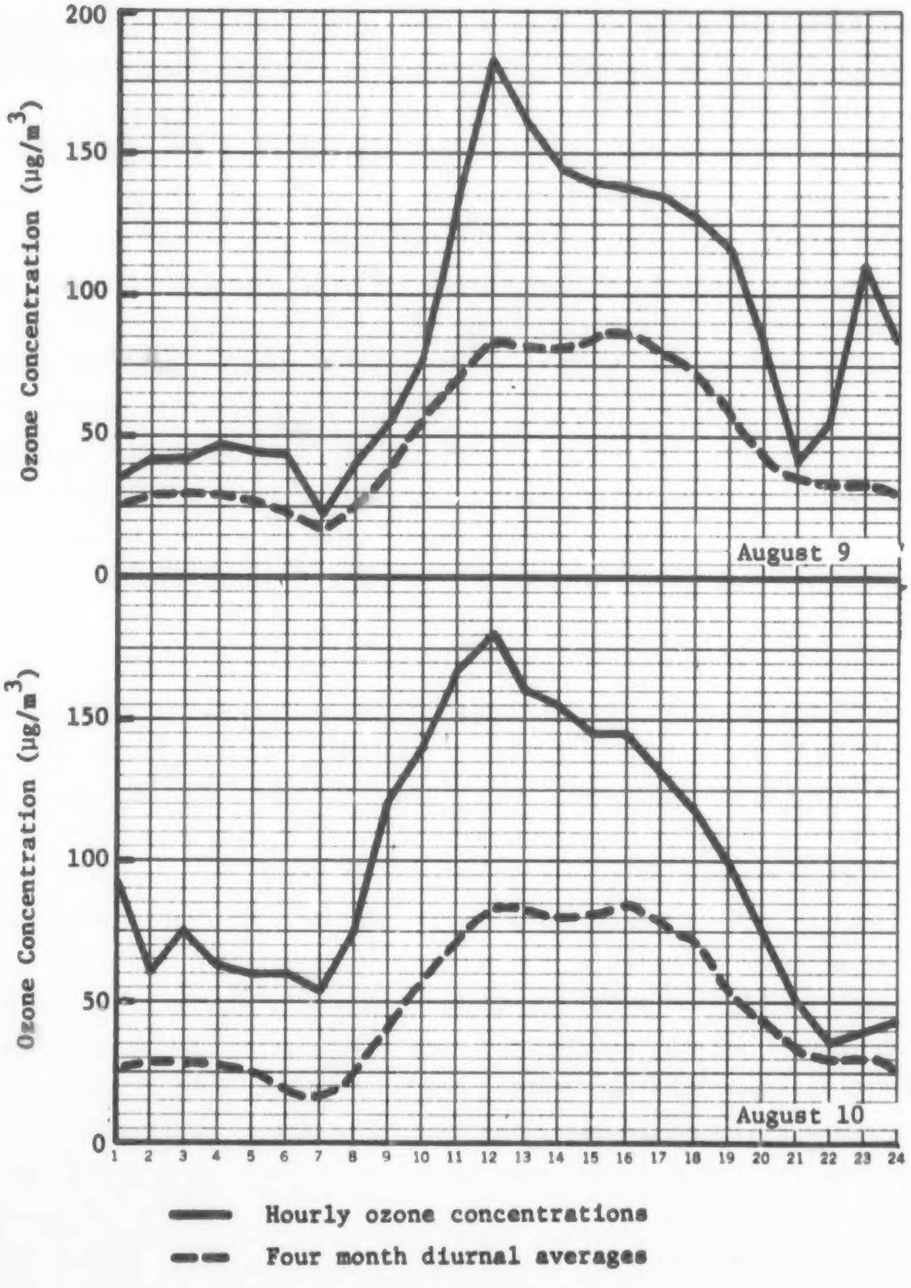

Figure 102. Hourly average ozone concentrations, August 9, 10, 1975 at Austin, Texas and the mean hourly average concentration for July 1 to October 31, 1975.

hours, exceeding the standard at 1200. By the next hour, concentrations had decreased. For the remainder of the afternoon, ozone slowly decreased until nightfall and returned to concentrations below 50 $\mu g/m^3$ briefly. The rapid rise of ozone coincides with the time the low-level inversion layer was dissipated by solar heating and when the mixing depth increases rapidly. The air arriving in the mixed layer in the morning was sampled the previous day and showed ozone concentrations of approximately 170 $\mu g/m^3$. Comparable concentrations were observed on the morning of the August 9 in Austin. The maximum concentration was more than twice the diurnal average for 1200 CDT. The rapid rate of increase of ozone during the morning is certainly not characteristic of the Austin area and implies that an abnormal source of ozone may be responsible. Since it was demonstrated that the air came from Houston over the past 48 hours, either ozone or ozone precursor materials from Houston have been injected into the Austin atmosphere.

The evidence suggests ozone, rather than ozone precursors, is mixed downward from just above the nocturnal radiation inversion. If it were the ozone precursors, then ozone generation processes would continue into the afternoon after the precursor materials have been mixed with the low-level emissions. The rapid increase of ozone with the breakup of the inversion suggests that the ozone is already present. As mixing continues the mixing volume apparently increases more rapidly than ozone can be synthesized, diluting the ozone concentration at the ground.

On the evening of August 9, ozone concentrations decreased rapidly with sunset but rose again to 100 $\mu g/m^3$ around 2300 before returning to values of 60 to 70 $\mu g/m^3$ on the morning of August 10. The early morning sounding from Victoria did not indicate a low-level stable layer; however, inland a very strong, stable layer was indicated in the first 300 m of the atmosphere at Dallas-Fort Worth. Clear skies and light winds during the night were conducive to reforming radiative inversion. Ground fog and haze, and the lowest temperature of the month, were reported in the early morning of the August 10. Temperatures increased rapidly, dissipating the inversion probably more rapidly than on the day before. Ozone concentrations began a steady rise shortly after sunrise and reached their peak at

1200 CDT. Concentrations again receded in the afternoon and decreased with nightfall. The rise of ozone during the morning suggests that vertical mixing again brought air down from above the radiation inversion to the ground giving the increased ozone concentrations. Previous samples of the air showed concentrations of about 160 $\mu g/m^3$. The air which had been sampled arrived in the Austin area after having had a transect over the metropolitan Houston area approximately 48 hours before.

2) September 3 and 4, 1975, Case Study

On September 2 and 3, a weak high pressure center was stationary in southeastern Texas. The winds were poorly organized in a weak anticyclonic circulation. Clear skies and very warm temperatures characterized the daytime hours. A subsidence temperature inversion near 2 km was over much of the area. Morning radiation inversions extended several hundred meters above ground level. The air flow arriving in Austin on these days are indicated in figure 103.

The winds shifted northerly and easterly during the day of the 3rd, remained there overnight before shifting southerly again by late afternoon of September 4. The first and last of these trajectories show air passing southwest of Houston. The middle two trajectories show air passing directly over Houston and near the Nederland petrochemical complex during the 24 hours prior to arrival at Austin. Ozone concentrations had been high at the Houston station on September 1, but had diminished on September 2 and 3. The lower values may have been a result of the more easterly flow changing the source-receptor orientation of the Aldene location. Other data from the Houston area were not available.

Hourly averaged concentrations of ozone in Austin on September 3 and 4 are shown in figure 104. In the early morning of September 3, ozone was very near the average values through 0900. Between 0900 and 1000, a large increase of ozone occurred and continued through 1200. By 1400, ozone concentrations had decreased to below 150 $\mu g/m^3$ and decreased during the late afternoon. Clear skies were reported all day, and maximum temperatures reached 96° F, giving favorable opportunity for ozone generation.

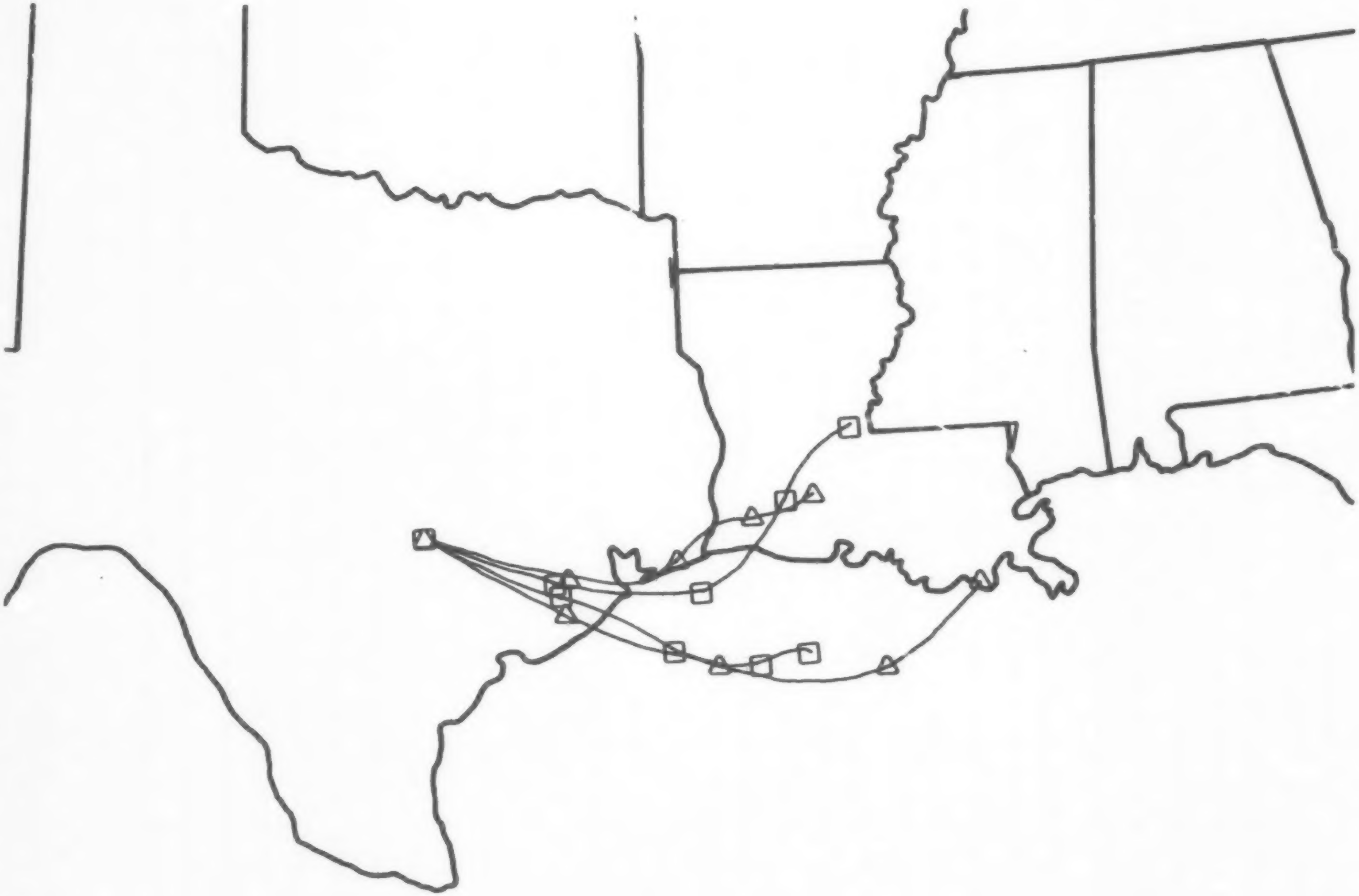

Figure 103. Air trajectories arriving in Austin, Texas on September 3-4, 1975 (□ - morning, Δ - evening).

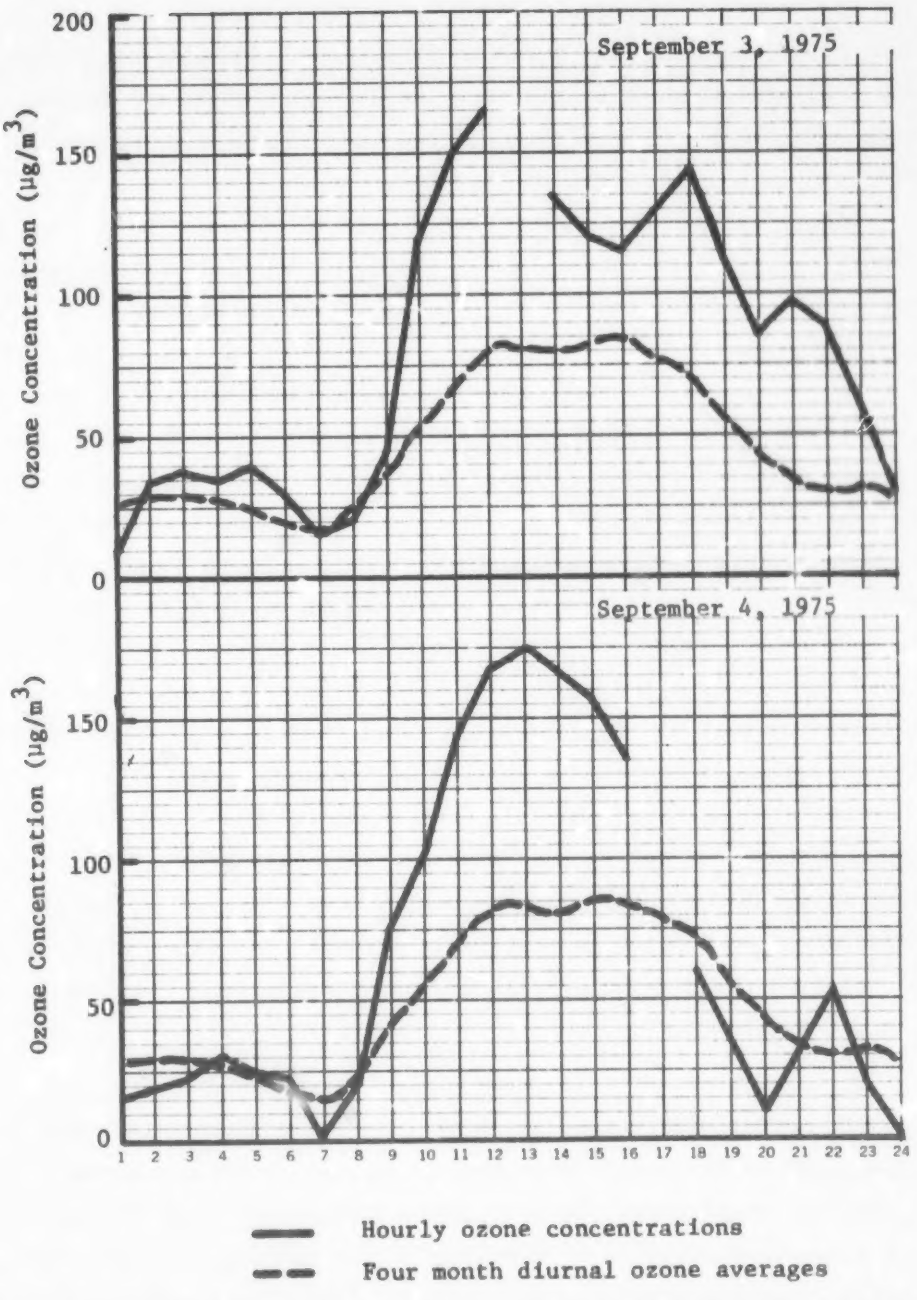

Figure 104. Hourly average ozone concentrations, September 3, 4, 1975 at Austin, Texas and the mean hourly average concentration from July 1 to October 31, 1975.

Shortly after sunrise on September 4, ozone concentrations increased at a more rapid than normal rate to a maximum value of 175 $\mu g/m^3$ at 1300. Ozone concentrations then began to decrease. A thundershower occurred at 1600 CDT, and ozone concentrations decreased and remained at very low values. Skies were clear on the morning of the 4th. Cloudiness increased during the afternoon as the thunderstorm activity developed.

Aircraft measurements were not available during this period, inhibiting identification of an ozone plume downwind of Houston or Nederland. Therefore, the case for transport is weaker and more tentative than in the previous case.

In both cases, however, ozone concentrations increased rapidly during the morning hours, reached their maxima at 1200 to 1300 hours, remained over the standard for less than 3 hours and had a trajectory from the Houston area where high ozone concentrations had been measured on one to two days previously. Rapid increases of ozone in midmorning apparently resulted from the same processes occurring in the August 9 and 10 cases, i.e., vertical mixing of boundary layer ozone downward to the ground after it had been transported aloft, insulated from the ground by the nocturnal radiation inversion. These sets of circumstances were encountered in the Ohio-Pennsylvania regions in an earlier investigation.[5/]

The meteorological conditions of these two cases are similar and are common occurrences during this time of year. The diurnal variations of ozone in these two cases are very similar but atypical to Austin. The trajectory from Houston is atypical. Transport of ozone and/or ozone precursors from the Houston area is strongly implicated as *one* cause of high ozone at Austin.

8.1.5 Summary of Gulf Coast Aerial Survey

Air moving slowly over areas of large hydrocarbon emissions was associated with upper decile ozone concentrations at urban and rural locations in the gulf coast area. In most cases, trajectory analysis showed air with high ozone arriving from nonprevailing directions. Air--which moved rapidly, had long overwater fetches, and showed weak anticyclonic curvature--

was associated with lower decile ozone concentrations at all of the ground monitoring locations.

In most cases, the highest ozone concentrations were attributed through trajectory analysis to the principal cities or areas of high precursor emissions. These observations suggested that ozone plumes commonly develop downwind of large precursor emission areas. The separation of urban and industrial centers of the area against a background of low emissions density facilitated identification of urban influence.

The double-box flight pattern very convincingly showed the development of an ozone plume downwind of a petrochemical complex. The plume apparently began downwind of the complex. The downwind distance is probably proportional to the product of time of travel (e.g., a time to generate ozone from emitted precursor material) and the wind speed, although that relationship cannot be established with the available data. Data from other flights also suggested that the maximum ozone will be found downwind of the emission data.

The location of the ozone monitor with respect to the precursor sources and the existing wind velocity (speed and direction) showed a substantial effect upon the ozone concentrations measured in the immediate vicinity of a large emission area. Winds from the prevailing direction tend to have higher speeds. Measurements of ozone along the axis of the prevailing wind direction downwind from a major source area may be biased because of the source-receptor distance and the increased ventilation normally associated with the prevailing wind speed.

Intercity transport of ozone or ozone precursor materials was associated with an urban plume and was shown as a possible cause of some violations of the NAAQS at Austin.

In the area survey flights, the mean ozone concentrations over water were usually less than those over the land, regardless of the level of ozone encountered. When elevated ozone concentrations were measured over the water, the trajectory analysis usually showed the air parcel had a recent (< 24 hr) history over continental areas, usually over high hydrocarbon emission areas.

When areawide ozone concentrations exceeded the NAAQS, vertical mixing was usually restricted by a stable layer below 2 km. That layer was usually associated with the subsidence within a high pressure system. Although the afternoon mixing height seldom exceeded 2 km, further vertical mixing was possible because stable layers occurred infrequently at higher levels. Vertical profiles of ozone concentration showed sharp transitions across the subsidence layer. The ozone below the stable layer was about twice the concentrations above.

8.2 Chemistry of Ozone Generation

The main purpose of the study in the gulf coast area was to document ozone behavior, especially the generation of high ozone concentrations. Much of the area under investigation has a large concentration of petroleum and petrochemical installations and a much smaller population density than the northeastern United States.

The basic reactions of the mechanism of ozone generation in the troposphere are assumed to be the photolysis of NO_2 to NO and O, the reaction of O with O_2 to form O_3 and the oxidation of some of the NO to NO_2 by a species other than O_3. The details of NO oxidation will vary mostly due to differences in identity of organic compounds present. Oil refineries are sources of both hydrocarbons and oxides of nitrogen. When the refineries provide a major portion of the precursor pollutants, it is anticipated that more propane will be observed than in an urban pollution system consisting mainly of automobile exhaust. On the other hand, acetylene should not provide a good index to automobile exhaust, since about 47 percent of the commercial acetylene production in the United States is located between Houston and New Orleans. Halocarbons are also manufactured in the gulf coast area.

Due to the proximity of the Gulf of Mexico, complex thermal layering of the air is a common occurrence. Photographs of the area taken from satellites have also shown that pollution from a point source can be transported great distances without losing the identity of thplume.

Major differences between the northern area of study and the gulf coast area as far as ozone generation is concerned are:

1. Source areas are discrete entities in the gulf coast area whereas source areas in the north tend to sprawl over great distances with considerable population in any apparent interstices.
2. The gulf coast is an oil-producing area, and refinery emissions tend to have a smaller alkene-to-alkane ratio than city hydrocarbons derived chiefly from the automobile.

One effect of the "clustering" of sources in the gulf coast area and the thermal layering of the maritime air is that a plume effect can occur in stable atmospheric conditions before a regionwide system of high ozone can be observed. Figures 105, 106, 107, and 108 show the different aspects of the ozone concentration picture. Figure 105 represents an aircraft flight on a day where low ozone concentrations were observed. Figure 106 represents a flight when conditions allowed only a few areas to generate high ozone concentration. Figure 107 depicts a flight where considerable stretches of countryside were covered by air with high ozone concentrations in the mixing layer. In figure 108 high ozone is evident in almost all areas covered by the flight path.

The average ozone concentration from June through October at DeRidder, the only fixed rural station in the gulf coast area, was 61 $\mu g/m^3$ (2,136 hours); nitric oxide was 2 and NO_2 5 $\mu g/m^3$ (2,444 cases). Seventeen of the 2,136 hours (0.8 percent) equaled or exceeded the NAAQS for photochemical oxidants. The frequency of ozone exceeding the standard (table 13) and the hydrocarbon data (tables 59, 60, and 61) are similar to that of the Midwest rural areas where high ozone concentration and low concentrations of NO_x occur. Probably the main difference is due to the difference in identity and the proximity to large numbers of all refineries and petrochemical installations.

The high ozone concentrations at DeRidder appear to be due both to ozone associated with area plumes (e.g., city plumes) and to air so generally polluted as to present high ozone concentrations as an air mass characteristic. The aircraft data presented in figures 109 and 110 show two cases where ozone was low everywhere in one case ($\leq$ 19 $\mu g/m^3$) and the other where ozone was high on the transition flight ($\geq$ 160 $\mu g/m^3$).

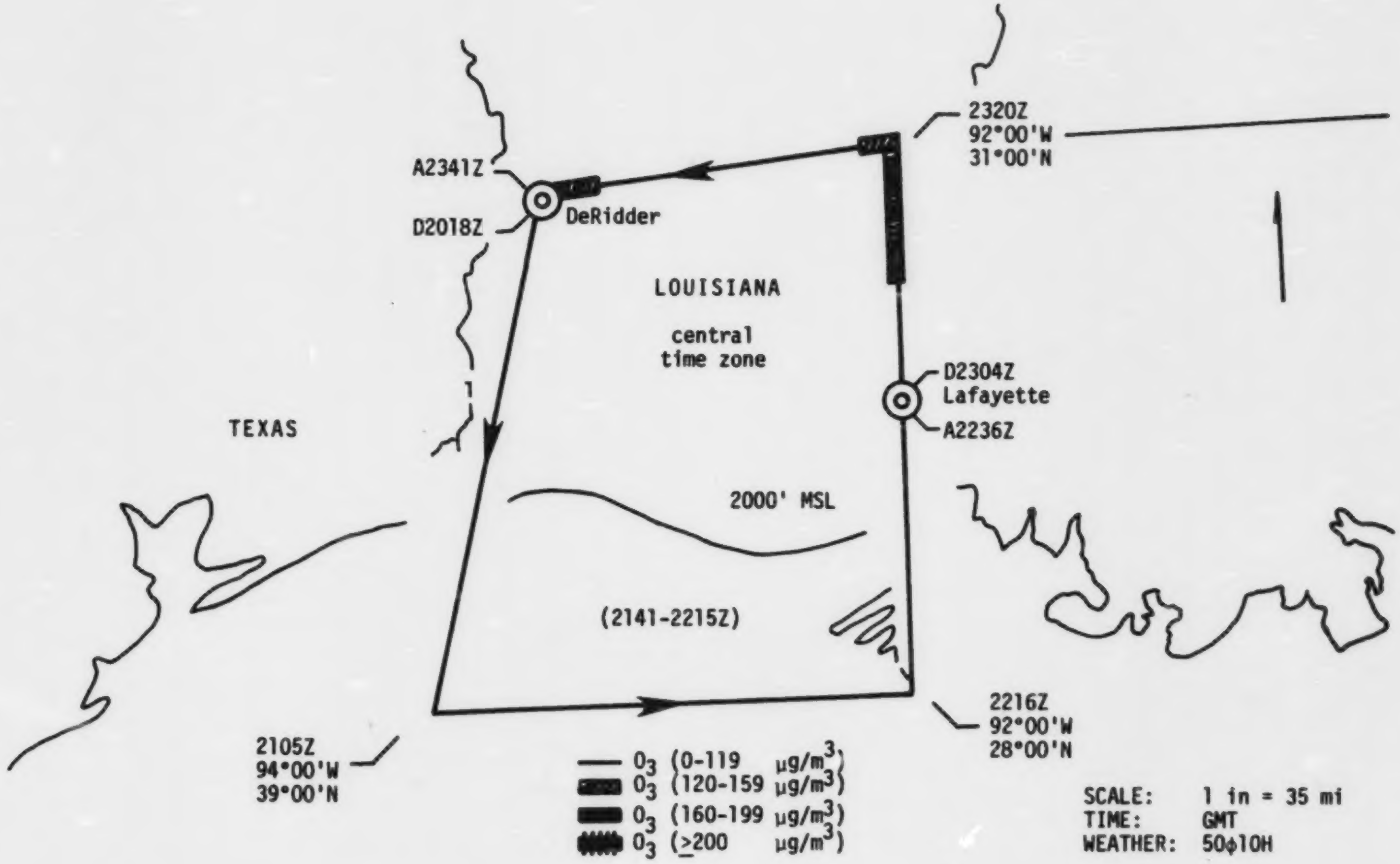
A2341Z
DeRidder
D2018Z
2320Z
92°00'W
31°00'N
LOUISIANA
central
time zone
D2304Z
Lafayette
A2236Z
TEXAS
2000' MSL
(2141-2215Z)
2105Z
94°00'W
39°00'N
2216Z
92°00'W
28°00'N
O_3 (0-119 μg/m^3)
O_3 (120-159 μg/m^3)
O_3 (160-199 μg/m^3)
O_3 (≥200 μg/m^3)
SCALE: 1 in = 35 mi
TIME: GMT
WEATHER: 50ϕ10H

Figure 105. Ozone concentrations observed on sea-breeze flight of September 19, 1975.

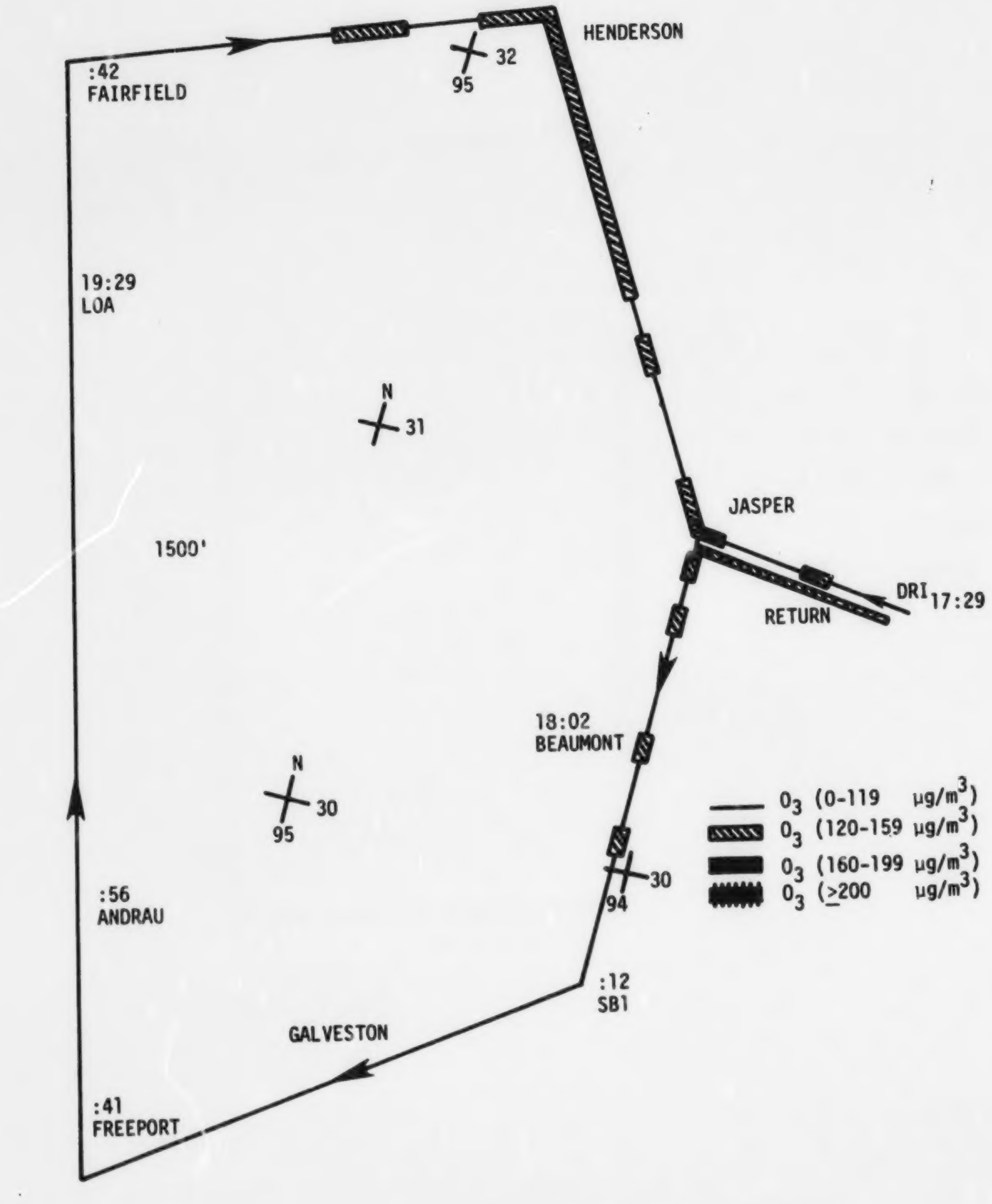
HENDERSON
:42
FAIRFIELD
32
95
19:29
LOA
N
31
1500'
JASPER
DRI
17:29
RETURN
18:02
BEAUMONT
N
30
95
30
94
:56
ANDRAU
:12
SB1
GALVESTON
:41
FREEPORT
O_3 (0-119 μg/m^3)
O_3 (120-159 μg/m^3)
O_3 (160-199 μg/m^3)
O_3 (≥200 μg/m^3)

Figure 106. Ozone concentrations observed on aerial survey flight on June 27, 1975.

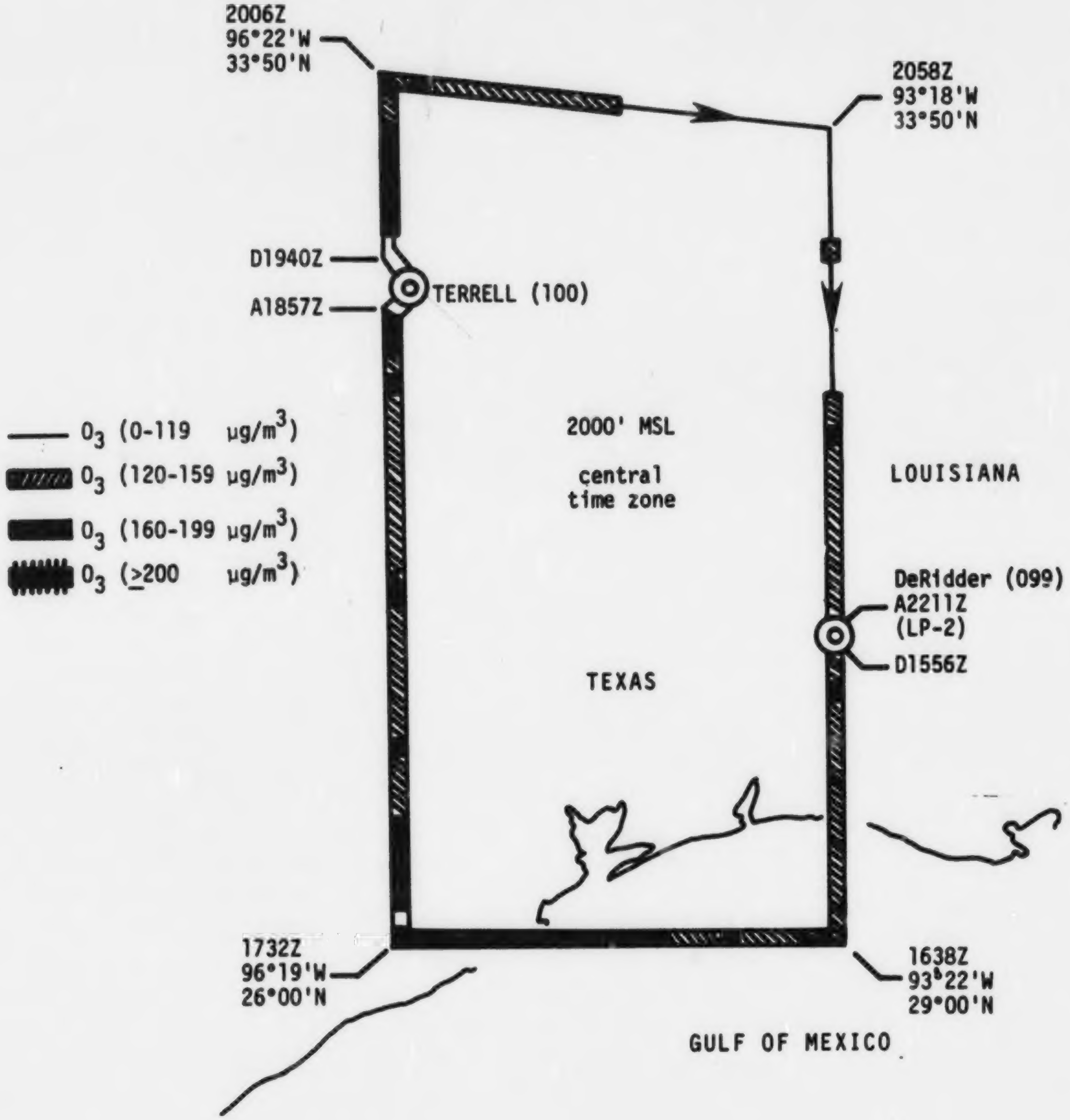
2006Z
96°22'W
33°50'N
2058Z
93°18'W
33°50'N
D1940Z
TERRELL (100)
A1857Z
O3 (0-119 μg/m3)
O3 (120-159 μg/m3)
O3 (160-199 μg/m3)
O3 (≥200 μg/m3)
2000' MSL
central time zone
LOUISIANA
DeRidder (099)
A2211Z
(LP-2)
D1556Z
TEXAS
1732Z
96°19'W
26°00'N
1638Z
93°22'W
29°00'N
GULF OF MEXICO

Flight 107. Ozone concentrations observed on box flight pattern on October 19, 1975.

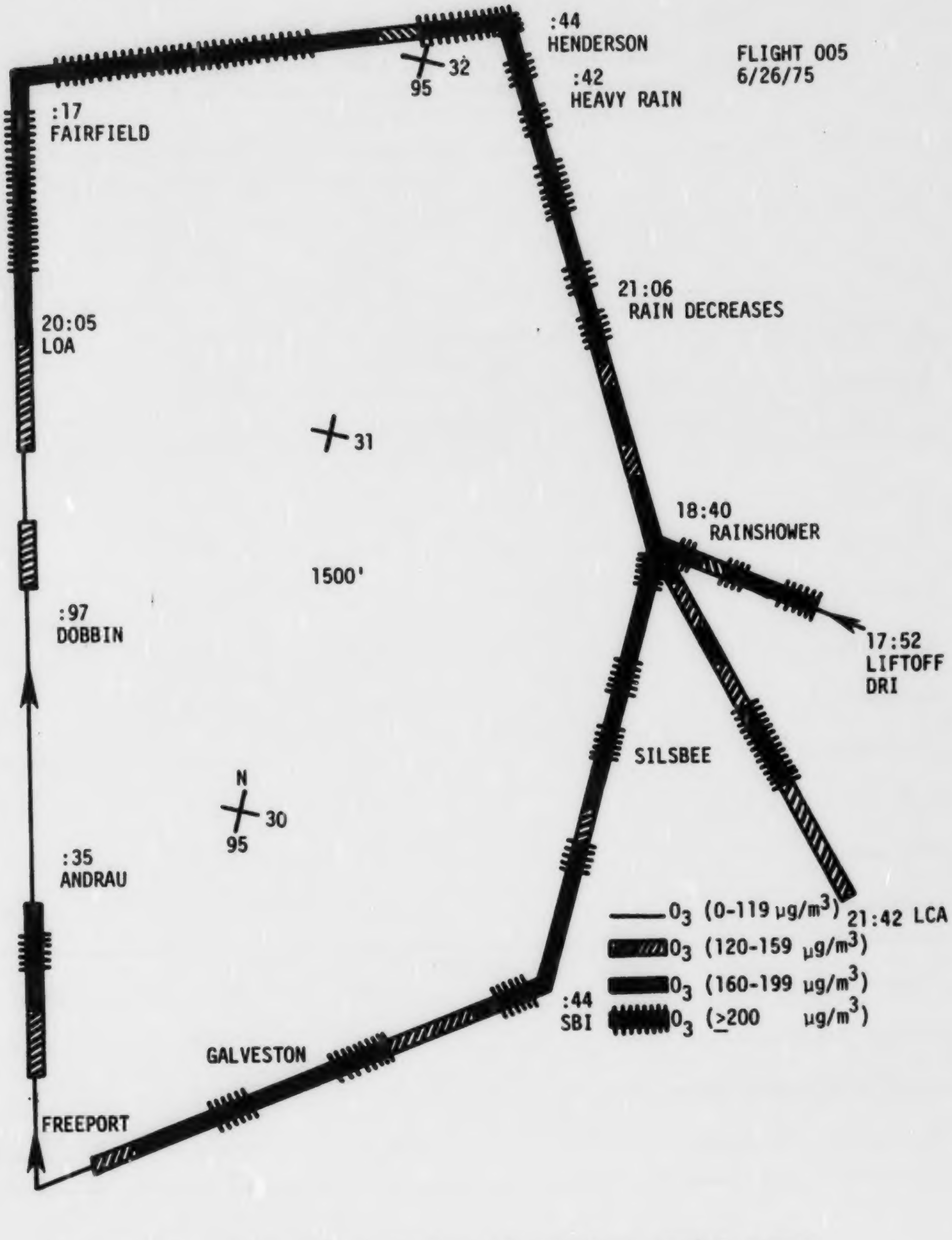
:44
HENDERSON
FLIGHT 005
6/26/75
:42
HEAVY RAIN
32
95
:17
FAIRFIELD
21:06
RAIN DECREASES
20:05
LOA
31
18:40
RAINSHOWER
1500'
:97
DOBBIN
17:52
LIFTOFF
DRI
SILSBEE
N
30
95
:35
ANDRAU
21:42 LCA
O3 (0-119 μg/m3)
O3 (120-159 μg/m3)
O3 (160-199 μg/m3)
O3 (≥200 μg/m3)
:44
SBI
GALVESTON
FREEPORT

Figure 108. Ozone concentrations observed on aerial survey flight on June 26, 1975.

Table 59. Mean hydrocarbon and halocarbon concentrations for ozone concentration ranges at DeRidder, Louisiana (July-October 1975)

Compound	O_3 Maximum Hourly Average Range			
	0-53 ($\mu g/m^3$)	54-107 ($\mu g/m^3$)	105-159 ($\mu g/m^3$)	≥ 160 ($\mu g/m^3$)
Ethylene/Ethane (ppbV)	No Samples Corresponding to Hourly Max. <54 $\mu g/m^3$	36.8	22.2	26.1
Propane		6.7	5.1	8.2
Propylene		1.6	2.4	1.5
Acetylene		3.2	3.1	2.7
n-Butane		2.4	3.0	3.5
1-Butene		0.1	0.1	0.2
Isobutane		2.0	2.1	2.6
Isopentane		1.1	1.9	2.1
Cyclopentane		0.2	0.2	<0.1
n-Pentane		3.2	2.8	1.4
Toluene		5.7	10.8	4.4
o-Xylene		0.9	0.9	1.0
Freon-11 (pptV)		376.0	371.0	291.0
Carbon Tetrachloride		85.0	71.0	51.0
1,1,1-Trichloroethane		1.5	1.3	1.1
Tetrachloroethylene		386.0	358.0	298.0

Table 60. Mean hydrocarbon and halocarbon concentrations for ozone concentration ranges, gulf coast - flights over land (July-October 1975)

Compound	O_3 Maximum Hourly Average Range			
	0-53 (μg/m³)	54-107 (μg/m³)	105-159 (μg/m³)	≥ 160 (μg/m³)
Ethylene/Ethane (ppbV)	5.9	46.0	19.2	18.7
Propane	0.3	3.6	4.4	7.2
Propylene	0.3	1.8	1.5	2.2
Acetylene	0.9	2.0	2.3	2.4
n-Butane	0.3	2.1	1.7	2.2
1-Butene	0.1	0.1	0.1	<0.1
Isobutane	0.1	1.0	0.9	2.1
Isopentane	Not Detected	3.9	4.5	1.6
Cyclopentane	Not Detected	0.1	0.5	Not Detected
n-Pentane	0.2	2.2	1.5	1.5
Toluene	3.4	11.4	12.4	10.6
o-Xylene	Not Detected	4.5	0.4	0.9
Freon-11 (pptV)	86.0	201.0	325.0	Not Detected
Carbon Tetrachloride	54.0	46.0	33.0	33.0
1,1,1-Trichloroethane	1.0	0.9	1.1	1.3
Tetrachloroethylene	78.0	141.0	158.0	129.0

Table 61. Average hydrocarbon and halocarbon concentrations for ozone concentration ranges, gulf coast - flights over water (July-October 1975)

Compound	O_3 Maximum Hourly Average Range			
	0-53 ($\mu g/m^3$)	54-107 ($\mu g/m^3$)	105-159 ($\mu g/m^3$)	$\geq$ 160 ($\mu g/m^3$)
Ethylene/Ethane (ppbV)	21.0	11.0	9.6	21.4
Propane	0.3	3.2	1.7	9.2
Propylene	0.8	2.4	0.7	2.7
Acetylene	0.5	1.2	1.2	2.2
n-Butane	1.3	7.3	0.8	4.2
1-Butene	Not Detected	0.9	Not Detected	0.1
Isobutane	0.2	0.6	0.4	3.4
Isopentane	2.7	5.8	0.8	4.0
Cyclopentane	Not Detected	0.4	Not Detected	1.4
n-Pentane	0.6	1.7	1.2	3.3
Toluene	22.5	10.6	7.3	10.9
o-Xylene	0.7	2.2	0.8	Not Detected
Freon-11 (pptV)	172.0	211.0	179.0	310.0
Carbon Tetrachloride	46.0	56.0	42.0	35.0
1,1,1-Trichloroethane	0.9	1.0	1.2 (12)	1.1
Tetrachloroethylene	75.0	119.0	138.0 (12)	167.0

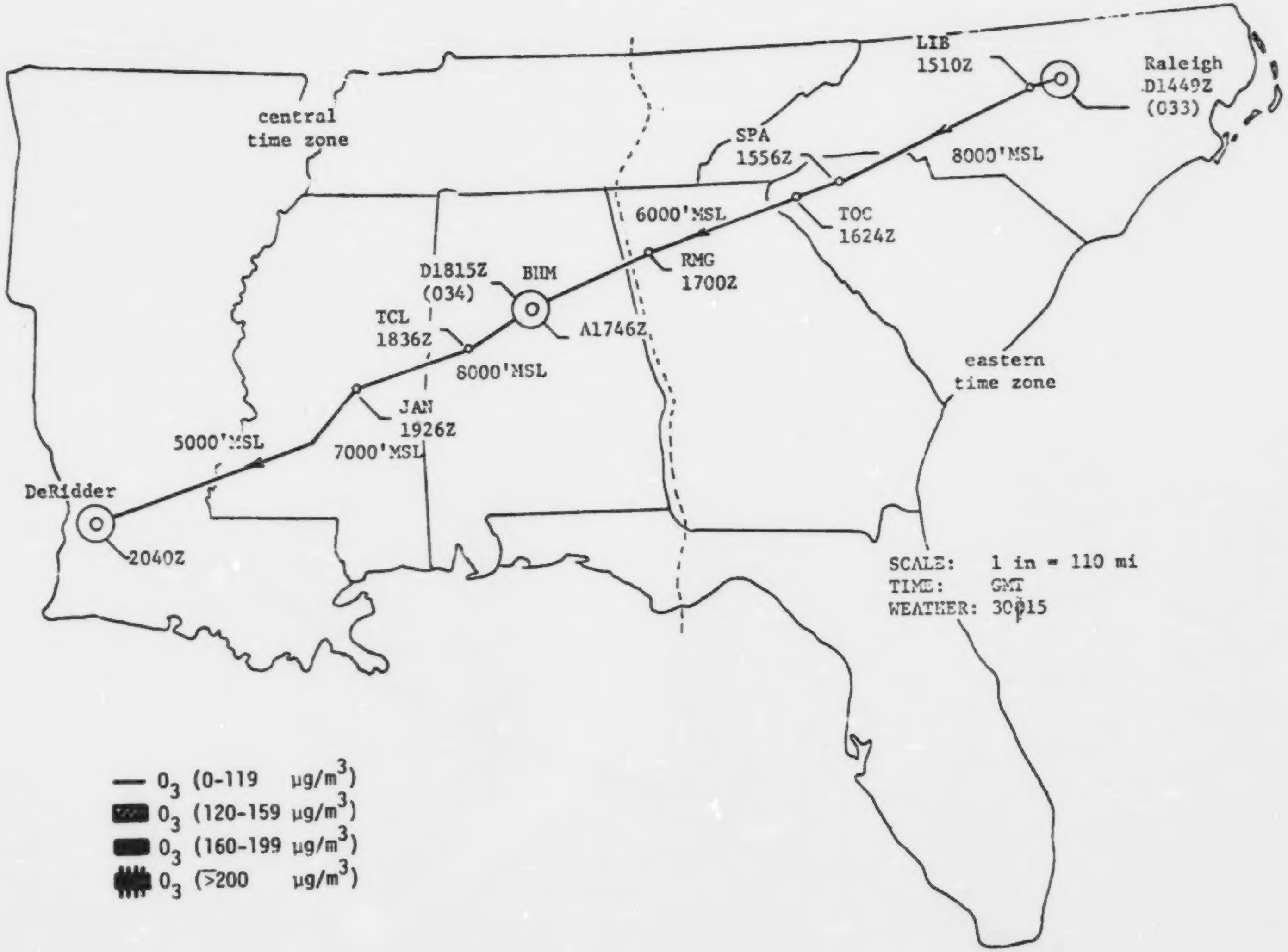
LIB
1510Z
Raleigh
D1449Z
(033)
8000'MSL
SPA
1556Z
TOC
1624Z
6000'MSL
RMG
1700Z
central
time zone
D1815Z
(034)
BHM
A1746Z
TCL
1836Z
8000'MSL
JAN
1926Z
7000'MSL
5000'MSL
DeRidder
2040Z
eastern
time zone
SCALE: 1 in = 110 mi
TIME: GMT
WEATHER: 30015
O_3 (0-119 μg/m^3)
O_3 (120-159 μg/m^3)
O_3 (160-199 μg/m^3)
O_3 (>200 μg/m^3)

Figure 109. Ozone concentrations, transitions flight on August 5, 1975.

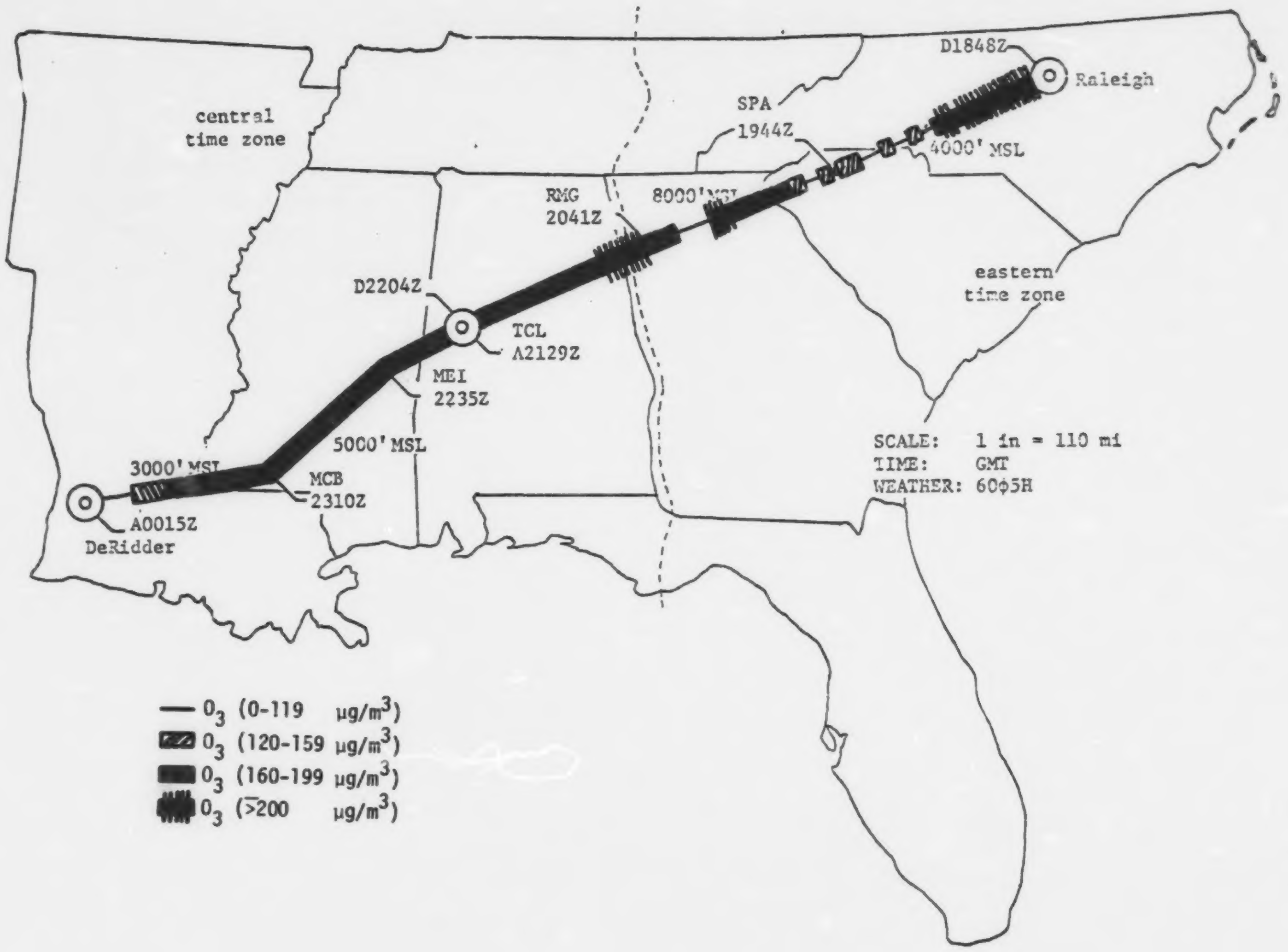
central
time zone
eastern
time zone
D1848Z
Raleigh
SPA
1944Z
4000' MSL
8000' MSL
RMG
2041Z
D2204Z
TCL
A2129Z
MEI
2235Z
5000' MSL
3000' MSL
MCB
2310Z
A0015Z
DeRidder
SCALE: 1 in = 110 mi
TIME: GMT
WEATHER: 6005H
— O_3 (0-119 μg/m^3)
▨ O_3 (120-159 μg/m^3)
■ O_3 (160-199 μg/m^3)
▩ O_3 (>200 μg/m^3)

Figure 110. Ozone concentrations, transition flight on June 25, 1975.

The population density of the Southeastern States over which the aircraft flights took place was ~63 persons mi^{-2} (1970 census) (table 62). Comparison of the ozone/population relationship with the northern stations is probably not valid largely because of the presence of the large oil fields, the refineries, the petrochemical installations, and longer smog seasons.

The average ozone concentration, as well as the average maximum, increased month by month in DeRidder from July through October. The general chemical system at DeRidder appears to be: low NO_x, high $NMHC/NO_x$ ratio with opportunity for reactant concentrations and reaction times to achieve concentration of ozone above the NAAQS. Ozone and hydrocarbon relationships are shown in tables 59, 60, and 61. Because of shifting relationships, discussed in more detail in section 7.2, there is little evidence of a one-to-one relationship between the hydrocarbon and ozone concentrations.

Table 62. Population density for southeastern States*

States	Population	Density of Population (By Square Mile, 1970)	Area (Sq. Miles)
Texas	11,196,730	42.7	262,134
Oklahoma	2,559,253	37.2	68,782
Arkansas	1,923,295	37.0	51,945
Louisiana	3,643,180	81.0	44,930
Tennessee	3,924,164	94.9	41,328
Mississippi	2,216,912	46.9	47,296
Alabama	3,444,165	67.9	50,708
North Carolina	5,082,059	104.1	48,798
South Carolina	2,590,516	85.7	30,225
Georgia	4,589,575	79.0	58,073
Florida	6,789,443	125.5	54,090
Total	47,959,292		
Average Density	63.2		

*U.S. Bureau of the Census, Census of Population and Housing; 1970, United States Summary.

8.2.1 Bag Irradiation Experiments

In October in DeRidder, a number of ambient air samples were taken in Teflon bags. One bag was irradiated with sunlight without additional reactants; a second bag, taken at the same time, was spiked with about 10 ppb of NO and irradiated at the same time as the first. Data obtained for October 18 and 19 experiments are shown in table 63. All data for both spiked- and unspiked-bag irradiation experiments are shown in figures 111 and 112. Obviously, in the ambient system, the added 10 ppb of NO increased the ozone-generative capability of the system, but none of the systems was sensitive enough to added NO that its addition would have generated ozone concentrations over the NAAQS.

8.2.2 Ozonesonde Releases

8.2.2.1 Introduction

Recent field measurements have shown frequent occurrences of ambient ozone concentrations at nonurban locations in excess of the NAAQS of 160 $\mu g/m^3$ for more than 1 hour per year.[5,26] These may arise from a combination of local generation, horizontal transport of ozone or ozone precursors, and from downward diffusion from the stratosphere. The role of the stratospheric ozone in the nonurban ozone problem is not fully understood. Analyses of the ozonesonde soundings reported by Hering and Borden[32] were concerned primarily with documentation of the stratospheric ozone. The analyses showed high ozone normally confined to the stratosphere, with a major increase just above the tropopause. Reiter's discussions[33] indicate occasions when large concentrations are brought from the stratosphere into the midtroposphere through folds or breaks in the tropopause. The implication is that the ozone could reach the ground in sufficient quantity to cause high concentrations. The conditions for these occurrences are usually found in late winter and early spring, when frontal systems are strong and deep and when the stratosphere is relatively ozone rich, rather than the summer and fall periods when most of the ozone concentrations exceeds the NAAQS at nonurban stations. Subsequent analysis of Reiter has indicated that the maximum 24-hour average of O_3 attributable to the stratosphere is not likely to be greater than 60-80 $\mu g/m^3$ [34].

Table 63. DeRidder Louisiana bag irradiation experiments, 1975, experimental data from bag irradiation

Experiment	Ambient Initial O_3 ppm	NO added ppm	Initial NO/NO_2 ppm	O_3 After 30 Min. Stabilization ppm	O_3 After Irradiation ppm	Net O_3 Generated ppm	Hydrocarbons Measured, ppbc at Time of Filling Bag
10/18/75	0.030	0.0	0/0	0.023	0.023	0.0	100.8
10/18/75	0.030	0.013	0/0	0.012	0.022	0.010	100.8
10/19/75	0.012	0.0	0/.001	0.008	0.019	0.011	259.1
10/19/75	0.012	0.013	0/.001	0.000	0.043	0.043	259.1

Weather:

Both days were clear and warm.

Conclusions:

In both these days' experiments, there was net production of O_3 in the NO-spiked bag. The experiments in spiked bags of 10/19 produced over 4 times as much ozone as that of 10/18. This is true even though the initial ozone was lower on the 19th than on the 18th. The main difference seems to be the hydrocarbon content of the sampled air. This may not be just a case of having more than twice as much carbon content on the 19th as the 18th but rather may be a matter of specific hydrocarbons.

There was a measurable initial amount of NO_2 on the 19th; although the added NO was only about 13 ppb, the presence of the NO_2 could have helped get O_3 production started sooner (i.e., crossover of NO and NO_2 concentrations occurred earlier) and thus attained a higher value by the day's end.

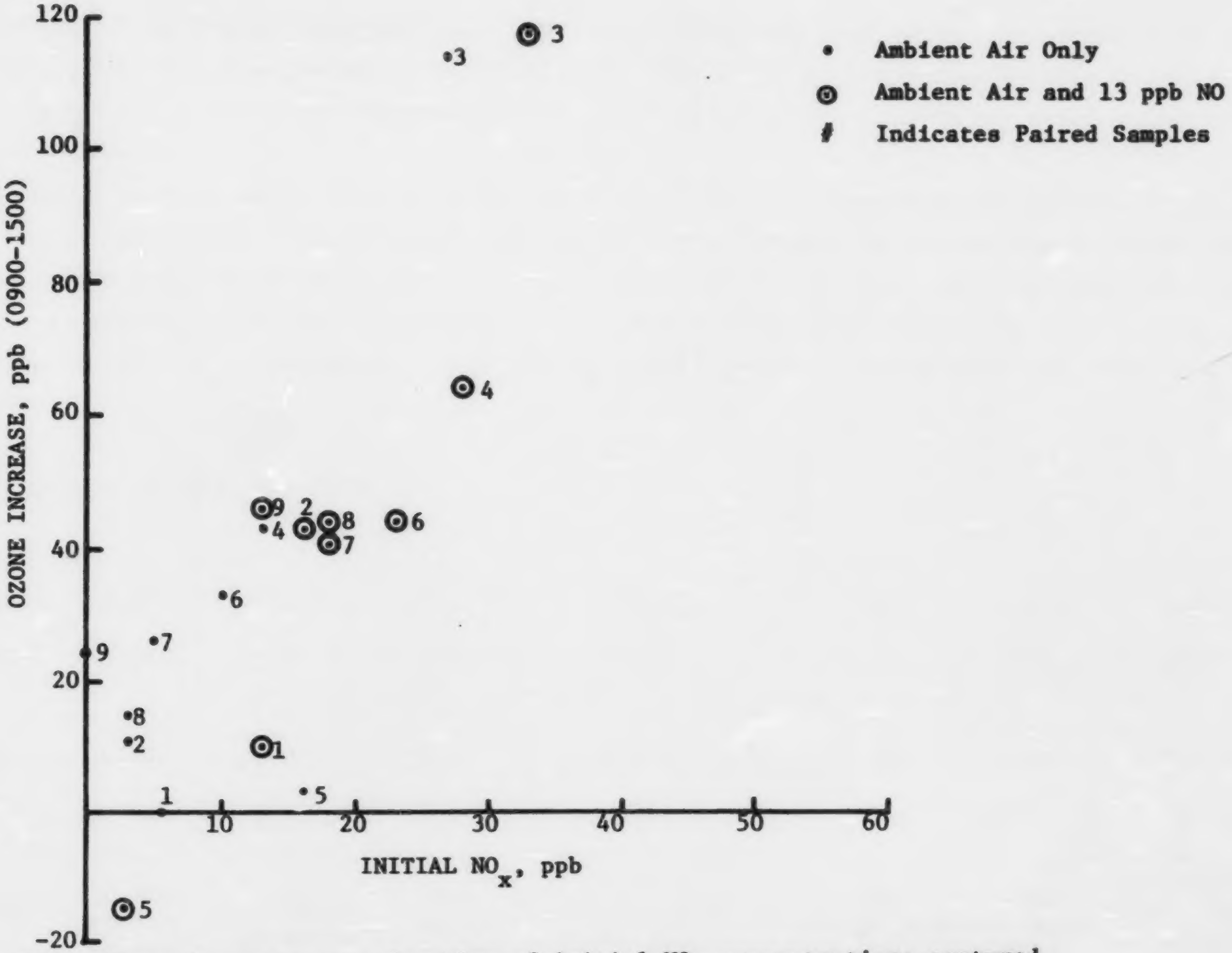

Figure 111. Ozone increase as a function of initial NO$_x$ concentration; captured air irradiation experiments, DeRidder, Louisiana (October 1-31, 1975).

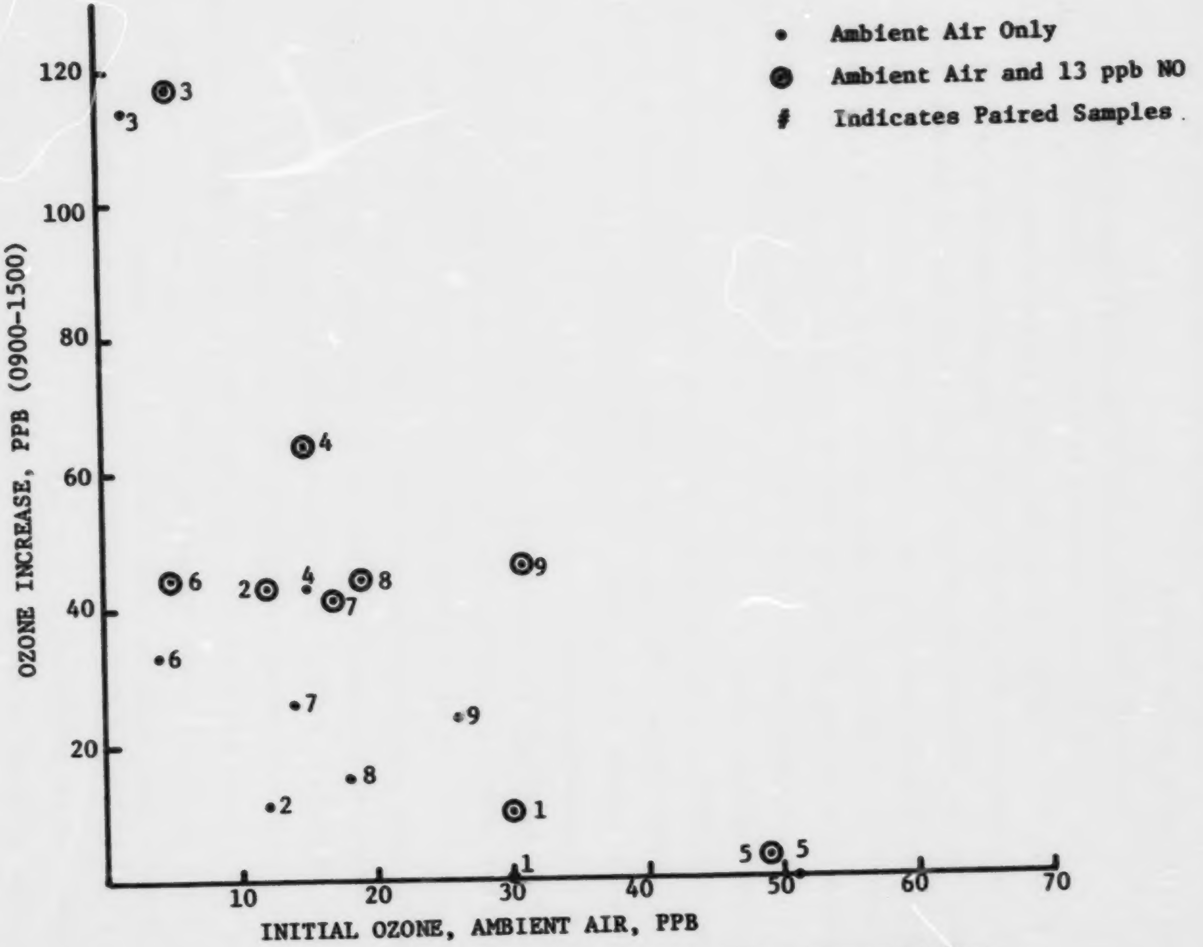

Figure 112. Ozone increase as a function of initial ozone concentration; captured air irradiation experiments, DeRidder, Louisiana (October 1-31, 1975).

Thunderstorms or other mechanisms of strong vertical mixing have been suggested as avenues for bringing stratospheric ozone to the ground.[35/] Lightning discharges associated with the thunderstorms also produce ozone. Few occurrences of high ozone at nonurban locations have been reported to be associated with thunderstorms.

8.2.2.2 Ozonesonde Releases at DeRidder, Louisiana, October 24-27, 1975

Ozonesonde releases were conducted at DeRidder, Louisiana, during the period October 24-27, 1975. On October 24, a fairly strong front was moving steadily southeastward across Oklahoma and central Texas into central Louisiana. About 0100 EDT on October 25, the front passed DeRidder and stalled before passing Lake Charles. Heavy rains ensued over the next 24 hours, before the front began to move again. Skies slowly cleared as the front moved to northwest Florida by late afternoon of October 25. A ridge of high pressure established itself along a northeastward axis lying slightly north of the DeRidder area.

One ozonesonde was released at 2300 CDT on October 24, several hours before the front passed. The sounding operations were suspended on October 25 because of intense rain. Three ozonesondes were released on October 26, and two more ozonesondes were released on October 27.

8.2.2.3 Stratosphere-Troposphere Ozone Distribution

The time-altitude cross-section of potential temperature and ozone from the ground to 100 mb is given in figure 113. Only the first four postfrontal ozone concentrations were used in this analysis.

The changes of atmospheric structure as the front passed Lake Charles were quite dramatic. Potential temperature from the Lake Charles, Louisiana, rawinsondes augmented the DeRidder measurements.

The ozone increases with altitude above 700 mb in all of the soundings, but the ozone isopleths cross the adiabats rather than paralleling them. It then appears that ozone is being produced in the upper troposphere. The major increase occurs after 0600 on October 26 and continues until night (1800) before decreasing in the night.

The time-altitude cross-section for higher altitudes is shown in figure 114. The tropopause is near 85 mb (~57,000 ft) where minimum temperature of -70° C were encountered. The atmosphere began to stabilize

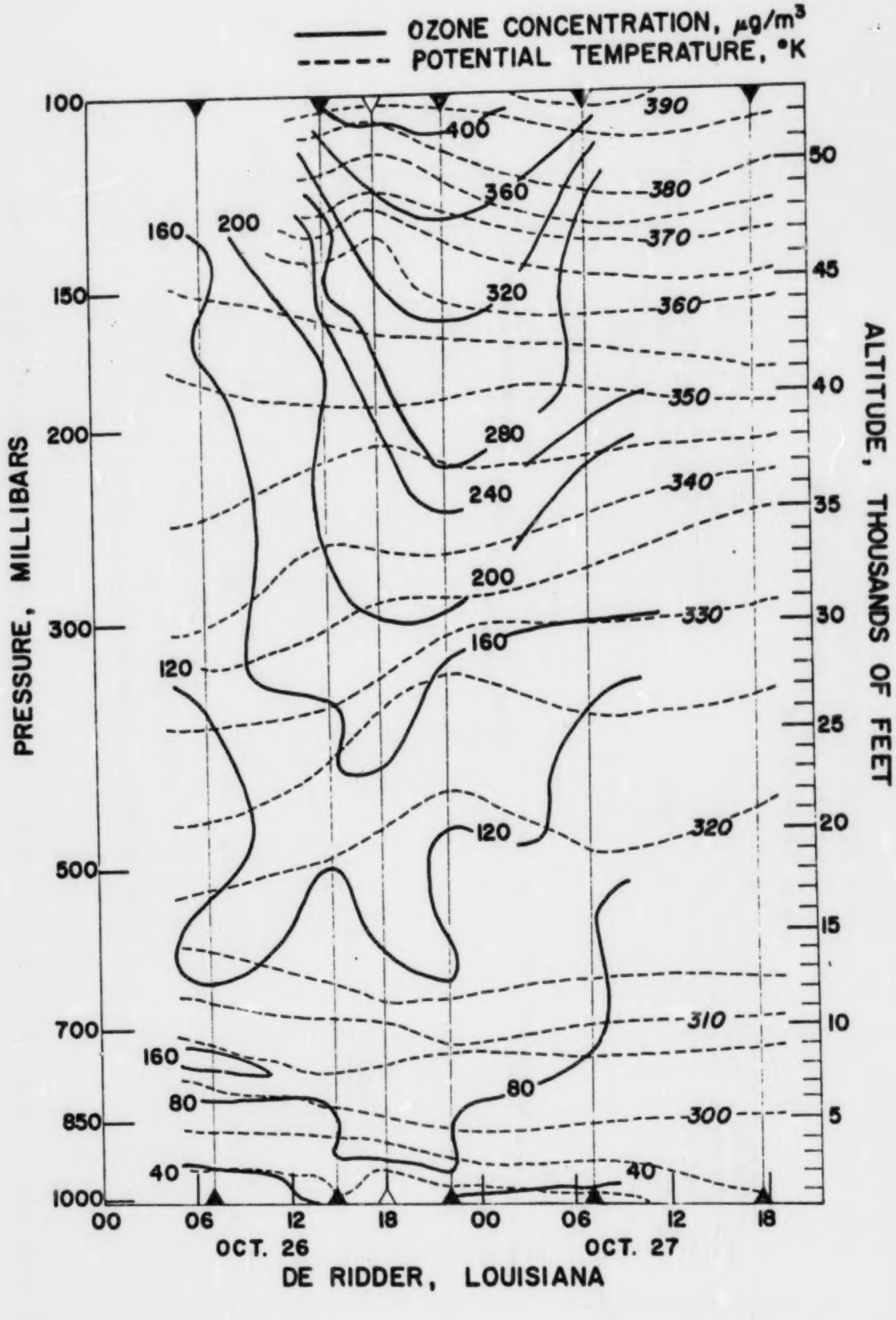

Figure 113. Time-altitude cross section of ozone and potential temperature, lower portion.

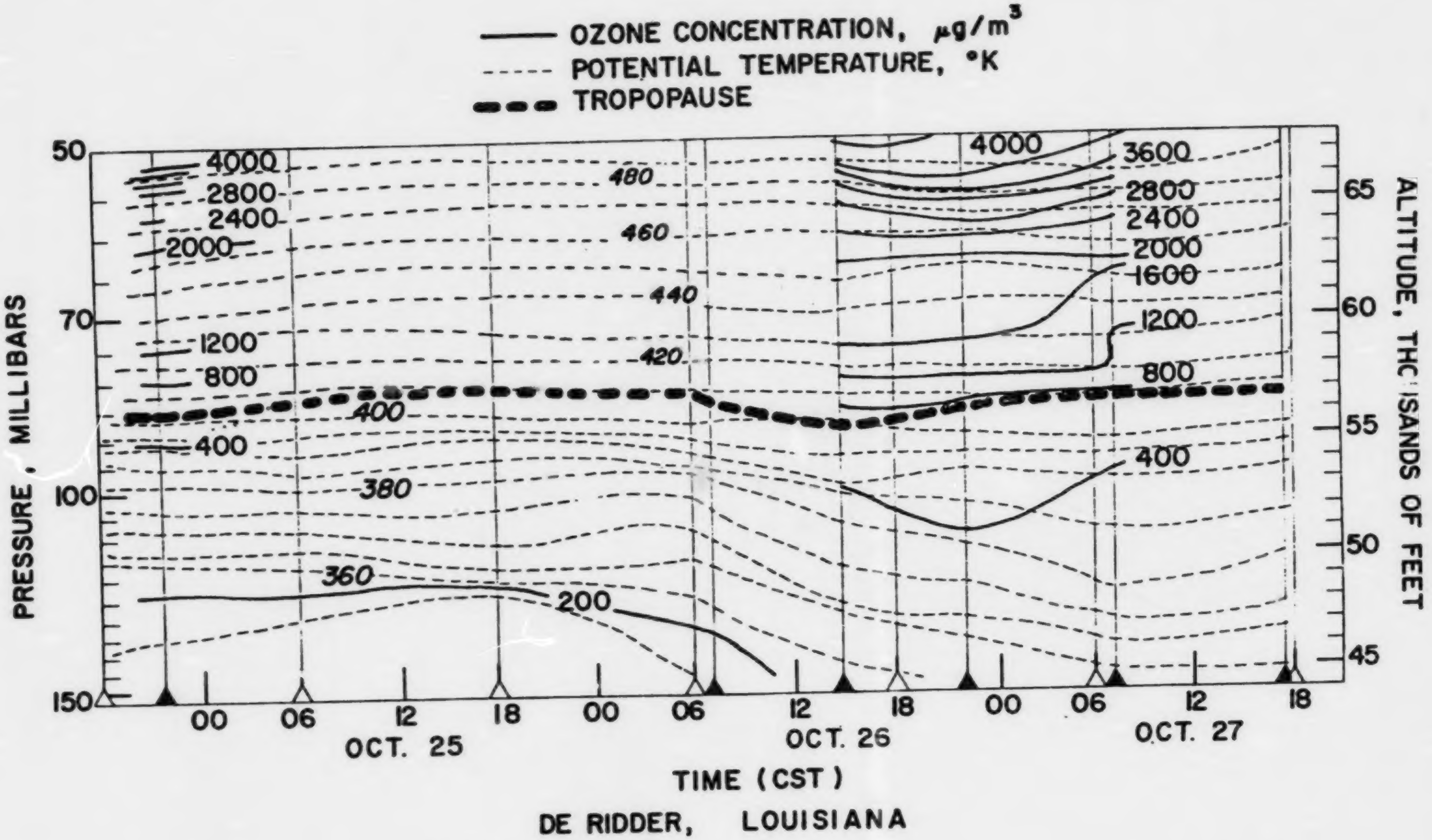

Figure 114. Time-altitude cross section of ozone and potential temperature, upper portion.

just below 100 mb. Because of the strong stratification, the prefrontal sounding was included in this analysis. Within the stabilized layer, the ozone is very stratified, following the adiabats, giving no indication of transport across the tropopause.

8.2.2.4 Low Altitude Distribution of Ozone

The analysis of the five postfrontal ozonesonde data show (figure 85) that the ozone concentration, $[O_3]$, increased almost linearly when plotted against the logarithm of pressure, P. A least-squares regression fit to the equation

$$[O_3] = a + b \log (P/1000) \quad P \geq 100 \text{ mb}$$

gave the dashed line of figure 115 and the regression parameters, a and b, and correlation coefficients of table 64.

The slope of the regression, b, changes slightly from one sounding to another. The slope of the last sounding is two to three times the slope of the other soundings, while the linear correlation remains high. If the regression trend is removed from the sounding, then departures from

Table 64. Average daily total suspended particulate (TSP) by month at DeRidder, Louisiana (1975)

Month	Average daily TSP, $\mu g/m^3$
	DeRidder
July	55.0
August	31.0
September	38.5
October	42.8
Overall Average	42.3

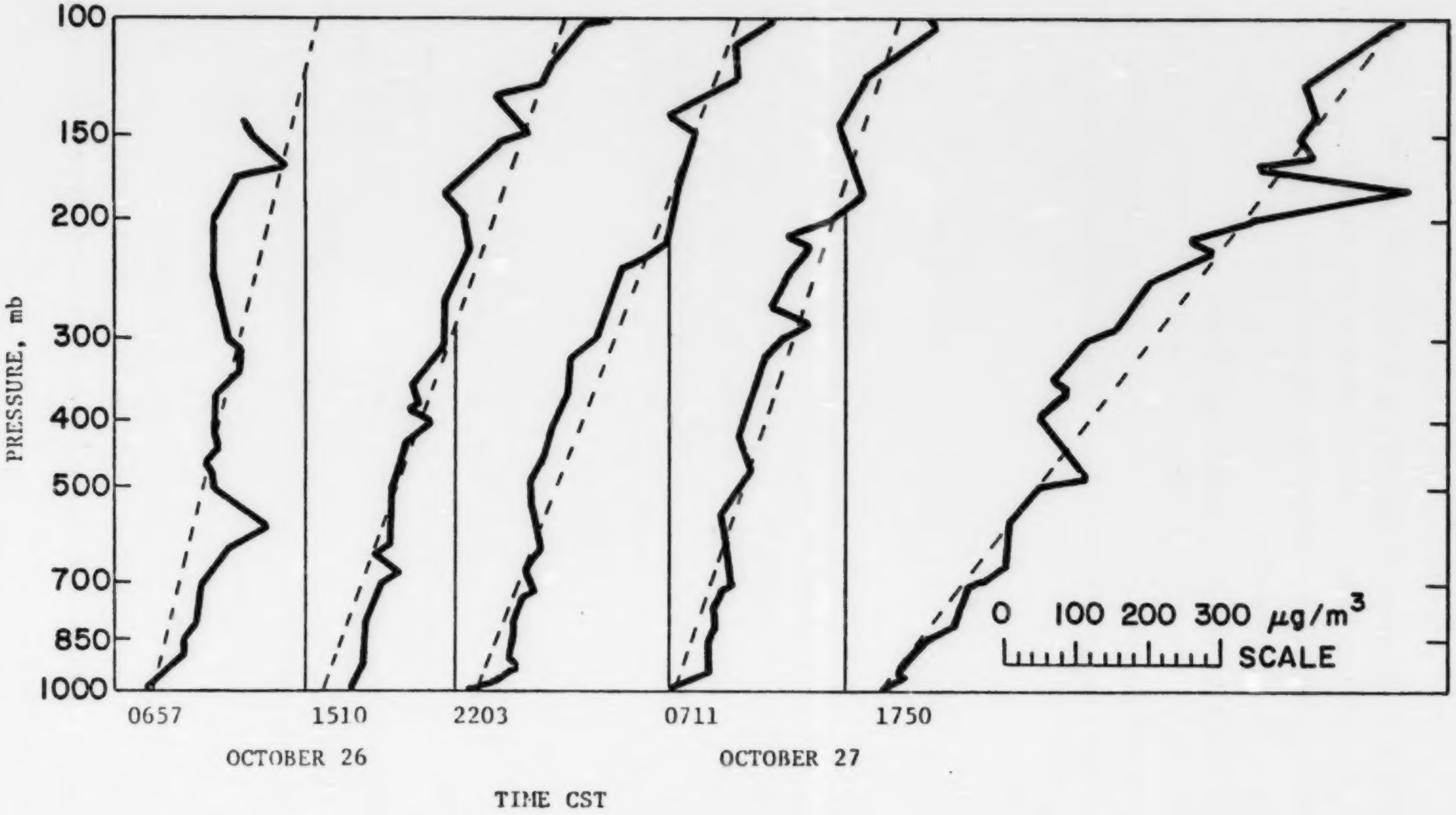

Figure 115. Vertical profile of ozonesonde data (solid) and best fit profile (dashed) 1000 to 100 mb.

the trend, $[O_3']$, show a close relationship with stable layers in all five soundings. In figure 116 the stable layer between the 308° K and 312° K potential temperatures persists during the analysis period. In each sounding, the $[O_3']$ increases in that layer. A stable layer develops between the 292° K and 295° K values and $[O_3']$ increases through it. Obviously, persistent stable layers appear to maintain an excess of ozone. While these stable layers do not appear to influence surface ozone concentration, a mechanism for transport of ozone, near the surface is verified.

This analysis suggests that the ozonesondes probably provide a good measure of relative change from one sounding point to another. Absolute concentrations are harder to establish.

8.2.3 Hydrocarbons and Halocarbons

8.2.3.1 Theoretical Considerations

The major purpose in making hydrocarbon measurements for both the gulf coast and the northern high pressure studies was to verify that anthropogenic pollution was present in the atmosphere when samples were collected. All samples analyzed contained acetylene and selected halocarbons. Since these samples were collected in a spatial and temporal manner, the conclusion could be drawn that all the air with high ozone concentrations contained anthropogenic pollution.

Difficulties are encountered in trying to relate hydrocarbons to ozone on a one-to-one basis. The fact that alkene to alkane ratios tend to be lower in rural air than in city air is a characteristic of a "spent" photochemical system. The fact that there is always some alkene material and that specific alkene/alkane ratios vary from place to place and time to time is an indication that some new pollutant material is continually being injected into the air.

Another indication of the continual injection of new material is that sequential hydrocarbon samples taken along the flight path show no progression at all in the concentrations of individual hydrocarbons. In other words each sample appears to come from a different microsystem with a different history of injection and atmospheric residence time.

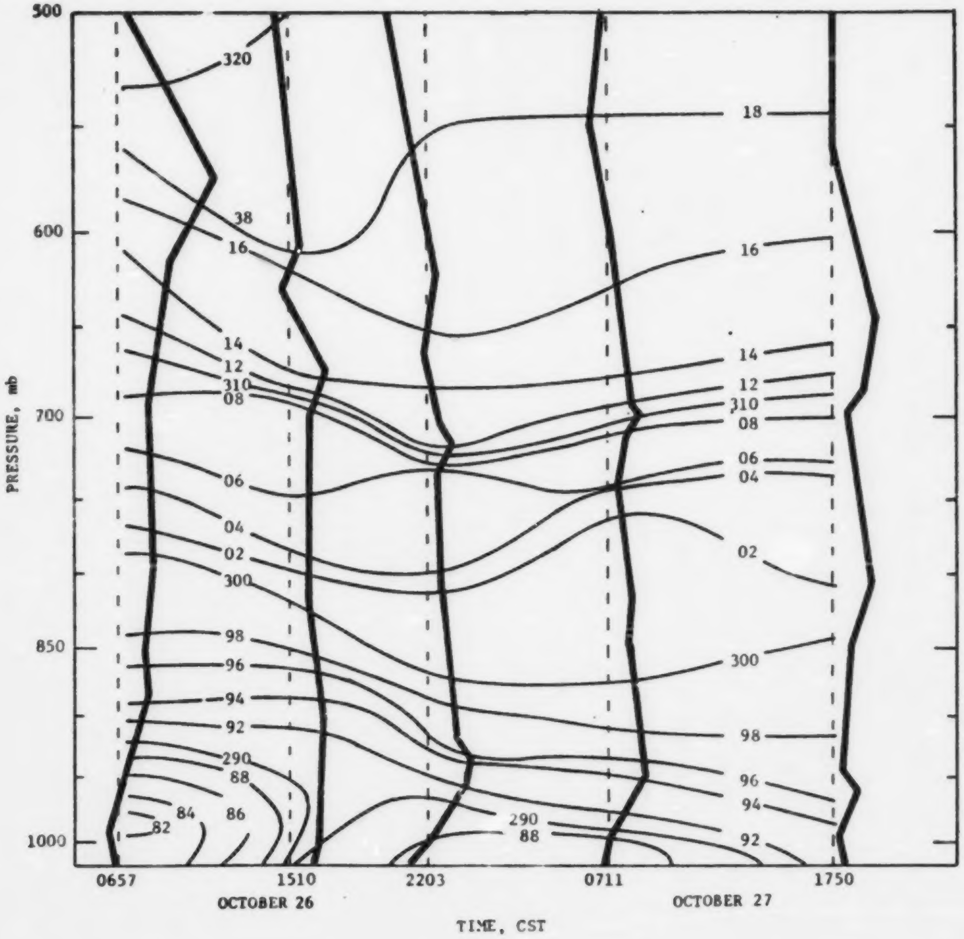

Figure 116. Vertical profile of ozone departures from best fit profile and time-altitude cross section of potential temperature.

There are no good figures for natural organic emissions from the areas covered by this study, but there are estimates for primary production. Primary production is the amount is the amount of carbon fixed by plants per unit land area per unit time. Since, in the long run, the amount of gaseous organic emissions is a fraction of the new plant tissue produced, a comparison of primary production should fairly accurately represent the relative values of the natural organic emissions.

The primary production along the gulf shore where the study was conducted was 1.5 to 2.0 kg m^{-2} yr^{-1}, with a change to 1.0 to 1.5 not far inland.[36] Natural organic emissions on a yearly basis should be more than twice the emissions at Wolf Point, and somewhat larger than the emissions at Creston and Bradford. An absolute number cannot, however, be assigned at this time. Aside from the difficulties in determining rates of primary production, the nature of the plant cover might cause a difference in seasonal released of organics from the plants. The Gulf Coast area around DeRidder is characterized by grassy land and mixed decidious and coniferous trees.

8. .3.2 Variation of Selected Hydrocarbons

A. Acetylene

Acetylene occurred in all ground-level samples. The averages for Saturday and Sunday were lower than for weekdays, but since a large portion of the United States production and commercial utilization of acetylene occurs in this area, acetylene is not a good index to the proportion of automobile exhaust emitted. Figure 117 shows the average acetylene concentration by day of the week.

B. Propane

Propane is a hydrocarbon not found in automobile exhaust. Its presence can, thus, be associated with industry, petrochemical processes, natural gas, or other natural emissions sources. Before the study, it was predicted that, due to the proximity of oil-producing and -processing installations, the propane concentrations would be higher or in higher ratio to other compounds at DeRidder than at the northern sites. This proved to be the case. Higher values of propane were expected in this area of the country since

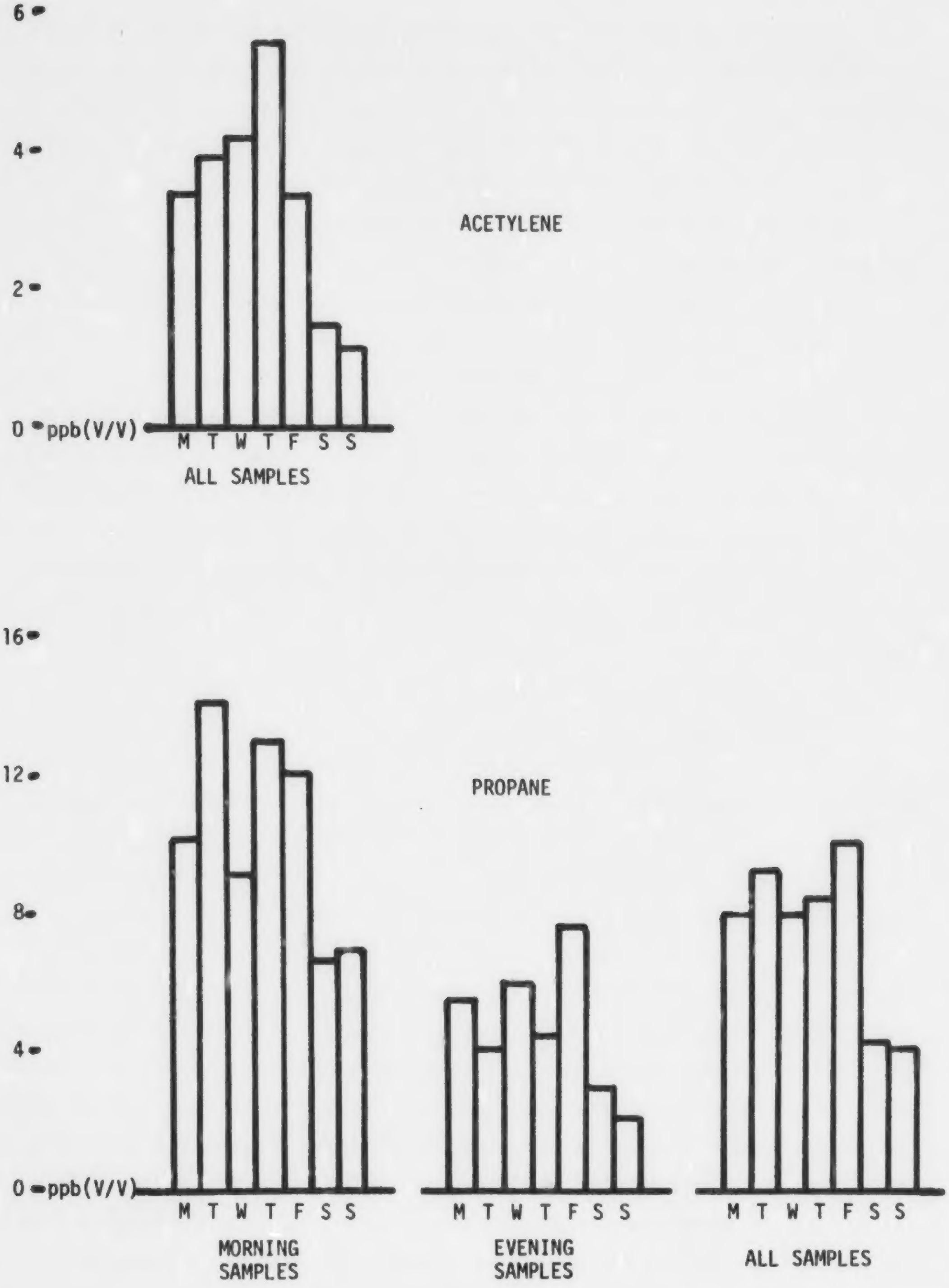

Figure 117. Bar graph showing acetylene and propane concentrations by day of week at DeRidder, Louisiana (July-October 1975).

there are many natural gas seeps as well as heavy concentration of refineries and hydrocarbon users here. Figure 117 shows the average propane concentration for each day of the week. These data suggest that propane is not due entirely to natural emissions or evaporative losses (which would be expected to be constant 7 days per week) but is also influenced by weekday activities unrelated to automobile exhaust.

C. Isopentane

Isopentane is one of the most abundant hydrocarbons in automobile exhaust. The acetylene-to-isopentane ratio in auto exhaust has been reported to be approximately 2. Due to the photochemical activity of isopentane, the ratio in ambient air samples should be slightly higher. The acetylene/isopentane ratio was calculated for each sample and averaged over the month for all samples. The acetylene/isopentane ratio at the DeRidder site for July, August, September, and October were 1.4, 2.4, 1.1, and 1.4, respectively. Only during the month of August did the ratio exceed 2. These data suggest that both compounds are not necessarily related to automobile emissions (table 18, section 6.1).

D. Toluene

A gradual increase in toluene concentration was observed from July to October. This trend does not follow the trends observed by other compounds, such as acetylene and isopentane. The increase cannot be associated with the increase of aromatic production, since o-xylene concentrations do not increase during the same time period (table 18, section 6.1).

E. Halocarbons

Selected halocarbons were analyzed in grab samples collected in DeRidder. There was considerable variance in their concentrations, which indicates that the mean concentration of short integrated samples may not be representative of the air mass. Halocarbon concentrations changed rapidly by several orders of magnitude during the study period (table 18, section 6.1). Even though the DeRidder station was located in a rural area, it is surrounded from the east to the south and southwest by large petrochemical centers and urban areas.

8.2.4 Particulates

8.2.4.1 Total Suspended Particulates; Sulfate, Nitrate, Ammonium

Total suspended particulate (TSP) samples were collected on a daily basis at the DeRidder site from July through October 1975 by the 24-hour, integrated high-volume method. Selective analyses for sulfate, nitrate, and ammonium ions were also made. Table 65 summarizes the average daily TSP levels by month. The highest TSP concentration occurred in July.

TSP averages by day of the week show the highest concentration on Thursday (51.2 $\mu g/m^3$); the lowest value on Saturday (35.4 $\mu g/m^3$). Chemical analysis of the particulate samples gave these average concentrations: sulfate, 5.6 $\mu g/m^3$ (13 percent of TSP); nitrate, 1.4 $\mu g/m^3$ (3.3 percent of TSP); and, ammonium, 0.03 $\mu g/m^3$ (0.07 percent of TSP).

Sulfate and nitrate data from the DeRidder site were also expressed as percent of TSP by month as follows (month, percent sulfate, percent nitrate): July, 10.6, 3.5; August, 17.6, 3.1; September, 13.2, 3.1; and October, 13.3, 3.7. Sulfate was also averaged by day of the week as a percentage of TSP. The sulfate percentage of TSP was consistent during the week.

Comparison of these percentages with data taken from the National Air Sampling Network (table 55, section 7.3) classifies the DeRidder site as a nonurban site intermediate in distance from sulfate and nitrate sources.

8.2.4.2 Gulf Coast Aircraft Particulate Samples

High-volume particulate samples were collected by the aircraft on nine of the Gulf Coast area flights. Sample collection occurred during the entire flight. These flights are listed in table 66 with the corresponding analyses for nitrate and sulfate.

The flights from DeRidder, Louisiana, which extended over the Gulf of Mexico, were much lower in nitrate and sulfate than the corresponding southern flights over land surfaces. The highest concentrations of nitrate and sulfate in the gulf coast flights occurred on the flight which surveyed the Port Arthur, Texas, area (fig. 66). The lowest concentrations occurred on flights over the Gulf of Mexico.

Table 65. Selected particulate constituents as percentages of gross suspended particulates (1966-1967)*

	Urban		Nonurban					
	(217 Stations)		Proximate[a] (5)		Intermediate (15)		Remote[b] (10)	
	μg/m³	%	μg/m³	%	μg/m³	%	μg/m³	%
Suspended Particulates	102.0		45.0		40.0		21.0	
Benzene soluble Organics	6.7	6.6	2.5	5.6	2.2	5.4	1.1	5.1
Ammonium ion	0.9	0.9	1.22	2.7	0.28	0.7	0.15	0.7
Nitrate ion	2.4	2.4	1.40	3.1	0.85	2.1	0.46	2.2
Sulfate ion	10.1	9.9	10.0	22.2	5.29	13.1	2.51	11.8
Copper	0.16	0.15	0.16	0.36	0.078	0.19	0.060	0.28
Iron	1.43	1.38	0.56	1.24	0.27	0.67	0.15	0.71
Manganese	0.073	0.07	0.026	0.06	0.012	0.03	0.005	0.02
Nickel	0.017	0.02	0.008	0.02	0.004	0.01	0.002	0.01
Lead	1.11	1.07	0.21	0.47	0.096	0.24	0.022	0.10

*Data from United States National Air Sampling Network, 1966-1967.

[a] Near urban areas.

[b] Far from urban areas.

Table 66. Nitrate and sulfate concentrations for samples collected during gulf coast flights

Date	Flight	Altitude (ft)	NO_3^- ($\mu g/m^3$)	$SO_4^=$ ($\mu g/m^3$)
9/19	DeRidder to Sea (075, 076)	1000/500	1.9	0.7
9/21	DeRidder to Sea (078, 079)	4000/500	3.2	9.7
10/10	DeRidder to Sea (094, 095)	500	2.4	2.8
10/13	DeRidder to Sea (096)	2000/500	2.1	2.9
10/14	Alabama (097, 098)	2000	2.7	8.6
10/19	Texas (099, 100)	2000	4.4	8.4
10/20	Louisiana (101, 102)	2000	5.1	11.4
10/30	Port Arthur, Texas (109)	2000	10.6	25.5
10/31	Texas (110)	2000	5.7	11.2
Overall Average			4.2	9.0
Average of 2000 ft. Flights			5.7	13.0
Average of Sea Flights			2.4	4.0

8.2.5 Summary of Ozone Generation (Gulf Coast Oxidant Study)

The gulf coast area produces all the necessary precursors for tropospheric ozone generation. These come from the urban areas and from the petroleum and petrochemical industry, which is concentrated in the east Texas and west Louisiana regions. Oil refineries are sources not only of hydrocarbons but of NO_x also.

The cities and industries in this region represent discrete sources and are not sprawling megalopolises nor thickly settled rural areas, and certain aspects of the high ozone generation show this. With good atmospheric ventilation the whole southeast exhibits ozone concentrations which can be considered at or near natural background levels (i.e., $\leq 70\ \mu g/m^3$). With less favorable conditions, a gradient of high ozone concentrations can be observed, progressing from plumes of high concentration and covering more and more areas until the high ozone concentrations become virtually an air mass characteristic.

9.0 CONCLUSIONS

The following conclusions derived from the data are listed separately for each of the two study areas. Section numbers are provided to refer to the section of the report that pertains to each conclusion.

A. Conclusions: Northern High Pressure Oxidant Study

1. In the summer, high concentrations of ozone (i.e., $\geq 160\ \mu g/m^3$) in the rural boundary layer and in the eastern portions of the United States are most often found within high pressure systems. Sustained periods of high ozone are associated with macroscale high pressure systems that persist for more than 20 days. (Section 7.2.2)

2. Highest concentrations of ozone were found in the back side of a high pressure system. A relative minimum is observed in the front side or near the center. (Section 7.2.3)

3. Locations of maximum and minimum ozone concentrations in a moving high pressure system correlate with the location of air having maximum and minimum residence time in that system. (Section 7.2.3)

4. The air initially in the northeastern quadrant of an eastward moving high pressure system has the longest residence time in that system. (Section 7.2.4)

5. Oxides of nitrogen concentrations in rural areas in the western section of the study area were apparently too low to promote the generation of ozone concentration equal to or greater than the NAAQS. (Section 7.3.1)

6. High ozone concentrations and the frequency of exceeding the NAAQS for photochemical oxidants are associated with increased population density (i.e., both increased from west to east). (Section 7.3.1)

B. Conclusions: Gulf Coast Oxidant Study

1. Ozone concentrations over the Gulf of Mexico usually were less than those over land. High ozone concentrations (i.e., $\geq 160\ \mu g/m^3$) that were measured over water or in air flowing off the Gulf of Mexico were associated with air that had previously passed over continental sources of pollution. (Section 8.1.3)

2. Changes in the vertical structure of ozone concentrations below 3 km are primarily controlled by boundary layer processes. (Section 8.1.2)

3. Elevated ozone concentrations (i.e., $\geq 160\ \mu g/m^3$) are frequently measured in plumes downwind of potential ground sources of precursors, i.e., cities, major refineries, and petrochemical installations. (Section 8.1.3)

4. Upper decile concentrations of ozone are associated with slow moving air that had passed over high precursor emission areas and arrived from a nonprevailing wind direction; lower decile concentrations are associated with faster moving air, having a long over-water fetch with a weak anticyclonic trajectory. (Sections 8.1.3 and 8.1.4)

10.0 REFERENCES

1. Federal Register, "National Primary and Secondary Ambient Air Quality Standards," April 30, 1971.

2. L. A. Ripperton, H. E. Jeffries, and J. J. B. Worth, "Relationship of Measurements in Non-Urban Air to Air Pollution: Ozone and Oxides of Nitrogen," Proceedings, Second International Clean Air Congress, Academic Press, N. Y., pp. 386-390 (1971).

3. Research Triangle Institute, "Investigation of High Ozone Concentration in the Vicinity of Garrett County, Maryland, and Preston County, West Virginia," issued as Environmental Protection Agency Report No. EPA-R4-73-019.

4. Research Triangle Institute, "Investigation of Ozone and Ozone Precursor Concentrations at Non-Urban Locations in the Eastern United States, Phase I," issued as Environmental Protection Agency Report No. EPA-450/3-74-034 (May 1974).

5. Research Triangle Institute, "Investigation of Rural Oxidant Levels as Related to Urban Hydrocarbon Control Strategies," issued as Environmental Protection Agency Report No. EPA-450/3-75-035 (March 1975).

6. D. A. Craven and D. J. Johnson, Yellow Pine Study, Texas Air Control Board, Technical Support Program, Air Quality Evaluation Division (1975).

7. W. N. Stasiuk and P. E. Coffey, "Rural and Urban Ozone Relationships in New York State," J.A.P.C.A., 24:564-568 (1974).

8. California Air Resources Board, Air Quality Data, Indio, July 1972.

9. P. R. Muller, M. H. McCutchan, and H. P. Milligan, "Oxidant Air Pollution in the Central Valley, Sierra Nevada Foothills and Mineral King Valley of California," Atmospheric Environment, 6:603-633 (1972).

10. C. E. Junge, "Air Chemistry and Radioactivity," N. Y. Academic Press, pp. 37-59 (1963).

11. H. G. Richter, Special Ozone and Oxidant Measurement in the Vicinity of Mt. Storm, West Virginia, Research Triangle Institute, Task Report, Task No. 3, NAPCA Contract No. 70-147 (1970).

12. T. Y. Canby, "Skylab, Outpost on the Frontier of Space," National Geographic, 146:441-493 (1974).

13. Texas Air Control Board, "Background Concentrations of Hydrocarbons in the Atmosphere of the Northwest Gulf of Mexico, Air Quality Evaluation (1973).

14. E. F. Gibich, D. J. Johnson, and R. Wallis, "Ambient Air Quality Survey," Corpus Christi, Texas, Texas Air Control Board, Technical Support Program, Air Quality Evaluation Division (1973).

15. D. J. Johnson, "Texas Ambient Air Quality Continuous Monitoring Network," Texas Air Control Board, Technical Support Program, Air Quality Evaluation Division (1973).

16. R. Wallis, J. H. Price, G. K. Tannahill, and J. P. Gise, "Ozone Concentrations in Rural and Industrial-Urban Cities in Texas," Texas Air Control Board, Air Quality Evaluation Division (1975).

17. C. E. Decker, T. M. Royal, and J. B. Tommerdahl, Development and Testing of an Air Monitoring System, Final Report, Research Triangle Institute, Research Triangle Park, North Carolina, issued as Environmental Protection Agency Report No. EPA-650/2-74-019.

18. EPA-650/2-74-056, "Development of an Acetylene Monitor at the PPB Level," Final Report, Beckman Instrument Company (August 1974).

19. Federal Register, "Ambient Air Quality Standards: Reference Method for Determination of Nitrogen Dioxide" (June 8, 1973).

20. W. D. Komhyr and T. B. Harris, "Development of an ECC Ozonesonde," NOAA TR ERL 200-APCL 18, Boulder, Colorado, February (1971).

21. A. J. Wagner, "Weather and Circulation of June 1975," Mon. Wea. Rev., 103, 932-939 (1975).

22. R. E. Taubensee, "Weather and Circulation of September 1975," Mon. Wea. Rev., 103, 1143-1148 (1975).

23. R. R. Dickson, "Weather and Circulation of August 1975," Mon. Wea. Rev., 103, 1027-1031 (1975).

24. A. J. Wagner, "Weather and Circulation of October 1975," Mon. Wea. Rev., 104, 107-113 (1976).

25. S. M. Brunty, W. S. Cleveland, T. E. Graedel, B. Kleiner, and J. L. Warner, "Ozone Concentrations in New Jersey and New York: Statistical Association with Related Variables," Science, 186, 257-258, 1974.

26. W. D. Bach, Jr., Investigation of Ozone and Ozone Precursor Concentrations at Nonurban Locations in the Eastern United States, Phase II, Meteorological Analysis, Research Triangle Institute, Research Triangle Park, N. C., Report No. EPA-450/3-74-034a (February 1975).

27. W. S. Hering and T. R. Borden, Jr., "Ozonesonde Observations over North America," 4, Air Force Cambridge Research Laboratories, Office of Aerospace Research, 1967.

28. H. E. Jeffries, An Experimental Method for Measuring the Rate of Synthesis, Destruction and Transport of Ozone in the Lower Atmosphere, E.S.E. Publication No. 285, Ph.D. Thesis, Department of Environmental Science and Engineering, University of North Carolina, Chapel Hill, North Carolina, 1971.

29. F. M. Vukovich, "Some Observations of the Variations of Ozone Concentrations at Night in the North Carolina Piedmont Boundary Layer," J. E. R., 78, 4458-4462, 1973.

30. J. L. Heffter and A. D. Taylor, "A Regional-Continental Scale Transport Diffusion and Deposition Model, Part I, Trajectory Model," NOAA TM ERL-ARL-50, Silver Springs, Maryland, 1975, 16 pp.

31. K. MacKenzie, Personal Communication, Health Department, Houston, Texas.

32. W. S. Hering and T. R. Borden, Jr., "Ozonesonde Observations over North America," 2, 3, Air Force Cambridge Research Laboratories Reports AFCRL-64-30 (II, III, IV), (1964, 65).

33. E. R. Reiter, Atmospheric Transport Processes, Part 2: Chemical Tracers, U. S. Atomic Energy Commission, Division of Technical Information Extension, Oak Ridge, Tennessee, pp. 113-154 (1971).

34. E. R. Reiter, "Significance of Stratospheric Ozone for Ground Level Ozone for Ground Level Ozone Concentrations." Report to Stanford Research Institute, April 7, 1976. Prepared pursuant to EPA contract no. 68-02-2084.

35. D. R. Davis and C. E. Dean, "Meteorological Aspects of Atmospheric Ozone as a Potential Threat to the Forest Industry of North Florida," J. Environ. Qual., 1, pp. 438-441 (1972).

36. H. Leith, "Primary Production: Terrestrial Ecosystems," Human Ecology, 1:303-332 (1973).

APPENDIX A

CALIBRATION SYSTEMS/PROCEDURES

Preceding page blank

APPENDIX A

CALIBRATION SYSTEMS/PROCEDURES

Dynamic calibration procedures were used to calibrate all analyzers used during the field measurement program. Monthly calibrations were performed on each instrument using the procedures described below.

A-1. General

Because the five stations were at elevations above mean sea level, adjustments to the data were necessary to reduce values to reference condition of 25° C (298° K) and 760 mmHg. Adjustments to volume measurements were made using the following equation:

$$V_R = V \times \frac{P}{760} \times \frac{298}{t + 273}$$

where

V_R = volume of air at reference conditions, liters,

V = volume of air at sampling conditions, liters,

P = barometric pressure at sampling conditions, mmHg, and

t = temperature at sampling conditions, °C.

Table A-1 summarizes the sampling conditions used for each site.

Table A-1. Altitude-pressure relationship for sampling sites

Station	Altitude above mean sea level meters	Altitude above mean sea level feet	Room temperature, °C	Barometric pressure mmHg	Volume of 1 liter at reference conditions (25°C, 760 mmHg)-liters
Bradford, Pa.	653	2,143	25 ± 2°	701.9	0.92
Lewisburg, W. Va.	702	2.301	25 ± 2°	697.7	0.92
Creston, Ia.	394	1,293	25 ± 2°	724.2	0.95
Wolf Point, Mont.	605	1,985	25 ± 2°	706.1	0.93
DeRidder, La.	62	203	25 ± 3°	751.3	0.99

Derived from table p. 9-4, Handbook of Air Pollution, PHS Publication No. 999-AP-44, "Barometric Pressure at Various Altitudes."

The same adjusted volume was used each time a calibration was performed. A basic step-wise procedure was employed for dynamic calibration of all air quality analyzers as follows:

1. Verify operational status of each analyzer prior to beginning calibration.
2. Connect instrument inlet line or instrument calibration inlet line, as the case may be, to the manifold of the calibration apparatus or, for hydrocarbon instruments, directly to cylinders containing calibration gas.
3. Allow instrument to sample zero air (i.e., air minus the pollutant of concern) for a period of time sufficient to establish a valid zero output. Average the instrument output for zero input concentration for at least 15 minutes. Record voltage and/or chart readings as dictated by the type of data acquisition system used.
4. Introduce a pollutant calibration concentration equal to approximately 80 percent of the operating range and adjust the span of instrument as required upon initial setup of the instrument. This adjustment is normally required only upon initial setup of an instrument or if excessive span drift occurred during the evaluation period. Omit step 4, except on initial setup of analyzer.
5. Introduce successive pollutant calibration concentrations of 10, 20, 40, 60, and 80 percent of the operating range of the instrument being calibrated. Allow sufficient time to establish a valid instrument output for each calibration concentration, and average the instrument output for that input calibration concentration for at least 15 minutes. Record the voltage and/or chart reading for that calibration point and proceed to the next higher calibration concentration and repeat the sequence of events.
6. Return the instrument inlet line to the ambient air sampling manifold and compute a transfer equation, which relates

pollutant concentration input to instrument voltage output, for each instrument.

7. Document thoroughly all parameters required to complete the calibration record sheet designed for each analyzer.

A-2. Ozone Analyzers

A dynamic calibration system producing ozone by ultraviolet irradiation of oxygen[A-1] was used to calibrate the gas phase chemiluminescent ozone analyzers. The ozone generator consisted of a shielded mercury vapor lamp (20.3 cm in length) which irradiated clean compressed air flowing through a quartz tube (1.5 cm in diameter). By varying the length of the lamp exposed to the air and the total flow of compressed air (usually set at 5.0 l/min), ozone concentrations from zero to approximately 1 ppm (1960 $\mu g/m^3$) were produced.

A portable calibration unit consisting of a regulated power supply, zero air source, calibrated rotameter, ozone generator, mass flowmeter for nitric oxide mixtures, and a glass manifold with sampling ports was assembled. This unit was transported from site to site for calibration of each ozone (as well as nitrogen dioxide) analyzer. A schematic diagram of the ozone calibration system is shown in figure A-1.

In order to obtain a reference measure of the ozone output of the calibration unit, the neutral-buffered KI analysis method[A-2] was used for each calibration point. A diagram of the calibration system is shown in figure A-1. The analyzer and the bubbler train sampled simultaneously from the glass manifold. A diagram of the KI sampling train and apparatus used to calibrate the sample flow rate is shown in figure A-2.

A-3. Nitrogen Oxides Analyzer

The NO-NO_2-NO_x analyzer was calibrated by gas phase titration.[A-3] The technique utilizes the rapid gas phase reaction between NO and O_3 to produce a stoichiometric quantity of NO_2. A schematic diagram showing components of the parts of the calibration system is presented in figure A-3.

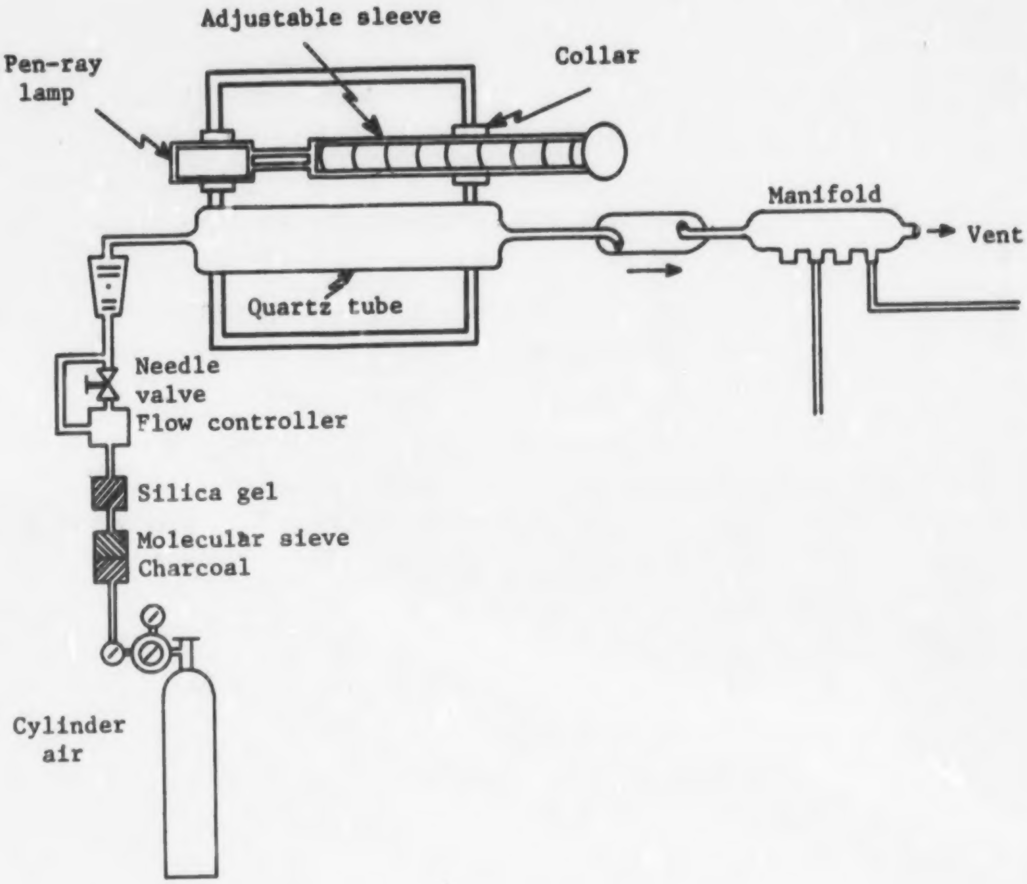
Adjustable sleeve
Pen-ray lamp
Collar
Manifold
Vent
Quartz tube
Needle valve
Flow controller
Silica gel
Molecular sieve
Charcoal
Cylinder air

Figure A-1. Ozone calibration system.

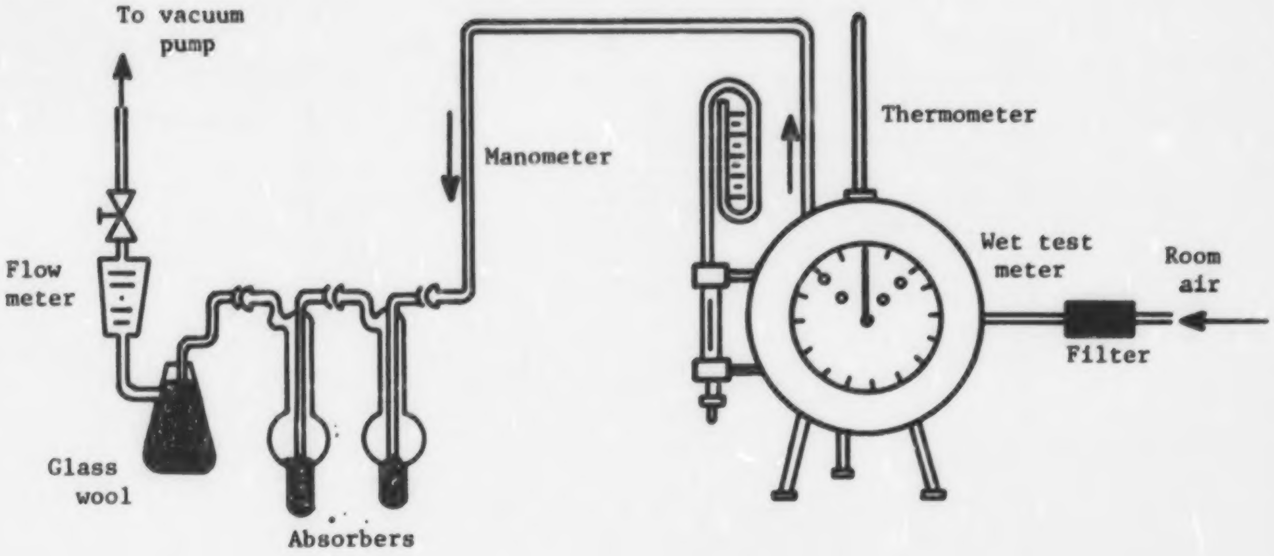
To vacuum pump
Thermometer
Manometer
Flow meter
Wet test meter
Room air
Filter
Glass wool
Absorbers

Figure A-2. KI sampling train and apparatus for calibration of flow rate under operational conditions.

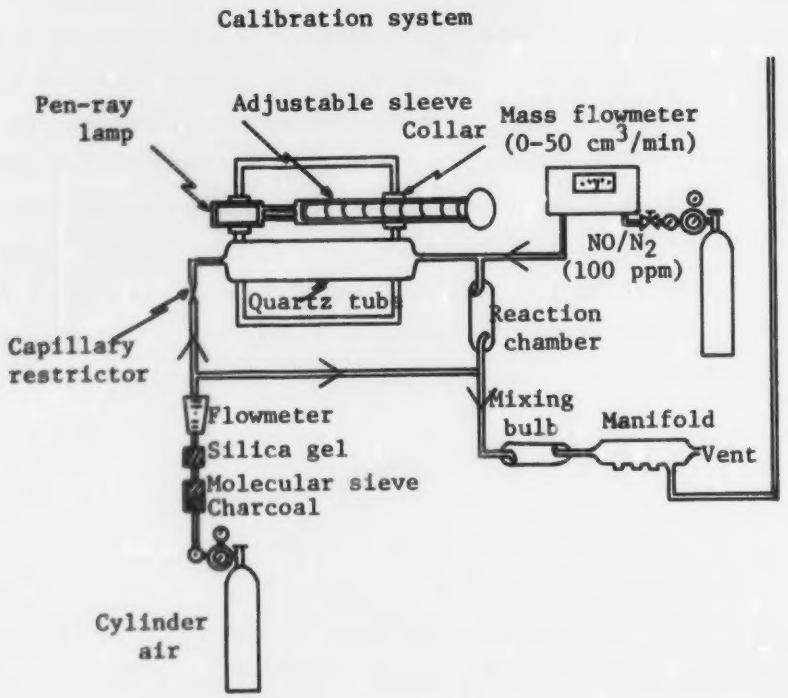
Calibration system
Pen-ray lamp
Adjustable sleeve
Collar
Mass flowmeter (0-50 cm^3/min)
NO/N$_2$ (100 ppm)
Quartz tube
Capillary restrictor
Reaction chamber
Mixing bulb
Manifold
Vent
Flowmeter
Silica gel
Molecular sieve
Charcoal
Cylinder air

Figure A-3. Gas phase titration system.

After the preliminary zero and span checks, the first step in the final calibration is the introduction of zero air into the analyzer. After 10 minutes, a zero reading is taken on the NO, NO_2, and NO_x channels.

Before transporting the NO calibration gas cylinders to the field, the NO concentration of the contained calibration gases was verified using the technique of Hodgeson and associates.[A-3/] The procedure consisted of titrating an NO concentration of 1.0 ppm with successive concentrations of ozone (0-0.8 ppm) produced by an ozone generator referenced to the neutral-buffered KI procedure. The resultant NO detector outputs, after stabilization at each titration points (i.e., 0.0, 0.1, 0.2, ... 0.8 ppm ozone added), were plotted as concentration ppm (y-axis) versus O_3 concentration added, ppm (x-axis). A straight line drawn through the linear portion of the titration curve was extrapolated to the x-axis. The concentration of the x-axis intercept, C_O', was the O_3 concentration equivalent to the initial diluted NO concentration. An example of a typical gas phase titration curve is presented in figure A-4. The cylinder NO concentration was then calculated as follows:

$$C_{NO} = \frac{F_O \times C_O'}{F_{NO}}$$

where

C_{NO} = cylinder NO concentration, ppm
F_{NO} = measured NO flow, ml/min,
C_O' = equivalence point O_3, concentration, ppm, and
F_O = total clean air flow, ml/min.

The NO portion of the analyzer was calibrated by dynamic flow dilution of the cylinder gas. This was accomplished by metering the NO from the cylinder through a calibrated mass flowmeter and then into the dilution system of the ozone generator. To calibrate the NO_2 portion of the analyzer, a constant NO concentration of approximately 940 $\mu g/m^3$ (0.5 ppm) was produced by dilution. Ozone was added in increments from the generator.

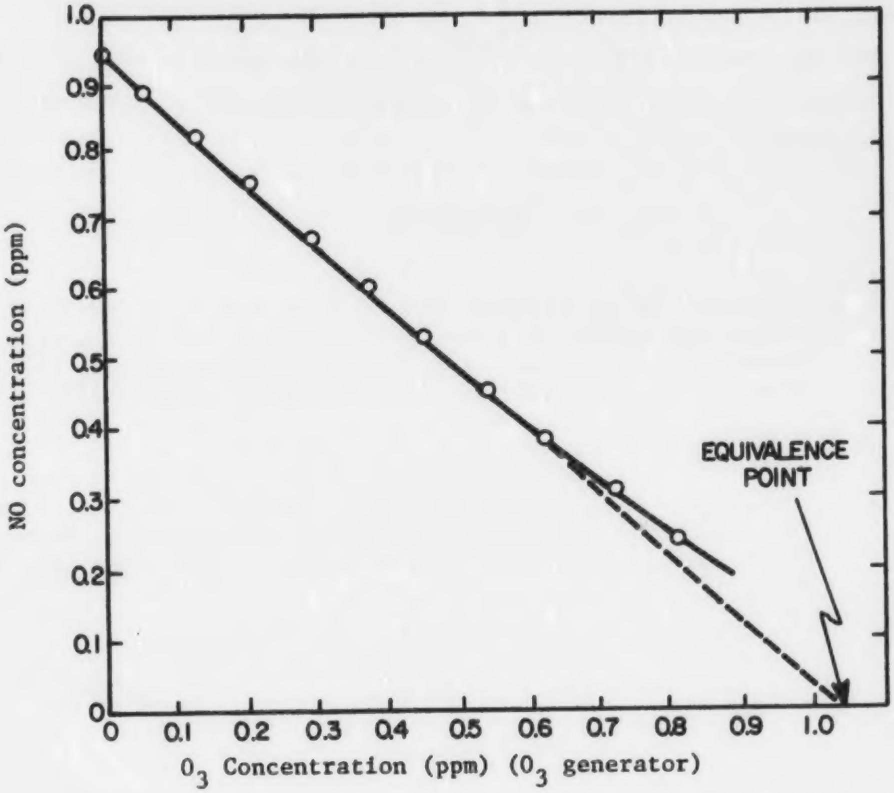

Figure A-4. Gas phase titration of NO with O_3.

Decrements observed on the spanned NO detector are then equivalent to the NO_2 concentration produced by the O_3 source. Since the NO_2 produced was equivalent to O_3 consumed, the calibrated O_3 source served as a calibrated NO_2 source when NO was present in excess. After adequate time (~10 min) for stabilization at each point, the mV output of each channel was recorded.

The NO_2 concentration was deduced from the decrease of the NO signal, and a calibration curve relating NO_2 concentration and analyzer mV output was constructed.

REFERENCES

A-1. J. A. Hodgeson, R. K. Stevens, and B. E. Martin, "A Stable Ozone Source Applicable as a Secondary Standard for Calibration of Atmospheric Monitors," Air Quality Instrumentation, Vol. 1, John Scales, ed., 149-150, ISA, Pittsburgh, Pa., 1972.

A-2. 40 CFR 50, Appendix D.

A-3. J. A. Hodgeson, R. E. Baumgardner, B. E. Martin, and K. A. Rehme, "Stoichiometry and Neutral Iodometric Procedure for Ozone by Gas-Phase Titration with Nitric Oxide," Anal. Chem. 43. 1123-1126, 1971.

APPENDIX B

PERFORMANCE CHARACTERISTICS AND OPERATIONAL SUMMARIES FOR INSTRUMENTS

APPENDIX B

PERFORMANCE CHARACTERISTICS AND OPERATIONAL SUMMARIES FOR INSTRUMENTS

B-1. Instrument Performance Characteristics.

Minimum detectable concentrations, ranges, and precisions for the air quality monitoring instruments used in this study are summarized in table B-1.

B-2. Operational Summaries for Instruments by Station.

Operational data are summarized for each analyzer by station during this study in table B-2. For this program, operational time is divided into the following categories:

(1) Percent operational time, and

(2) Percent downtime.

Percent operational time includes all categories or operational status other than downtime, which includes routine maintenance, awaiting repair, or repair. The data presented in table B-2 include percent operational time--which is synonymous with percent valid data--percent downtime, and number and nature of failures. Urban station ozone data provided to EPA by state/local agencies did not always include reasons for or the nature of instrument failures. Therefore, the data summary in table B-2 may not reflect anything other than percent valid data reported for each station.

Table B-1. Instrument performance characteristics

Instrument	Parameter	Minimum detectable concentration		Range		Precision (% of indicated concentration)
		$\mu g/m^3$	ppm	$\mu g/m^3$	ppm	
Bendix Model 8002 Chemiluminescent Ozone Analyzer	O_3	4.0	0.002	0-392	0-0.2	± 2%
Bendix Model 8101-B Chemiluminescent $NO-NO_x-NO_2$ Analyzer	NO, NO_x, NO_2	9.4	0.005	0-940	0-0.5	± 2%
Perkin-Elmer Model 900 Gas Chromatograph	Selected Hydrocarbons	sub-ppb		ppb-ppm		± 1%

Table B-2. Operational summary for instruments by station

Station	Instrument	Operational period (days)	Operational time (%)	Downtime (%)	Failures	Nature of failure
Bradford, Pennsylvania*	Bendix O_3	96	100.0	0.0	0	--
	Bendix NO_x	96	98.0	2.0	1	c
Lewisburg, West Virginia*	Bendix O_3	128	92.5	7.5	4	a, b, b, c
Creston, Iowa*	Bendix O_3	92	95.8	4.2	2	a, d
	Bendix NO_x	92	97.9	2.1	2	a, e
Wolf Point, Montana*	Bendix O_3	90	100.0	0.0	0	--
	Bendix NO_x	90	98.8	1.2	1	c
DeRidder, Louisiana*	Bendix O_3	123	100.0	0.0	0	--
	Bendix NO_x	123	97.8	2.2	1	b
Pittsburgh, Pennsylvania**	Bendix O_3	121	97.8	2.2	f	f
Columbus, Ohio**	Bendix O_3	121	99.3	0.7	f	f
Poynette, Wisconsin**	Rem O_3	122	90.9	9.1	f	f
DesMoines, Iowa**	Bendix O_3	107	98.4	1.6	f	f
Cedar Rapids, Iowa**	Bendix O_3	121	95.8	4.2	f	f
Omaha, Nebraska**	Rem O_3	93	80.0	20.0	f	f
Nederland, Texas**	McMillian O_3	121	93.5	6.5	f	f
Austin, Texas**	McMillian O_3	121	86.2	13.8	f	f
Houston, Texas**	McMillian O_3	121	72.5	27.5	f	f
Port O'Connor, Texas**	McMillian O_3	130	93.3	6.7	f	f

*Rural stations
**Urban stations
a - power failure
b - flow system problem
c - electronic circuitry problem
d - detector cell failure
e - excessive zero/span drift
f - not stated by state/local agency

APPENDIX C

AIRBORNE PLATFORM AIR SAMPLING SYSTEM DESIGN

APPENDIX C

AIRBORNE PLATFORM AIR SAMPLING SYSTEM DESIGN

C-1 System Description

The aircraft air-sampling system was designed to collect atmospheric samples with a minimum of sample disturbance and then to provide a known environment in which these samples could be measured. The system was designed for sampling in steady, level flight in a light aircraft. In addition to the air-sampling function, the system was to provide accurate meteorological data. In particular, measurements of atmospheric pressure and temperature, indicated and true air speed, and Mach number were of interest. The principal objectives in designing the sampling apparatus were gas analyzer measurements and accurate meteorological data. A secondary objective was to develop a system that would also be adequate for particulate sampling.

A schematic of the overall system is shown in figure C-1. The sampling probe was straight, except for a slight, large radius bend approximately midway along its length, which was necessary to avoid the aircraft radar unit located in the forward nose section. This bend should not have an influence on particle sampling. The outboard section of the probe extended approximately 0.3 m beyond the nose. Further extension was limited due to the possibility of interference with the radar system. At this forward location there was minimal aerodynamic disturbance and little likelihood of aircraft contamination in the air.

The probe was joined to a transition diffuser and stagnation manifold on board the aircraft. This unit decelerated the incoming air to stagnation conditions to provide an almost quiescent environment in which to take sample measurements. An exhaust damper was provided to adjust the exchange rate of the air inside the system and to maintain a positive pressure relative to the aircraft cabin to eliminate the possibility of contaminants entering from the cabin through the manifold exhaust. Measurements of pressure, temperature, and dew point, along with gas analyzer samples, particle analyzer samples, and hot wire anemometer readings, were then taken from the manifold.

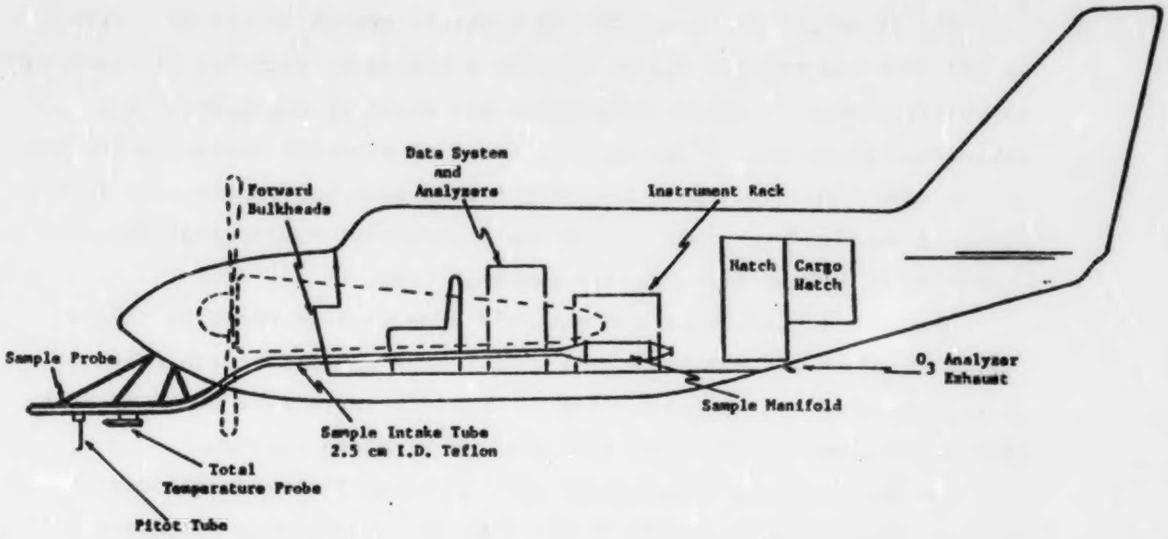
Data System and Analyzers
Forward Bulkheads
Instrument Rack
Hatch
Cargo Hatch
Sample Probe
O_3 Analyzer Exhaust
Sample Manifold
Sample Intake Tube 2.5 cm I.D. Teflon
Total Temperature Probe
Pitot Tube

Figure C-1. Functional layout of airborne sampling system.

The outboard total temperature and pitot-static probes were intended to provide data on the ambient static pressure (altitude), the stagnation pressure excess (velocity or Mach number), and the total temperature (ambient) static temperature). Quantities in parentheses were determined by calibration or calculation from the actual measurements. Air lines and electrical leads from the outboard instruments were brought into the cabin, where appropriate transducers were used to provide the dc signals necessary for the onboard recorder system. The probes were mounted on the aircraft so as to minimize aircraft aerodynamic error.

An atmospheric particulate sampler, which utilized aerodynamic pressure to cause air flow at approximately 35 cfm (1 m^3/min) through a standard high volume glass filter, was designed and installed midway through this program. The system required no power and was mounted externally.

The various elements of the system illustrated above are described in detail in the following sections with appropriate specifications and design methodology. Sections are also included on calibration and data reduction.

C-2 Sampling Probe and Onboard Stagnation Manifold

The objective of the probe and manifold system described briefly in the previous section was to provide a straight, ram-type air-sampling capability, which samples undisturbed air ahead of the plane. The system had particular advantages in avoiding aircraft contamination and, at the same time, providing a straight flow path for particulate detection. A manifold was used to provide a quiescent environment for measurements with an adjustable air exchange rate.

A sketch of the probe and manifold apparatus is shown in figure C-2. The probe was essentially a Teflon tube mounted inside a steel structural tube. Teflon was used to preclude extraneous chemical reaction effects and to minimize side wall particulate capture.

The manifold was constructed with an inlet diverging diffuser section to allow a deceleration of the flow to a manageable velocity. Design conditions were chosen to be 25° C and a nominal air speed of 90 m/sec (200 mph). At this speed, the ambient-to-stagnation temperature ratio is

$$\frac{T}{T_o} = 0.9886$$

and the Mach number is 0.24. Therefore, the velocity of the air inside the manifold is

$$V_m = \sqrt{kRg_c T/0.9886} \cdot M_m \tag{1}$$

where M_m is the manifold Mach number. The result is

$$V_m = 1144\ M_m \tag{2}$$

The final sizing of the manifold was accomplished by assuming the flow through the apparatus is isentropic and recognizing the equality of the flow rate in the inlet and manifold. Thus, $\dot{W}_{in} = \dot{W}_m$ and

$$A_i f_w(M) = f_w(M_m) \cdot A_m \tag{3}$$

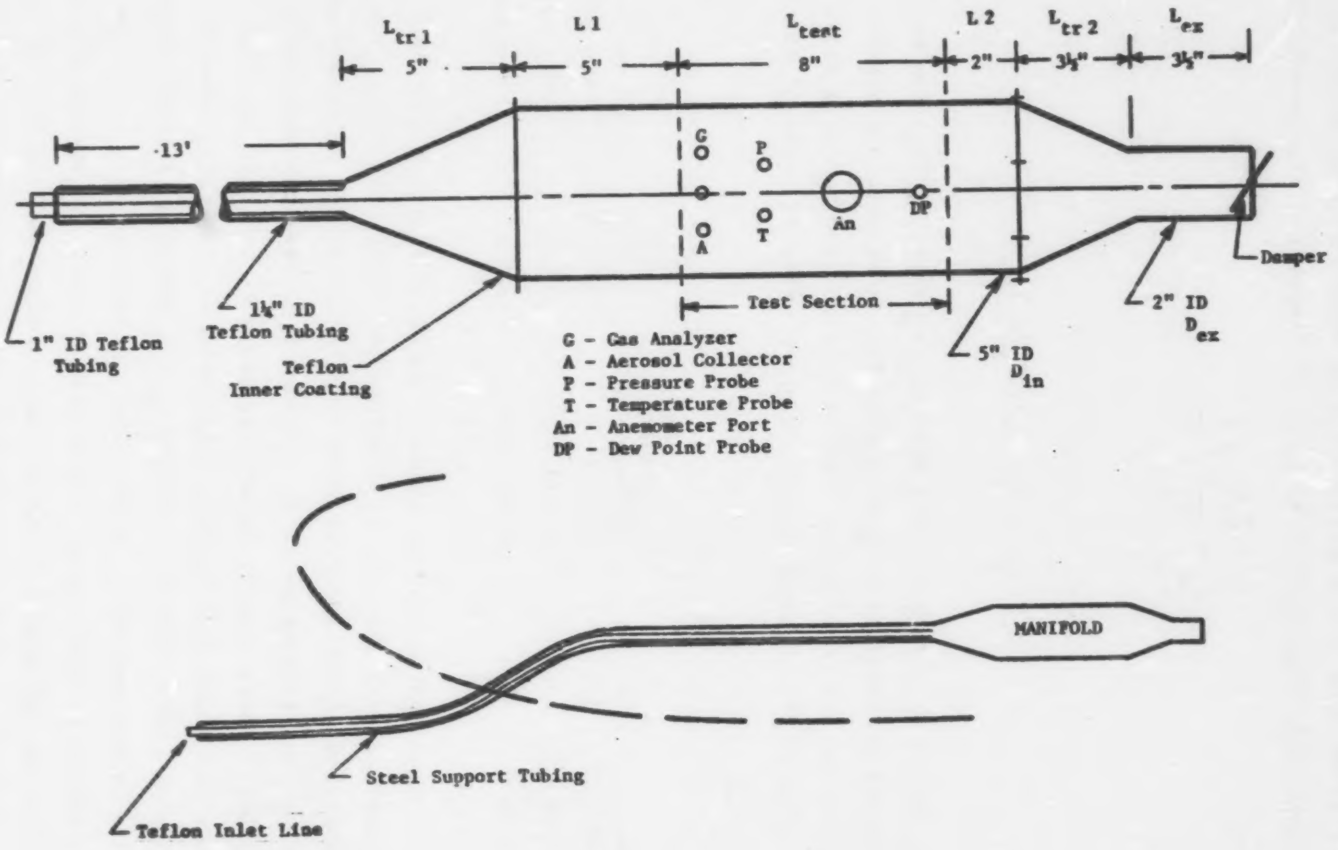

$L_{tr\,1}$
L 1
L_{test}
L 2
$L_{tr\,2}$
L_{ex}
5"
5"
8"
2"
3½"
3½"
13'
G
P
An
DP
A
T
1" ID Teflon Tubing
1¼" ID Teflon Tubing
Teflon Inner Coating
Test Section
5" ID D_{in}
2" ID D_{ex}
Damper
G - Gas Analyzer
A - Aerosol Collector
P - Pressure Probe
T - Temperature Probe
An - Anemometer Port
DP - Dew Point Probe
MANIFOLD
Steel Support Tubing
Teflon Inlet Line

Figure C-2. Sketch of onboard manifold and sampling tube.

where the isentropic flow function, f_w, is dependent only on the Mach number, and, when defined in terms of stagnation properties, it is

$$f_w = \frac{\dot{W}\sqrt{T_o}}{AP_o}\sqrt{\frac{R}{g_c}} \tag{4}$$

Thus,

$$f_w\ (M_m) = f_w\ (M_\infty)/(A_m/A_i) \tag{5}$$

where f_w (0.24) = 0.27438. For a given A_m/A_i ratio, $f_w(M_m)$ can be calculated and the corresponding M_m read from the isentropic air tables. The air velocity in the manifold is then calculated from M_m using equation 2. A table of some of the calculations is shown below in terms of manifold diameter, D_m.

D_m	A_m/A_i	$f_w(M_m)$	M_m	V_m
102 cm	16/1	$1.715(10)^{-2}$	0.0145	5.0 m/sec
12.7 cm	25/1	$1.098(10)^{-2}$	0.009	3.1 m/sec
15.2 cm	36/1	$0.763(10)^{-2}$	0.007	2.4 m/sec

It is seen that a 12.7-cm diameter manifold provides a nominal 3 m/sec manifold velocity for an unobstructed isentropic flow. The actual system would be expected to behave in a slightly different manner, as there are inefficiencies in the diffusion process and pressure losses in the probe. These losses, in effect, serve to obstruct the inlet flow and reduce the inlet Mach number, which reduces the actual velocity with the manifold. Back pressure, imposed on the manifold from the cabin, would also reduce the manifold velocity. A manifold with a 12.7-cm inside diameter should provide enough theoretical velocity to accommodate a loss due to friction and also provide a range of adjustability with an exhaust damper. That is, a 12.7-cm manifold should provide from 1.5 to 3 m/sec, which can then be adjusted with a damper to provide a velocity down to zero if desired. Any velocity down to 0.3 to 0.6 m/sec would probably provide a sufficiently short residence time, although 1.5 m/sec is recommended to insure no exhaust contamination.

Several instruments were located in the manifold for data collection. A gas analyzer probe was located nearest the entrance, but yet at a distance sufficiently far from the entrance diffuser to allow flow development. The gas analyzer probe was essentially a 1/4-in. diameter suction tube which was aligned to receive the incoming air. A hot-wire anemometer was centrally located to provide a visual indication of the manifold velocity, an adjustment of which was then obtained by adjusting the exit damper. The air velocity in the manifold could be maintained constant at varying altitudes and air speeds in this manner. A static pressure tap, temperature thermistor, and dew point sensor were also centrally located in the manifold to provide continuous recordings of manifold pressure and temperature data. Dew point measurements were taken to provide data from which ambient dew point could be determined. The primary use of the manifold pressure and temperature data was for correcting the volumetric gas analyzer's data to equivalent ambient conditions. The location of the sensors and sampling probes on the manifold is shown in figure C-2.

C-3 Outboard Pitot-Static Probe

The purpose of the outboard pitot-static probe was to provide continuous measurements of the ambient static pressure in the atmosphere, altitude, indicated air speed, and Mach number. These standard aircraft measurements have meteorological as well as air sampling applications, and therefore it was important that they be taken and recorded as accurately as possible. The pitot-static probe was used to accomplish these measurements, becoming an integral part of the air sampling system and thus avoiding the alternative of relying on typically less accurate light aircraft flight instrumentation.

The location of the pitot-static probe was an extremely important consideration. If improperly located, the indication of the static pressure would be erroneous because of the aerodynamic distortions by the aircraft. A typical pressure distribution is illustrated in figure C-3. The two locations which are usually recommended for a pitot-static probe are mountings on a nose boom and a wing tip boom. The latter was inconvenient by the difficulty in running air lines through the wing sections. A nose location was complicated by the difficulty in gettin gsufficiently far out from the nose without interfering with the nose radar. An estimate of the distance out from the nose necessary to obtain an undisturbed measurement was made by treating the forward air flow as an imcompressible flow around a half-body nose geometry. Two half-body profiles are shown in figure C-4, each with a different source location. The outer profile corresponds to a source location at $\bar{R}_o$ from the stagnation point and the inner profile corresponds to a source location at $\bar{R}_i$. It can be seen that the outer profile best fits the actual aircraft profile downstream whereas the inner profile best fits the aircraft profile near the nose. Both, however, are blunter near the nose than the actual skin profile. Thus, estimates based on these profiles near the nose are probably overestimates. The equation for the pressure field around the half-body profiles is

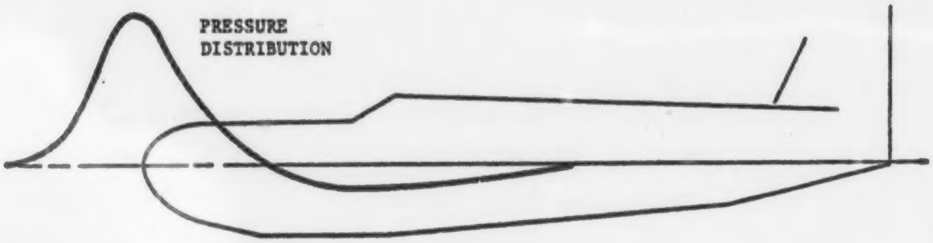

Figure C-3. Pressure distribution around aircraft.

$$\frac{P(r,\Theta)-P}{\frac{\rho V^2}{2g_c}} = \left(\frac{\bar{R}}{r}\right)^3 \left[2-\left(\frac{\bar{R}}{r}\right)\right] \qquad (6)$$

where P is the true static pressure and $P(r,\Theta)$ is the actual pressure in the vicinity of the aircraft. With the pitot-static tube location as shown

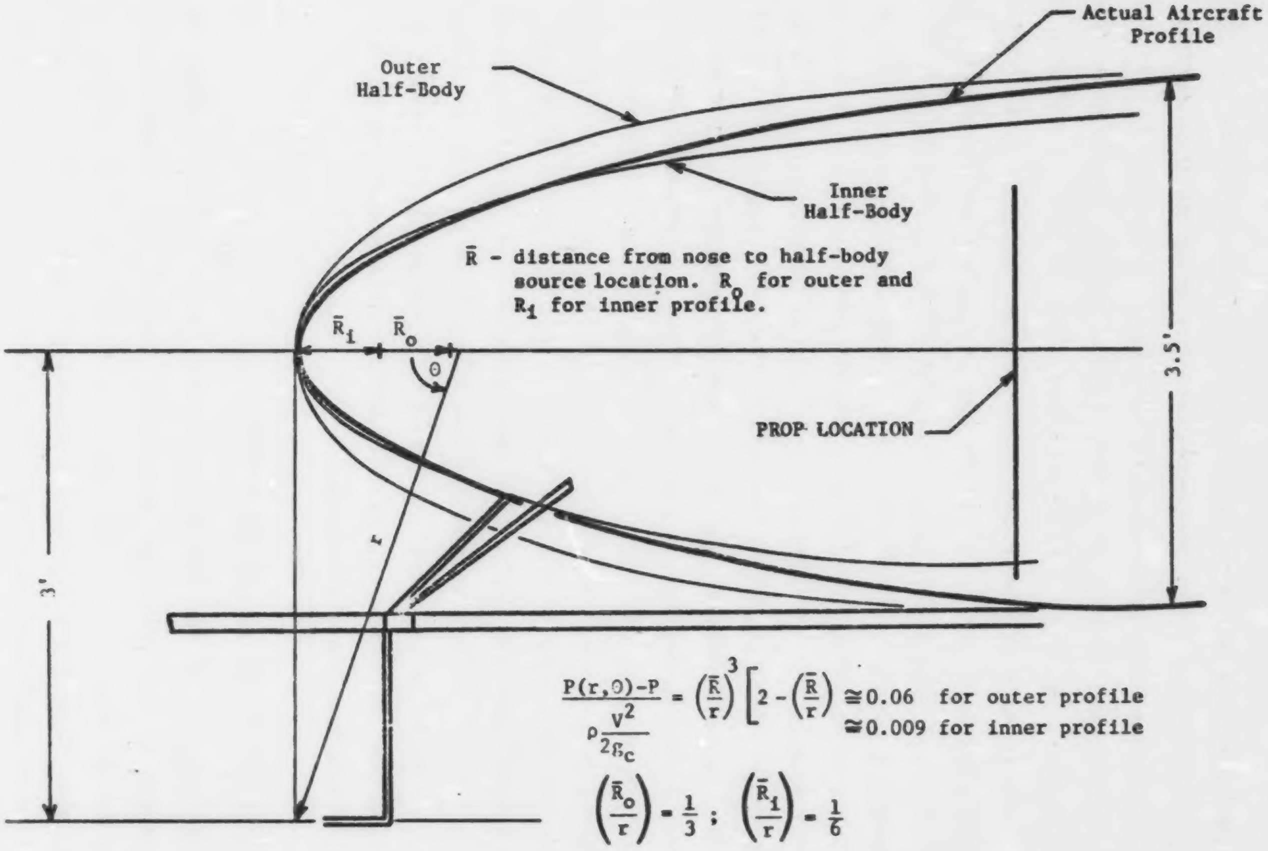
Actual Aircraft Profile
Outer Half-Body
Inner Half-Body
$\bar{R}$ - distance from nose to half-body source location. R_o for outer and R_1 for inner profile.
$\bar{R}_1$
$\bar{R}_o$
Θ
r
PROP LOCATION
3.5'
3'

$$\frac{P(r,\Theta)-P}{\rho\frac{V^2}{2g_c}} = \left(\frac{\bar{R}}{r}\right)^3\left[2-\left(\frac{\bar{R}}{r}\right)\right. \begin{array}{l}\cong 0.06 \text{ for outer profile}\\ \cong 0.009 \text{ for inner profile}\end{array}$$

$$\left(\frac{\bar{R}_o}{r}\right) = \frac{1}{3}\,;\ \left(\frac{\bar{R}_1}{r}\right) = \frac{1}{6}$$

Figure C-4. Estimate of aerodynamic pitot-static error.

in figure C-4, the outer profile estimate indicates an excess pressure of 6 percent of the total pressure, and the inner profile estimate indicates an excess pressure of 0.9 percent. The inner profile is probably a closer estimate at this location, with a nominal systematic error of 1 to 2 percent probably a good estimate. An error of 1 percent indicated on the static side of the pitot-static probe will indicate the true static pressure plus 0.01 (P_o - P), where the latter factor is approximately 0.5 psi at 200 mph. Thus, the overprediction is 0.005 psi which corresponds to about 3 m of altitude at sea level. Thus, the location of the pitot-static probe as shown should indicate altitude to within 3 to 6 m.

Any standard pitot-static tube designed to operate in the Mach number range of 0 to 0.25 is satisfactory. An inexpensive one which has been used successfully is the model manufactured by Airflow/Davis Instrument Company, Baltimore, Maryland. This instrument has a 30.5 cm length, a 4 mm tube diameter and an ellipsoidal nose geometry.

The pitot-static probe itself was located on the air-sampling tube beyond the nose of the aircraft. Metal air lines were then brought back into the cabin from the "static" and "total" connections on the probe and attached along the length of the air sampling tube. A schematic is shown in figure C-5, which illustrates the recommended manner of instrumenting the pitot-static probe, along with some of the electrical specifications.

C-4 Outboard Total Temperature Probe

The purpose of the total temperature probe was to achieve an accurate measurement of the adiabatic stagnation temperature of the air relative to the moving aircraft. With this measurement and a determination of the Mach number from the pitot-static probe, the actual static or "ambient" temperature could be determined. Manufactured total temperature probes are normally designed for high subsonic civilian applications as well as supersonic military applications. These commercial probes, such as that manufactured by the Rosemount Company, are somewhat overdesigned for the

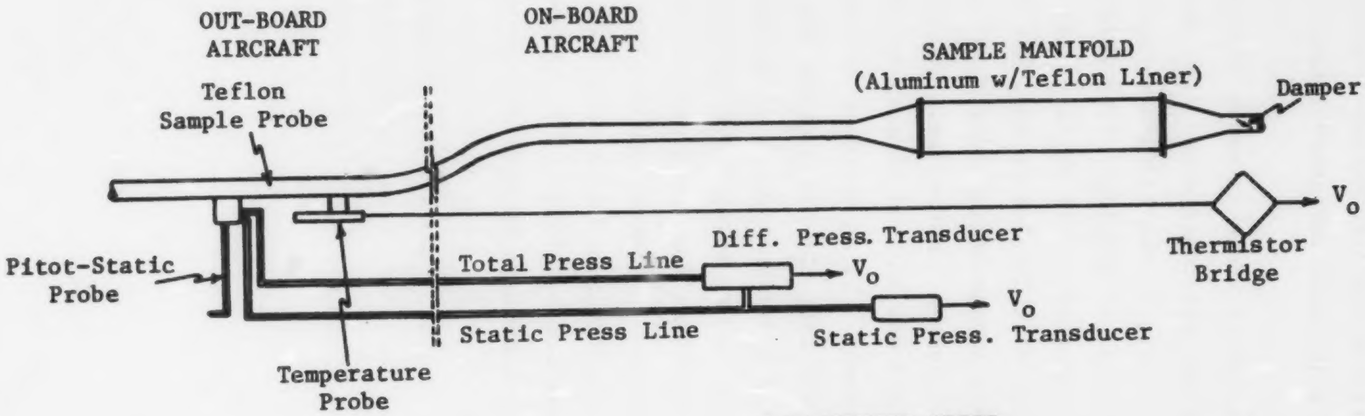
OUT-BOARD AIRCRAFT
ON-BOARD AIRCRAFT
SAMPLE MANIFOLD (Aluminum w/Teflon Liner)
Damper
Teflon Sample Probe
V_o
Diff. Press. Transducer
Thermistor Bridge
Pitot-Static Probe
Total Press Line
V_o
V_o
Static Press Line
Static Press. Transducer
Temperature Probe

TRANSDUCER SPECS:

Absolute (Sensotec, Model TJE)
0-15 psia, 0.1% FS Accuracy

Differential (Sensotec, Model Z)
±2 psid, 0.25% FS Accuracy

TEMPERATURE SENSOR:

Thermistor (Y.S.I. Part No. 44018)
-30 to +100° C, ±0.15°C

Figure C-5. Block diagram, sampling system, pressure and temperature measurement system.

low subsonic application here and excessively priced for the need. Therefore, a probe was designed to provide the information required and was specifically intended for low subsonic and steady-state, level-flight measurements.

A drawing of the total temperature probe is shown in figure C-6. It was designed as a small diffuser and was constructed from nylon material, which has a low thermal conductivity. It was taped externally with a silver reflecting tape to minimize solar heating. With this construction, it is not thought that the air compression will deviate significantly from an adiabatic process. Small holes were drilled in the rear of the diffuser to allow internal air movement and a ventilation sufficient to minimize extraneous heating effects on the sensed temperature. The probe was not designed for rapid measurements and was allowed to come to temperature equilibrium prior to each measurement. Using standard heat transfer computational methods, it was found that the above probe should require approximately 1.5 minutes to allow a dissipation of 95 percent of the heat energy contained in the nylon and to bring it to equilibrium with the new conditions. This time allowance for the probe adjustment should preclude any possibility of error due to thermal inertial delay.

The sizing of the probe was accomplished in a manner similar to that used in the sizing of the air-sampling manifold. The inlet area was somewhat arbitrary and was chosen small to eliminate excessive angle of attach sensitivity but sufficiently large to allow adequate internal ventilation. A diffuser area ratio of 25 to 30 to 1 was adequate to stagnate the incoming air, and an outlet area of 1/3 of the inlet area allowed adequate ventilation around the thermistor head. Three small holes were provided at the rear for this purpose.

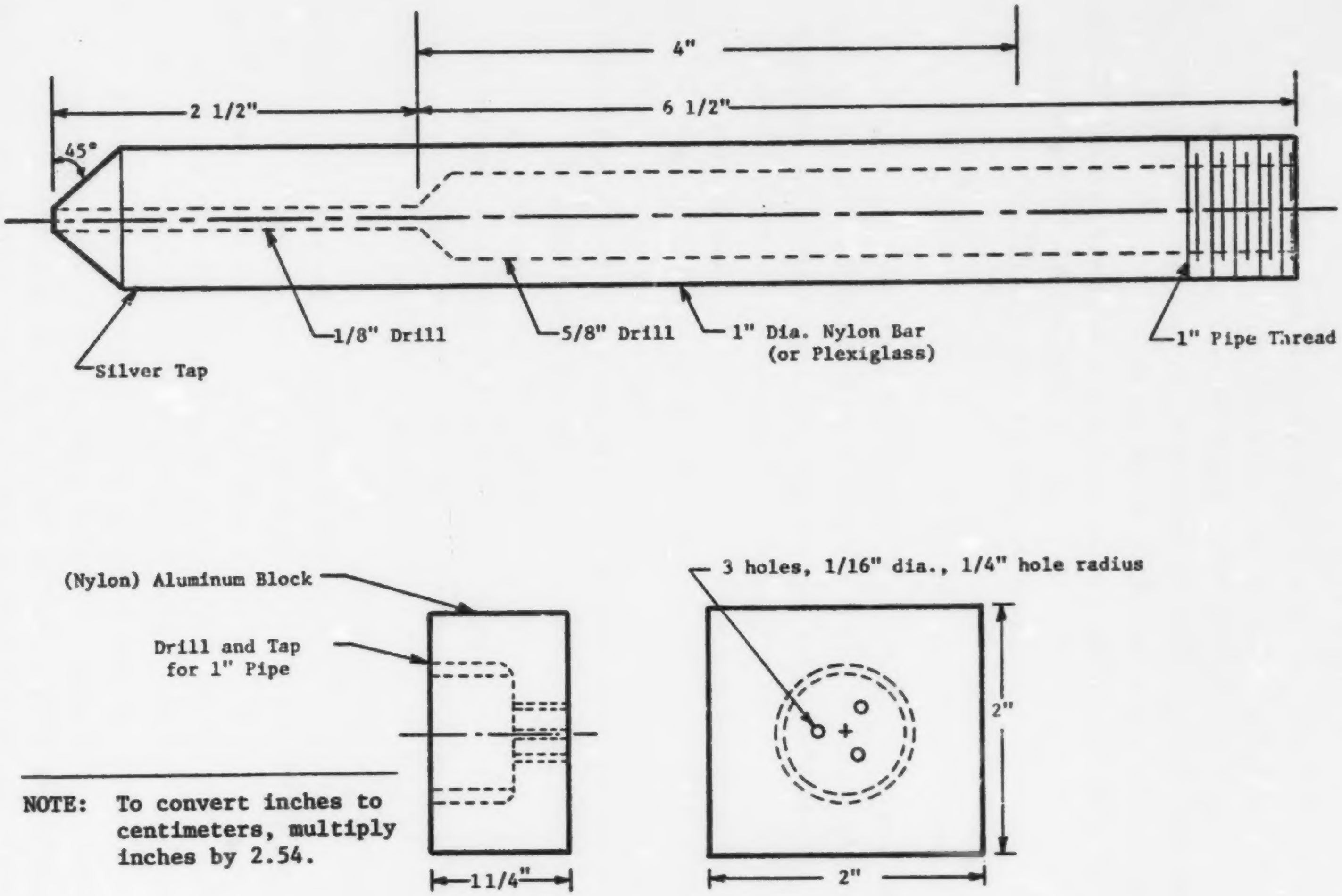
4"
2 1/2"
6 1/2"
45°
Silver Tap
1/8" Drill
5/8" Drill
1" Dia. Nylon Bar
(or Plexiglass)
1" Pipe Thread
(Nylon) Aluminum Block
Drill and Tap
for 1" Pipe
11/4"
3 holes, 1/16" dia., 1/4" hole radius
2"
2"

NOTE: To convert inches to centimeters, multiply inches by 2.54.

Figure C-6. Schematic of total temperature probe.

The specifications for the probe are shown on the drawing, some of which were modified for convenience in mounting, etc. The location of the probe on the aircraft was not important as long as it was not near the engines and located outside of the skin boundary layer. The location near the forward end of the sampling tube was ideal.

The probe was designed to be used with a thermistor sensor, an instrument which has a relatively slow response time and was therefore very compatible with the probe itself in terms of responsiveness.

C-5 Airborne High-Volume Sampler

An atmospheric particulate sampler which utilizes the High Volume Air Sampler Method was designed and used in an airborne application in conjunction with the air sampling system described previously. The sampler was used primarily in the collection of airborne sulfates and nitrates and utilizes the standard glass-fiber filter. The unit was mounted on the forward side of the aircraft nose section, placing it well in front of engine and prop contamination with a remotely operated flow control apparatus.

Several important considerations played a role in the design configuration for the sampler. A summary of these are given below.

First, in air sampling, the air must be slowed relative to the aircraft in such a way as to minimize the disturbance of the actual particulate concentration and distribution in the air. That is, the sample that passes through the high volume filter must be as representative of the condition of the quiescent air as possible.

It was necessary to make use of aerodynamic pressures to provide the flow through the filter rather than using powered devices to create the sample flow due to the large power requirements of a large air pump. In order to achieve the maximum flow through the filter possible by aerodynamic pressure, the diffuser action within the sampler which decelerates the air must be as efficient as possible in order to avoid pressure losses. Also, the nozzle action around the exterior and rearward sides of the unit should be preserved in order to provide the maximum rearward suction.

The volume rate of sampling must be measured continuously and a remote control apparatus designed to control the flow rate, including a shut-off during take-off, landing, etc. The quantity of flow through the filter must be sufficiently great to allow efficient filtration and at the same time sufficiently rapid to allow a large enough volume to be sampled in the available flight time.

The flow rate versus pressure drop characteristics for the clean glass-fiber filter material was estimated by assuming the pressure drop across the standard high volume filter calibration orifice and eighteen-hole plate assembly was approximately that which would occur across the clean filter material itself. This is the basis of the flow meter calibrations which are used with the standard units. The CFM per unit of filter area was then plotted versus pressure drop for the standard orifice. Using orifice formulae, a similar curve was plotted for the eighteen-hole plate. For any flow rate, then, the total pressure drop is the sum of that which occurs across the orifice and that which occurs across the plate. This sum should be approximately equal to the pressure drop across a clean filter with the same CFM per unit of its area. This plot is shown in Figure C-7 along with the CFM for the standard filter. It can be seen that a pressure drop of approximately 28 in. (71 cm) of water is required to produce the nominal 60 CFM through the standard filter in a clean state.

The aircraft motion will produce an aerodynamic pressure drop which can be used to drive the flow through the filter. This pressure drop will be approximately constant at constant air speed and should not vary appreciably with changing conditions within the filter. Thus, a prediction of this pressure drop should yield, using the previous flow rate curve, an estimate of the flow rate per unit of clean filter area. This predicted flow rate for the clean condition, then, is used to decide the sufficiency of the flow generated in this manner. It is assumed at the outset that heavy accumulation on the filter will not occur above ground level and that, basically, trace quantities are sought. Thus, a clean filter calculation should provide a good criteria.

At an air speed of 200 mph and an altitude of 1,000 feet (205 m), the total ram pressure is approximately 19 in. (48 cm) of water. Approximately 2.5 cm of this will probably be lost at the entrance and about 1.25 cm left as dynamic pressure at the filter. Thus, the raw pressure which

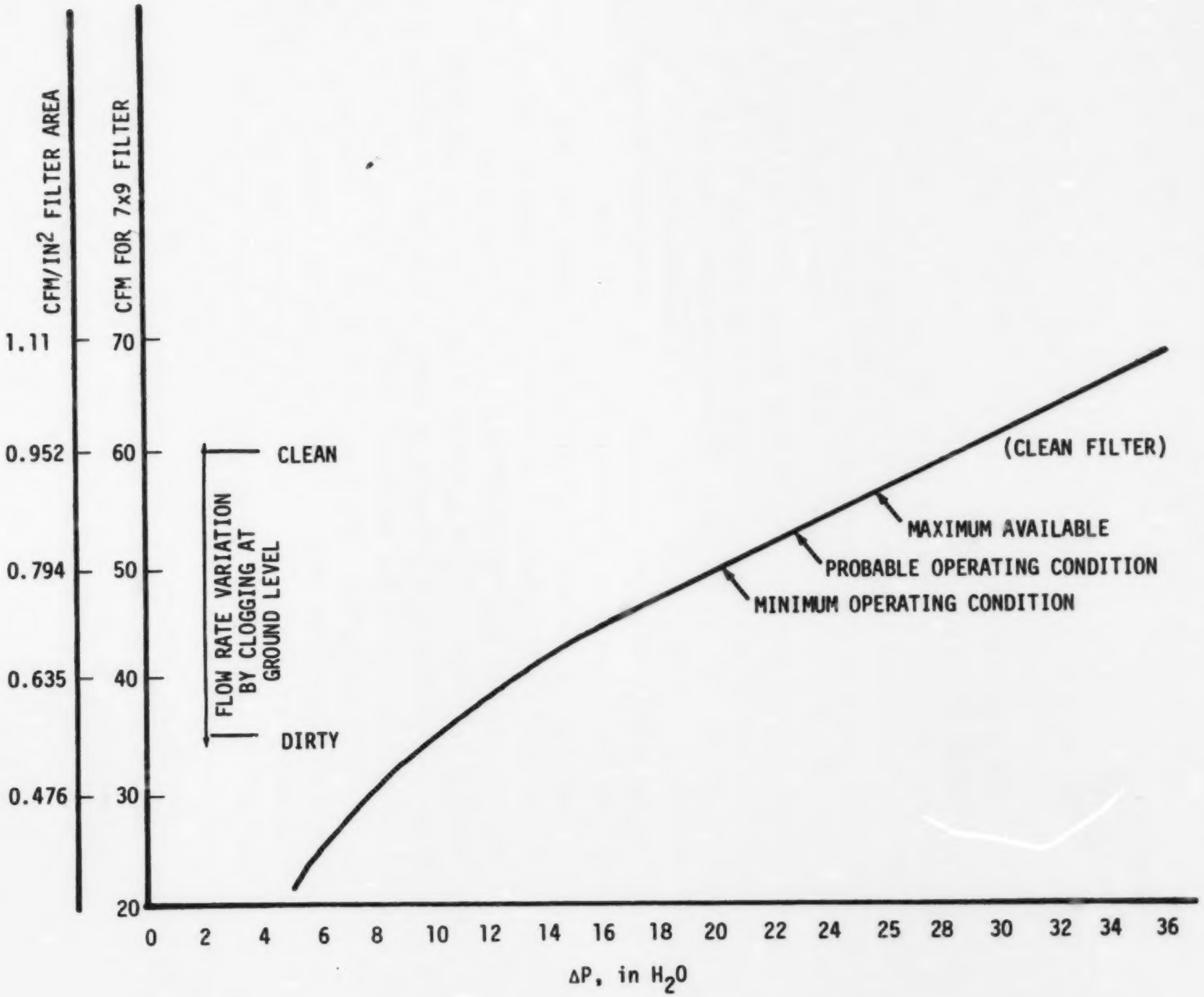

Figure C-7. Expected filter pressure drop.

might be available at the filter is approximately 17.5 in. (44.5 cm) of water. Estimating a suction pressure of 40% of the freestream dynamic pressure [i.e., approximately 7.5 in. (19 cm) of water] produces a total pressure drop available to the filter of approximately 25 in. (63.5 cm) of water. From the filter calibration curve, this corresponds to approximately 0.9 CFM/in^2 or 58 CM for the standard filter. Even though this pressure drop will be approximately constant for constant flight conditions, the flow rate will decrease some as the filter becomes clogged. These figures are all shown on the filter calibration curve. It is readily seen that the operating characteristics of the entire unit will be greatly dependent upon the aerodynamics of the design. That is, entrance losses should be minimized, internal diffuser losses must be minimized and, just as important, the external aerodynamics must not be interfered with in order to preserve the rearward suction pressure. An estimated operating range of flow rate is shown on the figure to account for uncertainties in design. The unit should operate around 30-35 CFM for a 7-in. (17.8 cm) diameter filter.

The diverging diffuser arrangement was used because it offers least disturbance to the air in deceleration. That is, the air stream does not impinge on any surface other than the filter itself and therefore suffers no turning difficulties with the associated particulate losses. The forward opening is just sufficient to admit that amount of air which can pass through the filter at the operating pressure drop. In order to make use of the full deceleration in the diverging section and avoid unnecessary pressure loss, assurance had to be made that flow separation did not occur. This was avoided by specifying a 5° cone angle, a criteria within the separation angle. The sizing of the inlet area was accomplished using standard gas dynamic calculations and tables of the properties of air. The specifications which resulted are shown on figure C-8. Note that suction at the rear of the sampler is accomplishbd by allowing the external flow to accelerate uninterrupted around the sampler.

An additional advantage which the above design offered was the relatively easy means by which the volume flow rate could be measured. A loss coefficient of 0.95 for this diverging apparatus is a relatively well accepted figure. Thus, the flow rate can be calculated from Bermoulli's equation if the pressure rise from the inlet to the filter is monitored.

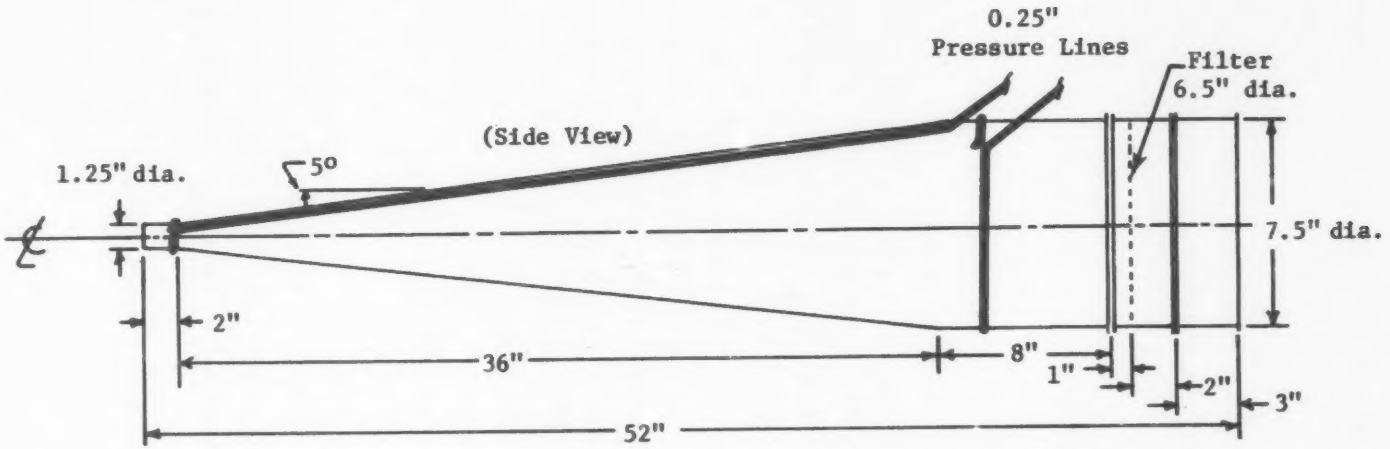
0.25"
Pressure Lines
Filter
6.5" dia.
(Side View)
5°
1.25" dia.
7.5" dia.
2"
36"
8"
1"
2"
3"
52"

NOTE: To convert inches to centimeters, multiply inches by 2.54.

Figure C-8. High volume sampler.

Thus, pressure taps were located at the inlet and just upstream from the filter. Three taps were equally spaced around the periphery at each of these two locations to provide the peripherally averaged static pressure. At the design flow rate of approximately 0.75 CFM/in^2 of filter area, the pressure rise should be approximately 1.9 cm of water.

C-6 Calibration of System and Components

The most important developmental aspect of the entire system is the calibration of both components and the assembled system under flight conditions. Each of these is discussed below.

This measurement relies on two devices: the static side of the pitot-static probe and a strain gage absolute pressure transducer. Each must be checked for accuracy. A pressure transducer can be calibrated with a dead weight tester, a water column, or other device. Even with the transducer working properly, there is no assurance that the pitot-static probe is aligned properly, etc. Thus, after the transducer itself is calibrated, the probe was checked in flight to make sure that a correct pressure was being recorded. This was done by flying down the runway a known height above the ground and checking the static pressure reading (altitude). A 0 - 15 psia transducer which is accurate to ±0.1% of F.S. should be able to resolve at least ± 9.1 meters of elevation.

The differential pressure transducer, with a range of ±2 psid and an accuracy of ±0.25% F.S., can be easily calibrated by manometer as a check on the manufacturer's calibration. An inflight calibration, however, is somewhat more complicated. Several timed, low level flights over a straight measured distance were conducted. A day was chosen with little or no air movement. The ground speed was then measured and used as the indicated air speed. If the velocity is low, it can be used directly in calculating the total pressure from

$$P_o = P + C_p \rho \frac{V^2}{2g_c} \tag{7}$$

where P is assumed at the test altitude, ρ is the density of the ambient air at that altitude, and V is the velocity. Several runs were made at varying speeds from as low as possible up to nominal cruise speed. A plot of $(P_o - P)/\rho\frac{V^2}{2g_c}$ versus V was developed and C_p determined as a calibration tion coefficient of pitot-static output versus indicated air speed. This indicated air speed will coincide with the true air speed as long as the above plot is flat with V. A V dependence indicates compressibility effects are present and should occur in the neighborhood of 150 mph, raising the desirability of a determination of "true" air speed in the range of 150 mph to 200 mph.

The type of pitot-static probe used actually minimizes the need for calibration since it has the modern ellipsoidal nose, with a C_p normally accepted to be within 1% of unity. The error is primarily introduced by misalignment, a characteristic which the ellipsoidal nose pitot-static probe is relatively insensitive to. The particular probe used here was checked and found to be stable with angles greater than $\pm 30^\circ$; thus this is not thought to be a problem. Therefore, in the above calibrations, runs in opposite directions were made to nullify wind effects and the data plotted and compared to unity. If a spread exists about unity, then this value should be accepted as the correct value for C_p. This type of calibration experiment primarily serves to corroborate and add credibility to a unit C_p but is not sufficiently controlled to provide data to alter C_p, even if the data indicates some alteration. Thus, in the following sections, C_p is taken as the commonly accepted 1.0 ± 1%.

The total temperature, measured with the total temperature probe, was calibrated in the same series of runs as those used for the total pressure calibration. Prior to the runs, a static temperature calibration was made by inserting the temperature probe into a water bath and checking against a calibrated thermometer.

C-7 Data Reduction Formulas

The following formulations can be used in reducing the transducer and thermistor outputs from the air sampling system:

Altitude - The 0.1% F.S., 0 - 15 psia pressure transducer should provide a ± 9.1 meters resolution of altitude at sea level and should remain

SYMBOLS

A - Flow area, ft^2,

A_{lt} - Altitude, ft,

A_1 - Sampling tube flow area, ft^2,

A_m - Manifold flow area, ft^2,

C - Ambient concentration in mass/vol.,

C_m - Manifold concentration in mass/vol.,

C_p - Total pressure calibration coefficient, approx. unity,

C_T - Total temperature calibration coefficient,

E - Ground elevation above mean sea level,

f_w - Isentropic flow function, equ. (4),

g_c - Gravitational constant, 32.2 $(lb_m\text{-}ft)/(lb_f\text{-}sec^2)$,

k - Specific heat ratio, =1.4,

K - Tabular conversion of psia to feet of altitude,

K_p - $1/\sqrt{C_p}$,

M - Mainstream Mach number, $V_{tr}/\sqrt{2g_c kRT}$,

M_m - Manifold Mach number,

P - Calibrated ambient static pressure output, psia,

(P_o-P) - Pitot-static probe output, psia,

P_o - Total pressure (= $P+(P_o-P)$, assuming $C_p = 1$),

P_m - Manifold pressure, psia,

P_{msl} - Ambient static pressure at mean sea level, psia,

$P(r,\theta)$ - Ambient static pressure field near aircraft,

R - Gas constant, 53.35 $(ft\text{-}lb_f)/(lb_m\text{-}{}^oR)$,

$\bar{R}$ - Nose radius, ft, as shown in Fig. 4,

r - Probe location, as shown in Fig. 4,

T - Ambient temperature, ^oR,

T_m - Manifold temperature, ^oR,

T_o - Stagnation temperature, ^oR,

T_{dp} - Dew point temperature, ^oF,

$T_{dp,m}$ - Manifold dew point temperature, ^oF,

V - Indicated air speed, ft/sec,

V_{tr} - True air speed, ft/sec,

V_m - Manifold velocity, ft/sec,

$\dot{W}$ - Mass flow rate, lb_m/sec

ρ - Ambient air density, 0.075 lb_m/ft^3 at msl and 70^oF, approximately this at most altitudes. The pitot-static output at mean sea level should be

$$P_{msl} = 14.696 \tag{10}$$

where P_{msl} is the output measured at mean sea level. Thus, the altitude relative to sea level is

$$(\text{Alt.})_{msl} = K \cdot \left(P_{msl} - P\right) = K(14.696 - P) \tag{11}$$

where K is a tabular conversion to feet of altitude and P is the actual static pressure output. The local ground elevation should be obtainable by taking a P reading on the ground. That is,

$$E = K\left(14.696 - P_{ground}\right) \tag{12}$$

Dew Point Correction - Because of the compression in the manifold, the indicated dew point temperature must be corrected to ambient conditions. This is done using the Clapeyron equation for the vapor pressure curve for water vapor. In the neighborhood of 70°F, this expression integrates to

$$\left(T_{dp,m} - T_{dp}\right) = T_{dp,m}^{\ \ 2} \left(1.05 \times 10^{-4}\right) \ln \left(\frac{P_m}{P}\right) \tag{13}$$

where $T_{dp,m}$ is the measured manifold dew point temperature and T_{dp} is the dew point corrected to ambient conditions. The dew point correction should not be greater than approximately 2°F.

Indicated Air Speed - The indicated air speed is developed from Bernoulli's equation

$$P_o - P = \rho V^2 / 2g_c \tag{14}$$

or

$$V_i = K_p \sqrt{\frac{2g_c(P_o - P)}{\rho}} \tag{15}$$

where ρ is the ambient density, P_o the total pressure, P the ambient static pressure, and K_p the calibration coefficient which should be close to unity, within 1%.

True Air Speed and Mach Number - The Mach number is computed from the relation

$$M = \sqrt{\frac{2}{k-1}}\left[\left(\frac{\Delta P}{P}+1\right)^{\frac{k-1}{k}} -1\right]^{\frac{1}{2}} \tag{16}$$

where ΔP is the $P_o - P$ above and K_P is approximately unity. The true air speed then becomes

$$V_{tr} = M \cdot \sqrt{g_c kRT} \tag{17}$$

where T is the ambient static temperature determined by the total temperature probe.

APPENDIX D

OZONE AND OXIDES OF NITROGEN ANALYZER EVALUATION AT REDUCED PRESSURE

Preceding page blank

APPENDIX D

OZONE AND OXIDES OF NITROGEN ANALYZER CALIBRATION AT REDUCED PRESSURE

D-1 Introduction and Summary

A series of tests were conducted in an altitude chamber at the EPA Environmental Monitoring & Support Laboratory at Las Vegas, Nevada. The purpose of these tests was to determine the characteristic behavior of a gas phase chemiluminescent ozone analyzer, Bendix Model 8002, and a gas phase chemiluminescent oxides of nitrogen analyzer, Bendix Model 8101-B, to changing altitude, as in an unpressurized aircraft.

The instruments were placed in the chamber and calibrated at ambient pressure. The chamber was then sealed and partially evacuated simulating a higher altitude environment. Calibration gases were generated externally from a calibration system operating at a constant ambient pressure, and drawn into the chamber to the gas analyzer inputs, to insure constant calibration levels with changing pressure. Tests were run over the range of pressures corresponding to ground level to an altitude of approximately 7,620 meters (25,000 feet) for the ozone analyzer and 5,790 meters (19,000 feet) for the oxides of nitrogen analyzer. Test results demonstrated that all instruments responded in a repeatable manner to variations in pressure. From these data, graphs were constructed whereby a single correction factor could be determined for each instrument at any given altitude over the test range. The effects of altitude on the instrument then could be compensated for by multiplying with the proper correction factor.

D-2 Test Set-up

The O_3 and $NO-NO_2-NO_x$ analyzers were mounted inside a Weber Pressure Chamber. A schematic diagram of the chamber is shown in figure D-1, illustrating the chamber controls, support gases and signal lines to the analyzers and the sample manifold system. The glass sample manifold was mounted inside the chamber, with the downstream end exhausted into the chamber. Teflon tubing was used to connect the sample inlet of each instrument to the manifold.

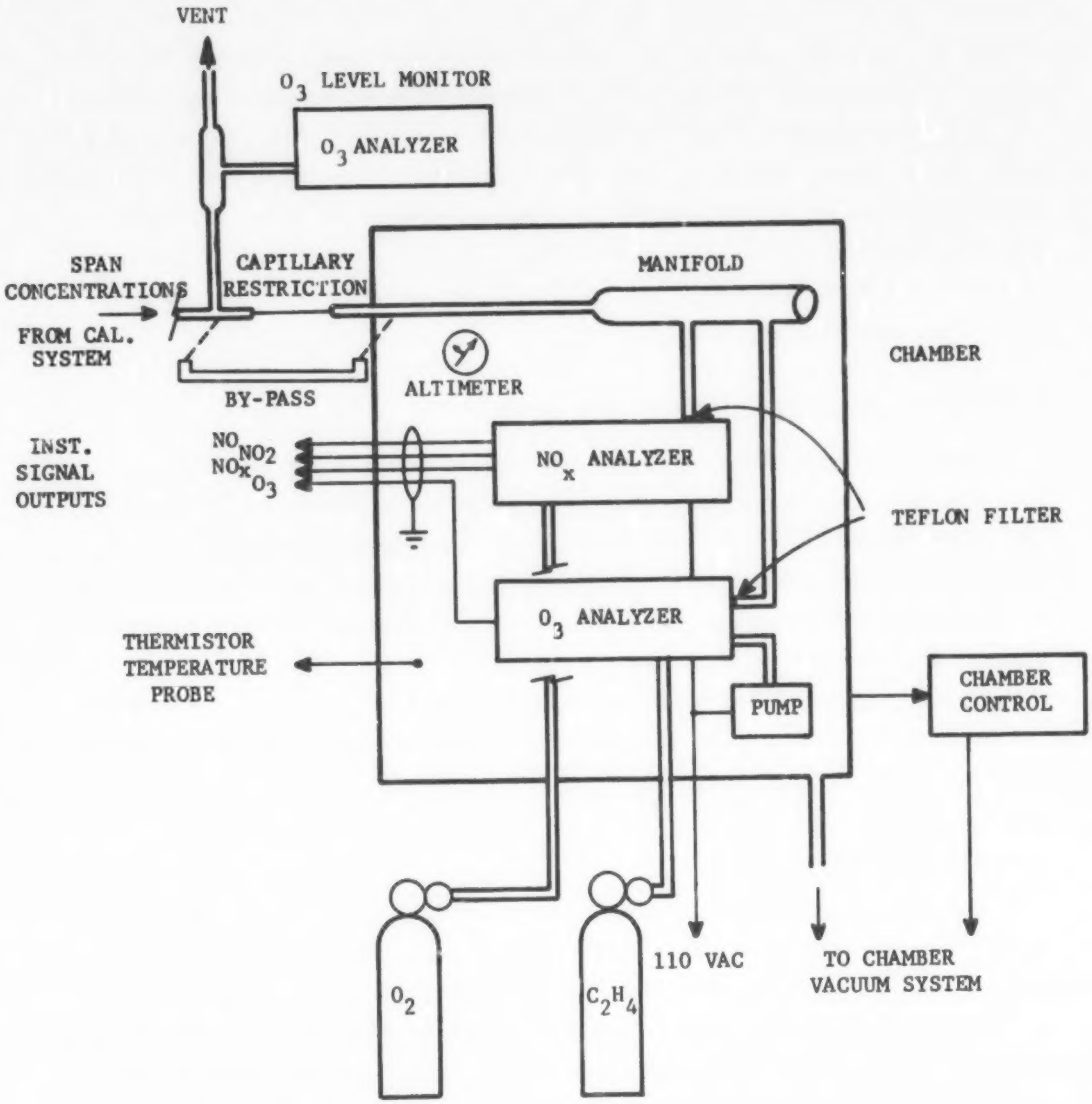
VENT
O_3 LEVEL MONITOR
O_3 ANALYZER
SPAN CONCENTRATIONS
FROM CAL. SYSTEM
CAPILLARY RESTRICTION
MANIFOLD
CHAMBER
ALTIMETER
BY-PASS
INST. SIGNAL OUTPUTS
NO
NO_2
NO_x
O_3
NO_x ANALYZER
TEFLON FILTER
O_3 ANALYZER
THERMISTOR TEMPERATURE PROBE
PUMP
CHAMBER CONTROL
O_2
C_2H_4
110 VAC
TO CHAMBER VACUUM SYSTEM

Figure D-1. Schematic diagram of test setup in pressure chamber.

Oxygen and ethylene gases were conveyed to the instruments inside the chamber, through s.s. tubing passed through bulkhead Swagelok connectors. The ethylene exhausted from the ozone analyzer was vented into the chamber after being passed through a catalytic converter.

A descriptive diagram of the calibration system is shown in figure D-2. The apparatus consists of a clean air source, compressed cylinder of nitric oxide in nitrogen, regulating valves, flow meters, an ozone generator, and mixing flasks.

D-3 Calibration Gases

Ozone concentrations in $\mu g/m^3$ for various ozone generator sleeve settings were determined using the Neutral-Buffered Potassium Iodide Method described in the April 30, 1971 Edition of the Federal Register.

Nitric oxide span concentrations were obtained by diluting pressurized NO in nitrogen with zero air. Nitrogen dioxide span concentrations were generated by the gas phase titration technique.

The NO concentration supplied by the manufacturer for the pressurized cylinder of NO used in this test was referenced to equivalent ozone concentrations added during titration.

D-4 Test Procedure

The units under tests were calibrated several times during the study at ambient conditions of temperature and pressure (25°C and 708 mm Hg). These calibrations were conducted by introducing the zero air and span concentrations directly to the sample manifold through the removable by-pass shown in figure D-1. The pressure differential between the manifold and ambient conditions during these tests was determined to be less than 0.6 cm of water. Subsequent calibrations were conducted with the chamber controlled at 25°C and at various simulated altitudes above ambient. During the reduced pressure tests, the sample manifold was maintained at chamber pressure by placing a capillary restriction upstream from the manifold and leaving the downstream end of the manifold open ended into the chamber (refer to fig. D-3).

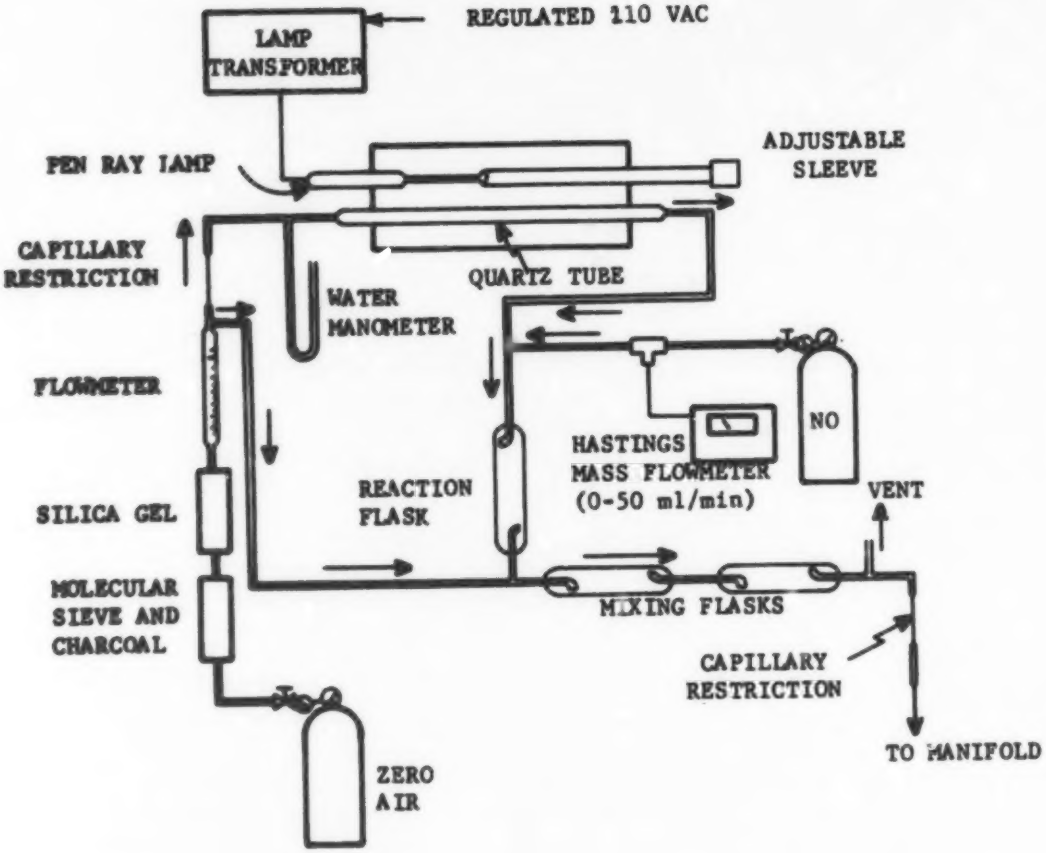
REGULATED 110 VAC
LAMP TRANSFORMER
PEN RAY LAMP
ADJUSTABLE SLEEVE
CAPILLARY RESTRICTION
QUARTZ TUBE
WATER MANOMETER
FLOWMETER
NO
HASTINGS MASS FLOWMETER (0-50 ml/min)
REACTION FLASK
SILICA GEL
VENT
MOLECULAR SIEVE AND CHARCOAL
MIXING FLASKS
CAPILLARY RESTRICTION
TO MANIFOLD
ZERO AIR

Figure D-2. Ozone generator/gas phase titration system for calibration of O_3 and NO-NO_x analyzers.

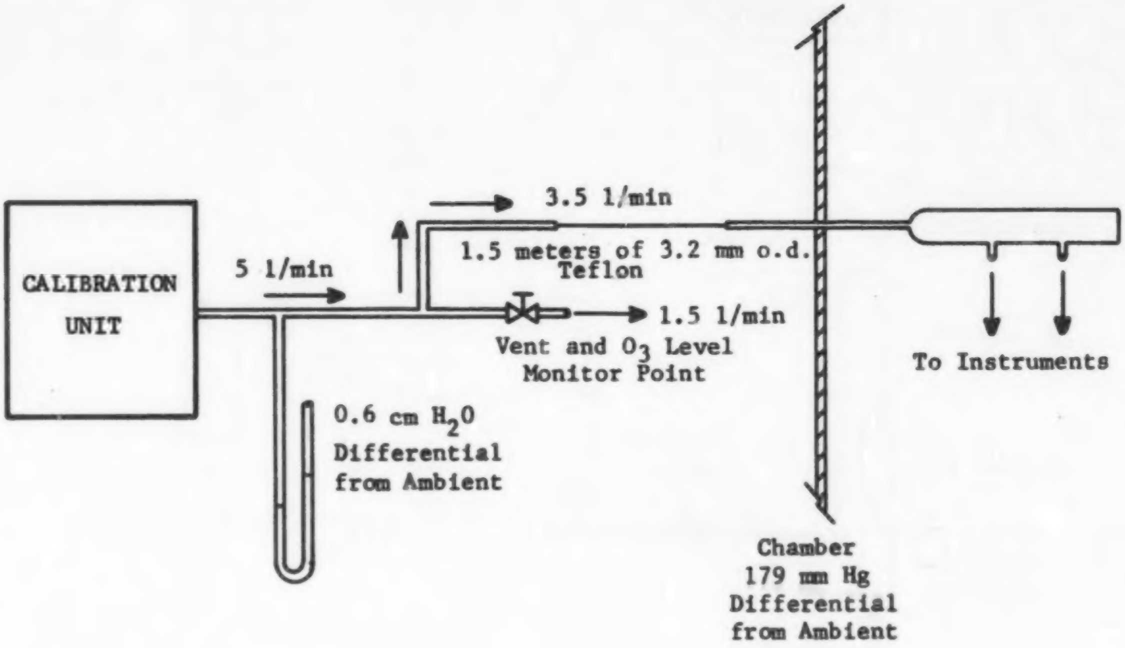
CALIBRATION UNIT
5 l/min
3.5 l/min
1.5 meters of 3.2 mm o.d. Teflon
1.5 l/min
Vent and O_3 Level Monitor Point
To Instruments
0.6 cm H_2O Differential from Ambient
Chamber 179 mm Hg Differential from Ambient

Figure D-3. Typical pressure and flow conditions for chamber setting at simulated altitude of 3048 meters (10k feet).

The sample was drawn into the chamber because the chamber was at a vacuum relative to the calibration system which was at ambient. The length of the Teflon capillary was adjusted so that the flow drawn into the chamber was 2.5 to 4 ℓ/min. The remainder of the calibrating gas, > 1ℓ/min, was vented into the room through an unrestricting vent to maintain a constant ambient pressure within the calibration system. This, in effect, provided for a known concentration of the calibration gas (O_3, NC, or NO_2 in this case) to be made available to the instrument at the pressure of interest based on measurements or calibration procedures conducted at ambient pressure. A second O_3 analyzer was used to monitor the ozone level at the room vent port, thus providing a second check on the concentration level of the calibration gas. Figure D-3 illustrates the typical pressure and flow conditions during a reduced pressure test with the chamber controlled at a simulated altitude of 3,048 meters (10,000 feet). A standard aircraft altimeter readable to tens of feet was used in the chamber to establish the altitude/pressure points at which data was taken. This same altimeter was used on the flights as well.

It was observed that the instruments adjusted much more rapidly to changes in pressure than did the entire system (instrument and calibration system) to changes in concentration. Therefore, these tests consisted of setting the system up for a single calibration gas level input and varying the pressure stepwise over the range being tested. Runs were repeated using the same input concentration levels on different days to determine repeatability. Also, different input concentrations were used to check linearity of the analyzers over the pressure range of interest.

D-5 Results of Tests

The response of O_3 and NO analyzers to different concentration of calibration gas and the respective altitude range were determined. These data were then normalized to an initial reading of unity at ambient pressure conditions in the laboratory. A best fit was then made for the respective sets of data, and these altitude correction curves are given in figures D-4 and D-5 for the O_3 and NO analyzers, respectively.

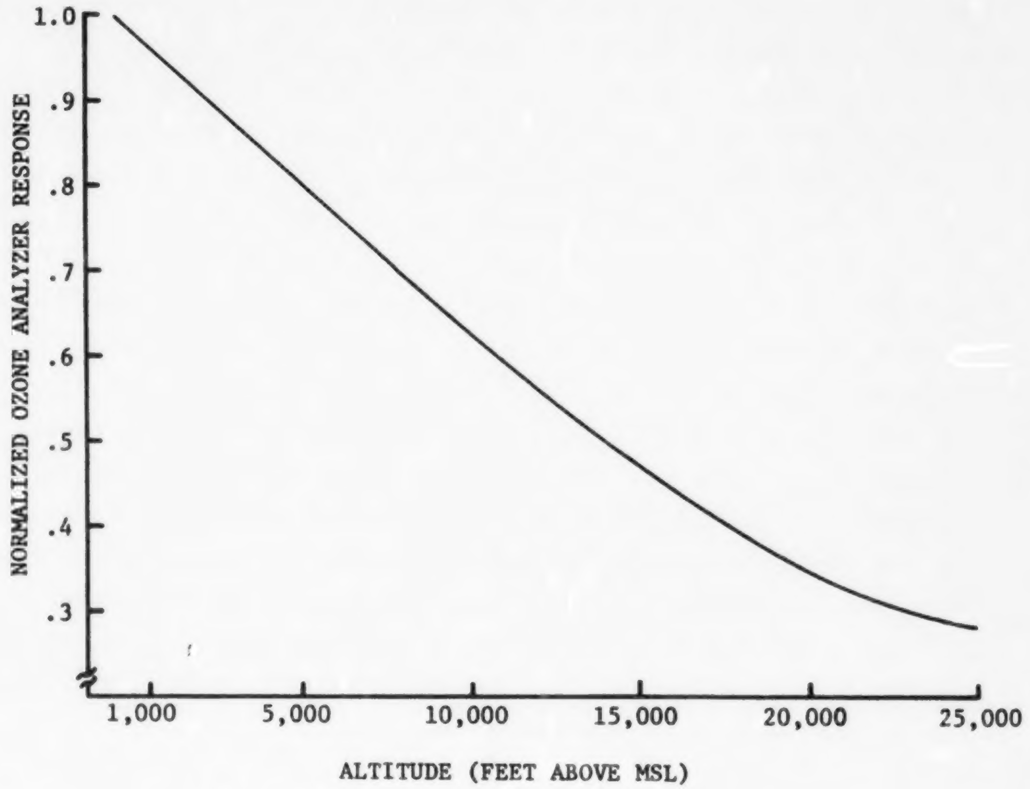

Figure D-4. Normalized response versus altitude for Bendix ozone analyzer.

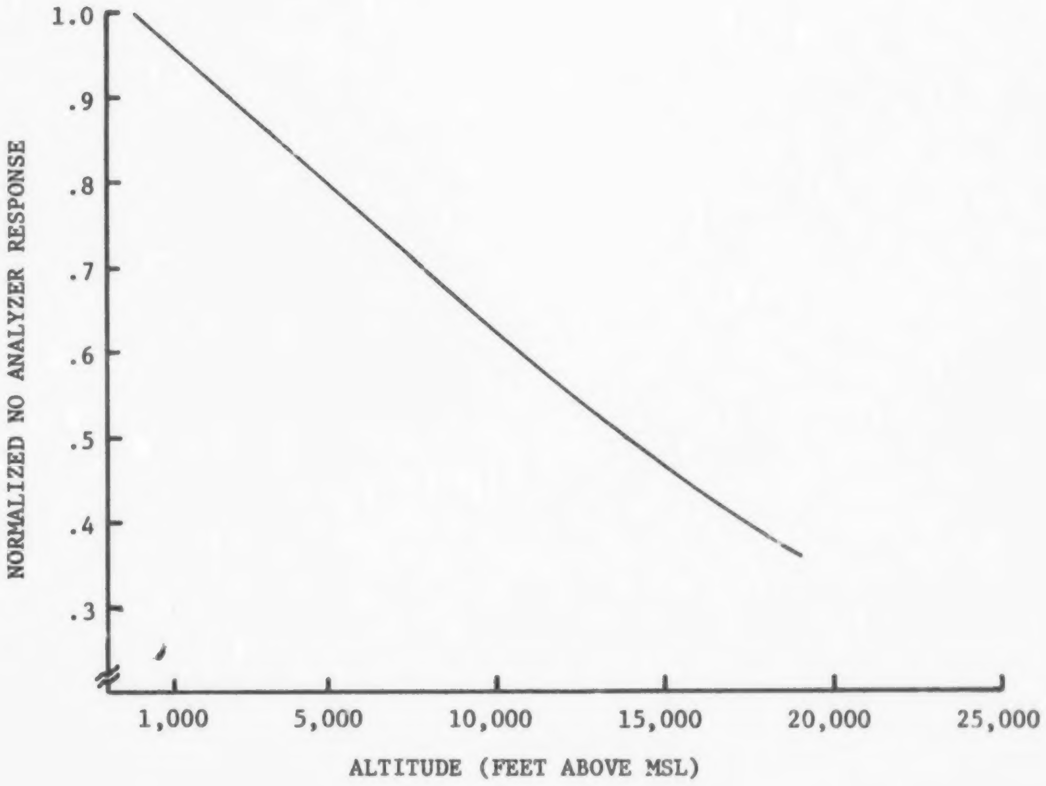

Figure D-5. Normalized response versus altitude for Bendix oxides of nitrogen analyzer.

APPENDIX E

SUMMARY SHEETS FOR AIRCRAFT DATA
AND SELECTED FLIGHTS

Preceding page blank

APPENDIX E

The following flight logs, summary sheets, and selected flights are included:

E-1 OTHER

- E-1a Flight Track Symbols & Designators
- E-1b List of Weather Symbols

E-2 LOGS AND SUMMARY SHEETS

- E-2a Grab Sample (Hydrocarbon) Log (Gulf Coast Area)
- E-2b Grab Sample (Hydrocarbon) Log (Northern Route)
- E-2c Selective Filter (Acetylene) Log (Gulf Coast Area)
- E-2d Selective Filter (Acetylene) Log (Northern Route)
- E-2e Sulfate Filter Log (Gulf Coast)
- E-2f Sulfate Filter Log (Northern Route)
- E-2g Summary Low Pass Data (Gulf Coast Area)

E-3 SULFATE SAMPLER DATA--TRACKS AND DATA

E-4 SELECTED FLIGHTS--TRACKS AND DATA

- E-4a Northern High Pressure System Survey (Flights 021 to 031)
- E-4b Down Wind Plume Flight No. 005 (Gulf Coast Area)
- E-4c Down Wind Plume Flight No. 006 (Gulf Coast Area)
- E-4d Sea-breeze Flight No. 075 (Gulf Coast Area)
- E-4e Sea-breeze Flight No. 076 (Gulf Coast Area)
- E-4f Box Pattern Flight No. 099-100 (Gulf Coast Area)
- E-4g Box Pattern Flight No. 109 (Gulf Coast Area)
- E-4h Box Pattern Flight No. 110 (Gulf Coast Area)

OTHER

E-1a Flight Track Symbols & Designators

E-1b List of Weather Symbols

Table E-1a. Flight Track Symbols and Designators

Symbol	Description
∘	Navigation Reference
◎	Landings & Takeoffs
	Vertical Profiles
◄··········►	Selective Filters
⬡	Grab Samples

Table E-1b. List of Weather Symbols

Symbol	Description	
0, C	Clear	0/10
ϕ	Scattered	1/10 to 5/10
◐, ◐	Broken	6/10 to 9/10
●, ⊕	Overcast	10/10
CB	Thunderstorm	
H	Haze	

EXAMPLE:

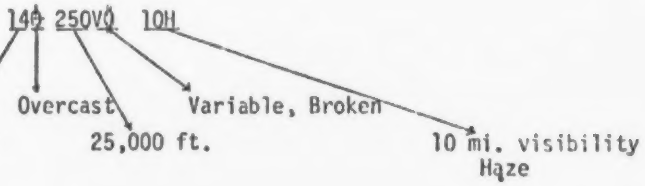
14⊕ 250V◐ 10H
Overcast
Variable, Broken
1400 ft
25,000 ft.
10 mi. visibility
Haze

LOGS AND SUMMARY SHEETS

E-2a Grab Sample (Hydrocarbon) Log (Gulf Coast Area)

Table E-2a. Grab sample (hydrocarbon) log (gulf coast area)

DATE (1975)	FLIGHT NO.	SAMPLE NO.	COLLECTION TIME (GMT)	
			START	STOP
6/30	010	0	1100	1102
"	"	1	1026	1028
"	"	2	1103	1106
"	011	1	1529	1533
8/6	035	1	1451	1453
"	"	2	1512	1514
"	"	3	1527	1529
"	"	4	1544	1546
8/7	037	1	1340	1342
"	"	2	1358	1400
"	"	3	1415	1417
"	"	4	1432	1434
8/9	040	1	1905	1907
"	"	2	2013	2015
"	"	3	2055	2057
8/10	041	1	1906	1908
"	"	2	2014	2016
9/19	075	1	1530	1532
"	"	2	1606	1608
"	"	3	1638	1640
"	"	4	1717	1719
"	"	5	1735	1737
9/19	076	1	2045	2047
"	"	2	2115	2117
"	"	3	2153	2155
"	"	4	2222	2224
9/20	077	1	1545	1547
"	078	1	1508	1510
"	"	2	1540	1542
"	"	3	1632	1634
"	"	4	1702	1704
"	"	5	1736	1738
9/21	079	1	1950	1952
"	"	2	2030	2032
"	"	3	2130	2132
"	"	4	2225	2227
10/10	094	1	1716	1718
"	"	2	1751	1753
"	"	3	1816	1818
"	"	4	1847	1849
"	095	1	2122	2124
"	"	2	2150	2152
"	"	3	2415	2417
10/13	096	1	1710	1712
"	"	2	1743	1745
"	"	3	1814	1816
"	"	4	1843	1845
"	"	5	1912	1914
"	"	6	1946	1948

Table E-2a. Grab sample (hydrocarbon) log (gulf coast area) (con.)

DATE (1975)	FLIGHT NO.	SAMPLE NO.	COLLECTION TIME (GMT)	
			START	STOP
10/14	097	1	1632	1634
"	"	2	1658	1660
"	"	3	1734	1736
"	"	4	1806	1808
"	"	5	1835	1837
"	098	1	2102	2104
"	"	2	2133	2135
"	"	3	2200	2202
"	"	4	2227	2229
10/19	099	1	1619	1621
"	"	2	1644	1646
"	"	3	1717	1719
"	"	4	1745	1747
"	"	5	1828	1830
"	100	1	1952	1954
"	"	2	2035	2037
"	"	3	2120	2122
10/20	101	1	1616	1618
"	"	2	1644	1646
"	"	3	1715	1717
"	"	4	1744	1746
"	102	1	1905	1907
"	"	2	1935	1937
"	"	3	2008	2010
"	"	4	2040	2042
10/21	103	1	2118	2120
"	"	2	2153	2155
"	"	3	2216	2218
"	"	4	2352	2354
10/30	109	1	1945	1947
"	"	2	2013	2015
"	"	3	2047	2049
"	"	4	2112	2114
"	"	5	2148	2150
"	"	6	2216	2218
10/31	110	1	1858	1860
"	"	2	1930	1932
"	"	3	2001	2003
"	"	4	2029	2031
"	"	5	2058	2100
"	"	6	2127	2129
"	"	7	2159	2201
"	"	8	2300	2302
"	"	9	2330	2332
11/1	111	1	1348	1350
"	"	2	1415	1417
"	"	3	1443	1445
"	"	4	1514	1516
"	"	5	1546	1548
"	"	6	1614	1616
"	"	7	1650	1652
"	"	8	1842	1844
"	"	9	1915	1917

E-2b Grab Sample (Hydrocarbon) Log (Northern Route)

Table E-2b. Grab sample (hydrocarbon) log (northern route flights)

DATE (1975)	FLIGHT NO.	SAMPLE NO.	COLLECTION TIME (GMT)	
			START	STOP
7/9	014	1	1142	1145
"	"	2	1932	1935
7/10	015	1	1303	1306
"	"	2	1458	1501
7/11	016	1	1233	1236
"	"	2	1415	1418
7/12	017	1	0934	0937
7/13	018	1	1116	1118
"	"	2	1402	1404
7/24	025	1	1719	1722
"	"	2	2149	2151
7/25	027	1	1708	1710
"	"	2	1924	1926
7/26	028	1	1643	1645
"	"	2	1910	1912
7/27	029	1	1550	1552
"	030	1	1918	1920
9/5	058	1	1713	1715
"	"	2	1745	1747
"	"	3	1811	1813
"	059	1	1942	1944
"	"	2	2053	2055
"	"	3	2116	2118
"	"	4	2148	2150
9/6	060	1	1733	1735
"	"	2	1810	1812
"	"	3	1844	1846
"	061	1	2031	2033
"	"	2	2102	2104
"	062	1	2255	2257
"	"	2	2323	2325
9/7	063	1	1647	1649
"	"	2	1720	1722
"	"	3	1743	1745
"	"	4	1823	1825
"	064	1	2113	2115
"	"	2	2144	2146
"	"	3	2216	2218
"	"	4	2242	2244
9/8	065	1	1506	1508
"	"	2	1530	1532
"	"	3	1616	1618
"	066	1	1745	1747
"	"	2	1817	1819
"	"	3	1848	1850
"	"	4	1920	1921

Table E-2b. Grab sample (hydrocarbon) log (northern route flights) (con.)

DATE (1975)	FLIGHT NO.	SAMPLE NO.	COLLECTION TIME (GMT)	
			START	STOP
9/12	069	1	1605	1607
"	"	2	1634	1636
"	070	1	1739	1741
"	"	2	1848	1850
"	"	3	1925	1927
"	"	4	1945	1947
9/27	084	1	1558	1600
"	"	2	1632	1634
"	"	3	1705	1707
"	"	4	1740	1742
"	"	5	1817	1819
"	085	1	2030	2032
"	"	2	2159	2161
"	"	3	2245	2247
9/28	086	1	1435	1437
"	"	2	1502	1504
"	"	3	1535	1537
"	"	4	1628	1630
"	087	1	1748	1750
9/29	088	1	1546	1548
"	089	1	1718	1720
"	"	2	1748	1750
"	"	3	1859	1901
9/30	090	1	1512	1514
"	"	2		1622
"	"	3	1715	1717
"	091	1	1835	1837
"	"	2	1906	1908
"	"	3	1940	1942

E-2c Selective Filter (Acetylene) Log (Gulf Coast Area)

Table E-2c. Selective filter (acetylene) log (gulf coast area)

DATE (1975)	FLIGHT NO.	FILTER NO.	SAMPLE COLLECTION TIME (GMT)		TOTAL SAMPLE TIME (MIN)	SAMPLE FLOW RATE (cc/min)
			FROM	TO		
8/11	041	1-18	1837	1855	18	46
"	"	2-31	1915	1925	10	75
"	"	3-42	1932	2002	30	25
"	"	4-58	2005	2045	40	18
"	"	5-61	2047	2153	16	20
9/19	075	1-70	1511	1538	27	22.6
"	"	2-0	1541	1615	34	21.8
"	"	3-134	1624	1655	31	20.7
"	"	4-79	1657	1727	30	15.5
"	"	5-50	1730	1756	26	23.1
"	076	1-53	2025	2055	30	21.0
"	"	2-145	2100	2131	31	21.8
"	"	3-82	2135	2204	29	23.6
"	"	4-118	2209	2259	50	12
9/20	077	1-40	1530	1602	32	24
9/21	078	1-10	1450	1522	32	26
"	"	2-36	1527	1557	30	23.5
"	"	3-40	1602	1631	29	19
"	"	4-113	1634	1702	32	24
"	"	5-24	1705	1736	31	23
"	079	1-55	1924	1955	31	16
"	"	2-108	1959	2035	36	17.6
"	"	3-132	2117	2135	18	21.4
"	"	"	2157	2210	13	"
"	"	4-142	2215	2240	25	22.6
10/9	092	1-14	1906	1940	34	22.2
"	"	2-59	1944	2019	35	21.8
"	"	3-34	2025	2054	29	20
"	"	4-01	2057	2127	30	23.1
"	093	1-66	2159	2232	33	21
"	"	2-150	2238	2309	31	22.6
"	"	3-30	2314	2346	32	21.4
"	"	4-87	2352	2420	28	20
10/10	094	1-13	1652	1726	34	25
"	"	2-44	1730	1802	32	13.9 MAX
"	"	3-74	1806	1834	28	22.2
"	"	4-91	1836	1902	26	24
"	"	5-75	1906	1938	32	20
"	095	1-11	2109	2136	25	20
"	"	2-18	2140	2212	32	23.1
"	"	3-49	2308	2328	32	22.6
"	"	"	2356	2408	"	"
"	"	4-106	2412	2438	26	21.8
10/13	096	1-52	1648	1724	26	21.8
"	"	2-94	1730	1757	27	26.7
"	"	3-81	1759	1826	27	27.3
"	"	4-33	1831	1557	26	23.1
"	"	5-78	1859	1931	32	19.4
"	"	6-1	1934	1954	20	24.5
10/14	097	1-60	1617	1649	32	26.7
"	"	2-103	1655	1722	27	18.8
"	"	3-14	1724	1753	29	23.1
"	"	4-110	1755	1820	25	19.0
"	"	5-113	1825	1855	30	17.6
"	"	6-68	1858	1931	33	22.2

Table E-2c. Selective filter (acetylene) log (gulf coast area) (con.)

DATE (1975)	FLIGHT NO.	FILTER NO.	SAMPLE COLLECTION TIME (GMT)		TOTAL SAMPLE TIME (MIN)	SAMPLE FLOW RATE (cc/min)
			FROM	TO		
10/14	098	1-35	2043	2114	31	20
"	"	2-67	2117	2150	33	21.8
"	"	3-72	2152	2281	29	19.4
10/19	099	1-29	1601	1631	30	7.0
"	"	2-69	1633	1651	28	25
"	"	3-58	1702	1730	28	26.5
"	"	4-131	1733	1805	32	21.4
"	"	5-61	1808	1850	42	15.2
"	100	1-70	1938	2005	27	24.4
"	"	2-7	2008	2037	29	24.5
"	"	4-172	2040	2110	30	22.6
10/20	101	1-42	1558	1627	29	27.3
"	"	2-55	1630	1658	28	15.4
"	"	3-134	1656	1727	28	30
"	"	4-132	1730	1756	26	24
"	102	1-82	1851	1923	32	16.4
"	"	2-118	1926	2002	36	7.5
"	"	3-50	2004	2027	25	20.7
10/21	103	1-79	2107	2134	27	20
"	"	2-149	2136	2208	32	21.4
"	"	3-333	2210	2235	25	23.1
"	"	4-103	2237	2249	30	18.8
"	"	"	2347	2405	"	"
10/30	109	1-40	1928	1958	30	26.1
"	"	2-53	2000	2038	28	27.6
"	"	3-10	2030	2059	29	27.2
"	"	4-43	2101	2129	28	23.1
"	"	5-136	2131	2200	29	21.8
"	"	6-140	2202	2232	30	23.1
10/31	110	1-139	1846	1918	32	19.6
"	"	2-99	1920	1946	26	18.8
"	"	3-64	1948	2016	28	23.1
"	"	4-26	2018	2045	27	20.7
"	"	5-327	2047	2114	27	17.6
"	"	5A-146	Control	-	-	-
"	"	6-56	2118	2142	24	18.5
"	"	7-121	2145	2200	29	22.6
"	"	"	2231	2245	29	27.6
"	"	8-97	2247	2314	27	19.8
"	"	9-2	2315	2338	23	22.2
11/1	111	1-20	1336	1359	23	22.2
"	"	2-119	1401	1430	29	23.1
"	"	3-112	1432	1455	23	21.4
"	"	4-31	1501	1530	29	25.5
"	"	5-76	1533	1601	28	21.8
"	"	6-14	1603	1633	30	22.6
"	"	7-16	1635	1703	28	21.4
"	"	8-144	1829	1905	36	24.5

E-2d Selective Filter (Acetylene) Log (Northern Route)

Table E-2d. Selective filter (acetylene) log (northern route flights)

DATE (1975)	FLIGHT NO.	FILTER NO.	SAMPLE COLLECTION TIME (GMT) FROM	TO	TOTAL SAMPLE TIME (MIN)	SAMPLE FLOW RATE (cc/min)
9/5	058	1-40	1656	1725	29	24
"	"	2-110	1729	1755	26	26
"	"	3-15	1802	1828	26	18.9
"	059	1-50	1925	1955	30	24
"	"	2-125	1957	2011	29	18
"	"	"	2050	2104	"	"
"	"	3-19	2106	2138	32	17.9
"	"	4-53	2140	2215	35	23
9/6	060	1-7	1724	1755	31	20
"	"	2-61	1759	1825	26	18.5
"	"	3-35	1827	1854	27	21.8
"	061	1-69	2015	2045	30	17.4
"	"	2-79	2051	2144	53	14
"	062	1-134	2239	2310	31	22.6
"	"	2-42	2312	2338	26	23.5
9/7	063	1-93	1636	1705	29	21.5
"	"	2-58	1707	1734	24	22.6
"	"	3-143	1736	1805	29	24.0
"	"	4-132	1808	1840	32	21.5
"	064	1-92	2057	2131	34	22.6
"	"	2-131	2133	2159	26	23.0
"	"	3-142	2201	2230	29	20.0
"	"	4-124	2235	2302	27	21.4
9/8	065	1-43	1447	1516	29	21.8
"	"	2-108	1519	1558	39	15.2
"	"	3-140	1604	1635	31	17.6
"	"	4-55	1637	1647	43	12.5
"	"	"	1728	1801	"	"
"	066	1-136	1803	1829	26	24.4
"	"	2-101	1835	1906	31	24.5
"	"	3-10	1908	1931	23	20
9/12	069	1-69	1549	1620	31	27.9
"	"	2-35	1623	1655	32	21.8
"	"	3-7	1738	1751	30	19.4
"	"	"	1658	1715	"	"
"	070	1-61	1833	1905	34	19.7
"	"	"	1753	1755	"	"
"	"	2-23	1910	1958	48	12.0
9/27	084	1-61	1543	1615	32	18.5
"	"	2-69	1647	1715	28	23.5
"	"	3-7	1728	1801	32	24
"	085	1-308	2021	2059	38	17.6
"	"	2-35	2205	2338	33	19.8
9/28	086	1-140	1506	1540	34	25
"	"	2-131	1615	1646	31	26.1
"	087	1-92	1805	1835	30	22.2
9/29	089	1-110	1708	1732	24	22.6
"	"	2-142	1735	1708	33	18.8
"	"	3-52	1845	1915	30	20
9/30	090	1-125	1500	1527	27	20
"	"	2-29	1607	1637	30	18.9
"	"	3-67	1700	1728	28	23.1
"	091	1-72	1818	1847	29	20.7
"	"	2-68	1915	1948	33	20.3

Table E-2e. Sulfate filter log
(gulf coast area)

DATE (1975)	FLIGHT NO.	FILTER NO.	COLLECTION TIME (GMT) START	COLLECTION TIME (GMT) STOP	TOTAL COLLECTION TIME (HRS)
9/19	075	9000041	1509	1812	
"	076	"	2020	2343	6.43
9/21	078	9000019	1446	1756	
"	079	"	1915	2240	6.58
10/9	092	9000042	1853	2127	
"	093	"	2152	2425	5.1
10/10	094	9000043	1642	1938	
"	095	"	2106	2444	6.6
10/13	096	9000018	1643	1954	3.2
10/14	097	9000054	1614	1930	
"	098	"	2038	2236	5.23
10/19	099	9000053	1552	1852	
"	100	"	1937	2208	5.52
10/20	101	9000052	1554	1755	
"	102	"	1850	2059	4.17
10/30	109	9000051	1926	2238	3.2
10/31	110	9000050	1845	2200	
"	"	"	2230	2335	4.33
11/1	111	9000049	1334	1708	
"	"	"	1826	1935	4.72

E-2f Sulfate Filter Log (Northern Route)

Table E-2f. Sulfate filter log (northern route flights)

DATA (1975)	FLIGHT NO.	FILTER NO.	COLLECTION TIME (GMT)		TOTAL COLLECTION TIME (HRS)
			START	STOP	
9/4	055	9000012	2158	0115	5.72
"	056	"	0228	0454	"
9/5	058	9000013	1652	1825	4.33
"	059	"	1928	2215	"
9/6	060	9000014	1725	1905	4.4
"	061	"	2016	2158	"
"	062	"	2237	2339	
9/7	063	9000015	1637	1927	4.98
"	064	"	2054	2303	"
9/8	065	9000016	1444	1931	4.12
"	"	"	1728	1648	"
9/11	067	9000017	1635	2032	7.82
"	068	"	2116	0108	"
9/12	069	9000035	1547	1715	4.0
"	070	"	1738	2010	"
9/15	071	9000036	2055	2302	5.4
"	072	"	0015	0232	"
9/27	084	9000037	1532	1833	5.5
"	085	"	2020	2249	"
9/28	086	9000038	1428	1652	3.47
"	087	"	1732	1836	"
9/29	088	9000039	1530	1610	3.83
"	089	"	1659	2009	"
9/30	090	9000046	1444	1727	6.2
"	091	"	1815	2144	"

E-2g Summary Low Pass Data (Gulf Coast Area)

Table E-2g. Summary low pass data
(gulf coast area)

DATE (1975)	FLIGHT NO.	TIME (GMT)	LOCATION	OZONE CONCENTRATION ($\mu g/m^3$)	
				AIRCRAFT	STATION
6/26	005	1757	DeRidder	191	-
6/27	006	1729	"	121	63
6/28	007	1440	"	72	78
"	"	1745	"	68	101
6/29	008	1042	"	82	72
"	"	1213	"	84	59
"	009	1801	"	93	46
8/6	035	1331	"	51	44
"	"	1335	"	51	48
"	036	2417	"	80	72
"	"	2422	"	82	78
8/7	037	1239	"	29	16
"	"	1244	"	29	12
"	"	1441	"	102	118
"	"	1445	"	102	120
8/7	038	1815	"	83	134
"	"	2030	"	83	122
8/8	039	1840	"	95	122
"	"	2219	"	117	136
8/9	040	1826	"	64	93
"	"	2200	"	81	85
8/11	041	1826	"	141	138
"	"	2153	"	115	144
9/21	078	1444	"	72	60
"	079	1920	"	92	106
10/10	094	1640	"	111	144
"	"	1938	"	140	126
"	095	2104	"	154	128
10/13	096	1639	"	118	104
"	"	1951	"	131	118
10/14	097/098	1611	"	107	112
"	"	2238	"	125	116
10/19	099/100	1554	"	118	114
"	"	2207	"	118	119
10/20	101/102	1557	"	180	164
"	"	2103	"	180	178
10/21	103	2248	"	183	178
"	"	2325	"	178	178
10/22	104	1643	"	110	118
"	"	1658	"	115	120
10/24	105	2145	"	72	72
10/26	107	2018	"	77	68
"	"	2132	"	56	72
10/30	109	1926	"	96	104
"	"	2238	"	108	108
10/31	110	1722	"	104	108
"	"	2322	"	142	132

SULFATE SAMPLER DATA--TRACKS AND DATA

Table E-3. Sulfate samples

Date (1975)	Flight No.	Filter No.	NH_4^+ ($\mu g/m^3$)	NO_3^- ($\mu g/m^3$)	$SO_4^=$ ($\mu g/m^3$)
9/4	055,056,057	9000012	B.D.	2.7	6.5
9/6	060,061,062	9000014	B.D.	2.4	1.4
9/7	063,064	9000015	B.D.	3.9	14.5
9/11	067,068	9000017	B.D.	1.3	0.7
9/12	069,070	9000035	B.D.	1.1	B.D.
9/15	071,072	9000036	B.D.	0.6	B.D.
9/19	075,076	9000041	B.D.	1.9	0.7
9/21	078,079	9000019	B.D.	3.2	9.7
9/27	084,085	9000037	B.D.	6.6	21.2
9/28	086,087	9000038	B.D.	9.8	22.2
9/29	088,089	9000039	B.D.	1.5	0.2
9/30	090,091	9000046	B.D.	5.6	18.6
10/9	092,093	9000042	B.D.	2.1	8.6
10/10	094,095	9000043	B.D.	2.4	2.8
10/13	096	9000018	B.D.	2.1	2.9
10/14	097,098	9000054	B.D.	2.7	8.6
10/19	099,100	9000053	B.D.	4.4	8.4
10/20	101,102	9000052	B.D.	5.1	11.4
10/30	109	9000051	0.2	10.6	25.5
10/31	110	9000050	B.D.	5.7	11.2
11/1	111	9000049	B.D.	1.6	1.4

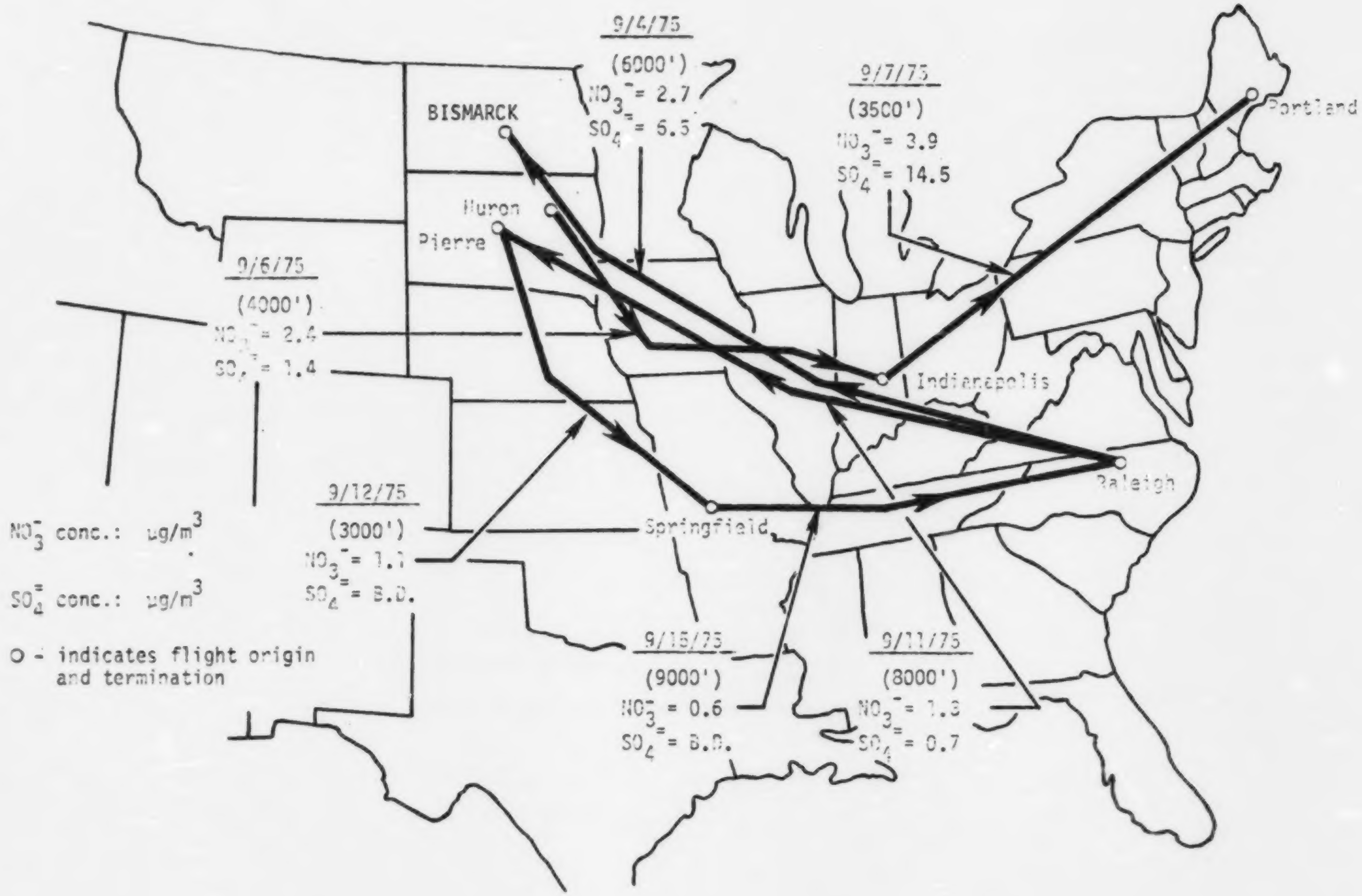
9/4/75
(6000')
$NO_3^- = 2.7$
$SO_4^= = 6.5$
9/7/75
(3500')
$NO_3^- = 3.9$
$SO_4^= = 14.5$
BISMARCK
Huron
Pierre
Portland
9/6/75
(4000')
$NO_3^- = 2.4$
$SO_4^= = 1.4$
Indianapolis
Raleigh
9/12/75
(3000')
$NO_3^- = 1.1$
$SO_4^= =$ B.D.
Springfield
NO_3^- conc.: µg/m^3
$SO_4^=$ conc.: µg/m^3
○ - indicates flight origin and termination
9/15/75
(9000')
$NO_3^- = 0.6$
$SO_4^= =$ B.D.
9/11/75
(8000')
$NO_3^- = 1.3$
$SO_4^= = 0.7$

Reproduced from best available copy.

Figure E-3-1. AIRCRAFT FLIGHTS, 9/4/75-9/15/75 high volume filter measurements for sulfate and nitrates.

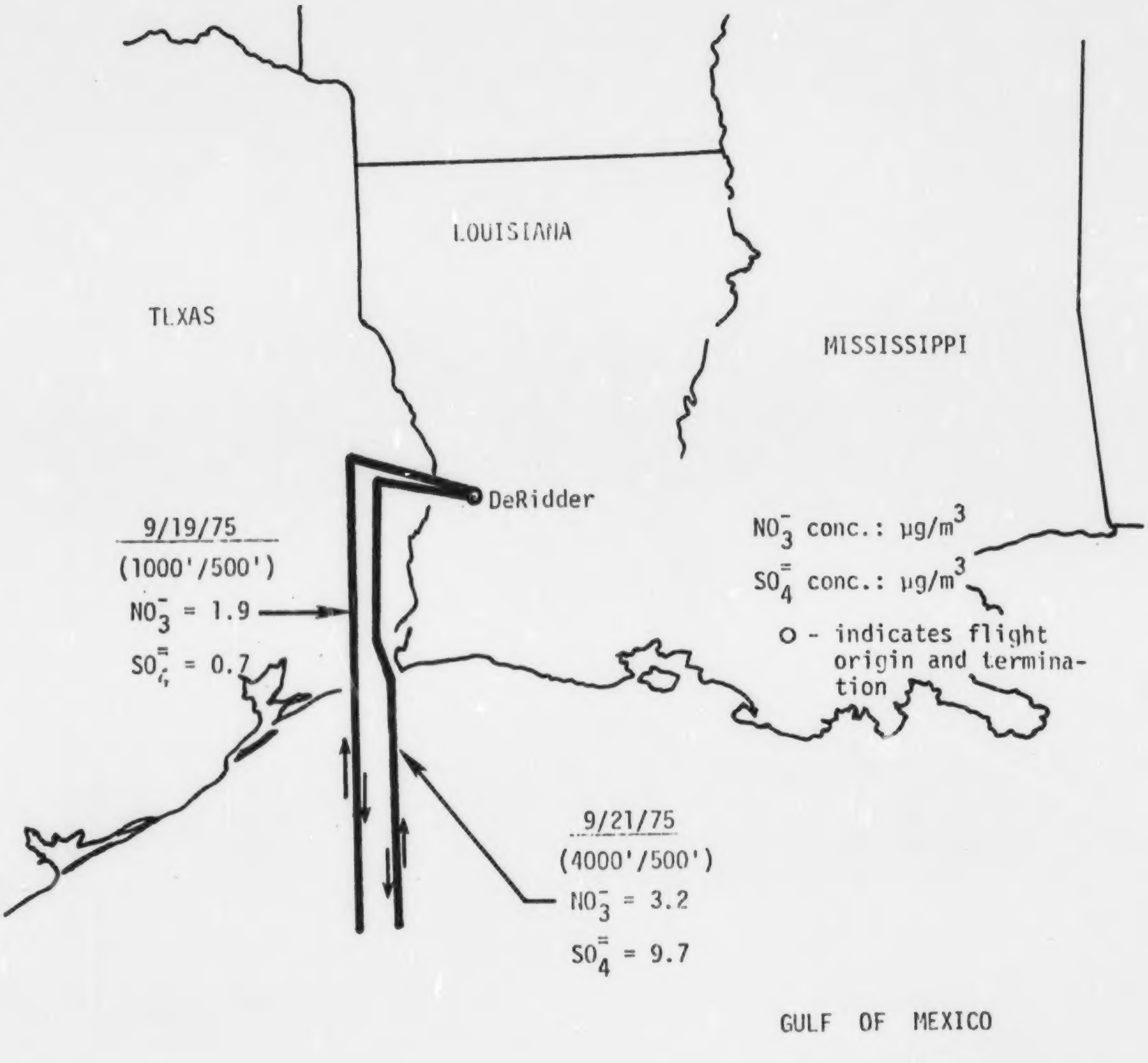
LOUISIANA
TEXAS
MISSISSIPPI
DeRidder
9/19/75
(1000'/500')
$NO_3^- = 1.9$
$SO_4^= = 0.7$
NO_3^- conc.: μg/m^3
$SO_4^=$ conc.: μg/m^3
O - indicates flight origin and termination
9/21/75
(4000'/500')
$NO_3^- = 3.2$
$SO_4^= = 9.7$
GULF OF MEXICO

Figure E-3-2. AIRCRAFT FLIGHTS, 9/19/75-9/21/75 high volume filter measurements for sulfate and nitrates.

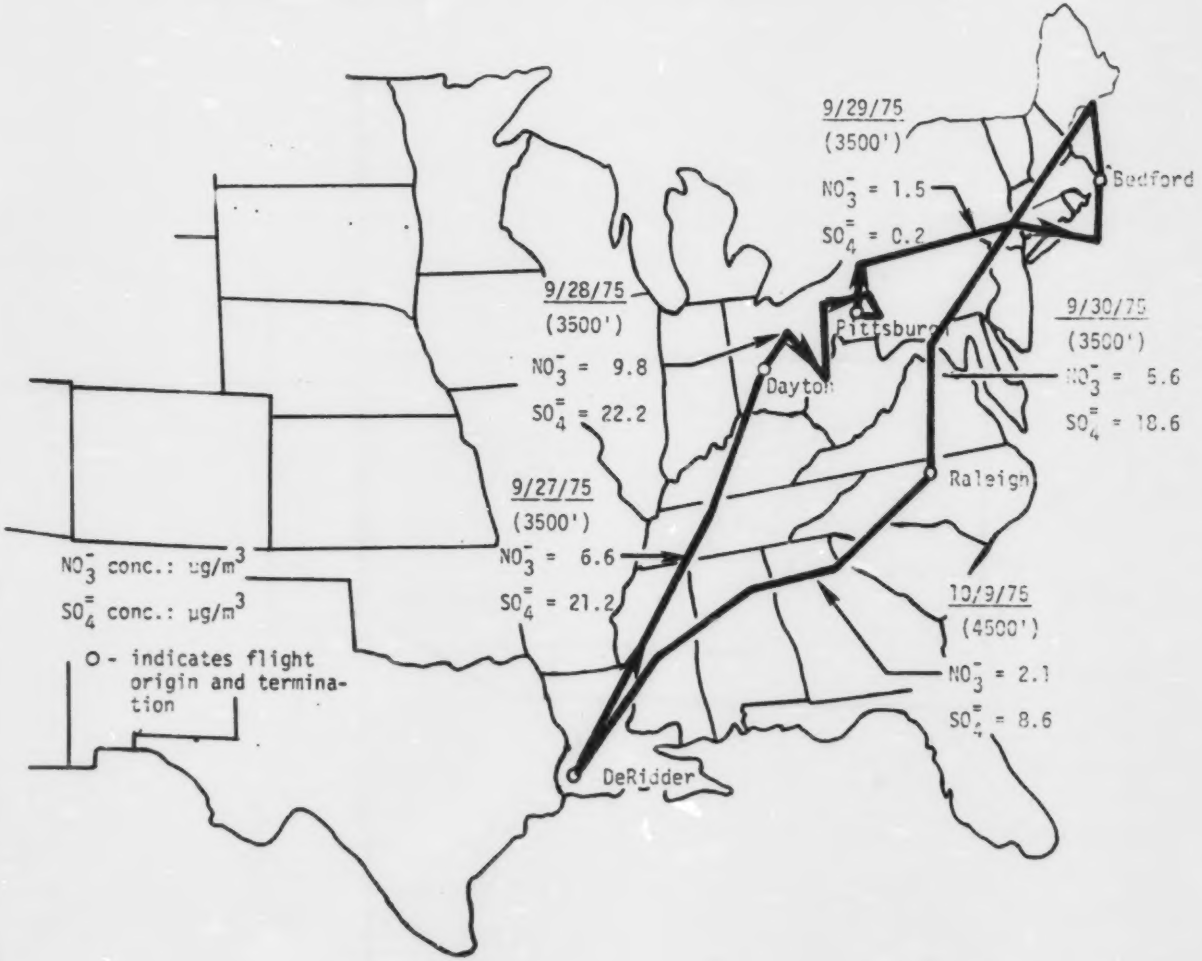
9/29/75
(3500')
NO_3^- = 1.5
$SO_4^=$ = 0.2
Bedford
9/28/75
(3500')
NO_3^- = 9.8
$SO_4^=$ = 22.2
Pittsburgh
Dayton
9/30/75
(3500')
NO_3^- = 5.6
$SO_4^=$ = 18.6
Raleigh
9/27/75
(3500')
NO_3^- = 6.6
$SO_4^=$ = 21.2
10/9/75
(4500')
NO_3^- = 2.1
$SO_4^=$ = 8.6
NO_3^- conc.: μg/m^3
$SO_4^=$ conc.: μg/m^3
O - indicates flight origin and termination
DeRidder

Figure E-3-3. AIRCRAFT FLIGHTS, 9/27/75-10/9/75 high volume filter measurements for sulfate and nitrates.

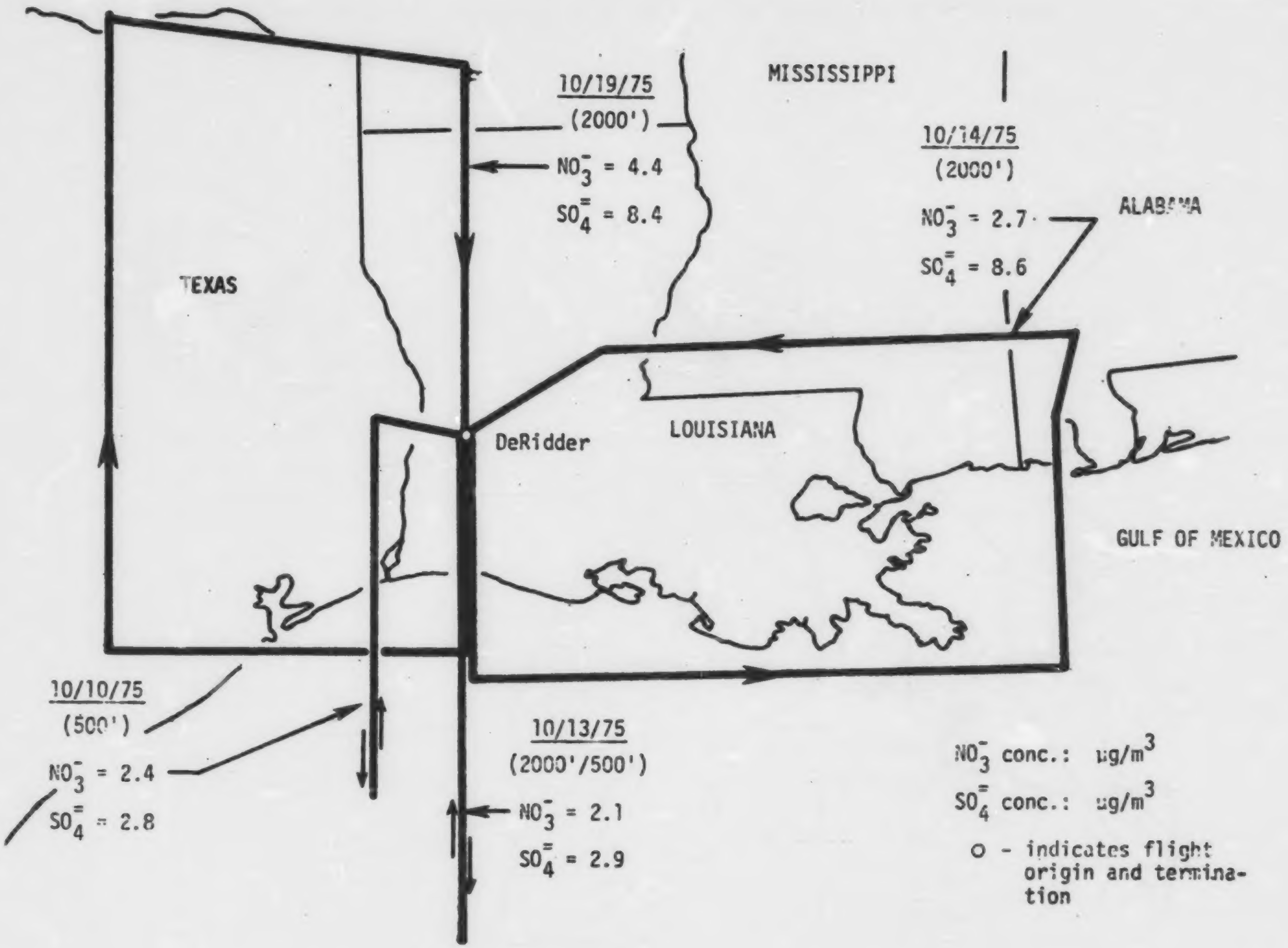
10/19/75
(2000')
NO_3^- = 4.4
$SO_4^=$ = 8.4
MISSISSIPPI
10/14/75
(2000')
NO_3^- = 2.7
$SO_4^=$ = 8.6
ALABAMA
TEXAS
DeRidder
LOUISIANA
GULF OF MEXICO
10/10/75
(500')
NO_3^- = 2.4
$SO_4^=$ = 2.8
10/13/75
(2000'/500')
NO_3^- = 2.1
$SO_4^=$ = 2.9
NO_3^- conc.: $\mu g/m^3$
$SO_4^=$ conc.: $\mu g/m^3$
o - indicates flight origin and termination

Figure E-3-4. AIRCRAFT FLIGHTS, 10/10/75-10/19/75 high volume filter measurements for sulfate and nitrates.

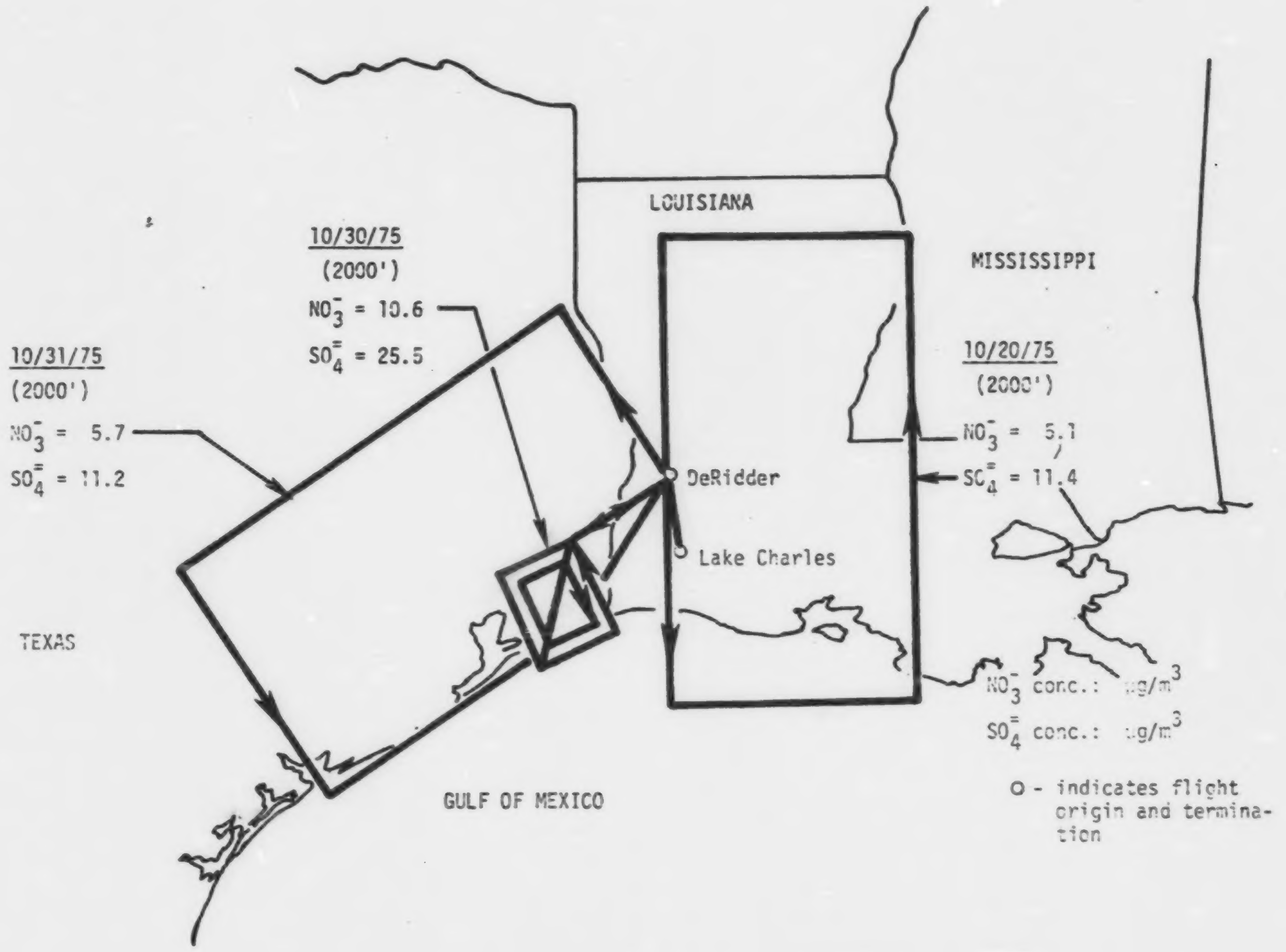

LOUISIANA
MISSISSIPPI
TEXAS
GULF OF MEXICO
DeRidder
Lake Charles
10/31/75
(2000')
$NO_3^- = 5.7$
$SO_4^= = 11.2$
10/30/75
(2000')
$NO_3^- = 10.6$
$SO_4^= = 25.5$
10/20/75
(2000')
$NO_3^- = 5.1$
$SO_4^= = 11.4$
NO_3^- conc.: μg/m^3
$SO_4^=$ conc.: μg/m^3
o - indicates flight origin and termination

Figure E-3-5. AIRCRAFT FLIGHTS, 10/20/75-10/31/75 high volume filter measurements for sulfate and nitrates.

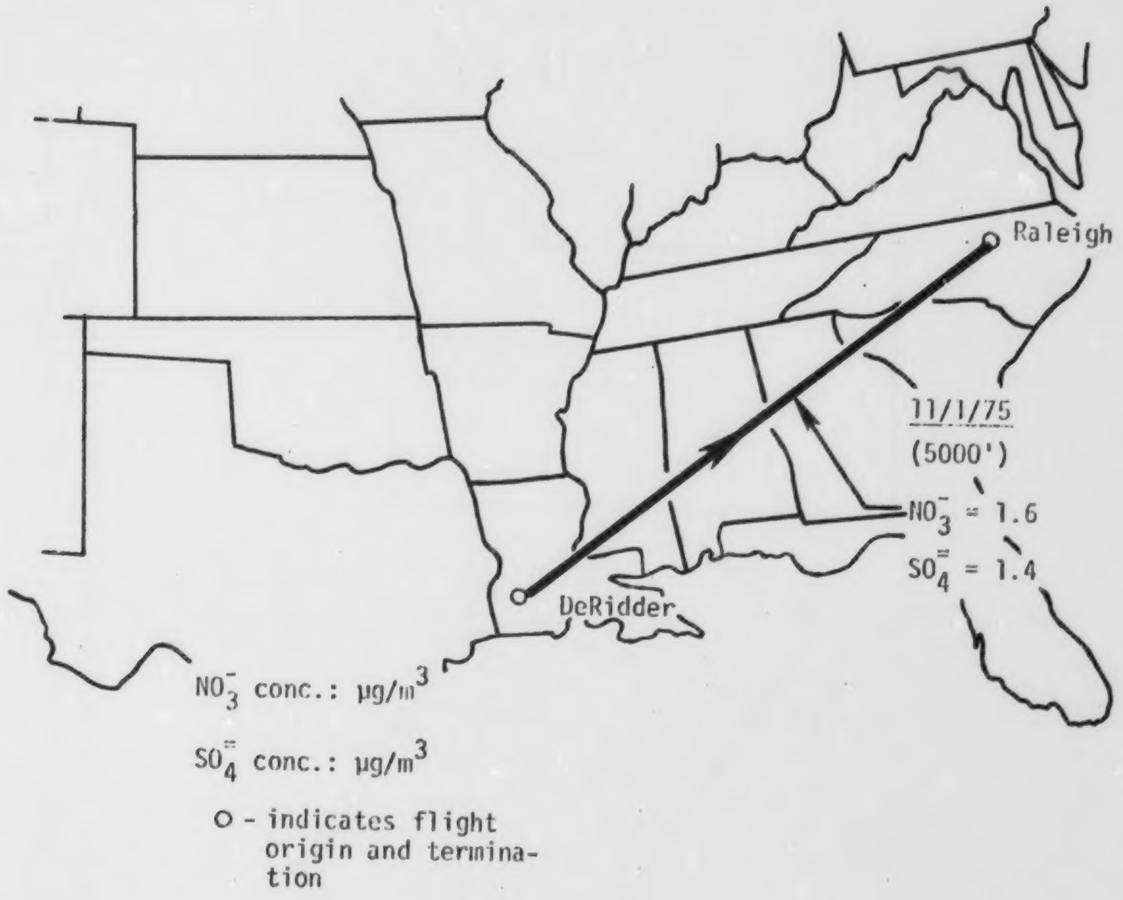
Raleigh
DeRidder
11/1/75
(5000')
$NO_3^- = 1.6$
$SO_4^= = 1.4$
NO_3^- conc.: μg/m^3
$SO_4^=$ conc.: μg/m^3
o - indicates flight origin and termination

Figure E-3-6. AIRCRAFT FLIGHT, 11/1/75
high volume filter measurements for sulfate and nitrates.

SELECTED EXAMPLE OF NORTHERN HIGH PRESSURE SYSTEM SURVEY FLIGHT - NORTHERN HIGH PRESSURE OXIDANT STUDY

E-4A--Northern High Pressure Survey-Flights No. 021 through 031; July 22 to July 27, 1975

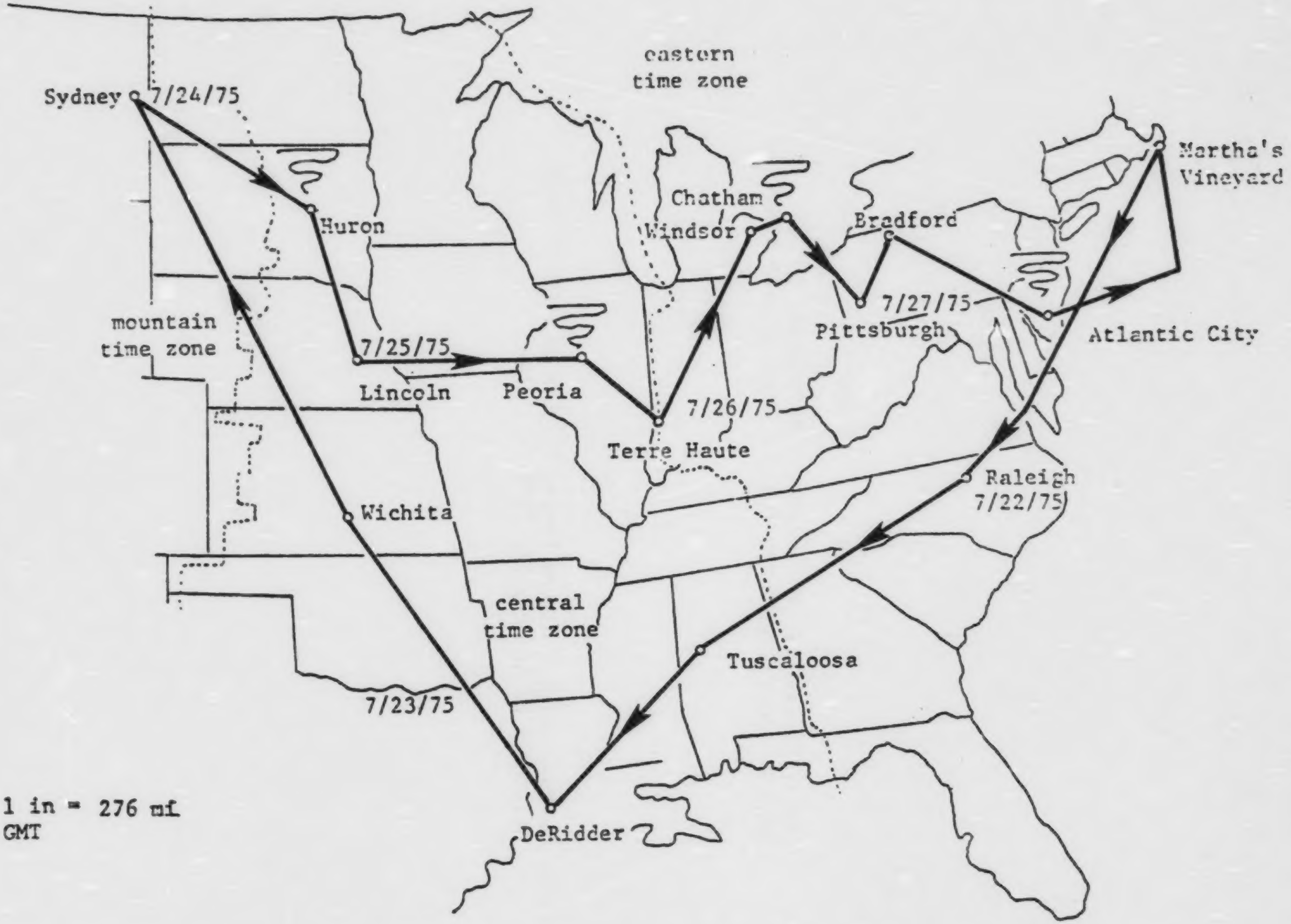
eastern time zone
mountain time zone
central time zone
Sydney
7/24/75
Huron
7/25/75
Lincoln
Peoria
Terre Haute
7/26/75
Windsor
Chatham
Bradford
Pittsburgh
7/27/75
Atlantic City
Martha's Vineyard
Raleigh
7/22/75
Tuscaloosa
DeRidder
7/23/75
Wichita

SCALE: 1 in = 276 mi
TIME: GMT

Figure E-4A-1. High pressure survey flights (021-031), 7/22/75-7/27/75.

Reproduced from best available copy.

Table E-4a. Tabulated data: transition flight, RDU-LCH (021-022), 7/22/75

TIME (GMT)	POSITION	HEADING	ALTITUDE observed (ft)	O_3 ($\mu g/m^3$)	TEMP. observed (°C)	TRUE AIR SPEED observed (mph)
(Flight 021)						
18:22	RDU	TAKEOFF	436	-	34	140
24	"	269°	-	-	-	-
42		"	-	87	-	-
43	LIB	100°	10000	-	-	200
44		"	"	80	-	-
46		"	"	80	-	-
48		"	"	80	-	-
50		"	"	87	-	-
52		"	"	87	-	-
54		"	"	101	-	-
56		"	"	94	-	-
58		"	"	80	-	-
19:00		"	"	80	-	-
02		"	"	94	-	-
04		"	"	87	-	-
06		"	"	80	-	-
08		"	"	73	-	-
09	CLT	259°	"	-	-	-
10		"	"	80	-	-
12		"	"	80	-	-
14		"	"	73	-	-
16		"	"	73	-	-
18		"	"	73	-	-
20		"	"	73	-	-
22		"	"	73	-	-
24		"	"	73	-	-
26	SPA	256°	"	73	-	-
28		"	"	66	-	-
30		"	"	73	-	-
32		"	"	73	-	-
34		"	"	73	-	-
36		"	"	73	-	-
38		"	"	73	-	-
40		"	"	73	-	-
42		"	"	73	-	-
44		"	"	73	-	-
46		"	"	73	-	-
48		"	"	73	-	-
50	TOC	254°	"	73	-	-
52		"	"	73	-	-
54		"	"	73	-	-
56		"	"	73	-	-
58		"	"	80	-	-
20:00		"	"	73	-	-
02		"	"	73	-	-
04		"	"	80	-	-
06		"	"	80	-	-
08		"	"	87	-	-
10	Nello XN	239°	"	87	-	-
12		"	"	94	-	-

Table E-4a. Tabulated data: transition flight, RDU-LCH (021-022), 7/22/75 (con.)

TIME (GMT)	POSITION	HEADING	ALTITUDE observed (ft)	O_3 ($\mu g/m^3$)	TEMP. observed (°C)	TRUE AIR SPEED observed (mph)
20:14		"	"	87	-	-
16		"	"	94	-	-
18		"	"	101	-	-
20		"	"	94	-	-
22		"	"	94	-	-
23	RMG	251°	"	-	-	-
24		"	"	80	-	-
26		"	"	80	-	-
28		"	"	80	-	-
30		"	"	115	-	-
32		"	"	122	-	-
34		"	"	115	-	-
36		"	"	94	-	-
38		"	"	94	-	-
40		"	"	87	-	-
42		"	"	87	-	-
44		"	"	94	-	-
46		"	"	108	-	-
48		"	"	122	-	-
50		"	"	122	-	-
52		"	"	170	-	-
54		"	"	156	-	-
55	BHM	230°	"	-	-	-
56		"	"	149	-	-
58		"	-	115	-	-
21:00		"	-	135	-	-
02		"	-	170	-	-
11	TCL	LANDING	169	-	-	-
(Flight 022)						
22:03	TCL	TAKEOFF	169	-	33	140
04	"	228°	-	-	-	-
18		"	8000	82	-	200
20		"	"	82	-	-
22		"	"	88	-	-
24		"	"	88	-	-
26		"	"	88	-	-
28		"	"	88	-	-
30		"	"	88	-	-
32		"	"	88	-	-
34	MEI	216°	"	88	-	-
36		"	"	88	-	-
38		"	"	88	-	-
40		"	"	88	-	-
42		"	"	95	-	-
44		"	"	95	-	-
46		"	"	95	-	-
48	MZE XN	229°	"	95	-	-
50		"	"	95	-	-
52		"	"	95	-	-

Table E-4a. Tabulated data: transition flight, RDU-LCH (021-022), 7/22/75 (con.)

TIME (GMT)	POSITION	HEADING	ALTITUDE observed (ft)	O_3 ($\mu g/m^3$)	TEMP. observed (°C)	TRUE AIR SPEED observed (mph)
22:54		"	"	88	-	-
56		"	"	82	-	-
58		"	"	88	-	-
23:00		"	"	101	-	-
02		"	"	88	-	-
04		"	"	88	-	-
06		"	"	76	-	-
07	MCB	239°	"	-	-	-
08		"	"	76	-	-
10		"	"	70	-	-
12		"	"	70	-	-
14		"	"	70	-	-
16		"	"	70	-	-
18		"	"	70	-	-
20		"	"	76	-	-
22		"	"	76	-	-
24		"	"	76	-	-
26		"	"	70	-	-
28		"	"	70	-	-
30		"	"	70	-	-
32		"	"	70	-	-
34		"	"	76	-	-
36		"	"	76	-	-
38		"	"	76	-	-
40		"	"	76	-	-
42		"	"	70	-	-
44		"	"	76	-	-
46		"	"	70	-	-
48		"	"	40	-	-
50		"	"	64	-	-
52		"	"	82	-	-
		"	"	82	-	-
56		"	"	88	-	-
58		"	-	101	-	-
24:07	LCH	LANDING	16	-	-	-

Table E-4a-1. Tabulated data: transition flight, LCH-SDY (023-024), 7/23/75

TIME (GMT)	POSITION	HEADING	ALTITUDE observed (ft)	O_3 ($\mu g/m^3$)	TEMP. observed (^{o}C)	TRUE AIR SPEED observed (mph)
(Flight 023)						
16:17	LCH	TAKEOFF	16	-	28	140
18	"	323^{o}	-	-	-	-
32		"	-	66	-	-
34		"	10000	66	-	200
36		"	"	80	-	-
38		"	"	80	-	-
40		"	"	66	-	-
42		"	"	60	-	-
44		"	"	59	-	-
46		"	"	59	-	-
48		"	"	66	-	-
50		"	"	73	-	-
52		"	"	73	-	-
54		"	"	80	-	-
56		"	"	80	-	-
58		"	"	73	-	-
17:00		"	"	66	-	-
02		"	"	73	-	-
04		"	"	73	-	-
06		"	"	73	-	-
08		"	"	73	-	-
10		"	"	73	-	-
12		"	"	73	-	-
14		"	"	73	-	-
16		"	"	80	-	-
17	GGG	335^{o}	"	-	-	-
18		"	"	80	-	-
20		"	"	80	-	-
22		"	"	66	-	-
24		"	"	66	-	-
26		"	"	66	-	-
28		"	"	66	-	-
30		"	"	66	-	-
32		"	"	66	-	-
34		"	"	73	-	-
36		"	"	73	-	-
38		"	"	73	-	-
40		"	"	66	-	-
42		"	"	66	-	-
44		"	"	80	-	-
46		"	"	73	-	-
48		"	"	59	-	-
50		"	"	59	-	-
52		"	"	59	-	-
54		"	"	66	-	-
56		"	"	59	-	-
58		"	"	59	-	-
18:00		"	"	66	-	-
02		"	"	52	-	-
04		"	"	52	-	-

Table E-4a-1. Tabulated data: transition flight, LCH-SDY (023-024), 7/23/75 (con.)

TIME (GMT)	POSITION	HEADING	ALTITUDE observed (ft)	O_3 (μg/m^3)	TEMP. observed (°C)	TRUE AIR SPEED observed (mph)
18:06		"	"	52	-	-
08	MLC	323°	"	52	-	-
10		"	"	52	-	-
12		"	"	52	-	-
14		"	"	45	-	-
16		"	"	52	-	-
18		"	"	52	-	-
20		"	"	45	-	-
22		"	"	52	-	-
24		"	"	52	-	-
26		"	"	52	-	-
28		"	"	59	-	-
30		"	"	66	-	-
32		"	"	73	-	-
34		"	"	66	-	-
36		"	"	66	-	-
38		"	"	73	-	-
40		"	"	73	-	-
42		"	"	73	-	-
44	PER	338°	"	73	-	-
46		"	"	73	-	-
48		"	"	66	-	-
50		"	"	52	-	-
52		"	-	38	-	-
54		"	-	45	-	-
56		"	-	38	-	-
58		"	-	52	-	-
19:00		"	-	73	-	-
02		"	-	87	-	-
04		"	-	66	-	-
06		"	-	-	-	-
08		"	-	-	-	-
09	ICT	LANDING	1332	-	-	-
(Flight 024)						
21:06	ICT	TAKEOFF	1332	-	-	140
08	"	334°	-	-	-	-
22		"	10500	61	-	-
24		"	"	68	-	-
26		"	"	76		
28		"	"	76	-	-
30		"	"	68	-	-
32		"	"	68	-	-
34		"	"	68	-	-
36		"	"	68	-	-
38		"	"	68	-	-
40		"	"	68	-	-
42		"	"	76	-	-
44		"	"	83	-	-
46		"	"	76	-	-

Table E-4a-1. Tabulated data: transition flight, LCH-SDY (023-024), 7/23/75 (con.)

TIME (GMT)	POSITION	HEADING	ALTITUDE observed (ft)	O_3 ($\mu g/m^3$)	TEMP. observed (^oC)	TRUE AIR SPEED observed (mph)
21:48		334°	10500	83	-	-
50		"	"	76	-	-
52		"	"	76	-	-
54		"	"	76	-	-
56		"	"	76	-	-
58	TKO	325°	"	76	-	-
22:00		"	"	76	-	-
02		"	"	76	-	-
04		"	"	68	-	-
06		"	"	61	-	-
08		"	"	61	-	-
10		"	"	61	-	-
12		"	"	61	-	-
14		"	"	61	-	-
16		"	"	54	-	-
18		"	"	61	-	-
20		"	"	61	-	-
22	EAR	"	"	61	-	-
24		"	"	54	-	-
26		"	"	61	-	-
28		"	"	47	-	-
30		"	"	47	-	-
32		"	"	40	-	-
34		"	"	47	-	-
36		"	"	47	-	-
38		"	"	40	-	-
40		"	"	47	-	-
42		"	"	40	-	-
44		"	"	47	-	-
46		"	"	40	-	-
48		"	"	47	-	-
50		"	"	47	-	-
52		"	"	47	-	-
54		"	"	47	-	-
56		"	"	54	-	-
58		"	"	54	-	-
23:00		"	"	54	-	-
02		"	"	54	-	-
04		"	"	61	-	-
06		"	"	68	-	-
08		"	"	76	-	-
09	ANW	321°	"	-	-	-
10		"	"	68	-	-
12		"	"	76	-	-
14		"	"	76	-	-
16		"	"	68	-	-
18		"	"	61	-	-
20		"	"	54	-	-
22		"	"	61	-	-
24		"	"	61	-	-

Table E-4a-1. Tabulated data: transition flight, LCH-SDY (023-024), 7/23/75 (con.)

TIME (GMT)	POSITION	HEADING	ALTITUDE observed (ft)	O_3 ($\mu g/m^3$)	TEMP. observed (°C)	TRUE AIR SPEED observed (mph)
23:26		"	"	61	-	-
28		"	"	61	-	-
30		"	"	61	-	-
32		"	"	61	-	-
34		"	"	61	-	-
36		"	"	61	-	-
38		"	"	61	-	-
40		"	"	61	-	-
42		"	"	61	-	-
44		"	"	61	-	-
46		"	"	61	-	-
48		"	"	61	-	-
50		"	"	61	-	-
52		"	"	61	-	-
54		"	"	61	-	-
56		"	"	61	-	-
58		"	"	61	-	-
00:00		"	"	61	-	-
02		"	"	61	-	-
04		"	"	61	-	-
06		"	"	68	-	-
08		"	"	68	-	-
10		"	"	68	-	-
12		"	"	68	-	-
14		"	"	76	-	-
15	DPR	315°	"	-	-	-
16		"	"	76	-	-
18		"	"	76	-	-
20		"	"	76	-	-
22		"	"	76	-	-
24		"	"	76	-	-
26		"	"	68	-	-
28		"	"	68	-	-
30		"	"	68	-	-
32		"	"	68	-	-
34		"	"	68	-	-
36		"	"	68	-	-
38		"	"	68	-	-
40		"	"	68	-	-
42		"	"	61	-	-
44		"	"	61	-	-
46		"	"	61	-	-
48		"	"	61	-	-
50		"	"	61	-	-
52		"	"	61	-	-
54		"	"	61	-	-
56		"	"	61	-	-
58		"	"	61	-	-
01:00		"	"	54	-	-
02		"	"	54	-	-

Table E-4a-1. Tabulated data: transition flight, LCH-SDY (023-024), 7/23/75 (con.)

TIME (GMT)	POSITION	HEADING	ALTITUDE observed (ft)	O_3 ($\mu g/m^3$)	TEMP. observed (°C)	TRUE AIR SPEED observed (mph)
01:04		"	"	54	-	-
06		"	-	47	-	-
08		"	-	47	-	-
10		"	-	47	-	-
12		"	-	47	-	-
14		"	-	47	-	-
16		"	-	47	-	-
18		"	-	47	-	-
20		"	-	54	-	-
22		"	-	54	-	-
24		"	-	54	-	-
26		"	-	54	-	-
28		"	-	54	-	-
30		"	-	54	-	-
31	SDY	LANDING	1983	-	-	-

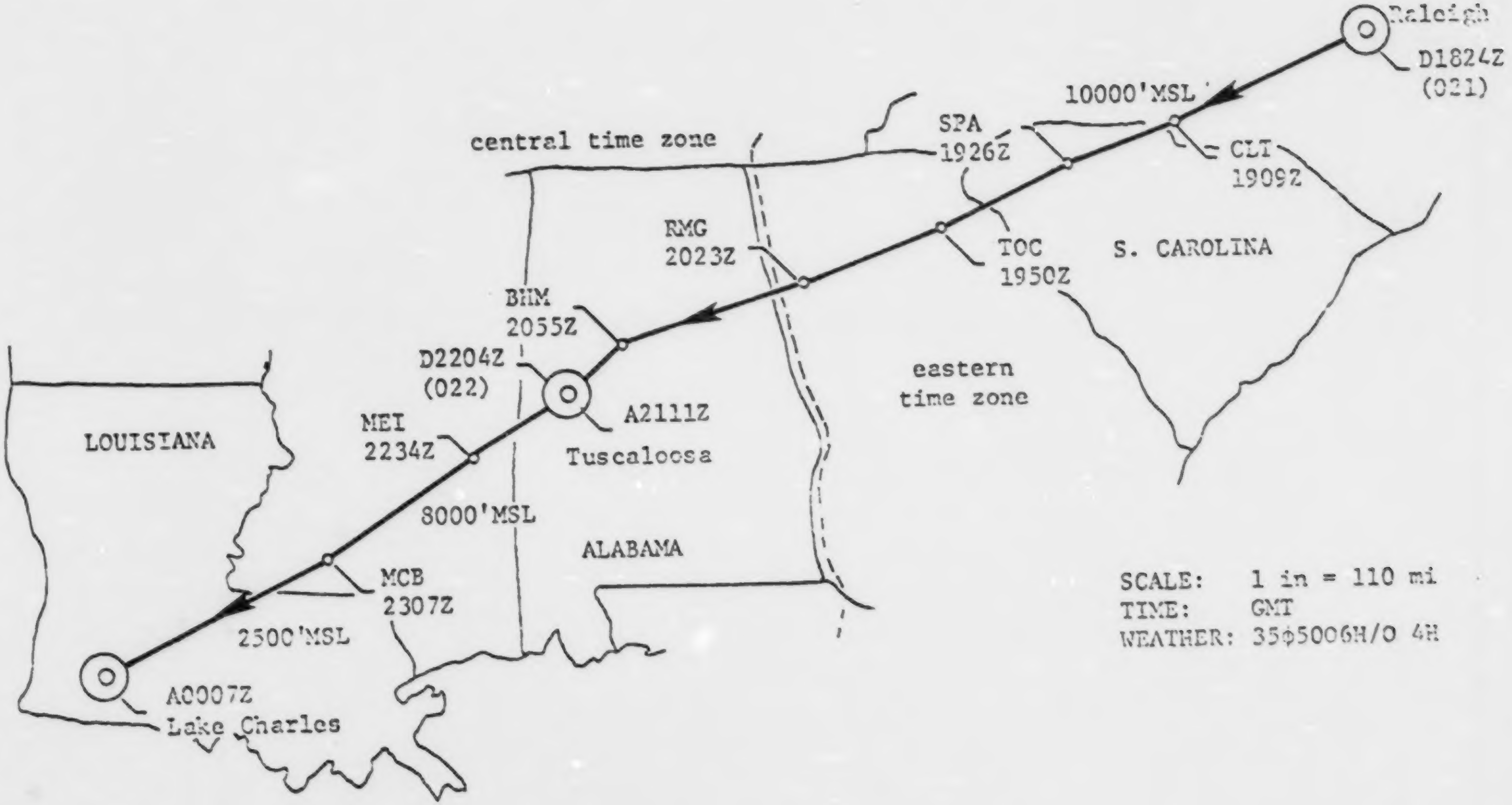
Raleigh
D1824Z
(021)
10000'MSL
CLT
1909Z
SPA
1926Z
TOC
1950Z
S. CAROLINA
central time zone
eastern
time zone
RMG
2023Z
BHM
2055Z
D2204Z
(022)
A2111Z
Tuscaloosa
MEI
2234Z
8000'MSL
ALABAMA
LOUISIANA
MCB
2307Z
2500'MSL
A0007Z
Lake Charles
SCALE: 1 in = 110 mi
TIME: GMT
WEATHER: 35ϕ5006H/0 4H

Figure E-4A-2. Transition flight, RDU-LCH (021-022), 7/22/75.

Table E-4a-2. Tabulated data: high pressure survey flight (025-026), 7/24/75

TIME (GMT)	POSITION	HEADING	ALTITUDE observed (ft)	O_3 ($\mu g/m^3$)	TEMP. observed (°C)	TRUE AIR SPEED observed (mph)
(Flight 025)						
17:07	SDY	TAKEOFF	1983	-	-	-
08	"	-	-	-	-	170
10	"	LOW PASS	2033	-	-	-
12	"	-	-	-	-	-
14	"	117°	-	-	-	-
16		"	-	-	-	-
18		"	4000	-	-	190
20		"	"	42	-	-
22		"	"	37	-	-
24		"	"	37	-	-
26		"	"	37	-	-
28		"	"	42	-	-
30		"	"	37	-	-
32		"	"	37	-	-
34		"	"	37	-	-
36		"	"	37	-	-
38	BELFIELD	118°	"	37	-	-
40		"	"	42	-	-
42		"	"	42	-	-
44		"	"	42	-	-
46		"	"	42	-	-
48		"	"	42	-	-
50		"	"	42	-	-
52		"	"	37	-	-
54		"	"	37	-	-
56		"	"	37	-	-
58		"	"	37	-	-
18:00		"	"	37	-	-
02		"	"	37	-	-
04		"	"	37	-	-
06		"	"	37	-	-
08		"	"	37	-	-
10		"	"	37	-	-
12		"	"	42	-	-
14		"	"	37	-	-
16		"	"	37	-	-
18		"	"	37	-	-
20		"	"	37	-	-
22		"	"	37	-	-
24		"	"	37	-	-
26		"	"	37	-	-
28		"	"	37	-	-
30		"	"	37	-	-
32	RIDGEVIEW	"	"	37	-	-
34		"	"	37	-	-
36		"	"	37	-	-
38		"	"	37	-	-
40		"	"	37	-	-
18:42		"	"	37	-	-
44		"	"	42	-	-

Table E-4a-2. Tabulated data: high pressure survey flight (025-026), 7/24/75 (con.)

TIME (GMT)	POSITION	HEADING	ALTITUDE observed (ft)	O_3 ($\mu g/m^3$)	TEMP. observed (^oC)	TRUE AIR SPEED observed (mph)
18:46		"	"	42	-	-
48		"	"	42	-	-
50	PIR	076°	4000	42	-	190
52		"	"	42	-	-
54		"	"	42	-	-
56		"	"	42	-	-
58		"	"	42	-	-
19:00		"	"	42	-	-
02		"	"	42	-	-
04		"	"	37	-	-
06		"	"	37	-	-
08		"	"	37	-	-
10		"	"	37	-	-
12		"	"	32	-	-
14		"	"	32	-	-
16		"	"	32	-	-
18	HON	VERTICAL	"	-	-	-
20		"	5000	34	-	-
23		"	6000	36	11	-
28		"	8000	52	10	-
33		"	10000	87	-	-
39		"	12000	52	5	-
44		"	10000	-	-	-
49		"	8000	64	10.5	-
56		"	6000	36	12	-
20:00		"	5000	34	-	-
04		"	4000	32	18	-
06		"	-	-	-	-
08		"	-	-	-	-
09	HON	LANDING	1287	-	-	-
(Flight 026)						
21:32	HON	TAKEOFF	1287	-	31	140
34	"	152°	-	-	-	-
42		"	5500	-	15	190
44		"	"	40	-	-
46		"	"	40	-	-
48		"	"	40	-	-
50		"	"	40	-	-
52		"	"	45	-	-
54		"	"	45	-	-
56		"	"	45	-	-
58		"	"	45	-	-
22:00		"	"	45	-	-
02		"	"	45	-	-
04		"	"	45	-	-
06		"	"	45	-	-
08		"	"	50	-	-
10		"	"	56	-	-
12		"	"	56	-	-
14		"	"	56	-	-
16		"	"	56	-	-

Table E-4a-2. Tabulated data: high pressure survey flight (025-026), 7/24/75 (con.)

TIME (GMT)	POSITION	HEADING	ALTITUDE observed (ft)	O_3 ($\mu g/m^3$)	TEMP. observed (^{o}C)	TRUE AIR SPEED observed (mph)
22:18		"	"	61	-	-
20		"	"	61	-	-
24	RANDOLPH	"	"	-	-	-
44		"	-	-	-	-
57	LINCOLN	LANDING	1198	-	-	-

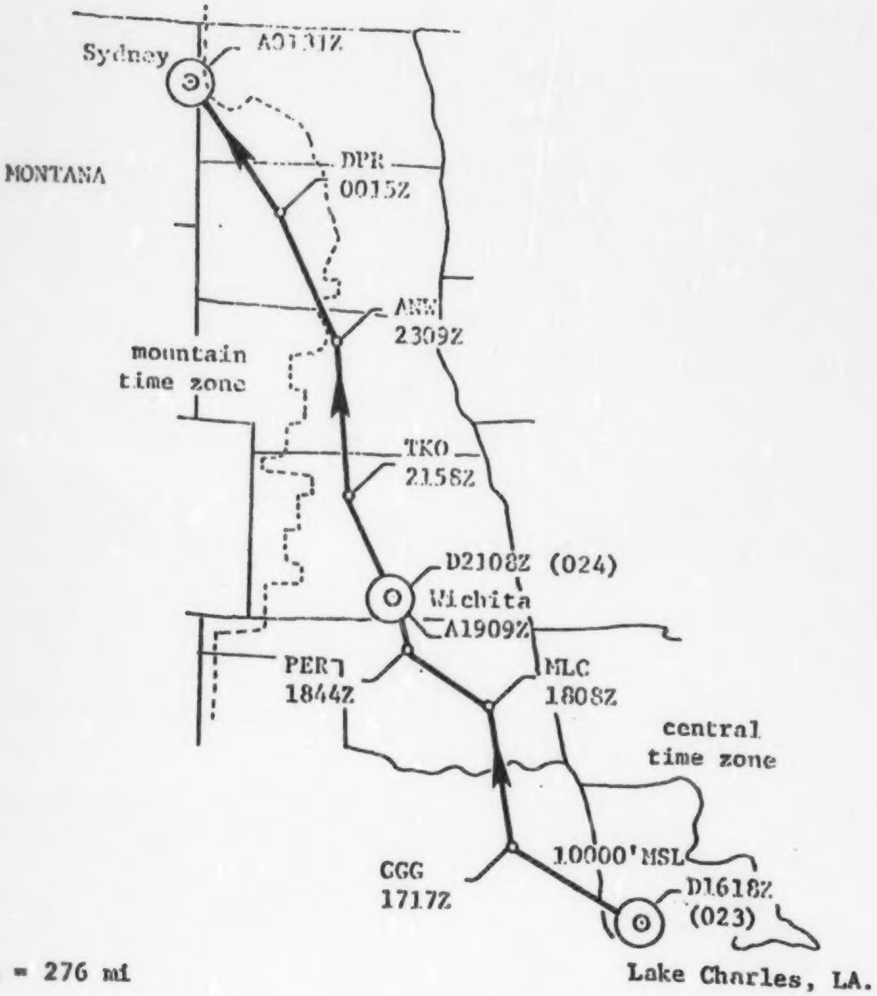
Sydney
A0131Z
MONTANA
DPR
0015Z
ANW
2309Z
mountain
time zone
TKO
2158Z
D2108Z (024)
Wichita
A1909Z
PER
1844Z
MLC
1808Z
central
time zone
10000'MSL
GGG
1717Z
D1618Z
(023)
Lake Charles, LA.

SCALE: 1 in = 276 mi
TIME: GMT
WEATHER: O 8+H/120015+H

Figure E-4A-3. Transition flight, LCH-SDY (023-024), 7/23/75.

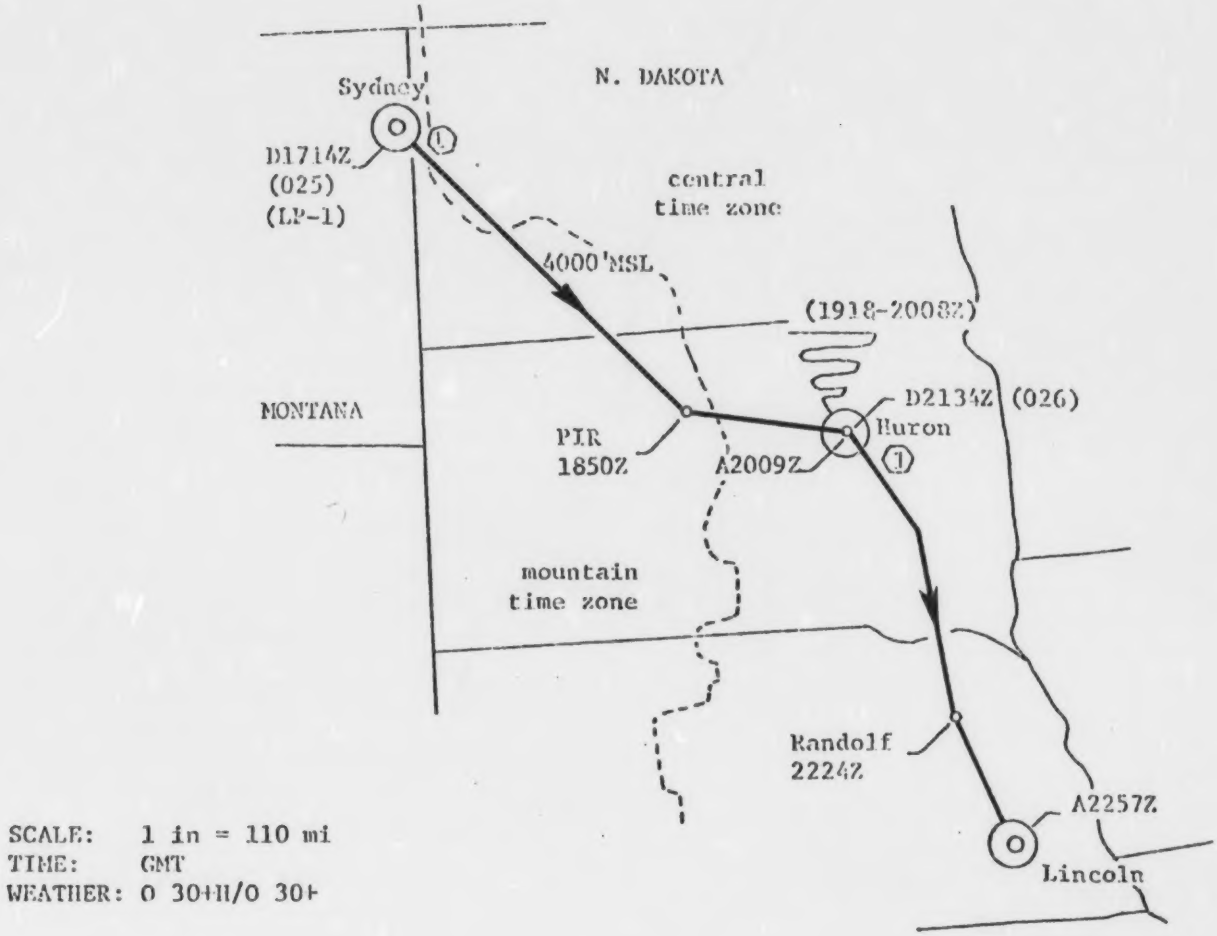
Sydney
N. DAKOTA
D1714Z
(025)
(LP-1)
①
central
time zone
4000'MSL
(1918-2008Z)
MONTANA
PIR
1850Z
D2134Z (026)
Huron
A2009Z
①
mountain
time zone
Randolf
2224Z
A2257Z
Lincoln
SCALE: 1 in = 110 mi
TIME: GMT
WEATHER: O 30+H/O 30+

Figure E-4A-4. High pressure survey flight (025-026), 7/24/75.

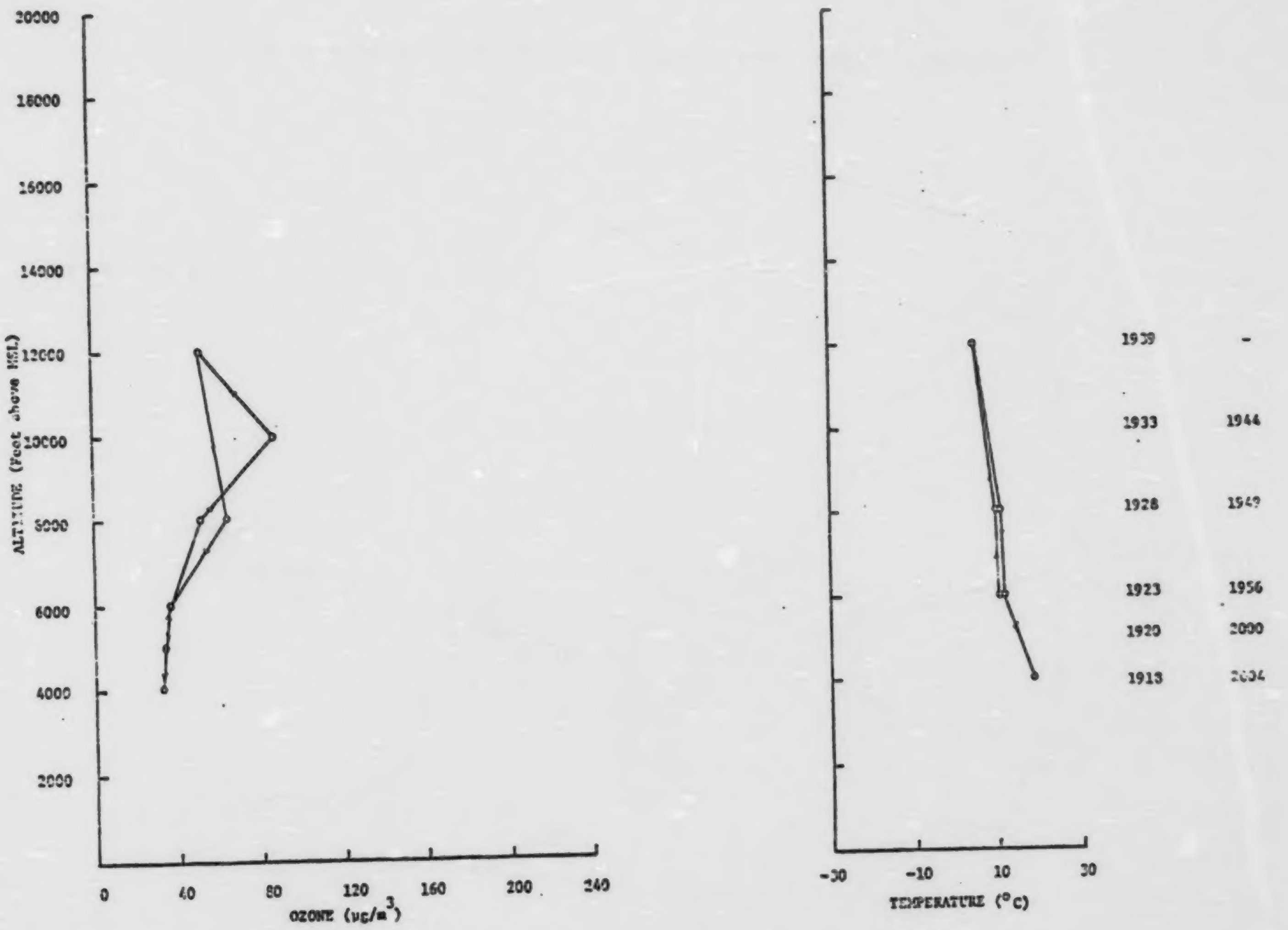

Figure E-4A-5. Vertical profile, Huron, South Dakota (025), 7/24/75.

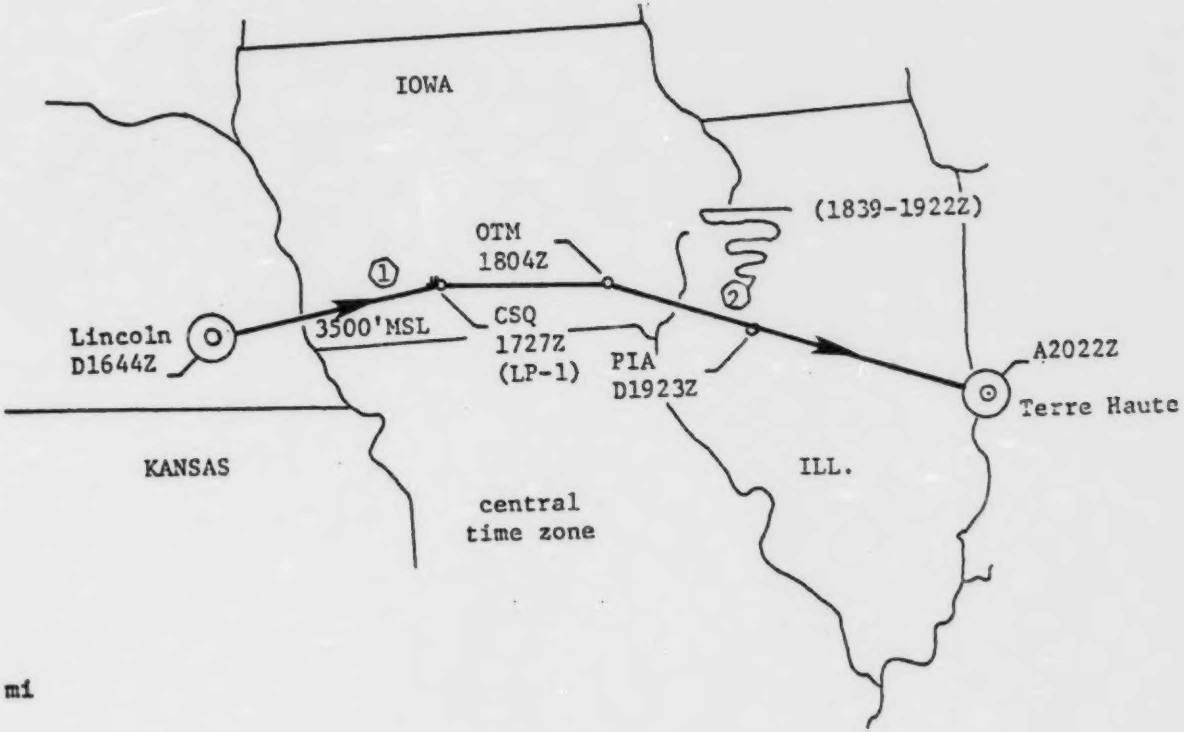
IOWA
(1839-1922Z)
OTM
1804Z
①
②
Lincoln
D1644Z
3500'MSL
CSQ
1727Z
(LP-1)
PIA
D1923Z
A2022Z
Terre Haute
KANSAS
ILL.
central
time zone

SCALE: 1 in = 110 mi
TIME: GMT
WEATHER: O 20+H

Figure E-4A-6. High pressure survey flight (027), 7/25/75.

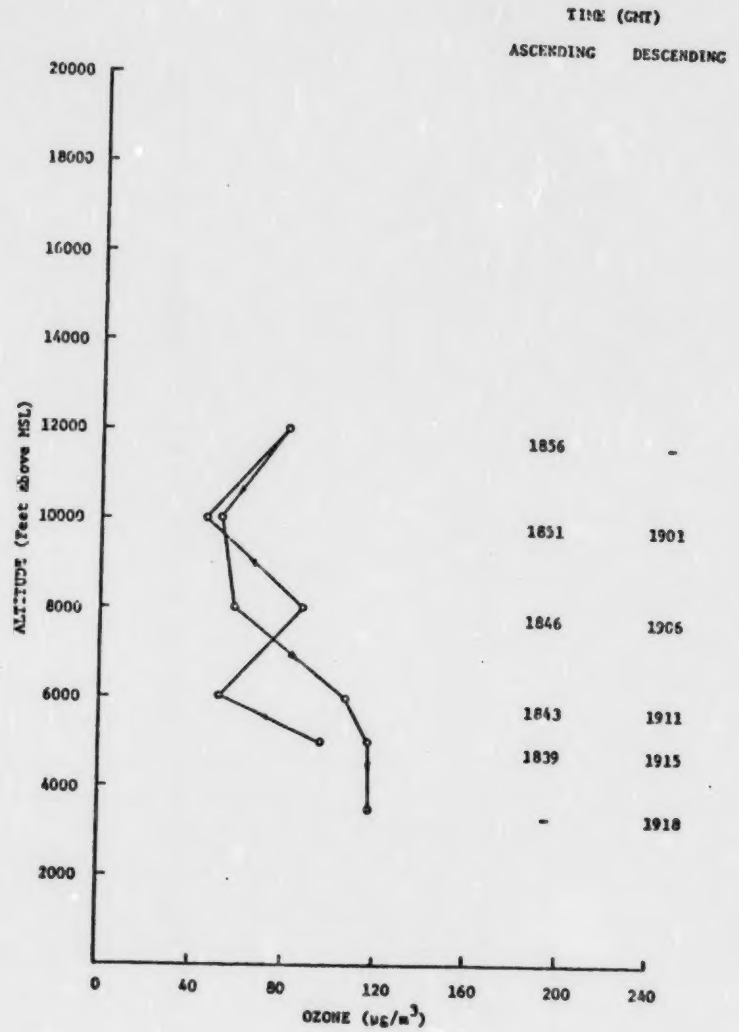

Figure E-4A-7. Vertical profile, Peoria, Illinois (027), 7/25/75.

Table E-4a-3. Tabulated data: high pressure survey flight (027), 7/25/75

TIME (GMT)	POSITION	HEADING	ALTITUDE observed (ft)	O_3 ($\mu g/m^3$)	TEMP. observed (°C)	TRUE AIR SPEED observed (mph)
16:43	LNK	TAKEOFF	1198	-	-	140
44	"	078°	-	-	-	-
50		"	3500	-	-	190
52		"	"	99	-	-
54		"	"	99	-	-
56		"	"	94	-	-
58		"	"	94	-	-
17:00		"	"	89	-	-
02		"	"	94	-	-
04		"	"	94	-	-
06		"	"	89	-	-
08		"	"	84	-	-
10		"	"	84	-	-
12	RED OAK	"	"	84	-	-
14		"	"	84	-	-
16		"	"	84	-	-
18		"	"	84	-	-
20		"	"	84	-	-
22		"	"	84	-	-
24		"	-	-	-	-
26		"	-	-	-	-
27	CSQ	LOW PASS	-	81	-	-
28	"	-	-	-	-	-
30	"	078°	3500	79	-	-
32		"	"	79	-	-
34		"	"	79	-	-
36		"	"	79	-	-
38		"	"	79	-	-
40		"	"	70	-	-
42		"	"	75	-	-
44		"	"	75	-	-
46		"	"	75	-	-
48		"	"	75	-	-
50		"	"	79	-	-
52		"	"	79	-	-
54		"	"	84	-	-
56		"	"	84	-	-
58		"	"	84	-	-
18:00		"	"	84	-	-
02		"	"	84	-	-
04	OTM	100°	3500	89	17	-
06		"	"	84	-	-
08		"	"	75	-	-
10		"	"	84	-	-
12		"	"	84	-	-
14		"	"	79	-	-
16		"	"	79	-	-
18		"	"	79	-	-
20		"	"	79	-	-
22		"	"	79	-	-

Table E-4a-3. Tabulated data: high pressure survey flight (027), 7/25/75 (con.)

TIME (GMT)	POSITION	HEADING	ALTITUDE observed (ft)	O_3 ($\mu g/m^3$)	TEMP. observed (°C)	TRUE AIR SPEED observed (mph)
18:24		"	"	79	-	-
26		"	"	79	-	-
28	BRL	088°	3500	84	-	-
30		"	"	-	-	-
32		"	"	-	-	-
34		"	"	-	-	-
36		"	-	-	-	-
39	PIA	VERTICAL	5000	96	-	-
43	"	"	6000	52	-	-
46	"	"	8000	88	-	-
51	"	"	10000	45	-	-
56	"	"	12000	80	5	-
19:01	"	"	10000	52	-	-
06	"	"	8000	58	-	-
11	"	"	6000	106	-	-
15	"	"	5000	117	-	-
18	"	"	3500	118	-	-
20	"	"	"	108	-	-
22	"	"	"	108	-	-
23	"	117°	"	-	-	-
24		"	"	108	-	-
26		"	"	108	-	-
28		"	"	104	-	-
30		"	"	108	-	-
32		"	"	36	-	-
34		"	"	108	-	-
36		"	"	123	-	-
38		"	"	89	-	-
40		"	"	89	-	-
42		"	"	89	-	-
44		"	"	89	-	-
46		"	"	89	-	-
48		"	"	94	-	-
50		"	"	89	-	-
52		"	"	79	-	-
54		"	"	89	-	-
56		"	"	89	-	-
58		"	"	89	-	-
20:00		"	"	104	-	-
02		"	"	104	-	-
04		"	"	108	-	-
06		"	"	108	-	-
08		"	"	118	-	-
10		"	"	108	-	-
12		"	"	108	-	-
14		"	"	108	-	-
15		140°	"	-	-	-
16		"	"	113	-	-
18		"	"	104	-	-
20		"	"	99	-	-
22	TERRE HAUTE	LANDING	585	-	-	-

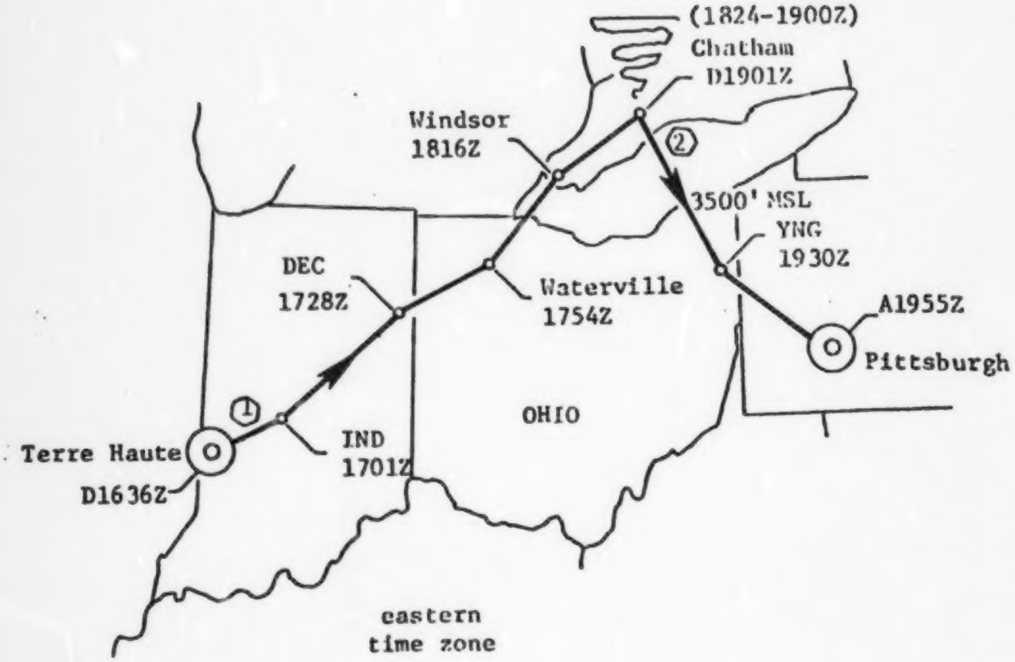
(1824-1900Z)
Chatham
D1901Z
Windsor
1816Z
②
3500' MSL
YNG
1930Z
DEC
1728Z
Waterville
1754Z
A1955Z
Pittsburgh
①
OHIO
Terre Haute
IND
1701Z
D1636Z
eastern
time zone

SCALE: 1 in = 110 mi
TIME: GMT
WEATHER: 5008+H

Figure E-4A-8. High pressure survey flight (028), 7/26/75.

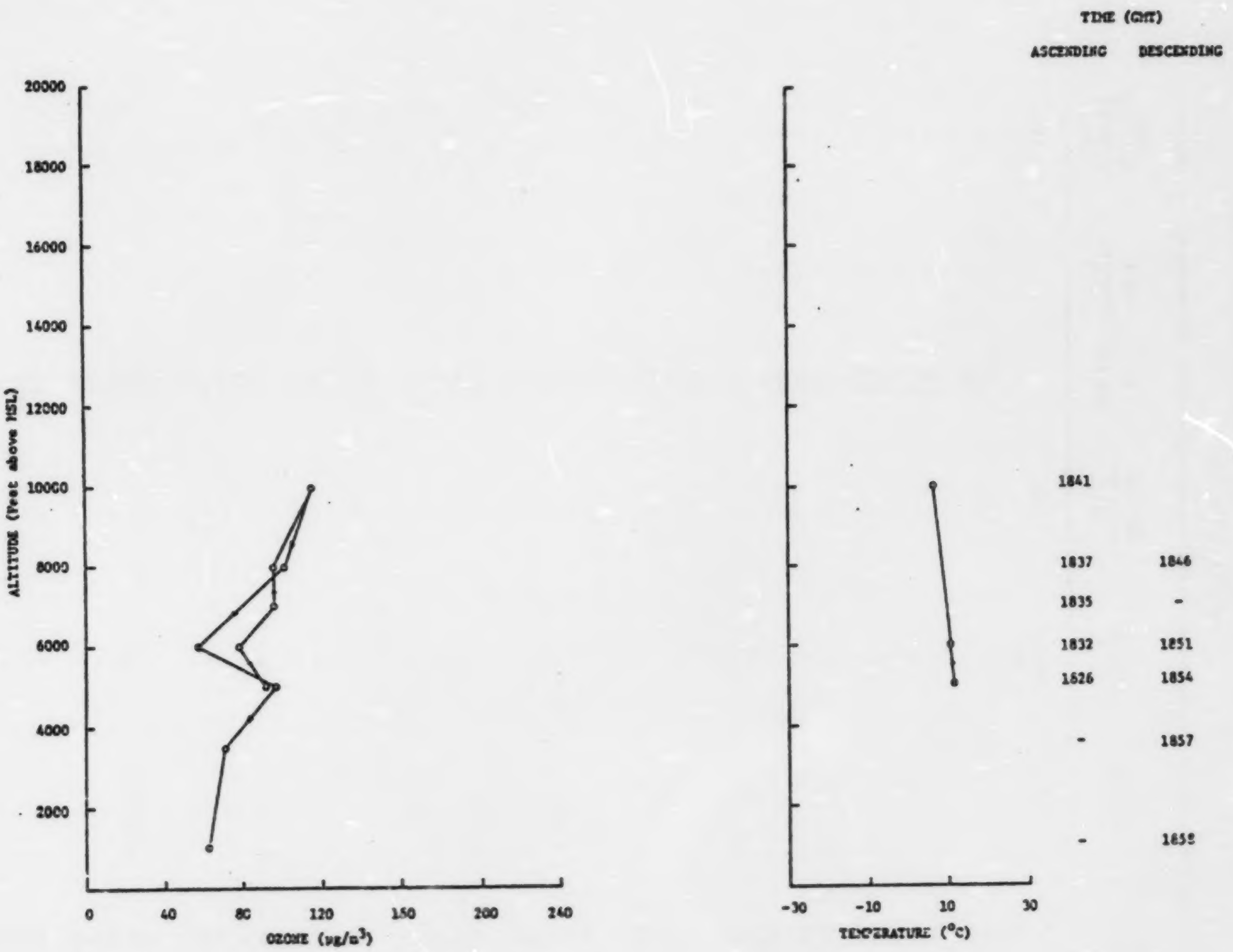

Figure E-4A-9. Vertical profile, Chatham (028), 7/26/75.

Table E-4a-4. Tabulated data: high pressure survey flight (028), 7/26/75

TIME (GMT)	POSITION	HEADING	ALTITUDE observed (ft)	O_3 ($\mu g/m^3$)	TEMP. observed (°C)	TRUE AIR SPEED observed (mph)
16:35	HUF	TAKEOFF	585	-	-	140
36	"	053°	-	-	-	-
38		"	-	-	-	-
40		"	3500	118	-	190
42		"	"	108	-	-
44		"	"	108	-	-
46		"	"	108	-	-
48		"	"	104	-	-
50		"	"	113	-	-
52		"	"	118	-	-
54		"	"	118	-	-
56		"	"	118	-	-
58		"	"	128	-	-
17:00		"	"	113	-	-
01	IND	"	"	-	-	-
02		"	"	108	-	-
04		"	"	108	-	-
06		"	"	108	-	-
08		"	"	104	-	-
10		"	"	104	-	-
12		"	"	99	-	-
14		"	"	99	-	-
16		"	"	99	-	-
18		"	"	99	-	-
20		"	"	99	-	-
22		"	"	104	-	-
24		"	"	104	-	-
26		"	"	104	-	-
28		"	"	108	-	-
29	DEC	"	"	-	-	-
30		"	"	113	-	-
32		"	"	113	-	-
34		"	"	108	-	-
36		"	"	104	-	-
38		"	"	104	-	-
40		"	"	108	-	-
42		"	"	108	-	-
44		"	"	113	-	-
46		"	"	113	-	-
48		"	"	118	-	-
50		"	"	104	-	-
52		"	"	104	-	-
54	WATERVILLE	040°	"	104	-	-
56		"	"	104	-	-
58		"	"	89	-	-
18:00		"	"	104	-	-
02		"	"	128	-	-
04		"	"	157	-	-
06		"	"	-	-	-
08		"	"	84	-	-
10		"	"	65	-	-

Table E-4a-4. Tabulated data: high pressure survey flight (028), 7/26/75 (con.)

TIME (GMT)	POSITION	HEADING	ALTITUDE observed (ft)	O_3 ($\mu g/m^3$)	TEMP. observed (°C)	TRUE AIR SPEED observed (mph)
18:12		"	"	75	-	-
14		"	"	80	-	-
16	WINDSOR	077°	"	89	-	-
18		"	"	84	-	-
20		"	"	84	-	-
22		"	"	89	-	-
24	CHATHAM	VERTICAL	-	-	-	-
26	"	"	5000	91	12	-
32	"	"	6000	79	11	-
35	"	"	7000	95	-	-
37	"	"	8000	95	-	-
41	"	"	10000	115	7	-
46	"	"	8000	101	-	-
51	"	"	6000	57	-	-
54	"	"	5000	96	-	-
57	"	"	3500	70	-	-
58	"	"	1000	62	-	-
19:00	"	"	-	-	-	-
01	"	145°	1000	65	-	-
02		"	"	75	-	-
04		"	-	80	-	-
06		"	-	-	-	-
08		"	-	-	-	-
10		"	3500	-	-	-
12		"	"	65	-	-
14	LOST NATION	"	"	60	-	-
16		"	"	55	-	-
18		"	"	65	-	-
20		"	"	80	-	-
22		"	"	-	-	-
24		"	"	99	-	-
26		"	"	84	-	-
28		"	"	99	-	-
30	YNG	"	"	99	-	-
32		"	"	113	-	-
34		"	"	113	-	-
36		"	"	137	-	-
38		"	"	128	-	-
40		"	"	104	-	-
42		"	"	99	-	-
44		"	"	104	-	-
46		"	"	108	-	-
48		"	"	128	-	-
50		"	-	-	-	-
55	ALLEGHENY	LANDING	1252	-	-	-

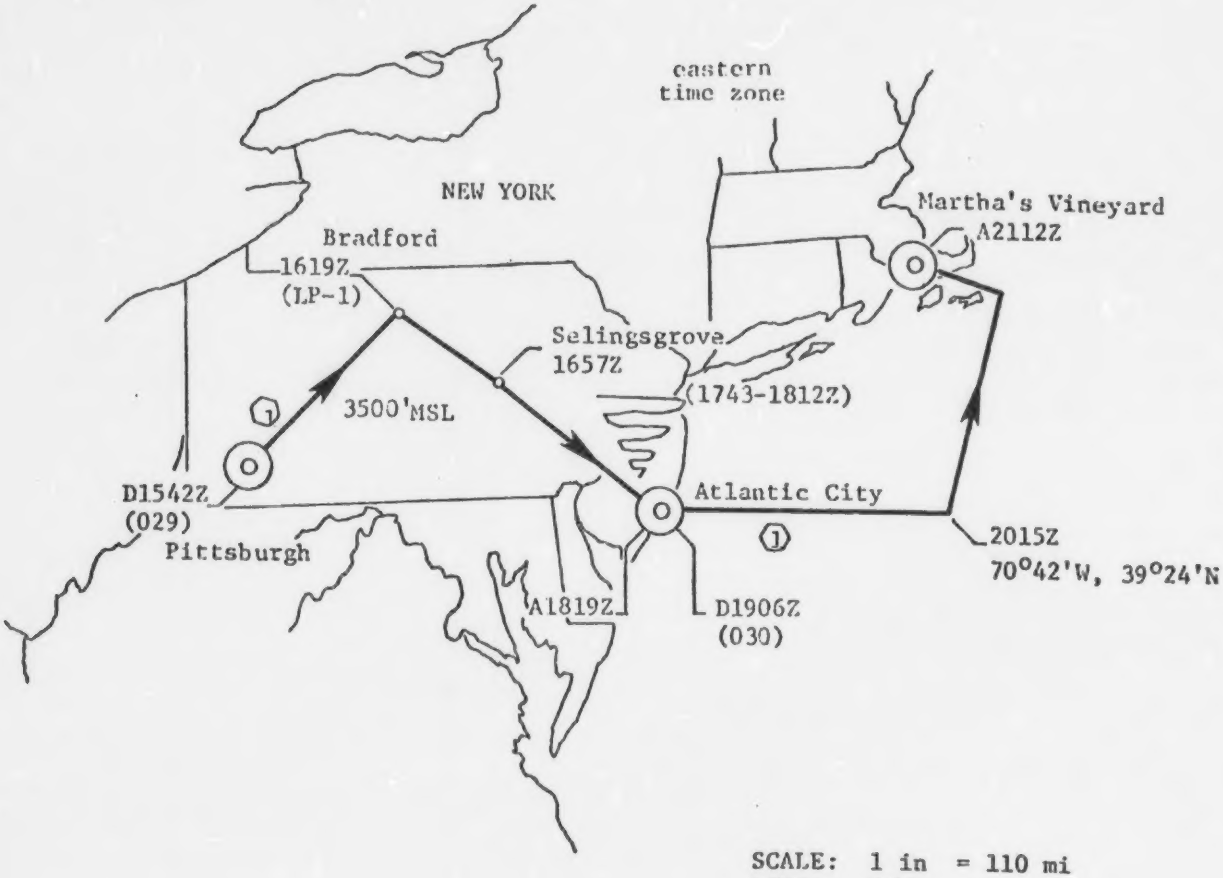
eastern time zone
NEW YORK
Bradford
1619Z
(LP-1)
Martha's Vineyard
A2112Z
Selingsgrove
1657Z
(1743-1812Z)
1
3500'MSL
D1542Z
(029)
Pittsburgh
Atlantic City
1
2015Z
70°42'W, 39°24'N
A1819Z
D1906Z
(030)

SCALE: 1 in = 110 mi
TIME: GMT
WEATHER: 5004KH/700

Figure E-4A-10. High pressure survey flight (029-030), 7/27/75.

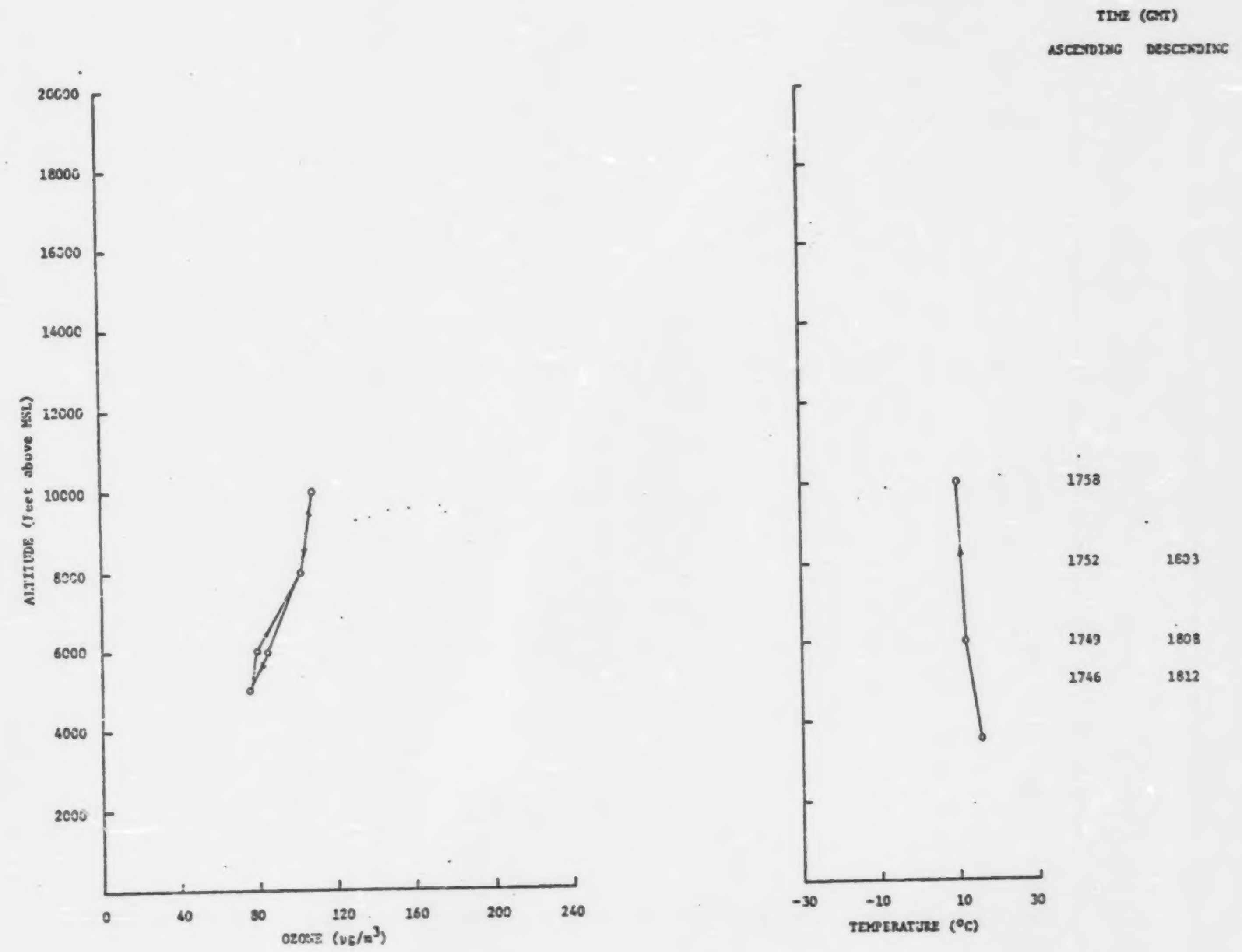

Figure E-4A-11. Vertical profile, Atlantic City, New Jersey (029), 7/27/75.

Table E-4a-5. Tabulated data: high pressure survey flight (029-030), 7/27/75

TIME (GMT)	POSITION	HEADING	ALTITUDE observed (ft)	O_3 (μg/m^3)	TEMP. observed (°C)	TRUE AIR SPEED observed (mph)
(Flight 029)						
15:40	AGC	TAKEOFF	1252	-	-	140
42	"	040°	-	-	-	-
44		"	3500	137	-	190
46		"	"	-	-	-
48		"	"	161	-	-
50		"	"	161	-	-
52		"	"	171	-	-
54		"	"	166	-	-
56		"	"	161	-	-
58		"	"	161	-	-
16:00		"	"	157	-	-
02		"	"	152	-	-
04		"	"	147	-	-
06		"	"	152	-	-
08		"	"	152	-	-
10		"	"	147	-	-
12		"	"	147	-	-
14		"	"	147	-	-
16		"	-	147	-	-
18		"	-	147	-	-
19	BFD	LOW PASS	-	-	-	-
20	"	"	-	122	18	-
21	"	040°	-	-	-	-
22		"	-	147	-	-
24		"	3500	147	-	-
26		"	"	142	-	-
28		"	"	142	-	-
30		"	"	137	-	-
32		"	"	142	-	-
34		"	"	137	-	-
36		"	"	137	-	-
38		"	"	147	-	-
40		"	"	157	-	-
42		"	"	132	-	-
44	PIPER MEMORIAL	"	"	147	-	-
46		"	"	157	-	-
48		"	"	142	-	-
50		"	"	137	-	-
52		"	"	128	-	-
54		"	"	147	-	-
56		"	"	137	-	-
57	SELINGSGROVE	137°	"	-	16	-
58		"	"	-	-	-
17:00		"	"	161	-	-
02		"	"	147	-	-

Table E-4a-5. Tabulated data: high pressure survey flight (029-030), 7/27/75 (con.)

TIME (GMT)	POSITION	HEADING	ALTITUDE observed (ft)	O_3 ($\mu g/m^3$)	TEMP. observed (^oC)	TRUE AIR SPEED observed (mph)
17:14		"	"	118	-	-
16		"	"	123	-	-
18		"	"	128	-	-
20		"	"	118	-	-
22		"	"	118	-	-
24		"	"	118	-	-
26		"	"	132	-	-
28		"	"	132	-	-
30		"	"	166	-	-
32		"	"	-	-	-
34		"	"	214	-	-
36		"	"	157	-	-
38		"	"	176	-	-
40		"	"	176	-	-
42		"	"	166	16	-
43	ACY	VERTICAL	-	-	-	-
46	"	"	5000	75	-	-
49	"	"	6000	79	12	-
52	"	"	8000	101	-	-
58	"	"	10000	108	10	-
18:03	"	"	8000	101	-	-
08	"	"	6000	85	-	-
12	"	"	5000	75	-	-
19	"	LANDING	76	-	-	-
(Flight 030)						
19:05	ACY	TAKEOFF	76	-	-	140
06	"	112°	-	-	-	-
08		"	-	-	-	-
09	COAST	"	3000	-	-	190
10		"	"	-	-	-
12		"	"	153	-	-
14		"	"	139	-	-
16		"	"	139	-	-
18		"	"	78	-	-
20		"	"	115	-	-
22		"	"	120	-	-
24		"	"	125	-	-
26		"	"	110	-	-
28		"	"	120	-	-
30		"	"	115	-	-
32		"	"	115	-	-
34		"	"	115	-	-
36		"	"	106	-	-
38		"	"	87	-	-
40		"	"	73	-	-
42		"	"	87	-	-
44		"	"	82	-	-
46		"	"	97	-	-
48		"	"	101	-	-
50		"	"	82	-	-

Table E-4a-5. Tabulated data: high pressure survey flight (029-030), 7/27/75 (con.)

TIME (GMT)	POSITION	HEADING	ALTITUDE observed (ft)	O_3 ($\mu g/m^3$)	TEMP. observed (^oC)	TRUE AIR SPEED observed (mph)
19:52		"	"	82	-	-
54		"	"	78	-	-
56		"	"	78	-	-
58		"	"	55	-	-
20:00		"	-	-	16	-
02		"	3500	46	18	-
04		"	"	46	-	-
06		"	"	70	-	-
08		"	"	55	-	-
10		"	"	70	-	-
12		"	"	80	-	-
14		"	"	65	-	-
15	70°42'W,39°24'N	355°	-	-	-	-
16		"	"	70	-	-
18		"	"	67	-	-
20		"	"	75	-	-
22		"	"	80	-	-
24		"	"	80	-	-
26		"	"	60	-	-
28		"	"	70	-	-
30		"	"	55	-	-
32		"	"	70	-	-
34		"	"	65	-	-
36		"	"	46	-	-
38		"	"	51	-	-
40		"	"	46	-	-
42		"	"	46	-	-
44		"	"	46	-	-
46		"	"	51	-	-
48		"	"	51	-	-
50		"	"	51	-	-
52		"	"	51	-	-
54		"	"	51	-	-
56		"	"	46	-	-
58	NANTUCKET	"	"	51	-	-
21:00		"	"	46	-	-
02		"	"	75	-	-
04		"	"	84	-	-
05		"	-	-	-	-
12	MARTHA'S VINEYARD	LANDING	68	-	-	-

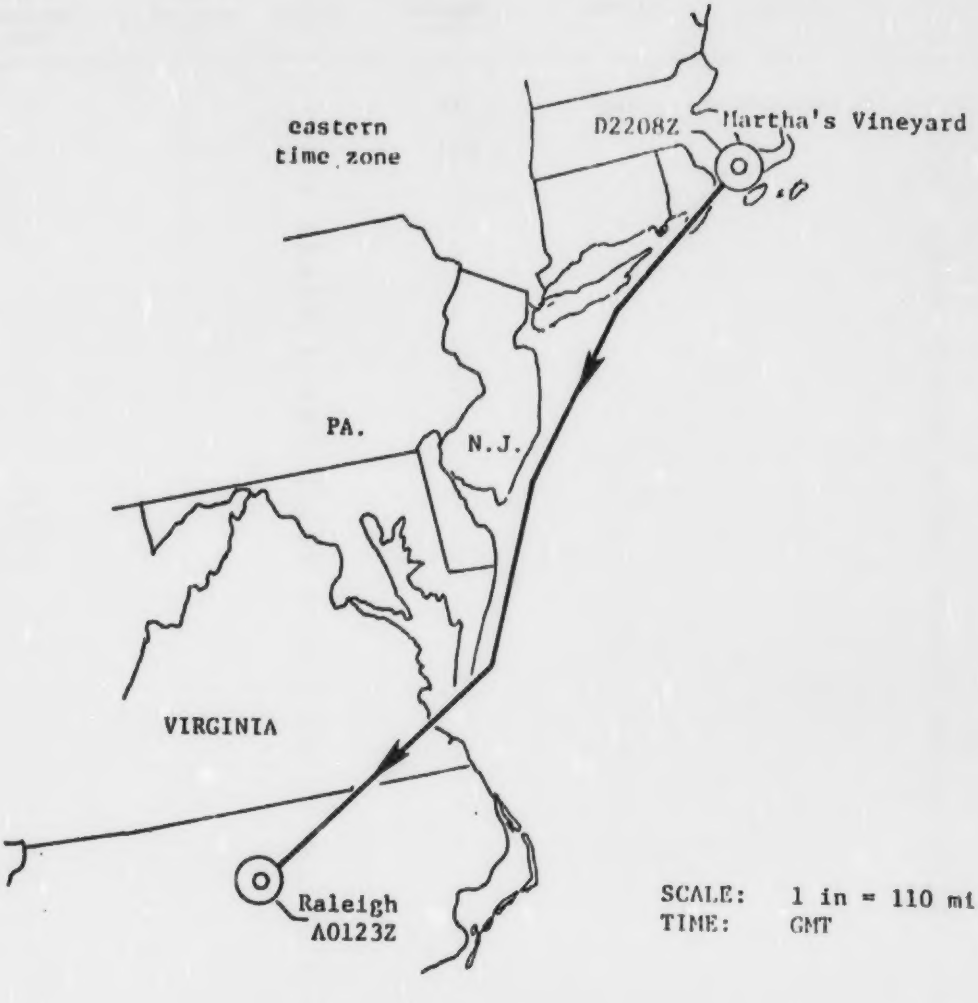

eastern
time zone
D2208Z
Martha's Vineyard
PA.
N.J.
VIRGINIA
Raleigh
A0123Z
SCALE: 1 in = 110 mi
TIME: GMT

Figure E-4A-12. Transition flight, ACK-RDU (031), 7/27/75.

Table E-4a-6. Tabulated data: transition flight, ACK-RDU (031), 7/27/75

TIME (GMT)	POSITION	HEADING	ALTITUDE observed (ft)	O_3 (μg/m^3)	TEMP. observed (°C)	TRUE AIR SPEED observed (mph)
22:08	MARTHA'S VINEYARD	TAKEOFF	68	-	-	140
10	"	260°	-	-	-	-
12		"	4500	-	-	190
14		"	"	-	-	-
16		"	"	94	-	-
18		"	"	88	-	-
20		"	"	104	-	-
22		"	"	88	-	-
24		"	"	104	-	-
26		"	"	114	-	-
28		"	"	99	-	-
30		"	"	-	-	-
32		"	"	94	-	-
34		"	"	99	-	-
36		"	"	109	-	-
38		"	"	104	-	-
40		"	"	104	-	-
42		"	"	109	-	-
44		"	"	88	-	-
46		"	"	88	-	-
48		"	"	83	-	-
50		"	"	83	-	-
52		236°	"	78	-	-
54		"	"	78	-	-
56		"	"	78	-	-
58		"	"	78	-	-
23:00		"	"	78	-	-
02		"	"	73	-	-
04		"	"	73	-	-
06		"	"	73	-	-
08		"	"	78	-	-
10		"	"	73	-	-
12		"	"	73	-	-
14		"	"	73	-	-
16		"	"	78	-	-
18		"	"	78	-	-
20		"	"	78	-	-
22		"	"	78	-	-
24		"	"	78	-	-
26		"	"	78	-	-
28		"	"	83	-	-
30		"	"	83	-	-
32		"	"	78	-	-
34		"	"	94	-	-
36		"	"	124	-	-
37		218°	"	-	-	-
38		"	"	124	-	-
40		"	"	129	-	-
42		"	"	149	-	-
44		"	"	144	-	-

Table E-4a-6. Tabulated data: transition flight, ACK-RDU (031), 7/27/75 (con.)

TIME (GMT)	POSITION	HEADING	ALTITUDE observed (ft)	O_3 ($\mu g/m^3$)	TEMP. observed (°C)	TRUE AIR SPEED observed (mph)
23:46		"	"	134	-	-
48		"	"	119	-	-
50		"	"	119	-	-
51		"	"	-	-	180
52		"	"	-	-	-
54		"	"	-	-	-
56		"	"	-	-	-
58		"	"	-	-	-
24:00		"	6500	98	-	190
02		"	"	93	-	-
03		240°	"	-	-	-
04		"	"	98	-	-
06		"	"	98	-	-
08		"	"	93	-	-
10		"	"	104	-	-
12		"	"	104	-	-
14		"	"	104	-	-
16		"	"	104	-	-
18		"	"	109	-	-
20		"	"	115	-	-
22		"	"	121	-	-
24		"	"	121	-	-
26		"	"	121	-	-
28		"	"	126	-	-
30		"	"	126	-	-
32		"	"	115	-	-
34		"	"	115	-	-
36		"	"	109	-	-
38		"	"	109	-	-
40		"	"	109	-	-
42		"	"	109	-	-
44		"	"	115	-	-
46	FRANKLIN	246°	"	121	-	-
48		"	"	121	-	-
50		"	"	121	-	-
52		"	"	126		
54		"	"	115	-	-
56		"	"	115	-	-
58		"	"	115	-	-
01:00		"	"	115	-	-
02		"	"	115	-	-
04		"	"	115	-	-
06		"	"	121	-	-
08		"	"	137	-	-
10		"	"	137	-	-
12		"	-	154	-	-
14		"	-	165	-	-
16		"	-	154	-	-
18		"	-	149	-	-
20		"	-	137	-	-
22		"	-	137	-	-
23	RDU	LANDING	436	-	-	-

SELECTED EXAMPLES OF THE DOWN WIND PLUME FLIGHT - GULF COAST OXIDANT STUDY

E-4B--Flight No. 005 on June 26, 1975.

E-4C--Flight No. 006 on June 27, 1975.

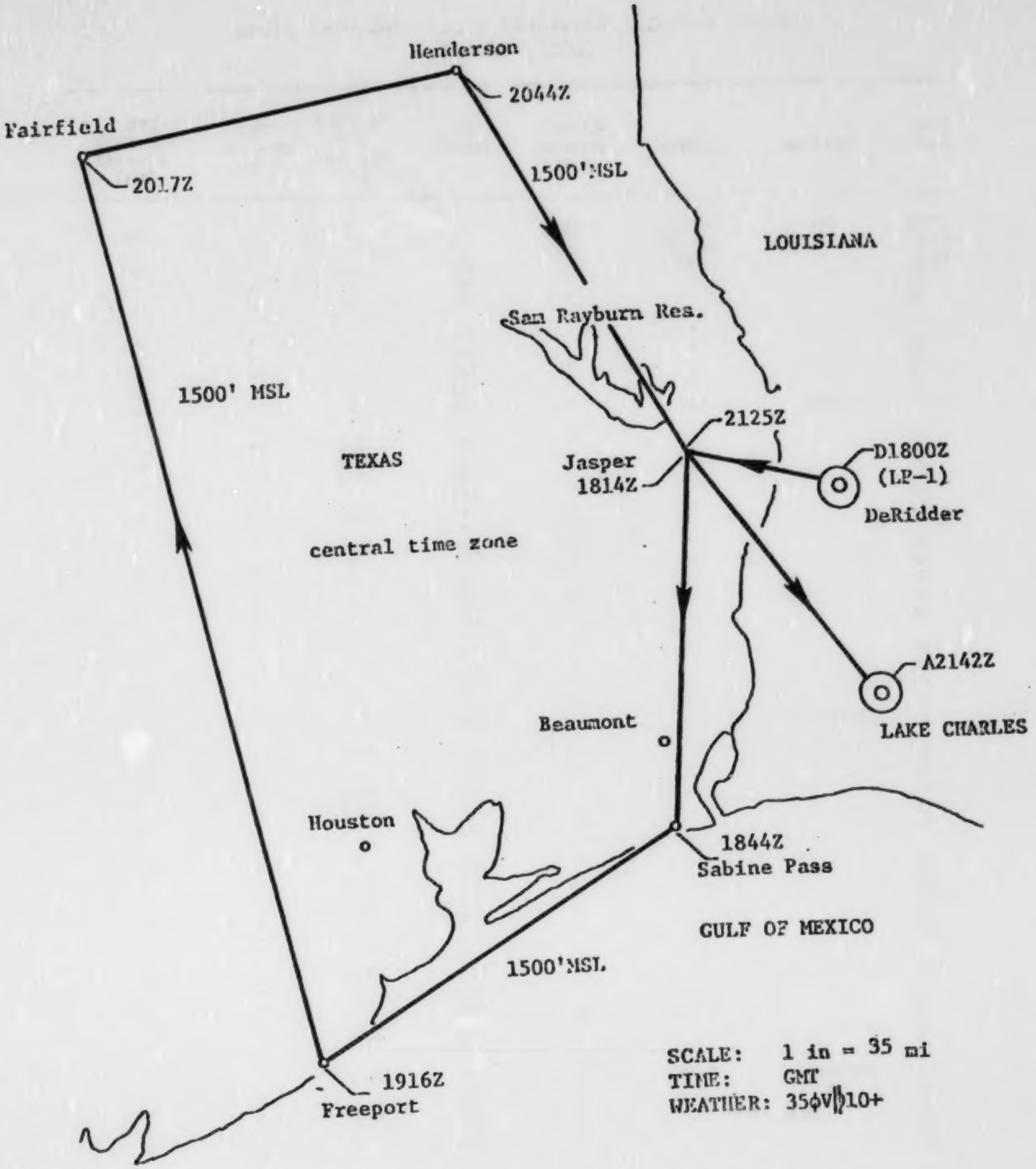
Henderson
2044Z
Fairfield
2017Z
1500'MSL
LOUISIANA
San Rayburn Res.
1500' MSL
2125Z
Jasper
1814Z
D1800Z
(LP-1)
DeRidder
TEXAS
central time zone
A2142Z
LAKE CHARLES
Beaumont
Houston
1844Z
Sabine Pass
GULF OF MEXICO
1500'MSL
SCALE: 1 in = 35 mi
TIME: GMT
WEATHER: 350V⊕10+
1916Z
Freeport

Figure E-4B-1. Downwind plume flight (005), 6/26/75.

Table E-4b-1. Tabulated data: downwind plume (005), 6/26/75

TIME (GMT)	POSITION	HEADING	ALTITUDE observed (ft)	O_3 ($\mu g/m^3$)	MANIFOLD TEMP. observed (°C)	TEMP. observed (°C)	TRUE AIR SPEED observed (mph)
17:52	ORI	TAKEOFF	203	-	-	-	160
17:57	"	LOW PASS	253	191	-	-	-
18:00	"	285°	1500	204	-	-	180
02		"	"	182	-	-	-
04		"	"	182	-	-	-
06		"	"	200	-	-	-
08		"	"	196	-	-	-
10		"	"	187	-	-	-
12		"	"	196	-	-	-
14	JASPER	185°	"	174	-	-	-
16		"	"	200	28.6	-	-
18		"	"	187	28.0	-	-
20		"	"	182	25.3	-	-
22		"	"	204	"	-	-
24		"	"	191	25.9	-	-
26		"	"	209	26.4	-	-
28		"	"	178	"	-	-
30		"	"	174	"	-	-
32		"	"	138	"	-	-
34		"		200	"	-	-
36		"	"	196	"	-	-
38		"	"	182	"	-	-
40		"	"	178	"	-	-
42		"	"	174	"	-	-
44	SABINE PASS	240°	"	182	"	-	-
46		"	"	244	"	-	-
48		"	"	191	"	-	-
50		"	"	152	25.9	-	-
52		"	"	147	26.4	-	-
54		"	"	156	"	-	-
56		"	"	213	"	-	-
58		"	"	261	27.0	-	-
19:00		"	"	182	28.6	-	-
02		"	"	174	"	-	-
04		"	"	191	"	-	-
06		"	"	204	29.6	-	-
08		"	"	165	"	-	-
10		"	"	160	"	-	-
12		"	"	130	"	-	-
14		"	"	116	29.1	-	-
16	FREEPORT	345°	"	112	28.6	-	-
18		"	"	103	"	-	-
20		"	"	116	28.0	-	-
22		"	"	116	"	-	-
24		"	"	121	"	-	-
26		"	"	121	"	-	-
28		"	"	169	27.5	-	-
30		"	"	310	"	-	-
32		"	"	191	"	-	-
34		"	"	116	"	-	-

Table E-4b-1. Tabulated data: downwind plume (005), 6/26/75 (con.)

TIM (GM	POSITION	HEADING	ALTITUDE observed (ft)	O_3 ($\mu g/m^3$)	MANIFOLD TEMP. observed (°C)	TEMP. observed (°C)	TRUE AIR SPEED observed (mph)
19:		"	"	112	28.0	-	-
		"	"	99	"	-	-
		"	"	99	27.5	-	-
		"	"	90	28.0	-	-
		"	"	112	"	-	-
		"	"	112	"	-	-
		"	"	108	27.5	-	-
		"	"	147	"	-	-
		"	"	121	"	-	-
		"	"	116	"	-	-
		"	"	86	27.5	-	-
		"	"	121	27.0	-	-
20:		"	"	143	26.4	-	-
		"	"	147	"	-	-
		"	"	182	"	-	-
		"	"	178	"	-	-
		"	"	204	"	-	-
10		"	"	226	27.0	-	-
12		"	"	209	26.4	-	-
14		"	"	204	25.3	-	-
16		"	"	178	"	-	-
17	FAIRFIELD	080°	"	-	"	-	-
18		"	"	196	"	-	-
20		"	"	200	"	-	-
22		"	"	226	"	-	-
24		"	"	209	"	-	-
26		"	"	222	"	-	-
28		"	"	218	"	-	-
30		"	"	204	25.9	-	-
32		"	"	204	26.4		
34		"	"	196	"	-	-
36		"	"	182	"	-	-
38		"	"	143	27.5	-	-
40		"	"	235	"	-	-
42		"	"	226	"	-	-
44	HENDERSON	150°	"	235	"	-	-
46		"	"	182	24.3	-	-
48		"	"	222	23.7	-	-
50		"	"	187	23.2	-	-
52		"	"	226	"	-	-
54		"	"	191	"	-	-
56		"	"	231	"	-	-
58		"	"	218	"	-	-
21:00		"	"	191	23.7	-	-
02		"	"	182	24.3	-	-
04		"	"	209	"	-	-
06		"	"	169	24.8	-	-
08		"	"	222	"	-	-
10		"	"	174	"	-	-
12		"	"	156	25.3	-	-

Table E-4b-1. Tabulated data: downwind plume (005), 6/26/75 (con.)

TIME (GMT)	POSITION	HEADING	ALTITUDE observed (ft)	O_3 ($\mu g/m^3$)	MANIFOLD TEMP. observed (^oC)	TEMP. observed (^oC)	TRUE AIR SPEED observed (mph)
21:14		"	"	160	"	-	-
16		"	"	165	"	-	-
18		"	"	165	"	-	-
20		"	"	156	"	-	-
22		"	"	165	25.9	-	-
24		"	"	165	26.4	-	-
25	JASPER	145°	"	-	"	-	-
26		"	"	196	"	-	-
28		"	"	156	"	-	-
30		"	"	165	"	-	-
32		"	"	147	"	-	-
34		"	"	239	"	-	-
36		"	"	244	"	-	-
38		"	-	143	-	-	-
42	LCH	LANDING	16	-	-	-	-

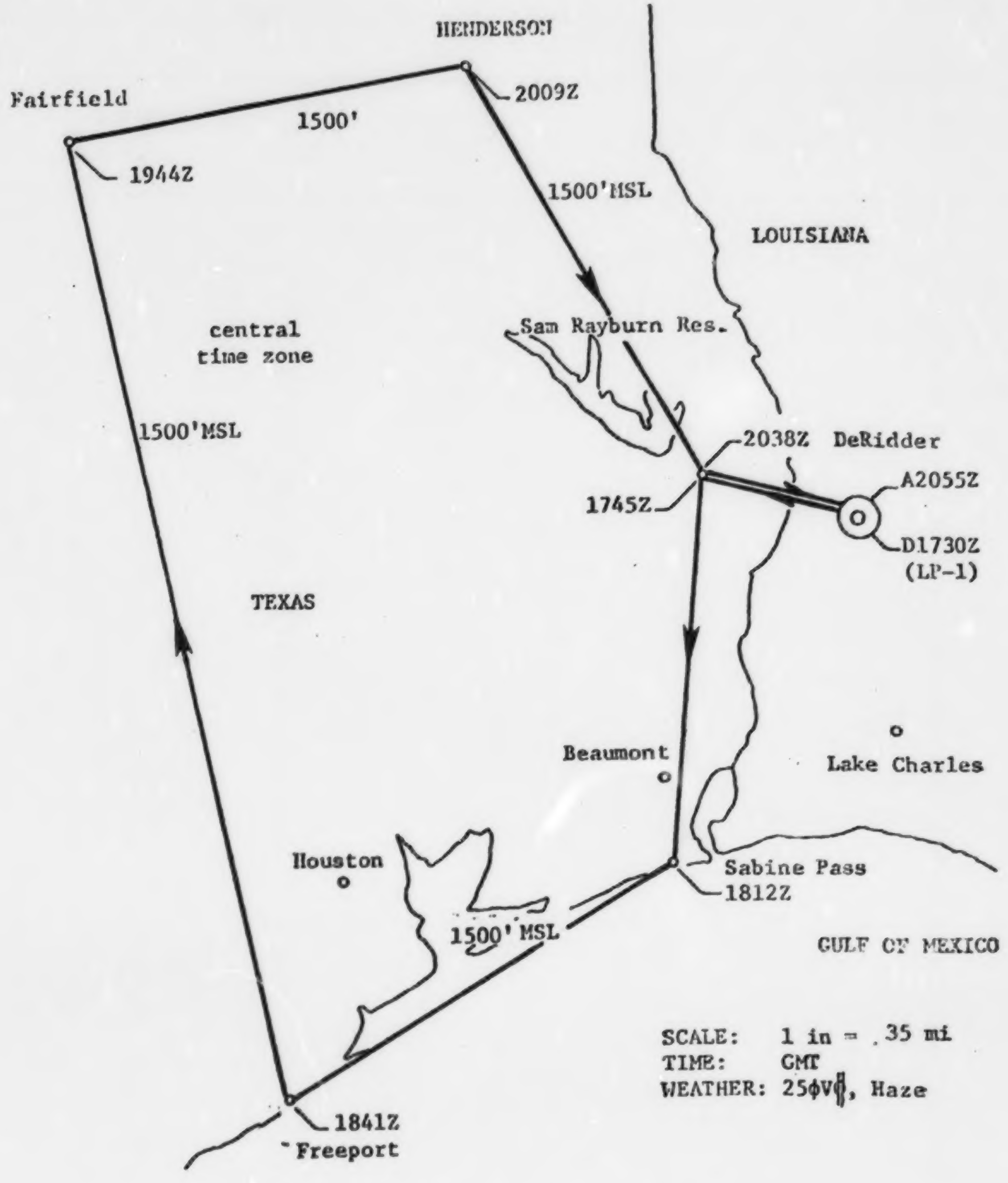
HENDERSON
Fairfield
2009Z
1500'
1944Z
1500'MSL
LOUISIANA
central
time zone
Sam Rayburn Res.
1500'MSL
2038Z
DeRidder
A2055Z
1745Z
D1730Z
(LP-1)
TEXAS
Beaumont
Lake Charles
Houston
Sabine Pass
1812Z
1500' MSL
GULF OF MEXICO
SCALE: 1 in = 35 mi
TIME: GMT
WEATHER: 250V0, Haze
1841Z
Freeport

Figure E-4C-1. Downwind plume flight (006), 6/27/75.

Table E-4c-1. Tabulated data: downwind plume (006), 6/27/75

TIME (GMT)	POSITION	HEADING	ALTITUDE observed (ft)	O_3 ($\mu g/m^3$)	MANIFOLD TEMP. observed (°C)
17:26	DRI	TAKEOFF	203	-	-
28	"	-	-	-	-
29	"	LOW PASS	253	121	-
30	"	286°	-	-	-
32		"	1500	130	-
34		"	"	116	-
36		"	"	121	-
38		"	"	99	-
40		"	"	81	-
42		"	"	95	-
44		"	"	143	29.6
45	JASPER	185°	"	-	"
46		"	"	116	"
48		"	"	134	"
50		"	"	112	"
52		"	"	121	"
54		"	"	103	"
56		"	"	95	"
58		"	"	99	"
18:00		"	"	99	"
02		"	"	125	"
04		"	"	86	"
06		"	"	147	"
08		"	"	95	"
10		"	"	55	"
12	SABINE PASS	242°	"	59	"
14		"	"	20	"
16		"	"	-	"
18		"	"	-	"
20		"	"	-	"
22		"	"	-	"
24		"	"	-	29.1
26		"	"	73	"
28		"	"	95	28.6
30		"	"	59	"
32		"	"	59	"
34		"	"	68	"
36		"	"	59	28.0
38		"	"	55	"
40		"	"	51	"
41	FREEPORT	349°	"	-	28.6
42		"	"	55	"
44		"	"	64	"
46		"	"	55	"
48		"	"	55	28.0
50		"	"	55	27.5
52		"	"	68	"
54		"	"	77	"
56		"	"	86	"
58		"	"	73	"

Table E-4c-1. Tabulated data: downwind plume (006), 6/27/75 (con.)

TIME (GMT)	POSITION	HEADING	ALTITUDE observed (ft)	O_3 ($\mu g/m^3$)	MANIFOLD TEMP. observed (^oC)
19:00		"	"	73	26.4
02		"	"	86	25.9
04		"	"	77	26.4
06		"	"	68	"
08		"	"	73	"
10		"	"	86	"
12		"	"	86	27.5
14		"	"	68	"
16		"	"	68	"
18		"	"	77	"
20		"	"	64	"
22		"	"	64	"
24		"	"	64	"
26		"	"	95	27.5
28		"	"	95	"
30		"	"	59	"
32		"	"	59	"
34		"	"	64	28.0
36		"	"	68	"
38		"	"	95	28.6
40		"	"	86	"
42		"	"	81	"
44	FAIRFIELD	80°	"	99	29.1
46		"	"	77	29.6
48		"	"	90	"
50		"	"	95	"
52		"	"	99	"
54		"	"	112	"
56		"	"	112	"
58		"	"	125	"
20:00		"	"	125	29.6
02		"	"	112	"
04		"	"	112	30.2
06		"	"	125	"
08		"	"	165	"
09	HENDERSON	152°	"	-	"
10		"	"	174	"
12		"	"	169	"
14		"	"	147	"
16		"	"	169	"
18		"	"	121	30.7
20		"	"	156	30.2
22		"	"	147	30.7
24		"	"	130	"
26		"	"	116	"
28		"	"	121	"
30		"	"	95	"
32		"	"	95	"
34		"	"	112	"
36		"	"	134	"

Table E-4c-1. Tabulated data: downwind plume (006), 6/27/75 (con.)

TIME (GMT)	POSITION	HEADING	ALTITUDE observed (ft)	O_3 ($\mu g/m^3$)	MANIFOLD TEMP. observed (^0C)
20:38	JASPER	104°	"	130	"
40		"	"	156	"
42		"	"	147	"
44		"	"	138	"
46		"	"	125	"
48		"	"	121	"
50		"	"	-	31.8
52		"	-	-	32.9
55	DRI	LANDING	203	-	-

SELECTED EXAMPLES OF THE SEA-BREEZE FLIGHTS-
GULF COAST OXIDANT STUDY

E-4D--Flight No. 075 (Morning Flight) on October 19, 1975.

E-4E--Flight No. 076 (Afternoon Flight) on October 19, 1975.

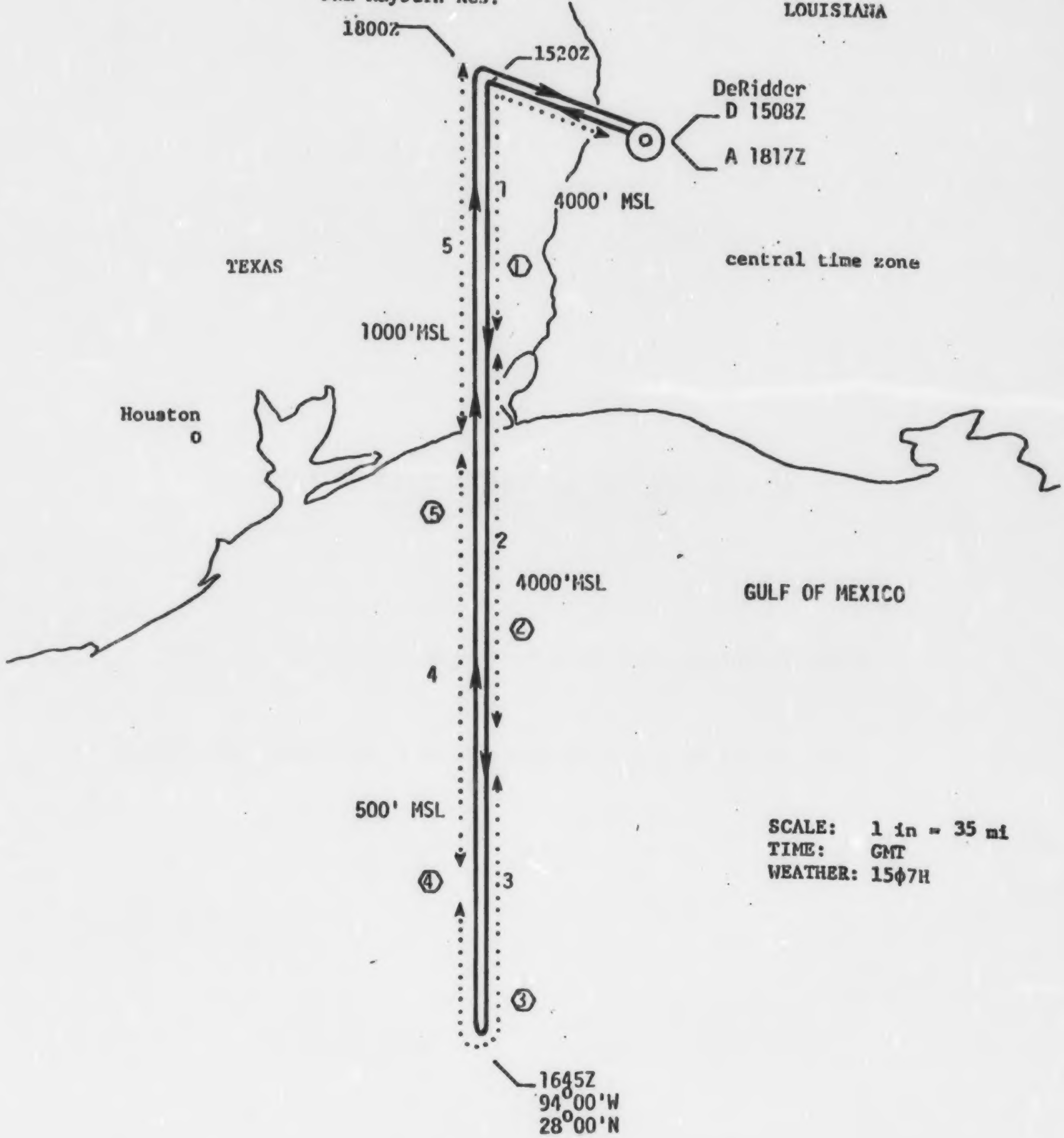

Sam Rayburn Res.
1800Z
1520Z
LOUISIANA
DeRidder
D 1508Z
A 1817Z
4000' MSL
1
5
①
TEXAS
central time zone
1000'MSL
Houston
⑤
2
4000'MSL
GULF OF MEXICO
②
4
500' MSL
④
3
③
1645Z
94°00'W
28°00'N
SCALE: 1 in = 35 mi
TIME: GMT
WEATHER: 15ϕ7H

Figure E-4D-1. Sea-breeze flight (075), 9/19/75.

Table E-4d-1. Tabulated data: sea-breeze flight (075), 9/19/75

TIME (GMT)	POSITION	HEADING	ALTITUDE (ft)	O_3 ($\mu g/m^3$)	TEMP. (°C)	DEWPT. (°C)	MANIFOLD TEMP. (°C)	TRUE AIR SPEED (mph)
15:03	DRI	TAKEOFF	203	-	-	-	-	-
08	"	280°	1183	66	24.7	20.2	28.2	158
10		"	-	66	-	-	-	-
12		"	3394	30	20.9	12.6	25.1	140
14		"	-	42	-	-	-	-
16		"	4108	66	18.8	9.3	23.6	178
18		"	-	66	-	-	-	-
20	SAM RAYBURN RES.	170°	4132	66	19.5	5.2	24.1	183
22		"	-	60	-	-	-	-
24		"	-	30	-	-	-	-
38		"	-	42	-	-	-	-
40		"	4124	48	18.6	12.3	22.6	183
42		"	-	48	-	-	-	-
44		"	4096	48	18.4	11.3	22.8	186
46		"	-	54	-	-	-	-
48		"	4131	54	18.6	12.0	22.9	185
50		"	-	54	-	-	-	-
52		"	4140	54	18.7	11.1	22.7	184
54		"	-	54	-	-	-	-
56		"	4323	60	18.9	12.1	22.8	173
58		"	-	48	-	-	-	-
16:00		"	4128	60	18.4	13.5	22.5	183
02		"	-	54	-	-	-	-
04		"	4072	60	18.1	13.0	22.7	184
06		"	-	60	-	-	-	-
08		"	4062	60	18.4	13.0	23.1	183
10		"	-	54	-	-	-	-
12		"	4088	48	18.4	13.5	22.8	183
14		"	-	54	-	-	-	-
16		"	4073	48	18.2	14.4	22.9	182
18		"	-	48	-	-	-	-
20		"	4062	42	18.4	12.9	23.0	183
22		"	-	48	-	-	-	-
24		"	4078	48	18.5	12.3	23.2	183
26		"	-	42	-	-	-	-
28		"	4098	42	18.6	11.5	23.3	184
30		"	-	36	-	-	-	-
32		"	4080	36	18.7	12.3	23.0	183
34		"	-	30	-	-	-	-
36		"	4090	30	18.9	11.5	23.6	180
38		"	-	36	-	-	-	-
40		"	4088	30	18.8	11.6	23.4	182
42		"	-	30	-	-	-	-
44		"	-	-	-	-	-	-
45	94°W,28°N	350°	4077	30	18.5	13.1	23.3	183
46		"	-	30	-	-	-	-
48		"	3028	30	18.5	13.0	24.3	209

Table E-4d-1. Tabulated data: sea-breeze flight (075), 9/19/75 (con.)

TIME (GMT)	POSITION	HEADING	ALTITUDE (ft)	O_3 (μg/m^3)	TEMP. (°C)	DEWPT. (°C)	MANIFOLD TEMP. (°C)	TRUE AIR SPEED (mph)
50		350°	-	30	-	-	-	-
52		"	923	42	23.3	22.5	27.6	199
54		"	-	36	-	-	-	-
56		"	460	36	26.3	21.6	29.6	180
58		"	-	41	-	-	-	-
17:00		"	455	41	26.6	21.4	30.2	176
02		"	-	61	-	-	-	-
04		"	519	61	26.4	21.7	30.2	179
06		"	-	56	-	-	-	-
08		"	473	56	26.6	21.6	30.3	177
10		"	-	51	-	-	-	-
12		"	484	51	26.4	21.6	30.3	177
14		"	-	46	-	-	-	-
16		"	472	46	26.4	21.6	30.4	178
18		"	-	46	-	-	-	-
20		"	513	46	26.4	21.5	30.4	176
22		"	-	46	-	-	-	-
24		"	525	41	26.5	21.6	30.2	176
26		"	-	41	-	-	-	-
28		"	501	47	26.4	21.4	30.5	176
30		"	-	47	-	-	-	-
32		"	933	47	26.7	20.6	30.2	166
34		"	-	68	-	-	-	-
36		"	1038	68	25.9	20.3	30.2	184
38		"	-	72	-	-	-	-
40		"	503	83	28.0	19.9	31.3	183
42		"	-	78	-	-	-	-
44		"	646	78	28.3	18.9	31.8	174
46		"	-	83	-	-	-	-
48		"	723	83	28.1	19.4	31.7	173
50		"	-	67	-	-	-	-
52		"	734	57	27.6	19.0	31.7	178
54		"	-	62	-	-	-	-
56		"	1042	78	27.1	18.5	31.2	177
58		"	-	78	-	-	-	-
18:00	SAM RAYBURN RES.	100°	870	88	27.4	18.7	31.4	176
02		"	-	78	-	-	-	-
04		"	946	62	27.0	12.9	31.1	178
06		"	-	78	-	-	-	-
08		"	928	98	27.0	18.4	31.0	181
10		"	-	109	-	-	-	-
12		"	928	114	27.0	18.0	31.1	180
14		"	-	114	-	-	-	-
17	DRI	LANDING	203	-	-	-	-	-

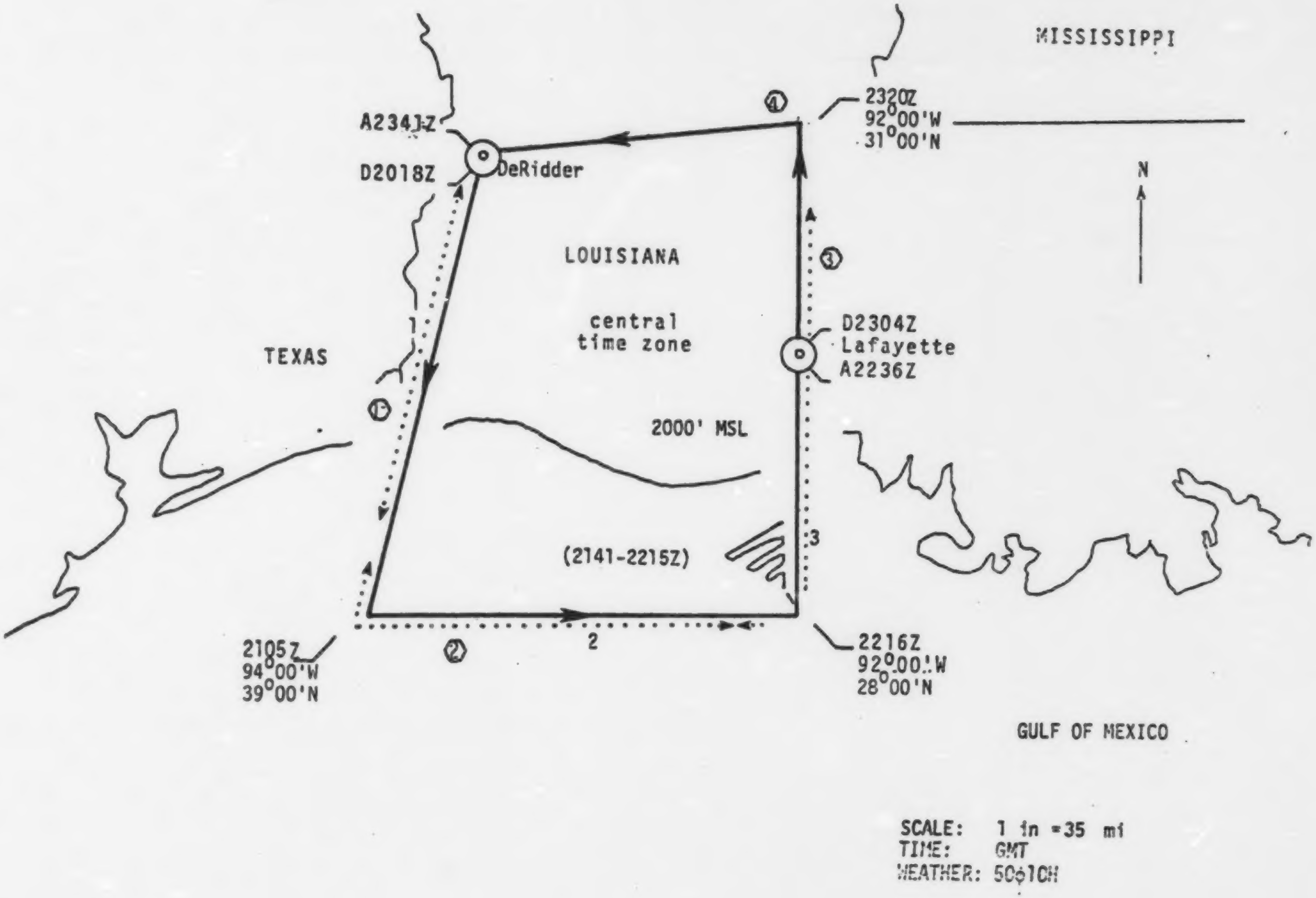
MISSISSIPPI
A2341Z
D2018Z
DeRidder
2320Z
92°00'W
31°00'N
N
LOUISIANA
central
time zone
TEXAS
D2304Z
Lafayette
A2236Z
2000' MSL
(2141-2215Z)
1
2
3
①
②
③
④
2105Z
94°00'W
39°00'N
2216Z
92°00'W
28°00'N
GULF OF MEXICO
SCALE: 1 in =35 mi
TIME: GMT
WEATHER: 50¢1CH

Figure E-4E-1. Sea-breeze flight (076), 9/19/75.

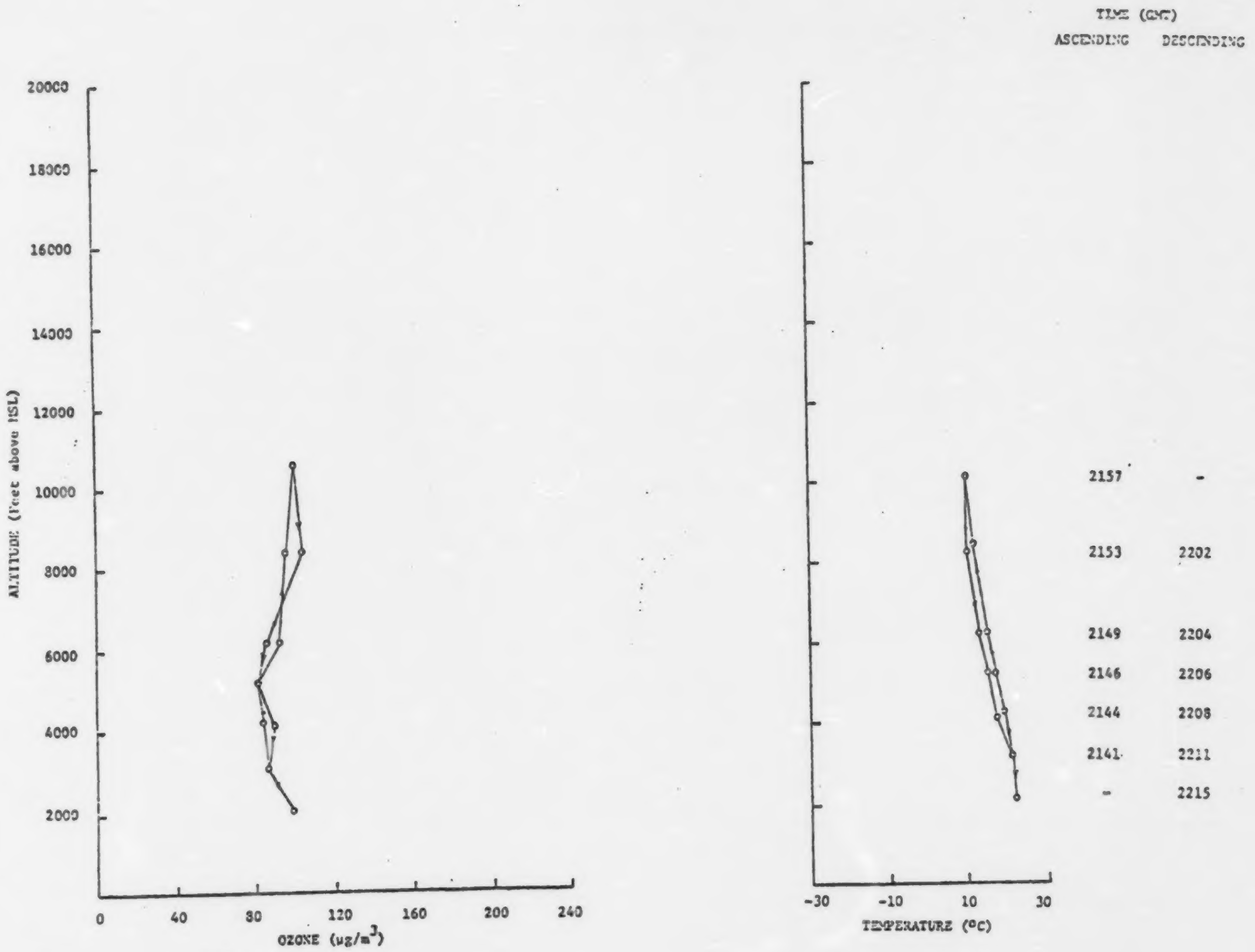

Figure E-4E-2. Vertical profile flight, 92°W, 28°N (076), 9/19/75.

Table E-4e-1. Tabulated data: sea-breeze flight (076), 9/19/75

TIME (GMT)	POSITION	HEADING	ALTITUDE (ft)	O_3 ($\mu g/m^3$)	TEMP. (°C)	DEWPT. (°C)	MANIFOLD TEMP. (°C)	TRUE AIR SPEED (mph)
20:17	DRI	TAKEOFF	203	-	-	-	-	-
18	"	198°	642	102	29.1	17.2	33.6	161
20		"	-	104	-	-	-	-
22		"	2123	109	25.7	16.8	30.8	172
24		"	-	98	-	-	-	-
26		"	2078	93	24.7	16.4	29.8	179
28		"	-	98	-	-	-	-
30		"	2056	98	24.2	18.5	29.5	183
32		"	-	98	-	-	-	-
34		"	2031	87	24.0	19.1	28.6	174
36		"	-	82	-	-	-	-
38		"	2030	87	23.1	20.0	29.1	181
40		"	-	87	-	-	-	-
42		"	2030	65	23.0	19.0	28.0	180
44		"	-	60	-	-	-	-
46		"	2025	49	23.2	16.6	27.6	179
48		"	-	55	-	-	-	-
50		"	2026	49	22.4	19.7	27.2	176
52		"	-	55	-	-	-	-
54		"	1989	60	22.5	19.2	27.1	175
56		"	-	55	-	-	-	-
58		"	2014	60	22.6	20.0	27.7	177
21:00		"	-	55	-	-	-	-
02		"	1979	49	22.7	19.2	34.2	176
04			-	55	-	-	-	-
05	94°W; 29°N	090°	-	-	-	-	-	-
06		"	2136	55	22.4	19.4	27.4	175
08		"	-	55	-	-	-	-
10		"	2137	55	22.5	19.6	27.5	175
12		"	-	65	-	-	-	-
14		"	2115	76	22.0	20.4	27.2	180
16		"	-	60	-	-	-	-
18		"	2135	65	22.2	18.9	27.4	177
20		"	-	71	-	-	-	-
22		"	2135	71	22.2	19.5	27.2	176
24		"	-	82	-	-	-	-
26		"	2140	87	22.1	20.0	26.9	175
28		"	-	87	-	-	-	-
30		"	2139	87	21.9	19.4	26.9	177
32		"	-	87	-	-	-	-
34		"	2115	87	22.0	19.8	27.1	176
38	92°W; 28°N	VERTICAL	-	-	-	-	-	-
41	"	"	3115	86	20.7	10.6	26.0	180
44	"	"	4187	84	19.2	9.5	24.9	182
46	"	"	5201	82	16.9	6.1	23.0	186
49	"	"	6208	93	15.2	5.1	21.6	182
53	"	"	8377	96	11.9	1.2	19.2	188
57	"	"	10619	101	10.4	-3.6	17.2	163
22:01	"	"	8202	104	10.2	0.6	17.6	209
04	"	"	6177	86	13.1	3.7	19.6	200
06	"	"	5190	82	14.8	5.2	20.9	197
08	"	"	4091	90	17.2	10.0	22.5	195
11	"	"	3106	86	20.5	12.2	24.9	183
15	"	"	2086	98	22.2	19.6	26.3	179

Table E-4e-1. Tabulated data: sea-breeze flight (076), 9/19/75 (con.)

TIME (GMT)	POSITION	HEADING	ALTITUDE (ft)	O_3 ($\mu g/m^3$)	TEMP. (°C)	DEWPT. (°C)	MANIFOLD TEMP. (°C)	TRUE AIR SPEED (mph)
22:16	92°W;28°N	360°	2080	104	22.2	18.4	26.6	180
10		"	-	87	-	-	-	-
20		"	2108	98	22.7	17.3	27.1	181
22		"	-	98	-	-	-	-
24		"	2125	98	23.3	13.6	27.9	183
26		"	-	98	-	-	-	-
28		"	1378	104	24.0	18.9	28.7	185
30		"	-	115	-	-	-	-
32		"	-	115	28.9	19.1	30.1	
36	LFT	LANDING	42	-	-	-	-	-
23:03	LFT	TAKEOFF	42	-	-	-	-	-
04	"	360°	2141	153	23.9	16.8	29.2	182
06		"	-	142	-	-	-	-
08		"	2144	131	24.3	16.3	29.2	183
10		"	-	136	-	-	-	-
12		"	2144	136	24.3	16.7	29.1	179
14		"	-	136	-	-	-	-
16		"	2168	120	24.2	16.8	28.7	180
18		"	-	120	-	-	-	-
20	92°W;31°N	262°	2150	125	24.3	15.7	29.1	180
22		"	-	125	-	-	-	-
24		"	2151	109	24.4	17.2	29.0	178
26		"	-	115	-	-	-	-
28		"	2158	98	24.6	15.5	29.1	180
30		"	-	104	-	-	-	-
32		"	2134	109	24.6	17.3	29.2	181
34		"	-	109	-	-	-	-
36		"	2145	109	24.4	18.3	29.2	181
38		"	-	125	-	-	-	-
40		"	1533	158	24.9	18.7	29.7	193
41	DRI	LANDING	203	-	-	-	-	-

SELECTED EXAMPLES OF THE BOX PATTERN FLIGHTS- GULF COAST OXIDANT STUDY

E-4F--Flights No. 099, 100 on October 19, 1975.

E-4G--Flight No. 109 on October 30, 1975.

E-4H--Flight No. 110 on October 31, 1975.

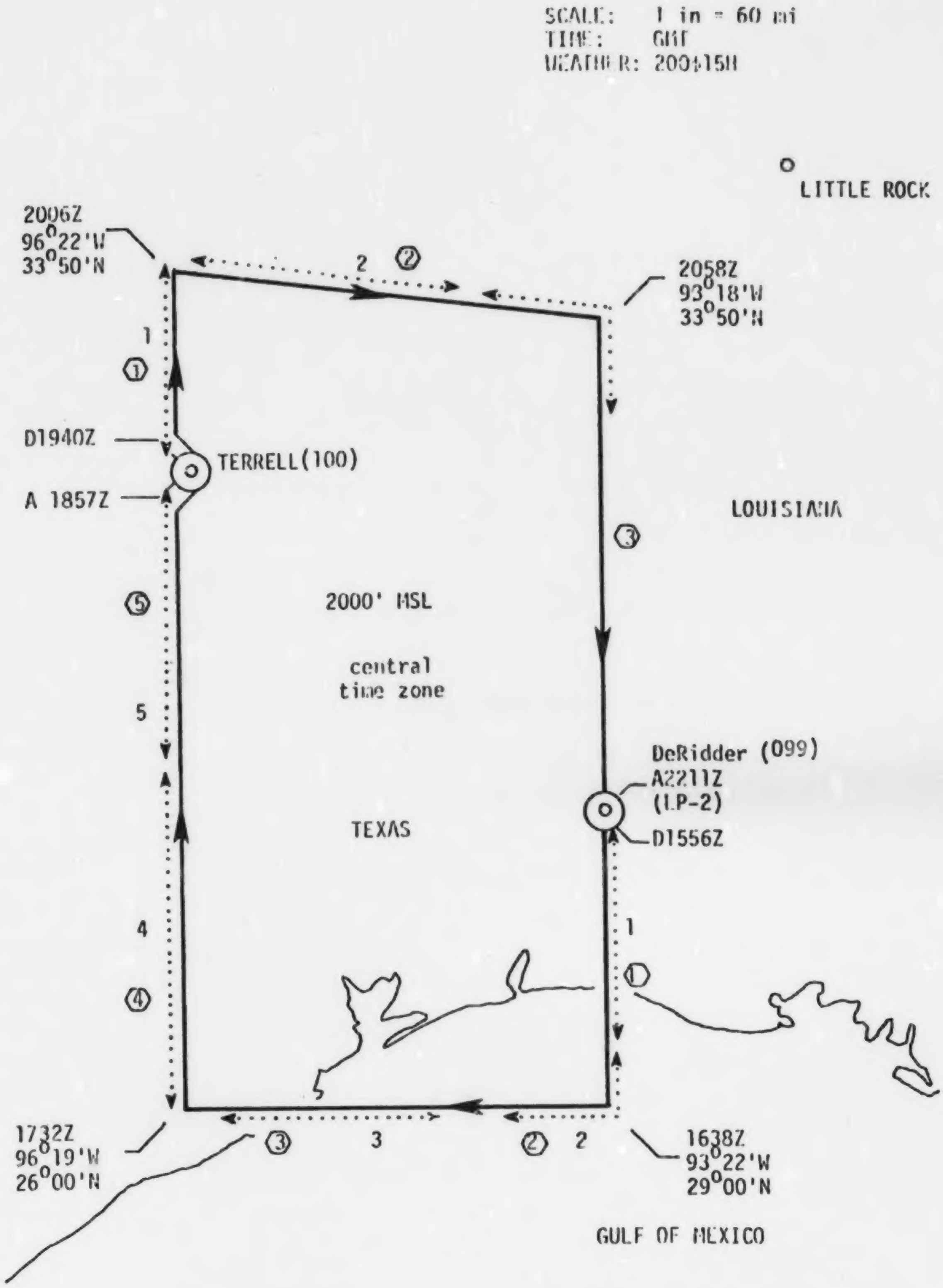
SCALE: 1 in = 60 mi
TIME: GMT
WEATHER: 200⊕15H
LITTLE ROCK
2006Z
96°22'W
33°50'N
2 ②
2058Z
93°18'W
33°50'N
1
①
D1940Z
TERRELL(100)
A 1857Z
LOUISIANA
③
⑤
2000' MSL
central
time zone
5
DeRidder (099)
A2211Z
(LP-2)
D1556Z
TEXAS
4
1
①
④
1732Z
96°19'W
26°00'N
③
3
②
2
1638Z
93°22'W
29°00'N
GULF OF MEXICO

Figure E-4F-1. Box pattern flights (099-100), 10/19/75.

Table E-4f-1. Tabulated data: box pattern flights (099-100), 10/19/75

TIME (GMT)	POSITION	HEADING	ALTITUDE (ft)	O_3 ($\mu g/m^3$)	NO ($\mu g/m^3$)	TEMP. (°C)	DEWPT. (°C)	MANIFOLD TEMP. (°C)	TRUE AIR SPEED (mph)
(Flight 099)									
15:51	DRI	TAKEOFF	203	-	-	-	-	-	-
54	"	LOW PASS	253	118	-	17.0	4.5	32.9	154
56	"	175°	-	125	-	-	-	-	-
58		"	1744	125	-	14.4	2.3	32.4	188
16:00		"	-	131	-	-	-	-	-
02		"	1751	131	17	14.5	0.9	-	188
04		"	-	131	-	-	-	-	-
06		"	1721	142	17	14.5	1.0	32.2	187
08		"	-	147	-	-	-	-	-
10		"	1750	153	17	14.3	2.2	31.7	187
12		"	-	158	-	-	-	-	-
14		"	1755	174	17	14.3	2.0	31.8	187
16		"	-	142	-	-	-	-	-
18		"	1761	142	10	14.2	2.5	32.4	187
20		"	-	147	-	-	-	-	-
22		"	1768	142	6	14.4	5.2	31.8	188
24		"	-	142	-	-	-	-	-
26		"	1709	142	4	14.4	4.7	31.9	185
28		"	-	136	-	-	-	-	-
30		"	1757	136	-	14.6	5.2	31.9	186
32		"	-	131	-	-	-	-	-
34		"	1769	131	-	14.5	7.1	31.9	188
36		"	-	125	-	-	-	-	-
38	93°22'W,29°N	263°	1745	131	8	14.5	7.9	32.0	186
40		"	-	125	-	-	-	-	-
42		"	1771	131	0	14.8	8.1	32.0	187
44		"	-	136	-	-	-	-	-
46		"	1772	142	0	15.1	7.5	32.7	183
48		"	-	147	-	-	-	-	-
50		"	1771	142	14	14.9	6.8	32.0	185
52		"	-	142	-	-	-	-	-
54		"	1766	153	17	15.0	5.7	31.8	185
56		"	-	164	-	-	-	-	-
58		"	1827	158	22	15.3	6.4	31.7	185
17:00		"	-	153	-	-	-	-	-
02		"	1813	153	8	15.0	5.3	31.6	185
04		"	-	153	-	-	-	-	-
06		"	1825	147	9	15.0	5.4	31.5	187
08		"	-	174	-	-	-	-	-
10		"	1791	164	9	15.2	5.0	31.5	184
12		"	-	169	-	-	-	-	-
14		"	1801	174	3	15.8	2.8	31.3	186
16		"	-	153	-	-	-	-	-
18		"	1846	169	0	16.4	2.2	31.3	184
20		"	-	169	-	-	-	-	-
22		"	1834	174	0	16.4	2.7	31.3	188
24		"	-	164	-	-	-	-	-
26		"	1822	180	0	16.4	1.9	31.3	183
28		"	-	174	-	-	-	-	-
30		"	1835	164	0	16.5	2.4	-	183

Table E-4f-1. Tabulated data: box pattern flights (099-100), 10/19/75 (con.)

TIME (GMT)	POSITION	HEADING	ALTITUDE (ft)	O_3 ($\mu g/m^3$)	NO ($\mu g/m^3$)	TEMP. (°C)	DEWPT. (°C)	MANIFOLD TEMP. (°C)	TRUE AIR SPEED (mph)
17:32	96°19'W,29°N	350°	-	164	-	-	-	-	-
34		"	1850	158	0	16.1	2.7	32.2	188
36		"	-	164	-	-	-	-	-
38		"	1821	169	0	16.2	2.1	31.8	189
40		"	-	164	-	-	-	-	-
42		"	1835	164	0	16.5	2.3	-	190
44		"	-	164	-	-	-	-	-
46		"	1825	164	0	16.8	1.1	31.9	181
48		"	-	153	-	-	-	-	-
50		"	1867	158	5	16.8	1.7	31.2	184
52		"	-	153	-	-	-	-	-
54		"	1856	164	6	16.9	1.7	31.0	181
56		"	-	158	-	-	-	-	-
58		"	1935	158	9	17.1	1.7	32.1	182
18:00		"	-	153	-	-	-	-	-
02		"	1837	147	10	16.9	1.6	31.8	182
04		"	-	147	-	-	-	-	-
06		"	1855	153	10	16.8	0.1	32.8	182
08		"	-	153	-	-	-	-	-
10		"	1921	158	8	16.8	0.7	32.2	184
12		"	-	158	-	-	-	-	-
14		"	1833	147	9	17.2	0.9	32.3	181
16		"	-	147	-	-	-	-	-
18		"	1838	147	15	17.0	1.6	31.3	181
20		"	-	147	-	-	-	-	-
22		"	1861	147	20	16.9	1.7	31.4	186
24		"	-	142	-	-	-	-	-
26		"	1857	147	20	17.1	1.2	31.5	183
28		"	-	142	-	-	-	-	-
30		"	1865	147	20	17.5	1.6	31.6	181
32		"	-	153	-	-	-	-	-
34		"	1914	153	20	17.5	0.6	32.2	176
36		"	-	153	-	-	-	-	-
38		"	1870	153	4	17.3	1.1	33.0	178
40		"	-	158	-	-	-	-	-
42		"	1821	158	0	17.2	0.9	32.4	182
44		"	-	158	-	-	-	-	-
46		"	1860	169	4	16.7	1.6	31.3	187
48		"	-	158	-	-	-	-	-
50		"	1716	164	6	16.6	1.5	31.3	185
52		018°	-	164	-	-	-	-	-
54		"	-	164	-	20.0	1.5	31.6	104
57	TERRELL	LANDING	479	-	-	-	-	-	-

Table E-4f-1. Tabulated data: box pattern flights (099-100), 10/19/75 (con.)

TIME (GMT)	POSITION	HEADING	ALTITUDE (ft)	O_3 (μg/m^3)	NO (μg/m^3)	TEMP. (°C)	DEWPT. (°C)	MANIFOLD TEMP. (°C)	TRUE AIR SPEED (mph)
(Flight 100)									
19:38	TERRELL	TAKEOFF	479	-	-	-	-	-	-
40	"	300°	2043	164	0	18.8	3.5	31.8	161
42		350°	-	169	-	-	-	-	-
44		"	1912	169	0	17.4	0.8	31.9	186
46		"	-	180	-	-	-	-	-
48		"	1847	180	0	17.4	0.9	32.2	187
50		"	-	180	-	-	-	-	-
52		"	1883	169	0	17.4	1.0	32.1	184
54		"	-	169	-	-	-	-	-
56		"	1997	158	0	17.4	0.8	32.9	187
58		"	-	153	-	-	-	-	-
20:00		"	1832	153	0	17.9	0.8	32.9	183
02		"	-	153	-	-	-	-	-
04		"	1807	142	0	17.7	1.2	32.3	183
06	96°22'W, 33°50'N	080°	-	136	-	-	-	-	-
08		"	1913	142	0	17.5	1.0	32.6	183
10		"	-	142	-	-	-	-	-
12		"	1833	136	0	17.1	1.0	34.2	188
14		"	-	131	-	-	-	-	-
16		"	1976	131	0	16.9	0.6	34.4	187
18		"	-	131	-	-	-	-	-
20		"	1957	131	0	16.9	0.4	33.4	183
22		"	-	136	-	-	-	-	-
24		"	1901	125	0	16.6	-1.6	33.6	187
26		"	-	125	-	-	-	-	-
28		"	-	-	0	-	-	-	-
30		"	-	125	-	-	-	-	-
32		"	1976	125	0	16.1	-1.9	34.8	186
34		"	-	115	-	-	-	-	-
36		"	1872	115	0	15.8	-3.1	34.1	187
38		"	-	104	-	-	-	-	-
40		"	1976	109	0	16.1	-2.8	-	186
42		"	-	104	-	-	-	-	-
44		"	1972	109	0	15.5	-1.8	32.3	187
46		"	-	109	-	-	-	-	-
48		"	1968	98	0	14.9	-4.3	-	195
50		"	-	109	-	-	-	-	-
52		"	1949	109	0	15.6	-4.5	32.8	188
54		"	-	98	-	-	-	-	-
56		"	1800	98	0	15.6	-6.4	32.0	182
58	93°18'W, 33°50'N	174°	-	98	-	-	-	-	-
21:00		"	1915	98	0	14.9	-4.7	35.8	185
02		"	-	104	-	-	-	-	-
04		"	1907	104	0	15.7	-5.3	35.6	175
06		"	-	109	-	-	-	-	-
08		"	1911	104	0	15.3	-5.0	-	185
10		"	-	104	-	-	-	-	-
12		"	1878	131	0	15.8	-3.7	-	183
14		"	-	115	-	-	-	-	-
16		"	1862	109	0	16.0	-6.2	-	187

Table E-4f-1. Tabulated data: box pattern flights (099-100), 10/19/75 (con.)

TIME (GMT)	POSITION	HEADING	ALTITUDE (ft)	O_3 (µg/m^3)	NO (µg/m^3)	TEMP. (°C)	DEWPT. (°C)	MANIFOLD TEMP. (°C)	TRUE AIR SPEED (mph)
21:18		"	-	115	-	-	-	-	-
20		"	1967	115	0	16.5	-6.6	-	184
22		"	-	109	-	-	-	-	-
24		"	1860	115	0	16.7	-5.6	-	180
26		"	-	109	-	-	-	-	-
28		"	1841	115	0	16.5	-3.8	-	186
30		"	-	125	-	-	-	-	-
32		"	2092	136	0	16.3	-3.1	-	182
34		"	-	158	-	-	-	-	-
36		"	1799	169	0	16.5	-2.6	33.8	187
38		"	-	153	-	-	-	-	-
40		"	1824	131	0	16.7	-0.4	-	187
42		"	-	125	-	-	-	-	-
44		"	1802	125	0	17.0	-1.2	33.1	186
46		"	-	125	-	-	-	-	-
48		"	1828	125	0	17.3	-0.3	34.2	187
50		"	-	125	-	-	-	-	-
52		"	1822	125	0	17.3	-0.4	35.0	187
54		"	-	125	-	-	-	-	-
56		"	1829	131	0	17.5	-0.3	35.1	183
58		"	-	131	-	-	-	-	-
22:00		"	1847	125	0	17.5	1.0	-	183
02		"	-	125	-	-	-	-	-
04		"	549	125	0	20.3	2.2	-	182
07	DRI	LOW PASS	253	118	-	-	-	-	-
08	"	-	-	-	0	23.6	2.0	33.6	-
11	"	LANDING	203	-	-	-	-	-	-

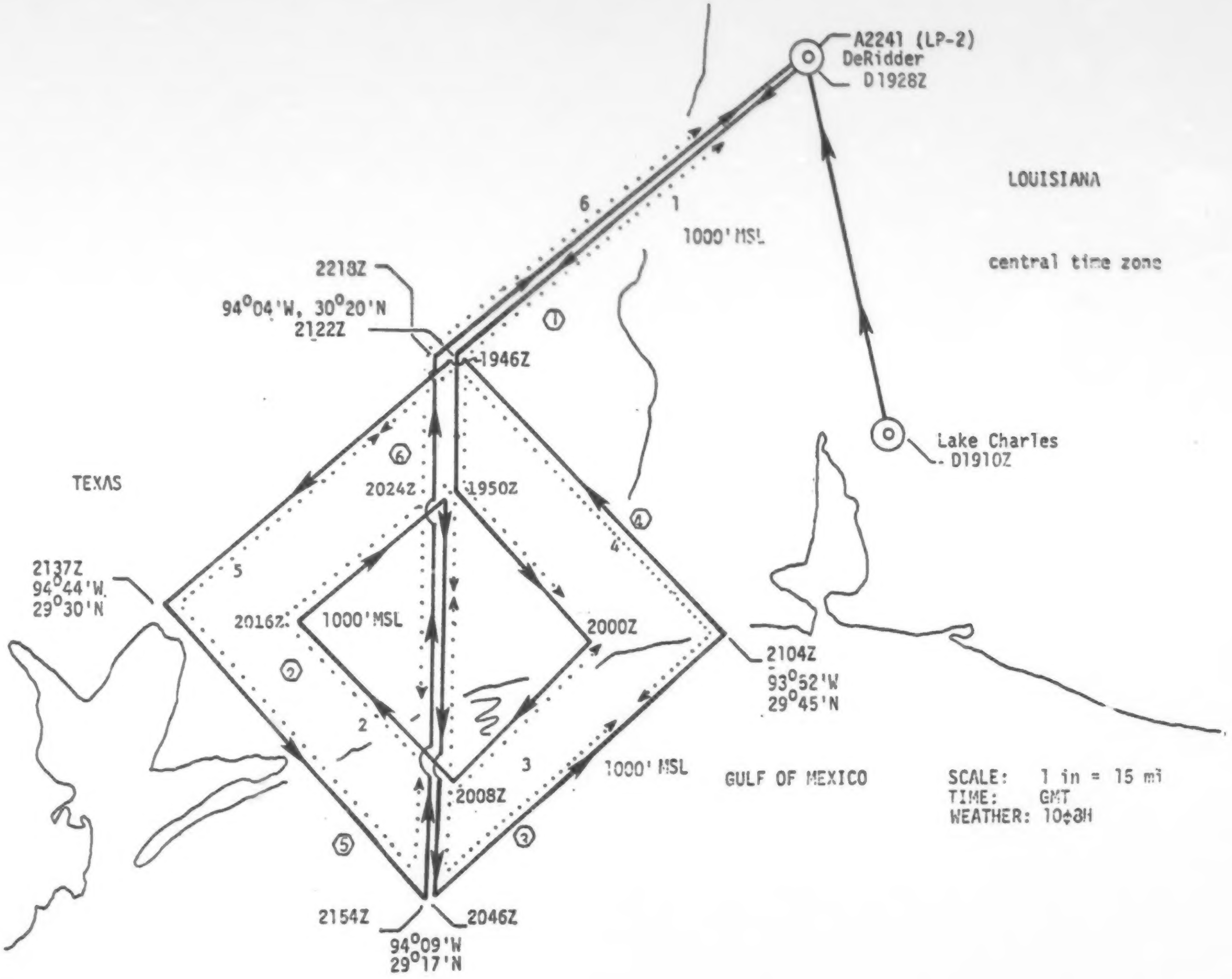
A2241 (LP-2)
DeRidder
D1928Z
LOUISIANA
central time zone
Lake Charles
D1910Z
6
1
1000' MSL
2218Z
94°04'W, 30°20'N
2122Z
1946Z
①
TEXAS
⑥
2024Z
1950Z
④
4
2137Z
94°44'W
29°30'N
5
2016Z
1000' MSL
2000Z
2104Z
93°52'W
29°45'N
②
2
3
1000' MSL
2008Z
GULF OF MEXICO
⑤
③
2154Z
2046Z
94°09'W
29°17'N
SCALE: 1 in = 15 mi
TIME: GMT
WEATHER: 10⊕3H

Figure E-4G-1. Box pattern flight (109), 10/30/75.

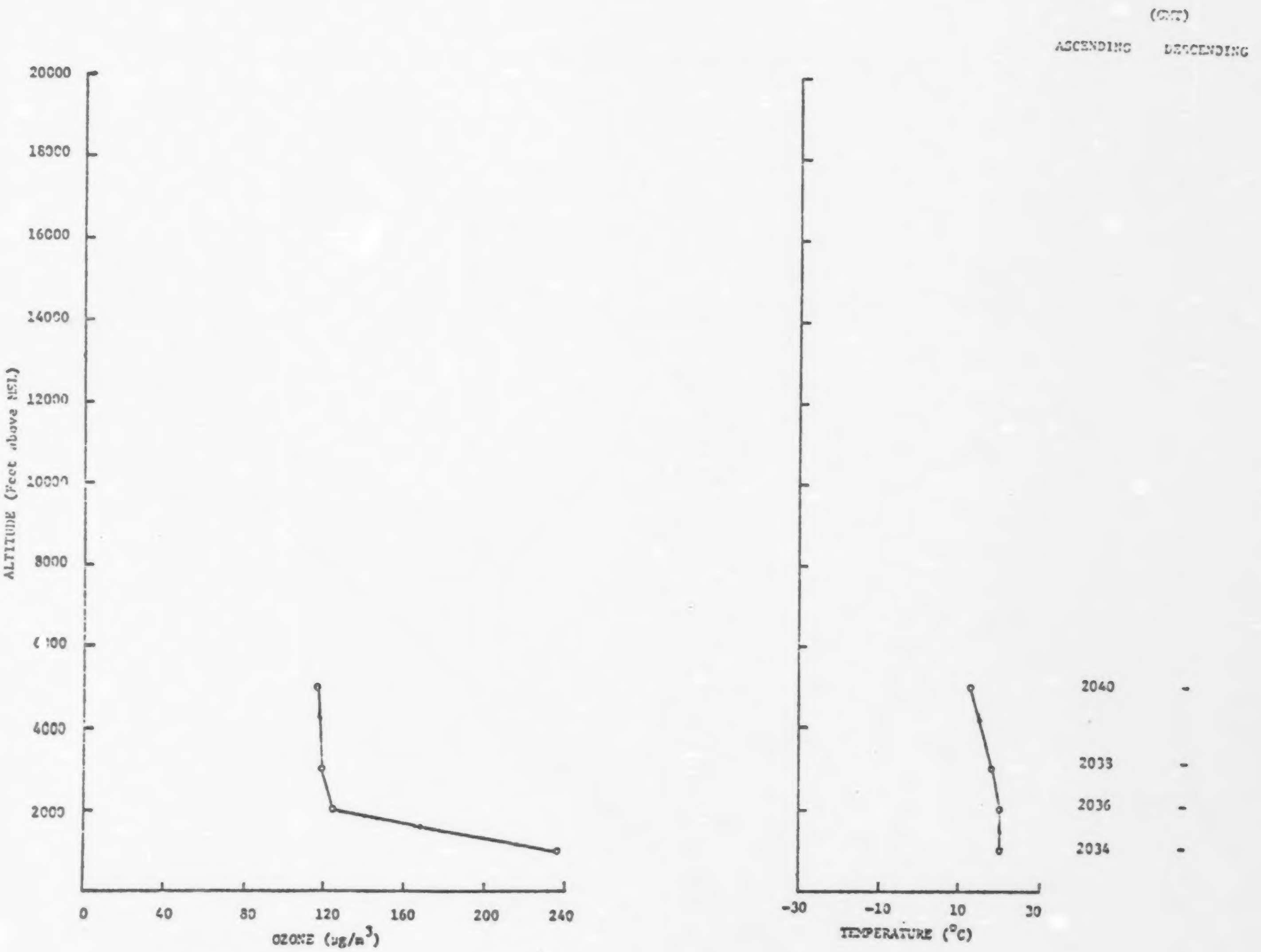

Figure E-4G-2. Vertical profile, S.W. Beaumont (109), 10/30/75.

Reproduced from best available copy.

Table E-4g-1. Box pattern flight (109), 10/30/75

TIME (GMT)	POSITION	HEADING	ALTITUDE observed (ft)	O_3 ($\mu g/m^3$)	TEMP. observed (°C)	DEWPT. (°C)	TRUE AIR SPEED observed (mph)
19:08	LCH	TAKEOFF	16	-	-	-	-
10	"	340°	-	100	20.0	15.7	179
12		"	-	98	-	-	-
14		"	1000	98	-	13.0	-
16		"	"	98	20.0	-	173
18		"	"	98	-	12.1	-
20		"	"	98	-	-	-
22		"	"	100	-	8.0	-
24		"	"	100	-	-	-
26	DRI	LOW PASS	253	96	24.0	7.1	180
28	"	255°	"	98	-	-	-
30		"	"	108	-	8.2	-
32		"	"	108	-	-	-
34		"	"	104	-	12.6	-
36		"	"	100	-	-	-
38		"	"	100	-	13.7	-
40		"	"	98	-	-	-
42		"	"	98	-	14.8	-
44		"	"	100	-	-	-
46	SILSBEE	178°	"	100	20.5	15.0	179
48		"	"	100	-	-	-
50		132°	"	100	20.5	15.0	180
52		"	"	92	-	-	-
54		"	"	98	-	15.8	-
56		"	"	116	-	-	-
58		"	"	108	-	15.8	-
20:00		228°	"	140	19.5	-	178
02		"	"	144	-	15.7	-
04		"	"	190	-	-	-
06		"	"	206	-	16.1	-
08		312°	"	256	-	-	-
10		"	"	156	20.5	16.3	180
12		"	"	156	-	-	-
14		"	"	120	-	16.9	-
16		045°	"	112	20.5	-	178
18		"	"	116	-	15.6	-
20		"	"	116	-	-	-
22		"	"	112	-	15.8	-
24		178°	"	104	20.5	-	176
26		"	"	100	-	15.6	-
28		"	"	128	-	-	-
30		"	"	152	-	16.2	-
32		"	"	174	-	-	-
34	S.W. BEAUMONT	VERTICAL/178°	"	236	-	16.5	-
36		"	2000	124	20.0	11.9	170
38		"	3000	118	18.0	10.9	165
40		"	5000	116	13.0	6.2	166
42		178°	-	-	-	-	-
44		"	-	-	-	-	-
46		038°	1000	-	20.0	-	190

Table E-4g-1. Box pattern flight (109), 10/30/75 (con.)

TIME (GMT)	POSITION	HEADING	ALTITUDE observed (ft)	O_3 ($\mu g/m^3$)	TEMP. observed (°C)	DEWPT. (°C)	TRUE AIR SPEED observed (mph)
20:48		"	"	186	-	-	-
50		"	"	156	-	-	-
52		"	"	164	-	-	-
54		"	"	186	-	-	-
56		"	"	128	-	-	-
58		"	"	-	-	15.5	-
21:00		"	"	124	19.5	-	180
02		"	"	156	-	16.1	-
04		312°	"	198	20.5	-	183
06		"	"	116	-	16.2	-
08		"	"	116	-	-	-
10		"	"	100	-	15.5	-
12		"	"	120	-	-	-
14		"	"	104	-	15.5	-
16		"	"	100	21.0	-	179
18		"	"	104	-	15.3	-
20		"	"	100	-	-	-
22	Silsbee	225°	"	104	-	14.7	-
24		"	"	108	-	-	-
26		"	"	112	21.5	15.5	181
28		"	"	112	-	-	-
30		"	"	112	22.0	15.1	180
32		"	"	104	-	-	-
34		"	"	100	-	16.8	-
36			"	104	-	-	-
37		132°	"	-	-	-	-
38		"	"	100	21.0	16.9	178
40		"	"	108	-	-	-
42		"	"	116	-	16.8	-
44		"	"	144	-	-	-
46		"	"	170	-	16.8	-
48		"	"	178	-	-	-
50		"	"	280	-	15.8	-
52		"	"	198	-	-	-
54		358°	"	280	20.0	16.1	180
56		"	"	248	-	-	-
58		"	"	226	-	16.3	-
22:00		"	"	194	22.0	-	180
02		"	"	186	-	16.8	-
04		"	"	186	-	-	-
06		"	"	148	-	16.8	-
08		"	"	116	-	-	-
10		"	"	100	-	15.6	-
12		"	"	100	-	-	-
14		"	"	100	22.0	15.2	181
16		"	"	104	-	-	-
18	SILSBEE	075°	"	104	22.0	14.1	180
20		"	"	104	-	-	-
22		"	"	108	-	13.3	-
24		"	"	116	-	-	-
26		"	"	116	-	6.0	-

Table E-4g-1. Box pattern flight (109), 10/30/75 (con.)

TIME (GMT)	POSITION	HEADING	ALTITUDE observed (ft)	O_3 ($\mu g/m^3$)	TEMP. observed (°C)	DEWPT. (°C)	TRUE AIR SPEED observed (mph)
22:28		"	"	112	-	-	-
30		"	"	112	22.0	7.0	183
32		"	"	112	-	-	-
34		"	"	112	-	5.9	-
36		"	"	112	22.0	-	185
38	DRI	LOW PASS	253	108	24.0	6.7	183
41	"	LANDING	16	-	-	-	-

Oxides of nitrogen below the minimum detectable. concentration of the analyzer.

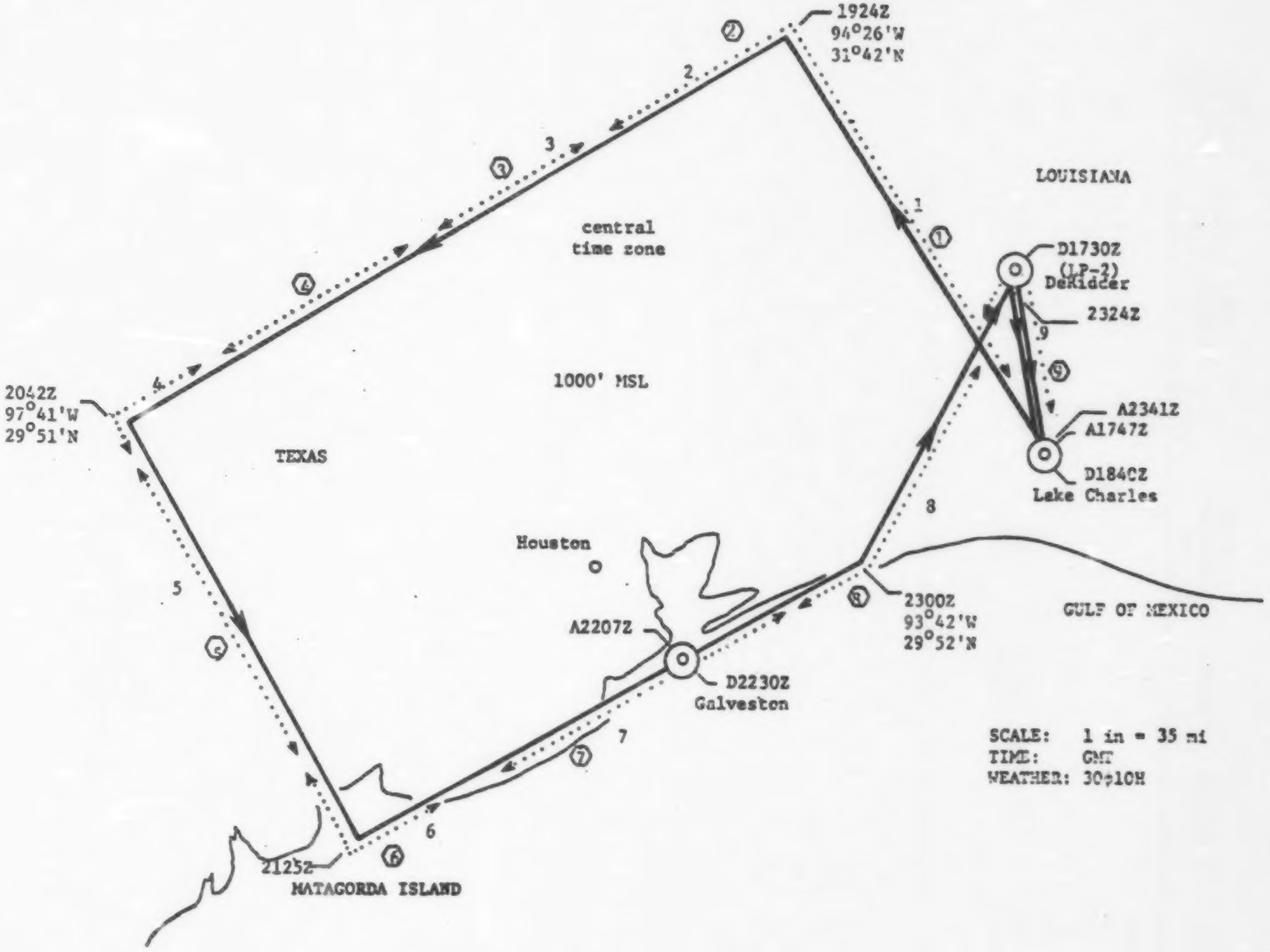
1924Z
94°26'W
31°42'N
②
2
3
③
④
4
2042Z
97°41'W
29°51'N
5
⑤
21252
MATAGORDA ISLAND
⑥
6
⑦
7
TEXAS
central
time zone
1000' MSL
Houston
A2207Z
D2230Z
Galveston
⑧
2300Z
93°42'W
29°52'N
8
GULF OF MEXICO
LOUISIANA
1
①
D1730Z
(LP-2)
DeRidder
2324Z
9
⑨
A2341Z
A1747Z
D1840Z
Lake Charles
SCALE: 1 in = 35 mi
TIME: GMT
WEATHER: 30⌀10H

Figure E-4H-1. Box pattern flight (110), 10/31/75.

Table E-4h-1. Tabulated data: box pattern flight (110), 10/31/75

TIME (GMT)	POSITION	HEADING	ALTITUDE observed (ft)	O_3 ($\mu g/m^3$)	TEMP. observed (^{o}C)	DEWPT. (^{o}C)	TRUE AIR SPEED observed (mph)
17:18	DRI	TAKEOFF	203	104	19.0	-	-
20	"	-	600	104	-	-	176
22	"	LOW PASS	253	104	20.5	5.4	180
24	"	-	1000	100	-	-	-
26	"	-	"	104	-	4.0	-
28	"	-	"	104	-	-	-
30	"	165°	"	104	18.0	5.5	182
32		"	"	104	-	-	-
34		"	"	112	-	5.3	-
36		"	"	120	-	-	-
38		"	"	128	20.0	7.5	184
40		"	"	120	-	-	-
42		"	"	132	-	8.7	-
44		"	-	128	-	-	-
46		"	-	130	-	10.2	-
47	LCH	LANDING	16	-	-	-	-
18:37	LCH	TAKEOFF	16	-	-	-	-
38	"	-	-	138	-	-	-
40	"	322°	1000	178	-	-	-
42		"	"	174	19.5	2.1	171
44		"	"	174	-	-	-
46		"	"	182	-	10.0	-
48		"	"	154	-	-	-
50		"	"	224	-	8.5	-
52		"	"	202	-	-	-
54		"	"	152	-	8.0	-
56		"	"	-	-	-	-
58		"	"	132	-	6.6	-
19:00		"	"	132	21.0	-	176
02		"	"	136	-	6.0	-
04		"	"	132	-	-	-
06		"	1200	126	21.0	3.7	178
08		"	"	126	-	-	-
10		"	"	130	-	4.6	-
12		"	"	126	-	-	-
14		"	"	122	-	5.9	-
16		"	1500	120	20.5	-	177
18		"	"	120	-	1.4	-
20		"	"	120	-	-	-
22		"	"	116	-	4.8	-
24	94°26'W,31°42'N	230°	"	116	-	-	-
26		"	"	120	21.0	3.9	180
28		"	"	124	-	-	-
30		"	"	124	21.0	3.8	182
32		"	"	128	-	-	-
34		"	"	140	-	4.8	-
36		"	"	128	-	-	-
38		"	"	132	-	6.6	-
40		"	"	136	-	-	-
42		"	"	140	-	7.6	-

Table E-4h-1. Tabulated data: box pattern flight (110), 10/31/75 (con.)

TIME (GMT)	POSITION	HEADING	ALTITUDE observed (ft)	O_3 (μg/m^3)	TEMP. observed (°C)	DEWPT. (°C)	TRUE AIR SPEED observed (mph)
19:44		"	"	136	-	-	-
46		"	"	136	21.5	-	181
48		"	"	136	-	-	-
50		"	"	148	-	9.5	-
52		"	"	148	-	-	-
54		"	"	148	-	10.2	-
56		"	"	164	-	-	-
58		"	"	152	-	8.9	-
20:00		"	"	168	22.5	-	180
02		"	"	188	-	10.2	-
04		"	"	222	-	-	-
06		"	"	266	-	12.2	-
08		"	"	200	-	-	-
10		"	"	172	-	12.4	-
12		"	"	156	-	-	-
14		"	"	152	-	12.5	-
16		"	"	148	23.0	-	178
18		"	"	152	-	13.4	-
20		"	"	148	-	-	-
22		"	"	140	-	13.9	-
24		"	"	124	-	-	-
26		"	"	124	-	14.2	-
28		"	"	128	-	-	-
30		"	"	132	23.5	13.6	182
32		"	"	132	-	-	-
34		"	"	132	-	13.5	-
36		"	"	136	-	-	-
38		"	"	132	-	13.7	-
40		"	"	128	-	-	-
42	97°41'W,29°51'N	140°	"	116	24.0	14.1	182
44		"	"	120	-	-	-
46		"	"	120	23.5	14.4	181
48		"	"	124	-	-	-
50		"	"	128	-	14.7	-
52		"	"	128	-	-	-
54		"	"	128	-	14.2	-
56		"	"	128	-	-	-
58		"	"	128	-	14.1	-
21:00		"	"	132	22.0	-	180
02		"	"	132	-	14.7	-
04		"	"	128	-	-	-
06		"	"	128	-	15.0	-
08		"	"	124	-	-	-
10		"	"	128	-	15.4	-
12		"	"	128	-	-	-
14		"	"	124	-	14.9	-
16		"	1000	124	23.0	-	183
18		"	"	124	-	14.7	-
20		"	"	128	-	-	-
22		"	"	128	-	15.5	-

Table E-4h-1. Tabulated data: box pattern flight (110), 10/31/75 (con.)

TIME (GMT)	POSITION	HEADING	ALTITUDE observed (ft)	O_3 ($\mu g/m^3$)	TEMP observed (°C)	DEWPT. (°C)	TRUE AIR SPEED observed (mph)
21:24		"	"	-	-	-	-
25		050°	"	-	-	-	-
26		"	"	128	23.0	15.4	180
28		"	"	128	-	-	-
30		"	"	136	22.5	14.6	178
32		"	"	144	-	-	-
34		"	"	144	-	14.0	-
36		"	"	148	-	-	-
38		"	"	144	22.5	14.6	181
40		"	"	140	-	-	-
42		"	"	144	-	13.3	-
44		"	"	144	-	-	-
46		"	"	148	22.0	12.0	181
48		"	"	148	-	-	-
50		"	"	144	-	10.6	-
52		"	"	144	-	-	-
54		"	"	148	-	15.2	-
56		"	"	148	-	-	-
58		"	"	148	-	14.8	-
22:00		"	"	148	21.5	-	-
02		"	"	152	-	13.8	-
04		"	"	152	-	-	-
06		"	"	156	-	14.0	-
07	GALVESTON	LANDING	-	-	-	-	-
22:29	GALVESTON	DPR	-	-	-	-	-
30	"	050°	1000	128	-	33.1	-
32		"	"	148	20.5	-	178
34		"	"	148	-	9.5	-
36		"	"	144	-	-	-
38		"	"	148	-	12.0	-
40		"	"	160	-	-	-
42		"	"	160	-	11.7	-
44		"	"	156	-	-	-
46		"	"	156	20.5	11.9	180
48		"	"	152	-	-	-
50		"	"	152	-	11.6	-
52		"	"	152	-	-	-
54		"	"	152	-	11.6	-
56		"	"	152	-	-	-
58		"	"	144	-	11.7	-
23:00	93°42'W,29°52'N	280°	"	144	20.0	-	180
02		"	"	148	-	11.4	-
04		"	"	152	-	-	-
06		"	"	148	-	10.7	-
08		"	"	152	-	-	-
10		"	"	162	-	10.7	-
12		"	"	174	-	-	-
14		"	"	174	-	8.1	-
16		"	"	166	20.5	-	181

Table E-4h-1. Tabulated data: box pattern flight (110), 10/31/75 (con.)

TIME (GMT)	POSITION	HEADING	ALTITUDE observed (ft)	O_3 ($\mu g/m^3$)	TEMP observed (°C)	DEWPT. (°C)	TRUE AIR SPEED observed (mph)
23:18		"	"	182	-	7.1	-
20		"	"	166	-	-	-
22	DRI	LOW PASS	253	142	22.0	6.0	190
24	"	160°	1000	166	20.5	7.6	178
26		"	"	178	-	-	-
28		"	"	182	-	8.0	-
30		"	"	170	21.0	-	181
32		"	"	174	-	5.1	-
34		"	"	174	-	-	-
36		"	"	170	-	7.1	-
38		"	"	166	20.0	-	180
40		"	-	166	-	11.6	-
41	LCH	LANDING	16	-	-	-	-

Oxides of nitrogen below the minimum detectable concentration of the analyzer.

APPENDIX F

BACKGROUND DATA AND EMISSION STUDY FOR TEXAS GULF COASTAL AREA

APPENDIX F

BACKGROUND DATA AND EMISSION STUDY
FOR TEXAS GULF COASTAL AREA

F-1. Background Data and Emission Study for Texas Gulf Coastal Area

A partial analysis of historical data was initiated using ozone data for Nederland, Texas from July 1 to September 30, 1972 and for Houston, Texas from August 1 to September 30, 1972 as reported by Johnson, et al.[1/]. Meteorological data from the Local Climatological Data for Jefferson County Airport and Houston Intercontinental Airport and from the Daily Weather Map, Weekly Series were examined. The Nederland ozone station is located at the Jefferson County Airport. The Houston ozone station is located in the Houston Ship Channel area, about 29 km south of the airport. Concentrations of ozone less than 100 $\mu g/m^3$ were not reported. During the measurement periods, the ozone exceeded NAAQS on 43 percent of the days at both locations.

The resultant wind direction (i.e., net transport wind direction) for those days when the ozone exceeded the NAAQS (160 $\mu g/m^3$) for at least one hour were compared with the occurrences of the resultant wind direction in all circumstances. The data presented in figure F-1 seem to indicate that the relatively infrequent occurring northwest quadrant daily resultant wind is disproportionately associated with high ozone concentrations at both Houston and Nederland. In the summer of 1972, these winds--west (250°-290°), northwest (300°-330°), and north (340°-020°)--occurred only 10 percent of the days at Houston and 15 percent of the days at Nederland. Table F-1 ranks all maximum daily one hour average ozone concentrations above 300 $\mu g/m^3$ at the two sites. The underlined values indicate days when there was a northwest quadrant resultant wind. There was no consistent association of wind speed with ozone concentration.

During the respective study periods, the following conditions were found to exist at the respective locations:

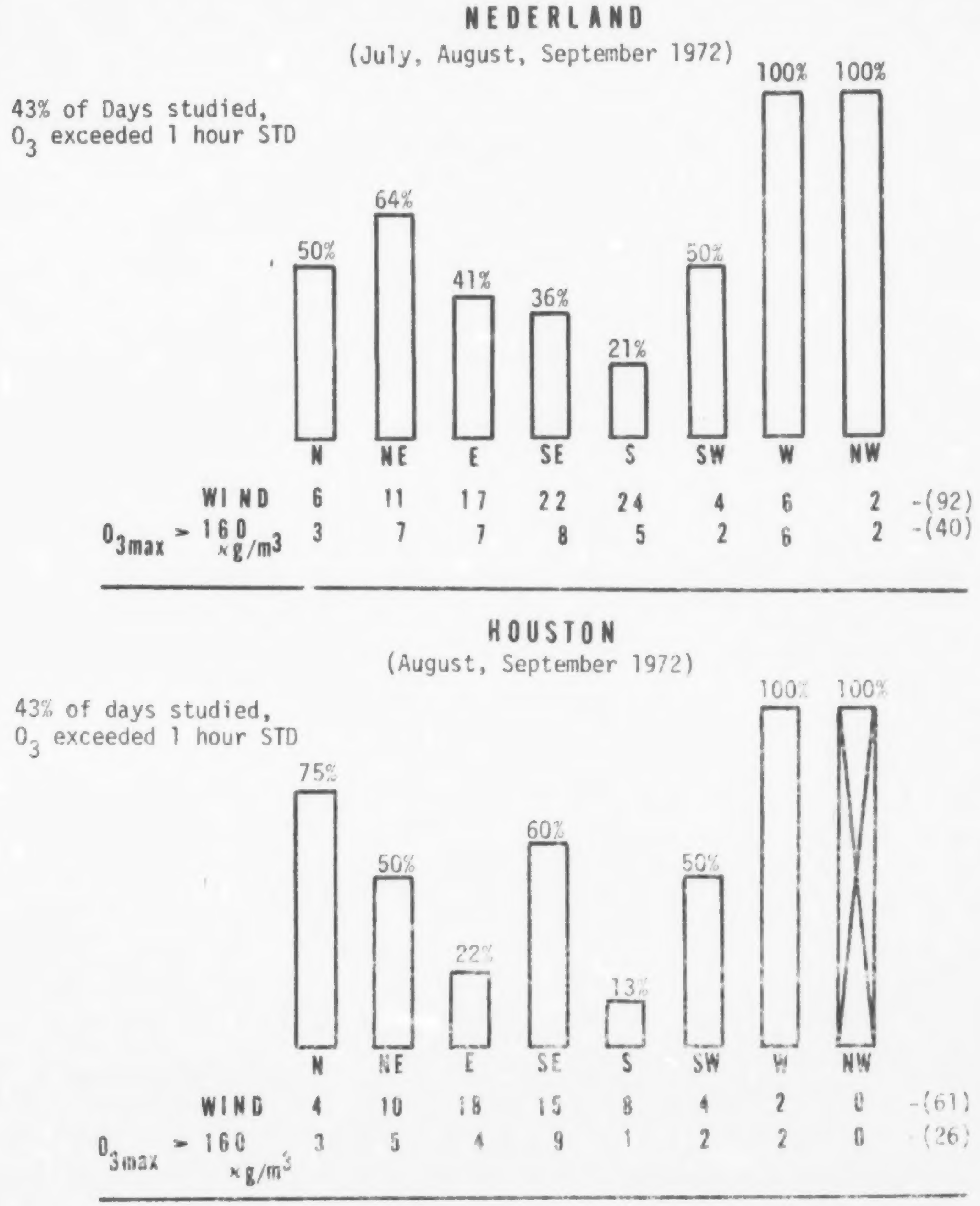

Figure F-1. Ratio of daily resultant wind direction occurrences when ozone concentration exceeded NAAQS to all occurrences of the daily resultant wind direction.

Table F-1. Ranking of maximum daily ozone concentration exceeding 300 $\mu g/m^3$

RANK	NEDERLAND		HOUSTON	
1)	715*	(9/9)**	715	(8/5)
2)	615		515	
3)	600	(8/5)	450	(9/21)
4)	500		445	
5)	425		445	
6)	410	(7/25)	425	(9/3)
7)	405		405	
8)	390		375	
9)	380	(9/21)	365	
10)	375		345	
11)	365		315	
12)	360	(8/20)		
13)	355			
14)	355			
15)	335			
16)	325	(8/21)		
17)	320			
18)	315			
19)	305	(8/6)		
20)	300	(8/22)		
21)	300			

*Underlined concentrations associated with NW resultant winds.

**Date of Occurrence.

A. NEDERLAND:

1) Seventy-nine percent of the time a NW quadrant resultant wind occurred and the maximum one hour ozone concentration exceeded 160 $\mu g/m^3$.
2) Fifty-seven percent of the time a NW quadrant resultant wind occurred and the maximum one hour ozone concentration exceeded 300 $\mu g/m^3$.
3) The maximum daily one hour average ozone concentration exceeded 300 $\mu g/m^3$ twenty-one times, eight days of which (38 percent) had a NW quadrant resultant wind.
4) The maximum daily one hour average ozone concentration exceeded 400 $\mu g/m^3$ seven times, three days of which (43 percent) had a NW quadrant resultant wind.
5) The following six days had NW quadrant resultant winds and maximum ozone less than 300 $\mu g/m^3$.

8/15	270 $\mu g/m^3$
7/29	260 $\mu g/m^3$
9/5	205 $\mu g/m^3$
7/5 and 9/30	$<$ 100 $\mu g/m^3$ (following the only cold fronts which passed during the study).
8/27	Missing Data

B. HOUSTON:

1) Eighty-three percent of the time a NW quadrant resultant wind occurred and the maximum one hour ozone concentration exceeded 160 $\mu g/m^3$.
2) Fifty percent of the time a NW quadrant resultant wind occurred and the maximum one hour ozone concentration exceeded 300 $\mu g/m^3$.
3) In August and September, the maximum daily one hour average ozone concentration exceeded 300 $\mu g/m^3$ eleven times, three days of which (27 percent) had a NW quadrant resultant wind.

4) In August and September, the maximum daily one hour average ozone concentration exceeded 400 $\mu g/m^3$ seven times, three days of which (43 percent) had a NW quadrant resultant wind.

5) The following three days had NW quadrant resultant winds and maximum ozone less than 300 $\mu g/m^3$:

8/27	290 $\mu g/m^3$
8/6	190 $\mu g/m^3$
9/30	$<$ 100 $\mu g/m^3$ (frontal passage)

The maximum hourly ozone concentrations were compared on those days when both locations reported more than 100 $\mu g/m^3$ concentrations. The data are shown in figure F-2. The least squares regression gives the Nederland (NED) concentration as a function of the Houston (HOU) concentration as:

$$\text{NED} = 0.6\ (\text{HOU}) + 155\ \mu g/m^3$$

The linear correlation coefficient is 0.61. These two results verify the impression of visual inspection of the data that the maximum Houston and Nederland ozone concentrations are not well correlated.

An inventory of available hourly ozone concentrations in the SAROAD data file was obtained. The inventory contained only measurements made by the chemiluminescent method in the states of Alabama, Mississippi, Arkansas, Louisiana and Texas.

The data were examined for the date and time of ozone concentrations greater than the NAAQS, for apparent relationships among several nearby stations and for such occurrences over widespread areas. Historic surface weather maps were used in an attempt to quantify the attendant meteorological conditions.

While the data were interesting, it was extremely difficult to relate the ozone measurements at a station among stations, or to weather conditions in a systematic manner. Research efforts were redirected to activities of the field research programs.

Dates: August & September, 1972

Conditions: Maximum 24 hour ozone concentrations exceeding 100 micrograms per cubic meter at both Houston and Nederland sites.

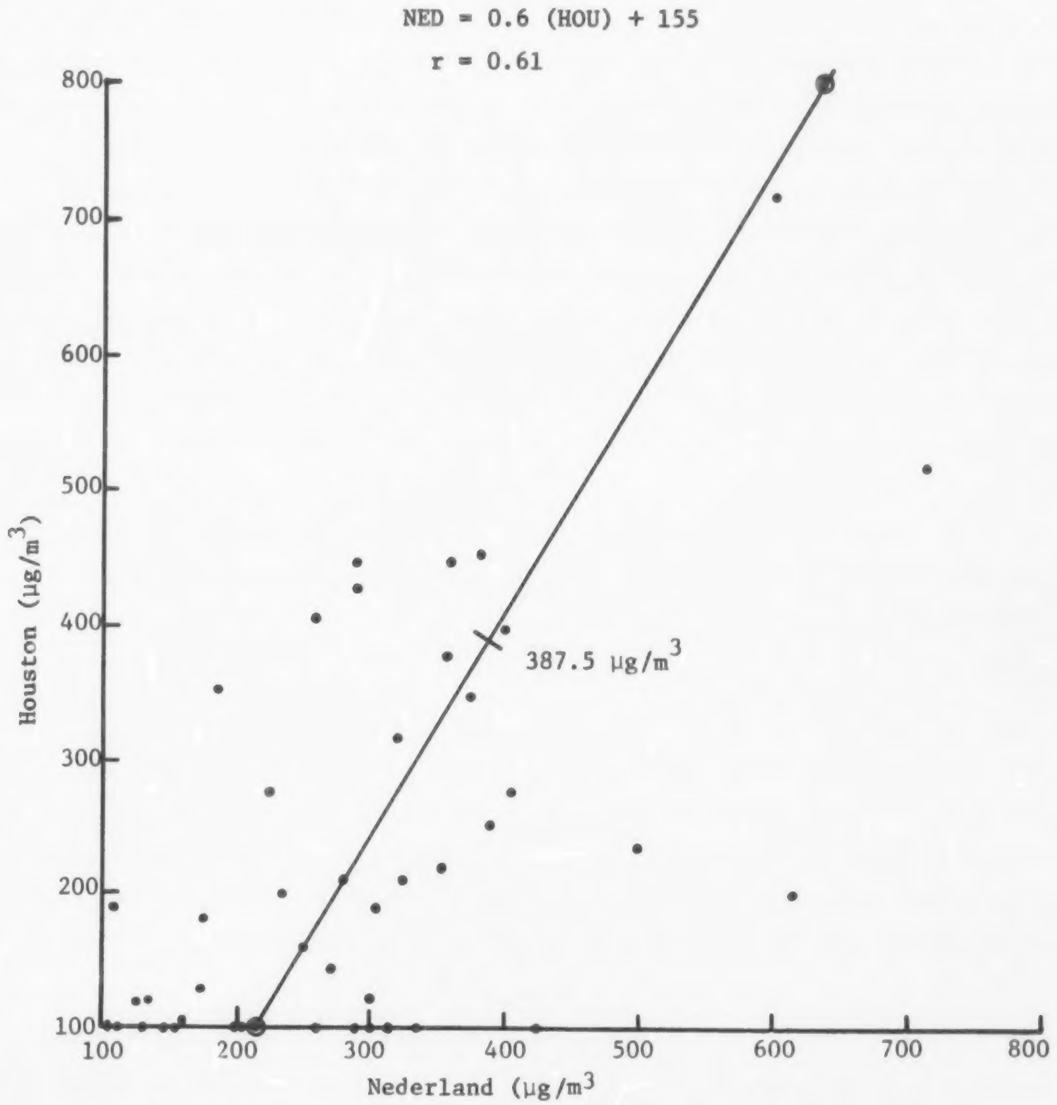

Figure F-2. Scatter diagram of maximum daily ozone concentrations (>100 $\mu g/m^3$) at Nederland and Houston, August, September, 1972.

F.2. Hydrocarbon Emission Data

Annual average hydrocarbon emission data (tons/year) for each county of each state bordering or east of the Rocky Mountains were requested from the NEDS data file. A priority was assigned at RTI to the needed data. The lowest was assigned to those states where analyses of hydrocarbon data had been done previously. A higher priority was given to those states, outside of the primary study area (e.g., South Carolina, Georgia) that had not been analyzed. The highest priority was given to the remaining states. The annual emissions by county and annual emission density (tons per square mile) were computed for the two higher priority states. The logarithm of those values were computed and plotted. A manual analysis of the resulting distribution was made at unit increments of the logarithm, i.e., at order of magnitude intervals of emission or emission density. The emission density map is available from RTI through the EPA Project Officer.

The emissions by county in Ohio, as tabulated and plotted previously, were compared with the latest data from the NEDS files. The regression equation is

$$E_{70} = 1.155\ E_{75}$$

where E_{70} and E_{75} are the 1970 and 1975 emissions, respectively. The linear correlation coefficient is 0.998. The reduced emissions in the 1975 data occur primarily in the six largest population centers. In the remainder of the counties, the emission changes are minimal. The high correlation coefficient and the small changes of emissions suggested that reanalysis of the data in the previously analyzed states was unnecessary.

F.3. Reference

1. Johnson, C. E., D. J. Johnson and R. R. Wallis, "Ozone Concentrations on the Upper Texas Gulf Coast, July, August, September 1972", Air Quality Evaluation Program, Texas State Department of Health, Austin, Texas, March 1973.